12 / 88

GEORGIA INSTITUTE OF TECHNOLOGY
OFFICE OF CONTRACT ADMINISTRATION

NOTICE OF PROJECT CLOSEOUT

Date 10/16/89

roject No. G-41-614 Center No. R5436-5A1

roject Director M. R. Flannery School/Lab Physics

ponsor Air Force

ontract/Grant No. AFOSR-84-0233 GTRC XX GIT ___

rime Contract No. N/A

itle Termolecular Association of Ions in Gases

ffective Completion Date 7/31/89 (Performance) 9/30/89 (Reports)

loseout Actions Required:

___ None
X Final Invoice or Copy of Last Invoice
X Final Report of Inventions and/or Subcontracts- Patent questionnaire sent to P/I.
X Government Property Inventory & Related Certificate
___ Classified Material Certificate
X Release and Assignment
___ Other

ncludes Subproject No(s).

bproject Under Main Project No.

ntinues Project No. Continued by Project No.

stribution:

X Project Director
X Administrative Network
X Accounting
X Procurement/GTRI Supply Services
X Research Property Management
_ Research Security Services

X Reports Coordinator (OCA)
X GTRC
X Project File
2 Contract Support Division (OCA)
___ Other

REPORT DOCUMENTATION PAGE

1a. REPORT SECURITY CLASSIFICATION UNCLASSIFIED	1b. RESTRICTIVE MARKINGS
2a. SECURITY CLASSIFICATION AUTHORITY	3. DISTRIBUTION / AVAILABILITY OF REPORT Approved for public release; distribution unlimited.
2b. DECLASSIFICATION / DOWNGRADING SCHEDULE	
4. PERFORMING ORGANIZATION REPORT NUMBER(S) GIT-85-014	5. MONITORING ORGANIZATION REPORT NUMBER(S) N/A
6a. NAME OF PERFORMING ORGANIZATION Georgia Institute of Technology 6b. OFFICE SYMBOL (If applicable)	7a. NAME OF MONITORING ORGANIZATION Air Force Office of Scientific Research (AFOSR) Directorate of Physical and Geophysical Sciences
6c. ADDRESS (City, State, and ZIP Code) School of Physics Georgia Institute of Technology Atlanta, Georgia 30332	7b. ADDRESS (City, State, and ZIP Code) AFOSR/NP Bolling Air Force Base, Bldg. 410 Washington, D. C. 20332-6448
8a. NAME OF FUNDING / SPONSORING ORGANIZATION AFOSR 8b. OFFICE SYMBOL (If applicable) NP	9. PROCUREMENT INSTRUMENT IDENTIFICATION NUMBER AFOSR-84-0233
8c. ADDRESS (City, State, and ZIP Code) Building 410 Bolling AFB, D. C. 20332-6448	10. SOURCE OF FUNDING NUMBERS PROGRAM ELEMENT NO: 61102F; PROJECT NO: 2301; TASK NO: A4; WORK UNIT ACCESSION NO: N/A
11. TITLE (Include Security Classification) TERMOLECULAR RECOMBINATION IN GASES	
12. PERSONAL AUTHOR(S) M. R. Flannery	
13a. TYPE OF REPORT Annual Technical Report	13b. TIME COVERED FROM 7/1/87 TO 7/30/88
14. DATE OF REPORT (Year, Month, Day) 10/31/88	15. PAGE COUNT 48
16. SUPPLEMENTARY NOTATION	

17. COSATI CODES		
FIELD	GROUP	SUB-GROUP
N/A	N/A	N/A

18. SUBJECT TERMS (Continue on reverse if necessary and identify by block number)
Termolecular, Association, Master Equation, Bottleneck, Diffusion, Variational.

19. ABSTRACT (Continue on reverse if necessary and identify by block number)

During this fourth year of the grant, research has been initiated and completed on Termolecular Recombination in Gases. An exact low gas density treatment was presented, an exact Master Equation and an equivalent-Variational Method. Various approximations to the exact treatment - strong collision method, bottleneck method, diffusional method, coupled nearest-neighbor limit and uncoupled intermediate levels limit - were deduced, implemented and tested.

20. DISTRIBUTION / AVAILABILITY OF ABSTRACT ☒ UNCLASSIFIED/UNLIMITED ☐ SAME AS RPT ☐ DTIC USERS	21. ABSTRACT SECURITY CLASSIFICATION UNCLASSIFIED
22a. NAME OF RESPONSIBLE INDIVIDUAL Dr. Ralph E. Kelley	22b. TELEPHONE (Include Area Code) (202) 767-4980 22c. OFFICE SYMBOL NP

DD FORM 1473, 84 MAR 83 APR edition may be used until exhausted. All other editions are obsolete.

Contents

Abstract

During this fourth year of the grant, research has been initiated and completed on Termolecular Recombination in Gases. An exact low gas density treatment was presented: an exact Master Equation and an equivalent Variational Method. Various approximations to the exact-treatment - strong collision method, bottleneck method, diffusional method, coupled nearest-neighbor limit and uncoupled intermediate levels limit - were deduced, implemented and tested.

1. Research Completed and Published (July 1, 1987 - Aug. 30, 1988)

The following four papers have been published in Journal of Chemical Physics (J. Chem. Phys.).

(A) "Termolecular Recombination at low gas density: Strong Collision, bottleneck and exact treatments", by M. R. Flannery and E. J. Mansky, J. Chem. Phys. 88, 4228-4241 (1988); April 1, 1988 issue.

(B) "Variational Principle for Termolecular Recombination in a gas", by M. R. Flannery, J. Chem. Phys. 89, 214-222 (1988); July 1, 1988 issue.

(C) "Termolecular Recombination: Coupled nearest-neighbor limit and uncoupled intermediate levels limit", by M. R. Flannery and E. J. Mansky, J. Chem. Phys. 89, 4086-4091 (1988); October 1, 1988 issue.

(D) "Diffusional Theory of Termolecular Recombination and association of atomic species in a gas", by M. R. Flannery, J. Chem. Phys. 87, 6947-6956 (1987); December 15, 1987 issue.

In addition the following research appeared as a Chapter in a book.

(E) "Macroscopic and Microscopic Perspectives of Termolecular Association of Atomic Reactants in a Gas", by M. R. Flannery, in Recent Studies in Atomic and Molecular Processes (A. E. Kingston, ed.) Plenum Press, pp. 167-191 (1987).

Six reprints each of (D) and (E) above have been submitted previously to AFOSR on 3/1/88 under Performing Organization Report Numbers GIT-85-012 and GIT-85-013.

Six reprints each of (A), (B) and (C) above are submitted together with this report (GIT-85-014) as Report numbers GIT-85-015, GIT-85-016 and GIT-85-017 respectively. They are also contained in Appendices A, B and C of this report.

2. Summary of Completed Research

A. Termolecular Recombination at low gas density.

On introducing the probabilities for association as a function of internal separation R and internal energy E of the associating (A-B) species the strong collision model is thoroughly investigated and compared, as a case study, with the exact treatment of termolecular ion-ion recombination at low gas densities. A bottleneck model is also investigated. Analytical expressions for the one way equilibrium energy-change rates at fixed R are also provided.

B. Variational Principle for Termolecular Recombination

A variational principle for the rates of termolecular processes is proposed and then applied to recombination between atomic ions with excellent results. The variational expression when minimized with respect to stabilization probabilities is capable of providing rates identical to those determined from the quasi-steady-state solution of the full Master equation. Connection is made with electrical networks and with the principle of least dissipation.

C. Coupled nearest-neighbor limit and uncoupled intermediate levels limit

Two extreme limits of collisional coupling in termolecular recombination are investigated. The coupled nearest neighbor (CNN) limit includes only couplings between neighboring excited energy levels of the associating species AB^*, while the uncoupled intermediate levels (UIL) limit includes only couplings between the fully dissociated reactants A^+ and B^- and each of the (assumed uncoupled) excited levels of AB^*, which are then coupled to the fully associated products AB. Comparison is made with results of previous exact and diffusion treatments.

D. Diffusional Theory of Termolecular Association

A diffusional treatment of termolecular association of atomic species A and B in a low density gas is presented and applied to positive ion-negative ion recombination over the full range of masses of reactants for various classes of ion-neutral interactions. In contrast to rates given by the diffusional current, excellent results are obtained for general mass species provided a more basic expression for the association is introduced.

Full technical details of the above work appear as Appendices (A), (B), (C) and (D) of this report.

3. Invited and Contributed Papers Presented at Professional Scientific Meetings

3.1 An invited paper entitled "Termolecular Recombination", by M. R. Flannery was presented at the 40th Annual Gaseous Electronics Conference, Atlanta, Georgia, October 13-16, 1987. It is published in Bull. Amer. Phys. Soc. 33, #2 (1988) p. 122.

3.2 A contributed paper entitled "Orientation and Alignment Parameters for e + He ($2^{1,3}S$) → e + He ($3^{1,3}P$, $3^{1,3}D$) Collisions", by E. J. Mansky and M. R. Flannery, was presented at the 40th Annual Gaseous Electronics Conference, Atlanta, Georgia, October 13-16, 1987. It is published in Bull. Amer. Phys. Soc. 33, #2 (1988) p. 141.

3.3 A contributed paper entitled "Termolecular Recombination and Electrical Networks", by M. R. Flannery and E. J. Mansky was presented at the 1988 Spring Meeting of the American Physical Society (APS) held in conjunction with the Annual Meeting of the APS Division of Atomic and Molecular and Optical Physics. It is published in Bull. Amer. Phys. Soc. 33, 4 (1988) p. 1006.

The abstracts are included in the following sections.

4. Abstracts of Papers Presented

A-4 Termolecular Recombination*, M. R. FLANNERY, Georgia Tech - Theoretical description of termolecular ion-ion recombination and termolecular ion-atom association between atomic species in a gas will be presented. The underlying physics and dependence with gas density will be discussed. Results of various models - strong collision, diffusion and bottleneck - will be compared at low gas densities with the exact treatment.

*Research supported by AFOSR grant No. AFOSR-84-0233.

HB-3 Orientation and Alignment Parameters for $e^- + He(2^{1,3}S, 2^{1,3}P) \rightarrow e^- + He(3^{1,3}P, 3^{1,3}D)$ Collisions†, E. J. MANSKY II and M. R. FLANNERY, Georgia Institute of Technology - The multichannel eikonal theory results for the coherence and alignment parameters characterizing the decay of the metastable $3^{1,3}P$ and $3^{1,3}D$ states of helium, excited in the $2^{1,3}S \rightarrow 3^{1,3}P$ and $2^{1,3}P \rightarrow 3^{1,3}D$ transitions respectively, are examined. A detailed examination of the resulting λ, χ parameters (for the $3^{1,3}P$ states) and the λ, μ, χ, ψ parameters (for the $3^{1,3}D$ states) provides a clear picture of the effect interchannel couplings within the target basis set have upon the final state probabilities. The pattern of the coherence and alignment parameters for these transitions also provides a direct, physical explanation of the qualitative behavior of the integral cross sections for the $2^{1,3}S \rightarrow 3^{1,3}P$ and $2^{1,3}P \rightarrow 3^{1,3}D$ transitions.

†Research supported by U.S. Air Force Office of Scientific Research under Grant No. AFOSR-84-0233.

EX 100 Termolecular Recombination and Electrical Networks*, M. R. FLANNERY AND E. J. MANSKY, Georgia Tech - Analogy with an equivalent electrical network provides a very effective means not only to analyze the complicated dynamics intrinsic to termolecular recombination, A+B+M → AB+M, in a different light but also to readily construct physically appealing models. Two extreme limits are treated - the nearest neighbor limit where collisional couplings between excited levels n and n-1 are only included - and the one level limit which includes connections between the source of fully dissociated states and each individual excited state n and between n and the sink of fully associated products. Comparison with the exact Master Equation Method, the Variational Method and the Diffusional Method will be presented.

*Research supported by AFOSR grant No. AFOSR-84-0233.

Appendix A

"Termolecular Recombination at low gas density:

Strong Collision, bottleneck and exact treatments"

by

M. R. Flannery and E. J. Mansky

(J. Chem. Phys. 88, 4228-4241 (1988))

Termolecular recombination at low gas density: Strong collision, bottleneck, and exact treatments

M. R. Flannery and E. J. Mansky
School of Physics, Georgia Institute of Technology, Atlanta, Georgia 30332

(Received 23 November 1987; accepted 24 December 1987)

On introducing the probabilities for association as a function of internal separation R and internal energy E of the associating (A–B) species the strong collision model is thoroughly investigated and compared, as a case study, with the exact treatment of termolcular ion–ion recombination at low gas densities. A bottleneck model is also investigated. Analytical expressions for the one way equilibrium energy-change rates at fixed R are provided in the Appendix.

I. INTRODUCTION

The theory of termolecular ion–ion recombination,

$$\mathrm{A}+\mathrm{B}+\mathrm{M}\underset{k}{\overset{\alpha}{\rightleftarrows}}\mathrm{AB}+\mathrm{M} \tag{1.1}$$

between positive and negative atomic ions A and B in a low density gas thermal M is now well established.[1–5] The distribution $n_i(E_i,t)$ per unit interval dE_i of recombining pairs AB with internal energy E_i a time t is governed by the collisional input–output Master equation[1–5]:

$$\begin{aligned}\frac{d}{dt}n_i(E_i,t)&=\frac{\partial n_i}{\partial t}-F_i\\&=-\int_{-D}^{\infty}[n_i\nu_{if}-n_f\nu_{fi}]\,dE_f\\&=-\frac{\partial}{\partial E_i}J_i(E_i,t),\end{aligned} \tag{1.2}$$

where ν_{if} is the frequency per unit interval dE_f for $E_i\to E_f$ transitions by collisions between AB and M, where J_i is the upward current in energy space past level E_i and where $-D$ is the energy of the lowest vibrational level of AB relative to the dissociation limit taken as zero energy. For dissociated pairs with $E_i\geqslant 0$, F_i is the net flux per unit interval dE_i of (contracting) AB pairs generated with energy E_i at infinite internal separation R. For bound pairs with $E_i<0$, F_i is zero. The net rate for association is[4]

$$\begin{aligned}R^{A}(t)&=\int_{-D}^{\infty}P_i^S\left(\frac{dn_i}{dt}\right)dE_i\\&=\alpha N_{\mathrm{A}}(t)N_{\mathrm{B}}(t)-kn_s(t),\end{aligned} \tag{1.3}$$

where P_i^S is the probability that E_i pairs are collisionally connected to the product channel, i.e., have been stabilized against dissociative collisions with thermal M. The effective two-body rate constant for the association of A and B with (cm^{-3}) concentrations $N_{\mathrm{A}}(t)$ and $N_{\mathrm{B}}(t)$ is α ($\mathrm{cm}^3\,\mathrm{s}^{-1}$), and k (s^{-1}) is the frequency for dissociation of those tightly bound pairs of concentration $n_s(t)$, which are considered to be fully associated with energies E_i within a block $\mathscr{S}$ of low lying fully stabilized levels in a range $-S\geqslant E_i\geqslant -D$ within which the stabilization probability P_i^S is calculated to be unity. When the quasi-steady-state (QSS) condition $dn_i/dt=0$ is satisfied for pairs in a block $\mathscr{E}$ of highly excited levels in the energy range $0\geqslant E\geqslant -S$ between the dissociation limit at zero energy and level $-S$ the rate (1.3) reduces to[4]

$$\begin{aligned}R^{A}(t)&=\int_{-D}^{-S}\left(\frac{dn_i}{dt}\right)dE_i\\&=\int_0^{\infty}F_i\,dE_i=-\int_{-E}^{\infty}\left(\frac{dn_i}{dt}\right)dE_i\\&=-J(-E,t)\end{aligned} \tag{1.4}$$

for a steady-state ($\partial n_i/\partial t=0$) distribution of pairs in the block $\mathscr{C}$ of fully dissociated states in the energy range $0\leqslant E\leqslant\infty$, over which the stabilization probability P_i^S vanishes. The rate (1.3) therefore reduces[4] under QSS to the downward current $-J(-E,t)$ of pairs past energy level $-E$ in bound block $\mathscr{E}$.

At low gas densities the expansion[4]

$$\begin{aligned}\gamma_i(t)&=\frac{n_i(E_i,t)}{\tilde{n}_i(E_i)}=P_i^D(E_i)\left[\frac{N_{\mathrm{A}}(t)N_{\mathrm{B}}(t)}{\tilde{N}_{\mathrm{A}}\tilde{N}_{\mathrm{B}}}\right]\\&\quad+P_i^S(E_i)\left[\frac{n_s(t)}{\tilde{n}_s}\right]\end{aligned} \tag{1.5a}$$

$$\equiv P_i^D(E_i)\gamma_c(t)+P_i^S(E_i)\gamma_s(t) \tag{1.5b}$$

permits separation of variables E_i and t in the collisional part of Eq. (1.2). Here γ_i, γ_c, and γ_s are the various time-dependent distributions of states in blocks $\mathscr{E}$, $\mathscr{C}$, and $\mathscr{S}$ normalized to their respective equilibrium values $\tilde{n}_i,\tilde{N}_{\mathrm{A,B}}$, and $\tilde{n}_s$. For $\mathscr{E}$ states, P_i^S and $P_i^D=1-P_i^S$ are the probabilities that state i is collisionally connected to the sink $\mathscr{S}$ and to the source $\mathscr{C}$. For $\mathscr{C}$ states at low gas densities P_i^D, the collision survival probability is unity when equilibrium conditions in E_i and R can be assumed in the collision part of Eq. (1.2). When Eq. (1.5) is inserted the collisional part of Eq. (1.2), then Eqs. (1.4) and (1.3) yield the expressions[4]

$$\begin{aligned}\alpha\tilde{N}_{\mathrm{A}}\tilde{N}_{\mathrm{B}}&=-j(-E)=k\tilde{n}_s\\&=\int_{-E}^{\infty}dE_i\int_{-D}^{-E}(P_f^S-P_i^S)C_{if}\,dE_f\end{aligned} \tag{1.6}$$

for the rate coefficients α and k in Eq. (1.1). The collision kernel C_{if} is the collisional rate $\tilde{n}_i\nu_{if}$ ($\mathrm{cm}^3\,\mathrm{s}^{-1}$) per unit element $dE_i\,dE_f$ for $E_i\to E_f$ transitions and varies linearly with the gas density N. At low N, α is linear in N so that P_i^S, P_i^D are required only to zero order in N. The net downward time-dependent collisional current across arbitrary level $-E$ in block $\mathscr{E}$ separates as

 0021-9606/88/074228-14$02.10

$$-J(-E,t) = -j(-E)\left[N_A(t)N_{B(t)}/\tilde{N}_A\tilde{N}_B - n_s(t)/\tilde{n}_s\right] \quad (1.7)$$

which under conditions of full thermodynamic equlibrium tends therefore to zero.

The multicollisional stochastic aspect of the theory becomes apparent by correctly identifying the (time-independent and density-independent) stabilization probability as

$$P_i^S(E_i) = \left[\int_{-D}^{0} (n_i\nu_{if})\, P_f^S\, dE_f\right] \Big/ \left[\int_{-D}^{\infty} n_i\nu_{if}\, dE_f\right] \quad (1.8a)$$

which is the fraction of all collisions which result in association. Equation (1.8a) is consistent with the concept of a Markov element chain, and when rewritten in the form of an integral equation

$$P_i^S \int_{-D}^{\infty} C_{if}\, dE_f = \int_{-D}^{0} C_{if} P_f^S\, dE_f \quad (1.8b)$$

is seen, after substituting Eq. (1.5b) in Eq. (1.2), to be equivalent to the assumption of a quasi-steady-state (QSS) E_i distribution of pairs with energy within the highly excited block $\mathscr{E}$.

The rate (1.6) holds for $E=0$ and $E=S$ to give, respectively,

$$\alpha\tilde{N}_A\tilde{N}_B = -j(0) = \int_0^{\infty} dE_i \int_{-D}^{0} C_{if}P_f^S\, dE_f = k\tilde{n}_s \quad (1.9)$$

as the collisional rate from the fully dissociated states i to bound states f which are then collisionally stabilized with probability P_f^S, and

$$\alpha\tilde{N}_A\tilde{N}_B = j(-S) = \int_{-D}^{-S} dE_i \int_{-S}^{\infty} C_{if}P_f^D\, dE_f = k\tilde{n}_s \quad (1.10)$$

as the collisional rate from the fully associated states i to levels f which are then collisionally disrupted with probability P_f^D. Note that Eq. (1.9) or Eq. (1.6) is the QSS rate for association of a full equilibrium concentration $\tilde{N}_A\tilde{N}_B$ of dissociated pairs into a perfectly absorbing sink $\mathscr{S}$ maintained at zero population, i.e., $\gamma_c = 1$ and $\gamma_s = 0$ in Eq. (1.5b). Similarly Eq. (1.10) is the QSS rate for dissociation which would result from an equilibrium population $\tilde{n}_s$ of associated $\mathscr{S}$ pairs being dissociated into states $\mathscr{E}$ maintained at zero population, i.e., $\gamma_c = 0$ and $\gamma_s = 1$ in Eq. (1.5b).

In this paper two simplifications to the above exact treatment at low gas densities N are investigated in detail. In the strong collision and bottleneck models, the probabilities P_i^S are preassigned without recourse to Eq. (1.8). The first model assumes that P_i^S for all bound pairs with internal separation R is unity for R within the range $0 \leqslant R \leqslant R_T$, where R_T is some preassigned radius, outside which P_i^S is zero. In this strong collision (or Thomson-style[7]) model, bound pairs with $R \leqslant R_T$ are therefore considered to be fully associated and those with $R \geqslant R_T$ cannot be stabilized. In the bottleneck model, P_i^S for bound pairs at all accessible R is unity for $E_i \leqslant E^*$, and is zero for $E \geqslant E^*$ and E^* is a (bound) energy level within $\sim 2kT$ below the dissociation limit and past which the one-way equilibrium rate is a minimum which therefore acts as a bottleneck to the current. The level E^* is, in effect, a transition state. Each model therefore subdivides the two dimensional (R,E) space into regions of some physical signficance. The Thomson model has previously been addressed via a Monte Carlo simulation method[8] and indirectly by an analytical approach[9] based on collisional deactivation of dissociated pairs to levels lower than various bound levels. A more exhaustive and detailed investigation is undertaken here. The bottleneck model has also received some previous consideration.[1,2]

Not only will these models elucidate interesting dynamics underlying the recombination mechanism (1.1) at low gas densities N, but subsequent modification to cover higher gas densities proves quite valuable towards a study (in progress) of the variation of the recombination rate α with gas density N.

II. THEORY

The detailed investigation of the strong-collision model requires the generalization of the Master equation (1.2) to $(\mathbf{R},E)$ space and use of the frequencies $\nu_{if}(R)$ for $E_i \to E_f$ transitions per unit interval $d\mathbf{R}\, dE_f$ by collisions between M and the pair AB *at fixed internal separation* R. The appropriate input–output Master equation satisfied by the distribution $n_i(\mathbf{R})$ of (A–B)$_i$ pairs per unit interval $d\mathbf{R}\, dE_i$ has been shown[10] to be the continuity equation

$$\frac{d}{dt}n_i(\mathbf{R},t) = \frac{\partial n_i}{\partial t} + \frac{1}{R^2}\frac{\partial}{\partial R}\left[R^2 j_i^d(R)\right]_{E_i}$$
$$= -\int_{V(R)}^{\infty} \left[n_i(\mathbf{R})\nu_{if}(R) - n_f(\mathbf{R})\nu_{fi}(R)\right] dE_f$$
$$\equiv -\int_{V(R)}^{\infty} S_{if}(R)\, dE_f, \quad (2.1)$$

where $j_i^d(R)$ is the net outward transport current of pairs expanding at R, where S_{if} is the net two level collisional-absorption rate, and where $V(R)$ is the energy of interaction between A and B. Integration of Eq. (2.1) over all accessible R yields the customary Master equation (1.2) for dissociated and bound states.

A. Rates and stabilization probabilities

The steady-state rate (1.4), with the aid of Eq. (2.1), is

$$R^A(t) = -\int_0^{\infty} \lim_{R_T \to \infty} \left[4\pi R_T^2 j_i^d(R_T)\right] dE_i$$
$$= \int_0^{\infty} dE_i \int_0^{\infty} d\mathbf{R} \int_{V(R)}^{0} S_{if}(R)\, dE_f \quad (2.2)$$

which either is the net inward flux of dissociated pairs contracting by transport across a sphere of infinite radius R_T or is the net collisional downflow across the dissociation limit at $E_i = 0$.

Now assume (a) that there is a finite radius R_T for which all E_i pairs with $R \geqslant R_T$ are in energy equilibrium at each R, i.e.,

$$\frac{n_i(\mathbf{R})}{n(\mathbf{R})} = \frac{\tilde{n}_i(\mathbf{R})}{\tilde{n}(\mathbf{R})}, \quad R \geqslant R_T, \quad (2.3a)$$

where

$$n(\mathbf{R}) = \int_{V(R)}^{\infty} n_i(\mathbf{R}) dE \tag{2.3b}$$

is the concentration per unit interval $d\mathbf{R}$ of all pairs with separation R. Thus S_{if} in Eq. (2.2) vanishes for $R \geqslant R_T$ to yield

$$R^{A}(t) = \int_0^{\infty} dE_i \int_0^{R_T} d\mathbf{R} \int_{V(R)}^{0} S_{if}(R) dE_f \tag{2.4}$$

which is the steady-state rate of association of dissociated pairs with $R \leqslant R_T$.

Association of R_T complex: At low gas densities N, the distribution $n_i(\mathbf{R})$ is independent of N so that the collision term S_{if} remains linear in N. On the right-hand side of Eq. (2.1) $n_i(R)$ is equilibrium with respect to $\mathbf{R}$, so that

$$\frac{n_i(\mathbf{R},E_i)}{n_i(E_i)} = \frac{\tilde{n}_i(\mathbf{R},E_i)}{\tilde{n}_i(E_i)}, \tag{2.5a}$$

where the distribution per unit interval dE_i is

$$n_i(E_i) = \int_0^{R_i} n_i(\mathbf{R}) d\mathbf{R} \tag{2.5b}$$

and R_i is the classical turning point of E_i motion. The separation (1.5) is then valid so that Eq. (2.4) yields

$$\alpha \tilde{N}_A \tilde{N}_B = \int_0^{\infty} dE_i \int_0^{R_T} d\mathbf{R} \int_{V(R)}^{0} C_{if}(R) P_f^S dE_f = k_s \tilde{n}_s \tag{2.6}$$

for the rate of association of dissociated pairs in the complex of radius R_T. The required one-way equilibrium rate

$$C_{if}(R) = \tilde{n}_i(R) v_{if}(R) = C_{fi}(R) \tag{2.7}$$

at each R is related to the $\mathbf{R}$-averaged rate C_{if} previously used[1-3] in Eq. (1.6) by

$$C_{if} = \tilde{n}_i v_{if} = \int_0^{R_{if}} \tilde{n}_i(\mathbf{R}) v(R) d\mathbf{R} = \int_0^{R_{if}} C_{if}(R) d\mathbf{R}, \tag{2.8}$$

where R_{if} is the lesser of the two outermost turning points R_i and R_f associated with levels E_i and E_f, of which one at least is bound. Detailed expressions for $C_{if}(R)$ are presented in the Appendix.

Strong collision rate: In addition to Eq. (2.3a), assume (b) that all bound states f with $R \leqslant R_T$ are fully stabilized, i.e.,

$$P_f^S = 1, \quad R \leqslant R_T, \; E_f \leqslant 0 \tag{2.9}$$

so that the required strong collision rate is

$$\alpha(R_T) \tilde{N}_A \tilde{N}_B = \int_0^{\infty} dE_i \int_0^{R_T} d\mathbf{R} \int_{V(R)}^{0} C_{if}(R) dE_f \tag{2.10}$$

which is the one-way equilibrium rate that dissociated pairs with $R \leqslant R_T$ are collisionally deexcited across the dissociation limit. The "complex" assumption (2.3a) is equivalent either to assigning in Eq. (2.2) zero probability $P_f^S = 0$ for $R \geqslant R_T$ and $E_f \leqslant 0$, i.e., to the overall neglect of association or to inclusion in Eq. (2.4) of upward equilibrating transitions past $E_i = 0$ for $R \geqslant R_T$. The *strong-collision* assumption (2.9) is equivalent to the neglect in Eq. (2.4) of the rate $\int_V^0 n_f(R) v_{fi}(R) dE_f$ for upward redissociation of pairs with $R \leqslant R_T$.

The physical basis to the two assumptions (2.3) and (2.9) can be illustrated by Fig. 1. Bound states at large R arise from highly elliptical Coulomb orbits with low angular momenta where the possible velocity vectors for relative (A–B) motion lie within a narrowly focused region. Upon collision with the gas, the velocity vector is mainly deflected into directions outside this region so that the post-collision velocity vector cannot be consistent with bound states at large R. Collisional dissociation of these highly excited levels at large R is therefore most likely to occur,[8] and stabilization of bound levels f is not viable so that $P_f^S \; (R \geqslant R_T) = 0$ in keeping with assumption (2.3) underlying complex formation for association to proceed.

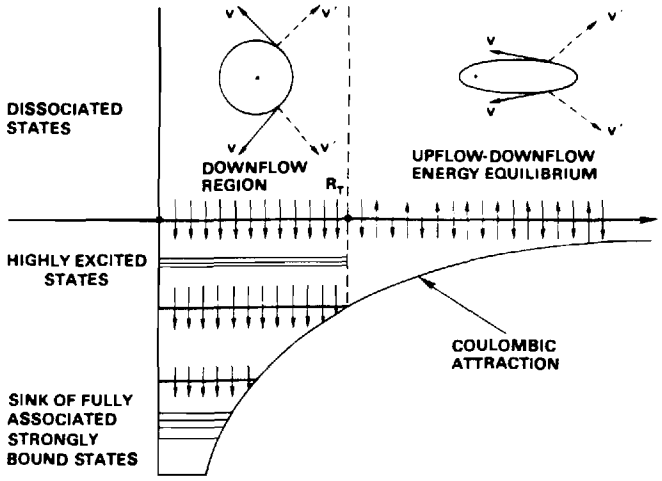

FIG. 1. Schematic basis for strong collisions within an assumed complex of radius R_T. A–B relative motion in circular and highly elliptical (large R) orbits with speeds v and v' before and after ion–neutral collision.

For intermediate R, however, the post-collision velocity can be accomodated by many angular-momentum bound orbits, more final angular momentum levels are accessible at these $R \simeq e^2/2|E_i|$, the radius of the circular orbit, and the number of accessible orbits at a given R increase with increasing binding. Collisional deexcitation of highly excited levels at smaller R therefore tends to occur and pairs with $R \leqslant R_T$ in all bound levels can be fully stabilized, in keeping with the strong-collision assumption (2.9).

The averaged kernels (2.8) have been previously derived for symmetrical resonance charge transfer,[1] hard-sphere,[2] and polarization[3] binary collisions between either ion A or B and the gas M. The R-dependent one-way equilibrium kernels $C_{if}(R)$ are not only required for this sudy but also for ongoing investigations of the nonlinear variation of α with gas density N. They are provided in the Appendix as a comprehensive package for present and future use and reference.

The exact low density rate (1.6) and the strong-collision rate (2.10) reduce to a sum[9,11] of rates α_A and α_B, each arising from A–M and B–M binary collisions, respectively, and α_A can be presented[1-3,5,9] as a universal function [cf. Eq. (A55)] of the mass parameter

$$a = \frac{M_B M_g}{M_A (M_A + M_B + M_g)}, \tag{2.11}$$

where M_A, M_B, and M_g are the masses of the reacting atomic ions and gas atoms, respectively.

Calculation of Eq. (1.6), the exact low density rate α_E,

and of the variation of the strong collision rate (2.10) with R_T can now be performed. For the exact rate (1.6), highly accurate converged solutions P_i^S of the integral equation (1.6), discretized as in Ref. 3 into an equivalent set of 100 algebraic equations, have been obtained. Previous results[1-3] were based on 36 coupled equations at most. Convergence of α_E to within 0.5% is found to be much more rapid for intermediate mass parameters a ($\sim 1/3$) than for small and large a which required 100 coupled equations for convergent rates.[5]

In contrast to ion–atom association where the radius R_T may, with some justification, be identified with the location of the centrifugal barrier, no such assignment for ion–ion recombination (without any centrifugal barrier) exists, although Thomson[7] suggested $R_T = 2e^2/3kT$ where the relative kinetic energy ($\frac{3}{2}kT + e^2/R$) is reduced to $\frac{3}{2}kT$ upon collision. Hence bound pairs with $E_f = e^2(1/R_T - 1/R) \leqslant 0$ can be formed within $R \leqslant R_T$.

The variation with R_T of the ratio $\alpha(R_T)/\alpha_E$ for the recombination of *equal-mass* ions via symmetrical resonance charge–transfer (CX), polarization (POL), and hard-sphere (HS) collisions with an *equal-mass* gas ($a = 1/3$) is displayed in Fig. 2. The ratio is unity for R_T in the range (0.48–0.55) (e^2/kT), in good agreement with Thomson's suggestion. The neglect in Eq. (2.6) of a positive contribution to association from possible collisional stabilization of those bound levels with $R \geqslant R_T \approx 0.5$ (e^2/kT) is effectively offset by the neglect in Eq. (2.10) via Eq. (2.9) of a negative contribution arising from redissociation of those bound states with $R \leqslant R_T$.

The strong collision model is therefore capable of high accuracy *provided* R_T can be preassigned; realistic assignment to R_T for recombination being only feasible[9] after the exact treatment is performed! The radius R_T, once assigned, may however be adopted in models under development for variation of α with gas density N.

As R_T becomes large the rate (2.10) however tends rapidly to

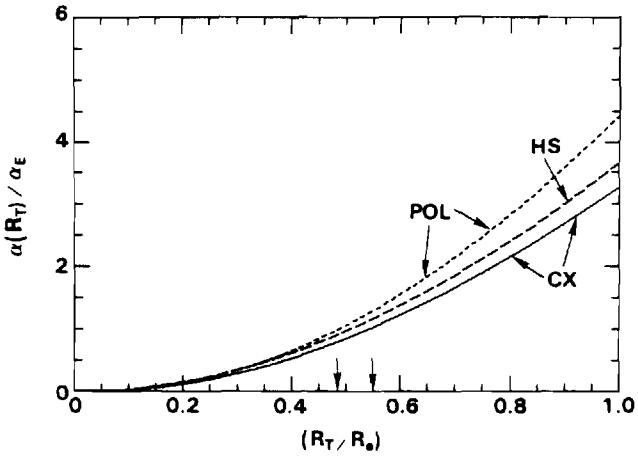

FIG. 2. R_T variation of $\alpha(R_T)$, the strong-collision rate (2.10) normalized to α_E, the exact rate (1.6), for equal-mass components and model ion–neutral interactions (POL: polarization; HS: hard sphere; CX: symmetrical resonance charge transfer). Arrows indicate where $\alpha(R_T) = \alpha_E$ for POL and CX in units of $R = e^2/kT$.

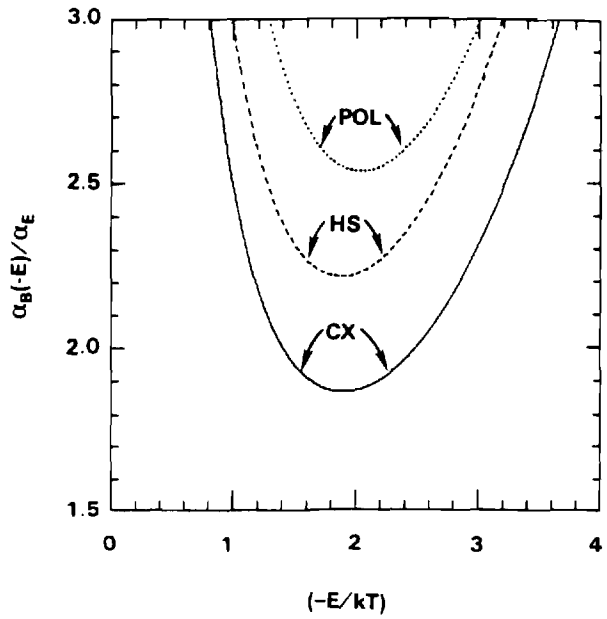

FIG. 3. One-way equilibrium rates $\alpha_{BN}(-E)$, Eq. (2.13), normalized to α_E, the exact rate (1.6), across energy level $-E$ for model ion–neutral interactions POL, HS, and CX.

$$\alpha(R_T \to \infty)\tilde{N}_A\tilde{N}_B = \int_0^\infty dE_i \int_{-D}^0 C_{if}\, dE_f \qquad (2.12)$$

which is of course infinite owing to the divergence, as $E_i \to 0$, of the equilibrium density $\tilde{n}_i(E_i) \sim |E_i|^{-5/2}\exp(-E_i/kT)$ of Coulomb bound states per unit interval dE_i. As $R_T \to \infty$, the physical basis for adopting the one-way equilibrium rate (2.10) becomes untenable since bound states with large R_T are more readily redissociated (cf. Fig. 1). Upward collisions past the dissociation limit must therefore be included for large R_T. The strong collision assumption is therefore no longer justified for large R_T.

This divergence can be eliminated not only by maintaining R_T finite but also by considering the one-way equilibrium rate

$$\alpha_{BN}(-E)\tilde{N}_A\tilde{N}_B = \int_{-E}^\infty dE_i \int_{-D}^{-E} C_{if}\, dE_f \qquad (2.13)$$

across any bound level $-E$ in block $\mathscr{E}$. Figure 3 illustrates that this rate decreases from the infinite limit (2.12) at $E = 0$ to a pronounced minimum at an energy $E^* = 2kT$ below the dissociation limit. Since Eq. (2.13) is an upper limit to the exact rate by taking $P_i^S(E_i > -E)$ and $P_f^S(E_f < -E)$ within Eq. (1.6) to be zero and unity, respectively, then its minimum value $\alpha_{BN}(-E^*)$ is the least upper limit and is the one-way rate past the effective bottleneck to the curent at $-E^*$ which, in effect, is a transition state. Although this bottleneck model (2.13) is physically different from the previous strong collision model (2.10), it is worth noting that $E^* = 2kT$ corresponds to a turning point R_T of $\frac{1}{2}(e^2/kT)$ for which the strong collision model is effectively exact (cf. Fig. 2). Figure 3 shows that the bottleneck result is however a factor of 1.9–2.5 times larger than the exact rate α_E. In contrast to the strong-collision model (2.10), Eq. (2.13) is always an upper limit since in order to obtain the bottleneck result (2.13) from Eq. (1.6), the ne-

glected terms cannot cancel since they always remain negative. This search for the least upper limit to the one-way equilibrium rate across transition state E^* is identical in principle to the variational phase-space theory of Keck[13] as applied to termolecular ion–ion recombination. The strong collision (Fig. 2) and bottleneck pictures (Fig. 3) have been previously displayed in a recent review[12]; the present CX results in Fig. 2 correct those in Ref. 12.

B. Association probabilities

To obtain these, the low density rate (2.6) for association of dissociated pairs in the R_T complex may also be expressed with the aid of Eq. (2.2) as

$$\alpha(R_T)\tilde{N}_A\tilde{N}_B = \int_0^\infty [4\pi R_T^2 \bar{j}_i^-(R_T)]P_i^A(R_T)dE_i, \tag{2.14}$$

the net inward transport rate across the R_T sphere where

$$P_i^A(R_T) = [\tilde{n}_i^-(R_T) - n_i^+(R_T)]/\tilde{n}_i^-(R_T) \tag{2.15}$$

now specifies the desired probability that fully dissociated E_i pairs which are originally contracting at R_T will associate within the spherical complex of radius R_T. The distribution of dissociated pairs contracting at R_T is $\tilde{n}_i^-(\mathbf{R}_T)$, the equilibrium value characteristic of low gas densities N, and is a nonequilibrium value $n_i^+(\mathbf{R}_T)$ for pairs expanding at R_T. The one-way incident current at temperature T and pertinent to low N is the one-way equilibrium current

$$\bar{j}_i^-(R)dE_i = \tfrac{1}{2}\tilde{n}_i^-(\mathbf{R})v_i(R)dE_i = \tfrac{1}{4}\tilde{n}_i(R)v_i(R)dE_i \tag{2.16}$$

$$= \frac{1}{4}\left(\frac{8kT}{\pi M_{AB}}\right)^{1/2}\tilde{N}_A\tilde{N}_B[1 - V(R)/E_i]$$

$$\times (E_i/kT)\exp(-E_i/kT)d(E_i/kT), \tag{2.17}$$

where M_{AB} is the reduced mass of the pair (A–B) and where $\tilde{n}_i$ is $\tilde{n}_i^+ + \tilde{n}_i^-$. By direct comparison of Eqs. (2.14) and (2.16) the exact association probability of fully dissociated pairs within $R \leqslant R_T$ at low gas densities is

$$P_i^{AE}(E_i \geqslant 0, R_T) = [\pi R_T^2 \tilde{n}_i(R_T)v_i(R_T)]^{-1}$$

$$\times \int_0^{R_T} d\mathbf{R}\int_{V(R)}^0 C_{if}(R)P_f^S(R)dE_f \tag{2.18}$$

which increases linearly with gas density N via C_{if}. The stabilization probabilities P_f^S which are solutions of Eq. (1.8) do not vary with N. As $R_T \to \infty$, Eq. (2.18) in Eq. (2.14) yields

$$\alpha_i(E_i \geqslant 0, R_T) = \pi R_T^2 \tilde{n}_i(R_T)v_i(R_T)P_i^{AE}(E_i \geqslant 0, R_T), \tag{2.19}$$

the rate per unit interval dE_i for association of dissociated E_i pairs with $R \leqslant R_T$. As $R_T \to \infty$, Eq. (2.19) saturates to the exact partial rate.

The association rate per unit dE_i for the highly excited bound E_i pairs in block $\mathscr{E}$ of the complex of radius R_T is

$$\alpha_i(E_i < 0, R_T) = [\pi R_T^2 \tilde{n}_i(R_T)v_i(R_T)]P_i^A(E_i < 0, R_T)$$

$$= \int_0^{R_T} d\mathbf{R}\left[\int_{V(R)}^0 C_{if}(R)P_f^S dE_f\right.$$

$$\left. - P_i^S\int_{V(R)}^\infty C_{if}(R)dE_f\right]. \tag{2.20}$$

As $R_T \to R_i$, the outermost turning point of E_i motion where $|E_i| = |V(R_i)|$, this rate (2.20) vanishes owing to the QSS requirement (1.8) of zero net gain of all E_i pairs with $R < R_i$ in block $\mathscr{E}$, a condition on which calculation of the stabilization probabilities P_i^S is based.

Strong collision and Thomson probabilities: The corresponding strong-collision association probability P_i^{ST} is given by Eq. (2.18) with $P_f^S = 1$, i.e., by the probability

$$P_i^{ST}(E_i \geqslant 0, R_T) = [\pi R_T^2 \tilde{n}_i(R_T)v_i(R_T)]^{-1}$$

$$\times \int_0^{R_T} d\mathbf{R}\int_{V(R)}^0 C_{if}(R)dE_f \tag{2.21}$$

for direct collisional formation of bound levels from a dissociated state of energy E_i. It overestimates the exact association probability by

$$P_i^{RD} \equiv P_i^{ST}(R_T) - P_i^{AE}(R_T)$$

$$= [\pi R_T^2 \tilde{n}_i(R_T)v_i(R_T)]^{-1}$$

$$\times \int_0^{R_T} d\mathbf{R}\int_{V(R)}^0 C_{if}(R)P_f^D dE_f \tag{2.22}$$

which in fact is the probability P_i^{RD} for subsequent redissociation of bound pairs formed with $R \leqslant R_T$ and which is inherently neglected by the strong-collision model. On defining the free path length[4] $\lambda_i(R)$ for continuum–bound transitions in A–M collisions during the (A–B) trajectory by

$$\lambda_i^{-1}(R) \equiv [\nu_i(R)/v_i]$$

$$= \left[\int_{V(R)}^0 C_{if}(R)dE_f\right]/[\tilde{n}_i(R)v_i(R)] \tag{2.23}$$

then the strong-collision probability (2.21) is redefined as in

$$\pi R_T^2[1 - V(R_T)/E_i]P_i^{ST}(R_T)$$

$$= \int_0^{R_T}[1 - V(R)/E_i]d\mathbf{R}/\lambda_i(R). \tag{2.24}$$

The corresponding strong collision rate (2.14) is now

$$\alpha_T(R_T) = \int_0^\infty G(E_i)dE_i$$

$$\times \int_0^{R_T} v_i[1 - V(R)/E_i]^{1/2}d\mathbf{R}/\lambda_i(R), \tag{2.25}$$

where the (Boltzmann) distribution of internal energies ($E_i \geqslant 0$) is

$$G(E_i)dE_i = \frac{2}{\sqrt{\pi}}(E_i/kT)^{1/2}\exp(-E_i/kT)d(E_i/kT). \tag{2.26}$$

When λ_i is assumed to be λ, independent of R and E_i, as for hard-sphere collisions, and when $V(R)$ is neglected, Eq. (2.24) yields

$$P_T^A(R_T) = \tfrac{1}{4}R_T/\lambda \tag{2.27}$$

the Thomson probability[7] for (A–M) collisions during recti-

linear A–B relative motion within $R \leqslant R_T$. Also Eq. (2.25) yields

$$\alpha_T(R_T) = \tfrac{4}{3}\pi R_T^3(\bar{v}/\lambda) \tag{2.28}$$

the Thomson rate[7] in terms of $\bar{v}$, the mean (A–B) relative speed $(8kT/\pi M_{AB})^{1/2}$. All of the rates calculated here and previously[1-3] are however normalized (cf. Appendix) to

$$\tilde{\alpha}_T = \frac{4}{3}\frac{\pi}{\lambda}\left(\frac{2}{3}\frac{e^2}{kT}\right)^3\left(\frac{3kT}{M_{AB}}\right)^{1/2}, \tag{2.29}$$

where the root-mean-square speed rather than $\bar{v}$ has been customarily used, and where $\frac{2}{3}(e^2/kT)$ is assigned for R_T. Unless otherwise noted, all of the following calculations in the following sections (II C–II E) refer to symmetrical resonance charge–transfer ion–neutral collisions involving equal-mass species $M_A = M_B$ in an equal mass gas.

C. Calculated stabilization and disruption probabilities, and partial rates

The stabilization and disruption probabilities P_f^S and $P_f^D = 1 - P_f^S$ are the stochastic probabilities that (A–B) pairs initially in a bound level E_f of block $\mathscr{E}$, will either become fully associated or disrupted by multicollisions with the thermal gas. For a quasi-steady-state distribution of bound pairs in block $\mathscr{E}$, P_f^S are numerical solutions of the integral equation (1.8) and are illustrated in Fig. 4. The probabilities P_f^S increase from zero at the dissociation limit to near unity for binding energy $|E_f| \geqslant 5kT$. Note that $P_f^S \approx 1/2 \approx P_f^D$ for $E_f \sim -2kT$, the bottleneck energy E^* (cf. Fig. 3) based on the assumption in Eq. (2.13) that P_f^S is zero for $E \geqslant E^*$ and unity for $E_i \leqslant -E^*$. The probabilities $P_f^D = (1 - P_f^S)$ for multistep collisional disruption of these pairs decrease fairly rapidly with binding energy $|E|$ and are negligible for binding $|E| \geqslant 5\ kT$. Since block $\mathscr{S}$ of fully stabilized levels is characterized by unit P_f^S, Fig. 4 suggests that the block $\mathscr{S}$ is composed of all levels with binding $\gtrsim 10kT$. Since the deexcitation frequency ν_{if} from the continuum directly to the strongly bound levels with $E_f \lesssim -10kT$ of block $\mathscr{S}$ is vanishingly small, association given by Eq. (1.9) therefore occurs primarily via multistep transitions to the block $\mathscr{E}$ of levels E_f within the range $0 \geqslant E_f \geqslant -10kT$, which are then connected stochastically with probability P_f^S to the fully associated block $\mathscr{S}$ via a Markov-element chain.[6]

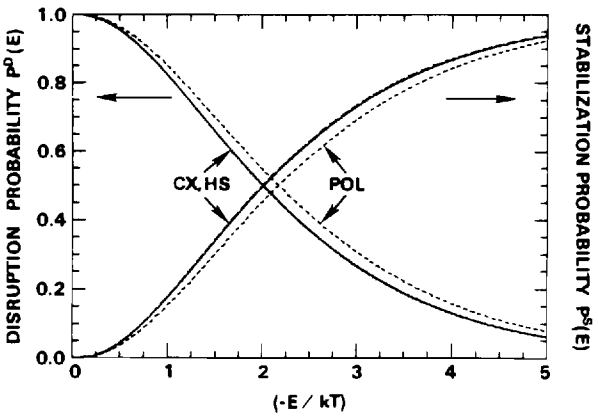

FIG. 4. Stabilization and disruption probabilities, solutions of Eq. (1.8) for equal mass components.

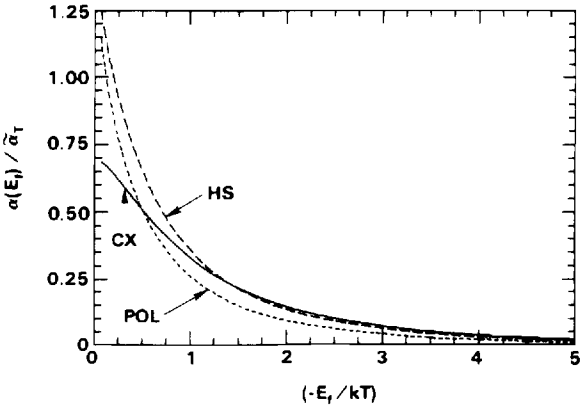

FIG. 5. Partial rates (2.30a) per final bound level $-E_f$ normalized to $\tilde{\alpha}_T$, the Thomson rate (2.29).

Figure 5 for the partial rate

$$\alpha(E_f)\tilde{N}_A\tilde{N}_B = \left(\int_0^\infty C_{if}\, dE_i\right) P_f^S(E_f) \equiv C_f P_f^S \tag{2.30a}$$

normalized to $\tilde{\alpha}_T$, which is the contribution per unit normalized interval (dE_f/kT) from level E_f to the full association rate of all dissociated pairs, illustrates that levels in general within kT of the dissociation limit, are mainly responsible for the association process. This is less so however for CX since deactivation by symmetrical resonance charge transfer involves larger energy reductions[1-3] than for the case of polarization and hard-sphere collisions. The very rapid increase of $\alpha(E_f)$ from zero at $E_f = 0$, not shown in Fig. 5, and subsequent decrease arises from the combination of the monotonic increase from zero of the stabilization probabilities P_f^S and the rapid decrease from infinity of C_f, the collisional rate from the continuum to a bound level f.

Figure 6 for the E_i-partial contribution

$$\alpha(E_i)\tilde{N}_A\tilde{N}_B = \int_{-D}^{0} C_{if} P_f^S\, dE_f \tag{2.30b}$$

to the exact rate for association of dissociated E_i pairs per unit interval (dE_i/kT) illustrates a monotonic increase as $E_i > 0$ approaches the dissociated limit at zero energy. This

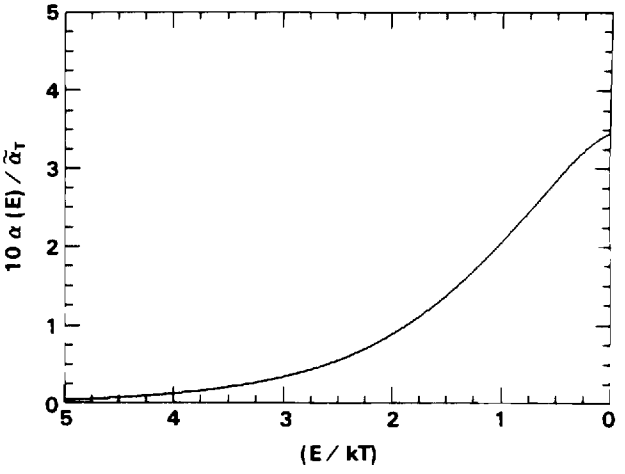

FIG. 6. Partial rate (2.30b) per initial continuum state E_i, normalized to $\tilde{\alpha}_T$, the Thomson rate (2.29).

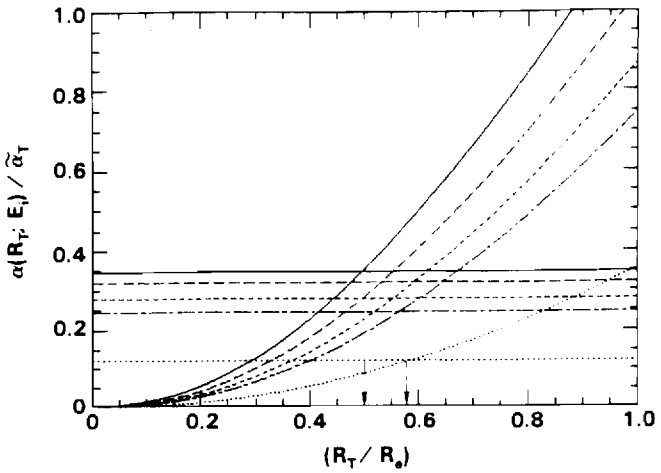

FIG. 7. Partial strong continuum rate $\alpha(R_T;E_i)$, Eq. (2.31), per initial continuum state E_i, normalized to $\tilde{\alpha}_T$, the Thomson rate (2.29). Exact normalized partial rates are indicated by straight lines. $E_i/kT = 0, 0.26, 0.529, 0.734$, and 1.646 ordered sequentially from top to bottom.

is expected since C_{if} for a given bound level E_f increases quite rapidly as the energy difference $(E_i - E_f)$ is reduced. The full rate (1.9) is the E_i-integrated area of Fig. 6.

Variations of the partial E_i contributions

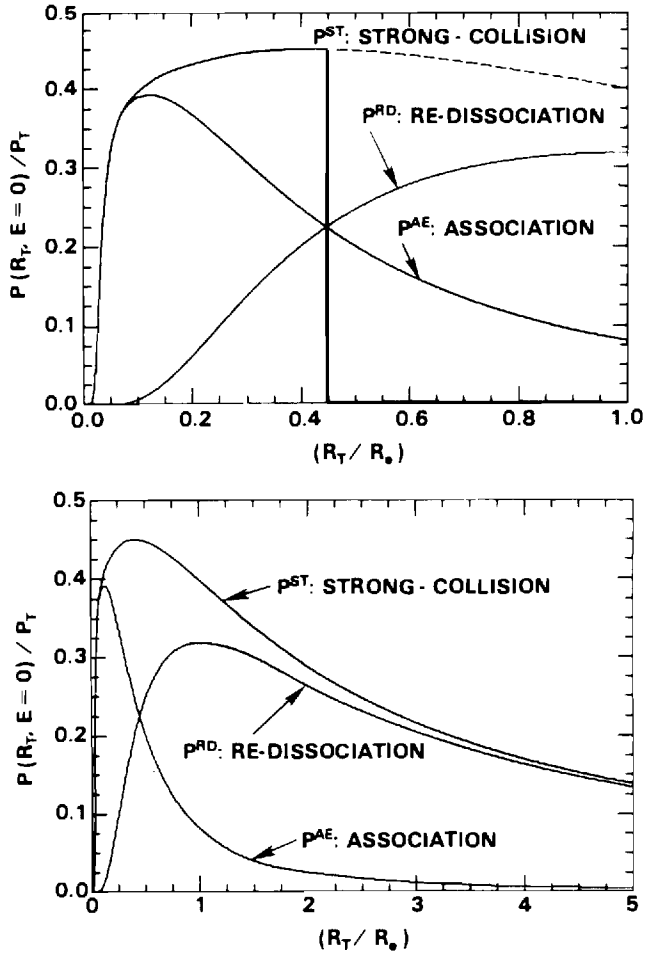

FIG. 8. (a),(b) Probabilities P^{ST}, P^{AE}, and P^{RD} for strong collisions (2.21), association (2.18), and redissociation (2.22) of (A–B) pairs with energy $E = 0$. Probabilities are normalized to the Thomson probability P_T, Eq. (2.27) and are presented as a function of R_T (normalized to $R_e = e^2/kT$).

$$\alpha(R_T;E_i)\tilde{N}_A\tilde{N}_B = \int_0^{R_T} d\mathbf{R} \int_{V(R)}^{0} C_{if}(R)dE_f \quad (2.31)$$

to the strong-collision rate (2.10) with R_T are displayed in Fig. 7. They intersect the corresponding exact partial rates (2.31a), represented as straight lines at R_T, in the range $0.5R_e \leqslant R_T \leqslant 0.6R$, a result consistent with the E_i-integrated rates of Fig. 2 where $R_T \sim 0.55R_e$.

D. R variation of calculated probabilities for multistep association

Figure 8 illustrates variation with R_T of P_i^{AE}, the exact probability (2.18) for multistep association via bound levels of $E_i = 0$ pairs with $R \leqslant R_T$, and of P_i^{ST}, the corresponding strong-collision probability (2.21). The probabilities are normalized to P_T, the Thomson probability (2.27). Also shown [Fig. 8(a)] is P_i^{RD}/P_T, the normalized probability (2.22) for redissociation of the bound pairs so formed with $R \leqslant R_T$. Figure 8(a) emphasizes that association dominates redissociation within smaller $R_T \ll (e^2/kt) \equiv R_e$ so that the exact and strong probabilities P_i^{AE} and P_i^{ST}, respectively, are equal. Figure 8(b) emphasizes that pairs within larger $R_T \gg R_e$ are mainly redissociated. The strong-collision probability P_i^{ST} accurately represents either P_i^{AE}, the association probability at small R_T, or P_i^{RD}, the redissociation probability at larger R_T, thereby providing the actual physical basis for Fig. 1.

Within radius $R_T \sim 0.45R_e$, there is as much association as redissociation [Fig. 8(a)] so that the strong rate is twice the exact rate for association of pairs with $R \leqslant 0.45R_e$. The contribution of pairs with $R \geqslant 0.45R_e$ to the exact rate is however equal to the contribution from $R \leqslant 0.45R_e$, so that the exact rate form all R and the strong rate from $R \leqslant 0.45R_e$ are fortuitously equal. This balance is the essential basis for agreement with the strong-collision model as previously illustrated by Figs. 2 and 7. Figure 8(a) also suggests that the R_T variation of the strong collision probability (2.21) is represented fairly well by P_T^A, the Thomson result (2.27), over the region $R \leqslant R_e$ important to association, although the magnitude is overestimated by a factor of $\lesssim 2.5$.

As the energy E_i of the dissociated pairs increases from

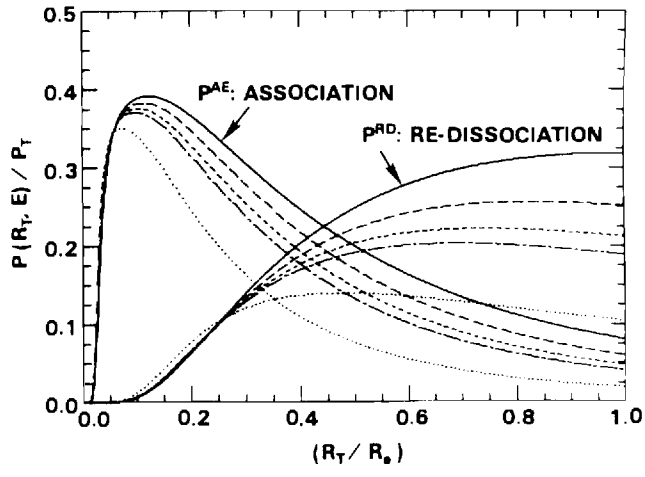

FIG. 9. As in Fig. 8 but for various continuum energies ($E/kT = 0, 0.529, 1.09, 1.56$, and 4.7 ordered sequentially from top to bottom).

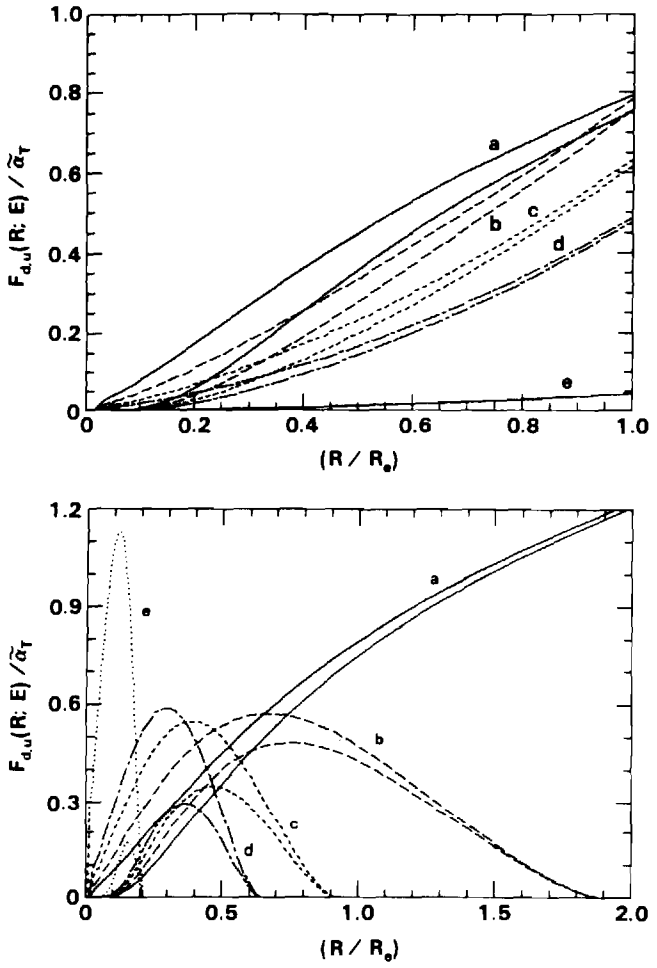

FIG. 10. R dependence of downward F_d and upward F_u normalized flux, Eqs. (2.32) and (2.33), upper and lower curves of each set, across various continuum energies [$E/kT = 0$, 0.529, 1.09, 1.56, and 4.7, (a)–(e), respectively] and across various bound energies [$-E/kT = 0$, 0.529, 1.09, 1.56, and 4.7, (a)–(e), respectively] in (b).

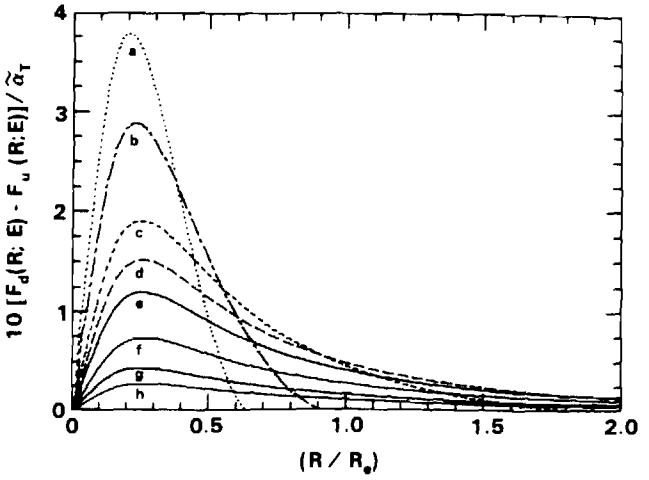

FIG. 11. R dependence of the net flux ($F_d - F_u$) downward across various continuum [$E/kT = 0, 0.529, 1.09, 1.56$; (e)–(h), respectively] and bound [$-E/kT = 0.26, 0.529, 1.09, 1.56$; (d)–(a), respectively] energy levels.

zero, Fig. 9 shows that the probabilities for association of these pairs and for subsequent redissociation decreases monotonically with E_i and that the R_T region over which association exceeds redissociation becomes somewhat smaller. As before, the strong collision probability P_i^{ST}, the sum ($P_i^{AE} + P_i^{RD}$) of each pair of curves, tends to P_i^{AE} at small R_T, to P_i^{RD} at large R_T. The sum is fairly constant for the range $0.2R_e \leqslant R_T \leqslant R_e$, as in Fig. 8(a).

E. (R,E) variation of calculated flux and rates

In Figs. 10(a) and 10(b) are shown the variation with R of the downward differential flux ($dF = FdR$),

$$F_d(R;E) = 4\pi R^2 \int_E^\infty (1 - P_i^S)dE_i \int_{V(R)}^E C_{if}(R)dE_f \tag{2.32}$$

per unit interval dR across various continuum [Fig. 10(a)] and bound [Fig. 10(b)] energy levels E, and of the corresponding upward flux

$$F_u(R;E) = 4\pi R^2 \int_E^\infty dE_i \int_{V(R)}^E (1 - P_f^S)C_{fi}(R)dE_f \tag{2.33}$$

with both normalized to the Thomson rate (2.29). For small $R \leqslant 0.3R_e$, F_d increases more rapidly from zero and remains greater for all R than F_u which eventually tends at large R to F_d from below. This limiting behavior at small and large R also elucidate the physical basis for the separate R regions in Fig. 1. For bound levels [Fig. 10(b)], both F_d and F_u across state (R,E) increase from zero to a maximum and then decrease as expected to zero at the turning points associated with energy E.

Variation with R in Fig. 11 of $F(R)$, the *net* differential flux ($F_d - F_u$) across both bound and continuum energy levels E exhibits a peak at roughly the same $R \sim (0.2\text{–}0.3)R_e$ for all E. As E decreases through the continuum the flux, and R-integrated flux, $\int_0^\infty F(R)dR$, increases. For bound E, the net flux increases and then decreases to zero at the classical turning points $R_i = e^2/|E|$. The net R-integrated flux across the highly excited bound levels remains constant, i.e., the area under each of the bound curves remains constant in accord with the QSS condition [$dn_i(t)/dt = 0$] in block $\mathscr{E}$, so that the flux becomes constricted into more restricted R space as E decreases through the bound levels. The resulting increase exhibited in Fig. 11 of the net differential flux as E decreases is therefore expected. The E variation of the normalized R-integrated net flux

$$F(E) = \begin{cases} \int_0^\infty [F_d(R;E) - F_u(R;E)]dR, & E \geqslant 0 \\ \int_0^{R_t} [F_d(R;E) - F_u(R;E)]dR, & E \leqslant 0 \end{cases} \tag{2.34}$$

is illustrated in Fig. 12. That $F(E \leqslant 0)$ is constant simply reflects the QSS condition or constant flux through the highly excited block $\mathscr{E}$.

Figure 13 illustrates the variation with R_T of α_i the exact partial rates (2.19) and (2.20) for the association of dissociated pairs ($E_i \geqslant 0$) and of highly excited bound pairs ($E_i < 0$), respectively, within the sphere of radius R_T. The former rate increases with R_T and saturates fairly rapidly for large R_T to the exact rate for association which, in order to

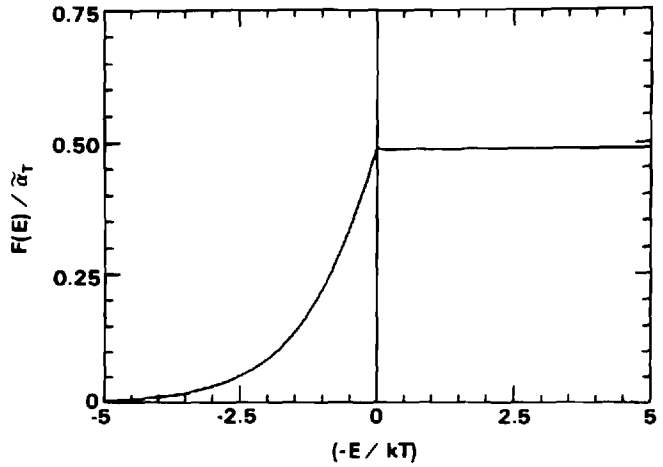

FIG. 12. Energy dependence of exact current, Eq. (2.34), normalized to $\bar{\alpha}_T$, for the association of equal mass species under charge–transfer ion–neutral collisions. Exact rate is the constant current across bound levels.

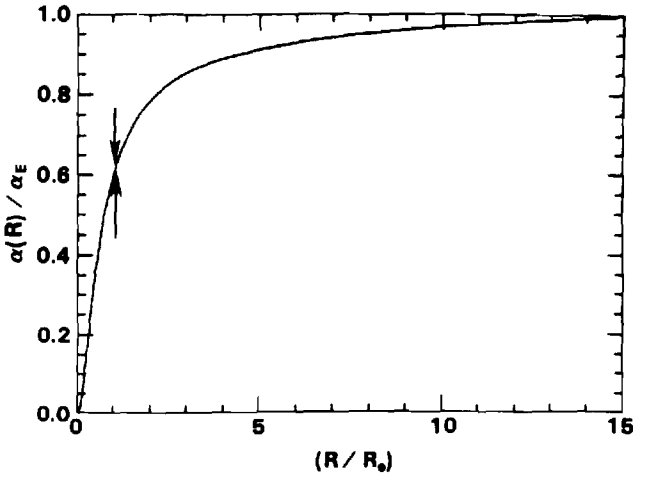

FIG. 14. Rate that fully dissociated pairs (with a Maxwellian energy distribution) recombine within a sphere of radius R. The exact rate is α_E.

maintain a steady-state $\mathscr{C}$ block, is the rate of generation of net inward E_i pairs with infinite separation.

The rates that bound E_i pairs are lost also increase with R_T due to continual downwards output, but reach a maximum when the upward input from other levels becomes competitive, and then decrease as a result to zero at the classical point R_i of classical motion. There is a net loss of bound E_i pairs with small R and a net gain of pairs with larger $R \leqslant R_i$ so that the R-integrated distribution (2.5b) remains constant in time. The zero rate at the apocenter R_i in Fig. 13 reflects the QSS condition (1.8) in Eq. (2.20) for no net loss or gain of R-integrated bound E_i pairs in block $\mathscr{E}$.

The rate $\alpha(R)$ of volume recombination within a sphere of radius R, the rates of Fig. 13 integrated over $E \geqslant 0$ is given in Fig. 14 as a function of R. It is worth noting that 60% of the exact rate $\alpha_E = \alpha(R \to \infty)$ is achieved within the sphere of the natural (Onsager) radius $R_e = e^2/kT$ as designated by the arrows.

III. MASS EFFECT IN STRONG-COLLISION MODEL

Figures 2 and 7 illustrate the ratio of the strong collision result (2.10) to the exact result α_E for equal mass species recombining in an equal mass gas, i.e., a, the mass parameter (2.11), is (1/3). In Fig. 15 is displayed variation of the same ratio over the full range of a. Small $a \approx 10^{-3}$ implies heavy particle recombination in a vanishingly light gas, while electron–ion recombination in a normal gas is characterized by large $a \approx 10^3$. It is noted that the radius R_T^*, where $\alpha(R_T) = \alpha_E$ increases from $\sim 0.1R_e$ to $\sim 0.5R_e$ as the parameter a increases to unity, and then decreases back again as the parameter a further increases. For greatly mismatched species, i.e., in the limits of small and large a the energy-change collision dynamics is weak, and vanishingly small energy changes are involved particularly for deactivating transitions across the dissociation limit at $E_i = 0$. The stabilization probability P_J^S in Eq. (2.6) and Fig. 4 is therefore of prime significance. To invoke the strong-collision assumption (2.9) for these bound levels close to the dissociation limit and important at small and large a is therefore without validity. Although some physical significance can be attached to R_T^*, where $\alpha(R_T)$ and α_E are equal, for intermediate $a \sim 1$, as previously discussed in Sec. II, no such significance exists in the limits of small and large a. The essential reason why $R_T^* \sim 0.1R_e$ becomes unacceptably small at

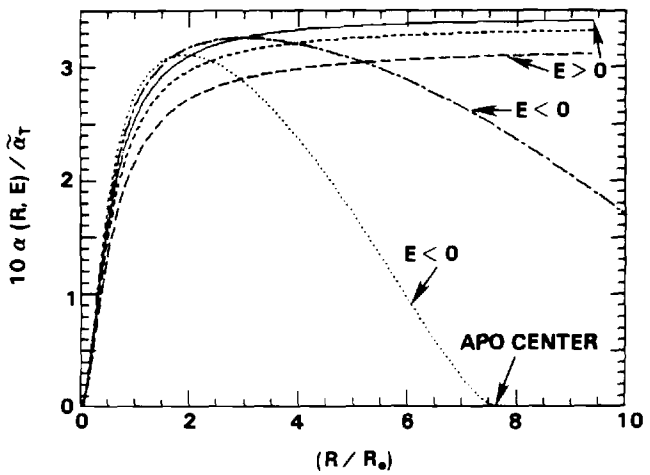

FIG. 13. Normalized rate equations (2.19) and (2.20) that pairs in continuum and bound energy levels E recombine within a sphere of radius R.

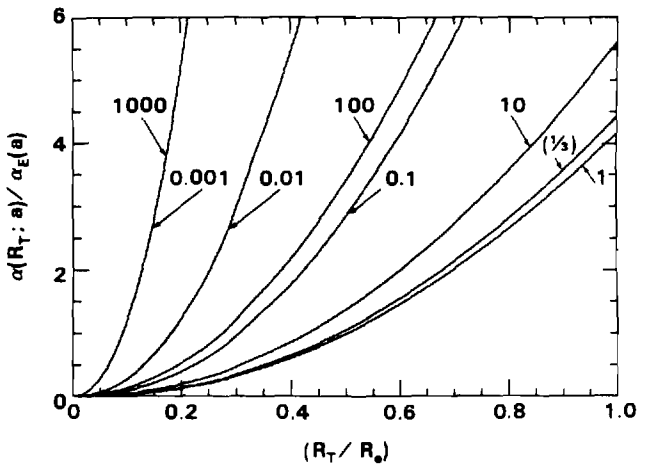

FIG. 15. Mass effect in strong-collision model: R_T variation of the strong-collision rate (2.31) normalized to the exact rate α_E, Eq. (1.6), for recombination of systems with various mass parameters a, Eq. (2.11).

these limits is that small R_T^* effectively (numerically) offsets the large addition to the inner integral of Eq. (2.10) entailed by the strong collision assumption ($P_f^S = 1$) in Eq. (2.6). The smaller exact values of P_f^S (cf. Fig. 4) are more appropriate to the important levels in the vicinity of the dissociation limit for large and small a.

IV. RECOMMENDED LOW-DENSITY TERMOLECULAR RATES

Due to the long-range Coulombic attraction and to the use of shorter-range ion–neutral interactions [charge–transfer (CX), polarization (POL), and hard sphere (HS)], rates for the termolecular ion–ion recombination,

$$A^+ + B^- + M \rightarrow AB + M \tag{4.1}$$

between general atomic species in a general atomic gas may be characterized[9] by a universal function of the mass parameter (2.11) and of the gas temperature T [cf. Eqs. (A40)–(A55)]. This universality does not extend to ion–atom association which, due to the closer interactions involves, demands individual calculations for specific systems. As previously mentioned, rates (1.6) or (1.9) or (1.10) have been obtained numerically from Eq. (A55) via the highly accurate numerical solutions P_f^S to the integral equation (1.8) for the stabilization probabilities. Converged probabilities for small and large mass parameters a in particular were obtained only when the integral equation (1.8b) was discretized into 100 algebraic equations via the efficient procedure of Ref. 3. Previous results[1–3] adopted 36 equations at most.

Recommended values of the ratio[1–3]

$$\mathcal{R}(a) = (M_A/M_{AB})[\alpha_E^{(A)}(a,T)/\tilde{\alpha}_T(T)], \tag{4.2}$$

where $\alpha_E^{(i)}$ is the exact numerical rate (A55a) originating from $(i - M)$ collisions alone, are presented at closely spaced a in Table I. The exact low density rate can be represented to a high degree of accuracy by[9]

$$\alpha = \alpha_E^{(A)} + \alpha_E^{(B)}. \tag{4.3}$$

Although the partial rates $\alpha_E^{(i)}$ are tabulated here to four significant figures, the recombination rule (4.3) as previously tested was then shown to be accurate to three figures at best or two figures at worst. The test however relies on the accuracy of the solutions to the integral equations (1.8b) with C_{if} taken as $C_{if}^{(A)}, C_{if}^{(B)}$ and $[C_{if}^{(A)} + C_{if}^{(B)}]$ where $C_{if}^{(A),(B)}$ is the one-way equlibrium rate which results from individual A–M and B–M collisions, respectively. Since the present converged probabilities P_i^S have been determined by a numerical procedure[3] more accurate and efficient than that[9] previously used for the test, the accuracy of rule (4.3) is being updated.

TABLE I. Normalized partial rates 10 $(M_A/M_{AB})(\alpha_E^A/\tilde{\alpha}_T)$ for termolecular recombination $A^+ + B^- + M \rightarrow AB + M$ as a function of mass parameter $a = M_A M_B/M_A(M_A + M_B + M_g)$ for various interactions (CX: symmetrical resonance charge transfer: HS: hard sphere; POL: polarization attraction) in collision between A and gas atoms of mass M_g.

a	CX[a]	HS[b]	POL[b]	a	HS[b]	POL[b]
0.0010	1.291	1.278	1.029	1.5000	9.452	6.751
0.0020	1.816	1.818	1.472	2.0000	8.593	6.044
0.0030	2.208	2.221	1.800	2.5000	7.877	5.472
0.0040	2.530	2.554	2.071	3.0000	7.276	5.003
0.0050	2.807	2.841	2.304	3.5000	6.766	4.611
0.0060	3.053	3.098	2.512	4.0000	6.328	4.280
0.0070	3.274	3.329	2.699	4.5000	5.947	3.994
0.0080	3.476	3.542	2.870	5.0000	5.613	3.746
0.0090	3.662	3.739	3.029	5.5000	5.317	3.529
0.0100	3.835	3.923	3.177	6.0000	5.053	3.336
0.0200	5.115	5.313	4.288	6.5000	4.815	3.164
0.0300	5.959	6.264	5.039	7.0000	4.601	3.010
0.0400	6.581	6.986	5.603	7.5000	4.406	2.871
0.0500	7.066	7.565	6.049	8.0000	4.228	2.744
0.0600	7.456	8.042	6.414	8.5000	4.065	2.629
0.0700	7.778	8.444	6.719	9.0000	3.914	2.523
0.0800	8.047	8.789	6.976	9.5000	3.775	2.426
0.0900	8.276	9.086	7.197	10.0000	3.646	2.336
0.1000	8.471	9.347	7.387	12.0000	3.212	2.036
0.2000	9.459	1.078, + 1	8.377	14.0000	2.875	1.806
0.3000	9.709	1.127, + 1	8.644	16.0000	2.604	1.624
0.3333	9.727	1.134, + 1	8.666	18.0000	2.382	1.476
0.4000	9.709	1.140, + 1	8.652	20.0000	2.196	1.353
0.5000	9.600	1.136, + 1	8.547	50.0000	1.029	6.064, − 1
0.6000	9.446	1.124, + 1	8.389	100.0000	5.535, − 1	3.177, − 1
0.7000	9.269	1.107, + 1	8.206	500.0000	1.195, − 1	6.582, − 2
0.8000	9.045	1.087, + 1	8.013	1000.0000	6.029, − 2	3.253, − 2
0.9000	8.860	1.067, + 1	7.818			
1.0000	8.678[c]	1.046, + 1	7.625			

[a] In CX small a implies $M_B \ll M_A = M_g$; $a = 1$ implies $M_B \gg M_A = M_g$.

[b] In HS and POL small a implies recombination in a vanishingly light gas and large a ($\approx 10^3$) implies electron–ion recombination in a normal mass gas.

[c] For CX, the maximum value of a is 0.998.

The partial rates (4.2) are very insensitive to a realistic choice of either the level $-S$ ($\lesssim -10kT$), below which the stabilization probability P_i^S is calculated as unity, or the lowest level $-D$ since the one-way coupling C_{if} connecting the dissociated states i to any bound level f decreases extremely rapidly and is quite negligible for states with binding energies D as low as $30\,kT$, which is much smaller, in general, than dissociation energies of normal molecules.

The temperature dependence of $\alpha_E^{(i)}$ follows that of $\bar{\alpha}_T$, the Thomson rate (A40) with Eqs. (A41)–(A44). Results of a recent diffusional treatment[5] are in close agreement with those of Table I.

In conclusion, via an exhaustive investigation of the strong-collision and bottleneck methods of the termolecular process (4.1), interesting underlying physics and dynamics of the basic process have been uncovered and studied. Highly accurate rates have been presented (Table I) for future use.

ACKNOWLEDGMENT

This research is supported by the U.S. Air Force of Scientific Research under Grant No. AFOSR-84-0233.

APPENDIX: ONE-WAY EQUILIBRIUM COLLISION KERNELS $C_{if}(T)$

The one-way equilibrium rate per unit interval $d\mathbf{R}\,dE_i\,dE_f$ for $E_i \to E_f$ transitions in the microscopic process,

$$(\text{A–B})_{E_i,R} + \text{M} \to (\text{A–B})_{E_f,R} + \text{M} \tag{A1}$$

at specified internal separation R of the pair AB is

$$C_{if}(R) = \bar{n}_i(\mathbf{R})\nu_{if}(R) = \bar{n}_i\left[\nu_{if}^{(1)}(R) + \nu_{if}^{(2)}(R)\right]. \tag{A2}$$

The equilibrium distribution $\bar{n}_i(R)$ per unit interval $d\mathbf{R}$ of (A–B) pairs with internal energy E_i, internal kinetic energy T_{12}, and reduced mass M_{12} is

$$\frac{\bar{n}_i(\mathbf{R})dE_i}{\tilde{N}_\text{A}\tilde{N}_\text{B}} = \frac{2}{\pi^{1/2}}\left(\frac{T_{12}}{kT}\right)^{1/2}\exp(-E_i/kT)d(T_{12}/kT) \tag{A3}$$

at temperature T. The frequency ν_{if} per unit interval dE_f for $E_i \to E_f$ transitions is assumed in Eq. (A2) to be the sum $\nu_{if}^{(1)} + \nu_{if}^{(2)}$ of the separate contributions $\nu_{if}^{(j)}$ that arise from (A–M), $j=1$, and (B–M), $j=2$, binary collisions at fixed $\mathbf{R}$. The species A, B, and M denoted by indices 1, 2, and 3, respectively, have masses M_i, reduced masses M_{ij} and velocities $\mathbf{v}_i$ and $\mathbf{v}_i'$ before and after the (1–3) elastic collision with differential cross section $\sigma(g,\psi)$ which changes the (1–3) relative velocity from $\mathbf{g}$ along the polar axis to $\mathbf{g}'(\psi,\phi)$. Hence the (1–3) energy-change collision frequency is

$$\nu_{if}^{(1)}(R)dE_f = \left[\int N_0(\mathbf{v}_3)d\mathbf{v}_3\int_{\psi^-}^{\psi^+} g\sigma(g,\psi)d(\cos\psi)\right]d\phi, \tag{A4}$$

where the integration is over the $(\mathbf{v}_3,\psi)$ region of velocity space accessible to $E_i \to E_f$ transitions. The velocity distribution of gas species with concentration N (cm^{-3}) over the kinetic energy

$$T_3 = \tfrac{1}{2}M_s v_3^2 \tag{A5}$$

of AB–M relative motion is the Maxwellian

$$N_0(\mathbf{v}_3)d\mathbf{v}_3 = NG(T_3)dT_3\left[\frac{1}{4\pi}d(\cos\theta_3)d\phi_3\right], \tag{A6}$$

where the distribution

$$G(T_3)dT_3 = \frac{2}{\sqrt{\pi}}(T_3/kT)^{1/2}\exp(-T_3/kT)d(T_3/kT) \tag{A7}$$

represents thermodynamic equilibrium at temperature T between 3 and the (1–2) center of mass.[14] The reduced mass of the AB–M system is

$$M_s = (M_1+M_2)M_3/(M_1+M_2+M_3) = aM = (1+a)M_{13}, \tag{A8}$$

where a convenient mass parameter[9] for (1–3) collisions is

$$a = M_2M_3/M_1(M_1+M_2+M_3). \tag{A9}$$

The (1–2) center of mass is at rest before the (1–3) collision which changes both the kinetic energy

$$T_{12} = \tfrac{1}{2}M_{12}(\mathbf{v}_1-\mathbf{v}_2)^2 = \tfrac{1}{2}Mv_1^2;\quad M = M_1(1+M_1/M_2) \tag{A10}$$

of (1–2) relative motion to T_{12}' and the internal energy

$$E_i = \tfrac{1}{2}Mv_1^2 + V(R) \tag{A11}$$

at a fixed R by

$$\epsilon = T_{12}' - T_{12} = \tfrac{1}{2}M_{12}\left[(\mathbf{v}_1'-\mathbf{v}_2)^2 - (\mathbf{v}_1-\mathbf{v}_2)^2\right]. \tag{A12}$$

The (1–3) relative momentum is changed by

$$\mathbf{P} = M_{13}(\mathbf{g}'-\mathbf{g}) = M_1(\mathbf{v}_1'-\mathbf{v}_1) = M_3(\mathbf{v}_3-\mathbf{v}_3') \tag{A13}$$

and the (1–3) relative energy T_{13} remains $\frac{1}{2}M_{13}g^2$. On following from analysis in Ref. 15 it can be shown that the Jacobian J_2 in the angle-kinetic energy transformation

$$d(\cos\theta_3)d\phi = J_2\,dT_{13}\,dT_{12}' \tag{A14}$$

is given by

$$J_2(\psi,T_{13},T_3;\epsilon) = \frac{(1+a)^2}{2a}\left[(T_{12}T_3T_{13})\times(T_{12}+T_3-T_{13})(\mu^+-\mu)(\mu-\mu^-)\right]^{-1/2}. \tag{A15}$$

The scattering ψ region accessible at fixed T_{13}, T_3, and ϵ is the range $\mu^- \leqslant \cos\psi \leqslant \mu^+$, with limits

$$\mu^\pm = (1-\Gamma_i^2)^{1/2}(1-\Gamma_f^2)^{1/2} \pm \Gamma_i\Gamma_f, \tag{A16}$$

where

$$\Gamma_i^2 = \left[(T_{13}^+ - T_{13})(T_{13}-T_{13}^-)\right]/\left[4T_{13}(T_{12}+T_3-T_{13})\right] \tag{A17a}$$

and

$$\Gamma_f^2 = [(\tilde{T}_{13}^{+} - T_{13})(T_{13} - \tilde{T}_{13}^{-})]/ [4T_{13}(T_{12} + T_3 - T_{13})]. \quad \text{(A17b)}$$

The accessible T_{13} region accessible for fixed T_3 and ϵ is the range

$$T^{-} = \max(T_{13}^{-}, \tilde{T}_{13}^{-}) \leqslant T_{13} \leqslant \min(T_{13}^{+}, \tilde{T}_{13}^{+}) = T^{+} \quad \text{(A18)}$$

which ensures real $\mu^{\pm}$, where

$$T_{13}^{\mp}(T_3;T_{12}) = (T_3^{1/2} \mp a^{1/2}T_{12}^{1/2})^2/(1+a) \quad \text{(A19a)}$$

is a function of the initial kinetic energies, and where

$$\tilde{T}_{13}^{\mp}(T_3';T_{12}') = (T_3'^{1/2} \mp a^{1/2}T_{12}'^{1/2})^2/(1+a) \quad \text{(A19b)}$$

is the same function of the final (1–2) and 3 kinetic energies

$$T_{12}' = T_{12} + \epsilon, \quad \text{(A20)}$$

$$T_3' = T_3 - \epsilon. \quad \text{(A21)}$$

Since

$$\frac{\tilde{n}_i(\mathbf{R})}{T_{12}^{1/2}} \frac{N_0(T_3)dT_3}{T_3^{1/2}} = \frac{4}{\pi} \frac{(\tilde{N}_A \tilde{N}_B)}{(kT)^2} \exp - (E/kT)d(E/kT), \quad \text{(A22)}$$

where

$$E = E_i + T_3 = (T_{12} + T_3) + V(R) = \tilde{T} + V(R) \quad \text{(A23)}$$

then the contribution to the one-way equilibrium rate (A2) from (1–3) collisions is

$$C_{if}^{(1)}(R) = \tilde{n}_i(\mathbf{R})\nu_{if}^{(1)}(R) = \frac{(1+a)^2}{a}\left(\frac{2}{M_{13}}\right)^{1/2} \times \frac{(\tilde{N}_A \tilde{N}_B N)}{\pi(kT)^2} \int_{E_0}^{\infty} \exp(-E/kT)d(E/kT) \times \int_{T^-}^{T^+} (\tilde{T} - T_{13})^{-1/2} dT_{13} \int_{\mu^-}^{\mu^+} \sigma(T_{13},\mu) \times [(\mu^+ - \mu)(\mu - \mu^-)]^{-1/2} d\mu, \quad \text{(A24)}$$

where T is $E - V(R)$, as defined in Eq. (A23), and where

$$E_0 = \min(E_i, E_f) \quad \text{(A25)}$$

ensures real T_3 and T_3' in Eq. (A18).

Case I: When the differential cross section σ is a function only of T_{13} as for spiralling ion–neutral collisions under pure polarization attraction when

$$\sigma(T_{13},\psi) = \left(\frac{\alpha_M e^2}{8T_{13}}\right)^{1/2}, \quad \text{(A26)}$$

where α_M is the polarizability of M, then

$$C_{if}^{(1)}(R) = \left(\frac{\alpha_M e^2}{M_{13}}\right)^{1/2} \times \frac{(1+a)^2(\tilde{N}_A \tilde{N}_B N)}{a(kT)^2} \int_{E_0}^{\infty} \exp(-E/kT) \times \left[\sin^{-1}\left(\frac{T^+}{\tilde{T}}\right)^{1/2} - \sin^{-1}\left(\frac{T^-}{\tilde{T}}\right)^{1/2}\right] \times d(E/kT), \quad \text{(A27)}$$

where $\tilde{T}$ is $T_{12} + T_3$ as in Eq. (A23). Integration over $\mathbf{R}$ yields an expression identical to that of Bates and Mendaš.[3]

Case II: For hard sphere collisions when

$$\sigma(T_{13},\psi) = \frac{\sigma_0}{4\pi} \quad \text{(A28)}$$

then[2]

$$C_{if}^{(1)}(R) = \frac{\sigma_0}{\pi} \frac{(\tilde{N}_A \tilde{N}_B N)}{(2M_{13})^{1/2}(kT)^2} \int_{E_0}^{\infty} \exp(-E/kT) \times [(\tilde{T} - T^-)^{1/2} - (\tilde{T} - T^+)^{1/2}]d(E/kT). \quad \text{(A29)}$$

Case III. When $\sigma(T_{13},\psi)$ is a function only of momentum change P as for the Born approximation or for pure Coulombic attraction when

$$\sigma(T_{13},\psi) = 4e^4 M_{13}^2/P^4 = \sigma(P) \quad \text{(A30)}$$

and by finding the Jacobean J_3 in

$$d(\cos\theta_3)\, d\phi\, d(\cos\psi) = J_3\, dT_{12}'\, dP\, dT_{13} \quad \text{(A31)}$$

then from previous analysis,[15] it can be shown that

$$C_{if}^{(1)}(R) = \frac{2^{1/2}(1+a)}{a^{1/2}M_{13}} \frac{(\tilde{N}_A \tilde{N}_B N)}{(kT)^2} \times \int_{E_0}^{\infty} \exp(-E/kT)d(E/kT) \int_{P^-}^{P^+} \sigma(P)dP, \quad \text{(A32)}$$

where the limits to the momentum change P for specified $v_1^{(1)}$, $v_3^{(1)}$, and ϵ are

$$P^-(v_1,v_3;\epsilon) = \max[M|v_1' - v_1|, M_s|v_3' - v_3|] \quad \text{(A33a)}$$

and

$$P^+(v_1,v_3;\epsilon) = \min[M(v_1' + v_1), M_s(v_3' + v_3)]. \quad \text{(A33b)}$$

Case IV. Symmetrical resonance charge–transfer (1–3) collisions

$$X^+ + X \rightarrow X + X^+ \quad \text{(A34)}$$

between an ion and its parent gas simply interchange $\mathbf{v}_1$ and $\mathbf{v}_3$. At thermal energies the integral cross section σ^x is essentially independent of relative speed g. It can then be shown that[1]

$$C_{if}^{(1)}(R) = \frac{[(1+c)/c]^{3/2}}{(2\pi M_{12})^{1/2}} \frac{(\tilde{N}_A \tilde{N}_B N)\sigma^x}{(kT)^{3/2}} \times \exp\left[-\frac{(1+c)}{(1+2c)}\frac{(E_i + E_f)}{kT}\right] \times \exp\left[-\frac{V(R)/kT}{(2c+1)}\right] \int_{E^-}^{E^+} G(E)dE, \quad \text{(A35)}$$

where

$$c = M_1/M_2$$

and where the fraction of Maxwell particles with energies E in the range $E^- \leqslant E \leqslant E^+$ with limits

$$E^{\pm} = [c(1+c)/(1+2c)][T_{12}^{1/2} \pm T_{12}'^{1/2}]^2 \quad \text{(A36)}$$

is

$$\int_{E^-}^{E^+} G(E)dE = \left[\mathrm{erfc}(E/kT)^{1/2} - \frac{2}{\sqrt{\pi}}(E/kT)^{1/2}\exp(-E/kT)\right]_{E^-}^{E^+}. \quad \text{(A37)}$$

The above rates (A24), (A27), (A29), (A32), and (A35) satisfy the detailed balance relation $C_{if}(R) = C_{fi}(R)$, and **R** integration of Eqs. (A27), (A29), and (A35) yields previous expressions.[1-3]

Computational equilibrium rates: C_{if} may be conveniently expressed for computational purposes in terms of dimensionless units,

$$\lambda = -E_i/kT, \quad \mu = -E_f/kT, \quad v(r) = -V(R)/kT, \quad r = R/R_e, \quad R_e = e^2/kT \quad \text{(A38)}$$

by

$$4\pi C_{if}(R)R^2\,dR\,|dE_i|dE_f| = \Gamma\tilde{\alpha}_T F(\lambda,\mu;r)r^2\,dr\,d\lambda\,du \ \ (\mathrm{cm^3\,s^{-1}}) \quad \text{(A39)}$$

in terms of specified mass factors Γ and the Thomson (low density) rates,

$$\tilde{\alpha}_T = \tfrac{4}{3}\pi(R_e/\beta)^3(3kT/M_{12})^{1/2}\sigma_0 N, \ \beta = 3/2, \quad \text{(A40)}$$

where σ_0 is the integral cross section for (1-3) collisions are relative energy $\frac{3}{2}kT$. The appropriate mass factors Γ in Eq. (A39) and cross section σ_0 in Eq. (A40) are

$$\Gamma^H = \left(\frac{3}{2}\right)^{1/2}\left(\frac{\beta^3}{\pi}\right)\frac{(1+a)^2}{a^{3/2}}\left(\frac{M_{12}}{M_1}\right); \quad \sigma_0 = \sigma_0^H \quad \text{(A41)}$$

for hard-sphere (1-3) collisions with integral cross section σ_0^H,

$$\Gamma^C = \frac{3a}{\pi(1+a)}\Gamma^H; \quad \sigma_0 = \sigma_0^c = \frac{1}{9}\pi R_e^2 \quad \text{(A42)}$$

for Coulomb (1-3) collisions with integral cross section σ_0^c which corresponds to Coulomb scattering by angles $\psi \geqslant \pi/2$, and to energy transfers $\epsilon \geqslant (3/2)kT$ for equal mass species. For (1-3) polarization attraction/core repulsion for collisions within the orbiting radius,

$$\Gamma^P = \left(\frac{3}{2}\right)\left(\frac{\beta^3}{\pi}\right)\frac{(1+a)^{5/2}}{a^{3/2}}\left(\frac{M_{12}}{M_1}\right); \quad \sigma_0 = \sigma_0^P = 2\pi(\alpha_M R_e/3)^{1/2} \quad \text{(A43)}$$

and σ_0^P adopted in Thomson's rate (A40) is the corresponding integral (elastic or momentum transfer) collisional cross section at $(3/2)kT$ relative energy. For (1-3) charge–transfer collisions,

$$\Gamma^X = \left(\frac{3}{2}\right)^{1/2}\left(\frac{\beta^3}{\pi}\right)\left(\frac{1+c}{c}\right)^{3/2}; \quad \sigma_0 = 2\sigma^X, \quad \text{(A44)}$$

where σ_0 in Eq. (A44) is the corresponding momentum-transfer cross section, taken as twice the cross section σ^X for charge transfer.[1]

The corresponding dimensionless functions F in Eq. (A39) are symmetric in λ and μ and are

$$F^H(\lambda,\mu;r) = \int_{Y_0}^{\infty}\exp(-Y)dY\,[\tilde{P}_+ - \tilde{P}_-]; \quad Y_0 = \max(-\lambda,-\mu) \quad \text{(A45)}$$

for hard-sphere (1-3) collisions with (dimensionless) momentum-change limits $\tilde{P}_+ \geqslant \tilde{P}_-$, given by

$$\tilde{P}_-(\lambda,\mu;r) = \max\{[v(r)-\lambda]^{1/2} - [v(r)-\mu]^{1/2}; a^{1/2}[(Y+\lambda)^{1/2} - (Y+\mu)^{1/2}]\} \quad \text{(A46a)}$$

and

$$\tilde{P}_+(\lambda,\mu;r) = \min\{[v(r)-\lambda]^{1/2} + [v(r)-\mu]^{1/2}; a^{1/2}[(Y+\lambda)^{1/2} + (Y+\mu)^{1/2}]\}. \quad \text{(A46b)}$$

For Coulomb (1-3) collisions,

$$F^C(\lambda,\mu;r) = \int_{Y_0}^{\infty}\exp(-Y)dY\left[\tilde{P}_-^{-3} - \tilde{P}_+^{-3}\right]. \quad \text{(A47)}$$

For polarization (1-3) collisions,

$$F^P(\lambda,\mu;r) = \int_{Y_0}^{\infty}\exp(-Y)dY \times [\sin^{-1}(G_2/A) - \sin^{-1}(G_1/A)], \quad \text{(A48)}$$

where

$$G_1(\lambda,\mu;r) = \max[|(Y+\lambda)^{1/2} - a^{1/2}[v(r)-\lambda]^{1/2}|; |(Y+\mu)^{1/2} - a^{1/2}[v(r)-\mu]^{1/2}|], \quad \text{(A49)}$$

$$G_2(\lambda,\mu;r) = \min[(Y+\lambda)^{1/2} - a^{1/2}[v(r)-\lambda]^{1/2}; (Y+\mu)^{1/2} - a^{1/2}[v(r)-\mu]^{1/2}],$$

and

$$A = (1+a)^{1/2}[v(r)+Y]^{1/2}. \quad \text{(A50)}$$

For charge–transfer (1-3) collisions

$$F^X(\lambda,\mu;r) = \exp\left[\left(\frac{1+c}{1+2c}\right)(\lambda+\mu)\right] \times \exp[-1/(1+2c)r] \times \left[\frac{\sqrt{\pi}}{2}\,\mathrm{erf}\,g - g\exp(-g^2)\right]_{g_-}^{g_+}, \quad \text{(A51)}$$

where

$$g_\pm^2(\lambda,\mu;r) = \frac{c(1+c)}{(1+2c)}\{[v(r)-\lambda]^{1/2} \pm [v(r)-\mu]^{1/2}\}^2. \quad \text{(A52)}$$

The universal expression (A39) is also valuable in that the one-way equilibrium current (rate) across an arbitrary bound level $\nu = -E/kT$ is simply

$$\alpha_{eq} = \Gamma\tilde{\alpha}_T\int_{-\infty}^{\nu}d\lambda\int_{\nu}^{\omega}F(\lambda,\mu)d\mu, \quad \text{(A53)}$$

where $\omega = -D/kT$ is the maximum binding energy in units of (kT) and where

$$F(\lambda,\mu) = \int_0^{r_m}F(\lambda,\mu;r)r^2\,dr, \quad r_m = 1/\max(\lambda,\mu). \quad \text{(A54)}$$

This equilibrium collisional rate displays a minimum at $\nu^* = (1\text{-}3)kT$, the location of a bottleneck (see Fig. 3). The QSS rates (1.9), (1.10), and (1.6) reduce simply to

$$\alpha = \Gamma\tilde{\alpha}_T \int_{-\infty}^{0} d\lambda \int_{0}^{\omega} F(\lambda,\mu) P^{S}(\mu) d\mu, \tag{A55a}$$

$$\alpha = \Gamma\tilde{\alpha}_T \int_{\epsilon}^{\omega} d\lambda \int_{-\infty}^{\epsilon} F(\lambda,\mu) P^{D}(\mu) d\mu, \tag{A55b}$$

$$= \Gamma\tilde{\alpha}_T \int_{-\infty}^{\nu} d\lambda \int_{\nu}^{\omega} [P^{S}(\mu) - P^{S}(\lambda)] F(\lambda,\mu) d\mu, \tag{A55c}$$

where $\epsilon = -S/kT$.

Also various energy-change moments,

$$D_i^{(m)}(E_i) = \frac{1}{m!} \int_{-D}^{\infty} (E_f - E_i)^m C_{if}\, dE_f \tag{A56}$$

are useful[5] in a Fokker–Planck reduction of the collision term (1.2). These can be expressed simply as

$$D_i^m(E_i) = \Gamma\tilde{\alpha}_T \tilde{N}_A \tilde{N}_B (kT)^{m-1} (-1)^m \mathscr{D}_i^{(m)}(\lambda), \tag{A57}$$

where the dimensionless moments

$$\mathscr{D}_i^{(m)}(\lambda) = \frac{1}{m!} \int_{-\infty}^{\omega} (\mu - \lambda)^m F(\lambda,\mu) d\mu \tag{A58}$$

are easily determined[5] on using one of the relevant expressions, (A45), (A47), (A48), or (A51), pertinent to the chosen binary A–M and B–M interactions of A and B with the gas M.

[1] M. R. Flannery, J. Phys. B **13**, 3649 (1980).
[2] M. R. Flannery, J. Phys. B **14**, 915 (1981).
[3] D. R. Bates and I. Mendaš, J. Phys. B **15**, 1949 (1982).
[4] M. R. Flannery, J. Phys. B **18**, L839 (1985).
[5] M. R. Flannery, J. Chem. Phys. **87**, 6947 (1987).
[6] M. R. Flannery, Ann. Phys. (N.Y.) **67**, 376 (1971).
[7] J. J. Thomson, Philos. Mag. **47**, 337 (1924).
[8] P. J. Feibelman, J. Chem. Phys. **42**, 2462 (1965).
[9] D. R. Bates and M. R. Flannery, Proc. R. Soc. London Ser. A **302**, 367 (1968).
[10] M. R. Flannery, J. Phys. B. **20**, 4929 (1987).
[11] M. R. Flannery and T. P. Yang, J. Chem. Phys. **73**, 3239 (1980).
[12] M. R. Flannery, *Recent Studies of Atomic and Molecular Processes*, edited by A. E. Kingston (Plenum, New York, 1987).
[13] J. C. Keck, in *Advances in Atomic and Molecular Physics*, edited by D. R. Bates and I. Estermann (Academic, New York, 1972), Vol. 8; Adv. Chem. Phys. **13**, 83 (1967).
[14] D. R. Bates, P. B. Hays, and D. Sprevak, J. Phys. B **4**, 962 (1971).
[15] M. R. Flannery, Phys. Rev. A **22**, 2408 (1980).

Appendix B

"Variational Principle for Termolecular Recombination in a gas"

by

M. R. Flannery

(J. Chem. Phys. 89, 214-222 (1988))

Variational principle for termolecular recombination in a gas

M. R. Flannery
School of Physics, Georgia Institute of Technology, Atlanta, Georgia 30332-0430

(Received 29 February 1988; accepted 22 March 1988)

A variational principle for the rates of termolecular processes is proposed and then applied to recombination between atomic ions with excellent results. The variational expression when minimized with respect to stabilization probabilities is capable of providing rates identical to those determined from the quasi-steady-state solution of the full Master equation. Connection is made with electrical networks and with the principle of least dissipation.

I. INTRODUCTION

An important objective in chemical physics is the formulation of a variational theory of chemical reactions which is exact in the sense that the deduced variational expression will yield, upon variation of relevant parameters, the distributions n_i and rate constants which are identical with those obtained by direct solution of the exact Master equation for the particular process. The variational procedure of Wigner[1] and Keck[2] is "variational" in the sense that it yields a least upper bound to the rate of a chemical reaction as determined from a Master equation. The reaction is represented by the motion of a point $(\mathbf{p},\mathbf{q})$ in multidimensional phase space across a trial surface S which separates a block $\mathscr{C}$ of initial reactant states i from a block $\mathscr{S}$ of final product states f. The one-way rate R that representative phase points flow (downward) across S—or flux of trajectories—is an upper limit to the actual rate since (a) upward reexcitation to states i above S is ignored and since (b) a representative point which passes through S more than once is repeatedly included at each pass. The additional use of an equilbrium density $\bar{n}_i$ for the reacting states then provides a rigorous upper bound R_e to the reaction rate. A minimum—the least upper bound—to R_e is then obtained by variation of the trial surface S.

In termolecular electron-ion or ion-ion collisional recombination

$$A^+ + B^- + M \rightarrow AB + M \qquad (1.1)$$

at low gas densities, for example, the "surface", can be taken as some bound energy level $-E$ of the pair AB so that an upper bound to the two-body rate constant $\alpha(\mathrm{cm^3\ s^{-1}})$ for recombination (1.1) is

$$R_e(-E) = \int_{-E}^{\infty} dE_i \int_{-D}^{-E} C_{if}\, dE_f > \alpha \bar{N}_A \bar{N}_B\ , \qquad (1.2)$$

where $\bar{N}_A$ and $\bar{N}_B$ are the equilibrium concentrations of A^+ and B^- and where C_{if} is the one-way equilibrium collisional rate per unit interval $dE_i\ dE_f$ for transitions between energy levels E_i and E_f of AB pairs. The level $-E$ separates the "reactant" block $\mathscr{C}$ of states i with energies E_i in the range $-E \leqslant E_i \leqslant \infty$ from the "product" block $\mathscr{S}$ of states f with energies E_f in the range $-E \geqslant E_f \geqslant -D$, where $-D$ is the lowest energy level of the AB pair relative to a dissociation limit at zero energy. A minimum to R_e occurs at $-E = -E^*$ which therefore acts as a bottleneck or transition state. States above $-E^*$ are more likely to be excited by collision and hence are unstable with respect to association, while those below $-E^*$ tend to be deexcited and are therefore considered as stable. For this one-dimensional surface, the Wigner–Keck treatment is then identical with the bottleneck method proposed by Byron *et al.*[3] for three-body electron–ion recombination.[4] For termolecular recombination of arbitrary mass ions in a gas, this variational treatment yields rates[5] which are higher by factors of 2 to 8 than the exact rates[6] obtained from a Master equation.

What is desirable is a variational method which will yield a rate identical to that determined from solution of the full Master equation. This search requires the addition, as illustrated by Fig. 1, of a block $\mathscr{E}$ of highly excited states i for which the reaction can go either way. The block is characterized by the overall probability P_i^S for stabilization via downward ($\mathscr{E} \rightarrow \mathscr{S}$) transitions or by the overall probability $P_i^D = (1 - P_i^S)$ for disruption via upward ($\mathscr{E} \rightarrow \mathscr{C}$) transitions. This block $\mathscr{E}$ lies intermediate between the reactant and product blocks $\mathscr{C}$ and $\mathscr{S}$ which are separately characterized by $P_i^S = 0$ and $P_i^S = 1$, respectively.

In this paper such a method is proposed and is then applied as a case study to the well-developed example[6] of termolecular ion–ion recombination (1.1) in a low density gas M. Connection is then made with the principle of least

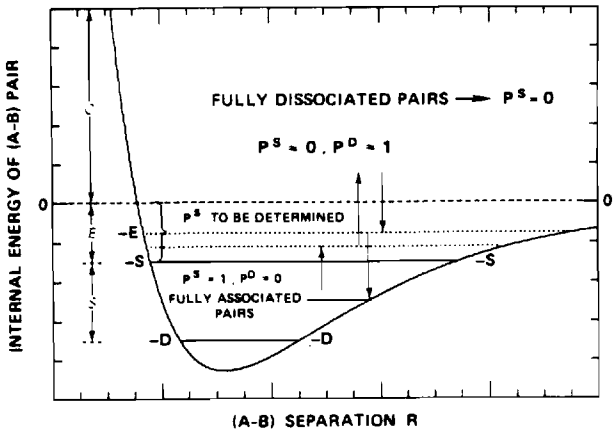

FIG. 1. Schematic diagram of energy blocks $\mathscr{C}$, $\mathscr{E}$, and $\mathscr{S}$ pertinent to recombination at low gas densities.

 0021-9606/88/130214-09$02.10

dissipation, well known in heat-conduction problems and in electrical networks. By analogy with this principle for a network of resistors, Bates[7] very perceptively postulated that a minimum would exist, with respect to variation in the normalized time-independent distributions $\gamma_i(E_i) = n_i/\tilde{n}_i$, in the time-independent measure:

$$\mathscr{M} = \int_{-D}^{\infty} dE_i \int_{-D}^{\infty} (\gamma_f - \gamma_i)^2 C_{if}\, dE_f \tag{1.3}$$

of the total rate of restoration to thermal equilibrium. Mendaš[8] then noted that minimum $\mathscr{M}$ is obtained for a quasi-steady-state distribution of excited levels determined by

$$\gamma_i \int_{-D}^{\infty} C_{if}\, dE_f = \int_{-D}^{\infty} \gamma_f C_{if}\, dE_f . \tag{1.4}$$

The present formulation permits the identification of this $\mathscr{M}$ so minimized with twice the actual (quasi-steady-state) rate constant

$$\alpha \tilde{N}_A \tilde{N}_B = \int_{-E}^{\infty} dE_i \int_{-D}^{-E} (\gamma_i - \gamma_f) C_{if}\, dE_f \tag{1.5}$$

which is the net downward constant energy-space current across any level $-E$, in the block $\mathscr{E}$ of excited levels in quasi-steady-state. A supplementary calculation of Eq. (1.5) with the variational result of Eq. (1.3) is then not required. Note that the upper bound [Eq. (1.2)] is recovered upon eliminating block $\mathscr{E}$ by assigning $\gamma_i(-E \leqslant E_i \leqslant \infty) = 1$ and $\gamma_f(-E \geqslant E_f \geqslant -D) = 0$ in either Eq. (1.3) or Eq. (1.5).

II. VARIATIONAL PRINCIPLE

The net rate for termolecular association

$$A + B + M \underset{k}{\overset{\alpha}{\rightleftarrows}} AB + M \tag{2.1}$$

between A and B in a gas M is[9]

$$R^{A}(t) = \int_{-D}^{\infty} P_i^S \left(\frac{dn_i}{dt}\right) dE_i \tag{2.2}$$

$$= \alpha N_A(t) N_B(t) - k n_s(t) , \tag{2.3}$$

where P_i^S is the stochastic probability that a pair AB with internal relative energy E_i is connected via a series of energy (state)-changing collisions to a sink $\mathscr{S}$ of fully associated AB pairs. The concentration $n_i(t)$ of AB pairs with internal energy E_i of relative motion in unit interval dE_i about E_i develops in time t according to the standard Master equation[9]

$$\frac{dn_i}{dt} = -\int_{-D}^{\infty} [n_i(t)\nu_{if} - n_f(t)\nu_{fi}]\, dE_f = -\frac{\partial J_i}{\partial E_i} , \tag{2.4}$$

where $-D$ is the energy of the lowest vibrational level of AB relative to the dissociation limit taken as zero energy.

The frequency per unit interval dE_f for $E_i \to E_f$ transitions in AB by collision with gas species M is ν_{if} which is linear in gas density N. At low gas densities, R^A is linear in N so that P_i^S is then only required to zero order in N. Over the range $0 \leqslant E_i \leqslant \infty$ which defines the $\mathscr{C}$ block of fully dissociated reactant states, n_i at low N can then be taken in the collisional part of Eq. (2.4) as its thermodynamic equilibrium value $\tilde{n}_i$, so that $P_i^S \approx 0$ for block $\mathscr{C}$. The effective two-body rate constant for the association of A and B with (cm^{-3}) concentrations $N_A(t)$ and $N_B(t)$ at time t is α ($cm^3\,s^{-1}$). The constant $k(s^{-1})$ is the frequency for dissociation of the tightly bound pairs in the product block $\mathscr{S}$ of levels with energies E_i in the range $-S \geqslant E_i \geqslant -D$, within which the stabilization probability P_i^S is unity. In the intermediate block $\mathscr{E}$ of "reacting" states with $0 \geqslant E_i \geqslant -S$ in Fig. 1, the probabilities P_i^S must be determined. The net rate for termolecular dissociation in the closed system is

$$R^{D}(t) = \int_{-D}^{\infty} P_i^D \left(\frac{dn_i}{dt}\right) dE_i = -R^{A}(t) , \tag{2.5}$$

where $P_i^D = 1 - P_i^S$ is the probability that state i is collisionally connected to fully dissociated channels (at infinite A–B separation).

The proposed variational principle now asserts that the probabilities $P_i^{S,D}$ and densities n_i have energy distributions which ensure that $R^{A,D}(t)$ of Eqs. (2.2) and (2.5) are extrema at time t.

A. The quasi-steady-state deduction

Rewrite Eq. (2.2) as

$$R^{A}(t) = -\int_{-D}^{\infty} P_i^S \left(\frac{\partial J_i}{\partial E_i}\right) dE_i \tag{2.6}$$

in terms of the net downward collisional current

$$-J(E,t) = \int_{E}^{\infty} dE_i \int_{-D}^{E} [n_i(t)\nu_{if} - n_f(t)\nu_{fi}]\, dE_f \tag{2.7}$$

past level E. Since J_i vanishes as E_i tends to both $-D$ and ∞, the rate is then

$$R^{A}(t) = \int_{-D}^{\infty} J_i(E,t) \left(\frac{dP_i^S}{dE_i}\right) dE_i . \tag{2.8}$$

Since P_i^S is constant (0 and 1 in blocks $\mathscr{E}$ and $\mathscr{S}$, respectively), Eq. (2.8) further reduces to

$$R^{A}(t) = \int_{-S}^{0} J_i(E,t) \left(\frac{dP_i^S}{dE_i}\right) dE_i . \tag{2.9}$$

A necessary condition for the integral

$$I = \int_{x_1}^{x_2} F[\mathbf{y}(x), \dot{\mathbf{y}}(x); x]\, dx, \quad \dot{\mathbf{y}} = d\mathbf{y}/dx \tag{2.10}$$

to exhibit an extremum is given in the calculus of variations by the Euler–Lagrange equation[10]

$$\frac{d}{dx}\left(\frac{\partial F}{\partial \dot{y}_i}\right) - \frac{\partial F}{\partial y_i} = 0, \quad i = 1,2,\ldots,N , \tag{2.11}$$

the solution of which determines $\mathbf{y}(x) \equiv [y_i(x)]$ over the fixed range $x_1 \leqslant x \leqslant x_2$. Write $x \equiv E_i$, $y_i \equiv P_i^S$ and $F(\dot{\mathbf{y}}(x); x) \equiv J(E_i)\,(dP_i^S/dE_i)$. The integral (2.9) is then an extremum provided

$$\frac{\partial J_i}{\partial E_i} = 0 = -\frac{dn_i}{dt}, \quad 0 \geqslant E_i \geqslant -S \tag{2.12}$$

for each level i within block $\mathscr{E}$. This is the quasi-steady-state (QSS) condition for pairs in block $\mathscr{E}$ with $n_i(t)$ distributed so that J, the current (2.7), is constant over all energies $(-E)$ of block $\mathscr{E}$. The extremum rate, obtained from Eq. (2.12) in Eq. (2.9), is then the net downward current across bound level $-E$ of block $\mathscr{E}$:

$$R^{A}_{*}(t) = -J(-E,t) = \int_{-E}^{\infty} dE_i \times \int_{-D}^{-E} [n_i(t)\nu_{if} - n_f(t)\nu_{fi}]\, dE_f , \quad (2.13)$$

which depends on the probabilities P_i^S only implicitly via n_i. As E tends from above to the dissociation limit at $E=0$, $-J(E,t)$ increases monotonically to this rate.[5]

B. Analysis

From Eq. (2.4) the distribution

$$\gamma_i(t) = n_i(E_i,t)/\tilde{n}_i(E_i) \quad (2.14)$$

normalized to the distribution $\tilde{n}_i$ for full thermodynamic equilibrium satisfies

$$\frac{dn_i}{dt} = \tilde{n}_i \frac{d\gamma_i}{dt} = -\int_{-D}^{\infty} [\gamma_i(t) - \gamma_f(t)]\, C_{if}\, dE_f , \quad (2.15)$$

where the one-way equilibrium rate

$$C_{if} = \tilde{n}_i\, \nu_{if} = \tilde{n}_f\, \nu_{fi} = C_{fi} \quad (2.16)$$

satisfies detailed balance and is linear in gas density N. On introducing the implicit dependence of n_i on the probabilities $P_i^{S,D}$ via the separation[9]

$$\gamma_i(t) = P_i^D \gamma_c(t) + P_i^S \gamma_s(t) , \quad (2.17)$$

where

$$\gamma_c(t) = n_c(t)/\tilde{n}_c = N_A(t) N_B(t)/\tilde{N}_A\, \tilde{N}_B \quad (2.18a)$$

and

$$\gamma_s(t) = n_s(t)/\tilde{n}_s \quad (2.18b)$$

are the respective concentrations $n_c(t)$ and $n_s(t)$ of fully dissociated pairs with energies E_i in the range $0 \leqslant E_i \leqslant \infty$ of block $\mathscr{C}$ and of fully associated pairs of block $\mathscr{S}$ normalized to their respective equilibrium concentrations $\tilde{n}_c$ and $\tilde{n}_s$, then Eq. (2.15) separates as[9]

$$\frac{dn_i}{dt} = [\gamma_c(t) - \gamma_s(t)] \times \int_{-D}^{\infty} (P_i^S - P_f^S) C_{if}\, dE_f = -\frac{\partial J_i}{\partial E_i} . \quad (2.19)$$

Hence the macroscopic rate (2.3) is now

$$R^{A}(t) = \alpha \tilde{N}_A\, \tilde{N}_B\, [\gamma_c(t) - \gamma_s(t)] = -R^{D}(t) , \quad (2.20)$$

where the association rate in units of the time-dependent difference $(\gamma_c - \gamma_s)$ is the rate constant

$$\alpha \tilde{N}_A\, \tilde{N}_B = k\tilde{n}_s , \quad (2.21a)$$

$$= \int_{-D}^{\infty} P_i^S\, dE_i \int_{-D}^{\infty} (P_i^S - P_f^S)\, C_{if}\, dE_f , \quad (2.21b)$$

$$= \frac{1}{2} \int_{-D}^{\infty} dE_i \int_{-D}^{\infty} (P_i^S - P_f^S)^2\, C_{if}\, dE_f \quad (2.21c)$$

which is now time independent and is always positive. The upward current J past energy E in Eq. (2.19) separates similarly as[9]

$$J(E,t) = [\gamma_c(t) - \gamma_s(t)]\, j(E) , \quad (2.22)$$

where

$$j(E) = \int_{E}^{\infty} dE_i \int_{-D}^{E} (P_i^S - P_f^S)\, C_{if}\, dE_f . \quad (2.23)$$

Since Eq. (2.20) is an extremum provided the QSS condition (2.12) holds, i.e., Eq. (2.19) vanishes in block $\mathscr{E}$ where Eq. (2.23) is constant, then the probabilities P_i^S satisfy the standard integral equation[9]

$$P_i^S \int_{-D}^{\infty} C_{if}\, dE_f = \int_{-D}^{\infty} C_{if}\, P_f^S\, dE_f . \quad (2.24)$$

When inserted in Eq. (2.21) the solutions P_i^S yield after some reduction the extremum rate constant,

$$R_{*} = \alpha_{*}\, \tilde{N}_A\, \tilde{N}_B = \int_{-E}^{\infty} dE_i \int_{-D}^{-E} (P_f^S - P_i^S)\, C_{if}\, dE_f , \quad (2.25a)$$

$$= \int_{0}^{\infty} dE_i \int_{-D}^{0} C_{if}\, P_f^S\, dE_f , \quad (2.25b)$$

$$= \int_{-S}^{\infty} dE_f \int_{-D}^{S} C_{if}\, P_f^D\, dE_i , \quad (2.25c)$$

where $-E$ is any level in block $\mathscr{E}$, including the $\mathscr{C}$–$\mathscr{E}$ and $\mathscr{E}$–$\mathscr{S}$ boundaries at 0 and $-S$, respectively. This extremum simply confirms the identification in Eq. (2.13) of rate with current. The nature (maximum or minimum) of the extremum becomes apparent on performing independent variations δP_i^S to P_i^S for each level in block $\mathscr{E}$ subject to the constraints

$$P_i^S = 0; \quad 0 < E_i < \infty , \quad (2.26)$$
$$= 1; \quad -D < E_i < -S ,$$

associated with blocks $\mathscr{C}$ and $\mathscr{S}$, respectively. The resulting change in Eq. (2.20) is

$$\delta R^{A}(t) = 2[\gamma_c(t) - \gamma_s(t)] \times \left[\int_{-S}^{0} dE_i\, \delta P_i^S \left\{ \int_{-D}^{\infty} (P_i^S - P_f^S)\, C_{if}\, dE_f \right\} + \frac{1}{4} \int_{-D}^{\infty} dE_i \int_{-D}^{\infty} (\delta P_i^S - \delta P_f^S)^2\, C_{if}\, dE_f \right] \quad (2.27)$$

to second order in δP_i^S. For an extremum the change δR^{A} to first order in δP_i^S vanishes so that Eq. (2.24) is recovered from Eq. (2.27). The change to second order in δP_i^S is determined by the sign of $(\gamma_c - \gamma_s)$. When $\gamma_c(t) > \gamma_s(t)$ so that the overall direction, according to Eq. (2.20), is association, then the extremum to R^{A} is a minimum; and the dissociation rate R^{D} in Eq. (2.20) is a negative maximum. When $\gamma_s(t) > \gamma_c(t)$ so that the overall direction is dissociation, then R^{A} is a negative maximum; and R^{D} is a minimum. The proposed variational principle governing Eqs. (2.2) and (2.5) thus asserts that the rate R^{A} or R^{D}, whichever corresponds to the overall direction, always adjusts itself to a min-

imum, i.e., the probabilities P_i^S are so distributed that they tend to counteract the change so as to impede the progress towards full equilibrium (when $\gamma_c \to \gamma_s \to 1$). The rate R_* in Eq. (2.25) is a minimum to Eq. (2.21).

Rather than inserting the numerical solution of the QSS integral equation (2.23) in Eq. (2.25a) for the rate constant, an alternative procedure is therefore a direct search of a minimum in the rate (2.21) with respect to variation of P_i^S, a procedure similar to that noted by Mendaš with respect to variation of Eq. (1.3) with respect to γ_i. The present variational principle however provides a variational expression (2.21) for the actual QSS rate (2.25) obtained otherwise from the Master equation.

Although the present analysis has been developed with termolecular ion–ion recombination (1.1) in mind, it may be easily generalized to include ion–atom association

$$A^+ + B + M \to AB^+ + M \tag{2.28}$$

between atomic species in a low density gas M. Here quasi-bound levels (E_i, L_i^2) of AB^+ can be formed with $E_i > 0$ within the centrifugal barrier associated with internal relative angular momentum (squared) L_i^2. By adopting the ansatz [Eq. (5.2) of Ref. 5] for the distribution $n_i(E_i, L_i^2)$ of AB^+ pairs in terms of the stabilization probability $P_i^S(E_i, L_i^2)$ then expression (2.21), generalized to include relevant integrations over L_i^2 and L_f^2, is varied with respect to $P_i^S(E_i, L_i^2)$ so as to provide a minimum which is then the required QSS rate.

C. Application to termolecular recombination

Since dP_i^S/dE_i tends to zero as $E_i \to 0$ and as $E_i \to -S$ (taken now to be $-\infty$), the simplest one-parameter (λ^*) trial function is provided by

$$\frac{dP^S(\lambda;\lambda^*)}{d\lambda} = A\lambda\, e^{-(\lambda/\lambda^*)}, \tag{2.29}$$

where $\lambda = -E_i/kT$ is the binding energy in units of kT, the mean energy of the gas M, and where the variational parameter λ^* is the location of the maximum at $\lambda = \lambda^*$ of Eq. (2.29). Since $P(\infty)$–$P(0)$ is unity, then integration yields the normalization parameter A to be $(1/\lambda^*)^2$ and

$$P^S(\lambda;\lambda^*) = 1-(1+x)\exp(-x); x = \lambda/\lambda^*. \tag{2.30}$$

Consider, as a case study, the well-developed example of termolecular ion–ion recombination[6]

$$X^+ + X^- + X \to X_2 + X \tag{2.31}$$

between equal mass species. Necessary integrations of Eq. (2.21) and solution[6] of the integral equation (2.24) are performed by choosing 72 pivots each in blocks $\mathscr{C}$ and $\mathscr{E}$ according to the procedure outlined in Ref. 11. When Eq. (2.30) is inserted into Eq. (2.21) and when λ^* is varied, the long-dashed curve in Fig. 2 is obtained for the ratio

$$r = R(\lambda = \lambda^*)/R_*, \tag{2.32}$$

where R_* is the exact QSS rate (2.25) determined from the direct solution[6] of Eq. (2.24). Not only does the single parameter $\lambda^* = 1.1624$ provide a minimum to R but it also yields the exact result to 1% accuracy with $r = 1.011$. Introduction of a more sophisticated three parameter (λ^*, a, b) trial function

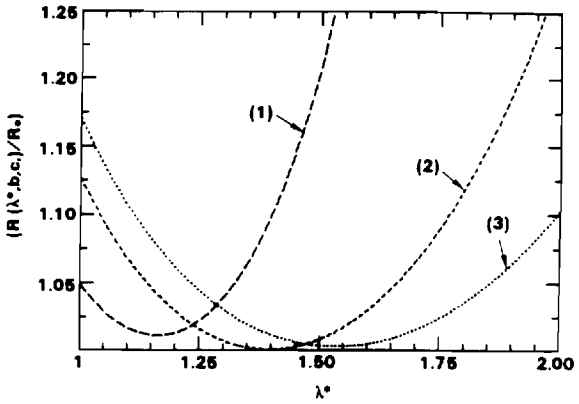

FIG. 2. Ratio of the variational rate (2.21) to the exact QSS rate (2.25) as a function of variational parameter λ^*. (1): One parameter function (2.30). (2) and (3): Two- and three-parameter functions (2.35) with $a = 1, b = 0$ and $a = 1, b = 0.7$, respectively.

$$dP^S(\lambda;\lambda^*,a,b)/d\lambda = A\lambda(1 + a\lambda + b\lambda^2)e^{-\lambda/\Lambda_*}, \tag{2.33}$$

where, in terms of the location at λ^* of the maximum to Eq. (2.33), Λ_* is the function

$$\Lambda(\lambda,a,b) = \lambda(1 + a\lambda + b\lambda^2)/(1 + 2a\lambda + 3b\lambda^2) \tag{2.34}$$

evaluated at $\lambda = \lambda^*$.

Integration of Eq. (2.33) subject to the constraints Eq. (2.26) determines the normalization factor A and yields

$$P^S(\lambda;\lambda^*,a,b) = 1 - [1 + x + x^2 g(x)^2]\exp(-x);$$
$$x = \lambda/\Lambda_*, \tag{2.35}$$

where

$$g(x;\Lambda_*,a,b) = \Lambda_*(a + 3b\Lambda_* + b\Lambda_* x)/$$
$$(1 + 2a\Lambda_* + 6b\Lambda_*^2). \tag{2.36}$$

The derivative is

$$\frac{dP^S(\lambda;\Lambda_*,a,b)}{d\lambda} = [(x + a\Lambda_* x^2 + b\Lambda_*^2 x^3)/$$
$$(1 + 2a\Lambda_* + 6b\Lambda_*^2)]\exp(-x). \tag{2.37}$$

Figure 2 illustrates that minima $r = 1.0008$ and $r = 1.0029$ are obtained for two-parameter ($\lambda^* = 1.3962$, $a = 1.0, b = 0$) and three-parameter ($\lambda^* = 1.5348, a = 1.0$, $b = 0.7$) trial functions, respectively, and that these minima agree with the calculation of the exact QSS rate (2.25). Comparison of the corresponding probabilities for all three variational cases with the exact QSS solution[6] of Eq. (2.24) is given in Fig. 3(a). The two-parameter function is graphically indistinguishable from the numerical QSS solution in Fig. 3(a). The agreement is in general very good for such simple variational functions, and could be easily improved at larger λ by insisting that $P_i^S \to 1$ as $E_i \to -S \approx -(10\text{–}20)\,kT$ rather than as $E_i \to -\infty$ in Eq. (2.35). Although the two-parameter function provides a slightly better representation we note from Fig. 2 that the rate (2.21) is not overly sensitive to the ..nall deviations in the probabilities.

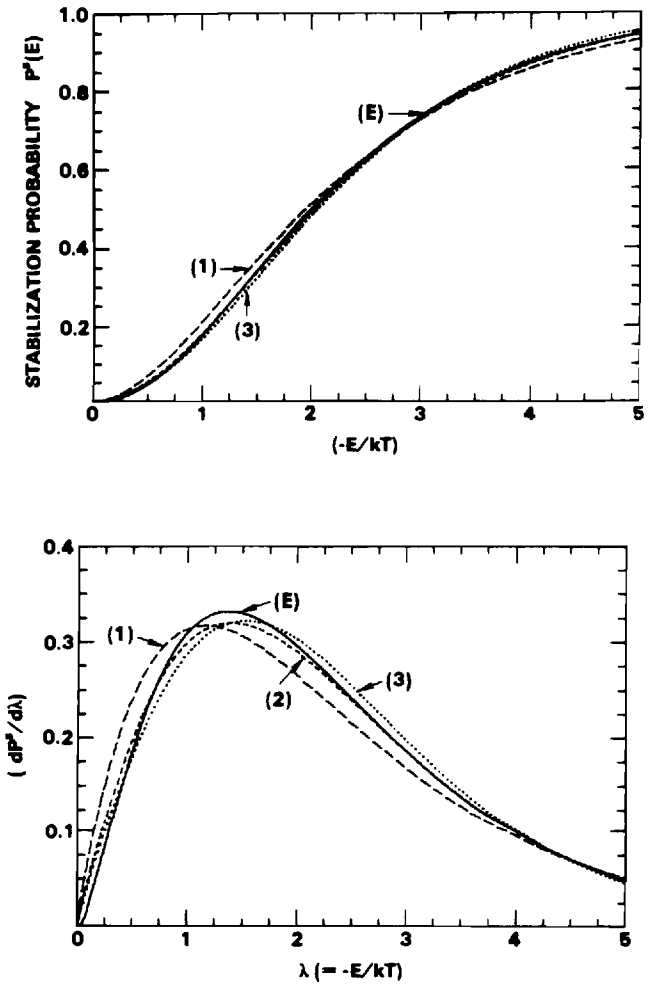

FIG. 3. (a) Variational probabilities (2.35), (1), (2), and (3) as a function of normalized bound energy $(-E/kT)$. Parameters (λ^*,a,b) given by (1.1624,0,0), (1.3962,1,0), and (1.5348,1,0.7), respectively. Exact QSS probability (2.24):(E). (b) Corresponding derivatives.

A more sensitive test[5] is provided in Fig. 3(b) which displays the corresponding comparison of the derivatives. All of these variational curves and the direct QSS solution of Eq. (2.24) display maxima almost equal and located in the same neighborhood. This location has physical significance and is perhaps key to the overall success obtained. This is most easily illustrated by expanding

$$P_f^S = P_i^S + (E_f - E_i)\left[\frac{dP_i^S}{dE_i}\right] + \tfrac{1}{2}(E_f - E_i)^2\left[\frac{d^2P_i^S}{dE_i^2}\right] + \cdots \tag{2.38}$$

in powers of the energy difference $(E_f - E_i)$ so that Eq. (2.19) yields

$$-[\gamma_c(t) - \gamma_s(t)]^{-1}\frac{dn_i}{dt} = D_i^{(1)}\left[\frac{dP_i^S}{dE_i}\right] + D_i^{(2)}\left[\frac{d^2P_i^S}{dE_i^2}\right] \tag{2.39}$$

to second order in the energy-change moments[5]

$$D_i^{(m)}(E_i) = \frac{1}{m!}\int_{-D}^{\infty}(E_f - E_i)^m C_{if}\, dE_f . \tag{2.40}$$

For QSS of block $\mathscr{E}$,

$$\left(\frac{d^2P_i^S}{dE_i^2}\right)\Big/\left(\frac{dP_i^S}{dE_i}\right) = -D_i^{(1)}/D_i^{(2)} \equiv -\chi_i(E_i) \tag{2.41}$$

so that (dP_i^S/dE_i) exhibits a maximum where $D_i^{(1)}$, the average energy increase per second, passes through zero, which in general occurs[5] at $E_i^* = -(1\text{–}2)\,kT$. The above trial expressions (2.29) and (2.33) therefore implicitly acknowledge the physical tendency for collisions to excite those pairs with $E > E_i^*$ and to degrade those with $E < E_i^*$. Once λ_i^* has been variationally determined by the present procedure, it will only coincide with the actual location of the zero in $D_i^{(1)}$ to the extent that approximation (2.39) is valid. If so the expressions then imply that the ratio (kT) $D_i^{(1)}/D_i^{(2)}$ may be represented quite accurately either by the simple form $(1/\lambda - 1/\lambda^*)$ or by the more complicated form $(1/\Lambda - 1/\Lambda_*$, respectively. Both forms yield zero at $\lambda = \lambda^*$. Interestingly enough, the zero of $D_i^{(1)}$ for symmetrical resonance charge transfer collisions occur at $\lambda_i^* = 1.329$ in close agreement with the two-parameter variational and exact calculations [cf. Fig. 3(b)].

The solution of Eq. (2.41) subject to Eq. (2.26) is

$$P^S(-E) = \left[\int_{-E}^{0} dE_f \exp\left\{\int_{-E_f}^{0}\chi_i\, dE_i\right\}\right] \times\left[\int_{-S}^{0} dE_f \exp\left\{\int_{-E_f}^{0}\chi_i\, dE_i\right\}\right]^{-1} \tag{2.42}$$

in block $\mathscr{E}$. When the approximation[5]

$$D_i^{(1)} = \frac{dD_i^{(2)}}{dE_i} \tag{2.43}$$

between moments $D_i^{(1)}$ and $D_i^{(2)}$ can be invoked, then

$$\exp\left[\int_{-E_f}^{0}\chi_i\, dE_i\right] = D^{(2)}(0)/D^{(2)}(-E_f) \tag{2.44}$$

so that Eq. (2.42) reduces to

$$P_d^S(-E_i) = \left[\int_{-E}^{0} dE_f/D^{(2)}(-E_f)\right] \times\left[\int_{-S}^{0} dE_f/D^{(2)}(-E_f)\right]^{-1} . \tag{2.45}$$

This expression (2.45) has been used in Eq. (2.21c) to provide accurate rates α_D in a previous diffusional treatment.[5] The more basic expression (2.42) is currently being tested.[12]

There are now two accurate treatments which provide accurate *analytical* representations of the collisional stabilization and disruption probabilities—the previous diffusional method[5] and the present (two-parameter) variational method. These results D from Eq. (2.45) and V from Eq. (2.35) are compared in Fig. 4 with the exact numerical solution E of Eq. (2.24). Due to a more accurate evaluation of $D_i^{(1)}$, the present diffusional results differ somewhat from those previously reported.[5] The resulting rates

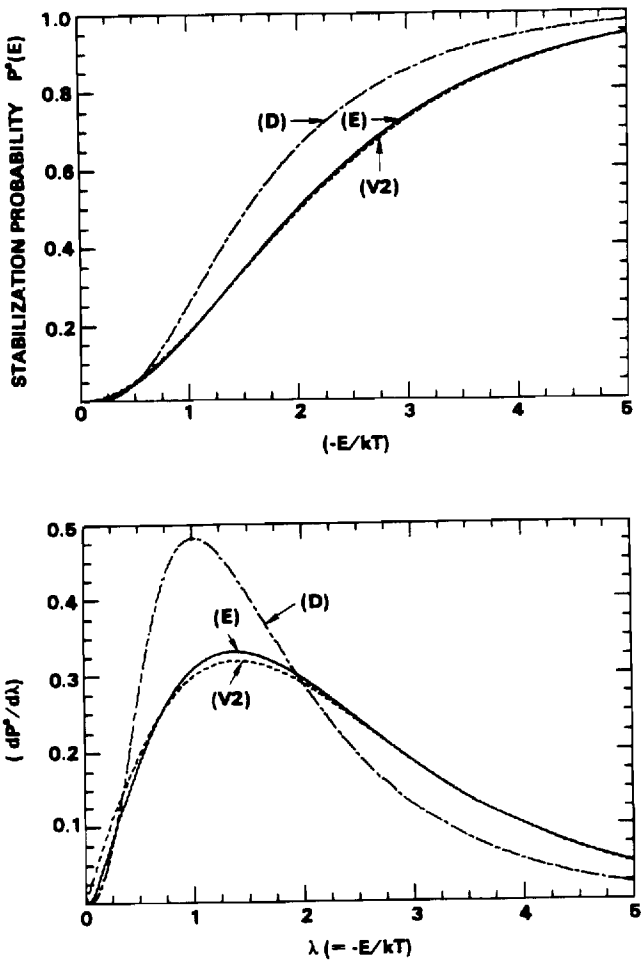

FIG. 4. (a) Probabilities and (b) corresponding derivatives in exact QSS (E), two-parameter ($\lambda^* = 1.3962$, $a = 1$) variational ($V2$), and diffusional (D) treatments, as a function of normalized bound energy ($-E/kT$).

($\alpha_D/\alpha_E = 1.08$, $\alpha_V/\alpha_E = 1$) are not that sensitive, as before, to the larger discrepancies in P_i^S resulting from the diffusional and variational treatments.

III. ANALOGY WITH (R,C) ELECTRICAL CIRCUIT AND WITH PRINCIPLE OF LEAST DISSIPATION

Bates[7] has already provided the interesting analogy with a network of resistors for the case when $\gamma_c(t) = 1 \gg \gamma_s(t)$ so that time dependencies can be omitted,[5] and has introduced the variational function $\mathscr{M}$, Eq. (1.3), as a measure of the restoration rate to thermodynamic equilibrium. Here capacitors are introduced (Sec. III A) so as to explicitly acknowledge time-dependent currents and voltages. The present approach allows us to identify (Sec. III B) the time-independent function $\mathscr{M}$ with $2\alpha\tilde{N}_A\tilde{N}_B$.

The Master equation (2.15) involves the internal energy E_f of relative (A–B) motion as a continuous variable since the spacing between bound levels are much smaller than the thermal energy (kT) of the thermal gas bath M. The discrete representation of Eq. (2.15) gives the net electrical current flowing outward from node i of a multimode system as

$$I_i(t) = -\frac{dn_i}{dt} = \sum_{f=-D}^{\infty} I_{if}(t)\,, \tag{3.1}$$

where the current in the $i \to f$ segment is

$$I_{if}(t) = [\gamma_i(t) - \gamma_f(t)]\, C_{if}\,. \tag{3.2}$$

This reduces under Eq. (2.16) to

$$I_{if}(t) = [\gamma_c(t) - \gamma_s(t)]\,(P_f^S - P_i^S)\, C_{if} \tag{3.3}$$

$$\equiv [\gamma_c(t) - \gamma_s(t)]\, i_{if}\,.$$

The formal structure of Eqs. (3.1) and (3.2) is identical[7] to an electrical network where the current I_{if} along the line element e_{if} from junction i to junction f in the network is equivalent to the time-dependent voltage drop

$$V_{if}(t) = [\gamma_i(t) - \gamma_f(t)] \tag{3.4}$$

$$= [\gamma_c(t) - \gamma_s(t)]\,(P_i^D - P_f^D) \tag{3.5}$$

times the conductivity $C_{if} = R_{if}^{-1}$ of the line element of resistance R_{if}.

Since, Eq. (3.2) is Ohm's law ($V_{if}(t) = I_{if}(t)\, R_{if}$)[7], a time-dependent potential

$$V_i(t) = \gamma_i(t) \tag{3.6}$$

can be associated with any level i. All states within the source block $\mathscr{C}$ are at equipotential $\gamma_c(t)$ and all levels within sink block $\mathscr{S}$ are at equipotential $\gamma_s(t)$. The potential γ_i of each $\mathscr{E}$ level i is below γ_c by an amount

$$V_{ci} = \gamma_c(t) - \gamma_i(t) = P_i^S\,[\gamma_c(t) - \gamma_s(t)] \tag{3.7}$$

or is above γ_s by an amount

$$V_{is} = \gamma_i(t) - \gamma_s(t) = P_i^D\,[\gamma_c(t) - \gamma_s(t)]\,. \tag{3.8}$$

Hence in units of $(\gamma_c - \gamma_s)$, P_i^S is the potential drop from $\mathscr{C}$ to i, P_i^D is the potential height of i above $\mathscr{S}$, and I_{if} is the current Eq. (3.3) along segment e_{if}. Since P_i^D within $\mathscr{E}$ increases with E_i continuously and monotonically from zero within $\mathscr{S}$ to unity within $\mathscr{C}$ then

$$\sum_{e_{if}} V_{if} = [\gamma_c(t) - \gamma_s(t)] \oint_{E_1}^{E_2} \left[\frac{dP_i^D}{dE_i}\right] dE_i = 0\,, \tag{3.9}$$

where the sum is over each segment e_{if} within any closed loop ($E_1 \to E_2 \to E_1$). Equation (3.9) as already noted,[7] is Kirchoff's voltage law (KVL) which is based on the uniqueness of the potential $\gamma_i(t)$ at a given time and which expresses *energy conservation* for any closed loop within the entire ($\mathscr{C}, \mathscr{E}, \mathscr{S}$) circuit at time t.

A. QSS simplification: (R,C) circuit

The QSS condition (2.12) for each level i of block $\mathscr{E}$ ($0 \geqslant E_i \geqslant -S$) is equivalent to

$$I_i(t) = \sum_{f=-D}^{\infty} I_{if}(t) = \sum_{f=-D}^{\infty} [\gamma_i(t) - \gamma_f(t)]\, C_{if} \tag{3.10a}$$

$$\equiv [\gamma_c(t) - \gamma_s(t)] \int_{-D}^{\infty} (P_f^S - P_i^S)\, C_{if}\, dE_f \tag{3.10b}$$

$$= 0, \quad i = 1, 2, N \tag{3.10c}$$

which[7] is Kirchoff's current law (KCL). The balance of currents I_{if} which exits and enters any junction i within block

$\mathscr{C}$ ($1 \leqslant i \leqslant N$) to all junctions ($f = N+1, N+2, \ldots \infty$, in block $\mathscr{C}$, $f = 1,2,\ldots,N$ in block $\mathscr{E}$ and $f = 0, -1, \ldots, -D$ in block $\mathscr{S}$) of the network is zero. This expresses *charge conservation* at junction i where there is no net buildup of density (charge) n_i. The ansatz (2.17) which enables the QSS condition (2.12) to be satisfied by a specified distribution P_i^S at all times provides the separation in Eqs. (3.3), (3.5), and (3.10b).

Under KCL or QSS, the voltages P_i^S satisfy

$$P_i^S \int_{-D}^{\infty} C_{if}\, dE_f = \int_{-D}^{0} C_{if}\, P_f^S\, dE_f . \tag{3.11}$$

The time-dependent $\mathscr{C}$ and $\mathscr{S}$ blocks of states are analogous to capacitors connected in parallel with their positive plates charged to

$$Q_1(t) = n_c(t) = \int_0^{\infty} n_i(t) dE_i \tag{3.12}$$

and

$$Q_2(t) = n_s(t) = \int_{-D}^{-S} n_i(t) dE_i , \tag{3.13}$$

at time t and held at voltages

$$V_1(t) = \gamma_c(t) \tag{3.14}$$

and

$$V_2(t) = \gamma_s(t) \tag{3.15}$$

above their negative plates. Since $Q = C/V$, their capacitances

$$C_1 = \tilde{n}_c = \int_0^{\infty} \tilde{n}_i\, dE_i \tag{3.16}$$

and

$$C_2 = \tilde{n}_s = \int_{-D}^{-S} \tilde{n}_i\, dE_i \tag{3.17}$$

are constant. The external capacitor $C_1 \equiv \mathscr{C}$ is connected to internal KCL node f (or energy level) by equivalent resis-

$$\frac{1}{R_{Cf}} = \sum_{i=N+1}^{\infty} \frac{1}{R_{if}} \equiv \int_0^{\infty} C_{if}\, dE_i = C_{Cf} \tag{3.18}$$

and directly to the external capacitor $C_2 \equiv \mathscr{S}$ by a resistance R_{CS} given by

$$\frac{1}{R_{CS}} = \sum_{i=N+1}^{\infty} \sum_{f=-D}^{0} \frac{1}{R_{if}} \equiv \int_0^{\infty} dE_i \int_{-D}^{-S} C_{if}\, dE_f = C_{CS} . \tag{3.19}$$

Each internal KCL node i of block $\mathscr{E}$ is coupled to internal node f by R_{if} and externally coupled to C_2 via R_{iS} given by

$$\frac{1}{R_{iS}} = \sum_{f=-D}^{0} \frac{1}{R_{if}} \equiv \int_{-D}^{-S} C_{if}\, dE_f = C_{iS} . \tag{3.20}$$

The above resistances R_{Cf}, R_{iS}, and R_{CS} are equivalent to a parallel network of resistances R_{if} connecting, respectively, all states $C(i = N+1, \ldots, \infty)$ of block $\mathscr{C}$ to the specified $\mathscr{E}$-block state f, each $\mathscr{E}$-block state i to all states $S(f = 0, -1, \ldots, -D)$ of block $\mathscr{S}$ and all states C to all states S, respectively. The electrical network which corresponds to the Master equation (3.10) for association is illustrated by Fig. 5. A time-varying current $I(t)$ from capacitor C_1 with initial charge $Q_1(0) = n_c(0)$ is subdivided along mainline channels R_{Cn} to enter a KCL network with N nodes, composed entirely of resistors R_{nj} and internal currents $I_{nj}(t)$, and is then reconstituted at C_2 via mainline exit channels R_{fS}.

B. Principle of least dissipation

The network of resistances R_{CS}, R_{Cf}, R_{iS}, and R_{if} may now be replaced by an equivalent resistance R with throughput current $I(t)$ determined from the power loss

$$I(t)^2 R = [\gamma_c(t) - \gamma_s(t)] I(t) \tag{3.21}$$

$$= \sum_{n=-D}^{\infty} \sum_{f>n}^{\infty} I_{nf}^2 R_{nf} \tag{3.22}$$

to be

$$I(t) \equiv \frac{1}{2} [\gamma_c(t) - \gamma_s(t)] \times \int_{-D}^{\infty} dE_i \int_{-D}^{\infty} (P_i^S - P_f^S)^2\, C_{if}\, dE_f . \tag{3.23}$$

The summations include external junctions $C(n = N+1, N+2, \ldots, \infty)$ and $S(n = -D, -D+1, \ldots, 0)$ at the source and sink capacitors and the internal junctions ($n = 1,2,\ldots,N$). By comparison with Eq. (2.20), the association rate $R^A(t)$ may now be identified with the electrical current $I(t)$ of Eq. (3.23), and the rate constant identified with

$$\alpha \tilde{N}_A\, \tilde{N}_B = \frac{1}{2} \int_{-D}^{\infty} dE_i \int_{-D}^{\infty} (P_i^S - P_f^S)^2\, C_{if}\, dE_f , \tag{3.24}$$

the effective conductivity R^{-1} of the network, or with the time-dependent electrical current $I(t)$, Eq. (3.23), per unit

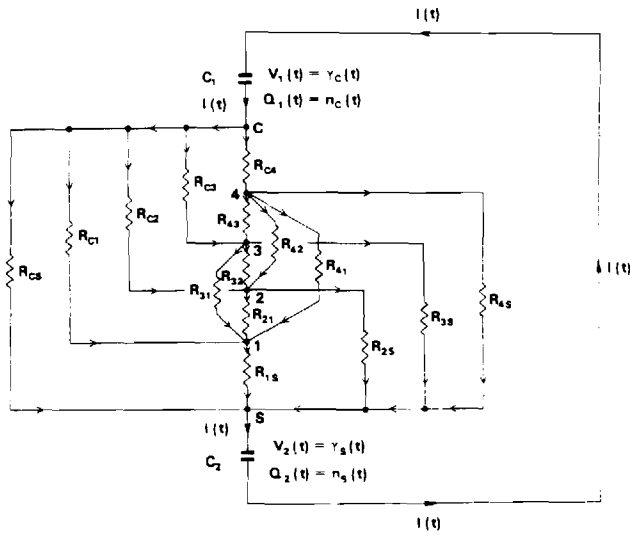

FIG. 5. (R,C) electrical diagram analogous to termolecular recombination.

voltage drop $[\gamma_c(t)-\gamma_s(t)]$. When the KCL condition (3.11) is used directly in Eq. (3.24) then the previous results (2.25) are obtained.

The power loss

$$I^2(t)R=[\gamma_c(t)-\gamma_s(t)]\,R^A(t)\geqslant 0 \tag{3.25}$$

is always positive. The present variational principle (VP) asserts that P_i^S, the voltage drop in units of $(\gamma_c-\gamma_s)$, are so distributed that the rate $R^A(t)$—the electrical current $I(t)$—is a minimum. When $\gamma_c(t)>\gamma_s(t)$, i.e., association occurs at positive rate $R^A(t)$, then VP implies that the power (3.25) dissipated by (A–B) and absorbed by the gas M is least. When R^A is negative, the net direction is dissociation which occurs at rate $R^D(t)=-R^A(t)$ when $\gamma_c<\gamma_s$, then VP implies that the power provided to AB *by* the gas M is least.

This principle of least dissipation is basic in many fields, e.g., thermodynamics, heat conduction, fluid mechanics. The principle for heat conduction was derived explicitly by Onsager.[13] For a current I entering a KVL and a KCL electrical network via R_{Cn} and exiting via R_{nS}, the currents within the KCL network are so distributed that the summed rate of dissipation of energy in the R_{Cn}, R_{nj}, and R_{nS} resistors is a minimum—Joule's law. With this law, Bates[7] postulated that a minimum would exist in the measure $\mathscr{M}$, Eq. (1.3) of the restoration rate of thermodynamic equilibrium by recombination in highly nonequilibrium systems [when $\gamma_c\gg\gamma_s$ and $\gamma_i=P_i^D$ in Eq. (2.17) so that explicit time dependences can be ignored[5]]. Mendaš[8] then noted that the distributions n_i associated with this minimum satisfy the QSS condition (1.4). From Eq. (3.23) it follows that this unnormalized time-independent measure $\mathscr{M}$ may now be uniquely identified as the rate $2\alpha\tilde{N}_A\tilde{N}_B$ so that the minimum of $\mathscr{M}$ yields the minimum rate (2.25a) directly, without the further need for substituting the final variational function $P_i^D=1-P_i^S$ in expression (2.23) for the current (2.25a) or in Eq. (1.5).

The present assertion that the rates (2.2) and (2.5) are extremum implies a principle of least dissipation for chemical reactions. The rates $R^{A,D}(t\to\infty)$ tend naturally to zero when thermodynamic equilibrium is obtained for the complete system. This is analogous to the electrical current I decaying to zero when the voltages across the capacitors C_1 and C_2 connected in series across R become equal.

C. Use of diagram

Various QSS results may be deduced rather readily from consideration of the electrical diagram (Fig. 5).

Result I: The mainline entrance current along R_{Cn} and entering KCL node n is

$$i_n^-=P_n^S\,C_{Cn} \tag{3.26}$$

in units of $(\gamma_c-\gamma_s)$. The total mainline current which enters all N nodes of KCL block $\mathscr{C}$ and node $n=0$ of block $\mathscr{S}$ from block $\mathscr{C}$ is

$$\alpha\tilde{N}_A\tilde{N}_B=\sum_{n=0}^{N}i_n^-\equiv\int_{-D}^{0}C_{Cf}\,P_f^S\,dE_f \tag{3.27}$$

which is the association rate $R^A(t)$ in units of $[\gamma_c(t)-\gamma_s(t)]$ in agreement with Eq. (2.25b).

Result II: The current which exits KCL node n along all the internal resistors R_{nf} and external resistors R_{nS} of Fig. 5 is

$$i_n^+=\sum_{f=0}^{N}(P_n^S-P_f^S)\,C_{nf}\,. \tag{3.28}$$

The total current exiting from all N-KCL nodes is then

$$\sum_{n=1}^{N}i_n^+=\sum_{n=1}^{N}(1-P_n^S)\,C_{ns}\equiv\int_{-S}^{0}C_{Sf}\,P_f^D\,dE_f \tag{3.29}$$

which when combined with the $\mathscr{C}$–$\mathscr{S}$ direct current, $i_0=C_{CS}$ yields

$$k\,\tilde{n}_s=\int_{-S}^{\infty}C_{Sf}\,P_f^D\,dE_f \tag{3.30}$$

in agreement with Eq. (2.25c). The KCL law, $I_n=i_n^+-i_n^-=0$, Eq. (3.10) applied to nodes $n=1,2,\ldots,N$ not only confirms the QSS condition (2.25) but also demands equality of Eqs. (3.27) and (3.30), which provides macroscopic detailed balance.

Result III: From Fig. 5, the total mainline entrance current to nodes below a designated KCL node N^*:

$$i_*^-(\leqslant N^*)=\sum_{n=0}^{N^*}i_n^-\equiv\int_{-D}^{-E}C_{Cf}\,P_f^S\,dE_f\,, \tag{3.31}$$

where the junction N^* is associated with energy level $-E$. The internal and mainline exit currents from nodes above N^* sum to

$$i_*^+(>N^*)=\sum_{n=N^*}^{N}i_n^+=\sum_{n=N^*}^{N}\sum_{f=0}^{N}(P_n^S-P_f^S)\,C_{nf} \tag{3.32}$$

$$\equiv\int_{-E}^{0}dE_i\int_{-D}^{0}(P_f^S-P_i^S)\,C_{if}\,dE_f \tag{3.33}$$

which reduces to

$$i_*^+=\int_{-E}^{0}dE_i\int_{-D}^{-E}(P_f^S-P_i^S)\,C_{if}\,dE_f\,. \tag{3.34}$$

Since $i_n^+=i_n^-$ for each KCL node the total current $(i_*^++i_*^-)$ in units of $[\gamma_c(t)-\gamma_s(t)]$ is

$$\alpha\tilde{N}_A\tilde{N}_B=\int_{-E}^{0}dE_i\int_{-D}^{-E}(P_f^S-P_i^S)\,C_{if}\,dE_f \tag{3.35}$$

in agreement with Eqs. (2.23) and (2.25).

Result IV: When C_1 with charge $Q_1(t)$ gains a charge dQ_1 and C_2 with charge $Q_2(t)$ gains a charge dQ_2 on their positive plates within time dt, the sum of the total electrostatic energy $(V_1dQ_1+V_2dQ_2)$ gained by the capacitors and the thermal energy (3.21) radiated must be zero. Since the charge

$$q_i=n_i(t)=n_i(0),\quad i=1,2,\ldots,N \tag{3.36}$$

at each junction i of the N junction KCL network remains constant then the total charge distributed among the capacitors of initial charges Q_{10} and Q_{20} is

$$Q_1(t)+Q_2(t)=Q_{10}+Q_{20} \tag{3.37}$$

and the discharging/charging current is

$$I=-\frac{dQ_1(t)}{dt}=\frac{dQ_2(t)}{dt}\,. \tag{3.38}$$

Hence the power equation is

$$(V_1 - V_2)\left[\frac{dQ_1}{dt}\right] + I^2R = 0 \tag{3.39}$$

which also follows from application of KVL, Eq. (3.9), to the (C_1,R,C_2) circuit at time t. Hence

$$R^{\mathcal{A}}(t) = -\frac{dQ_1(t)}{dt} = \frac{dQ_2(t)}{dt}$$

$$= \frac{1}{R}\left[Q_1(t)/C_1 - Q_2(t)/C_2\right] \tag{3.40}$$

which is the analog of Eq. (2.20) with $R^{-1} = \alpha\tilde{N}_A\,\tilde{N}_B$, $\gamma_c = Q_1(t)/C_1$, and $\gamma_s = Q_2(t)/C_2$. The equation is linear (rather than quadratic) in Q_1 since Eq. (2.7) renders the basic equation (2.2) linear in the (pair) distribution (3.12) of dissociated species AB. The solution of Eq. (3.40) subject to C_1 being initially uncharged ($Q_{10} = 0$) is

$$Q_1(t) = Q_{20}(C/C_2)[1 - \exp - t/RC\,]$$

$$\overset{t\to\infty}{\to} \frac{C_1}{(C_1 + C_2)}\,Q_{20} \tag{3.41}$$

and

$$Q_2(t) = Q_{20}[1 - (C/C_2)(1 - \exp - t/RC\,)]$$

$$\overset{t\to\infty}{\to} \frac{C_2}{(C_1 + C_2)}\,Q_{20}\,, \tag{3.42}$$

where C is $C_1C_2/(C_1 + C_2)$. As $t\to\infty$, the voltages across each pair of plates, $\gamma_c = Q_1/C_1$ and $\gamma_s = Q_2/C_2$ are equal (and opposite), no current flows and charging is complete (corresponding to thermodynamic equilibrium). When C_1 has infinite capacity for absorbing charge, i.e., when $C_1 \gg C_2$ then $C \to C_2$ so that

$$Q_1(t) \to Q_{20}(1 - \exp - t/RC_2) \tag{3.43}$$

and

$$Q_2(t) \to Q_{20}\exp - t/RC_2\,, \tag{3.44}$$

so that the dissociation frequency k can be related to the time constant for discharging of C_2 and charging of C_1 by

$$k = 1/RC_2 \tag{3.45}$$

as expected (since $C_2 = \tilde{n}_s$ and $1/R = \alpha\tilde{N}_A\,\tilde{N}_B = k\tilde{n}_s$). This rate constant governs only the rate of approach to, but not the magnitude of, the asymptotic limits.

In summary, appeal to the network (Fig. 5) provides results (3.27), (3.30), and (3.35) which are exact under KCL condition (3.11). For voltages which do not satisfy this KCL condition, then Eq. (3.24) is used for the electrical current in units of $(\gamma_c - \gamma_s)$.

IV. SUMMARY

A variational principle based on the search for a minimum to the net rate $R^{\mathcal{A}}(t)$ for association with respect to variation of the stabilization probabilities P_i^S has been proposed. It is capable (Sec. II B) of providing probabilities P_i^S and rate coefficients α identical with those determined from direct QSS solutions of the Master equation. In this sense the developed expression (2.21) provides a variational expression for the QSS approximation. Good trial representations (Sec. II B) for P_i^S exhibit a maximum in $|dP_i^S/dE_i|$ near the location E_i^* of a physical bottleneck.

By introduction of the additional block $\mathscr{E}$ of highly excited levels i sandwiched between the reactant and product zones $\mathscr{C}$ and $\mathscr{S}$, respectively, and characterized by forward and reverse (variational) probabilities P_i^S and P_i^D, respectively, the present variational method is more detailed and complete than the least-upper-bound variational method of Wigner[1] and Keck[2] which ignores this block.

The minimum with respect to variation in n_i of function (1.3) postulated by Bates[7] via analogy with an electrical network is identified here with $2\alpha\tilde{N}_A\,\tilde{N}_B$ so that the supplementary explicit calculation of the rate (1.5) is not required. Electrical diagrams (as Fig. 5) may be utilized very effectively not only to analyze (Sec. III C) the detailed dynamics of termolecular processes but also to facilitate the ready construction of various simplified approximate schemes.[14]

ACKNOWLEDGMENT

This research is supported by the U. S. Air Force Office of Scientific Research under Grant No. AFOSR-84-0233.

[1] E. P. Wigner, J. Chem. Phys. **5**, 720 (1937).
[2] J. C. Keck, J. Chem. Phys. **32**, 1035 (1960).
[3] S. Byron, R. C. Stabler, and P. I. Bortz, Phys. Rev. Lett. **8**, 376 (1962).
[4] B. Makin and J. C. Keck, Phys. Rev. Lett. **11**, 281 (1963).
[5] M. R. Flannery, J. Chem. Phys. **87**, 6947 (1987).
[6] M. R. Flannery and E. J. Mansky, J. Chem. Phys. **88**, 4228 (1988), and Refs. 1–3 therein.
[7] D. R. Bates, Proc. R. Soc. London. Ser. A **337**, 15 (1974).
[8] I. Mendaš, J. Phys. B **12**, L209 (1979).
[9] M. R. Flannery, J. Phys. B **18**, L839 (1985).
[10] See, for example, G. Arfken, *Mathematical Methods for Physicists*, 3rd ed. (Academic, New York, 1985), p. 937.
[11] D. R. Bates and I. Mendaš, J. Phys. B **15**, 1949 (1982).
[12] M. R. Flannery and E. J. Mansky (work in progress).
[13] L. Onsager, Phys. Rev. **37**, 405 (1931).
[14] M. R. Flannery and E. J. Mansky, J. Chem. Phys. (to be published).

Appendix C

"Termolecular Recombination: Coupled nearest-neighbor limit and uncoupled intermediate levels limit"

by

M. R. Flannery and E. J. Mansky

(J. Chem. Phys. 89, 4086-4091 (1988))

Termolecular recombination: Coupled nearest-neighbor limit and uncoupled intermediate levels limit

M. R. Flannery and E. J. Mansky
School of Physics, Georgia Institute of Technology, Atlanta, Georgia 30332

(Received 18 April 1988; accepted 15 June 1988)

Two extreme limits of collisional coupling in termolecular recombination are investigated. The coupled nearest neighbor (CNN) limit includes only couplings between neighboring excited energy levels of the associating species AB*, while the uncoupled intermediate levels (UIL) limit includes only couplings between the fully dissociated reactants A^+ and B^- and each of the (assumed uncoupled) excited levels of AB*, which are then coupled to the fully associated products AB. Comparison is made with results of previous exact and diffusion treatments.

I. INTRODUCTION

Analogy with a mathematically equivalent electrical network provides an effective framework whereby not only can the complicated multilevel collisional dynamics intrinsic to a master equation treatment of termolecular recombination

$$A^+ + B^- + M \rightarrow AB + M \qquad (1.1)$$

between atomic species A^+ and B^- in a gas M be analyzed in a different light[1,2] but also physically appealing models may be readily constructed. In previous reports,[2-4] the (exact) quasi-steady-state (QSS) master equation method,[3] the corresponding variational method,[2] and an approximate diffusional method[4] were considered. In this paper, two simple models prompted by considering the analogous electrical diagram (Fig. 1)are investigated. So as to emphasize the importance of collisional couplings between many excited levels in a realistic treatment of process (1.1), two extreme limits will be tested. The *coupled nearest-neighbor limit* includes only the coupling of a given excited level n with its lower neighboring level $n-1$. The limit of *uncoupled intermediate levels* includes only couplings from the (external) source block $\mathscr{C}$ of fully dissociated states of the reactants A^+ and B^- to each of the excited levels n assumed to be *uncoupled* within the (internal) block $\mathscr{E}$ and then the coupling from each of these uncoupled n to the (external) sink block $\mathscr{S}$ of fully associated levels of the products AB (cf. Fig. 1). The "*intermediate*" levels comprise block $\mathscr{E}$ which is *intermediate* between blocks $\mathscr{C}$ and $\mathscr{S}$.

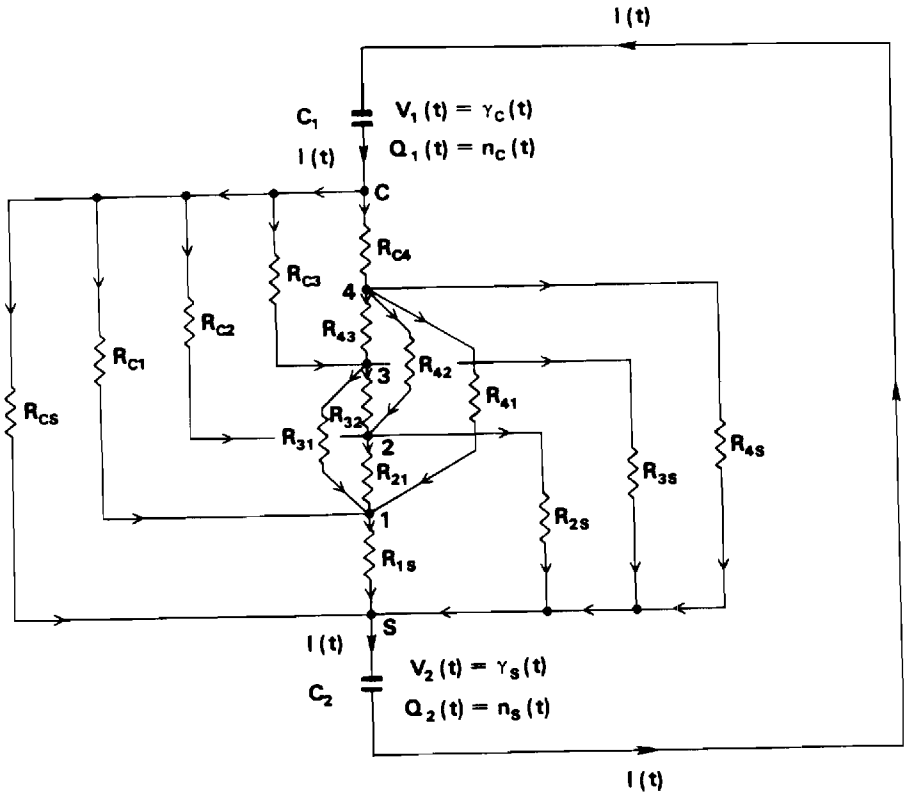

FIG. 1. (R, C) Electrical diagram (Ref. 2) appropriate to analysis of termolecular recombination, involving as an example, four excited levels ($n = 1,2,3,4$).

 0021-9606/88/194086-06$02.10

II. CONSTRUCTION

Termolecular recombination (1.1) may be described[4] via a *time-independent* treatment wherein equilibrium concentrations $\tilde{N}_A$ and $\tilde{N}_B$ of the fully dissociated atomic species A and B with relative energies E_i in the range $0 \leqslant E_i \leqslant \infty$, the reactant $\mathscr{C}$ block, are associated (a) by direct collisions into the product block $\mathscr{S}$ of fully associated molecular levels in the range $-S \geqslant E_i \geqslant -D$ maintained at zero population and (b) by a series of indirect transitions via the intermediate energy block $\mathscr{E}$ $(0 \geqslant E_i \geqslant -S)$ of highly excited levels. The indirect mechanism $\mathscr{C} \rightarrow \mathscr{E} \rightarrow \mathscr{S}$ is the most important[2-4] at thermal energies since the rate of the large energy transfers involved with direct $\mathscr{C} \rightarrow \mathscr{S}$ transitions is vanishingly small, by comparison. The lowest energy level of AB is $-D$, relative to the dissociated limit at zero energy, and $-S$ is a bound level below which the probability P_i^S of collisional stabilization of pairs in level E_i is by definition unity. The two key quantities are P_i^S which is unknown and the one-way equilibrium rate C_{if} which is given[3] in terms of the equilibrium number density of $\tilde{n}_i$ of levels of energy E_i per unit interval dE_i and the frequency ν_{if} for $E_i \rightarrow E_f$ transitions per unit interval dE_f by $\tilde{n}_i\, \nu_{if}$.

A hierarchy of approximate schemes are apparent via consideration[2] of process (1.1) in terms of the analogous electrical diagram displayed in Fig. 1. Here N discrete junctions ($\mathscr{E}$-block levels) n are at time-independent potentials P_n^S *below* the $\mathscr{C}$ block junctions C, all maintained at unit equipotential (due to the assumed equilibrium concentrations of A and B), or equivalently are at potentials $P_n^D = 1 - P_n^S$ *above* the zero potential of the $\mathscr{S}$ block junctions S (due to assumed zero concentration of AB). In terms of these voltages and of the conductances $C_{if} = R_{if}^{-1}$ of each element of resistance R_{if}, the rate constant deduced[2] from the power equation is then the effective conductance R^{-1} of the mathematically equivalent network. It follows from consideration of the power loss in the circuit that[2]

$$\alpha \tilde{N}_A \tilde{N}_B = \frac{1}{2} \int_{-D}^{\infty} dE_i \int_{-D}^{\infty} (P_i^S - P_f^S)^2 C_{if}\, dE_f \equiv R^{-1} . \tag{2.1}$$

Since the overall voltage drop is unity in the time-independent treatment, Eq. (2.1) is also the throughput electrical current. Only when the N nodes i in block $\mathscr{E}$ obey the Kirchoff current law, (KCL), or the following quasi-steady-state (QSS) equivalent condition for excited pairs:

$$P_i^S \int_{-D}^{\infty} C_{if}\, dE_f = \int_{-D}^{0} C_{if} P_f^S\, dE_f \tag{2.2}$$

does Eq. (2.1) reduce to $-j(0)$, the energy-space current

$$\alpha(0) \tilde{N}_A \tilde{N}_B = \int_0^{\infty} dE_i \int_{-D}^{0} C_{if} P_f^S\, dE_f = -j(0) \tag{2.3a}$$

across the dissociation limit at zero internal energy, or in general to

$$\alpha(-E) \tilde{N}_A \tilde{N}_B = \int_{-E}^{\infty} dE_i \int_{-D}^{-E} (P_f^S - P_i^S) C_{if}\, dE_f = -j(-E) , \tag{2.3b}$$

the constant energy-space downward current $-j(-E)$, across any arbitrary level of energy $-E$ in block $\mathscr{E}$. Two extreme limits may now be constructed.

(A) *Uncoupled intermediate levels (UIL) limit*: When the mainline entrance and exit channels of resistances R_{Cn} and R_{nS} defined in terms of collisional couplings by

$$R_{Cn}^{-1} = \int_0^{\infty} C_{in}\, dE_i \equiv C_{Cn} \tag{2.4}$$

and

$$R_{nS}^{-1} = \int_{-D}^{-S} C_{nf}\, dE_f \equiv C_{nS} , \tag{2.5}$$

respectively, are only included in the network for indirect passage between the reactant and product blocks $\mathscr{C}$ and $\mathscr{S}$ via junction n, the current I_n flowing past any of the uncoupled junctions n is given by

$$I_n [R_{Cn} + R_{nS}] = 1 , \tag{2.6}$$

since the voltage drop ($\mathscr{C} \rightarrow \mathscr{S}$) is unity and since n is not coupled to any other junction n' of intermediate block $\mathscr{E}$. The direct ($\mathscr{C} \rightarrow \mathscr{S}$) current

$$I_0 = R_{CS}^{-1} = \int_0^{\infty} dE_i \int_{-D}^{-S} C_{if}\, dE_f \tag{2.7}$$

is normally negligible but can be given by expression (2.6) since R_{fS} vanish for all nodes f in block $\mathscr{S}$. The voltage drop between junctions C and each isolated n is then

$$P_n^S = I_n R_{Cn} = \frac{C_{nS}}{C_{Cn} + C_{nS}} , \tag{2.8}$$

to be used in the basic power expression (2.1) for the rate constant.

Although expression (2.8) violates the KCL condition (2.2) required for reduction of Eq. (2.1) to Eq. (2.3), the QSS rate (2.3a) nonetheless provides the rate

$$\alpha_1(0) \tilde{N}_A \tilde{N}_B = \int_{-D}^{0} \left[\frac{C_{Cf} C_{fS}}{(C_{Cf} + C_{fS})} \right] dE_f \tag{2.9a}$$

$$= \left[\int_{-D}^{0} \alpha_f\, dE_f \right] \tilde{N}_A \tilde{N}_B \tag{2.9b}$$

which has several exemplary features. This rate is also the effective conductance obtained from the total electrical current $\Sigma_{n=0}^{N} I_n$ flowing between nodes C and S maintained at unit potential difference. Although invalid when compared to Eq. (2.8) in Eq. (2.1), expression (2.9) illustrates quite effectively (a) that the partial rate α_f of a reaction which proceeds via the series sequence $\mathscr{C} \rightarrow f$ and $f \rightarrow \mathscr{S}$ of transitions is given by the conductance

$$C_f = R_f^{-1} = [R_{Cf} + R_{fS}]^{-1} = \frac{C_{Cf} C_{fS}}{C_{Cf} + C_{fS}} \tag{2.10}$$

due to resistances R_{Cf} and R_{fS} connected in series and (b) that the overall rate α_1 of the reaction which proceeds via the parallel sequence involving each f is given by the conductance

$$C = R^{-1} = \sum_{f=0}^{N} R_f^{-1} = \sum_{f=0}^{N} C_f \tag{2.11}$$

of the effective network with resistances R_f $(f = 1,2,...,N)$ connected in parallel. The resistance, $R_0 = R_{CS}$, of the $\mathscr{C}$–

$\mathscr{S}$ direct connection is included in Eq. (2.11). Expressions (2.9) provide illustrations of the theorem due to Bates.[1] The approximate QSS rate $\alpha_1(-E)$ as a function of $\mathscr{E}$ block energy $-E$ is obtained by inserting Eq. (2.8) in Eq. (2.3b). The first rate under test is given by the probability (2.8) inserted in the power expression (2.1).

(*B*) *Coupled nearest-neighbor (CNN) limit*: When resistors $R_{n,n-1}$ are only included in block $\mathscr{E}$, the throughput current I is given by

$$I=\left[R_{\mathrm{CN}}+\sum_{n=1}^{N} R_{n,n-1}\right]^{-1}, \tag{2.12}$$

where junctions in block $\mathscr{S}$ are again denoted by $n=0$. As the highest excited bound level $N\to\infty$, R_{CN} vanishes, and the voltage drop between junctions C and f is then

$$P_f^S = I\sum_{n=f+1}^{\infty} R_{n,n-1} = \left[\sum_{n=f+1}^{\infty} C_{n,n-1}^{-1}\right]\left[\sum_{n=1}^{\infty} C_{n,n-1}^{-1}\right]^{-1}, \tag{2.13}$$

which, when inserted in the power equation (2.1) yields the second rate under investigation. A simplified rate given by the effective conductance (or electrical current) in Eq. (2.12) is

$$\alpha_2\tilde{N}_A\tilde{N}_B = R^{-1} = \left[\sum_{n=1}^{\infty} C_{n,n-1}^{-1}\right]^{-1}, \tag{2.14}$$

which again illustrates the reaction-in-series principle of Bates.[1] The approximation (2.14) has been previously obtained for $(e\text{-}A^+)+e$ recombination.[5] In contrast to Eq. (2.9), the result (2.14) cannot be obtained from the energy-space current (2.3a) since connections between C and the various n are ignored.

Note that the key approximations CNN, Eq. (2.13), and UIL, Eq. (2.8), satisfy the correct boundary conditions

$$P_i^S(E_i=0)=0,$$
$$P_i^S(E_i=-S)=1 \tag{2.15}$$

for the probability P_i^S.

III. RESULTS

As a test of the above approximations the case of termolecular ion–ion recombination (1.1) is adopted since the association (exact) rate α_E has been well studied (cf. Ref. 3) over full variation of the mass parameter

$$a=\frac{M_B M_g}{M_A(M_A+M_B+M_g)} \tag{3.1}$$

pertinent to A^+–M collisions and over the following model (A^+–M) interactions: symmetrical resonance charge transfer (CX), polarization attraction (POL), and hard-sphere repulsion (HS). The masses of A^+, B^-, and M are M_A, M_B, and M_g, respectively.

The approximate probabilities labeled UIL and CNN are calculated from the limit (2.8) for uncoupled-intermediate levels and the limit (2.13) for coupled-nearest-neighbor, respectively. They are compared in Fig. 2(a) with the exact quasi-steady-state (QSS) solution of Eq. (2.2). The results, which pertain to termolecular recombination of equal mass species ($a=\frac{1}{3}$) for A^+–M collisions under polarization attraction (POL), are quite representative of other cases. Closer agreement of CNN with the exact results indicates that association tends to proceed via a sequence of small energy-changing transitions down the ladder of intermediate levels n, as expected, rather than via the indirect ($\mathscr{E}\to n\to\mathscr{S}$) larger energy-changing transitions of UIL, which involves each intermediate level n presumed uncoupled from one another. Moreover, both approximations appear robust with respect both to the number N ($=36$ and 72) of intermediate levels n adopted in block $\mathscr{E}$ and to the consequent decrease in spacing between the levels. The N pivots and spacings are selected by the highly accurate method prescribed in Ref. 6.

Since both approximations CNN and UIL are seen to satisfy the correct constraints (2.15), the overall agreement in Fig. 2(a) may however mask certain deficiencies. A more sensitive quantity of greater significance to recombination is the gradient (dP_i/dE_i), since, in the limit of small energy transfers, the energy-space current (2.3b) across $\mathscr{E}$ block level $-E$ reduces[4] to the diffusional current

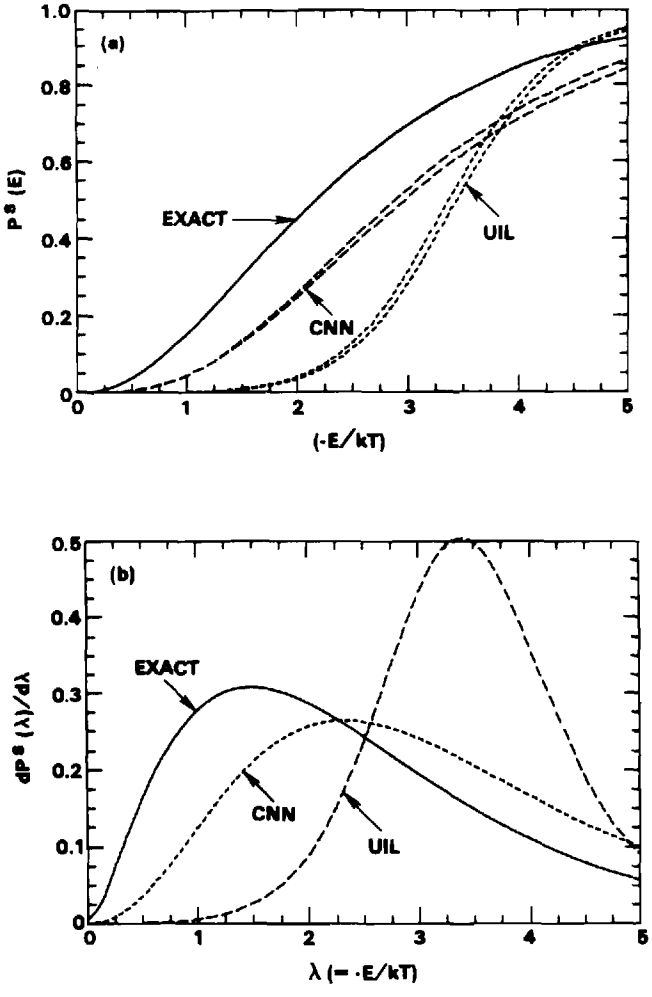

FIG. 2. (a) Stabilization probabilities (voltage drops) as a function of binding energy ($-E/kT$): EXACT [Eq. (2.2)]; CNN [Eq. (2.13)]; and UIL [Eq. (2.8)] with 72 pivots (upper curve) and 36 pivots (lower curve). (b) Corresponding derivatives.

$$j_d(-E) = D_i^{(2)}\left[\frac{dP_i^S}{dE_i}\right], \tag{3.2}$$

where the second-order energy-change moment is

$$D_i^{(2)}(E_i) = \frac{1}{2}\int_{-D}^{\infty}(E_f - E_i)^2 C_{if}\, dE_f . \tag{3.3}$$

The gradients shown in Fig. 2(b) are therefore expected to provide more reliable indicators of the extent of expected agreement between the corresponding rates.

This sensitivity is indeed confirmed in Figs. 3(a) and 3(b) which illustrate the quite different shapes for the variations with E of $-j(-E)$, the downward energy-space current (2.3b), obtained from both approximations. The currents (2.3b) are normalized to the exact QSS rate calculated from the numerical solution of Eq. (2.2) in Eq. (2.3b). Although α_E is then by definition, constant with respect to E variation, the E variation of the rate (2.3b) with the approximate probabilities (2.8) and (2.13) indicates the severe breakdown of QSS, due to the differences displayed in Figs. 2(a) and 2(b). The following points may now be noted.

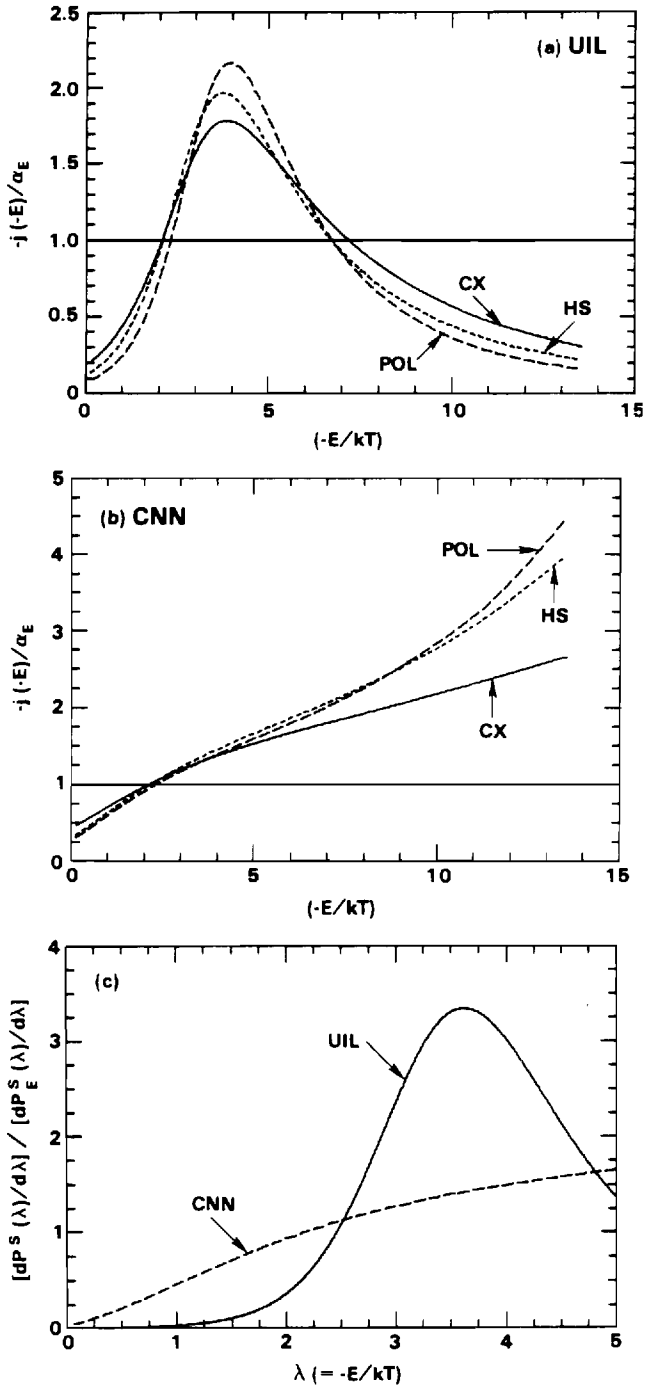

FIG. 3. Energy-space currents (2.3b), normalized to exact QSS rate α_E [Eq. (2.3b) with (2.2)] per unit $\tilde{N}_A\tilde{N}_B$ across bound energies ($-E/kT$): for model A–M interactions POL, HS, and CX. (a) UIL, with Eq. (2.8); (b) CNN, with Eq. (2.13); (c) ratio of approximate to exact derivatives, Eq. (3.4).

First, assigning the rate either at the dissociation limit $E = 0$ (the $\mathscr{C}$–$\mathscr{E}$ interface) or at the lower association limit $-S$ (the $\mathscr{E}$–$\mathscr{S}$ interface) represents a highly inaccurate procedure for the case of non-QSS probabilities, as previously noted[4] for the diffusional results. Choosing the rate at $\sim 2kT$ below the dissociation limit yields the exact QSS rate for both approximations, a coincidence mainly due to the agreement in Fig. 2(b) of the derivatives (dP_i^S/dE_i) at $E_i \sim -2kT$.

Second, the different shape of Fig. 3(a) from that in Fig. 3(b) can be explained with the aid of Fig. 2(b). From Eq. (3.2), the ratio of the downward energy-space current to the exact rate is

$$-j_d^{(A)}(E_i)/\alpha_E \approx \left[\frac{dP^S}{d\lambda}\right]_A \left[\frac{dP^S}{d\lambda}\right]_E^{-1}, \tag{3.4}$$

where A and E label approximate and exact quantities, respectively. As $\lambda = -E_i/kT$ increases to 2, Fig. 3(c) shows that the ratio (3.4) increases to unity for both CNN and UIL. With further increase of λ, the CNN ratio continues to increase while the UIL ratio increases until λ approaches ~ 3.5 and then falls below unity past $\lambda \sim 7$. The different shapes in Figs. 3(a) and 3(b) are a direct reflection of the variation for each approximation of the ratio (3.4) and confirms the physical importance and significance of the gradients (dP_i^S/dE_i).

In spite of its attractive illustrative features, the UIL energy current (2.9) yields rates which are much smaller than α_E by factors ranging from ~ 10 to $\sim 10^4$ as the mass parameter a of Eq. (3.1) varies from (1/3) for equal masses to $10^{\pm 3}$. The simplified CNN result (2.14) varies from a factor of 3 higher for $a = 10^{-2}$, to a factor of 10 smaller at $a = 1/3$, to a factor of 17 higher at $a = 10^3$, the limit for e-ion recombination in a gas.

As previously noted, the power expression (2.1), rather than Eq. (2.3), must be used when approximate (non-QSS) probabilities as Eq. (2.8) and (2.13) are adopted. Since the QSS probabilities provided[2] a minimum α_E to Eq. (2.1), all other approximate rates must be higher than α_E. This is indeed confirmed by Figs. 4(a) and 4(b), which also show that the CNN rates are much closer to α_E than the UIL rates, as expected from the closer gradients in Fig. 2(b). The maximum deviation occurs at $a = 1/3$ where the CNN rates are only $\sim 25\%$ higher than the exact QSS rates α_E. All of the rates are normalized to the Thomson rate $\tilde{\alpha}_T$, as defined in the previous reports.[3,4]

In addition to the exact QSS treatment, there are now three accurate methods available for termolecular rates: (a) the previous variational procedure[2] which provides, in fact, an alternative route to the QSS rates; (b) the previous diffu-

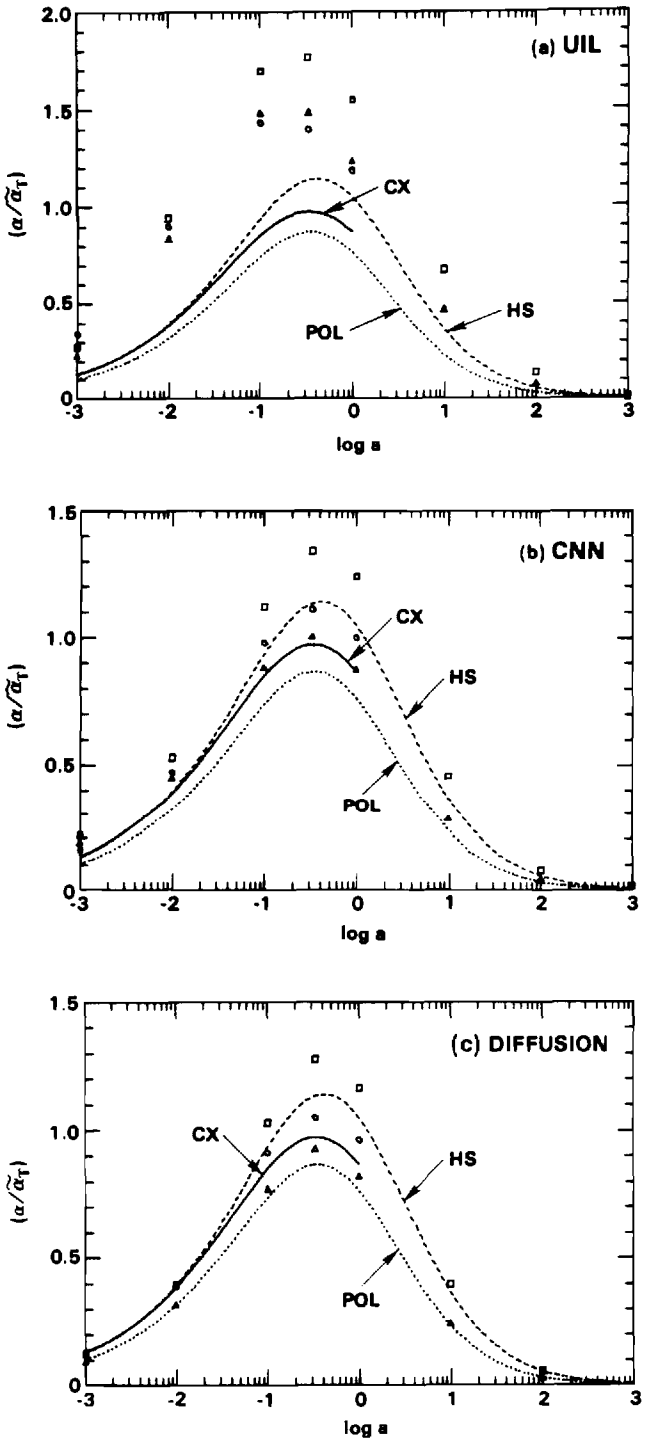

FIG. 4. Normalized partial rates $(M_A/M_{AB})(\tilde{\alpha}/\alpha_T)$ for termolecular recombination $A^+ + B^- + M \rightarrow AB + M$ resulting from $(A^+$–M) collisions as a function of mass parameter a for various model interactions (CX and ○: symmetrical resonance charge transfer; HS and □: hard-sphere; POL and Δ: polarization attraction). (a) UIL, Eq. (2.1) with (2.8); (b) CNN, Eq. (2.1) with Eq. (2.13); (c) diffusion method, Eq. (2.1) with Eq. (3.6).

sional method[4] D; and (c) the present CNN method. Methods CNN and D are in effect similar in spirit in that CNN also includes upward and downward transitions, and also emphasizes the role of small energy changes between neighboring levels. The diffusion method, however, does not impose, as does CNN, an immediate cutoff to transitions which involve larger energy changes. The CNN probability (2.13) relies only on evaluation of the collision kernel $C_{n,n-1}$ via the relation

$$P_n^S = P_{n+1}^S + C_{n+1,n}^{-1}\left[\sum_{n=0}^{\infty} C_{n+1,n}^{-1}\right] \tag{3.5}$$

which is simpler to implement than the diffusion method,[4] for which

$$P_f^S(E_f) = P_i^S(E_i) + \left[\int_{E_i}^{E_f} \frac{dE}{D^{(2)}(E)}\right]\left[\int_{-s}^{0} \frac{dE}{D^{(2)}(E)}\right]^{-1} \tag{3.6}$$

which requires highly accurate[2] evaluation of the energy-change moment $D^{(2)}(E)$ given by Eq. (3.3).

Figure 4(c) shows the rates of the diffusion method obtained from calculations of $D_i^{(2)}$ which are more accurate than those previously determined in Ref. 4. Comparison between Figs. 4(b) and 4(c) indicates that comparable rates are achieved by the diffusion and CNN methods. The more sophisticated diffusion method, however, is, in principle, more accurate in the limits of small and large mass parameters a where the collision dynamics is weak so that the rates are then more sensitive to the stabilization probabilities P_i^S near the dissociation limit. The diffusion method is also more accurate for intermediate $a \sim 1/3$ since the larger energy transfers tend to be more influential and are included. In spite of these shortcomings, the CNN method yields rates, just slightly less good than the diffusion treatment.

IV. SUMMARY AND CONCLUSION

With the aid of an electrical diagram (Fig. 1) two extreme limits of collisional coupling are investigated in order to elucidate the role of various classes of transitions. A given level n is directly coupled only to its neighbor in CNN while, in UIL, each n is assumed coupled only to the fully dissociated and fully associated states of the reactant $\mathscr{E}$ and product $\mathscr{S}$ channels, respectively. The CNN approximation furnishes closer stabilization probabilities P_i^S and association rates α, thereby indicating that recombination tends to proceed more down an energy ladder of coupled levels than by larger energy jumps $\mathscr{E} \rightarrow n \rightarrow \mathscr{S}$ involving each intermediate level n. As in the case for all approximate P_i^S, the power equation (2.1) furnishes[7] the required rate (which is always higher than the exact QSS rate), rather than $j(-E_i)$ the energy-space current (2.3b) which holds[7] only for quasi-steady-state probabilities (2.2). The E_i variation of the energy-space currents $j(-E_i)$ deduced from non-QSS probabilities P_i^S is mainly determined by the derivatives (dP_i^S/dE_i), as in Eq. (3.4). When assessing via comparison with the exact QSS rate the effectiveness of the underlying physical mechanism in each approximate model (CNN, UIL, or diffusion) it is important to use the power expression (2.1). Otherwise, use of Eq. (2.9b), (2.14), or even of the energy-space currents (2.3b) as in Figs. 3(a) and 3(b) can lead to incorrect conclusions regarding the efficacy of the basic physical assumption.

In conclusion, the nearest-neighbor limit CNN appears to be a satisfactory approximation for termolecular ion–ion recombination over the full range of mass parameter and

interactions associated with (A^+–M) collisions. It is similar in spirit to the more sophisticated diffusion method, yields comparable rates, and yet it is much simpler to implement.

ACKNOWLEDGMENT

This research is supported by the U.S. Air Force Office of Scientific Research under Grant No. AFOSR-84-0233.

[1]D. R. Bates, Proc. R. Soc. London Ser. A **337**, 15 (1974).
[2]M. R. Flannery, J. Chem. Phys. **89**, 214 (1988).
[3]M. R. Flannery and E. J. Mansky, J. Chem. Phys. **88**, 4228 (1988).
[4]M. R. Flannery, J. Chem. Phys. **87**, 6947 (1987).
[5]D. R. Bates and A. E. Kingston, Proc. Phys. Soc. **83**, 43 (1964).
[6]D. R. Bates and I. Mendaš, J. Phys. B **5**, 1949 (1982).
[7]M. R. Flannery, J. Phys. B **18**, L839 (1985).

Appendix D

"Diffusional Theory of Termolecular Recombination and association of atomic species in a gas"

by

M. R. Flannery

(J. Chem. Phys. 87, 6947-6956 (1987))

Diffusional theory of termolecular recombination and association of atomic species in a gas

M. R. Flannery
School of Physics, Georgia Institute of Technology, Atlanta, Georgia 30332

(Received 10 June 1987; accepted 10 September 1987)

A diffusional treatment of termolecular association of atomic species A and B in a low density gas is presented and applied to positive ion–negative ion recombination over the full range of masses of reactants for various classes of ion–neutral interactions. In contrast to rates given by the diffusional current, excellent results are obtained for general mass species *provided* a more basic expression for the association rate is introduced.

I. INTRODUCTION

The picture of electron–ion recombination, of termolecular positive ion–negative ion recombination, and of termolecular ion–atom association:

$$\mathrm{A} + \mathrm{B} + \mathrm{M} \underset{k}{\overset{\alpha}{\rightleftharpoons}} \mathrm{AB} + \mathrm{M}, \tag{1.1}$$

involving subsystems (A–B) associating in a thermal bath of dilute gas M as proceeding via diffusion in energy space has stimulated[1–7] a great deal of interest, in principle, valuable to elucidation of the dynamics of association processes and to many examples of decay of laser-produced plasmas, of reaction processes in flames, of shock wave propagation, etc. In a classic paper on electron–ion recombination, Pitaevskii[1] derived a rather elegant analytical expression for the two-body rate coefficient α ($\mathrm{cm^3\ s^{-1}}$) in Eq. (1.1). Because of its inherent simplicity over more sophisticated and therefore time consuming procedures based on a collisional input–output Master equation,[8–12] the result has been applied to heavy-particle recombination[3–5] which proceeds three orders of magnitude faster than collisional electron–ion recombination[1,7] for which the result was originally intended. In spite of its attractive features, the diffusion picture as formulated[1–6] achieved remarkably disappointing results for heavy-particle termolecular ion–ion recombination.[3–6]

Apart from recognition that diffusion methods (based on a Fokker–Planck reduction of the input–output collision integral) are likely to be valid only when the collisional changes in energy are small, the basic intrinsic defect for application of the Pitaevskii expression to general mass sytems remains as yet undetected. Moreover, that a much less sophisticated "bottleneck" model[13] originally designed also for electron–ion recombination achieved much closer agreement[10] with the exact results of the Master equation[8–10] for ion–ion recombination presents a puzzle.

In this paper, the foundation of the diffusion approach as applied to processes (1.1) will be examined and the basic defect in previous applications will become apparent. The proposed theory is valid for termolecular ion–ion recombination[8–11] and ion–atom association[14] at low gas densities and as a case study will be applied here to ion–ion recombination. Association at rate coefficient α ($\mathrm{cm^3\ s^{-1}}$) and dissociation at frequency k ($\mathrm{s^{-1}}$) in Eq. (1.1) are treated in a unified way so that equilibrium can eventually be established.

II. RATES AND CURRENT

The distribution $n_i(E_i,t)$ per unit interval dE_i of pairs AB with internal energy E_i at time t is governed by the collisional input–output Master equation[2,8–11,15]

$$\frac{d}{dt} n_i(E_i,t) = -\int_{-D}^{\infty} S_{if}\, dE_f = -\int_{-D}^{\infty} [n_i(t)\nu_{if} - n_f(t)\nu_{fi}]\, dE_f, \tag{2.1}$$

where $-D$ is the energy of the lowest vibrational level of AB relative to the dissociation limit taken as zero energy, and where ν_{if} is the frequency per unit interval dE_f for $E_i \to E_f$ transitions by collisions between AB and M. For bound states $dn_i/dt = \partial n_i/\partial t$, and for dissociated states $dn_i/dt = (\partial n_i/\partial t + F_i)$ where F_i is the net flux of contracting E_i pairs created with infinite separation. A basic expression for the rate $R^A(t)$ of association has already been derived.[16] In the interests of elucidation and completeness of the present discussion (in Secs. III C and IV) and of direct comparison with the diffusional quasi-steady-state approach, the key steps therein are provided below. The first step involves writing the net rate for association as[16]

$$R^A(t) = \int_{-D}^{\infty} P_i^S \left(\frac{dn_i}{dt}\right) dE_i = \alpha N_A(t) N_B(t) - k n_s(t), \tag{2.2}$$

where P_i^S is the probability of stabilization of E_i pairs by subsequent multicollisions with M. The effective two-body rate constant for the association of A and B with ($\mathrm{cm^{-3}}$) concentrations $N_A(t)$ and $N_B(t)$ is α ($\mathrm{cm^3\ s^{-1}}$), and k ($\mathrm{s^{-1}}$) is the frequency for dissociation of those tightly bound pairs of concentration $n_s(t)$ which are considered to be fully associated with energies E_i within a block of $\mathscr{S}$ of low lying levels in a range $-S \geqslant E_i \geqslant -D$ within which the stabilization probability P_i^S is calculated to be unity.

The separation between the energy levels of AB is sufficiently small compared to the thermal energy (kT) of the gas bath so that the levels form a quasicontinuum. Thus,

$$\frac{d}{dt} n_i(E_i,t) = -\frac{\partial}{\partial E_i} J(E_i,t), \tag{2.3}$$

so that the upward current past level E at time t is

$$J(E,t) = \int_E^\infty dE_i \int_{-D}^{E} S_{fi}(t)\,dE_f, \tag{2.4}$$

since J vanishes at the end points $(-D,\infty)$ and since $S_{if} + S_{fi} = 0$.

On introducing the normalized distribution

$$\gamma_i(t) = n_i(E_i,t)/\tilde{n}_i(E_i), \tag{2.5}$$

where $\tilde{n}_i$ is the pair distribution under full thermodynamic equilibrium with the gas, the Master equation (2.1) is

$$\frac{d}{dt} n_i(E_i,t) = -\int_D^\infty [\gamma_i(t) - \gamma_f(t)]\, C_{if}\, dE_f$$

$$= -\frac{\partial}{\partial E_i} J_i(E_i,t), \tag{2.6}$$

where the one-way equilibrium collisional rate

$$C_{if} = \tilde{n}_i \nu_{if} = \tilde{n}_f \nu_{fi} = C_{fi} \tag{2.7}$$

satisfied detailed balance. The second step is to introduce the ansatz[16]

$$\gamma_i(t) = P_i^D \left[\frac{N_A(t) N_B(t)}{\tilde{N}_A \tilde{N}_B}\right] + P_i^S \left[\frac{n_s(t)}{\tilde{n}_s}\right]$$

$$\equiv P_i^D \gamma_c(t) + P_i^S \gamma_s(t) \overset{t\to\infty}{\to} 1, \tag{2.8}$$

which holds at low gas densities. The equilibrium concentrations of A and B are $\tilde{N}_A$ and $\tilde{N}_B$. The probability that state i is a stabilized state, or is a destabilized state with respect to association is P_i^S or $P_i^D = 1 - P_i^S$, respectively, and γ_c and γ_s are the normalized distribution of pairs in the fully dissociated (source) block $\mathscr{C}$, $0 \leqslant E_i \leqslant \infty$, where P_i^D is unity, and in the fully associated (sink) block $\mathscr{S}$, $-S \geqslant E_i \geqslant -D$, where P_i^S is unity. Hence, the Master equation (2.6), current (2.4), and rate (2.2) separate as[16]

$$\frac{dn_i}{dt} = [\gamma_c(t) - \gamma_s(t)]$$

$$\times \int_{-D}^{\infty} (P_i^S - P_f^S) C_{if}\, dE_f = -\frac{\partial J_i}{\partial E_i}, \tag{2.9}$$

$$J(-E,t) = [\gamma_c(t) - \gamma_s(t)]$$

$$\times \int_{-E}^{\infty} dE_i \int_{-D}^{-E} (P_f^S - P_i^S) C_{if}\, dE_f, \tag{2.10}$$

and

$$R^A(t) = [\gamma_c(t) - \gamma_s(t)]$$

$$\times \int_{-D}^{\infty} P_i^S\, dE_i \int_{-D}^{\infty} (P_i^S - P_f^S) C_{if}\, dE_f. \tag{2.11}$$

From Eq. (2.9), the loss rates of fully dissociated and of fully associated species of energy E_i are, respectively,

$$-\frac{dn_i}{dt} = [\gamma_c(t) - \gamma_s(t)]$$

$$\times \int_{-D}^{0} C_{if} P_f^S\, dE_f, \quad E_i \geqslant 0 \tag{2.12}$$

and

$$-\frac{dn_i}{dt} = [\gamma_s(t) - \gamma_c(t)]$$

$$\times \int_{-S}^{\infty} C_{if} P_f^D\, dE_f, \quad -S \geqslant E_i \geqslant -D, \tag{2.13}$$

which illustrate quite effectively the significance of both the stabilization and disruption probabilities P_f^S and P_f^D.

From Eqs. (2.9) and (2.10),

$$\frac{dn_i}{dt} = -[\gamma_c(t) - \gamma_s(t)] \left(\frac{\partial j_i}{\partial E_i}\right), \tag{2.14}$$

where the time-independent background current downward across E is

$$-j(-E) = \int_{-E}^{\infty} dE_i \int_{-D}^{-E} (P_f^S - P_i^S) C_{if}\, dE_f. \tag{2.15}$$

From Eq. (2.11) the time-independent macroscopic coefficients α and k for association and dissociation in Eq. (2.2) are, therefore, given by the basic expression,

$$\alpha \tilde{N}_A \tilde{N}_B = \int_{-D}^{\infty} P_i^S\, dE_i \int_{-D}^{\infty} (P_i^S - P_f^S) C_{if}\, dE_f = k\tilde{n}_s \tag{2.16}$$

and satisfy (macroscopic) detailed balance.

The expressions (2.10) and (2.11), or equivalently Eqs. (2.15) and (2.16) for the current j and rate coefficient α are in general not identical unless the following additional requirement is satisfied.

A. Quasi-steady-state (QSS)

As Eqs. (2.12) and (2.13) illustrate, the distribution of pairs in blocks $\mathscr{C}$ and $\mathscr{S}$ are time dependent, until full thermodynamic equilibrium is established when $\gamma_{c,s} \to 1$ from above and below, respectively. Since $dn_i/dt = \partial n_i/\partial t$ for the intermediate block $\mathscr{E}$ of highly excited levels with energy E_i in the range $0 \geqslant E \geqslant -S$ then quasi-steady-state (QSS) in block $\mathscr{E}$ requires

$$\frac{dn_i}{dt} = 0, \quad 0 \geqslant E_i \geqslant -S \tag{2.17}$$

so that the stabilization probabilities in Eq. (2.9) then rigorously satisfy the integral equation

$$P_i^S \int_{-D}^{\infty} C_{if}\, dE_f = \int_{-D}^{0} C_{if} P_f^S\, dE_f; \quad 0 \geqslant E_i \geqslant -S. \tag{2.18}$$

The stochastic probability for stabilization P_i^S of state i is therefore the fraction of all collisions which eventually result in association. Under this circumstance it readily follows that the rate (2.11) reduces to

$$R^A(t) = -J(-E,t), \tag{2.19}$$

the downward current (2.10), and that the rate coefficient (2.16) is given by

$$\alpha \tilde{N}_A \tilde{N}_B = -j(-E), \tag{2.20}$$

where E is an arbitrary energy level in block $\mathscr{E}$ $(0 \geqslant E \geqslant -S)$.

The rate of association (2.16) may be identified with the

current (2.15) only when the QSS-condition (2.17) for the probabilities is satisfied.[16] Use of Eq. (2.17) from the outset in Eq. (2.2) also illustrates this relation,

$$R^A(t) = \int_{-D}^{-S} \left(\frac{dn_i}{dt}\right) dE_i = -J(-S,t) = -J(-E,t), \tag{2.21}$$

although the basic expression (2.16) for α cannot then be deduced. An exact expression which emphasizes the role of the current J is obtained from Eqs. (2.2) and (2.3) to give

$$R^A(t) = -\int_{-D}^{\infty} P_i^S \left(\frac{\partial J_i(t)}{\partial E_i}\right) dE_i = \int_{-S}^{0} J_i(t) \left(\frac{\partial P_i^S}{\partial E_i}\right) dE_i, \tag{2.22}$$

since J_i vanishes as $E_i \to -D$ and ∞, and since P_i^S is constant (0 and 1 within blocks $\mathscr{C}$ and $\mathscr{S}$, respectively). Only when Eq. (2.10) for J is constant over block $\mathscr{C}$, i.e., when QSS Eq. (2.18) is satisfied, does Eq. (2.22) reduce to Eq. (2.19). It may be shown (work in progress) that the QSS-condition (2.18) corresponds to a minimum[18] in Eq. (2.16) for α. Any approximate P_i^S which does not rigorously satisfy Eq. (2.18) will therefore yield higher rates α.

The QSS (minimum) rate coefficients are therefore given by

$$\alpha_* \tilde{N}_A \tilde{N}_B = \int_{-E}^{\infty} dE_i \int_{-D}^{-E} (P_f^S - P_i^S) C_{if}\, dE_f = -j(-E) \tag{2.23}$$

$$= \int_{0}^{\infty} dE_i \int_{-D}^{0} C_{if} P_f^S\, dE_f = -j(0) \tag{2.24}$$

$$= \int_{-D}^{-S} dE_i \int_{-S}^{\infty} C_{if} P_f^D\, dE_f = -j(-S) = k_* \tilde{n}_s, \tag{2.25}$$

which are, in general, different from Eq. (2.16) *unless* the probabilities P_f^S *exactly* satisfy[16] the QSS-condition (2.18). Note that Eq. (2.24) is the QSS rate for association that would result from the full equilibrium concentration $\tilde{N}_A \tilde{N}_B$ of dissociated pairs and zero population of fully associated $\mathscr{S}$ pairs i.e., $\gamma_c = 1$ and $\gamma_s = 0$ in Eq. (2.8). Similarly, Eq. (2.25) is the QSS rate for dissociation which would result from an equilibrium population $\tilde{n}_s$ of associated $\mathscr{S}$ pairs and zero population of dissociated pairs, i.e., $\gamma_c = 0$ and $\gamma_s = 1$ in Eq. (2.8).

The aim is now to derive a simple analytic but approximate expression for $j(-E)$ by converting Eq. (2.15) from an integral representation to a differential representation so that approximate expressions for the probabilities P_i^S may be derived, in contrast to the exact numerical solutions of Eq. (2.18).

III. FOKKER–PLANCK REDUCTION FOR ION–ION RECOMBINATION AT LOW GAS DENSITIES

The conversion of the integral operator in Eq. (2.13) into a differential operator achieved by a Fokker–Planck analysis[1,2] is useful when the collision kernel C_{if} favors small changes in energy. Here the current J_i in Eq. (2.6) can be determined to fourth order, rather than to the customary second order.[2]

A. Fokker–Planck current to fourth order in energy-change moments

On introduction of an arbitrary but well-behaved function $\Phi_i(E_i)$ whose derivatives vanish at the end points $[\infty, -D]$, then, with the aid of Eq. (2.6),

$$\int_{-D}^{\infty} \Phi_i \frac{dn_i}{dt} dE_i = \int_{-D}^{\infty} \gamma_i\, dE_i \int_{-D}^{\infty} (\Phi_f - \Phi_i) C_{if}\, dE_f. \tag{3.1}$$

On expanding the difference

$$\Phi_f - \Phi_i = \sum_{n=1}^{\infty} \frac{1}{n!} (E_f - E_i)^n \left[\frac{\partial^n \Phi_i}{\partial E_i^n}\right] \tag{3.2}$$

as a Taylor series in energy change $(E_f - E_i)$, assumed small, and on integration by parts with the explicit recognition that $(\partial^n \Phi_i / \partial E_i^n) \to 0$ for $n \geqslant 1$ as $E_i \to [\infty, -D]$, then Eq. (3.1) can be expressed as

$$\int_{-D}^{\infty} \Phi_i \frac{dn_i}{dt} dE_i = [J_i \Phi_i]_{-D}^{\infty} - \int_{-D}^{\infty} \Phi_i \frac{\partial J_i}{\partial E_i} dE_i, \tag{3.3}$$

where the current is

$$J_i(E_i,t) = \sum_{n=0}^{\infty} (-1)^n \frac{\partial^n [\gamma_i D_i^{(n+1)}]}{\partial E_i^n} \tag{3.4}$$

in terms of the normalized distributions γ_i and the energy change moments[2-4]

$$D_i^{(m)}(E_i) = \frac{1}{m!} \int_{-D}^{\infty} (E_f - E_i)^m C_{if}\, dE_f, \tag{3.5}$$

with respect to the one-way equilibrium rate for $E_i \to E_f$ transitions. The number per second of all collisions with an equilibrium distribution of E_i pairs in unit interval dE_i and unit volume is $D_i^{(0)}$; and $D_i^{(1)}$ and $2D_i^{(2)}$ are the average energy change and average energy change squared *per second*, $d\langle \Delta E \rangle / dt$ and $d\langle \Delta E^2 \rangle / dt$, respectively. The ratios $D_i^{(1)}/D_i^{(0)}$ and $2D_i^{(2)}/D_i^{(0)}$ specify $\langle \Delta E_i \rangle$ and $\langle \Delta E_i^2 \rangle$ *per collision*, respectively.

Evaluation of these moments can be facilitated by adopting the expressions for C_{if} which correspond to various A–M and B–M binary interactions (symmetrical resonance charge–transfer,[8-10] hard-sphere,[10] polarization[11]). They can be collected under a universal form (work in progress). These moments are normalized[10] to the quantity $(-1)^m \Gamma \alpha_T (kT)^{m-1} \tilde{N}_A \tilde{N}_B$ where α_T is the Thomson rate [Eq. (4.1) below], where Γ is a dimensionless mass factor[10] and where T is the temperature of the gas bath.

Figures 1(a) and 1(b) illustrate the general trend of these moments calculated here for the specific case[8,10] where internal-energy changes in an ion pair $(X^+ - X^-)$ are due to symmetrical resonance charge–transfer $(X^{\pm} - X)$ collisions with a parent gas X. In this case, the velocity vectors of the

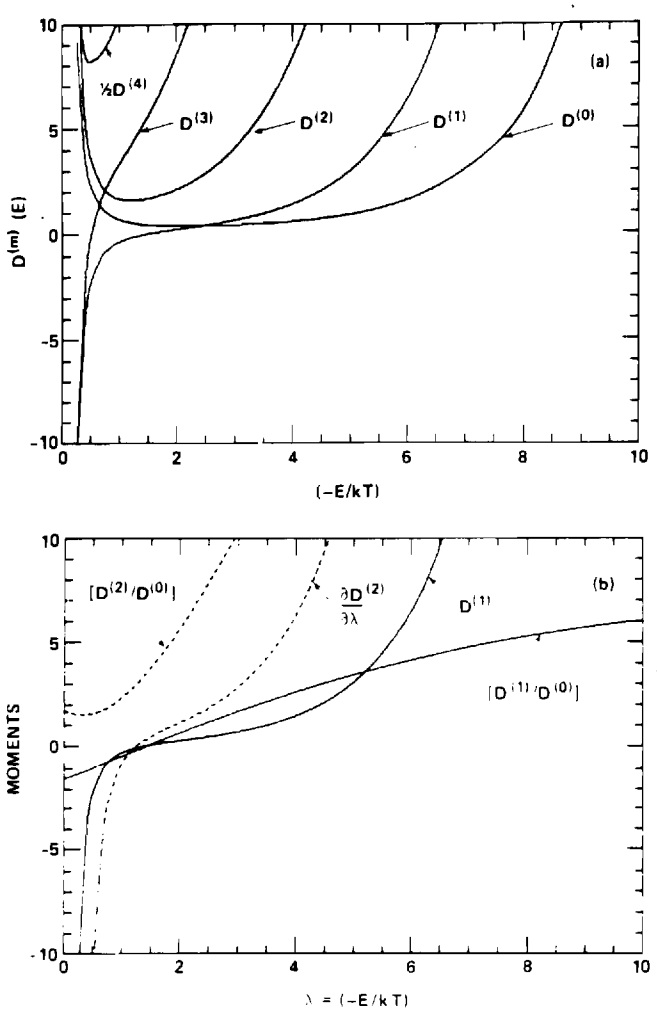

FIG. 1. (a) Normalized moments $D^{(m)}$ of energy change rate (energy^m s^{-1}), $m = 0$–4, as a function of internal energy $E_i = -\lambda(kT)$ of the bound ion pair. (b) Averaged energy change and energy-change squared $D^{(m)}/D^{(0)}$ per collision, $D^{(1)}$ and derivative of $D^{(2)}$. Equal-mass species and charge–transfer ion–neutral collisions are assumed and moments are normalized to the quantity $(-1)^m \Gamma \alpha_r (kT)^{m-1} \bar{N}_A \bar{N}_B$.

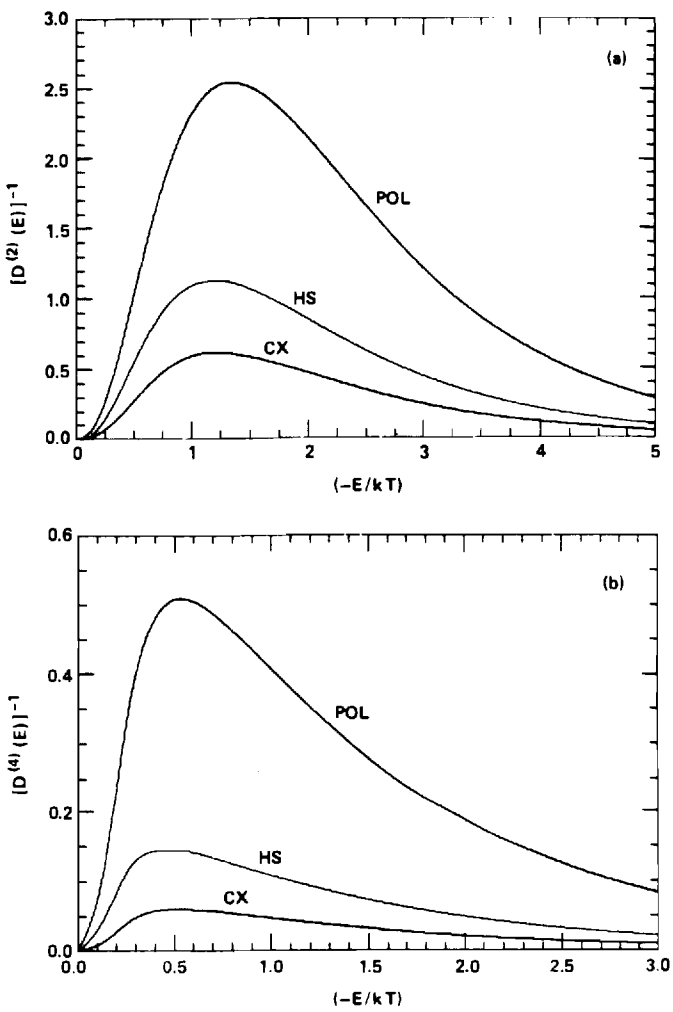

FIG. 2. Inverses of moments (a) $D^{(2)}(\lambda)$ and (b) $D^{(4)}(\lambda)$ as a function of internal energy $E_i = -\lambda kT$ of the ion pair for various ion–neutral interactions: POL (polarization), HS (hard-sphere), CX (charge–transfer). Equal mass species are assumed.

(fast) ion X^+ and the (thermal) neutral X are interchanged.[8] Large transfers of energy are therefore involved, as is confirmed by $D_i^{(2)}$, the averaged energy change squared $\langle \Delta E_i^2 \rangle$ *per second* shown in Fig. 1(a). This case will therefore provide a most stringent test of the weak-collision (diffusion) procedure adopted here.

As the binding energy $-E_i$ decreases from the dissociation limit (at zero energy), the equilibrium density $\tilde{n}(E_i) \sim |E_i|^{-5/2} \exp(-E_i/kT)$ per unit interval dE_i decreases from infinity, reaches a minimum at $E_i = -2.5kT$ and then increases exponentially.[10] Since the energy change frequency ν_{if} for each pair decreases rapidly with increase of binding, the overall shapes of the equilibrium moments $D_i^{(m)}$ in Figs. 1(a) and 1(b) reflect the variation of the product $\tilde{n}_i \nu_{if}$. Note that the equilibrium collisional rate $D_i^{(0)}$ is relatively constant in the range (1.8–4)kT of binding. Also $D_i^{(1)} \approx d/dt \langle \Delta E \rangle$ is positive for $E_i > -1.4kT = E^*$, so that these pairs on average become less tightly bound upon collision. Pairs with $E_i < -1.4kT$ become more tightly bound upon collision (since $D_i^{(1)} < 0$). This critical energy specifies the location of E^* of a bottleneck where the averaged energy change vanishes and where the region $E_i > E^*$ where excitation is greater is separated from the region $E_i < E^*$ where deexcitation is greater. Note also that the even moments $D_i^{(m)}$ display minima which become sharper with increase of m, as expected, and that the minimum in $D_i^{(2)} \approx \frac{1}{2} d/dt \langle \Delta E_i^2 \rangle$ coincides with the zero of $D_i^{(1)} \sim d/dt \langle \Delta E_i \rangle$ at E^*, as is clearly shown in Fig. 1(b). These features are quite general for the various ion–neutral interactions and are utilized below.

Figures 2(a) and 2(b) illustrate the variation of $[D_i^{(2)}]^{-1}$ and $[D_i^{(4)}]^{-1}$ for different interactions of A and B with M (charge–transfer CX, hard-sphere HS, and polarization POL). The bottleneck to $D_i^{(2)}$ occurs where the $\langle \Delta E_i^2 \rangle$ rate is least and in roughly in the same location ($E_i \sim 1.25kT$) for all the interactions. The $\langle \Delta E_i^2 \rangle$ rate is greatest for the charge–transfer interaction and weakest for the polarization attraction, as expected. The moment $D_i^{(4)}$ exhibits similar but more rapidly varying behavior.

Since C_{if} is symmetrical in i and f—the detailed-balance

relation (2.7)—then C_{if}, when expressed as a function of the energy-mean $\bar{E} = \frac{1}{2}(E_f + E_i)$ and the energy change $\Delta = E_f - E_i$, is such that $C_{if} = C_{if}\ (\bar{E}, |\Delta|)$ as previously noted by Keck and Carrier.[2] On expanding C_{if} about E_i in terms of the expansion parameter Δ, which is assumed small, then

$$C_{if}(\bar{E} = E_i + \tfrac{1}{2}\Delta, |\Delta|) = \sum_{n=0}^{\infty} \frac{\Delta^n}{n!} \left(\frac{1}{2}\right)^n \left(\frac{\partial^n C_i}{\partial E_i^n}\right), \tag{3.6}$$

where C_i is $C_{if}(\bar{E} = E_i, |\Delta|)$. The general moments (3.5) are therefore determined from

$$m! D_i^{(m)}(E_i) = \sum_{n=1,3,5}^{\text{odd}} (2^n n!)^{-1} \left[\frac{\partial^n F_i^{(m+n)}}{\partial E_i^n}\right]; \quad m \text{ odd}, \tag{3.7a}$$

$$= \sum_{n=0,2,4}^{\text{even}} (2^n n!)^{-1} \left[\frac{\partial^n F_i^{(m+n)}}{\partial E_i^n}\right]; \quad m \text{ even}, \tag{3.7b}$$

which involves only the terms

$$F_i^{(s)}(E_i) = \int_{-D}^{\infty} \Delta^s C_i(E_i, |\Delta|) dE_f, \tag{3.8}$$

with s even. Terms with s odd vanish since D is effectively infinite (~ 5 eV).

For equilibrium, γ_i in Eq. (3.4) is unity and the equilibrium current can then be expressed, with the aid of Eq. (3.7) as

$$\tilde{J}_i = \sum_{n=0}^{\infty} (-1)^n \left[\frac{\partial^n D_i^{(n+1)}}{\partial E_i^n}\right] = \sum_{n=0,2}^{\text{even}} \sum_{j=0,2}^{\text{even}} (n-2j)[2^{j+1}(n+2)!(j+1)!]^{-1} \times \frac{\partial^{j+n+1} F_i^{(j+n+2)}}{\partial E_i^{j+n+1}}. \tag{3.9}$$

This new form clearly shows that the coefficient of its first term $\partial F_i^{(2)}/\partial E_i$, which arises from the leading term of the expansion (3.7) for both $D_i^{(1)}$ and $\partial D_i^{(2)}/\partial E_i$, is identically zero. The coefficient of the second term $\partial^3 F_i^{(4)}/\partial E_i^3$, which is the net balance of the second term in the expansion (3.7) for both $D_i^{(1)}$ and $\partial D_i^{(2)}/\partial E_i$ and of the leading term in the expansion (3.7) for both $\partial^2 D_i^{(3)}/\partial E_i^2$ and $\partial^3 D_i^{(4)}/\partial E_i^3$, is also zero. The leading nonvanishing contribution to Eq. (3.9) is $[-\frac{1}{576}\partial^5 F_i^{(6)}/\partial E_i^5]$ which is the net balance of the third terms in the expansion (3.7) for both $D_i^{(1)}$ and $\partial D_i^{(2)}/\partial E_i$ and of the second terms in the expansion (3.7) for both $\partial^2 D_i^{(3)}/\partial E_i^2$ and $\partial^3 D_i^{(4)}/\partial E_i^3$. The consistent neglect of $\partial^4 D_i^{(5)}/\partial E_i^4 \sim \partial^5 F_i^{(6)}/\partial E_i^5$ and higher-order derivatives demands both the neglect in Eq. (3.4) of terms with $n > 4$ and the neglect in Eqs. (3.7a) and (3.7b) of terms with $n > 5$ and $n > 4$, respectively. Hence, the equilibrium current

$$\tilde{J}_i \approx D_i^{(1)} - \frac{\partial D_i^{(2)}}{\partial E_i} + \frac{\partial^2 D_i^{(3)}}{\partial E_i^2} - \frac{\partial^3 D_i^{(4)}}{\partial E_i^3} \equiv 0 \tag{3.10}$$

is exact to fourth order in the moments and is identically zero! Relationships between even and odd moments can be obtained from Eq. (3.7) by neglecting $F_i^{(6)}$ and higher terms, i.e., $D_i^{(5)}$ and higher moments, to give

$$D_i^{(1)} = \frac{\partial}{\partial E_i}\left[D_i^{(2)} - \frac{\partial^2 D_i^{(4)}}{\partial E_i^2}\right] \tag{3.11a}$$

and

$$D_i^{(3)} = 2\frac{\partial}{\partial E_i} D_i^{(4)}, \tag{3.11b}$$

which also ensure zero equilibrium current. In view of Eq. (3.11) note that equilibrium ($\tilde{J}_i = 0$) is obtained only when the current (3.4) is expanded to even order.

With the aid of Eq. (3.10), the nonequilibrium current (3.4) to fourth order in moments $D_i^{(m)}$ is

$$J_i^{(4)}(E_i,t) = -\left[D_i^{(2)} - 2\frac{\partial D_i^{(3)}}{\partial E_i} + 3\frac{\partial^2 D_i^{(4)}}{\partial E_i^2}\right]\left[\frac{\partial \gamma_i}{\partial E_i}\right] + \left[D_i^{(3)} - 3\frac{\partial D_i^{(4)}}{\partial E_i}\right]\left[\frac{\partial^2 \gamma_i}{\partial E_i^2}\right] - D_i^{(4)}\left[\frac{\partial^3 \gamma_i}{\partial E_i^3}\right] \tag{3.12}$$

which is the differential representation (up to and including the fourth-order moment $D_i^{(4)}$) of the double integral

$$J(E,t) = \int_E^{\infty} dE_i \int_{-D}^{E} [\gamma_f(t) - \gamma_i(t)] C_{if}\, dE_f \tag{3.13}$$

for the exact current (2.4). The differential form (3.12) is the Fokker–Planck current to fourth order since the general Fokker–Planck expansion can be employed for any variable whose changes are small in comparison with averaged characteristic values, e.g., the collisional energy change Δ here is assumed small relative to the thermal energy kT of the gas bath.

Upon use of the approximations (3.11), which are internally consistent to neglect of moments higher than $D_i^{(4)}$, Eq. (3.12) reduces to

$$J_i^{(4)}(E_i,t) = -\left[D_i^{(2)} - \frac{\partial^2 D_i^{(4)}}{\partial E_i^2}\right]\left[\frac{\partial \gamma_i}{\partial E_i}\right] - \frac{1}{2} D_i^{(3)}\left[\frac{\partial^2 \gamma_i}{\partial E_i^2}\right] - D_i^{(4)}\left[\frac{\partial^3 \gamma_i}{\partial E_i^3}\right]. \tag{3.14}$$

Inserting the ansatz (2.8) in Eq. (3.12), then Eq. (2.6) with Eq. (3.12) yields

$$\frac{dn_i(E_i,t)}{dt} = -[\gamma_c(t) - \gamma_s(t)]\frac{\partial j_i(E_i)}{\partial E_i}, \tag{3.15}$$

where in terms of the stochastic probability P_i^D that state i dissociates, the time-independent background current to fourth order is

$$j_i^{(4)}(E_i) = -\left[D_i^{(2)} - 2\frac{\partial D_i^{(3)}}{\partial E_i} + 3\frac{\partial^2 D_i^{(4)}}{\partial E_i^2}\right]\left[\frac{\partial^3 P_i^D}{\partial E_i}\right] + \left[D_i^{(3)} - 3\frac{\partial D_i^{(4)}}{\partial E_i}\right]\left[\frac{\partial^2 P_i^D}{\partial E_i^2}\right] - D_i^{(4)}\left[\frac{\partial^3 P_i^D}{\partial E_i^3}\right]. \tag{3.16}$$

B. Diffusion equation and current for termolecular recombination

On ignoring moments $D_i^{(3)}$ and higher, the (diffusional) current (3.16) is

$$j_d(E_i) = -D_i^{(2)} \frac{\partial P_i^D}{\partial E_i} = D_i^{(2)} \frac{\partial P_i^S}{\partial E_i}, \tag{3.17}$$

so that Eq. (3.15) is

$$\frac{dn_i(E_i,t)}{dt} = [\gamma_c(t) - \gamma_s(t)] \frac{\partial}{\partial E_i}\left[D_i^{(2)} \frac{\partial P_i^D}{\partial E_i}\right], \tag{3.18}$$

which is a diffusion equation in energy space. The moment $D_i^{(2)} = \frac{1}{2}d/dt \ \langle \Delta E_i^2 \rangle$ is the diffusion coefficient (energy^2 s^{-1}) in energy space. This type of streaming equation has been previously derived via other techniques by Pitaevskii[1] for electron–ion recombination under highly nonequilibrium conditions when $\gamma_c \gg \gamma_s$ so that $\gamma_i = P_i^D \gamma_c$ in Eq. (2.6), and by Keck and Carrier[2] for heavy-particle association/dissociation. It has been investigated by Landon and Keck,[3] by Mahan[5], and by Bates and Zundi[6] for highly nonequilibrium ($\gamma_c \gg \gamma_s$) termolecular ion–ion recombination. By explicitly including here the factor $(\gamma_c - \gamma_s)$ via the ansatz (2.8), Eqs. (3.15) and (3.18) for all $\gamma_{c,s}$ help to emphasize the evolution via termolecular recombination and dissociation (into ion products) of the subsystems (A–B) towards thermodynamic equilibrium with the gas M, attained when $\gamma_c \to \gamma_s \to 1$.

Another advantage of the ansatz (2.8) is that the intermediate block of highly excited levels can be taken to be in quasi-steady-state (QSS), i.e., $\partial n_i/\partial t \approx 0$ in either Eq. (2.9) or (3.18), *for all times*. The QSS-diffusional current (3.17) is constant over $\mathscr{E}$, so that the solution of Eq. (3.17) subject to conditions,

$$P_i^D(-S) = 0, \quad P_i^S(-S) = 1 \tag{3.19}$$

is

$$P_d^D(E_i) = -j_d\left[\int_{-S}^{E_i} dE/D^{(2)}(E)\right] = 1 - P_d^S(E_i), \tag{3.20}$$

where the subscript d denotes quantities associated with the diffusion equation (3.18). Various levels of approximation readily follow:

(a) Since

$$P_i^D(0) = 1, \quad P_i^S(0) = 0, \tag{3.21}$$

then Eq. (3.20) yields

$$-j_d^{(P)} = \left[\int_{-S}^{0} dE/D^{(2)}(E)\right]^{-1} = \alpha_P \tilde{N}_A \tilde{N}_B \tag{3.22}$$

for the downward diffusional current which, when compared with Eq. (2.20) provides the recombination rate α_P of Pitaevskii,[1] adopted for ion–ion recombination by Landon and Keck[3] and by Mahan.[5] Note that the current (3.22) is the inverse of the area under the curves in Fig. 2(a), and that Eq. (3.20) for the stabilization and disruption probabilities $P_i^{S,D}$ at energy E_i are the respective ratios of the areas which correspond to the energy ranges $(0 \to E_i)$ and $(E_i \to -S)$ to the total area.

(b) Rather than requiring Eq. (3.21) for the probabilities, j_d in Eq. (3.20) can be fixed by inserting Eq. (3.20) directly into Eq. (2.24) for $j(0)$ to give

$$-j(0) = \int_0^\infty dE_i \int_{-D}^{0} C_{if}\, dE_f + j_d \int_0^\infty dE_i \times \int_{-D}^{0} C_{if}\, dE_f \left\{\int_{-S}^{E_f} dE/D^2(E)\right\}. \tag{3.23}$$

On equating the exact current $j(0)$ in Eq. (3.23) with the diffusional current j_d, then

$$-j_d^{(k)}(0) = \left[\int_0^\infty dE_i \int_{-D}^{0} C_{if}\, dE_f\right]\left\{1 + \int_0^\infty dE_i \times \int_{-D}^{0} C_{if}\, dE_f \int_{-S}^{E_f} dE/D^{(2)}(E)\right\}^{-1} = \alpha_K \tilde{N}_A \tilde{N}_B, \tag{3.24}$$

which yields the expression of Keck[4] for α. The term in braces, $\{\ \}^{-1}$ is simply the ratio of the downward diffusional current to the one-way equilibrium current across the dissociation neck.

(c) Another possibility in similar vein to (b) is to insert Eq. (3.20) directly into Eq. (2.25) for $j(-S)$ to give

$$j_d(-S) = \left[\int_{-D}^{-S} dE_i \int_{-S}^{\infty} C_{if}\, dE_f\right] \times \left\{1 + \int_{-D}^{-S} dE_i \int_{-S}^{0} C_{if}\, dE_f \times \int_{-S}^{E_f} dE/D^2(E)\right\}^{-1} = \alpha_K \tilde{N}_A \tilde{N}_B, \tag{3.25}$$

where the term in braces, $\{\ \}^{-1}$, is simply the ratio of the upward diffusional current across $-S$ to the one-way equilibrium current upward across $-S$.

The feature common to all the above procedures (a)–(c) is that the required current (3.17) depends upon the accuracy of the gradient (dP_i^D/dE_i) which, due to the neglect of higher derivatives in Eq. (3.16), is described by the diffusion equation (3.18) less precisely than are the actual diffusion QSS solutions, i.e., Eq. (3.18) may furnish accurate P_i^D but relatively inaccurate derivatives. More importantly, however, is that Eq. (2.20), which is valid only under exact QSS-condition (2.18) of the exact Master equation (2.19) has been invoked for the diffusional currents $j_d^{(P)}$ of Eq. (3.22) and $j_d^{(k)}$ of Eq. (3.24) which are QSS solutions of the different and approximate diffusional equation (3.18).

The QSS solution of Eq. (3.18) subject to both constraints (3.19) and (3.21) is

$$P_d^S(E_i) = \left\{\int_{E_i}^{0} dE/D^{(2)}(E)\right\}\left\{\int_{-S}^{0} dE/D^{(2)}(E)\right\}^{-1} \tag{3.27}$$

for the probability that any level E_i in block $\mathscr{E}$, once accessed by collision, has "associative" character. The probability that level E_i has "dissociative" character is the complementary function

$$P_d^D(E_i) = \left\{\int_{-S}^{E_i} dE/D^{(2)}(E)\right\}\left\{\int_{-S}^{0} dE/D^{(2)}(E)\right\}^{-1}. \tag{3.28}$$

Thus, both functions are constrained to vary monotonically between zero and unity as does the exact numerical solution to the integral equation (2.18) so that, when compared with the exact numerical values, will involve less error than their corresponding derivatives

$$\frac{\partial P_i^{A,D}}{\partial E_i} = \mp\{D_i^{(2)}(E_i)\}^{-1} j_d^{(\rho),k} \tag{3.29}$$

appropriate to currents (3.22) and (3.24) in schemes (a) and (b) above.

C. Calculations for termolecular recombination at low N

The well developed case[8-12] of termolecular ion–ion recombination

$$A^+ + B^- + M \rightarrow AB + M \tag{3.30}$$

serves as a case study for assessing the accuracy of the diffusion approaches of Secs. III A and III B. The recombination coefficient α has previously been represented[9,17] very accurately by the sum

$$\alpha = \alpha_1 + \alpha_2 \tag{3.31}$$

of coefficients α_i obtained by considering separate contributions from (A^+–M) and (B^-–M) *binary* collisions ($i = 1$ and 2, respectively). The exact numerical rates α_i are obtained by inserting the exact numerical solution of the integral equation (2.18), the QSS condition into Eq. (2.32) for the current $j(-E_i)$. The rates α_i have been tabulated[9-11] as a function of the mass-ratio parameter:

$$a_i = M_j M_3 / M_i (M_1 + M_2 + M_3), \tag{3.32}$$

where M_i are the masses of species A^+, B^-, and M, $i = 1, 2$, and 3, respectively and where the set (i, j) is equal to (1,2) or (2,1) for (1 − 3) or (2 − 3) collisions, respectively.

Expressions for the equilibrium rate C_{if} appropriate to the three classes—polarization,[11] charge–transfer,[8,10] and hard-sphere[10]—of ion–neutral interactions have been previously derived.[9-11] Calculations have been performed here for the exact QSS-rates α_E that rise from 1–3 collisions and for the corresponding diffusional rates, (3.22) for α_P and (3.24) for α_K of Pitaevskii[1] and Keck,[4] respectively. Little discernable difference was found between α_P and α_K which may now be simply called the diffusional rates α_D obtained when the diffusional current (3.17) is inserted in Eq. (2.20). Previous results[9-11] were based on the solution of, at most, 36 coupled algebraic equations, the discretized equivalent representation of Eq. (2.18). Present calculations solve 100 coupled equations required for convergence in α for small and large mass parameters (3.32).

Table I provides present values of the ratio α_D/α_E for the various interactions over the full range of mass parameter a_1. Small $a \approx 10^{-3}$ corresponds to collisional recombination of heavy ions ($M_1 \approx M_2 \gg M_3$) in a much lighter (electron) gas, intermediate $a(=1/3$ for $M_1 = M_2 = M_3)$ corresponds to normal mass components, and large $a = 10^3$ for $M_1 \ll M_2 \approx M_3$ corresponds to electron–ion recombination in an ambient gas. The cases of small and large a involve energy transfers which are very much less than the energy kT of the gas so that the diffusional (weak collision) approach is likely then to be valid.

As Table I shows, the diffusional rates are reliable, as expected, only for recombination in a vanishingly light gas ($a \approx 10^{-3}$) or for electron–ion recombination ($a \approx 10^3$) in a general gas, the case for which Pitaevskii[1] designed his diffusional treatment. The diffusional rates are higher by between a factor of 3–9 for intermediate $a \sim 1$. As the ion–neutral interaction varies from polarization attraction to hard-sphere repulsion and then to charge–transfer interaction, the energy change in the ion–neutral collision becomes progressively larger [see Fig. 2(a) and 2(b)] so that the diffusional rates (based on weak collisions) become less accurate, as shown directly by the variation of entries in Table I for a specified mass parameter a.

Since Eq. (3.17) predicts zero current in both the fully dissociated and fully associated blocks, $\mathscr{C}$ and $\mathscr{S}$, respectively, the diffusional current (3.17) is therefore discontinuous, zero in $\mathscr{C}$, j_d in $\mathscr{E}$ and zero in $\mathscr{S}$. The diffusion rates (3.22) of Pitaevskii and (3.24) of Keck are therefore expected to be valid only in the limit of vanishingly small currents and rates α of recombination. This is confirmed in Table I for

TABLE I. Variation of the ratio (α_D/α_E) and (α_{BN}/α_E) with mass-ratio parameter a for 1–3 collisions and with the various 1–3 interactions: polarization (POL), hard-sphere (HS), and symmetrical resonance charge–transfer (CX). The exact, diffusional, and bottleneck rates are α_E, α_D, and α_{BN}, respectively.

	α_D/α_E			α_{BN}/α_E		
a	POL[a]	HS[a]	CX[b]	POL	HS	CX
0.001	1.001	1.013	1.030	32.447	25.782	16.996
0.01	1.163	1.222	1.321	8.369	7.336	5.513
0.1	2.131	2.739	3.522	3.354	2.939	2.384
1/3	3.360	4.967	6.840	2.541	2.215	1.865
1.0	4.060	6.604	9.272	2.333	2.015	1.722
10.0	2.131	3.510	⋯	3.354	2.746	⋯
100.0	1.163	1.455	⋯	8.369	6.302	⋯
1000.0	1.001	1.093	⋯	32.447	20.233	⋯

[a] In POL and HS, small a implies ion–ion recombination in a vanishingly light gas and large a ($\sim 10^3$) implies electron–ion recombination in a normal-mass gas.

[b] In CX small a implies $M_2 \ll M_1 = M_3$ and $a = 1$ implies $M_2 \gg M_1 = M_3$.

the limiting cases of small and large a. Then the actual rate for electron–ion collisional recombination in a gas is[7] $\alpha_E \sim 10^{-9}\,\mathrm{cm^3\,s^{-1}}$ at STP, which is three orders of magnitude less than the rate $\alpha_E \sim 10^{-6}\,\mathrm{cm^3\,s^{-1}}$ at STP (cf. Ref. 19) for ion–ion recombination a similar mass gas.

Another reason for the inadequacy of the diffusion approach as previously applied to general-mass cases is also apparent. As Figs. 3(a) and 3(b) show, the diffusion equation (3.18) in general furnishes fairly accurate probabilities $P_i^{A,D}$, Eqs. (3.29) and (3.30), but less reliable gradients $dP_i^{A,D}/dE_i$.

In an effort to assess the relative importance between using relatively accurate distributions P_i^S within the integral (2.23) or differential (3.17) forms of the collision integral of the Master equation, assume that the intermediate block $\mathscr{E}$ between blocks $\mathscr{C}$ and $\mathscr{S}$ is absent, i.e.,

$$P^S(E_i) = \begin{cases} 0, & -E < E_i < \infty \\ 1, & -D < E_i < -E \end{cases}, \tag{3.33}$$

where $-E$ is some bound energy level. The current (2.15) then reduces to

$$-j_{\mathrm{BN}}(-E) = \int_{-E}^{\infty} dE_i \int_{-D}^{-E} C_{if}\, dE_f = \alpha_{\mathrm{BN}}(E)\tilde{N}_{\mathrm{A}}\tilde{N}_{\mathrm{B}}, \tag{3.34}$$

which is the one-way equilibrium downward current across level $-E$. As $-E$ is varied, this current achieves a minimum[10] at energy $-E^*$ ($\approx -2kT$) which therefore acts as a bottleneck[13] to the recombination which proceeds at rate $\alpha_{\mathrm{BN}}(E^*)$. The ratio of α_{BN} at the bottleneck E^* to the exact numerical rate α_E is displayed in Table I for the various interactions. The bottleneck method fails quite markedly for small and large mass parameters a, where the diffusion current is by contrast successful, and becomes much more reliable than the diffusion approach at intermediate $a(\approx 1)$. For a given a, less error is involved for stronger collisions in harmony with Eq. (3.34) being a strong collision approximation. Since Eq. (3.33) assumes the least possible knowledge of the probabilities P_i^S(subject to the constraints) but an integral form (3.34) to the collision rate, it follows that fairly accurate distributions are required at small and large a where the collision rate and dynamics are weak, so that the discontinuous integral form (2.23) does reduce indeed to the continuous streaming form (3.17). For intermediate a when the energy changes are certainly not weak, inclusion of the integral form (2.22) is apparently more important than the use of fairly accurate distributions (which in any event are constrained to vary between unity and zero at the boundaries of block $\mathscr{E}$). Note also that the diffusional and bottleneck results are always greater than the exact QSS rates, in accord with predictions of the variational principle recently proposed.[18] The bottleneck method provides the *least* of the one-way equilibrium rates—the least upper limit—across a bound level. The diffusion method incorporates the effect of the net downward–upward collisional transitions.

The closeness exhibited in Fig. 3(a) between the diffusional probabilities, (3.27) and (3.28), and the exact numerical probabilities may be utilized in two ways. First, an

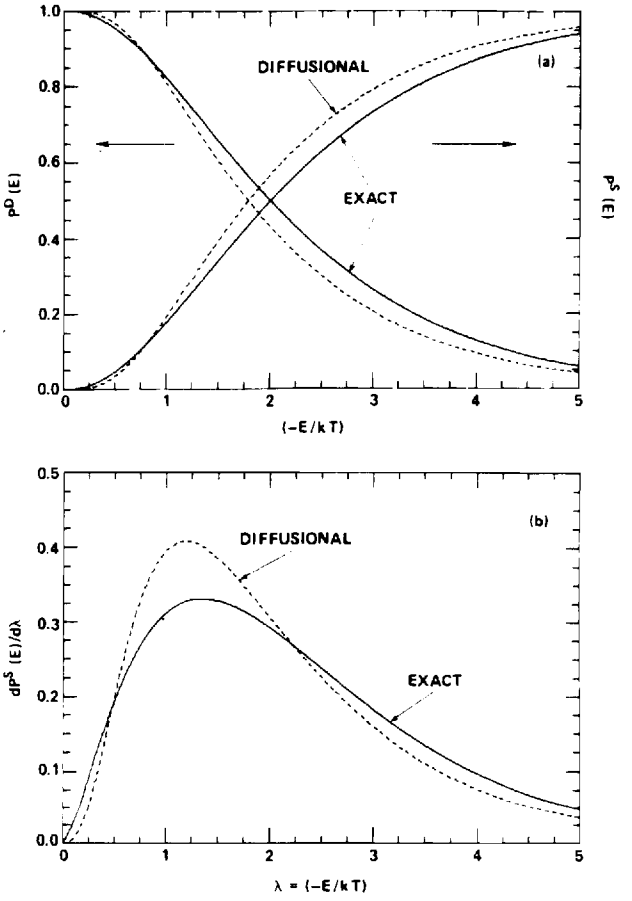

FIG. 3. (a) Probabilities $P^{S,D}$ for stabilization and dissociation of an ion-pair bound with energy $E_i = -\lambda kT$. Equal-mass species and charge-transfer ion–neutral collisions are assumed. —: Exact QSS solution of Eq. (2.18). - - -: Diffusional approximation, Eqs. (3.27) and (3.28). (b) Derivatives $(dP^S/d\lambda)$ of stabilization probability P^S. From numerical solution of Eq. (2.18) and from diffusional approximation, Eq. (3.29).

iterative procedure[4]

$$P^{(n+1)}(E_i)\int_{-D}^{\infty} C_{if}\, dE_f = \int_{-D}^{\infty} P^{(n)}(E_f) C_{if}\, dE_f \tag{3.37}$$

to the solution of the integral equation (2.18) can be developed by using the diffusional analytical probabilities (3.27) as the starting ($n = 0$) solution. It is found here that convergence to within 1% of the exact solution can be in general achieved after five iterations, so that accurate rates can then be determined from Eqs. (2.23)–(2.25) since the QSS-condition (2.18) is satisfied.

Since the diffusional probabilities (3.27) and (3.28) are reasonably accurate, a second possibility is to insert them directly into the current (2.23). This procedure, at first sight attractive, is however inconsistent, in that the diffusional probabilities while satisfying quasi-steady-state (QSS) of the diffusional equation (3.18) in block $\mathscr{E}$, *do not* satisfy the condition (2.18) for QSS of the Master equation (2.9) on which Eq. (2.23) relies. The resulting current (2.15) will therefore not be a constant in block $\mathscr{E}$. This is demonstrated by Fig. 4 which compares the exact downward current $-j_E(E_i)$ past level E_i obtained from the solution of Eq.

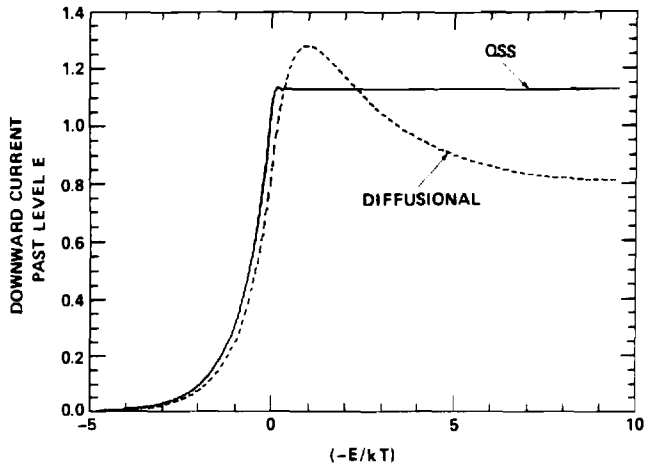

FIG. 4. Comparison of currents, Eq. (2.15), past energy level $-E=-\lambda kT$, obtained (—) from exact solution of Eq. (2.18) and from (- - -) diffusion probabilities Eq. (3.27). Equal-mass species and hard-sphere ion–neutral collisions are assumed. The current is normalized to $(2\alpha_T \tilde{N}_A \tilde{N}_B)$ where α_T is the Thomson rate, Eq. (4.1).

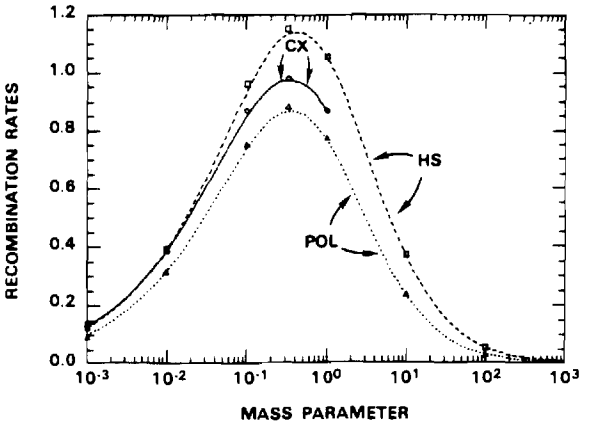

FIG. 5. Normalized rates R_T, Eq. (4.2), for ion–ion recombination in a dilute gas as a function of mass parameter a, Eq. (3.32) for various ion–neutral interactions: HS (hard-sphere), CX (charge–transfer) and POL (polarization). —: exact rates. □, ○, △: rates obtained with diffusional probabilities, Eq. (3.27), in basic Eq. (2.16) for HS, CX, and POL interactions.

(2.18) in Eq. (2.23) with the approximate downward current $-j_A(E_i)$ obtained by inserting Eq. (3.27) in Eq. (2.23). The diffusional current through the bound levels is far from constant over the block $\mathscr{E}$ of highly excited levels and hence, Eq. (2.20) cannot be used for steady-state rates. The figure also shows that assignment of a bound level E_i for determination of α from Eq. (2.23) is uncertain. Since the current $j(-E)$ exhibits a very rapid variation in the neighborhood of the dissociation limit (at zero energy), use of Eq. (2.24) for $j(0)$ is therefore a risky procedure, the exact value of $j(0)$ being $\sim 50\%$ higher than the approximate $j(0)$. Some defense can be made by calculating Eq. (2.23) at the bottleneck energy $E^* \sim -2kT$ where the diffusional and exact currents agree. This adoption is however not firmly based.

The basic reason for the inconsistency of using the diffusional probabilities (3.27) in Eq. (2.23) is not that the diffusional probabilities are not sufficiently accurate for useful application, but is that the expression (2.23) based on identifying the association rate with the current is not appropriate for the use of approximate probabilities, which do not satisfy the basic condition (2.18) for such identification.

IV. BASIC RATE WITH DIFFUSIONAL PROBABILITIES

The exact rates α_E obtained in Sec. III C from Eq. (2.18) in Eq. (2.23) for the various ion–neutral interactions are normalized[10,11] to the corresponding Thomson rate

$$\alpha_T = \tfrac{4}{3}\pi(R_e/\beta)^3(3kT/M_{12})^{1/2}\sigma_0 N, \quad \beta = 3/2, \quad (4.1)$$

where R_e is the natural unit (e^2/kT) for Coulombic attraction between the ions 1 and 2. The integral cross section σ_0 for 1–3 elastic collisions at relative energy $(\frac{3}{2}kT)$ is taken in Eq. (4.1) to be $2\sigma^X$, $2\pi(pR_e/3)^{1/2}$, and σ_0^H, respectively for symmetrical resonance charge–transfer collisions with cross section σ^X, for polarization (orbiting) collisions in terms of the polarizability p of the gas M, and for hard-sphere collisions with cross section σ_0^H.

Approximate rates α_A may now be determined by inserting P_i^S, the diffusional (approximate) probabilities (3.27) into the basic expression (2.16) which does not rely on the use of exact (QSS) P_i^S. Figure 5 displays a comparison of the corresponding ratios,

$$R_T = (M_1/M_{12})(\alpha/\alpha_T), \quad (4.2)$$

where α is taken as the exact rate α_E or the approximate rate α_A, which arises from 1–3 collisions. The exact rates reproduce those previously presented.[10,11] The present study adopts a 100-point quadrature throughout, rather than 36 and 18 used in Refs. 10 and 11, respectively, in order to obtain convergence at small and large a.

Excellent agreement between α_E and α_A is obtained over the full range of the mass parameter a, Eq. (3.32) for a_1 all the way, from $a \approx 10^{-3}$ for association of heavy ions in a light (electron) gas, to intermediate $a \approx 1/3$ for equal mass species and up to large $a \approx 10^3$ which corresponds to electron–ion recombination in a gas. As expected, greatest departures occur for the case of equal mass which involves the largest energy transfer so that the diffusional probabilities would also show their greatest departure from the exact probabilities as in Fig. 3(a). For this case $(a = 1/3)$, the diffusional result corresponding to hard-sphere collisions, which in turn involve largest energy transfers (cf. Fig. 2), exhibit the largest of small departures. The present diffusional treatment is also excellent over all of the various classes of 1–3 interaction considered.

V. ION–ATOM ASSOCIATION AT LOW GAS DENSITIES

The above theory may now be suitably modified to cover ion–atom association

$$A^+ + B + M \underset{k}{\overset{\alpha}{\rightleftarrows}} AB^+ + M \quad (5.1)$$

of atomic species A^+ and B in a low density gas M. In contrast to ion–ion recombination (3.30) where an equilibrium distribution over internal angular momentum L_i is established[12] the A^+–B attraction can support centrifugal barriers so that nonequilibrium distributions $n_i(E_i, L_i^2; t)$ over

both E_i and L_i^2 must be acknowledged. Thus, the ansatz (2.8) is replaced by

$$\gamma_i(E_i,L_i^2;t) = \frac{n_i(E_i,L_i^2;t)}{\tilde{n}_i(E_i,L_i^2)} = P_i^D(E_i,L_i^2)\gamma_c(t) + P_i^S(E_i,L_i^2)\gamma_s(t) \overset{t\to\infty}{\to} 1, \quad (5.2)$$

where $P_i^S = 1 - P_i^D$, the probability of stabilization of (E_i,L_i^2) pairs by subsequent multicollisions, is zero for dissociated pairs and unity for fully associated pairs.

Bates and McKibbin[14] found that a delta function approximation $\delta(L_i^2 - L_f^2)$ for $(E_i,L_i^2 \to E_f,L_f^2)$ transitions was quite satisfactory. The above analysis in Secs. III A and III B for energy change alone can then be immediately modified to yield corresponding results for the stabilization probabilities $P_i^S(E_i,L_i^2)$ for quasibound and bound states. Thus, the diffusion approximation for the bound and quasibound level yields

$$P_d^S(E_i,L_i^2) = \left[\int_{E_i}^{U_i} dE/D^{(2)}(E,L_i^2)\right] \times \left[\int_{-S}^{U_i} dE/D^{(2)}(E,L_i^2)\right]^{-1}, \quad (5.3)$$

where $U_i(L_i^2)$ is the energy at the top of the centrifugal barrier of the effective interaction

$$V_i(R) = V(R) + L_i^2/2mR^2. \quad (5.4)$$

In terms of C_{if} the one way equilibrium rate per unit $dE_i\,dL_i^2\,dE_f\,dL_f^2$ for $(E_i,L_i^2 \to E_f,L_f^2)$ collisional transitions, the diffusion coefficient is

$$D^{(2)}(E_i,L_i^2) = \frac{1}{2}\int_{-D}^{\infty}(E_f - E_i)^2\,dE_f \times \int_0^{L_{0f}^2} C_{if}(E_i,L_i^2;E_f,L_f^2)\,dL_f^2, \quad (5.5)$$

where L_{0f} is the maximum angular momentum for fixed E_f. For dissociated levels P_d^S is zero. The association rate corresponding to the basic rate (2.16) is then given by

$$\alpha\tilde{N}_A\tilde{N}_B = \int_{-D}^{\infty} dE_i \int_0^{L_{0i}^2} P_i^S\,dL_i^2 \int_{-D}^{\infty} dE_f \times \int_0^{L_{0f}^2} (P_i^S - P_f^S)C_{if}\,dL_f^2, \quad (5.6)$$

where the stabilization probabilities P_i^S are given by Eq. (5.3).

VI. SUMMARY

On introduction of stochastic probabilities $P_i^{S,D}(E_i)$ that ion pairs A–B with internal energy E_i will be stabilized or disrupted by collisions with a thermal bath of gas M, and upon the use of the ansatz (2.8) for their normalized distributions $\gamma_i(t)$ at time t, the basic Master equation (2.1), rate (2.2) and current (2.4) has been transformed into corresponding equations (2.9)–(2.11) which are separable in E_i and t. The diffusional equation (3.18), yields, for systems of general mass, accurate probabilities $P_i^{S,D}$ but very inaccurate currents (3.22)–(3.25) (cf. Fig. 3 and Table I). Identification as in Eq. (2.20) of association rates α with current, is valid only under QSS quasi-steady-state condition (2.18), appropriate to the original Master equation (2.9). Since the diffusional probabilities do not satisfy this condition, the diffusional current in general, may not be identified with the rate α. As Table I shows, the resulting diffusional rates (3.22)–(3.25), are therefore not reliable[2–6] except for those cases in which the current is relatively small, i.e., for collision electron–ion recombination[1] in a gas and for ion–ion recombination in a vanishingly light gas.

A new expression (2.11) or (2.16) derived[16] for the rates, is more appropriate for use under general conditions, as when QSS is not satisfied. When QSS is satisfied, Eq. (2.16) reduces to the current (2.23). The QSS rates are minimum (Ref. 18 and work in progress). The rate (2.16) is required when approximate probabilities are used, as here.

The diffusional probabilities can also be used in an iterative solution[4] of the QSS-condition (2.18) to provide highly accurate probabilities (to within 1%) after a few iterations and hence accurate QSS-rates (2.23)–(2.25).

Application of the diffusional equation (3.18) to general systems represents an accurate procedure provided the solutions $P_i^{S,D}$ are inserted in the appropriate and more basic expression (2.16) for the rate, rather than into the derived expressions (3.17) or (2.13) for the diffusional or exact currents. Excellent agreement with the exact numerical QSS results for various classes of ion–neutral interactions over the full range of mass parameters for general systems has been obtained.

Finally, generalization (Sec. V) of the above analysis Secs. II and III to cover the distributions $n(E_i,L_i^2,t)$ of A–B pairs over their internal energy E_i and angular momentum L_i is straightforward. The resulting equations are appropriate to consideration of ion–atom association of atomic species in a gas.

ACKNOWLEDGMENT

This research is supported by the U.S. Air Force of Scientific Research under Grant No. AFOSR-84-0233.

[1] L. P. Pitaevskii, Sov. Phys.–DETP **15**, 919 (1962); E. M. Lifshitz and L. P. Pitaevskii, in *Physical Kinetics* (Pergamon, Oxford, 1981), Chap. 2, pp. 89 and 102.
[2] J. C. Keck and G. Carrier, J. Chem. Phys. **43**, 2284 (1965).
[3] S. A. Landon and J. C. Keck, J. Chem. Phys. **48**, 374 (1968).
[4] J. C. Keck, in *Advances in Atomic and Molecular Physics*, edited by D. R. Bates and I. Estermann (Academic, New York, 1972) Vol. 8, p. 39.
[5] B. H. Mahan, J. Chem. Phys. **48**, 2629 (1968).
[6] D. R. Bates and Z. Jundi, J. Phys. B **1**, 1145 (1968).
[7] D. R. Bates and S. P. Khare, Proc. Phys. Soc. **85**, 231 (1965).
[8] D. R. Bates and R. J. Moffett, Proc. Soc. London Ser. A **291**, 1 (1966).
[9] D. R. Bates and M. R. Flannery, Proc. Soc. London Ser. A **302**, 367 (1968).
[10] M. R. Flannery, J. Phys. B **13**, 3649 (1980); **14**, 915 (1981).
[11] D. R. Bates and I. Mendaš, J. Phys. B **15**, 1949 (1982).
[12] D. R. Bates and I. Mendaš, J. Phys. B **8**, 1770 (1975).
[13] S. B. Byron, R. C. Stabler, and P. I. Bortz, Phys. Rev. Lett. **8**, 376 (1962).
[14] D. R. Bates and C. S. McKibbin, Proc. R. Soc. London Ser. A **339**, 13 (1974).
[15] M. R. Flannery, J. Phys. B **20**, 4929 (1987).
[16] M. R. Flannery, J. Phys. B **18**, L 839 (1985).
[17] M. R. Flannery and T. P. Yang, J. Chem. Phys. **73**, 3239 (1980).
[18] M. R. Flannery, in *Recent Studies in Atomic and Molecular Processes*, edited by A. E. Kingston (Plenum, New York, 1987), p. 167.
[19] M. R. Flannery, in *Applied Atomic Collision Physics*, edited by E. W. McDaniel and W. L. Nighan (Academic, New York, 1982), Vol. 3, p. 141.

ANNUAL TECHNICAL REPORT

ASSOCIATION/DISSOCIATION PROCESSES IN DENSE GASES

By

M. R. Flannery

Prepared for

AIR FORCE OFFICE OF SCIENTIFIC RESEARCH
BOLLING AIR FORCE BASE
WASHINGTON, D. C. 20332

Under

Grant No. AFOSR-84-0233

For Period July 1, 1984 – June 30, 1985

GEORGIA INSTITUTE OF TECHNOLOGY
A UNIT OF THE UNIVERSITY SYSTEM OF GEORGIA
SCHOOL OF PHYSICS
ATLANTA, GEORGIA 30332

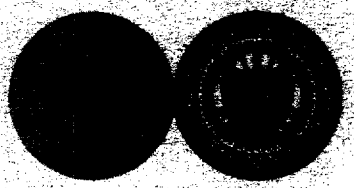

GEORGIA TECH 1885-1985

SECURITY CLASSIFICATION OF THIS PAGE

REPORT DOCUMENTATION PAGE

1a. REPORT SECURITY CLASSIFICATION UNCLASSIFIED	1b. RESTRICTIVE MARKINGS
2a. SECURITY CLASSIFICATION AUTHORITY	3. DISTRIBUTION/AVAILABILITY OF REPORT Approved for public release; distribution unlimited.
2b. DECLASSIFICATION/DOWNGRADING SCHEDULE	
4. PERFORMING ORGANIZATION REPORT NUMBER(S) GIT-85-001	5. MONITORING ORGANIZATION REPORT NUMBER(S) N/A
6a. NAME OF PERFORMING ORGANIZATION Georgia Institute of Technology 6b. OFFICE SYMBOL (If applicable)	7a. NAME OF MONITORING ORGANIZATION Air Force Office of Scientific Research (AFOSR) Directorate of Physical and Geophysical Sciences
6c. ADDRESS (City, State and ZIP Code) School of Physics Georgia Institute of Technology Atlanta, Georgia 30332	7b. ADDRESS (City, State and ZIP Code) AFOSR/NP Bolling Air Force Base, Bldg. 410 Washington, D. C. 20332-6448
8a. NAME OF FUNDING/SPONSORING ORGANIZATION AFOSR 8b. OFFICE SYMBOL (If applicable) NP	9. PROCUREMENT INSTRUMENT IDENTIFICATION NUMBER AFOSR-84-0233
8c. ADDRESS (City, State and ZIP Code) Building 410 Bolling AFB, D.C. 20332-6448	10. SOURCE OF FUNDING NOS. PROGRAM ELEMENT NO.: 61102F; PROJECT NO.: 2301; TASK NO.: A4; WORK UNIT NO.: N/A
11. TITLE (Include Security Classification) Association/Dissociation in Dense Gases (UNCL)	
12. PERSONAL AUTHOR(S) M. R. Flannery	
13a. TYPE OF REPORT Annual Technical Report 13b. TIME COVERED FROM 7/1/84 TO 6/30/85	14. DATE OF REPORT (Yr., Mo., Day) 8/16/85 15. PAGE COUNT 245
16. SUPPLEMENTARY NOTATION	

17. COSATI CODES			18. SUBJECT TERMS (Continue on reverse if necessary and identify by block number)
FIELD	GROUP	SUB. GR.	
N/A	N/A	N/A	

19. ABSTRACT (Continue on reverse if necessary and identify by block number)

A new basic microscopic theory of association/dissociation processes in dense gases has been developed. Expressions for the time-dependent rates $R^{A,D}(t)$ for the association/dissociation of atomic or molecular species A and B in a gas M are formulated in terms of the net probability $P_i^{A,D}$ for association/dissociation of bound energy level i of the pair (A-B).

A new Variational Principle for these rates is proposed and is applied to ion-ion recombination, as a benchmark, with very successful results.

The diffusional theory is examined and it is shown that highly accurate results can be obtained for general mass systems provided the new basic expression introduced here for $R_{A,D}(t)$ is adopted.

The microscopic basis of the macroscopic Debye-Smoluchowski Equation (DSE) is examined and analytical expressions for rates are derived for general interactions between A and B.

(continued)

20. DISTRIBUTION/AVAILABILITY OF ABSTRACT	21. ABSTRACT SECURITY CLASSIFICATION
UNCLASSIFIED/UNLIMITED ☒ SAME AS RPT. ☐ DTIC USERS ☐	UNCLASSIFIED

22a. NAME OF RESPONSIBLE INDIVIDUAL	22b. TELEPHONE NUMBER (Include Area Code)	22c. OFFICE SYMBOL
Dr. Ralph E. Kelley	(202) 767-4908	NP

DD FORM 1473, 83 APR EDITION OF 1 JAN 73 IS OBSOLETE.

SECURITY CLASSIFICATION OF THIS PAGE

19. Abstract (continued)

A valuable relationship between the rates of recombination appropriate to the cases of ions generated with uniform frequency within a reaction volume and ions which approach each other from infinite separation is derived.

Contents

Abstract

During this first year of the new grant, research has been initiated and conducted on the development and implementation of a new basic microscopic theory of association/dissociation processes in dense gases. Expressions for the time-dependent rates $R^{A,D}(t)$ for the association/dissociation of atomic or molecular species A and B in a gas M are formulated in terms of the net probability $P_i^{A,D}$ for association/dissociation of bound energy level i of the pair (A-B).

A new Variational Principle for these rates is proposed and is applied to ion-ion recombination, as a benchmark, with very successful results.

The diffusional theory is examined and it is shown that highly accurate results can be obtained for general mass systems provided the new basic expression introduced here for $R_{A,D}(t)$ is adopted.

The microscopic basis of the macroscopic Debye-Smoluchowski Equation (DSE) is examined and analytical expressions for rates are derived for general interactons between A and B.

A valuable relationship between the rates of recombination appropriate to the cases of ions generated with uniform frequency within a reaction volume and ions which approach each other from infinite separation is derived.

1. Research Initiated and Completed

1.1 List of Topics

During the first year (7/1/84 - 6/30/85) of the Grant, theoretical research on the following topics was completed and written up for publication in scientific journals:

(A) General Microscopic Theory of Association/Dissociation Non-Equilibrium Processes in Dense Gases.

(B) Diffusional Theory of Association/Dissociation Non-Equilibrium Processes for General Systems.

(C) Microscopic Basis and Analytical and Numerical Solutions of the Debye-Smoluchowski Equation.

(D) Ion-Ion Recombination at High Ion Density.

1.2 Summary of Topics

A summary of each of the above topics (A) - (D) now follows. Full details of each topic are presented in Appendices (A) - (D) of this report.

Topic (A): Sets of transport-collisional Master Equations for the two-particle non-equilibrium distribution function of subsystems (A-B) in a thermal bath of dense gas M are derived in various physical representations, corresponding to the full range of gas density. Expressions for time-dependent rates $R^{A,D}(t)$ for association/dissociation are formulated in terms of net probabilities $P_i^{A,D}$ for association/dissociation of bound energy level i of pair (A-B), so that association and dissociation are treated in a unified manner and that evolution in time t towards equilibrium is naturally achieved. The expressions for $R^{A,D}$ are also independent of whether or not a quasi-steady-state (QSS) distribution of highly excited levels is assumed and are particularly valuable when approximate probabilities $P_i^{A,D}$ are used. A

new Variational Principle for the rates $R^{A,D}(t)$ is proposed and is applied to ion-ion recombination, as a benchmark, with very successful results. Contact of this Variational Principle (in general for chemical reactions in a gas) is established with Tellegen's Theorem for electrical networks and with Onsager's Principle of Least Dissipation for heat conduction.

Topic (B): Upon re-examination of the foundations of the diffusional treatment of association/dissociation processes involving a non-equilibrium distribution of (A-B) pairs in a gas M, it is shown that highly accurate results may be obtained for general mass systems provided a new and more basic expression for the time-dependent association/dissociation rates $R^{A,D}(t)$ is introduced. These rates $R^{A,D}(t)$ are derived here in terms of the probability $P_i^{A,D}(E_i)$ that (A-B) pairs with internal energy E_i has associative or dissociative character and are obtained without appeal to the quasi-steady-state (QSS) condition for highly excited levels E_i. Then association and dissociation can be treated in a unified way and evolution towards equilibrium with the gas is naturally achieved. Comparison is made between the exact probabilities $P_i^{A,D}$ obtained from the QSS-condition to the Exact input-output Master Equation and those obtained from the derived diffusional equational. $R^{A,D}(t)$ reduces to the constant-in-energy current $J(t)$ through the excited levels only for exact QSS of the Master Equation. When approximate probabilities are adopted, identification of $R^{A,D}(t)$ with $J(t)$ is not justified. The basic expression here for $R^{A,D}(t)$ is appropriate for both exact and approximate (diffusional) probabilities and yields excellent results for ion-ion recombination in a dilute gas over the full range of masses of the species involved and over various classes of ion-neutral interaction (polarization, hard-sphere and charge-transfer).

Topic (C): By explicitly including collisions and by operating at a level more basic than the macroscopic Debye-Smoluchowski Equation (DSE), various assumptions within the DSE-treatment of transport-influenced reactions between A and B in a dense medium M become naturally exposed. The appropriate modification of DSE to description of the kinetics within the region of the sink is provided.

Analytical expressions for probability densities and rates are derived which are exact solutions of DSE (a) at all times t and large internal separations R of the pair (A-B), (b) at long times t and all R and (c) at short times t and all R. Not only are the transient rates $\alpha_S(t)$ and $\alpha_L(t)$ exact at short and long times, respectively, but they are naturally bounded for all times with $\alpha_S(t\to\infty)$ and $\alpha_L(t\to 0)$ tending to the correct limit, albeit with an incorrect transience. Comparison with exact numerical solutions of DSE illustrates the effectiveness of a proposed solution over the full range of time.

Topic (D): By appeal to a Thomson-type treatment of recombination, it is shown that the rate for recombination of ions generated with uniform frrequency within a reaction volume is a factor of (9/4) times greater than the rate for recombination of ions which approach each other from infinite separation. A valuable relationship connecting the two problems is uncovered. The analysis is pertinent to recombination involving dilute and high degrees of ionization.

1.3 Papers Presented at Scientific Meetings

1. "Association/Dissociation in Dense Gases and Adsorption/Desorption on Surfaces" by M. R. Flannery.
2. "Analytical and Numerical Solutions of the Time Dependent Debye-Smoluchowski Equation" by M. R. Flannery and E. J. Mansky.
3. "Electron-Excited Hydrogen and Helium Collisions" by E. J. Mansky and M. R. Flannery.
4. "Symmetric Charge-Transfer Cross Sections in Rare Gas (Rg^+-Rg) Systems" by E. J. Mansky and M. R. Flannery.

All of the above papers were presented at the 37th Annual Gaseous Electronics Conference, October 9-12, 1984, held at the University of Colorado in Boulder.

The abstracts of the above papers now follow.

1.4 Abstracts of Papers Presented

LD-13 Association/Dissociation in Dense Gases and Adsorption/Desorption on Surfaces,* M. R. FLANNERY, Georgia Institute of Technology--A new comprehensive theory[1] is described for the time evolution towards equilibrium of association and dissociation in a dense gas. Expressions are formulated and are illustrated for the net probabilities of association to stable vibrational levels and dissociation to the continuum from an arbitrary bound vibrational level via collision with the thermal gas bath. A general variational principle emerges: The rate which corresponds to the overall direction of the process always adjusts itself to a minimum and the time evolution towards equilibrium is hindered. Analogy is established with Kirchhoff's Laws and Tellegen's Theorem for electrical networks, and with the Principle of Least Dissipation basic to thermodynamics, heat conduction, and fluid mechanics. The theory can also be modified to provide the first basic microscopic account of Associative Desorption of atoms from and Dissociative Chemisorption of molecules to surfaces.

*Research supported by AFOSR under Grant AFOSR-84-0023.

[1]M. R. Flannery, Phys. Rev. A, (1985).

LD-2 Analytical and Numerical Solutions of the Time Dependent Debye-Smoluchowski Equation,* M. R. FLANNERY and E. J. MANSKY, Georgia Institute of Technology--The macroscopic Debye-Smoluchowski Equation (DSE) with a radiation boundary condition has been derived[1] from a basic microscopic theory of association/dissociation processes, A+B → AB, between A and B in a thermal gas bath. There are at present no exact analytical solutions of DSE for general interactions V(R) between A and B for all separations R and time t. We formulate here exact analytical solutions for the conditional probability density and reaction rates (a) at long and short times for all R and (b) at all times for large R and compare the results with direct numerical solutions. We also propose highly accurate working expressions for the rates of transport influenced reactions at all times.

*Research supported by AFOSR under Grant AFOSR-84-0233.

[1]M. R. Flannery, Phys. Rev. A (1985).

LC-1 Electron-Excited Hydrogen and Helium Collisions,* E. J. MANSKY and M. R. FLANNERY, Georgia Institute of Technology--The Multichannel Eikonal Treatment (MET) is modified so as to facilitate highly accurate description of various asymptotic long range dipole couplings important in electron excited atom collisions. MET is applied to excitation in e-H(2s), e-H(2p), e-He(2^1,^{3}S) and e-He(2^1,^{3}P) collisions at intermediate energies. Integral and differential cross sections together with various coherence and alignment parameters for the radiative decay of the n=2 and 3 collisionally-excited P and D states of H and He are determined from MET with 10 channels associated with n = 1, 2, and 3 sublevels. Comparison is made with various recent measurements.

*Research supported by AFOSR under Grant AFOSR-84-0233.

LD-12 Symmetric Charge-Transfer Cross Sections in Rare Gas (Rg^+-Rg) Systems,* E. J. MANSKY and M. R. FLANNERY, Georgia Institute of Technology--Symmetric resonance charge-transfer, elastic, diffusion and viscosity cross sections for the ion-atom collisions: $Rg^+ + Rg$, Rg = He, Ne, Ar, Kr, Xe are determined via a full quantal phase-shift analysis using the pseudopotential of Sinha, et al. [1] for He_2^+; and the spin-orbit ab-initio potentials of Cohen and Schneider [2] for Ne_2^+, Wadt [3] for Ar_2^+, Kr_2^+, and Xe_2^+; and Michels, et al. [4] for Ne_2^+, Ar_2^+, Kr_2^+, and Xe_2^+ at lab energies ranging from 0.001 eV to 1 keV. The long-range ion-atom polarization attraction is explicitly acknowledged in the full interaction and in a JWKB correction to the numerical asymptotic phase shift. Differential cross sections are also obtained. Comparison is made with existing experimental and theoretical data.

*Research supported by AFOSR under Grant AFOSR-84-0233.

[1] S. Sinha, S.L. Lin, and J.N. Bardsley, J. Phys. B 12 (1979) 1613.
[2] J.S. Cohen and B. Schneider, J. Chem. Phys. 61 (1974) 3230.
[3] W.R. Wadt, J. Chem. Phys. 68 (1978) 402.
[4] H.H. Michels, R.H. Hobbs, and L.A. Wright, J. Chem. Phys. 69 (1978) 5151.

1.5 List of Publications (in press and in preparation)

1. "General Microscopic Theory of Association/Dissociation Non-Equilibrium Processes in Dense Gases," M. R. Flannery (Phys. Rev. A).
2. "Diffusional Theory of Association/Dissociation Non-Equilibrium Processes for General Systems," M. R. Flannery (Phys. Rev. A).
3. "Microscopic Basis and Analytical and Numerical Solutions of the Debye-Smoluchowski Equation," M. R. Flannery and E. J. Mansky (Phys. Rev. A).
4. "Ion-Ion Recombination at High Ion Density," M. R. Flannery, J. Phys. B: Atom. Molec. Phys.
5. "Modified Multichannel Eikonal Treatment of Electron Excited Atom (H,He) Collisions," M. R. Flannery and E. J. Mansky (in preparation).
6. "Symmetrical Resonance Charge-Transfer in the Rare-Gas Sequence (Ne, Ar, Kr, Xe)," M. R. Flannery and E. J. Mansky (in preparation).
7. "Kinetic Theory Foundation of Ion-Ion Recombination in a Dense Plasma," M. R. Flannery and E. J. Mansky (in preparation).
8. "A Variational Principle in Dynamics of Relaxation," M. R. Flannery (in preparation).
9. "Classical Theory of Recombination," M. R. Flannery (in preparation).
10. "Selected Bibliography on Atomic Collisions: Data Collections, Bibliographies, Review Articles, Books, and Papers of Particular Tutorial Value," M. R. Flannery, E. W. Thomas and S. T. Manson, Atomic Data and Nuclear Data Tables 33 (1985) 1-148.

Papers #1-4 above are included as Appendices A-D of this report. Reprints of paper #10 will be sent to AFOSR under separate package. Papers #5-10 will be also sent to AFOSR when completed.

1.6 Ph.D. Thesis Supervised

Mr. E. J. Mansky has been a Ph.D. graduate student supervised by the Principal Investigator (M. R. Flannery) and supported by the present and previous AFOSR grants (AFOSR-84-0233 and AFOSR-80-0055). He has now completed his thesis and is expected to graduate with a Ph.D. on September 1985. Copies of his thesis are being prepared and will be submitted in due course to the AFOSR as a separate bound report.

Appendices

In the following Appendices A-D are contained preprints of the following articles submitted for publication to scientific journals.

(A) General Microscopic Theory of Association/Dissociation Non-Equilibrium Processes in Dense Gases.

(B) Diffusional Theory of Association/Dissociation Non-Equilibrium Processes for General Systems.

(C) Microscopic Basis and Analytical and Numerical Solutions of the Debye-Smoluchowski Equation.

(D) Ion-Ion Recombination at High Ion Density.

Appendix A

General Microscopic Theory of Association/Dissociation

Non-Equilibrium Processes in Dense Gases

General Microscopic Theory of Association/Dissociation Non-Equilibrium Processes in Dense Gases

M. R. Flannery
School of Physics,
Georgia Institute of Technology,
Atlanta, Georgia 30332

Abstract. Sets of transport-collisional Master Equations for the two-particle non-equilibrium distribution function of subsystems (A-B) in a thermal bath of dense gas M are derived in various physical representations, corresponding to the full range of gas density. Expressions for time-dependent rates $R^{A,D}(t)$ for association/dissociation are formulated in terms of net probabilities $P_i^{A,D}$ for association/dissociation of bound energy level i of pair (A-B), so that association and dissociation are treated in a unified manner and that evolution in time t towards equilibrium is naturally achieved. The expressions for $R^{A,D}$ are also independent of whether or not a quasi-steady-state (QSS) distribution of highly excited levels is assumed and are particularly valuable when approximate probabilities $P_i^{A,D}$ are used. A new Variational Principle for the rates $R^{A,D}(t)$ is proposed and is applied to ion-ion recombination, as a benchmark, with very successful results. Contact of this Variational Principle (in general for chemical reactions in a gas) is established with Tellegen's Theorem for electrical networks and with Onsager's Principle of Least Dissipation for heat conduction.

PACS: 34.10X, 34.50.1F., 82.20.Mj

I. Introduction

When a distribution of ion-ion ($A^+ + B^-$) pairs, or of ion-atom ($A^+ + B$) pairs or of any (ion or neutral) subsystem of dissociated species denoted in general by (A + B) is introduced in a dense gas of thermal species M, a highly non-equilibrium situation exists. In this paper, a set of Master Equations is formulated for the relaxation from some initial non-equilibrium distribution of dissociated subsystems A + B (or of molecules AB) towards equilibrium with a dense thermal gas M via the pertinent energy-change processes,

$$A + B + M \rightleftarrows AB + M \tag{1.1a}$$

$$A^+ + B + M \rightleftarrows AB^+ + M \tag{1.1b}$$

$$A^+ + B^- + M \rightleftarrows AB + M \tag{1.1c}$$

i.e., by the collisional association (recombination) of the dissociated species, the forward direction of (1.1), or by the reverse of (1.1), the collisional dissociation of molecules AB with an initial distribution characterized by temperature T_{AB} which is higher than the temperature T_M of the dense gas M. A key component of this theory is inclusion of the essential coupling[1] between the macroscopic effects of transport and reaction between A and B in M via a comprehensive microscopic treatment of the process. Evolution of the two particle correlation function for subsystem (A-B) is provided in terms of the internal energy E, internal angular momentum L and internal separation R of the subsystem by explicitly including streaming (diffusion and drift) and discontinuous collisions with the heat bath M.

The present theory is a natural development of that previously proposed[1]

for the rate of ion-ion recombination (1.1c) as a function of density N of the gas M. That theory[1] then emphasized the steady-state rate of recombination which can be expressed in terms of reaction and transport rates. Also the treatment intrinsically assumed that the relative speed v was purely radial and that the ratio of product concentrations of fully dissociated species, of concentration N_A and N_B, to their corresponding product $\tilde{N}_A\tilde{N}_B$ under thermodynamic equilibrium

$$N_A N_B/\tilde{N}_A\tilde{N}_B >> N_{AB}/\tilde{N}_{AB} \tag{1.2}$$

is much larger than the corresponding ratio $N_{AB}/\tilde{N}_{AB}$ for fully associated species. The overall direction of (1.1) is then forward i.e., the overall rate of association is much greater than the rate of dissociation which is then neglected, by comparison. The aim of the present paper is to remove those restrictions and thereby provide a comprehensive account of the time evolution towards equilibrium of a highly non-equilibrium situation via the dynamic balance as in (1.1) between association and dissociation processes, which may then be treated in a unified way.

Because it remains a very basic problem in atomic and molecular physics both in its detailed theoretical elucidation and in its central significance to many physical situations of great current interest, solution of the general problem represented by (1.1) as a function of gas density is considered as a prototype textbook study[1] of a process in which collision theory and statistical mechanics can be coupled via some unified microscopic treatment.

Association and recombination, the forward direction of (1.1), are important in many instances, as for example, in gaseous discharges,[2] in electron-beam pumped exciplex lasers[2,3] (KrF, XeCl etc.), and in the recent Optoacoustic Effect[4] where the acoustic wave is generated by the conversion

into translational heating of a dense gas via termolecular association of the photofragments A and B produced originally by photodissociation of a dense molecular gas AB. For overall dissociation the reverse direction of (1.1), externally-induced non-equilibrium distributions of AB in excited vibrational levels can be produced by absorption by AB but not by M of short-duration high-intensity thermal radiation with temperature $T \gg T_M$, or by the passage of a shock wave through the gas. Here the translational and rotational degrees of freedom of all species will relax to thermal equilibrium at temperature T_S immediately behind the shock wave more rapidly than the much slower relaxation of the vibrational distribution of AB associated with the original and final temperatures T_M and T_S, respectively. Charge-transfer between molecular species (AB^+ - AB) also produces[5] a non-equilibrium distribution of AB in various high vibrational levels. Absorption by AB of laser radiation will of course produce a vibrational distribution strongly peaked about a specific vibrational energy. The vibrational distribution will then relax by collisional association/dissociation processes.

In this paper, (1.1) is considered to be a closed system i.e., irreversible losses by curve crossings $AB \not\rightarrow A + B$, quantum tunnelling, or by mutual neutralization $(A^+ - B^-) \not\rightarrow A^* + B$ are specifically excluded. The concentrations N_A and N_B of subsystems are much less than the concentration N of the gas system M so that the main relaxation mechanisms are energy-changing collisions between the subsystem and gas. Relaxation via radiative transitions and subsystem-subsystem collisions may therefore be neglected. The gas is therefore regarded as a heat bath whose main function is to collisionally exchange energy and angular momentum with the subsystem, while maintaining its original thermodynamic state at temperature T_M at all times, thereby permitting the original dissociated or associated subsystems to relax

to eventual equilibrium at temperature T_M. The above three assumptions help to keep the theory tractable but may, in principle, be all or individually removed via straightforward generalization of what remains, however, a fairly comprehensive theory presented here.

In the limit of low gas densities N, mutual transport of A towards B in the gas M is very rapid so that the process (1.1) is determined by the rate limiting step of reaction. The previous collisional input-output Master Equations of Bates and Moffett[6], of Bates and Flannery[7], of Bates and Mendas[8], of Flannery,[2,9-11] for ion-ion recombination (1.1c), of Bates and McKibbin[12] for ion-atom association (1.1b) and the weak (diffusional) collision treatment of Keck and Carrier[13] and of Anderson and Shuler[14] for association/dissociation (1.1a) have all been designed specifically for reaction only in the limit of low gas densities N. As N is raised the transport rate decreases and the reaction rate increases until the rate limiting step of the overall process in the limit of high gas densities becomes transport. The present paper is therefore concerned with transport-influenced reactions and with the design of appropriate Master Equations which govern transport-reaction processes at all gas densities N. The Master Equation for the limit of low N is well documented and discussed[6-14] and the present theory yields this limit.

The organization of this paper is as follows. In § 2, various representations of the basic equation governing the mutual streaming (transport) of A towards B in the dense gas are presented. The corresponding transport-collisional (reaction) Master Equations for the non-equilibrium distributions are then developed in § 3. Simplifications introduced by assuming equilibrium associated with one or more of various physical variables as interseparation R, internal energy E, and internal angular momentum L of the pair A-B, are then discussed in § 4. Expressions for the rates of

association and dissociation are formulated in § 5 in terms of the solutions to the Master Equation. In § 6, the time evolution towards equilibrium is expressed in terms of the net probabilities of collisional association and dissociation of AB in high vibrational levels. A Variational Principle basic to evolution towards equilibrium then emerges and is discussed in §7. It is new and asserts that the conditional densities (or pair correlation functions) of pairs AB in various energy levels are so distributed that the rates $R^A(t)$ and $R^D(t)$ of association and dissociation, respectively, are extrema at time t. If conditions are such that the overall direction is association, then $R^A(t)$ is minimum and $R^D(t)$ is maximum; for overall direction of dissociation, $R^A(t)$ is maximum and $R^D(t)$ is minimum. Evolution towards eventual equilibrium is therefore hindered and the Principle of Least Dissipation (first derived by Onsager[15] for heat conduction) is satisfied. When equilibrium distributions are assumed for fully associated and dissociated pairs, the Variational Principle yields the quasi-steady state condition (i.e., a steady-state distribution of highly excited levels at all times) which rendered feasible the many pioneering studies[16] by Bates and colleagues of heavy-particle recombination[6-11] and of electron-ion collisional radiative recombination in a plasma[17,18] and in a gas.[19,20] Application of the Variational Principle to ion-ion recombination is made in §7.2.

Finally, in an effort to make this paper complete and comprehensive, Appendix A contains classical distributions corresponding to equilibrium in internal separation R, internal energy E and internal angular momentum L of the pair (A-B) together with various classical-quantal correspondences. In Appendix B are gathered various collision kernels and one-way equilibrium rates for energy-change collisions appropriate to various interactions (charge-transfer[6,10], hard-sphere,[11] polarization[8] and Coulombic) between the subsystem AB and the gas species M. The kernels are expressed in appropriate form for direct application of the present theory.

2. Various Representations of the Transport Equation

The present theory is a natural development and generalization of the microscopic theory recently proposed[1] for the rate of ion-ion recombination (or of any chemical reaction in general) as a function of gas density N. The proposed theory[1] bridged the density gap between the previous quasi-steady-state theories[6-13] based on energy-relaxation alone and therefore valid in the low-density limit, and the macroscopic mobility/diffusion theory[2], valid in the limit of high gas densities N. It was also shown[1] that the steady-state rate of recombination is determined by the well known relation $\alpha = \alpha_{TR}\,\alpha_{RN}/(\alpha_{TR} + \alpha_{RN})$, between the macroscopic rates α_{TR} and α_{RN} of mutual transport and of reaction between the species, respectively. At low N when $\alpha_{TR} >> \alpha_{RN}$ then $\alpha \to \alpha_{RN}$, the rate limiting step, while at high N when $\alpha_{RN} >> \alpha_{TR}$, then $\alpha \to \alpha_{TR}$, the limiting rate. This relationship is also a natural consequence of the macroscopic Debye-Smoluchowski Equation[1] where α_{RN} is regarded as an externally assigned parameter, in contrast to the microscopic theory[1] where α_{RN} is internally determined.

At low N, equilibrium with respect to the internal separation R of the (A-B) pair (ion-atom or atom-atom) is very quickly established in comparison to the much slower relaxation in time t of both the angular momentum L and the internal energy E of the pair. The appropriate time dependent master equation would involve only the set (E,L^2,t) of variables for ion-atom and atom-atom association. For ion-ion recombination, the Coulombic attraction does not support an angular momentum barrier and equilibrium in L^2 is then very quickly established in comparison to energy relaxation so that the master equation involves only (E,t), as in the previous quasi-steady-state treatments.[6-13]

As the gas density N is increased, relaxation in internal separation R occurs in a time comparable to relaxation in internal energy E so that both transport and reaction are coupled. It has already been established[1,21] that a "Boltzmann-like" equation governs the development of the pair correlation function, or conditional probability density $n(\underset{\sim}{R},\underset{\sim}{p},t)$, which is such that $n\, d\underset{\sim}{R}\, d\underset{\sim}{p}$

is the probability that the internal momentum, $\underset{\sim}{p} = m\underset{\sim}{v}$, and internal separation $\underset{\sim}{R}$ of the (A-B) pair of reduced mass m and relative velocity $\underset{\sim}{v}$, is within the interval $d\underset{\sim}{R}\, d\underset{\sim}{p}$ about $(\underset{\sim}{R},\underset{\sim}{p})$ at time t. Thus[1,2]

$$\frac{d}{dt} n(\underset{\sim}{R},\underset{\sim}{p},t) \equiv \frac{\partial n}{\partial t} + \underset{\sim}{v}\cdot\nabla_{\underset{\sim}{R}} n - \left(\frac{\partial V}{\partial R}\right) \hat{\underset{\sim}{R}}\cdot\nabla_{\underset{\sim}{p}} n \tag{2.1a}$$

$$= \sum_{i=1,2} \int_{\underset{\sim}{P}_M} d\underset{\sim}{P}_M \int_{\Omega'_i} d\Omega_i \left[n(\underset{\sim}{R},\underset{\sim}{p}';t) N_0(\underset{\sim}{P}_M') - n(\underset{\sim}{R},\underset{\sim}{p};t) N_0(\underset{\sim}{P}_M)\right]\left[g_{iM}\, \sigma_{iM}(g_{iM},\psi)\right]$$

$$- n(\underset{\sim}{R},\underset{\sim}{p};t)\, \nu(\underset{\sim}{R},\underset{\sim}{p}) \tag{2.1b}$$

where V(R) is the interaction between A and B, where the momentum $\underset{\sim}{P}_M$ of the gas species M is distributed according to a (time-independent) Maxwell distribution $N_0(\underset{\sim}{P}_M)$ at temperature Θ, and where $\sigma_{iM} d\Omega_i$ is the (center-of-mass) cross section for A-M (i = 1) or B-M (i = 2) elastic scattering at relative speed g_{iM} into solid angle $d\Omega_i$. If M is molecular, then σ_{iM} is augmented by the collisional inelastic cross section for rotational and vibrational transitions. The Ω_i-integration in (2.1b) is over that scattering region Ω'_i accessible for the production of all final scalar momenta $p'(\underset{\sim}{p},\underset{\sim}{P}_M,\Omega'_i)$ and $P_M'(\underset{\sim}{p},\underset{\sim}{P}_M,\Omega'_i)$ of the (A-B) pair and the gas, consistent with energy conservation and with fixed $\underset{\sim}{p}$ and $\underset{\sim}{P}_M$. Included also in (2.1b) is a term, $n\nu$ which specifies loss of bound or free pairs via irreversible chemical reaction, as mutual neutralization at frequency ν.

The emphasis of the earlier paper[1] was the steady state recombination rate for the case when there were many more dissociated A-B species than the associated neutrals such that the dominant process was association alone. In this paper, we focus on the time evolution towards equilibrium which is

established by the balance between collisional association of the free pairs and the collisional dissociation of the recombined pairs in a thermal gas bath. In order to facilitate appropriate theoretical development, the transport (streaming changes) portion (2.1a) and the collisional (discontinuous changes) portion (2.1b) of the above Master Equation will be formulated in various representations of physical interest.

2.1 $(\underset{\sim}{R},\underset{\sim}{p})$ Transport Equation.

With $\underset{\sim}{p}$ held fixed at angle θ to variable $\underset{\sim}{R}$, then after some analysis,

$$\underset{\sim}{p}\cdot\nabla_{\underset{\sim}{R}} n(\underset{\sim}{R},\underset{\sim}{p}) = \frac{1}{R^2}\ \frac{\partial}{\partial R}\ (R^2 np\cos\theta)_{p,\theta} + \frac{1}{R}\frac{\partial}{\partial(\cos\theta)}\ [np\ \sin^2\theta]_{p,R} \qquad (2.2)$$

$$+\ \frac{\sin\theta}{R}\ [\cos\phi\left(\frac{\partial n}{\partial\theta_R}\right) + \frac{\sin\phi}{\sin\theta_R}\left(\frac{\partial n}{\partial\phi_R}\right) - \sin\phi\ \cot\theta_R\left(\frac{\partial n}{\partial\phi}\right)\ ]$$

for general $n[\underset{\sim}{R}(R,\theta_R,\phi_R),\ \underset{\sim}{p}(p,\theta,\phi)]$, where $\underset{\sim}{p}(\theta,\phi)$ is directed along (θ,ϕ) of a spherical system with Z-axis along $\underset{\sim}{R}$ which, in turn, is directed along $(\theta_R,\ \phi_R)$ of a space-fixed spherical reference frame. Since the interaction $V(R)$ is radial, then the probability density n is a function only of R, p and θ, the angle between $\hat{\underset{\sim}{R}}$ and $\hat{\underset{\sim}{p}}$. Under azimuthal (ϕ,ϕ_R) symmetry, and with the aid of (2.2) together with the corresponding expression for $\hat{\underset{\sim}{R}}\cdot\nabla_{\underset{\sim}{p}} n$, (2.1a) can be expressed as

$$\frac{d}{dt}\, n(\underset{\sim}{R},\underset{\sim}{p};t) = \frac{\partial n}{\partial t} + \frac{1}{R^2}\frac{\partial}{\partial R}(R^2\ n\ v\ \cos\theta)_{p,\theta} + \frac{1}{R}\frac{\partial}{\partial(\cos\theta)}(n\ v\ \sin^2\theta)_{p,R}$$

$$-\left(\frac{\partial V}{\partial R}\right)[\frac{1}{p^2}\ \frac{\partial}{\partial p}\ (p^2\ n\ \cos\theta)_{R,\theta} + \frac{1}{p}\frac{\partial}{\partial(\cos\theta)}\ (n\ \sin^2\theta)_{p,R}]\ , \qquad (2.3a)$$

which may be cited as the conservative form of the transport equation in one dimensional spherical geometry, since the angular redistribution terms vanish when integrated over the full range $0 \leq \theta \leq \pi$ of the momentum direction $\hat{p}$ for fixed R. An alternative form of (2.3a) is

$$\frac{d}{dt} n(R,p;t) = \frac{\partial n}{\partial t} + v \cos\theta \left[\left(\frac{\partial n}{\partial R}\right)_{p,\theta} - \frac{m}{p} \left(\frac{\partial V}{\partial R}\right)\left(\frac{\partial n}{\partial p}\right)_{R,\theta} \right] \tag{2.3b}$$

$$+ \frac{1}{2} v \sin^2\theta \left[\frac{2}{R} - \frac{1}{(E-V)} \frac{\partial V}{\partial R} \right] \frac{\partial n}{\partial(\cos\theta)_{R,p}}$$

where the internal energy E of the AB pair is

$$E = p^2/2m + V(R) = 1/2\ mv^2 + V(R) = T + V(R) \tag{2.4}$$

in terms of relative kinetic energy T and relative speed v.

2.2 $(R,p,|\cos\theta|)$-Transport Equations

Introduce the superscripts $(\pm)$ to distinguish those pairs n^+ with $\hat{p}$ directed into the upper region, $0 < \theta < \frac{\pi}{2}$ where $\cos\theta > 0$ defines the positive (+) region, with outward directed radial speed, from those pairs n^- with $\hat{p}$ directed into the lower region, $\frac{\pi}{2} < \theta < \pi$ where $\cos\theta < 0$ defines the negative (-) region with inward directed radial speed. At $\theta = \frac{\pi}{2}$, the radial speed $v\cos\theta$ is zero (at the classical turning point of the relative motion).

The set of equations satisfied by,

$$n^{s,d}(R,p,|\cos\theta|;t) = n^+(R,p,|\cos\theta|;t) \pm n^-(R,p,|\cos\theta|;t), \tag{2.5a}$$

the sum (s) and difference (d) of the ϕ-integrated quantities,

$$n^{+}(\underset{\sim}{R},p,|\cos\theta|;t) = \int_{o}^{2\pi} n^{\pm}(\underset{\sim}{R},\underset{\sim}{p};t)d\phi \quad , \tag{2.5b}$$

is obtained from (2.3a) to yield,

$$\frac{d}{dt} n^{s}(\underset{\sim}{R},p,|\cos\theta|;t) = \frac{\partial n^{s}}{\partial t} + \frac{1}{R^2}\frac{\partial}{\partial R}(R^2 n^{d} v|\cos\theta|) + \frac{1}{R}\frac{\partial}{\partial(\cos\theta)}(n^{s} v \sin^2\theta)$$

$$-\left(\frac{\partial V}{\partial R}\right)\left[\frac{1}{p^2}\frac{\partial}{\partial p}(p^2 n^{d}|\cos\theta|) + \frac{1}{p}\frac{\partial}{\partial(\cos\theta)}(n^{s}\sin^2\theta)\right] \tag{2.6a}$$

and

$$\frac{d}{dt} n^{d}(\underset{\sim}{R},p,|\cos\theta|;t) = \frac{\partial n^{D}}{\partial t} + \frac{1}{R^2}\frac{\partial}{\partial R}(R^2 n^{s} v|\cos\theta|) + \frac{1}{R}\frac{\partial}{\partial(\cos\theta)}(n^{d} v \sin^2\theta)$$

$$-\left(\frac{\partial V}{\partial R}\right)\left[\frac{1}{p^2}\frac{\partial}{\partial p}(p^2 n^{s}|\cos\theta|) + \frac{1}{p}\frac{\partial}{\partial(\cos\theta)}(n^{d}\sin^2\theta)\right] \tag{2.6b}$$

2.3 $(\underset{\sim}{R},p)$-Transport Equations

Let

$$n^{\pm}(\underset{\sim}{R},p;t) = \int_{o}^{2\pi} d\phi \int_{0,-1}^{1,0} d(\cos\theta)\, n^{\pm}(\underset{\sim}{R},\underset{\sim}{p};t) \equiv \int_{(+,-)} n(\underset{\sim}{R},\underset{\sim}{p};t)d\hat{\underset{\sim}{p}} \tag{2.7}$$

be the conditional densities (per unit $d\underset{\sim}{R}\ p^2dp$) of pairs that are radially expanding (+) or radially contracting (-) across a fixed element of surface S at radius $\underset{\sim}{R}$. The corresponding intramolecular currents

$$j^{\pm}(\underset{\sim}{R},p;t) = v\int_{(+,-)} n(\underset{\sim}{R},\underset{\sim}{p};t)|\cos\theta|d\hat{\underset{\sim}{p}} \tag{2.8}$$

are the rates (per unit $d\underset{\sim}{R}\, p^2 dp$) that pairs expand (+) or contract (-) across a fixed surface S with normal $\hat{\underset{\sim}{e}}_S$ oriented along the fixed direction $\hat{\underset{\sim}{R}}$. In terms of (2.7) and (2.8), integration of the conservative form (2.3a) over each ($\pm$) region yields,

$$\frac{d}{dt}\, n^{\pm}(\underset{\sim}{R},p;t) = \frac{\partial n^{\pm}}{\partial t} \pm \frac{1}{R^2}\left[\left(\frac{\partial}{\partial R}\right)_p - \frac{m}{p^2}\left(\frac{\partial V}{\partial R}\right)_R p\right]\left[R^2\, j^{\pm}(\underset{\sim}{R},p;t)\right]$$

$$\mp \frac{1}{2}\, v\, n(\underset{\sim}{R},p,\ \theta = \tfrac{\pi}{2};t)\left[\frac{2}{R} - \frac{1}{(E-V)}\frac{\partial V}{\partial R}\right] \quad , \tag{2.9}$$

where, owing to ϕ-symmetry n ($\theta = \frac{\pi}{2}$) is $2\pi\, n^{\pm}(\underset{\sim}{R},\underset{\sim}{p};t)$ evaluated at $\theta = \frac{\pi}{2}$, which corresponds to turning point(s), the pericenter and apocenter (where appropriate) of the orbital motion.

This density $n(\frac{\pi}{2})$ corresponds to orbits (with angular momentum $L_t = |\underset{\sim}{R} \times \underset{\sim}{p}| = Rp$), which are tangential ($\theta = \frac{\pi}{2}$) to, but do not intersect the R-sphere i.e., $n(\frac{\pi}{2})$ is $n^-(\frac{\pi}{2})$ at the pericenter, and is $n^+(\frac{\pi}{2})$ at the apocenter of the appropriate orbits. As R increases from zero, the angular momentum L_t required to provide this tangential orbit must also increase, so that the orbit can only touch the R-sphere externally at its pericenter. For unbound orbits ($E > 0$), L_t can increase indefinitely so that $n(\frac{\pi}{2})$ remains $n^-(\frac{\theta}{2})$ for all R. For bound orbits of specified E, however, then $L_t = Rp$ required for a tangential orbit reaches a maximum at a radius A which is the root of

$$\frac{1}{R^2p^2}\left[\frac{\partial}{\partial R}\,(R^2p^2)\right]_E = \left[\frac{2}{R} - \frac{1}{(E-V)}\frac{\partial V}{\partial R}\right] \equiv \frac{2}{R} - \frac{1}{T}\frac{\partial V}{\partial R} = 0 \tag{2.10}$$

where T is the kinetic energy (E-V).

As R increases beyond this radius A, L_t decreases, and the required

L_t-orbits become internally tangential to the R-sphere at their apocenters; until R reaches the largest apocenter at R = B, the turning point of the L = 0 (straight line) motion determined by $|E| = |V(B)|$ for attractive interaction. Hence the density n in (2.9) is delineated as,

$$n(\underset{\sim}{R},p,\theta=\tfrac{\pi}{2};t) = \begin{cases} n^{-}(R,p,\theta=\tfrac{\pi}{2};t) \quad ; \; T > T^{*} = 1/2\, R\, (\partial V/\partial R) \\ \\ n^{+}(R,p,\theta=\tfrac{\pi}{2};t) \quad ; \; T < T^{*} = 1/2\, R\, (\partial V/\partial R) \end{cases} \tag{2.11}$$

Region I, characterized by $T < T^{*}$ corresponds to ($E > 0$, all R) and to ($E < 0$, $0 \leq R \leq A$) while Region II, characterized by $T < T^{*}$ corresponds to ($E < 0$, $A \leq R \leq B$).

Note that the coefficient of n in (2.9) vanishes at R = A and B. The radius of the bound circular orbit is given by the root of

$$\frac{\partial V_{eff}}{\partial R} \equiv \frac{\partial}{\partial R}\left[V + L^2/2mR^2\right]_L = 0 \tag{2.12}$$

which is identical with A, the root of (2.10) i.e., the circular orbit is associated with the largest value L_{max} of the allowed angular momentum, as expected. Hence, for $R < A$, the pericenters of all orbits with $L < L_t = Rp$ for given E lie within the R-sphere and that orbit with $L = L_t$ touches externally the R-sphere, and the apocenters for all L are all external to the R-sphere. For R = A, $L_t = L_{max}$ and the orbits are circular with the pericenters and apocenters lying on the R-sphere. For $R > A$, the pericenters of all L orbits

and the apocenters of those orbits with $L_t < L < L_{max}$ are within the R-sphere and the apocenters of orbits with $L < L_t$ lie without the R-sphere. The L_t-orbit is internally tangential to the R-sphere at the apocenter.

The radius A of the circular orbit for pure Coulomb attraction is $e^2/2|E|$ and the maximum turning point B is 2A. The turning points appropriate to fixed (E,L^2) are

$$R_{1,2}(E,L^2) = A[1 \pm \{1 - L^2/2m|E|A^2\}^{1/2}]; \; A=e^2/2|E|, \qquad (2.13)$$

such that, at $R_{1,2} = A$ then $L^2[= 2m|E|A^2 = 1/2\ me^4/|E|$ which is the maximum permissible value L^2_{max} of L^2 for a given $|E|]$ decreases with stronger binding $|E|$. For $L = 0$, $R_1 = 0$ and $R_2 = B = 2A$. Also $T > T^* = e^2/2R$ for $E > E^* = (-e^2/2R)$. Hence (2.11) shows that $n(\frac{\pi}{2})$ is n^- for $E > 0$ at all R, is n^- for $E < 0$ and $R < A$, and is n^+ for $E < 0$ and $R > A$.

With the sum (s) and differences (d)

$$n^{s,d}(\underset{\sim}{R},p;t) = n^+(\underset{\sim}{R},p;t) \pm n^-(\underset{\sim}{R},p;t) \qquad (2.14)$$

and with the <u>total</u> (s) current from, and with the <u>net</u> (d) outward current across,

$$j^{s,d}(\underset{\sim}{R},p;t) = j^+(\underset{\sim}{R},p;t) \pm j^-(\underset{\sim}{R},p;t), \qquad (2.15)$$

a fixed $\hat{\underset{\sim}{e}}_s$-surface, then (2.9) is equivalent to the set,

$$\frac{d}{dt}\, n^s(\underset{\sim}{R},p;t) = \frac{\partial n^s}{\partial t} + \frac{1}{R^2}\left[\left(\frac{\partial}{\partial R}\right)_p - \frac{m}{p^2}\left(\frac{\partial V}{\partial R}\right)\left(\frac{\partial}{\partial p}\right)_R p\right]\left[R^2 j^d(\underset{\sim}{R},p;t)\right] \qquad (2.16a)$$

and

$$\frac{d}{dt}\, n^d(\underset{\sim}{R},p;t) = \frac{\partial n^d}{\partial t} + \frac{1}{R^2}\left[\left(\frac{\partial}{\partial R}\right)_p - \frac{m}{p^2}\left(\frac{\partial V}{\partial R}\right)\left(\frac{\partial}{\partial p}\right)_R p\right]\left[R^2 j^s(\underset{\sim}{R},p;t)\right]$$

$$- \left[\frac{2}{R} - \frac{1}{(E-V)}\frac{\partial V}{\partial R}\right] n(\underset{\sim}{R},p;\ \theta = \tfrac{\pi}{2}\ ;t)v \qquad (2.16b)$$

in the $(\underset{\sim}{R},p)$-representation. The above forms are useful when $n^{\pm}(\underset{\sim}{R},p)$ are each independent of θ i.e., when the internal angular momentum states are in thermodynamic equilibrium (see Appendix A). Under this condition the set (2.16) with (2.7) and (2.8) reduces to

$$\frac{d}{dt}\, n^s(\underset{\sim}{R},p;t) = \frac{\partial n^s}{\partial t} + \frac{1}{2}\, v\left[\left(\frac{\partial n^d}{\partial R}\right)_p - \frac{m}{p}\left(\frac{\partial V}{\partial R}\right)\left(\frac{\partial n^d}{\partial p}\right)_R + \left(\frac{2}{R} - \frac{1}{(E-V)}\frac{\partial V}{\partial R}\right) n^d\right] \qquad (2.17a)$$

for the total density n^s and to

$$\frac{d}{dt}\, n^d(\underset{\sim}{R},p;t) = \frac{\partial n^d}{\partial t} + \frac{1}{2}\, v\left[\left(\frac{\partial n^s}{\partial R}\right)_p - \frac{m}{p}\left(\frac{\partial V}{\partial R}\right)\left(\frac{\partial n^s}{\partial p}\right)_R\right]$$

$$+ \frac{1}{2}\, v\left[n^s - 2n(\theta = \tfrac{\pi}{2})\right]\left[\frac{2}{R} - \frac{1}{(E-V)}\frac{\partial V}{\partial R}\right] \qquad (2.17b)$$

Since (2.17a) is appropriate to the L^2-equilibrium averaged value of $\underset{\sim}{v}$, it represents a generalization of Eqs. (2.12),(2.20) and (5.1a) of Ref. 1 which are associated only with the speed v_i along the radial direction $\hat{\underset{\sim}{R}}$.

2.4 $(\underset{\sim}{R},T)$-transport equations.

When the kinetic energy T (= $p^2/2m$) rather than E is used as a variable,

then the corresponding densities and currents (per unit $d\underset{\sim}{R}\ dT\ d\hat{\underset{\sim}{p}}$) are

$$n(\underset{\sim}{R},T,\hat{\underset{\sim}{p}};t) = m\ p\ n(\underset{\sim}{R},\underset{\sim}{p};t) \tag{2.18}$$

and

$$j(R,T,\hat{\underset{\sim}{p}};t) = m\ p\ j(\underset{\sim}{R},\underset{\sim}{p};t) = v\ n(R,T,\hat{\underset{\sim}{p}};t) \tag{2.19}$$

respectively, such that the $\hat{\underset{\sim}{p}}$-integrated quantities which correspond to (2.14) and (2.15) satisfy,

$$\frac{d}{dt}\, n^s(\underset{\sim}{R},T;t) = \frac{\partial n^s}{\partial t} + \frac{1}{R^2}\left[\left(\frac{\partial}{\partial R}\right)_T - \left(\frac{\partial V}{\partial R}\right)\left(\frac{\partial}{\partial T}\right)_R\right]\left[R^2\ j^d(\underset{\sim}{R},T;t)\right] \tag{2.20a}$$

$$\frac{d}{dt}\, n^d(\underset{\sim}{R},T;t) = \frac{\partial n^d}{\partial t} + \frac{1}{R^2}\left[\left(\frac{\partial}{\partial R}\right)_T - \left(\frac{\partial V}{\partial R}\right)\left(\frac{\partial}{\partial T}\right)_R\right]\left[R^2\ j^s(\underset{\sim}{R},T;t)\right]$$

$$- \left[\frac{2}{R} - \frac{1}{T}\frac{\partial V}{\partial R}\right] n(\underset{\sim}{R},T,\ \theta = \tfrac{\pi}{2}\ ;t)v \tag{2.20b}$$

In thermodynamic equilibrium (Appendix A) at temperature Θ, the conditional density factors as

$$\tilde{n}^s(\underset{\sim}{R},\underset{\sim}{p}) = (2\,\pi m\,k\,\Theta)^{-3/2}\ \exp(-p^2/2m)\ \exp(-V(R)/k\Theta), \tag{2.21}$$

and is independent of direction (such that $\tilde{n}^s = 2\tilde{n}^+$, $\tilde{n}^d = 0$). It therefore satisfies the set (2.17), where each term vanishes separately, and the set (2.20) as expected.

2.5 R-Transport Equations.

Integration of (2.16) over the full range $(0,\infty)$ of T therefore yields the set,

$$\frac{d}{dt}\, n^s(\underset{\sim}{R};t) = \frac{\partial n^s}{\partial t} + \frac{1}{R^2}\frac{\partial}{\partial R}\left[R^2 J^d(R)\right] \tag{2.22a}$$

and

$$\frac{d}{dt}\, n^d(\underset{\sim}{R};t) = \frac{\partial n^d}{\partial t} + \frac{1}{R^2}\frac{\partial}{\partial R}\left[R^2\, J^s(R)\right] - \left[\frac{2}{R} - \frac{2}{m}\frac{\langle v^{-1}\rangle}{\langle v\rangle}\left(\frac{\partial V}{\partial R}\right)\right] n(\underset{\sim}{R},\theta = \frac{\pi}{2};t)\ \langle v\rangle \tag{2.22b}$$

where the macroscopic (configuration) densities are

$$n^{s,d}(\underset{\sim}{R};t) = \int_0^\infty n^{s,d}(\underset{\sim}{R},T;t)\,dT \tag{2.23}$$

and the macroscopic (configuration) currents are

$$J^{s,d}(\underset{\sim}{R};t) = \int_0^\infty J^{s,d}(\underset{\sim}{R},T;t)\,dT \tag{2.24}$$

The averaged speeds $\langle v^n\rangle$ in (2.22b) are determined by,

$$n(\underset{\sim}{R},\theta = \tfrac{\pi}{2};t)\ \langle v^n\rangle = \int_0^{T^*} n^+(\underset{\sim}{R},T,\theta = \tfrac{\pi}{2};t)\ v^n\,dT + \int_{T^*}^\infty n^-(\underset{\sim}{R},T,\theta = \tfrac{\pi}{2};t)\ v^n\,dT \tag{2.25}$$

where $T^*(R) = \frac{1}{2}R(\partial V/\partial R)$ is either the kinetic energy of a bound circular orbit of radius R, as in (2.11), or else is zero for unbound orbits, and where

$$n(\underset{\sim}{R}, \theta = \tfrac{\pi}{2};t) = \int_0^{T^*} n^+(\underset{\sim}{R},T, \theta = \tfrac{\pi}{2};t)dT + \int_{T^*}^{\infty} n^-(\underset{\sim}{R},T, \theta = \tfrac{\pi}{2};t)dT \qquad (2.26)$$

is the total macroscopic density at the turning points (apocenter for $T < T^*$ and pericenter for $T > T^*$).

The variable sets $(\underset{\sim}{R},\underset{\sim}{p})$, $(\underset{\sim}{R},p)$, $(\underset{\sim}{R},T)$ and R are quite natural at higher gas densities N, since in the limit of high N, collisions are sufficiently rapid to establish equilibriun in p or T such that (2.3), (2.6), (2.16), (2.20) and (2.22) furnish quite naturally the appropriate non-equilibrium equations in the various variables. When there is T-equilibrium for example, $n^{\pm}$ are separately independent of p and satisfy the Maxwellian distribution

$$\frac{n^{\pm}(\underset{\sim}{R},T;t)}{n^{\pm}(\underset{\sim}{R};t)} = \frac{\tilde{n}^{\pm}(\underset{\sim}{R},T)}{\tilde{n}^{\pm}(\underset{\sim}{R})} = \frac{2}{\sqrt{\pi}} \frac{1}{(k\Theta)^{3/2}} T^{1/2} \exp(-T/k\Theta) \qquad (2.27)$$

where the tildas ($\sim$) denote equilibrium values and where the configurational density is

$$n^{\pm}(\underset{\sim}{R};t) = \int_0^{\infty} n^{\pm}(\underset{\sim}{R},T;t)dT \qquad (2.28)$$

The appropriate non-equilibrium equations for $n^{s,d}(\underset{\sim}{R},t)$ are then (2.22) where the currents are

$$J^{s,d}(\underset{\sim}{R},t) = 1/2\ n^{s,d}(\underset{\sim}{R};t)\ \bar{v} = 1/2\ [n^+(\underset{\sim}{R},t) \pm n^-(\underset{\sim}{R},t)]\ \bar{v} \qquad (2.29)$$

and where the averaged speed

$$\langle v \rangle = \bar{v} = (8\ k\ \Theta/\pi m)^{1/2} \qquad (2.30)$$

is simply the mean thermal speed. For T-equilibrium (2.27) holds such that

$$n(\underset{\sim}{R}, \theta = \tfrac{\pi}{2};t)\langle v\rangle = \bar{v}[n^{+}(\underset{\sim}{R},t) - n^{D}(\underset{\sim}{R},t)\{1 + (T^{*}/k\,\Theta)\exp(-T^{*}/k\Theta)\}] \quad (2.31)$$

and

$$\frac{2}{m}\, n(R, \theta = \tfrac{\pi}{2};t)\langle v^{-1}\rangle = (\bar{v}/k\theta)[n^{+}(\underset{\sim}{R},t) - n^{D}(\underset{\sim}{R},t)\exp(-T^{*}/k\theta)] \quad (2.32)$$

The macroscopic eq. (2.22b) therefore reduces to,

$$\frac{d}{dt}\, n^{d}(\underset{\sim}{R};t) = \frac{\partial n^{d}}{\partial t} + \frac{\bar{v}}{2R^{2}}\frac{\partial}{\partial R}\left[R^{2}\, n^{s}(R;t)\right]$$

$$- \frac{1}{2}\,\bar{v}\left[\frac{2}{R} - \frac{1}{k\Theta}\frac{\partial V}{\partial R}\right]\left[n^{s}(\underset{\sim}{R};t) + n^{d}(\underset{\sim}{R};t)\right] - \frac{2\bar{v}}{R}\, n^{d}(\underset{\sim}{R};t)\exp(-T^{*}(R)/k\Theta) \quad (2.33)$$

which is, of course, coupled to its companion (2.22a), with J^{d} given by (2.29).

In R-equilibrium, $n^{s}(\underset{\sim}{R},t)$ is the Boltzmann distribution

$$\tilde{n}(\underset{\sim}{R}) = \exp[-V(R)/k\Theta] \quad (2.34)$$

and $\tilde{n}^{s} = 2\,\tilde{n}^{+}(R)$, $n^{d} = 0$. Hence both (2.22a) with (2.29) and (2.33) are satisfied in equilibrium, as expected.

At the higher gas densities N where relaxation in R becomes the rate limiting step and where collisions are sufficiently fast to promote equilibrium in p or T, then the sets of equations (2.6), (2.16), (2.20) and

(2.22) derived above are appropriate for application from high N to intermediate N.

2.6 $(\underset{\sim}{R},E,\hat{\underset{\sim}{p}})$-Transport Equations

In the low N-limit, equilibrium in R (i.e., the Boltzmann distribution) is achieved instantaneously relative to the rate limiting step of collisional relaxation in the internal energy E. The set $(\underset{\sim}{R},E,\hat{\underset{\sim}{p}})$ of variables is therefore more natural to this situation. When the relaxation in E and in the internal angular momentum squared,

$$L^2 = R^2p^2 \sin^2\theta = 2m[E-V(R)]\, R^2 \sin^2\theta \tag{2.35}$$

are <u>both</u> slow in comparison with R-relaxation, then the set $(\underset{\sim}{R},E,L^2)$ of variables is more appropriate.

The probability densities germane to the various sets are related by (2.18) and by

$$n(\underset{\sim}{R},\underset{\sim}{p})d\underset{\sim}{R}\, d\underset{\sim}{p} \equiv n_1(\underset{\sim}{R},E,\hat{\underset{\sim}{p}})d\underset{\sim}{R}\, dE\, d\hat{\underset{\sim}{p}} \equiv n_2(\underset{\sim}{R},E,L^2)d\underset{\sim}{R}\, dE\, dL^2\, d\phi \tag{2.36}$$

for the probabilities $n\, d\underset{\sim}{p}$, $n_1\, dE\, d\hat{\underset{\sim}{p}}$ and $n_2\, dE\, dL^2\, d\phi$ that the pair with internal separation in the interval $d\underset{\sim}{R}$ about $\underset{\sim}{R}$ has the physical quantities $\underset{\sim}{p}$, $(E,\hat{\underset{\sim}{p}})$, or (E,L^2,ϕ) in the associated intervals. Hence the various probability densities are related by

$$n(\underset{\sim}{R},\underset{\sim}{p}) = R^2 n_1(\underset{\sim}{R},E,\hat{\underset{\sim}{p}})v/R^2p^2 = 2R^2\, n_2(\underset{\sim}{R},E,L^2)v\cos\theta \tag{2.37}$$

In what follows the ϕ-integrations are implied unless otherwise indicated. In (2.36) the bound levels (E,L^2) of the AB-pair are assumed to lie sufficiently close (relative to the thermal energy $k\Theta$ of the gas bath) that they form a quasi-continuum in energy E and angular momentum L. This restriction is not essential and can be removed by appropriate discretization of the continuous variables E and L^2.

With the recognition that

$$\left(\frac{\partial}{\partial R}\right)_E \equiv \left(\frac{\partial}{\partial R}\right)_p - \frac{m}{p}\left(\frac{\partial V}{\partial R}\right)\left(\frac{\partial}{\partial p}\right)_R \tag{2.38}$$

where the subscript denotes that quantity held constant throughout the appropriate differentiation, then the basic $(\underset{\sim}{R},\underset{\sim}{p})$-equation, (2.3) with (2.4) and (2.36), in the $(R,E,\hat{\underset{\sim}{p}})$-representation is equivalent to,

$$\frac{d}{dt}\, n_1(\underset{\sim}{R},E,\hat{\underset{\sim}{p}};t) = \frac{\partial n_1}{\partial t} + \left[\frac{1}{R^2}\frac{\partial}{\partial R}\left(R^2\, n_1\, v\cos\theta\right)_{E,\theta} + \right.$$

$$\left. \frac{1}{2}\, v\left\{\frac{2}{R} - \frac{1}{(E-V)}\frac{\partial V}{\partial R}\right\}\frac{\partial}{\partial(\cos\theta)}\left(n_1 \sin^2\theta\right)_{R,E}\right] \tag{2.39}$$

which is the conservative form similar to (2.3a), since the angular redistribution term, when integrated over the full range of θ, vanishes as with (2.3a).

2.7 $(\underset{\sim}{R},E,L^2)$-Transport Equations.

The transformation $\underset{\sim}{p} \to (E,L^2,\phi)$ in

$$n(\underset{\sim}{R},\underset{\sim}{p}) = n(\underset{\sim}{R},E(p,R),\, L^2(p,R,\theta),\, \phi) \tag{2.40}$$

may be accomplished via use of the derived identities,

$$\left(\frac{\partial n}{\partial R}\right)_{p,\theta} = \left(\frac{\partial n}{\partial R}\right)_{E,L^2} + \left(\frac{\partial n}{\partial E}\right)_{\underset{\sim}{R},L^2}\left(\frac{\partial E}{\partial R}\right)_{p} + \left(\frac{\partial n}{\partial L^2}\right)_{\underset{\sim}{R},E}\left(\frac{\partial L^2}{\partial R}\right)_{p,\theta} \tag{2.41a}$$

$$\left(\frac{\partial n}{\partial p}\right)_{\underset{\sim}{R},\theta} = \left(\frac{\partial n}{\partial E}\right)_{\underset{\sim}{p},L^2}\left(\frac{\partial E}{\partial p}\right)_{R} + \left(\frac{\partial n}{\partial L^2}\right)_{\underset{\sim}{R},E}\left(\frac{\partial L^2}{\partial p}\right)_{R,\theta} \tag{2.41b}$$

$$\left[\frac{\partial n}{\partial(\cos\theta)}\right]_{\underset{\sim}{R},p} = \left(\frac{\partial n}{\partial L^2}\right)_{\underset{\sim}{R},E}\left[\frac{\partial L^2}{\partial(\cos\theta)}\right]_{R,p} \tag{2.41c}$$

Also the derived identity

$$\left(\frac{\partial}{\partial R}\right)_{E,L^2} = \left(\frac{\partial}{\partial R}\right)_{E,\theta} + \frac{\sin^2\theta}{2\cos\theta}\left\{\frac{2}{R} - \frac{1}{(E-V)}\frac{\partial V}{\partial R}\right\}\left[\frac{\partial}{\partial(\cos\theta)}\right]_{R,E} \tag{2.41d}$$

is valuable for transformation between derivatives taken with respect to fixed L^2 and fixed θ, respectively.

Hence (2.3a) reduces after some analysis simply to

$$\frac{d}{dt}\, n(\underset{\sim}{R},\underset{\sim}{p};t) = \frac{\partial n}{\partial t} + v\cos\theta\left[\frac{\partial}{\partial R} n(\underset{\sim}{R},\underset{\sim}{p};t)\right]_{E,L^2} \tag{2.42a}$$

for $n(\underset{\sim}{R},\underset{\sim}{p};t)$, or with the aid of (2.37) for $n_1(\underset{\sim}{R},E,\hat{\underset{\sim}{p}})$ to

$$\frac{d}{dt}\, n_1(\underset{\sim}{R},E,\hat{\underset{\sim}{p}};t) = \frac{\partial n_1}{\partial t} + \frac{(R^2p^2\cos\theta)}{R^2}\frac{\partial}{\partial R}\left[R^2\, n_1(\underset{\sim}{R},E,\hat{\underset{\sim}{p}};t)v/R^2p^2\right]_{E,L^2} \tag{2.42b}$$

which, with the aid of (2.41d) can be shown to be identical with the conservative form (2.39) for $n_1(\underset{\sim}{R},E,\hat{\underset{\sim}{p}};t)$. In the $(\underset{\sim}{R},E,L^2)$-representation, (2.42a) is equivalent to

$$\frac{d}{dt}\, n_2(\underset{\sim}{R},E,L^2;t) = \frac{\partial n_2}{\partial t} + \frac{1}{R^2}\frac{\partial}{\partial R}\left[R^2\, n_2(\underset{\sim}{R},E,L^2;t)v\cos\theta\right]_{E,L^2} \tag{2.43a}$$

for $n_2(\underset{\sim}{R},E,L^2;t)$ of (2.36) in terms of quantities (E,L^2) which are naturally conserved in the absence of collisions with the gas. An equivalent and useful form of (2.42a) is obtained from (2.37) and (2.42b) as,

$$\frac{d}{dt}\, n_2(\underset{\sim}{R},E,L^2;t) = \frac{\partial n_2}{\partial t} + \frac{1}{2R^2}\frac{\partial}{\partial R}\left[n_1(\underset{\sim}{R},E,\hat{\underset{\sim}{p}};t)v/p^2\right]_{E,L^2} \tag{2.43b}$$

In contrast to (2.3) for $n(\underset{\sim}{R},\underset{\sim}{p})$, and to (2.39) for $n_1(\underset{\sim}{R},E,\hat{\underset{\sim}{p}})$, the microscopic vector current

$$\underset{\sim}{j}_2(\underset{\sim}{R},E,L^2;t) = n_2(\underset{\sim}{R},E,L^2;t)\underset{\sim}{v} \quad , \tag{2.44}$$

associated with the density n_2 of particles with fixed internal energy E and angular momentum L, across a fixed surface therefore satisfies the simple transport equation

$$\frac{dn}{dt} = \frac{\partial n}{\partial t} + \frac{1}{R^2}\frac{\partial}{\partial R}\,(R^2 J_R) \tag{2.45}$$

where $n = n_2(\underset{\sim}{R},E,L^2)$, the microscopic density, and J_R is the outward radial component of the microscopic current (2.44).

In spite of the neat simplicity of (2.45) this is the first time to the author's knowledge that the transport terms in the left-hand-side (2.3) of the Boltzmann-like equation (2.1), have been written as (2.43a) in terms of the conserved quantities (E,L^2) of a collisionless plasma being held fixed upon the R-differentiation. The form (2.45) is normally reserved <u>only</u> for the <u>macroscopic net</u> current $\underset{\sim}{J}(R)$ of all particles integrated over all vector momenta $\underset{\sim}{p}$ (in magnitude and in direction). In equilibrium, $(R^2\, n_2\, v\, \cos\theta)$ is

a function only of E (cf. Appendix A) such that the streaming (gradient) term in (2.43) vanishes, as expected.

Introduce $n_2^{\pm}(\underset{\sim}{R},E,L^2;t)$ to distinguish those pairs with the same values of $(\underset{\sim}{R},E,L^2)$ and therefore of

$$|\cos\theta| = [1 - L^2/R^2p^2]^{1/2} \quad , \tag{2.46}$$

but with $\hat{\underset{\sim}{p}}$ directed at θ with $\hat{\underset{\sim}{e}}_S$ into the positive (+) region, $0 < \theta < \frac{\pi}{2}$, or into the negative (-) region $\frac{\pi}{2} < \theta < \pi$. Under this distinction, the transport equation (2.43) is therefore equivalent to the set

$$\frac{d}{dt}\, n^{\pm}(\underset{\sim}{R},E,L^2;t) = \frac{\partial n^{\pm}}{\partial t} \pm \frac{1}{R^2}\frac{\partial}{\partial R}\left[R^2\, n^{\pm}(\underset{\sim}{R},E,L^2;t)v|\cos\theta|\right]_{E,L^2} \tag{2.47a}$$

for $n^{\pm}$, or to the set,

$$\frac{d}{dt}\, n^{s}(\underset{\sim}{R},E,L^2;t) = \frac{\partial n^{s}}{\partial t} + \frac{1}{R^2}\frac{\partial}{\partial R}\left[R^2\, j^{d}(\underset{\sim}{R},E,L^2;t)\right]_{E,L^2} \tag{2.47b}$$

$$\frac{d}{dt}\, n^{d}(\underset{\sim}{R},E,L^2;t) = \frac{\partial n^{d}}{\partial t} + \frac{1}{R^2}\frac{\partial}{\partial R}\left[R^2\, j^{s}(\underset{\sim}{R},E,L^2;t)\right]_{E,L^2} \tag{2.47c}$$

for the sum (s) and difference (d),

$$n^{s,d}(\underset{\sim}{R},E,L^2;t) = n_2^{+}(\underset{\sim}{R},E,L^2;t) \pm n_2^{-}(\underset{\sim}{R},E,L^2;t) \tag{2.48}$$

of those (E,L^2) pairs which are expanding (+) or contracting (-) across R with associated total (s) and net (d) currents

$$j^{s,d}(\underset{\sim}{R},E,L^2;t) = n^{s,d}(\underset{\sim}{R},E,L^2;t)v|\cos\theta| \tag{2.49}$$

with direction $\hat{\underset{\sim}{p}}$ at angle θ with the normal $\hat{\underset{\sim}{e}}_s$ to the fixed surface. The set (2.47) represents quite a formal simplification over the corresponding set (2.6) in the equivalent $(\underset{\sim}{R},p,|\cos\theta|)$-representation.

On integrating (2.43b) over the configuration volume between two spheres of radii $R_1(E,L^2)$ and $R_2(E,L^2)$, the turning points (pericenter and apocenter) for bound ($E < 0$) orbits and on recalling that n at R_1 and R_2 is n^- and n^+ respectively, then,

$$\frac{d}{dt}\, n^{\pm}(E,L^2;t) = \frac{\partial n^{\pm}}{\partial t} \pm 2\pi\left[(v_2/p_2^2)n\,(\underset{\sim}{R}_2,E,\theta=\pi/2;t) - (v_1/p_1^2)n^-(\underset{\sim}{R}_1,E,\theta=\pi/2;t)\right] \tag{2.50}$$

where p_i and v_i are the momenta and speeds at $R_i(i=1,2)$. Hence

$$n^{s,d}(E,L^2;t) \equiv n^+(E,L^2;t) \pm n^-(E,L^2;t) = \int_{R_1(E,L^2)}^{R_2(E,L^2)} n^{s,d}(\underset{\sim}{R},E,L^2;t)d\underset{\sim}{R} \tag{2.51}$$

satisfy the set

$$\frac{d}{dt}\, n^s(E,L^2;t) = \frac{\partial}{\partial t} n^s(E,L^2;t) \tag{2.52a}$$

and

$$\frac{d}{dt}\, n^d(E,L^2;t) = \frac{\partial n^d}{\partial t} + 4\pi\left[(v_2/p_2^2)n^+(\underset{\sim}{R}_2,E,\theta=\pi/2;t)\right.$$

$$\left. - (v_1/p_1^2)n^-(\underset{\sim}{R}_1,E,\theta=\pi/2;t)\right] \tag{2.52b}$$

The significance of the source/sink term in (2.52b) becomes transparent upon assuming $\underset{\sim}{R}$-equilibrium when (Appendix A),

$$\frac{n(\underset{\sim}{R},E,L^2;t)}{n(E,L^2;t)} = \frac{\tilde{n}(\underset{\sim}{R},E,L^2)}{\tilde{n}(E,L^2)} = \left[2\pi R^2\, v|\cos\theta|\tau_R(E,L^2)\right]^{-1} \tag{2.53}$$

where τ_R is the time to complete one radial orbit ($R_1 \to R_2 \to R_1$) for fixed E and L^2. With the aid of (2.37), (2.52b) therefore reduces to

$$\frac{d}{dt}\, n^d(E,L^2;t) = \frac{\partial n^d}{\partial t} + 4n^d(E,L^2;t)/\tau_R(E,L^2) \tag{2.54}$$

which with (2.51a) yields,

$$\frac{d}{dt}\, n^{\pm}(E,L^2;t) = \frac{\partial n^{\pm}}{\partial t} \pm 2(n^+ - n^-)/\tau_R(E,L^2); \quad E < 0 \tag{2.55a}$$

i.e., at every half periods, expanding (+) pairs in bound orbits are converted by transport at the apocenter into contracting-pairs, and contracting (-) pairs are converted at the pericenter into expanding (+) pairs. For unbounded (E > 0) orbits only the pericenter R_1 is relevant. Since $n^{\pm} \to \frac{1}{2}\tilde{n}$ as $R \to \infty$ then (2.55a) is replaced by

$$\frac{d}{dt}\, n^{\pm}(E,L^2;t) = \frac{\partial n^{\pm}}{\partial t} \mp 2n^-/\tau_R(E,L^2); \quad E > 0 \tag{2.55b}$$

such that transport converts contracting (-) pairs to expanding (+) pairs at the pericenter. Hence each set (2.50) or (2.52) of transport equations yields quite naturally the radial period under $\underset{\sim}{R}$-equilibrium and therefore contains rather instructive information, particularly useful when orbital and collisional times are to be compared.

2.8 (R,E)-Transport Equations

Since L^2 in (2.35) varies between 0 and $L_t^2 = R^2p^2$ for fixed R and E as $\hat{p}$ varies within each separate (+) or (-) region, the use of Leibnitz's rule[22] for R-differentiation of an integral with variable R-limits yields,

$$\int_0^{R^2p^2} \frac{1}{R^2}\frac{\partial}{\partial R}\left(R^2\, n_2\, v\cos\theta\right)_E dL^2 = \frac{1}{R^2}\frac{\partial}{\partial R}\left[R^2 \int_0^{R^2p^2} n_2\, v\cos\theta \;\; L^2\right]_E - \left[n_2\, v\cos\theta\right]_{\theta=\pi/2}\left[\frac{\partial}{\partial R}\left(R^2p^2\right)\right]_E \qquad (2.56)$$

With the aid of (2.37)

$$j(\underset{\sim}{R},E,L^2;t) = n_2(\underset{\sim}{R},E,L^2;t)\,v\,|\cos\theta| = n_1(\underset{\sim}{R},E,\theta;t)\,v/(2R^2p^2) \qquad (2.57)$$

and with the aid of (2.10), the L^2-integration of (2.43) over the range $(0 \to L_t^2)$ therefore yields

$$\frac{d}{dt}\,n^{\pm}(\underset{\sim}{R},E;t) = \frac{\partial n^{\pm}}{\partial t} \pm \frac{1}{R^2}\frac{\partial}{\partial R}\left[R^2\, j^{\pm}(\underset{\sim}{R},E;t)\right]_E \mp \frac{1}{2}\,v\left[\frac{2}{R} - \frac{1}{(E-V)}\frac{\partial V}{\partial R}\right] n_1(\underset{\sim}{R},E,\theta=\tfrac{\pi}{2};t) \qquad (2.58)$$

for the integrated densities

$$n^{\pm}(\underset{\sim}{R},E;t) = \int_0^{L_t^2} n_2^{\pm}(\underset{\sim}{R},E,L^2;t)\,dL^2 \qquad (2.59)$$

and currents

$$j^{\pm}(\underset{\sim}{R},E;t) = v \int_0^{L_t^2} n_2^{\pm}(\underset{\sim}{R},E,L^2;t)\,|\cos\theta|\,dL^2 \equiv n^{\pm}(\underset{\sim}{R},E;t)\; v\langle|\cos\theta|\rangle \tag{2.60}$$

The equivalent set of equations for

$$n^{s,d}(\underset{\sim}{R},E;t) = n^{+}(\underset{\sim}{R},E;t) \pm n^{-}(\underset{\sim}{R},E;t) \tag{2.61}$$

and the corresponding currents

$$j^{s,d}(\underset{\sim}{R},E;t) = j^{+}(\underset{\sim}{R},E;t) \pm j^{-}(\underset{\sim}{R},E,t) \tag{2.62}$$

which are the total (s) and net(d) rates (per unit $d\underset{\sim}{R}\,dE$) at which particles with speed v leave or cross a surface with normal $\hat{\underset{\sim}{e}}_S$ oriented along the fixed direction $\underset{\sim}{R}$, is

$$\frac{d}{dt}\, n^{s}(\underset{\sim}{R},E;t) = \frac{\partial n^{s}}{\partial t} + \frac{1}{R^2}\frac{\partial}{\partial R}\left[R^2\, j^{d}(\underset{\sim}{R},E;t)\right]_E \tag{2.63a}$$

and

$$\frac{d}{dt}\, n^{d}(\underset{\sim}{R},E;t) = \frac{\partial n^{d}}{\partial t} + \frac{1}{R^2}\frac{\partial}{\partial R}\left[R^2\, j^{s}(\underset{\sim}{R},E;t)\right]_E - v\left[\frac{2}{R} - \frac{1}{(E-V)}\frac{\partial V}{\partial R}\right] n_1(\underset{\sim}{R},E,\tfrac{\pi}{2};t) \tag{2.63b}$$

On integration of (2.39) for $n_1(\underset{\sim}{R},E,\hat{\underset{\sim}{p}};t)$ over the positive (+) region $0 < \theta < \frac{\pi}{2}$, and the negative (-), $\frac{\pi}{2} < \theta < \pi$, region of $\hat{\underset{\sim}{p}}$, the above set (2.58) for

$$n^{\pm}(\underset{\sim}{R},E;t) = \int_{(+,-)} n_1(\underset{\sim}{R},E,\hat{\underset{\sim}{p}};t)d\hat{\underset{\sim}{p}} \tag{2.64}$$

$$j^{\pm}(\underset{\sim}{R},E;t) = v \int_{(+,-)} n_1(\underset{\sim}{R},E,\hat{\underset{\sim}{p}};t)|\cos\theta|\, d\hat{\underset{\sim}{p}} \tag{2.65}$$

and the set (2.63) for $n^{s,d}$ also follow directly, since the $\underset{\sim}{R}$-differential operator in (2.39) and the $\hat{\underset{\sim}{p}}$-integral operator in (2.64) simply commute. On integrating (2.63) over the full range $-V(R) \leq E \leq \infty$ of energies E, and with the use of Leibnitz's rule, the macroscopic set (2.22) of equations, for

$$n^{s,d}(\underset{\sim}{R}) = \int_{-V(R)}^{\infty} n^{s,d}(\underset{\sim}{R},E;t)\, dE \tag{2.66}$$

and

$$J^{s,d}(\underset{\sim}{R}) = \int_{-V(R)}^{\infty} j^{s,d}(\underset{\sim}{R},E;t)\, dE \tag{2.67}$$

is also reproduced with the averaged speeds determined by

$$n_1(R, \theta = \tfrac{\pi}{2};t)\langle v^n\rangle = \int_{-V}^{E^*} n_1^{+}(R,E, \theta = \tfrac{\pi}{2};t)v^n\, dE + \int_{E^*}^{\infty} n_1^{-}(\underset{\sim}{R},E, \theta = \tfrac{\pi}{2};t)v^n\, dE \tag{2.68}$$

where

$$E^* = 1/2\ R\left(\frac{\partial V}{\partial R}\right) - V(R) \tag{2.69}$$

corresponds to T^* of (2.11), and is the energy of a bound circular orbit of radius R.

For pure Coulombic attraction, $E^* = -e^2/2R < 0$; for $V \sim R^{-2}$, E^* is zero; and for $V = -\alpha e^2/2R^4$ then E^* is $\alpha e^2/2R^4 > 0$.

2.9 E-Transport Equations

On integrating (2.63) over all accessible $\underset{\sim}{R}$, then the equations satisfied by,

$$n^{s,d}(E;t) = \int_0^{R_i} n^{s,d}(\underset{\sim}{R},E;t)\, d\underset{\sim}{R} \tag{2.70}$$

where R_i is either the outermost turning point B determined by $|E| = |V(R_i)|$ for $E < 0$ or is infinity for $E > 0$, are

$$\frac{d}{dt} n^s(E;t) = \frac{\partial}{\partial t} n^s(E;t) \tag{2.71a}$$

for n^s, since the <u>net</u> flux $4\pi R^2\, j^d(R,E;t)$ vanishes at both R_i and zero and

$$\frac{d}{dt} n^d(E \gtrless 0;t) = \frac{\partial n^d}{\partial t} + \lim_{R\to\infty} [4\pi R^2\, j^s(\underset{\sim}{R},E;t)] - 4\pi \int_0^{\infty} n_1^-(\underset{\sim}{R},E,\theta = \tfrac{\pi}{2};t) \times \left[\frac{v}{p^2} \frac{\partial}{\partial R} (R^2p^2)_E\right] dR \tag{2.71b}$$

$$\frac{d}{dt} n^d(E \lessgtr 0;t) = \frac{\partial n^d}{\partial t} - 4\pi\left[\int_0^A n_1^-(R,E,\theta = \tfrac{\pi}{2};t) + \int_A^{R_i} n_1^+(\underset{\sim}{R},E,\theta = \tfrac{\pi}{2};t)\right] \times \left[\frac{v}{p^2} \frac{\partial}{\partial R} (R^2p^2)_E\right] dR \tag{2.71c}$$

for n^d since the <u>total</u> current j^s vanishes at both 0 and R_i. Also A in

(2.71c) is the root of (2.10) for constant E i.e., where $\frac{\partial}{\partial R}\ (R^2p^2)_E$ vanishes.

The physical significance of the above terms becomes apparent upon examination under thermodynamic equilibrium in $\underset{\sim}{R}$ and θ when (Appendix A)

$$\frac{n(\underset{\sim}{R},E)}{n(E)} = \frac{\tilde{n}(\underset{\sim}{R},E)}{\tilde{n}(E)} \tag{2.72}$$

such that (2.71b,c) reduce in this limit to

$$\frac{d}{dt}\, n^d(E\gtrless 0;t) = \frac{\partial n^d}{\partial t} - n^-(E;t)\left[E-V(A)\right]A^2/\int_o^B pR^2dR \tag{2.73a}$$

exactly, since the total transport can be shown to vanish for $\underset{\sim}{R}$-equilibrium, and to

$$\frac{d}{dt}\, n^d(E<0;t) = \frac{\partial n^d}{\partial t} + n^d(E;t)[E-V(A)]A^2/\int_o^B p\ R^2\ dR \tag{2.73b}$$

For Coulombic attraction, $A = e^2/2|E|$ is the semi-major axis and

$$\left[E-V(A)\right]A^2\left[\int_o^B pR^2dR\right]^{-1} = \frac{1}{2}\,2\pi\left[\frac{e^2}{2|E|}\right]^{3/2}\left(\frac{m}{e^2}\right)^{1/2} = \frac{1}{2}\,\tau(|E|) \tag{2.73c}$$

is simply half the time period τ for a bound orbit of energy E. For Coulomb attraction therefore

$$\frac{d}{dt}\, n^d\,(E\gtrless 0;t) = \frac{\partial n^d}{\partial t} - 4n^-(E;t)/\tau(E) \tag{2.74a}$$

$$\frac{d}{dt}\, n^d\,(E<0;t) = \frac{\partial n^d}{\partial t} + 4n^d\,(E;t)/\tau(E) \tag{2.74b}$$

which, with (2.71a) yields

$$\frac{d}{dt}\, n^{+}_{-}(E>0;t) = \frac{\partial}{\partial t}\, n^{+}_{-} \mp 2n^{-}/\tau(E)$$

$$\frac{d}{dt}\, n^{+}_{-}(E<0;t) = \frac{\partial}{\partial t}\, n^{+}_{-} \pm 2(n^{+}-n^{-})/\tau(E) \qquad (2.75)$$

i.e., after every half-period $(\frac{\tau}{2})$ expanding (+) pairs in bound orbits ($E < 0$) are naturally converted at the apocenter into contracting (-) pairs which in turn (for bound and unbounded orbits) are converted at the pericenter into expanding (+) pairs. This result is quite general in that it can also be deduced from the corresponding eq. (2.54) for (E,L^2)-nonequilibrium in terms of the averaged radial frequency

$$\nu_R(E) = 1/\tau_R(E) = \int [n(E,L^2)/\,\tau(E,L^2)]dL^2/n(E) \qquad (2.76)$$

In this section the basic transport eq. (2.1a) has therefore been represented in various forms (2.6), (2.17), (2.20), 2.22), (2.39), (2.47), (2.52), and (2.63) appropriate, respectively, to the sets - $(\underset{\sim}{R},\underset{\sim}{p})$, $(\underset{\sim}{R},p)$, $(\underset{\sim}{R},T)$, $\underset{\sim}{R}$, $(\underset{\sim}{R},E,p)$, $\underset{\sim}{R},E,L^2)$, (E,L^2) and $(\underset{\sim}{R},E)$ - of variables all pertinent to various ranges of gas densities N. At low → intermediate N, the set $(\underset{\sim}{R},E,L^2)$ is more natural than the set $(\underset{\sim}{R},T)$ which in turn becomes more appropriate for intermediate → high N. The transport equation assumes for the set $(\underset{\sim}{R},E,L^2)$ a particularly simple form (2.43a) normally reserved only for configuration densities (i.e., phase densities $n(\underset{\sim}{R},\underset{\sim}{p})$ integrated over $\underset{\sim}{p}$). This form is also preserved by $n^s(\underset{\sim}{R},E;t)$ in (2.63a) but not by $n^d(\underset{\sim}{R},E;t)$ in (2.63b) due to the conversions at the turning points.

The coupled equations (2.22a) and (2.22b) must in principle be solved to yield the net current $j^d(R)$ in configuration space. It has already been shown[1] via the continuity and momentum equations [which are $\underset{\sim}{v}^s$ velocity

averaged moments (s = 0 and 1, respectively) of Boltzmann's eq. (2.1b)] that J^d may be expressed, to a very good approximation, in terms of the total density n^s, by

$$\underset{\sim}{J}^d(\underset{\sim}{R},t) = \int n(\underset{\sim}{R},\underset{\sim}{p};t)\underset{\sim}{v}\, d\underset{\sim}{p}$$

$$= - D \underset{\sim}{\nabla} n^s(\underset{\sim}{R},t) - (K/e)(\underset{\sim}{\nabla}V)n^s(\underset{\sim}{R};t) \qquad (2.76)$$

where $D = D_A + D_B$ is the diffusion coefficient and $K = K_A + K_B$ is the mobility for the relative diffusional-drift of A and B in the gas M, in terms of the individual coefficients $D_{A,B}$ and mobilities $K_{A,B}$ for each individual species A or B in the gas. This recognition permitted [1] the overall rate α of the process to be analyzed[1] in terms of rates, α_{RN} and α_{TR}, for reaction and transport rates, respectively, which provided great insight to the overall variation of α with gas density. It also helps to establish (§5.3) the microscopic foundation of the Debye-Smoluchowski Equation.

(THIS PAGE INTENTIONALLY LEFT BLANK)

3. Full Transport-Collisional Equations

The collisional rate (2.1b) in the basic equation (2.1) for the development of the two-particle correlation function $n(\underset{\sim}{R},\underset{\sim}{p};t)$ for (A-B) pairs has been transformed to the $(\underset{\sim}{R},E,L^2)$-representation in Appendix B. With the aid of (2.47a) the full Transport-Collisional Master Equation is then

$$\frac{d}{dt}\, n_i^{\pm}(\underset{\sim}{R},E_i,L_i^2;t) = \frac{\partial n_i^{\pm}}{\partial t} \pm \frac{1}{R^2}\frac{\partial}{\partial R}\left[R^2\, n_i^{\pm}(R,E_i,L_i^2;t)v|\cos\theta|\right]_{E_i,L_i^2}$$

$$= \int_{-V_i(R)}^{\infty} dE_f \int_{L_f^2=0}^{L_{tf}^2} dL_f^2 [n_f^{\pm}(\underset{\sim}{R};t)\nu_{if}(R) - n_i^{\pm}(\underset{\sim}{R};t)\nu_{fi}(R)] \qquad (3.1)$$

where the i-index specifies the combined internal energy E_i and internal angular momentum squared L_i^2 of the AB pair and where the direction cosine is

$$|\cos\theta| = |\hat{\underset{\sim}{R}}\cdot\hat{\underset{\sim}{p}}_i| = (1 - L^2/L_{ti}^2)^{1/2} \qquad (3.2)$$

in terms of the maximum internal angular momentum squared

$$L_{ti}^2 \equiv L_t^2(E_i,R) = 2m[E_i - V(R)]R^2 \qquad (3.3)$$

consistent with a fixed internal energy E_i and separation R. Also

$$V_i(R) = V(R) + L_i{}^2/2mR^2 \qquad (3.4)$$

is the effective radial interaction so that $-V_i(R)$ in (3.1) is the energy of the lowest vibrational level of AB consistent with separation R. The collision kernel $\nu_{if}(\underset{\sim}{R},E_i,L_i{}^2;E_f,L_f{}^2)dE_f dL_f{}^2$ is the frequency (s^{-1}) for the transitions

$(\underset{\sim}{R},E_i,L_i^2) \rightarrow (\underset{\sim}{R},E_f+dE_f,\ L_f^2+dL_f^2)$ in the AB pair by collision with the gas species M, under the assumption that $\underset{\sim}{R}$ remains fixed during the encounter between (A-B) and M, an excellent approximation[9] for ion-ion recombination. The superscripts $(\pm)$ indicate, as before, pairs which are radially-expanding (+), $\cos\theta > 0$, or radially-contracting (-), $\cos\theta < 0$, under the provision (2.11) that $n_i(R,E_i,L_{ti}^2;t)$ is $n_i^-(\frac{\pi}{2})$ when $E > E^*$ (region I) where

$$E^* = V + 1/2\ R(\partial V/\partial R) \tag{3.5}$$

and is $n_i^+(\frac{\pi}{2})$ when $E < E^*$ (region II). Since a closed system is assumed, the irreversible loss term $n_i \nu_i$ in (2.1b) can therefore be neglected in (3.1).

3.1 $\underline{(\underset{\sim}{R},E,L^2)\text{-Equations}}$.

Introduce the distribution

$$\gamma_i^{s,d}(\underset{\sim}{R};t) = n_i^{s,d}(\underset{\sim}{R},E_i,L_i^2;t)/\tilde{n}_i(\underset{\sim}{R},E_i,L_i^2) \tag{3.6a}$$

normalized to the conditional probability density $\tilde{n}_i$ for thermodynamic equilibrium (see Appendix A) so that

$$n_i^{\pm}(\underset{\sim}{R},E_i,L^2;t) = \frac{1}{2}\ (\gamma_i^s \pm \gamma_i^d)\ \tilde{n}_i(\underset{\sim}{R},E_i,L^2) \tag{3.6b}$$

The distribution γ_i is then independent of whatever variable $\underset{\sim}{R},E_i$ or L_i^2 is associated with equilibrium. With the aid of the appropriate set (2.47b,c) of transport equations, the Master Equation (3.1) therefore yields the set

$$\frac{d}{dt}\, n_i^s(\underset{\sim}{R},E_i,L_i^2;t) = \frac{\partial n_i^s}{\partial t} + \frac{1}{R^2}\frac{\partial}{\partial R}\left[R^2\, j_i^d(\underset{\sim}{R};t)\right]_{E_i,L_i^2}$$

$$= \int_{-V_i(R)}^{\infty} dE_f \int_0^{L_{tf}^2} dL_f^2 \left[\gamma_f^s(\underset{\sim}{R};t) - \gamma_i^s(\underset{\sim}{R};t)\right]\; C_{if}(\underset{\sim}{R},E_i,L_i^2;E_f,L_f^2) \quad (3.7a)$$

and

$$\frac{d}{dt}\, n_i^d(\underset{\sim}{R},E_i,L_i^2;t) = \frac{\partial n_i^d}{\partial t} + \frac{1}{R^2}\frac{\partial}{\partial R}\left[R^2\, j_i^s(\underset{\sim}{R};t)\right]_{E_i,L_i^2}$$

$$= \int_{-V_i}^{\infty} dE_f \int_0^{L_{tf}^2} dL_f^2 \left[\gamma_f^d(\underset{\sim}{R};t) - \gamma_i^d(\underset{\sim}{R};t)\right]\; C_{if}(\underset{\sim}{R},E_i,L_i^2;E_f,L_f^2) \quad (3.7b)$$

where $i \equiv (E_i,L_i^2)$. Also,

$$n_i^{s,d}(\underset{\sim}{R},E_i,L^2;t) = [n_i^+(\underset{\sim}{R},E_i,L^2;t) \pm n_i^-(\underset{\sim}{R},E_i,L^2;t)] = \gamma_i^{s,d}\, \tilde{n}_i(\underset{\sim}{R},E_i,L_i^2) \quad (3.8)$$

and

$$j_i^{s,d}(\underset{\sim}{R},E_i,L^2;t) = n_i^{s,d}(\underset{\sim}{R},E_i,L^2;t)\; v|\cos\theta| = \gamma_i^{s,d}\, \tilde{j}_i(\underset{\sim}{R},E_i,L_i^2) \quad (3.9)$$

are the densities and corresponding currents for fixed $(\underset{\sim}{R},E_i,L_i^2)$. The equilibrium rate for $i(E_i,L_i^2) \to f(E_f,L_f^2)$ collisional transitions at fixed internal separation $\underset{\sim}{R}$ is

$$C_{if}(\underset{\sim}{R},E_i,L_i^2;E_f,L_f^2) = \tilde{n}_i(\underset{\sim}{R})\, \nu_{if}(R) = \tilde{n}_f(R)\, \nu_{fi}(R) = C_{fi}(\underset{\sim}{R},E_f,L_f^2;E_i,L_i^2), \quad (3.10)$$

and satisfies detailed balance. Dependence on the density N of the thermal gas M occurs both via the (transport) coupling between n_i^s and n_i^d in (3.7) and the linear dependence on N of the collision frequency (per unit $d\underset{\sim}{R}\, dE_i\, dL_i^2$),

$$\nu_{if} = N\, k_{if}(\underset{\sim}{R}, E_i, L_i^2; E_f, L_f^2) \tag{3.11}$$

where k_{if} is the ($cm^3\ s^{-1}$) rate for $i \to f$ transitions by collision between one pair (A-B) with separation $\underset{\sim}{R}$ and one gas atom M (see Appendix B).

3.2 $(\underset{\sim}{R},E)$-Equations.

With the aid of the appropriate set of transport Eqns. (2.63a,b), integration of (3.7) over all accessible L_i^2 yields the set,

$$\frac{d}{dt}\, n_i^s(\underset{\sim}{R}, E_i; t) = \frac{\partial n_i^s}{\partial t} + \frac{1}{R^2}\frac{\partial}{\partial R}\left[R^2\, j_i^d(\underset{\sim}{R};t)\right]_{E_i} \int_{-V(R)}^{\infty} dE_f \left[\gamma_f^s(\underset{\sim}{R};t) - \gamma_i^s(\underset{\sim}{R};t)\right] C_{if}(\underset{\sim}{R}) \tag{3.12a}$$

$$\frac{d}{dt}\, n_i^d(\underset{\sim}{R}, E_i; t) = \frac{\partial n_i^d}{\partial t} + \frac{1}{R^2}\frac{\partial}{\partial R}\left[R^2 j_i^s(\underset{\sim}{R};t)\right]_{E_i} - n_1(\underset{\sim}{R}, E_i, \theta = \tfrac{\pi}{2}; t)\, v\left[\frac{2}{R} - \frac{1}{(E-V)}\frac{\partial V}{\partial R}\right]$$

$$= \int_{-V(R)}^{\infty} dE_f \left[\gamma_f^d(\underset{\sim}{R};t) - \gamma_i^d(\underset{\sim}{R};t)\right] C_{if}(R) \tag{3.12b}$$

in variables $\underset{\sim}{R}$ and E_i for the integrated densities,

$$n_i^{s,d}(\underset{\sim}{R}, E_i; t) = \int_0^{L_{ti}^2} n_i^{s,d}(\underset{\sim}{R}, E_i, L_i^2; t)\, dL_i^2 \tag{3.13}$$

and the integrated currents,

$$j_i^{s,d}(\underset{\sim}{R}, E_i; t) = v \int_0^{L_{ti}^2} n_i^{s,d}(\underset{\sim}{R}, E_i, L_i^2; t)\, |\cos\theta|\, dL_i^2 \tag{3.14}$$

$$= v \int n_1^{s,d}(R, E_i, L_i^2; t)\, |\cos\theta|\, d\hat{\underset{\sim}{p}} \equiv v\, n_i^{s,d}(\underset{\sim}{R}, E_i; t) \langle\cos\theta\rangle$$

Note in (3.12b) that n_1 is the angular density per unit $d\underset{\sim}{R}dE_i\ d(\cos\theta)$, as in (2.36), evaluated at $\theta = \frac{\pi}{2}$ i.e., at the turning points where $L_i^2 = L_{ti}^2$.

The collisional frequency $\nu_{if}(R)$ for $(E_i,\underset{\sim}{R}) \rightarrow (E_f,\underset{\sim}{R})$ transitions integrated over all angular-momentum changes (L_i^2,L_f^2) consistent with fixed E_i and E_f is given by

$$n_i(\underset{\sim}{R},E_i;t)\ \nu_{if}(R) = \int_0^{L_{ti}^2} dL_i^2\ n_i(R,E_i,L_i^2;t) \int_0^{L_{tf}^2} dL_f^2\ \nu_{if}(\underset{\sim}{R},E_i,L_i^2,E_f,L_f^2) \quad (3.15)$$

with corresponding equilibrium collisional rates

$$C_{if}(\underset{\sim}{R}) = \int_0^{L_{ti}^2} dL_i^2 \int_0^{L_{tf}^2} dL_f^2\ C_{if}(\underset{\sim}{R},E_i,L_i^2;E_f,L_f^2) \quad (3.16)$$

in (3.12). Expressions for the averaged rates (3.16) for various interactions between AB and M can be formulated directly from collision theory (refs. 6-12 and Appendix B).

The normalized distribution in (3.12) is

$$\begin{aligned}\gamma_i^{s,d}(\underset{\sim}{R},E_i;t) &= n_i^{s,d}(\underset{\sim}{R},E_i;t)/\tilde{n}_i(R,E_i) \\ &= \Big[\int_0^{L_{ti}^2} \gamma_i^{s,d}(\underset{\sim}{R},E_i,L_i^2;t)\ \tilde{n}_i(R,E_i,L_i^2)dL_i^2\Big]/\tilde{n}_i(\underset{\sim}{R},E_i) \end{aligned} \quad (3.17)$$

and becomes independent of E_i or $\underset{\sim}{R}$ when equilibrium is attained in E_i or $\underset{\sim}{R}$, respectively.

3.3 R-Equations.

On integrating (3.12) over the full range $-V(R) \leq E_i \leq \infty$ of E_i, then, on applying Leibnitz's rule, and on recognition of the null effect of collisions,

the following set

$$\frac{d}{dt} n^s(\underset{\sim}{R};t) = \frac{\partial n^s}{\partial t} + \frac{1}{R^2}\frac{\partial}{\partial R}\left[R^2 J^d(R)\right] = 0 \tag{3.18a}$$

$$\frac{d}{dt} n^d(\underset{\sim}{R};t) = \frac{\partial n^d}{\partial t} + \frac{1}{R^2}\frac{\partial}{\partial R}\left[R^2 J^s(R)\right] = n_1(\underset{\sim}{R},\tfrac{\pi}{2};t) \langle v\rangle \left[\frac{2}{R} - \frac{2}{m}\frac{\langle v^{-1}\rangle}{\langle v\rangle}\left(\frac{\partial V}{\partial R}\right)\right] \tag{3.18b}$$

is obtained for the macroscopic densities (2.66) and currents (2.67). The quantities $n_1 \langle v^n\rangle$ are determined by (2.68). When thermodynamic equilibrium exists in all variables except R, then J^d is E_i-independent and is given by (2.29) so that (3.7a) upon E_i-integration yields (3.18a) directly.

3.4 (E,L^2)-Equation

The appropriate set of transport-collisional equations is, with the use of (2.52),

$$\frac{d}{dt} n_i^s(E_i,L_i^2;t) = \frac{\partial n_i^s}{\partial t} = \int_{-D}^{\infty} dE_f \int_0^{L_{mf}^2} dL_f^2 \,(\gamma_f^s - \gamma_i^s)\, C_{if}(E_i,L_i^2;E_f,L_f^2) \tag{3.19a}$$

where i specifies (E_i,L_i^2), and

$$\frac{d}{dt} n_i^d(E_i,L_i^2;t) = \frac{\partial n_i^d}{\partial t} + 4\pi\left[(v_2/p_2^2)\, n_1^+(\underset{\sim}{R}_2,E_i,\theta=\tfrac{\pi}{2};t) - (v_1/p_1^2)\, n^-(\underset{\sim}{R}_1,E_i,\theta=\tfrac{\pi}{2};t)\right]$$

$$= \int_{-D}^{\infty} dE_f \int_0^{L_{mf}^2} dL_f^2 \,(\gamma_f^D - \gamma_i^D)\, C_{if}(E_i,L_i^2;E_f,L_f^2) \tag{3.19b}$$

where the equilibrium rate for i → f transitions,

$$C_{if} = \int_{R_1'}^{R_2'} C_{if}(\underset{\sim}{R},E_i,L_i^2;E_f,L_f^2)d\underset{\sim}{R} \tag{3.20}$$

is determined by $\underset{\sim}{R}$-integration of (3.10) between the limits $R_1' = \min[R_1(E_i,L_i^2), R_1(E_f,L_f^2)]$ and $R_2' = \min [R_2(E_i,L_i^2), R_2(E_f,L_f^2)]$. The lowest bound vibrational energy of the AB pair is -D and L_{mf}^2 is the square of the maximum angular momentum $(2m|E_f|A^2)$ for $E_f < 0$ or infinity for $E_f > 0$ for a given energy E_f.

3.5 E-Equations.

On integrating (3.12) over all accessible $\underset{\sim}{R}$ consistent with (E_i,E_f), and on adopting the appropriate transport equation (2.71), the densities

$$n_i^{s,d}(E_i;t) = \int_o^{R_i} n_i^{s,d}(\underset{\sim}{R},E_i;t)d\underset{\sim}{R} \tag{2.70}$$

per unit dE_i then satisfy

$$\frac{d}{dt} n_i^s(E_i;t) = \frac{\partial n_i^s}{\partial t} = \int_{-D}^{\infty} dE_f \left[\gamma_f^s(t) - \gamma_i^s(t)\right] C_{if}(E_i,E_f) \tag{3.21a}$$

where -D is the energy of the lowest bound level of AB, and either

$$\frac{d}{dt} n_i^d(E_i \gtrless 0;t) = \frac{\partial n_i^d}{\partial t} + \lim_{R\to\infty}[4\pi R^2 j_i^s(\underset{\sim}{R},E_i;t)] - 4\pi \int_o^{\infty} n_1^-(R,E_i,\theta=\tfrac{\pi}{2};t) \left\{\frac{v}{p^2}\frac{\partial}{\partial R}(R^2p^2)_{E_i}\right\} dR \tag{3.21b}$$

for $E \geq 0$, or

$$\frac{d}{dt} n_i^d(E_i<0;t) = \frac{\partial n_i^d}{\partial t} - 4\pi\Big[\int_o^A n^-(R,E,\theta=\tfrac{\pi}{2};t) + \int_A^B n^+(R,E,\theta=\tfrac{\pi}{2};t)$$

$$\frac{v}{p^2} \frac{\partial}{\partial R} (R^2p^2)_E \; dR \qquad (3.21c)$$

for $E < 0$, set equal to the collisional rate

$$\frac{d}{dt} n_i^d(E_i;t) = \int_{-D}^{\infty} dE_f [\gamma_f^d(t) - \gamma_i^d(t)] \, C_{if}(E_i,E_f) \quad . \qquad (3.21d)$$

The index i specifies only the energy E_i. The equilibrium rate C_{if} in (3.19) for $E_i \to E_f$ collisional transitions at all accessible R and angular momenta L^2 satisfies detailed balance and, in terms of (3.16), is

$$C_{if} = \int_o^{R_{if}} C_{if}(\underset{\sim}{R}) d\underset{\sim}{R} = C_{fi} \qquad (3.22)$$

where R_{if} is the minimum of the outermost turning points R_i and R_f associated with E_i and E_f, respectively. The normalized distributions in (3.21a,b) are

$$\gamma_i(t) = n_i(E_i;t)/\tilde{n}_i(E_i) = \int_o^{R_i} n_i(\underset{\sim}{R},E_i;t) d\underset{\sim}{R} / \int_o^{R_i} \tilde{n}_i(\underset{\sim}{R},E_i) d\underset{\sim}{R}$$

$$= \int_o^{R_i} \gamma_i(\underset{\sim}{R},E_i;t) \, \tilde{n}_i(\underset{\sim}{R},E_i) d\underset{\sim}{R} / \int_o^{R_i} \tilde{n}_i(\underset{\sim}{R},E_i) d\underset{\sim}{R} \qquad (3.23)$$

in terms of (3.17), and become independent of E_i for E_i-equilibrium in n_i. The collision rate (3.15) integrated over $\underset{\sim}{R}$ is

$$n_i(E_i;t)\ \nu_{if} = \int_0^{R_{if}} n_i(\underset{\sim}{R},E_i;t)\ \nu_{if}(R)d\underset{\sim}{R} \qquad (3.24)$$

which reduces to (3.22) for C_{if} under full equilibrium.

In contrast to the above derived transport-collision equations, (3.7) in $(\underset{\sim}{R},E_i,L^2)$, (3.12) in $(\underset{\sim}{R},E_i)$ and (3.18) in $\underset{\sim}{R}$, eq. (3.21a) for n_i^s appears uncoupled from (3.19b). It however remains complex in principle since the collisional rates (3.24) and (3.15) are determined by the solutions $n_i^{s,d}(\underset{\sim}{R},E_i,L^2;t)$ to the original set (3.7). The above sets are equations satisfied by the integrated quantities $n_i(\underset{\sim}{R};E_i;t)$, $n(\underset{\sim}{R};t)$ and $n_i(E_i;t)$ have all been derived from the basic set of Master Equations (3.7) for non-equilibrium in R, E and L_i^2. Assumption of equilibrium in at least one of the variables L_i^2, E_i and $\underset{\sim}{R}$ provides the following simplification via reduction in the dimensionality of the solutions.

4. Various Equilibrium Limits

4.1 L^2-equilibrium; $(\underset{\sim}{R},E)$-nonequilibrium

When thermodynamic equilibrium among the angular momentum levels is established in n_i^+ and n_i^- independently much more rapidly than equilibrium associated with the remaining variables, E_i and $\underset{\sim}{R}$, then (Appendix A)

$$\frac{n_i^{\pm}(\underset{\sim}{R},E_i,L_i^2;t)}{n_i^{\pm}(\underset{\sim}{R},E_i;t)} = \frac{\tilde{n}_i^{\pm}(\underset{\sim}{R},E_i,L_i^2)}{\tilde{n}_i^{\pm}(\underset{\sim}{R},E_i)} = \left[2R^2p^2|\cos\theta|\right]^{-1} \tag{4.1}$$

and hence the normalized distributions $\gamma_i^{s,d}(\underset{\sim}{R},E_i,L_i^2;t)$ are independent of L_i^2. The current (3.9), reduces to

$$j_i^{s,d}(\underset{\sim}{R},E_i,L_i^2;t) = 1/2\ v_i n_i^{s,d}(\underset{\sim}{R},E_i;t)/R^2p^2 \tag{4.2}$$

and is independent of L_i^2 so that the L_i^2-integrated current (3.14) is

$$j_i^{s,d}(\underset{\sim}{R},E_i;t) = 1/2\ v_i n_i^{s,d}(\underset{\sim}{R},E_i;t) = 1/2\ \gamma_i^{s,d}\ \tilde{j}_i \tag{4.3}$$

where $\gamma_i^{s,d}$ are the normalized distributions (3.17).

The equilibrium total current (Appendix A) and its gradient are

$$\tilde{j}_i(R) = \tilde{n}_i^s(\underset{\sim}{R},E_i)v_i = \frac{\exp(-E_i/k\Theta)}{\left[2\pi mk\Theta\right]^{3/2}} \left[8\pi m[E_i - V(R)]\right] , \tag{4.4a}$$

and

$$\frac{1}{R^2}\frac{\partial}{\partial R}(R^2\tilde{j}_i) = \left[\frac{2}{R} - \frac{1}{(E-V)}\frac{\partial V}{\partial R}\right]\tilde{j}_i \tag{4.4b}$$

a relation which is intimately connected with (2.10), since $R^{2\gamma}j_i$ for constant E varies as $L^2_{max} = R^2p^2$. The derivative vanishes at R = A, the radius of the sphere which intersects the maximum number of bound (E,L^2) orbits possible at a given energy $E < 0$.

For L^2-equilibrium (4.1), the directional density (2.37),

$$n_1(\underset{\sim}{R},E_i,\theta;t) = 2R^2p^2\cos\theta\, n_i(\underset{\sim}{R},E_i,L_i^2;t) = n_i^{\pm}(\underset{\sim}{R},E_i;t) \tag{4.5}$$

per unit $d\underset{\sim}{R}\, dE\, d(\cos\theta)$ is therefore independent of θ. The $(\underset{\sim}{R},E_i)$-set of Master Equations (3.12) reduce, with the aid of (4.3) - (4.5) for L^2-equilibrium, to

$$\frac{d}{dt} n_i^s(\underset{\sim}{R},E_i;t) = \frac{\partial n_i^s}{\partial t} + \frac{1}{R^2}\frac{\partial}{\partial R}\left[\frac{1}{2}R^2\,\gamma_i^d(\underset{\sim}{R};t)\tilde{j}_i(R)\right]_{E_i}$$

$$= \int_{-V(R)}^{\infty} dE_f \left[\gamma_f^s(R;t) - \gamma_i^s(R;t)\right] C_{if}(R) \tag{4.6a}$$

and to

$$\frac{d}{dt} n_i^d(\underset{\sim}{R},E_i;t) = \frac{\partial n_i^d}{\partial t} + \frac{1}{R^2}\frac{\partial}{\partial R}\left[\frac{1}{2}R^2\gamma_i(\underset{\sim}{R};t)\tilde{j}_i(R)\right]_{E_i} - (\gamma_i^s \mp \gamma_i^d)\frac{1}{R^2}\frac{\partial}{\partial R}\left(\frac{1}{2}R^2\,\tilde{j}_i\right)_{E_i}$$

$$= \int_{-V(R)}^{\infty} dE_f \left[\gamma_f^d(\underset{\sim}{R};t) - \gamma_i^d(\underset{\sim}{R};t)\right] C_{if}(R) \tag{4.6b}$$

where i now specifies E_i alone.

The upper (-) and lower (+) signs in the third term of (4.6b) respectively apply to region I ($E \geq 0$, all R; $E_i < 0$, $0 \leq R \leq A$) or to region II ($E < 0$, $A \leq B \leq B$). It is important to note that the four equations obtained by

Bates and Mendas[23] from conservation considerations in the interval dEdR and from detailed balance arguments can be rewritten compactly in the form (4.6) with the explicit time dependences $\partial n_i^{s,d}/\partial t$ ignored for all E_i and R. Since (Eq. (2.3)),

$$\frac{1}{R^2}\left[\frac{\partial}{\partial R}\left(R^2 j_i^d\right)\right]_{E_i} = \frac{1}{R^2}\frac{\partial}{\partial R}\left(R^2 j_i^d\right)_{p_i} - v\frac{\partial V}{\partial R}\left(\frac{\partial j_i^d}{\partial p_i}\right)_R$$

it is now apparent that consideration[23] of the variation with R of the flux appropriate to constant E_i is equivalent to consideration of both streaming terms which separately give rise to diffusion and drift, respectively, in contrast to that earlier thought (ref. 1, p 449).

For Coulombic attraction, $V(R) = -e^2/R$, for example, the set (4.6) yields the coupled set,

$$\frac{d}{dt} n_i^s(\underset{\sim}{R},E_i;t) = \frac{\partial n_i^s}{\partial t} + \frac{1}{2}\left[\frac{\partial \gamma_i^d}{\partial R} + \frac{(2E_i - V)}{R(E_i - V)}\gamma_i^d\right]\underset{\sim}{j}_i$$

$$= \int_{-V(R)}^{\infty} dE_f \left[\gamma_f^s(R;t) - \gamma_i^s(R;t)\right] C_{if}(R) \qquad (4.7a)$$

where i denotes E_i, and

$$\frac{d}{dt} n_i^d(\underset{\sim}{R},E_i;t) = \frac{\partial n_i^d}{\partial t} + \frac{1}{2}\left[\frac{\partial \gamma_i^s}{\partial R} + \frac{|2E_i - V|}{R(E_i - V)}\gamma_i^d\right]\underset{\sim}{j}_i$$

$$= \int_{-V(R)}^{\infty} dE_f \left[\gamma_f^d(R;t) - \gamma_i^d(R;t)\right] C_{if}(R) \qquad (4.7b)$$

which can be solved by numerical techniques.

Since $\underset{\sim}{R}$-equilibrium is established at low gas densities N where relaxation in internal energy E is the rate limiting step, the set (4.6) for non-equilibrium R and E is naturally more appropriate for low to intermediate N. In the limit of high N, (Maxwell) equilibrium in scalar momentum p, [or kinetic energy $T \equiv E_i - V(R)$]is established, and relaxation in the separation R is the rate limiting step. Hence, a more natural set of variables for intermediate-high N is (R,T) and the associated transport equation is provided by (2.20). For L^2-equilibrium, the appropriate set satisfied by

$$\gamma_i^{s,d}(\underset{\sim}{R},T_i;t) = n_i^{s,d}(\underset{\sim}{R},T_i;t)/\tilde{n}_i(\underset{\sim}{R},T_i) \tag{4.8}$$

is therefore

$$\frac{d}{dt}\, n_i^s(\underset{\sim}{R},T_i;t) = \frac{\partial n_i^s}{\partial t} + \frac{1}{R^2}\left[\left(\frac{\partial}{\partial R}\right)_{T_i} - \left(\frac{\partial V}{\partial R}\right)\left(\frac{\partial}{\partial T_i}\right)_R\right]\left\{\frac{1}{2}\, R^2 \gamma_i^d(\underset{\sim}{R},T_i;t)\ \tilde{j}_i(\underset{\sim}{R},T_i)\right\}$$

$$= \int_0^\infty dT_f \left[\gamma_f^s(\underset{\sim}{R};t) - \gamma_i^s(\underset{\sim}{R};t)\right] C_{if}(T_i,T_f) \tag{4.9a}$$

where the equilibrium rate C_{if} is simply a function only of T_i and T_f but not of R (see Appendix B), and

$$\frac{d}{dt}\, n_i^d(\underset{\sim}{R},T_i;t) = \frac{\partial n_i^d}{\partial t} + \frac{1}{R^2}\left[\left(\frac{\partial}{\partial R}\right)_{T_i} - \left(\frac{\partial V}{\partial R}\right)\left(\frac{\partial}{\partial T_i}\right)_R\right]\left\{\frac{1}{2}\, R^2 \gamma_i^s(\underset{\sim}{R},T_i;t)\tilde{j}_i(\underset{\sim}{R},T_i)\right\}$$

$$- \frac{1}{2}\,(\gamma_i^s \mp \gamma_i^d)\,\frac{1}{R^2}\,\frac{\partial}{\partial R}\left\{\left(R^2\tilde{j}_i(\underset{\sim}{R},T_i)\right\}_{T_i}\right.$$

$$= \int_0^\infty dT_f \left[\gamma_f^d(\underset{\sim}{R};t) - \gamma_i^d(\underset{\sim}{R};t)\right] C_{if}(T_i,T_f) \tag{4.9b}$$

where $\tilde{j}_i(\underset{\sim}{R},T_i)$ is given by (4.4a) with $T_i = E_i - V(R)$. Thus, the complexity is shifted from solution of Volterra-type[22] integro-differential equations (4.6) with the first order differential taken with respect to one variable, R and with the R-dependent function V(R) as an integration limit, to solution of integro-partial differential equations (4.9) with first-order differentials now taken with respect to two variables (R,T_i) but with fixed $(0,\infty)$ integration limits.

In the limit of high gas density N, the distribution in kinetic energy T

is Maxwellian (2.27), $\gamma_i^{s,d}(\underset{\sim}{R};t)$ are independent of T_i and the collision sides of (4.9) vanish. On integration over T_i, (4.9) then reduces to the coupled set (2.22a) and (2.33) with $\mathcal{J}^d(R)$ is given by (2.29).

4.2 $(L^2,\underset{\sim}{R})$-equilibrium; E-nonequilibrium

If, in addition to L^2-equilibrium, equilibrium in R is established for the <u>total</u> density n_i^s (but not for the <u>net</u> density n_i^d) so that relaxation in E is the rate limiting step, as at low gas densities N, then

$$\frac{n_i^s(\underset{\sim}{R},E_i;t)}{n_i^s(E_i;t)} = \frac{\tilde{n}_i(\underset{\sim}{R},E_i)}{\tilde{n}_i(E_i)} \tag{4.10}$$

and γ_i^s (but not γ_i^d) is therefore independent of R. The set (4.6) reduces in this limit to,

$$\frac{d}{dt}\, n_i^s(\underset{\sim}{R},E_i;t) = \frac{\partial n_i^s}{\partial t} + \frac{1}{R^2}\frac{\partial}{\partial R}\left[\frac{1}{2}R^2\,\gamma_i^d(\underset{\sim}{R};t)\tilde{j}_i\right] = \int_{-V(R)}^{\infty} dE_f\,[\gamma_f^s(t) - \gamma_i^s(t)]C_{if}(R) \tag{4.11a}$$

and to,

$$\frac{d}{dt}\, n_i^d(\underset{\sim}{R},E_i;t) = \frac{\partial n_i^d}{\partial t} \pm \frac{\gamma_i^d(R;t)}{R^2}\frac{\partial}{\partial R}\left[\frac{1}{2}R^2\tilde{j}_i\right] = \int_{-V(R)}^{\infty} dE_f\,[\gamma_f^d(\underset{\sim}{R};t) - \gamma_i^d(\underset{\sim}{R};t)]C_{if}(R) \tag{4.11b}$$

where (+) and (-) apply to regions I and II, respectively. Since $\gamma_i^d(R \to \infty,t)$ for $E_i \geq 0$, and $\tilde{j}_i$ at the turning point $R_i = B$ for bound levels ($E_i < 0$) both

vanish, then integration of (4.11) over all accessible R yields, in terms of the integrated equilibrium collisional rate (3.20),

$$\frac{d}{dt}\, n_i^S(E_i;t) = \frac{\partial n_i^S}{\partial t} = \int_{-D}^{\infty} dE_f \left[\gamma_f^S(t) - \gamma_i^S(t)\right]\, C_{if}(E_i,E_f) \qquad (4.12a)$$

for the total probability density which is decoupled both formally and in practice from its companion,

$$\frac{d}{dt}\, n_i^d(E_i;t) = \frac{\partial n_i^d}{\partial t} \mp \frac{1}{2} \int_o^{R_i} \underset{\sim}{j}_i(R) \left(\frac{\partial \gamma_i^d}{\partial R}\right) d\underset{\sim}{R}$$

$$= \int_{-D}^{\infty} dE_f \int_o^{R_i} d\underset{\sim}{R} \left[\gamma_f^d(\underset{\sim}{R};t) - \gamma_i^d(\underset{\sim}{R};t)\right]\, C_{if}(E_i,E_f,R) \qquad (4.12b)$$

for the net balance of expanding contracting pairs.

This set (4.12) corresponds to the case of equilibrium for n_i^S in $(\underset{\sim}{R},L_i^2)$, via (4.1) and (4.10), for n_i^d in L_i^2 alone via (4.1), and of non-equilibrium for both $n^{S,d}$ in E_i alone. This case is, in general, appropriate to ion-ion recombination at low gas densities N. It is not, however, appropriate to ion-atom or atom-neutral association since here, in contrast to Coulombic attraction in ion-ion recombination, the A-B interaction via the angular momentum barrier can support bound states with positive energies and angular momentum transitions are important.[12] When $\underset{\sim}{R}$-equilibrium is assumed for $n_i^{\pm}$, then γ_i^D in (4.12b) is zero.

Rates for association/dissociation can be determined directly (§ 5) from (4.12a) without recourse to (4.12b) which furnishes via (4.11b) the net densities $n_i^D(\underset{\sim}{R},E_i;t)$ and associated net currents (4.3). The above collisional input-output Master Equation, (4.12a), has been the governing basis of many studies of ion-ion recombination[6-11] and atom-atom association[13,14] at low gas

densities, and was there deduced from simple arguments based on the net rate of growth of pairs in energy level E_i. The complementary Eq. (4.12b) or its basis (4.10b) is new and serves to complete the picture of recombination at low gas densities.

4.3 $\underset{\sim}{R}$-equilibrium; (E,L^2)-nonequilibrium

Even in the limit of low gas densities N, L^2-equilibrium is in general not obtained except for the specific cases of interactions (as Coulombic) which cannot support an angular momentum barrier at positive energies. For ion-neutral[12] and atom-neutral association, it is essential[12] to acknowledge departure from L^2-equilibrium. Low N implies $\underset{\sim}{R}$-equilibrium in n_i^s, i.e.,

$$\frac{n_i^s(\underset{\sim}{R},E_i,L_i^2;t)}{n_i^s(E_i,L_i^2;t)} = \frac{\tilde{n}_i(\underset{\sim}{R},E_i,L_i^2)}{\tilde{n}_i(E_i,L_i^2)} = \left[2\pi v R^2 |\cos\theta| \tau_R\right]^{-1} \tag{4.13}$$

where $\tau_R(E_i,L_i^2)$ is the time (see Appendix B) to complete one radial round trip between the turning points R_1 and R_2. Both the flux, which then reduces to

$$R^2 j_i^s(\underset{\sim}{R},E_i,L_i^2;t) = [n_i^s(E,L_i^2;t)/2\pi \tau_R(E_i,L_i^2)] \tag{4.14}$$

and γ_i^s are then all independent of R. The $(\underset{\sim}{R},E_i,L_i^2)$-set (3.7) reduces to,

$$\frac{d}{dt} n_i^s(\underset{\sim}{R},E_i,L_i^2;t) = \frac{\partial n_i^s}{\partial t} + \frac{1}{R^2}\frac{\partial}{\partial R}\left[R^2 j_i^d(\underset{\sim}{R};t)\right]_{E_i,L_i^2}$$

$$= \int_{-V_i(R)}^{\infty} dE_f \int_0^{L_{tf}^2} dL_f^2 \left[\gamma_f^s(t) - \gamma_i^s(t)\right] C_{if}(R,E_i,L_i^2;E_f,L_f^2) \tag{4.15a}$$

where index i denotes (E_i,L_i^2), and to

$$\frac{d}{dt} n_i^d(\underset{\sim}{R},E_i,L_i^2;t) = \frac{\partial n_i^d}{\partial t} = \int_{-V_i(R)}^{\infty} dE_f \int_o^{L_{tf}^2} dL_f^2 \left[\gamma_f^d(\underset{\sim}{R},t) - \gamma_i^d(\underset{\sim}{R},t)\right]$$

$$C_{if}(\underset{\sim}{R},E_i,L_i^2;E_f,L_f^2) \qquad (4.15b)$$

which is fully decoupled from (4.14a).

The $\underset{\sim}{R}$-integration densities,

$$n_i^{s,d}(E_i,L_i^2;t) = \int_{R_1}^{R_2} n_i^{s,d}(R,E_i,L_i^2;t)d\underset{\sim}{R} \qquad (4.16)$$

therefore satisfy the set

$$\frac{d}{dt} n_i^s(E_i,L_i^2;t) = \frac{\partial n_i^s}{\partial t} = \int_{R_1}^{R_2} d\underset{\sim}{R} \int_{-V_i(R)}^{\infty} dE_f \int_o^{L_{tf}^2} dL_f^2 \left[\gamma_f^s(t) - \gamma_i^s(t)\right] \; C_{if}(R) \qquad (4.17a)$$

since the current j_i^d vanishes at the end points, and

$$\frac{d}{dt} n_i^d(E_i,L_i^2;t) = \frac{\partial n_i^d}{\partial t} = \int_{R_1}^{R_2} d\underset{\sim}{R} \int_{-V_i(R)}^{\infty} dE_f \int_o^{L_{tf}^2} dL_f^2 \left[\gamma_f^d(\underset{\sim}{R};t) - \gamma_i^d(\underset{\sim}{R};t)\right] \; C_{if}(R) \qquad (4.17b)$$

which are now fully decoupled from one another.

The integrations in (4.17a) may then be re-arranged to yield

$$\frac{d}{dt} n_i^s(E_i,L_i^2;t) = \int_{-D}^{\infty} dE_f \int_o^{L_{mf}^2} dL_f^2 \left[\gamma_f^s(t) - \gamma_i^s(t)\right] \int_{R_1'}^{R_2'} C_{if}(R)d\underset{\sim}{R} \qquad (4.18)$$

where $R_2' = \min\left[R_2(E_i,L_i^2),\ R_2(E_f,L_f^2)\right] > R_1' = \min[R_1(E_i,L_i^2),\ R_2(E_f,L_f^2)]$, where

L_{mf}^2 is the square of the maximum angular momentum, $(2m\,|E_f|\,A^2)$ for bound states or infinity for dissociated states], for fixed E_f and where -D is the energy of the lowest bound vibrational level of the AB pair.

Rates for association/dissociation can be obtained (§ 5) directly from (4.17a) without recourse in principle or in practice to its decoupled companion (4.17b), which yield the <u>net</u> densities $n_i^d(\underset{\sim}{R},E_i,L_i^2;t)$ and associated currents j_i^d.

In summary, coupled sets of Master Equations, (4.6), (4.9), (4.12), and (4.17) appropriate to non-equilibrium only in $(\underset{\sim}{R},E_i)$, $(\underset{\sim}{R},T_i)$, E_i, and (E_i,L_i^2) sets of variables have been systematically deduced from the basic set of Master Equations (3.7) for general $(\underset{\sim}{R},E_i,L_i^2)$-non equilibrium. Even for the most reduced case (4.12) of non-equilibrium in E_i alone, the subject of many previous treatments[6-14], the present procedure has uncovered an additional equation (4.12b) valuable for providing the full description of the recombination process at low gas densities.

5. Rates and the Macroscopic Transport-Collisional R-Equation

5.1 Various Energy Blocks

The full transport-collisional equation (3.12a) for the density $n_i^s(\underset{\sim}{R},E_i;t)$ of (3.13) in terms of the net current j_i^d of (3.14) is

$$\frac{d}{dt} n_i^s(\underset{\sim}{R},E_i;t) = \frac{\partial n_i^s}{\partial t} + \frac{1}{R^2}\frac{\partial}{\partial R}[R^2 j_i^d(R)]_{E_i} = -\int_{-V(R)}^{\infty} S_{if}(\underset{\sim}{R},t)\,dE_f \qquad (5.1)$$

where

$$S_{if}(\underset{\sim}{R},t) = n_i^s(\underset{\sim}{R},E_i;t)\,\nu_{if}(R) - n_f^s(\underset{\sim}{R},E_f;t)\,\nu_{fi}(R) = -S_{fi}(\underset{\sim}{R},t) \qquad (5.2)$$

is the <u>net</u> two level collisional rate of depletion of energy level E_i or net rate of production of E_f. The minimum energy level consistent with fixed R is -V(R) which always lies above -D, the lowest energy level.

Subdivide the full region of internal energy E_i into three blocks: the continuum block C with $0 \leq E_i \leq \infty$, an excited block E with $-S \leq E_i \leq 0$ and the block S of lowest excited levels in the range $-D \leq E_i \leq -S$. The block S in principle comprises all those levels between the lowest vibrational level -D ($\sim$5 eV $\approx$ 200 k (300/Θ) at both temperature Θ and an intermediate level -S defined as that level below which the <u>net</u> probability of direct dissociation by collision with the thermal bath is negligible. In practice, level -S arises naturally from the collisional mechanics via the cut-off effect of the Maxwellian distribution of the gas at temperature Θ and generally lies $\sim$ 10 kΘ below the dissociation limit (taken as zero energy). The central block E of highly excited bound levels is sandwiched (Fig. 1) between the continuum C - the fully dissociated block - and the fully associated block S and has no internal sources or sinks but is coupled by collision to both C and S. Each of C and S may be considered as a source/sink combination interconnected by E when

association is the dominant process, or as a sink/source combination when dissociation is dominant. Dissociation can therefore occur via stepwise collisional excitation through intermediate block E, as well as directly.

The macroscopic pair distributions

$$n_c(\underset{\sim}{R},t) = \int_0^\infty n_i\, s(\underset{\sim}{R},E_i;t)\,dE_i \tag{5.3a}$$

in block C,

$$n_e(\underset{\sim}{R},t) = \int_0^\infty n_i\, s(\underset{\sim}{R},E_i;t)\,dE_i \tag{5.3b}$$

in block E, and

$$n_s(\underset{\sim}{R},t) = \int_{-V(R)}^{-S} n_i\, s(\underset{\sim}{R},E_i;t)\,dE_i \tag{5.3c}$$

over those levels in the energy range $-V(R) \leq E_i \leq -S$ of block S accessible by collision at R, therefore satisfy

$$\frac{\partial}{\partial t} n_c(\underset{\sim}{R},t) + \underset{\sim}{\nabla}\cdot\underset{\sim}{J}_c = -\int_0^\infty dE_i \int_{-V}^\infty S_{if}(R,t)\,dE_f \quad , \quad \text{all } R \tag{5.4a}$$

$$\frac{\partial}{\partial t} n_e(\underset{\sim}{R},t) + \underset{\sim}{\nabla}\cdot\underset{\sim}{J}_e = -\int_{-S}^0 dE_i \int_{-V}^\infty S_{if}(R,t)\,dE_f \quad , \quad R \leq R_s \tag{5.4b}$$

$$\frac{\partial}{\partial t} n_s(\underset{\sim}{R},t) + \underset{\sim}{\nabla}\cdot\underset{\sim}{J}_s = -\int_{-V}^{-S} dE_i \int_{-V}^\infty S_{if}(R,t)\,dE_f \quad , \quad R \leq R_s \tag{5.4c}$$

where R_s is the classical turning point associated with level -S. The corresponding contributions from blocks C, E and S to the net radial current

$$J^d(R,t) = \int_{-V}^{\infty} j_i{}^d(R,E_i;t)dE_i = J_c(R,t) + J_e(R,t) + J_s(R,t) \tag{5.5}$$

are J_c, J_e and J_s, respectively. Since $S_{if} = -S_{fi}$ the upper limit to the integration over E_f in (5.4a) is, in effect 0 while the lower E_f-limit -V is, in effect, -S for (5.4c).

Since the net effect of collisions is null for this closed system, summation of 5.35(a)-(c) yields the continuity equation,

$$\frac{\partial}{\partial t}\left[n_c(\underset{\sim}{R},t) + n_e(\underset{\sim}{R},t) + n_s(\underset{\sim}{R},t)\right] + \underset{\sim}{\nabla}\cdot\underset{\sim}{J}^d = 0 \tag{5.6}$$

which agrees with (3.18a). For $R \geq R_s$, block *S* does not exist and

$$\frac{\partial}{\partial t} n_e(\underset{\sim}{R},t) + \underset{\sim}{\nabla}\cdot\underset{\sim}{J}_e = -\int_{-V}^{0} dE_i \int_{-V}^{\infty} S_{if}(R)dE_f \quad , R \geq R_s \tag{5.7}$$

holds instead of (5.4b,c). The lower E_f-limit-V in (5.7) is 0, in effect. Since $j_i{}^d$ vanishes at infinity (for $E_i \geq 0$) and at the classical turning point R_i (for $E_i < 0$), integration of (5.1) over all accessible R-space yields

$$\frac{\partial}{\partial t} n_i(E_i,t) = -\int_{0}^{R_i} \underset{\sim\sim}{dR} \int_{-V}^{\infty} S_{if}(R,t)dE_f = -\int_{-D}^{\infty} dE_f \int_{0}^{R_{if}} S_{if}(R,t)\underset{\sim\sim}{dR} \equiv -\int_{-D}^{\infty} S_{if}(t)dE_f \tag{5.8}$$

for the rate of change of density per unit energy interval. Within (5.8), the formal order of (R,E_f)-integrations has been interchanged, $R_{if} = \min(R_i,R_f)$ and

$$S_{if}(t) = \int_{0}^{R_{if}} S_{if}(R,t)\underset{\sim}{dR} = -S_{fi}(t) \tag{5.9}$$

is the net frequency (per unit $dE_i dE_f$) of collisional transitions ($i \to f$) between E_i and E_f. Hence, the rate of change in the configuration density

$$n_c(t) = \int_0^\infty n_c(\underset{\sim}{R},t)d\underset{\sim}{R} = \int_0^\infty d\underset{\sim}{R} \int_0^\infty n_i{}^s(\underset{\sim}{R},E_i;t)dE_i = \int_0^\infty n_i(E,t)dE_i \quad (5.10)$$

of free pairs is exactly,

$$\frac{\partial}{\partial t} n_c(t) = -\int_0^\infty dE_i \int_0^\infty d\underset{\sim}{R} \int_{-V}^{0} S_{if}(R,t)dE_f = -\int_0^\infty dE_i \int_{-D}^{0} S_{if}(t)dE_f$$

$$= \int_{-D}^{0} dE_i \int_0^\infty S_{if}(t)dE_f \quad (5.11)$$

which can also be obtained by R-integration of (5.4a). The corresponding rate of change in the density

$$n_s(t) = \int_0^{R_s} n_s(\underset{\sim}{R},t)d\underset{\sim}{R} = \int_0^{R_s} d\underset{\sim}{R} \int_{-V}^{-S} n_i{}^s(\underset{\sim}{R},E_i;t)dE_i = \int_{-D}^{-S} n_i(E_i,t)dE_i \quad (5.12)$$

of pairs bound in block S is exactly

$$\frac{\partial}{\partial t} n_s(t) = -\int_{-D}^{-S} dE_i \int_0^{R_i} dR \int_{-V}^{\infty} S_{if}(\underset{\sim}{R},t)dE_f = -\int_{-D}^{-S} dE_i \int_{-S}^{\infty} S_{if}(t)dE_f = \int_{-S}^{\infty} dE_i \int_{-D}^{-S} S_{if}(t)dE_f \quad (5.13)$$

which also follows from R-integration of (5.4c).

Integration of (5.1) over R from 0 to R_s yields,

$$\frac{\partial}{\partial t} \int_0^{R_s} n_i{}^s(\underset{\sim}{R},t)d\underset{\sim}{R} + 4\pi R_s{}^2 j_i{}^d(\underset{\sim}{R}_s,t) = -\int_0^{R_s} d\underset{\sim}{R} \int_{-V}^{\infty} S_{if}(\underset{\sim}{R},t)dE_f \quad (5.14)$$

which expresses continuity for each level E_i within the reaction sphere of radius R_s. Hence with the aid of (5.13),

$$\frac{\partial}{\partial t} \int_{-S}^{\infty} dE_i \int_0^{R_s} n_i{}^s(\underset{\sim}{R},t)d\underset{\sim}{R} + 4\pi R_s{}^2 \int_{-S}^{\infty} j_i{}^d(R_s,t)dE_i = -\int_{-S}^{\infty} dE_i \int_0^{R_s} d\underset{\sim}{R} \int_{-V}^{-S} S_{if}(\underset{\sim}{R},t)dE_f \quad (5.15a)$$

$$= -\int_{-S}^{\infty} dE_i \int_{-D}^{-S} S_{if}(t)dE_f \qquad (5.15b)$$

$$= -\partial n_s(t)/\partial t \qquad (5.15c)$$

Eq. (5.15b) simply states that the flux entering the sphere equals the sum of the collisional rate of production of S-pairs and the rate of increase of the contribution from the reaction volume to the density of C and E pairs. Eq. (5.15c) also follows from (5.6) without the intermediate collisional step. Integration of (5.1) over R from R_s to R_i, the classical turning point (for $E_i < 0$) or infinity (for $E_i \geq 0$) yields

$$\frac{\partial}{\partial t}\int_{R_s}^{R_i} n_i^s(\underset{\sim}{R},t)d\underset{\sim}{R} - 4\pi R_s^2 j_i^d(\underset{\sim}{R}_s,t) = -\int_{R_s}^{R_i} d\underset{\sim}{R} \int_{-V}^{\infty} S_{if}(\underset{\sim}{R},t)dE_f, R_i > R_s \qquad (5.16)$$

the continuity equation for each level E_i external to the reaction zone. Hence,

$$\frac{\partial}{\partial t}\int_{-S}^{\infty} dE_i \int_{R_s}^{R_i} n_i^s(\underset{\sim}{R},t)d\underset{\sim}{R} - 4\pi R_s^2 \int_{-S}^{\infty} j_i^d(\underset{\sim}{R}_s,t)dE_i = 0 \qquad (5.17)$$

due to the null effect of collisions. Addition of (5.15c) and (5.17) simply yields the conservation equation

$$\frac{\partial}{\partial t}[n_c(t) + n_e(t) + n_s(t)] = 0 \qquad (5.18)$$

for the sum of the densities (5.10) and (5.12) in blocks C and S and of

$$n_e(t) = \int_{-S}^{0} n(E_i,t)dE_i = \int_{-S}^{0} dE_i \int_{0}^{R_i} n_i(\underset{\sim}{R},E_i;t)d\underset{\sim}{R} \qquad (5.19)$$

the density of pairs in block E, as expected for this closed system.

5.2 Association and Dissociation Rates

From (5.11), the net rate of depletion of C-pairs (into all bound levels in E and S) is therefore

$$R_c(t) = -\int_0^{\infty}\left(\frac{\partial n_i}{\partial t}\right)dE_i = \int_0^{\infty} dE_i \int_{-D}^{\infty} S_{if}(t)dE_f = \int_0^{\infty} dE_i \int_{-D}^{0} S_{if}(t)dE_f \tag{5.20}$$

which is the net downward current across the dissociation neck at zero energy and which, with the aid of (5.9), equals the net rate of production

$$\int_{-D}^{0}\left(\frac{\partial n_i}{\partial t}\right)dE_i = -\int_{-D}^{0} dE_i \int_{-D}^{\infty} S_{if}dE_f \tag{5.21}$$

of E and S-pairs, as expected for this closed system. The net rate (5.13) of production of S-pairs alone is

$$R_s(t) = \int_{-D}^{-S}\left(\frac{\partial n_i}{\partial t}\right)dE_i = -\int_{-D}^{-S} dE_i \int_{-D}^{\infty} S_{if}(t)dE_f = \int_{-S}^{\infty} dE_i \int_{-D}^{-S} S_{if}(t)dE_f \tag{5.22}$$

so that, with the aid of (5.18),

$$R_c(t) = R_s(t) + \int_{-S}^{0}\left(\frac{\partial n_i}{\partial t}\right)dE_i \tag{5.23a}$$

$$= R_s(t) - \int_{-S}^{0} dE_i \int_{-D}^{\infty} S_{if}(t)dE_f \tag{5.23b}$$

Thus R_s and R_c are equal when $\partial n_i/\partial t \approx 0$ in block E i.e., constant (in energy) current flows through E which is in quasi-steady-state (QSS). For any fixed energies E_1 and E_2, then (5.9) yields

$$\int_{E_1}^{E_2} dE_i \int_{E_1}^{E_2} S_{if}(t)dE_f = 0 \tag{5.24}$$

which represents the null effect of collisions in the closed interval $E_1 \leq E_i \leq E_2$. The net downward current (5.20) across the dissociation neck can then be rearranged in terms of the net downward collisional current across arbitrary level -E as

$$R_c(t) = \int_{-E}^{\infty} dE_i \int_{-D}^{-E} S_{if}(t)dE_f + \int_{-E}^{o} (\partial n_i/\partial t)dE_i \tag{5.25}$$

and the net downward current (5.22) across level -S can be similarly rearranged as

$$R_s(t) = \int_{-E}^{\infty} dE_i \int_{-D}^{-E} S_{if}(t)dE_f - \int_{-S}^{-E} (\partial n_i/\partial t)dE_i \tag{5.26}$$

Note that (5.26) reduces to (5.22) directly when -E = -D, and that (5.25) reduces to (5.23a) and to (5.20) when -E = -S and when $-E \to \infty$ respectively. The expressions (5.25) and (5.26) provide alternative procedures which are valuable for accurate calculation of $R_c(t)$ and $R_s(t)$ particularly when block *E* is in QSS. In the absence of QSS, R_c and R_s are determined by the exact set (5.20) and (5.22) respectively.

On introduction of the (time-independent) probability P_i^A that pairs AB with internal energy E_i are considered as associated then the overall rate for association is,

$$R^A(t) = \int_{-D}^{\infty} P_i^A(E_i) \left(\frac{\partial n_i}{\partial t}\right) dE_i = R_s(t) + \int_{-S}^{o} P_i^A \left(\frac{\partial n_i}{\partial t}\right) dE_i \tag{5.27}$$

since P_i^A is unity in block *S* and is zero in block *C*. The overall rate for

dissociation is similarly,

$$R^D(t) = \int_{-D}^{\infty} P_i^D(E_i) \left(\frac{\partial n_i}{\partial t}\right) dE_i = - R_c(t) + \int_{-S}^{o} P_i^D \left(\frac{\partial n_i}{\partial t}\right) dE_i \qquad (5.28)$$

where the probability P_i^D that E_i-pairs are considered dissociated is unity in the continuum block C, and zero in the fully associated block S. Pairs in block E are in the process of associating and dissociating with probabilities $P_i^{A,D} < 1$. Expressions (5.27) and (5.28) are exact for $R^{A,D}(t)$ under all conditions (cf §7.1, §7.2).

Since

$$P_i^A(E_i) + P_i^D(E_i) = 1 \qquad (5.29)$$

addition of (5.27) and (5.28) yields, with the aid of (5.23a),

$$R^A(t) + R^D(t) = 0 \qquad (5.30)$$

as expected for this closed system.

Provided block E is in QSS (i.e., $\partial n_i/\partial t \approx 0$), the association rate $R^A(t)$ is therefore identical to $R_S(t)$, the net rate collisional rate (5.22) or (5.26) for formation of S-pairs and the dissociation rate $R^D(t)$ is identical to $-R_c(t)$, the net collisional rate for formation of C-pairs. As shown by (5.23a), R_s and R_c are then equal. Otherwise (5.27) and (5.28) must be used for $R^{A,D}(t)$.

In § 7, extrema $R_*^{A,D}(t)$ to the rates $R^{A,D}(t)$ at time t implies the QSS condition. Hence these extrema in addition to (5.30) satisfy

$$R_*^A(t) = R_s(t) = \partial n_s(t)/\partial t \qquad (5.31a)$$

$$= \alpha N_A(t)N_B(t) - k\, n_s(t) \tag{5.31b}$$

$$= \alpha N_A(t)N_B(t)\,[1 - \Gamma(t)] \tag{5.31c}$$

and

$$R_*^D(t) = -R_c(t) = \partial n_c(t)/\partial t \tag{5.32a}$$

$$= k\, n_s(t)\,[1 - \Gamma^{-1}(t)] \tag{5.32b}$$

where α is the effective two-body rate ($cm^3\ s^{-1}$) for association of dissociated species A and B with densities $N_{A,B}(t)$ cm^{-3} and where k is the frequency (s^{-1}) for dissociation of S-pairs AB with density $n_s(t)$. The quantity

$$\Gamma(t) = [\tilde{N}_A\tilde{N}_B/N_A(t)N_B(t)][n_s(t)/\tilde{n}_s] \tag{5.33}$$

is a measure of the departure of the densities from their corresponding time-independent values $\tilde{N}_{A,B}$ and $\tilde{n}_s$ achieved under full thermodynamic equilibrium ($\Gamma = 1$) with the gas bath M.

The QSS rate α is therefore determined by the equivalent expressions

$$R_*^A(t) = \alpha N_A(t)N_B(t)[1 - \Gamma(t)] = \int_{-S}^{\infty} dE_i \int_{-D}^{-S} S_{if}(t)\,dE_f \tag{5.34a}$$

$$= -R_*^D(t) = \int_{o}^{\infty} dE_i \int_{-D}^{o} S_{if}(t)\,dE_f \tag{5.34b}$$

$$= \int_{-E}^{\infty} dE_i \int_{-D}^{-E} S_{if}(t)\,dE_f \tag{5.34c}$$

which are respectively the rate R_s for formation of S-pairs, the rate R_c for depletion of C-pairs and the rate for formation of all pairs with energy $E_i \leqslant -E$. The QSS-frequency k for dissociation is provided by the detailed balance relation

$$k \tilde{n}_s = \alpha \tilde{N}_A \tilde{N}_B \tag{5.35}$$

Evaluation of the exact expressions (5.20) for $R_c(t)$ and (5.22) for $R_s(t)$ require solution in general of the time-dependent coupled set (3.7) for the microscopic densities $n_i(\underset{\sim}{R},E_i,L_i^2;t)$ or of the set (4.6) for $n_i(\underset{\sim}{R},E_i;t)$ when equilibrium in L_i^2 can be assumed. It is only when block E is in QSS that (5.27) and (5.28) for the association and dissociation rates $R^{A,D}(t)$ are equal to R_s and $-R_c$ respectively such that the coefficients α and k are determined directly from (5.34) and (5.35).

When block E is not in QSS, then the exact rates (5.27)and(5.28) with (5.8) yields,

$$R^{A,D}(t) = \int_{-D}^{\infty} P_i^{A,D} dE_i \int_{-D}^{\infty} S_{fi}(t) dE_f \tag{5.36}$$

which is exact and which reduces to (5.31a) and (5.32a) only when the QSS-condition

$$\int_{-D}^{\infty} S_{if}(t) dE_f = 0 \tag{5.37}$$

is satisfied in block E ($0 \geqslant E_i \geqslant -S$). When approximate or variational distributions (§7) are adopted, then (5.36), rather than (5.34), is the required expression.

5.3 Macroscopic Transport-Collisional R-Equation

With the aid of (5.4)-(5.7), the distribution

$$n(\underset{\sim}{R},t) = \int_{-S}^{\infty} n_i{}^{S}(\underset{\sim}{R},E_i;t)dE_i \equiv n_c(\underset{\sim}{R},t) + n_e(\underset{\sim}{R},t) \tag{5.38}$$

in combined blocks C and E, and the associated net current

$$J(\underset{\sim}{R},t) = \int_{-S}^{\infty} J_i{}^{d}(\underset{\sim}{R},E_i;t)dE_i \equiv J_c(\underset{\sim}{R},t) + J_e(\underset{\sim}{R},t) \tag{5.39}$$

then satisfy, for $R \geqslant R_s$.

$$\frac{\partial}{\partial t} n(\underset{\sim}{R},t) + \underset{\sim}{\nabla}\cdot\underset{\sim}{J} = 0 \quad , \quad R \geq R_s \tag{5.40a}$$

which agrees with (3.18a) since $n_s(R \geq R_s,t)$ vanishes. For $R \leqslant R_s$,

$$\frac{\partial}{\partial t} n(\underset{\sim}{R},t) + \underset{\sim}{\nabla}\cdot\underset{\sim}{J} = -\int_{-S}^{\infty} dE_i \int_{-V}^{-S} S_{if}(R,t)dE_f \quad , \quad R \leq R_s$$

$$\equiv -\nu(R)\, n(\underset{\sim}{R},t) \tag{5.40b}$$

wherein $\nu(R)$ is introduced as an effective frequency for collisional absorption into block S of C and E pairs with fixed $R \leq R_s$. Integration of (5.40a) yields,

$$\frac{\partial}{\partial t} \int_{R_s}^{\infty} n(\underset{\sim}{R},t)d\underset{\sim}{R} = 4\pi R_s{}^2\, J\,(\underset{\sim}{R}_s,t) \tag{5.41a}$$

with no flux at infinity . With the aid of (5.8) and (5.13), integration of (5.40b) yields

$$\frac{\partial}{\partial t} \int_{0}^{R_s} n(\underset{\sim}{R},t)d\underset{\sim}{R} + 4\pi R_s{}^2\, J(\underset{\sim}{R}_s,t) = -\int_{0}^{R_s} d\underset{\sim}{R} \int_{-S}^{\infty} dE_i \int_{-V}^{-S} S_{if}(R,t)dE_f \tag{5.41b}$$

$$\equiv - \int_{-S}^{\infty} dE_i \int_{-D}^{-S} S_{if}(t) dE_f \qquad (5.41c)$$

$$= - \quad \partial n_s(t)/\partial t \qquad (5.41d)$$

which agrees with (5.15) previously obtained from (E_i,R)-integration. The continuity equations (5.41a) and (5.41d) also follow from (5.6) since $J_s(R_s,t)$ and $n_s(R>R_s,t)$ both vanish. Addition of (5.41a) and (5.41d) yields

$$\frac{\partial}{\partial t} \int_o^{\infty} n(\underset{\sim}{R},t) d\underset{\sim}{R} + \frac{\partial}{\partial t} \; n_s(t) = 0 \qquad (5.42)$$

the conservation equation (5.18) appropriate for this closed system.

Define the averaged local rate α_3 ($cm^3\ s^{-1}$) for absorption within R_s by

$$\alpha_3 n(R_s,t) = \int_o^{R_s} \nu(R)\ n(\underset{\sim}{R},t) d\underset{\sim}{R} = \int_{-S}^{\infty} dE_i \int_{-D}^{-S} S_{if}(t) dE_f \qquad (5.43)$$

so that the net rate (5.31) with (5.13) for production of pairs in block S is therefore

$$\frac{\partial}{\partial t}\ n_s(t) = \alpha_3\ n(R_s,t) = \alpha\ N_A(t)\ N_B(t)\ [1 - r(t)] \qquad (5.44)$$

under quasi-steady-state (QSS) conditions in block E.

Evaluation of α still involves solution of the phase densities, $n_i^{\,s}(\underset{\sim}{R},E_i,L_i^{\,2};t)$, in general, or $n_i^{\,s}(\underset{\sim}{R},E_i;t)$ for L^2-equilibrium, from the appropriate set (3.7) or (4.6) of coupled equations.

5.3 Approximation and the Debye-Smoluchowski Equation

Assume in addition to QSS in block E where $\partial n_i/\partial t \approx 0$, that those pairs with $R \leq R_s$ in the combined blocks C and E are also in steady-state, i.e.,

$$\frac{\partial}{\partial t} \int_o^{R_s} n(\underset{\sim}{R}_s,t) d\underset{\sim}{R} = 0 \qquad (5.45)$$

so that (5.41c) with definition (5.43) reduces to

$$4\pi R_s^2 \, J(R_s,t) = - \alpha_3 \, n(R_s,t) = - \partial n_s(t)/\partial t \tag{5.46}$$

For $R \geq R_s$ the macroscopic current J can be approximated[1] by (2.76) i.e., by

$$\underset{\sim}{J}(R \geq R_s,t) = \underset{\sim}{J}^d(R \geq R_s,t) = -D\underset{\sim}{\nabla} n - [(K/e)\underset{\sim}{\nabla} V]n \tag{5.47}$$

since $J_s(R \geq R_s,t)$ and $n_s(R \geq R_s,t)$ both vanish. Provided the local rate α_3 for absorption is regarded as a pre-assigned external parameter, then (5.46) is, in effect, a radiation boundary condition to the solution $n(\underset{\sim}{R},t)$ of the macroscopic continuity equation (5.40a) with J given by (5.47). Since

$$n_s(t) - n_s(0) = \alpha_3 \int_0^t n(R_s,t)dt \tag{5.48}$$

$\Gamma(t)$ is therefore known from (5.33) so that the required rate of production of S-pairs is determined only by $n(R_s,t)$ via

$$\alpha N_A(t) \, N_B(t) = \alpha_3 \, n(R_s,t) \, [1 - \Gamma(t)]^{-1} \tag{5.49}$$

Hence under QSS in block *E*, the steady-state assumption (5.45) and a known local reaction rate α_3, the problem is reduced to one of transport alone. The combination (5.40a) with (5.47) for the current and the boundary condition (5.46) is referred to as the Debye-Smoluchowski Equation (DSE) familiar in the theory of reactions in condensed matter and of coagulation of colloids in solution. Apart from a previous account,[1] DSE has not to the author's knowledge ever been derived from a microscopic basic. If, however, α_3 is not known (as is usual) then the

present full microscopic treatment based on the coupled transport-collision equations of § 3 and § 4 for $n_i^{s,d}$ is required.

Refs. (24-27) provide preliminary reports[24-26] and a full detailed account[27] of the search for analytical solutions to DSE for general interaction V(R) between A and B.

6. Time Evolution Towards Equilibrium

Relaxation of a plasma,or of any subsystem (A,B,AB) in a bath of systems M,from any initial non-equilibrium distribution is, in principle, a time dependent process which proceeds towards equilibrium under various distinct time scales. A very fast initial transient characterizes Phase I, during which a new distribution in $(\underset{\sim}{R},E,L^2)$ is rapidly established. This is followed by a much slower Phase II, during which recombination, association or dissociation and chemical reactions based on the newly developed distribution of Phase I proceeds towards eventual equilibrium via a dynamic balance of collisional association and dissociation established in Phase III.

During Phase I, the $(\underset{\sim}{R},E,L^2)$-distribution collisionally relaxes within (collisional) time τ_1 to a quasi steady state of excited levels which persist throughout Phase II and is the distribution characteristic of the eventual equilibrium established as $t/\tau_1 \to \infty$. Phase II is characterized by (reaction) times $\tau_2 \approx \tau_R$, τ_A, or τ_D for recombination, association from non-equilibrium free states or dissociation from non-equilibrium bound levels (whichever pertains to the initial conditions). Since τ_1 is generally of the order of the inverse of the collisional frequency ν_{if}, and since association/dissociation proceeds on a much slower time scale, $\tau_1 << \tau_2$ such that the quasi steady-state distribution attained in Phase I persists throughout Phase II.

The beginning of the third Phase (III) association or dissociation depending on the overall direction as determined by initial densities, has produced a significant population of bound pairs AB or free pairs A + B such that the reverse process (dissociation or association) becomes important with the result that the subsystem relaxes toward eventual equilibrium.

Recognition of Phases I and II facilitated many pioneering and tractable

studies of recombination processes[6-12,17,18] in general, based on the solution of integral equations, and the study[13,14] via a diffusion (weak collision) approximation to association/dissociation processes at low gas densities.

The work of Bates et al.[6-8] and of Flannery[9-11] was concerned with the case of the concentrations $N_{A,B}$ of dissociated (charged) species >> N_{AB}, the concentration of bound systems, such that only Phase II and association were relevant. Also previous work on ion-ion recombination[6-11] dealt with low gas densities N. We are here concerned with theoretical development of both association and dissociation in Phases II and III at all gas densities N, for which the time dependent transport-collisional equations formulated in the previous sections (§ 2-4) are directly relevant.

6.1 Net Transition Probabilities for Association and Dissociation

As an aid to clarity of presentation, consider first the following analysis of eq. (3.21a) in which explicit dependence on the (R,L^2) variables has been systematically integrated out from the original basic eq. (3.7a). Eq. (3.21a) contains however implicit variation with (R,L^2) as characterized by (3.13) and (2.70) for n_i, and by (3.22) for γ_i. The $(\underset{\sim}{R},E,L_i^2)$ and $(\underset{\sim}{R},E)$ sets (3.7) and (3.12) respectively may then be similarly analyzed without any undue formal difficulty.

The governing equation for the conditional probability density n_i of AB systems per unit dE_i is

$$\frac{\partial}{\partial t} n_i(E_i,t) = \int_{-D}^{\infty} [n_f(t)\, \nu_{fi} - n_i(t)\nu_{if}]dE_f \equiv - \partial J_i(E_i,t)/\partial E_i \qquad (6.1a)$$

where ν_{if} is the frequency of $i \to f$ collisional transitions ($E_i \to E_f$) and -D is the energy of the lowest bound vibrational level of the AB pair.

Alternatively,

$$\partial n_i/\partial t = \int_{-D}^{\infty} [\gamma_f(t) - \gamma_i(t)] C_{if}\, dE_f \equiv -\partial J_i/\partial E_i \qquad (6.1b)$$

in terms of C_{if}, the equilibrium collisional rate (3.22), and of γ_i, the normalized distribution (3.23). Since the energy levels of AB be sufficiently close (relative to the thermal energy $k\Theta$ of the gas bath M), they form a quasi-continuum and $J_i(E_i,t)$ can then be interpreted as the net upward current (in energy space) across level E_i.

Introduce,

$$A_{fi} = \nu_{fi} - \delta(E_i - E_f) \int_{-D}^{\infty} \nu_{if}\, dE_f \,, \qquad (6.2)$$

the <u>net</u> probability/sec for $f \to i$ irreversible collisional transitions. Then (6.1a) can be compactly written as,

$$\partial n_i/\partial t = \int_{-D}^{\infty} n_f\, A_{fi}\, dE_f = -\int_{-D}^{\infty} S_{if}\, dE_f \qquad (6.3)$$

where S_{if} is defined by eqs. (5.2) and (5.9).

Since the AB-subsystem is closed, curve crossing and quantum tunnelling $AB \not\rightleftarrows A+B$ being precluded at present,

$$\int_{-D}^{\infty} (\partial n_i/\partial t)\, dE_i = (\partial/\partial t) \int_{-D}^{\infty} n_i\, dE_i = 0 \qquad (6.4)$$

When relaxation in L_i^2 and R is much faster that E_i- relaxation, assume by the end of Phase I that collisions have been sufficiently rapid to establish a Maxwell-Boltzmann distribution $f(E_i)$ in the energy $E_i \geq 0$ of the dissociated (A,B) species. The continuum distribution is then

$$\gamma_c(t) = [N_A(t)N_B(t)\ f(E_i)]/[\tilde{N}_A\tilde{N}_B\ f(E_i)] \xrightarrow{t\to\infty} 1, \quad E_i \geq 0 \tag{6.5}$$

where $N_{A,B}(t)$ are the time-dependent concentrations of the dissociated species (A and B) or free ions (X^+ and Y^-), which approach their constant equilibrium values $\tilde{N}_{A,B}$ as $t \to \infty$ in this closed system. The normalized distribution (6.5) is time-dependent but energy-independent. As association develops during phase II the pair concentration of the lowest bound levels, within the range $-S \geq E_i \geq -D$ defining energy-block S, grows. Within S, energy-equilibrium is maintained via collisions so that the S-block distribution, assumed to be

$$\gamma_s(t) = n_i(E_i,t)/\tilde{n}_i(E_i) = \int_{-D}^{-S} n_i\ dE_i \Big/ \int_{-D}^{-S} \tilde{n}_i\ dE_i$$

$$\equiv n_s(t)/\tilde{n}_s \to 1, \quad -S \geq E_i \geq -D \ , \tag{6.6}$$

is only time-dependent. In this closed system, let the E-block be coupled to the time-variations of C and S according to the ansatz,

$$\gamma_i(E_i,t) = P_i^{\,D}(E_i)\ \gamma_c(t) + P_i^{\,A}(E_i)\ \gamma_s(t) \xrightarrow{t\to\infty} 1 \tag{6.7}$$

where the coupling coefficients $P_i^{\,D}$ and $P_i^{\,A}$ which depend only on the energy will be later identified as being the <u>net</u> probabilities that bound AB pairs of energy E_i will be collisional dissociated into C or will be fully associated by collision into S. From the asymptotic conditions (6.5) - (6.7), the net probabilities satisfy the conservation of probability

$$P_i^{\,D} + P_i^{\,A} = 1 \tag{6.8}$$

as expected, since the complete subsystem is closed to mechanisms other than collisional association/dissociation.

Distributions (6.5) and (6.6) can be also incorporated within (6.7) since C and S are naturally characterized by unit net probability P_i^D $(E_i \geq 0)$ for dissociation, and unit net probability P_i^A $(E_i \leq -S)$ for association, respectively. Thus, (6.1b) yields,

$$\partial n_i/\partial t = -[\gamma_c(t) - \gamma_s(t)] \int_{-D}^{\infty} (P_f^A - P_i^A) C_{if}\, dE_f \tag{6.9a}$$

$$= [\gamma_c(t) - \gamma_s(t)] \int_{-D}^{\infty} (P_f^D - P_i^D) C_{if}\, dE_f \tag{6.9b}$$

which is separable in both time t and energy E_i, a natural result of the assumed form (6.7) subject to the asymptotic constraints (6.5) and (6.6).

The rate of change in the probability densities of pairs in each of the blocks C, E and S is respectively,

$$\partial n_i/\partial t = -[\gamma_c(t) - \gamma_s(t)][\int_{-D}^{0} P_f^A\, C_{fi}\, dE_f] \; ; \quad E_i \geq 0; \tag{6.10a}$$

for block C in a form natural when association ($\gamma_c > \gamma_s$) prevails,

$$\partial n_i/\partial t = [\gamma_c(t) - \gamma_s(t)][\int_{-S}^{\infty} P_f^D\, C_{fi}\, dE_f - P_i^D \int_{-D}^{\infty} C_{if}\, dE_f] \; ; \; 0 \geq E_i \geq -S \tag{6.10b}$$

for block E and

$$\partial n_i/\partial t = -[\gamma_s(t) - \gamma_c(t)][\int_{-S}^{\infty} P_f^D\, C_{fi}\, dE_f] \quad -S \geq E_i \geq -D \tag{6.10c}$$

for block S, in a form natural for dissociation controlled processes ($\gamma_s > \gamma_c$). Thus, the energy distribution P_i^D once established at the end of Phase I is then preserved at all future times in Phases II and III. Relaxation then proceeds in time at a rate determined by the established $P_i^{D,A}$ and $\gamma_i(t)$ towards eventual equilibrium when $\gamma_c \to \gamma_s \to 1$.

The upward current across any arbitrary level E is

$$J(E_i,t) = \int_{E_i}^{\infty} (\partial n_i/\partial t)dE_i = -\int_{-D}^{E} (\partial n_i/\partial t)dE_i \qquad (6.11)$$

since conservation (6.4) applies to the system, closed between -D and ∞, so that the currents $J(-D)$ and $J(\infty)$ across the end points both vanish.

Thus, the net current across a level E in block C is

$$J(E \geq 0,t) = -[\gamma_c(t) - \gamma_s(t)] \int_{E}^{\infty} dE_i \int_{-D}^{0} P_f^A \, C_{fi} \, dE_f \qquad (6.12a)$$

and the net current across a level E in block S is

$$J(-S \geq E \geq -D,t) = [\gamma_s(t) - \gamma_c(t)] \int_{-D}^{E} dE_i \int_{-S}^{\infty} P_f^D \, C_{fi} \, dE_f \qquad (6.12b)$$

which are directed down or up the energy ladder according as $\gamma_c > \gamma_s$ or $\gamma_c < \gamma_s$, respectively. Thus, the overall direction of the relaxation is determined by the inequality

$$\frac{N_A(t)N_B(t)}{\tilde{N}_A\tilde{N}_B} \gtrless \frac{n_s(t)}{\tilde{n}_s} \qquad (6.13)$$

which is originally established by the initial condition.

The net rate of growth of S-pairs or the downward current $-J(S,t)$ into the S-block is

$$\partial n_s(t)/\partial t = \int_{-D}^{-S} (\partial n_i/\partial t)\, dE_i \equiv -J(-S,t)$$

$$= [\gamma_c(t) - \gamma_s(t)]\alpha_s \tilde{N}_A \tilde{N}_B \qquad (6.14a)$$

which, with (6.5) and (6.6) for $\gamma_{c,s}$, yields

$$\partial n_s(t)/\partial t \equiv \alpha_s\, N_A(t) N_B(t) - k_s\, n_s(t) \qquad (6.14b)$$

The (time independent) rate α_s $(cm^3\ s^{-1})$ of association and the frequency k_s (s^{-1}) of dissociation in (6.14b) are hence given by,

$$\alpha_s\, \tilde{N}_A \tilde{N}_B = k_s\, \tilde{n}_s = \int_{-D}^{-S} \tilde{n}_i\, dE_i \int_{-S}^{\infty} P_f^D\, \nu_{if}\, dE_f \qquad (6.15)$$

and therefore satisfy (macroscopic) detailed balance. Characterization of P_f^D in (6.7) as the net probability of dissociation of level f once accessed by collision from level i is therefore appropriate, in keeping with (6.15). When conditions are such that $\gamma_c = N_A(t)N_B(t)/\tilde{N}_A\tilde{N}_B >> n([S],t)/\tilde{n}([S]) = \gamma_s \approx 0$, association is dominant, and γ_c decreases in time from a quantity >> 1 to unity at equilibrium, while γ_s increases essentially from zero to unity. In the reverse limit, $\gamma_s >> \gamma_c \approx 0$, for the case of a shock wave moving through a molecular gas, then dissociation prevails until equilibrium when $\gamma_{s,c} \approx 1$ and

the currents (6.14) vanish. The evolution toward equilibrium is described by (6.14b).

The net rate of growth of the C-pairs in (6.10a) or the upward current $J(0,t)$, (6.12a), entering block C is

$$\partial n_C(t)/\partial t = \int_0^\infty (\partial n_i/\partial t)dE_i \equiv J(0,t)$$

$$= [\gamma_S(t) - \gamma_C(t)]\, k_C\, \tilde{n}_S \qquad (6.16a)$$

which, with (6.5) and (6.6) for $\gamma_{C,S}$, yields

$$\partial n_C(t)/\partial t \equiv -\alpha_C\, N_A(t)N_B(t) + k_C\, n_S(t) \qquad (6.16b)$$

where (time-independent) rate α_C ($cm^3\ s^{-1}$) of association from the continuum and the frequency k_C (s^{-1}) of dissociation are given by

$$\alpha_C\, \tilde{N}_A\tilde{N}_B = k_C\, \tilde{n}_S = \int_0^\infty \tilde{n}_i\, dE_i \int_{-D}^{0} P_f^A\, \nu_{if}\, dE_f \qquad (6.17)$$

which satisfies detailed balance. Thus, P_f^A in (6.7) is uniquely identified in (6.17) as being the net probability of association of pairs in bound level f once collisionally accessed from the continuum C.

The above expressions (6.15) and (6.17) for the rate of change of free (fully dissociated) C-pairs, and of fully associated S-pairs, respectively, are exact, irrespective of any approximation used to determine the probabilities $P_i^{A,D}$ in the E-block ($0 \geq E_i \geq -S$).

In the quasi-steady-state (QSS) approximation, pioneered and used extensively by Bates and associates in many studies[6-8,16-20] of various types of recombination,

$$\frac{\partial n_i}{\partial t} = 0 \quad ; \quad \text{block } E \ (0 \gtrsim E_i \gtrsim -S) \tag{6.18}$$

since the frequencies of collisional production and destruction of a system i of energy E_i in block E are very large relative to the low frequency of explicit time decay of these excited levels i. The time-independent probabilities in (6.9) are therefore solutions to the integral equation

$$P_i^D \int_{-D}^{\infty} C_{if} dE_f = \int_{-S}^{\infty} P_f^D \, C_{if} dE_f \tag{6.19}$$

subject to the constraints $P_i^D(E_i \gtrsim 0) = 1$ and $P_i^D(E_i \lesssim -S) = 0$. Since the system is closed, (6.4) applies i.e.,

$$\partial n_c(t)/\partial t + \partial n_s(t)/\partial t = -\partial n_e(t)/\partial t = J(0,t) - J(-S,t) \tag{6.20}$$

In the QSS-approximation, (6.15) and (6.17) are therefore equivalent, the upward current J(-S,t) leaving block S being equal to the upward current J(0,t) entering the block C.

On invoking the null effect of collisions (cf. eq. (5.24))

$$0 = \int_{-E}^{\infty} dE_i \int_{-E}^{\infty} n_f \, \nu_{fi} \, dE_f - \int_{-E}^{\infty} n_i \, dE_i \int_{-E}^{\infty} \nu_{if} \, dE_f \equiv \int_{-E}^{\infty} dE_i \int_{-E}^{\infty} [\gamma_f(t) - \gamma_i(t)] C_{if} \, dE_f \tag{6.21}$$

for an arbitrary bound level of energy -E within block E, the net upward current (6.11) across -E is

$$J(-E,t) = -\alpha_e \quad N_A(t) N_B(t) + k_e \, n_s(t) \tag{6.22}$$

where both

$$\alpha_e = (\tilde{N}_A \tilde{N}_B)^{-1} \int_{-E}^{\infty} dE_i \int_{-D}^{-E} (P_i^D - P_f^D) C_{if}\, dE_f \tag{6.23}$$

and k_e satisfy the detailed balance relation

$$\tilde{N}_A \tilde{N}_B\, \alpha_e = \tilde{n}_s\, k_e \tag{6.24}$$

From (6.11),

$$J(0,t) = J(-E,t) + \int_{-E}^{0} (\partial n_i/\partial t) dE_i \tag{6.25}$$

$$J(-S,t) = J(-E,t) - \int_{-S}^{-E} (\partial n_i/\partial t) dE_i \tag{6.26}$$

which correspond to (5.25) and (5.26) the set (α_e, k_e) is identical to the exact set (α_s, k_s) appropriate to the current J(-S,t) of (6.14) out of *S* and to (α_c, k_c) for the current J(0,t) of (6.16) into *C*, <u>only</u> under quasi-steady-state conditions $(\partial n_i/\partial t) = 0$ in block *E*.

When initial conditions are such that

$$\gamma_c(t) = N_A(t) N_B(t)/\tilde{N}_A \tilde{N}_B >> 1 >> n_s(t)/\tilde{n}_s = \gamma_s(t) \approx 0, \tag{6.27}$$

then, the dissociation rate $k\, n_s(t)$ in (6.14b) and (6.16b), can only be neglected for times t (in Phase II) much shorter than the time required for the establishment of equilibrium when $\gamma_c = \gamma_s = 1$.

When Phase II is dominated by association ($\gamma_c >> \gamma_s$) the solution of (6.16b) is then,

$$\frac{1}{N_{A,B}(t)} = \frac{1}{N_{A,B}(0)} + \alpha_c t \tag{6.28}$$

the familiar macroscopic law of recombination[16] where time t is measured from the beginning of Phase II when it is assumed that the densities $N_A(0)$ and $N_B(0)$ of dissociated species are equal. Also the densities $n_s(t)$ of *S*-pairs are given by the solution of (6.14b) which yields,

$$n_s(t) + N_{A,B}(t) = n_s(0) + N_{A,B}(0) \tag{6.29}$$

when $\alpha_c = \alpha_s = \alpha$ i.e., the total number of pairs in blocks *C* and *S* are conserved under QSS-conditions in block *E*.

As t increases, $\gamma_c(t)$ decreases rapidly from a very large quantity, as

$$\gamma_c(t) = [N_{A,B}(0)/\tilde{N}_{A,B}]\,[1 + \alpha N_{A,B}(0)t]^{-1} \tag{6.30}$$

while γ_s increases slowly, essentially from zero as,

$$\gamma_s(t) = \left[\frac{\alpha N_{A,B}(0)t}{1+\alpha N_{A,B}(0)t}\right] \frac{N_{A,B}(0)}{\tilde{n}_s} + \left[\frac{n_s(0)}{\tilde{n}_s}\right] \tag{6.31}$$

The excited state distribution under (6.27) is

$$\gamma_i(t) \approx P_i^D \gamma_c(t) + \gamma_s(t) \approx P_i^D \gamma_c(t) \tag{6.32}$$

and is such that $\gamma_i \sim P_i^D \gamma_c$ only for those highly excited levels i at time t when $\gamma_s(t) \ll P_i^D \gamma_c$, as in Phase II.

All of the previous studies of recombination were concerned only with Phase II and dissociation was neglected. When dealing, however, with evolution towards eventual equilibrium (in Phase III) or with the enhancement of mutual neutralization (or curve crossings) by three body collisions the full distribution (6.7), rather than (6.32) is appropriate.

The solutions (6.30) and (6.31) which correspond to condition (6.27) are valid until a substantial fraction of associated pairs relative to their equilibrium concentration have been created, and dissociation becomes important.

When initial conditions and times are such that

$$\gamma_s(t) \gg 1 \gg \gamma_c(t) \approx 0 \tag{6.33}$$

then the net process is dominated by dissociation. The solution of (6.14b) yields for Phase II,

$$n_s(t) = n_s(0) \exp(-k_s t) \tag{6.34}$$

the familiar macroscopic law of dissociation, and the solution of (6.16b) yields the conservation requirement (6.27) when k_s and k_c are equal. As Phase III progresses, γ_c increases, association becomes important and equilibrium is achieved.

6.2 Multivariable Separation

The above strategy (6.7) for separation of the variables E_i and t can be easily generalized to cover multivariable separation. Define, for example

$$\gamma_i^{\pm}(\underset{\sim}{R},E_i;t) = P_i^{\pm}(R,E_i)\gamma_c(t) + [1 - P_i^{\pm}(R,E_i)]\,\gamma_s(t) \tag{6.35}$$

where $P_i^{\pm}$ is the net probability for eventual dissociation of an expanding (+) or contracting (-) pair with internal energy E_i and internal separation R. The set (4.6) therefore separates as

$$\frac{\partial}{\partial t} n_i^{\,s} + (\gamma_c-\gamma_s)\,\frac{1}{R^2}\frac{\partial}{\partial R}\left[\frac{1}{2} R^2 P_i^{\,d}(R)\,\tilde{j}_i(R)\right] = (\gamma_c-\gamma_s)\int_{-V}^{\alpha} dE_f\,[P_f^{\,s}(R)-P_i^{\,s}(R)]C_{if} \tag{6.36a}$$

and

$$\frac{\partial}{\partial t} n_i^{\,d} + (\gamma_c-\gamma_s)\left\{\frac{1}{R^2}\frac{\partial}{\partial R}\left[\frac{1}{2} R^2 P_i^{\,s}(R)\,\tilde{j}_i(R)\right] - (P_i^{\,s} \mp P_i^{\,d})\,\frac{1}{R^2}\frac{\partial}{\partial R}\left(\frac{1}{2} R^2\,\tilde{j}_i\right)\right\}$$

$$= (\gamma_c-\gamma_s)\int^{\infty} dE_f\,[P_f^{\,d}(R) - P_i^{\,d}(R)]\,C_{if} \tag{6.36b}$$

to be solved for the functions

$$P_i^{\,s}(R) = \frac{1}{2}\,[P_i^{\,+}(R,E_i) + P_i^{\,-}(R,E_i)] \tag{6.37a}$$

and

$$P_i^{\,d}(R) = \frac{1}{2}\,[P_i^{\,+}(R,E_i) - P_i^{\,-}(R,E_i)] \tag{6.37b}$$

In blocks *C* and *S*, respectively, $P_i^{\pm}$ is unity and zero, $P_i^{\,s}$ is unity and zero and $P_i^{\,d}$ is zero. If the quasi-steady condition (6.18a) is assumed in block *E*, (6.36a,b) can be solved independently of the functions $\gamma_{c,s}(t)$. The set (3.7) in R, E_i, $L_i^{\,2}$ and t may be similarly separated.

7. Variational Principles

7.1 Association/Dissociation Rates for non-QSS (Quasi-Steady-State) and for QSS.

Upon identification of $P_i^{A,D}$ in (6.7) as the net probabilities for association/dissociation of one AB-pair of energy E_i, the overall net probabilities/sec for association/dissociation are therefore

$$R^{A,D}(t) = \frac{\partial}{\partial t}\int_{-D}^{\infty} P_i^{A,D}(E_i)\, n_i(t)dE_i = \int_{-D}^{\infty} J_i(E_i,t)(\partial P_i^{A,D}/\partial E_i)\, dE_i \qquad (7.1a)$$

with the aid of (6.1b) and of integration by parts, since the current J_i vanishes at the end points to $E_i = (-D, \infty)$. Equivalent rates, obtained from (6.9) for $\partial n_i/\partial t$, are

$$\begin{aligned} R^A(t) &= \frac{\partial}{\partial t}\int_{-D}^{\infty} P_i^A n_i(t)dE_i = \int_{-D}^{\infty} P_i^A dE_i \int_{-D}^{\infty} S_{fi}(t)dE_f \\ &= [\gamma_c(t) - \gamma_s(t)] \int_{-D}^{\infty} P_i^A(E_i)dE_i \int_{-D}^{\infty} (P_i^A - P_f^A)C_{if}dE_f \end{aligned} \qquad (7.1b)$$

for association where $S_{if}(t)$ is given by (5.9) in terms of (5.2) and

$$\begin{aligned} R^D(t) &= \frac{\partial}{\partial t}\int_{-D}^{\infty} P_i^D n_i(t)dE_i = \int_{-D}^{\infty} P_i^D dE_i \int_{-D}^{\infty} S_{fi}(t)dE_f \\ &= -[\gamma_c(t) - \gamma_s(t)] \int_{-D}^{\infty} P_i^D(E_i)dE_i \int_{-D}^{\infty} (P_i^D - P_f^D)C_{if}dE_f \end{aligned} \qquad (7.1c)$$

for dissociation. In accord with probability conservation (6.8) then for the closed system (6.4),

$$R^A(t) + R^D(t) = 0 \qquad (7.2)$$

at all times, as expected. Subject to the constraints

$$P_i^D = 1 \quad ; \quad P_i^A = 0 \quad ; \quad C\text{-block } (E_i \geq 0) \; ; \tag{7.3a}$$

$$P_i^D = 0 \quad ; \quad P_i^A = 1 \quad ; \quad S\text{-block } (-S \leq E_i \leq -D) \; ; \tag{7.3b}$$

implicit in (6.5) and (6.6), assume that the probabilities $P_i^{A,D}$ are so distributed in energy space that the net rates $R^{A,D}(t)$ are extrema at all times.

From the calculus of variations[22] a necessary condition for the integral

$$I = \int f(y,\dot{y};x)dx \quad , \; \dot{y} = dy/dx \tag{7.4}$$

to be an extremum is the Euler-Lagrange equation[22]

$$\frac{d}{dx}\left(\frac{\partial f}{\partial \dot{y}}\right) - \frac{\partial f}{\partial y} = 0 \quad , \tag{7.5}$$

the solution of which determines $y(x)$.

Since $P_i^{A,D}$ remain constant in blocks C and S, then with $x = E_i$, $y = P_i^{A,D}$, and $f(\dot{y};x) = J(E_i)\, \dot{P}_i^{A,D}$ in (7.5), $R_i^{A,D}$ of (7.1a) is an extremum provided

$$\frac{\partial}{\partial E_i} J_i\,(E_i,t) = 0 = -\frac{\partial n_i}{\partial t} \quad ; \quad E\text{-block } (0 \geq E_i \geq -S) \tag{7.6}$$

in block E i.e., the quasi-steady-state condition (6.18) of constant-in-energy current $J_i = J_e(t)$ in block E. The equation (6.9) with (7.3) and (7.6) therefore reduces to

$$P_i^A \int_{-D}^{\infty} C_{if}\, dE_f = \int_{-D}^{\infty} P_f^A\, C_{if}\, dE_f \quad ; \quad \text{block } E \tag{7.7a}$$

for P_i^A and to

$$P_i^D \int_{-D}^{\infty} C_{if} dE_f = \int_{-S}^{\infty} P_f^D C_{if} dE_f \quad ; \quad \text{block} \tag{7.7b}$$

for P_i^d. Since $(\partial P_i/\partial E_i)$ vanishes in blocks C and S and since the current is constant J_e in block E - self consistent conditions (6.3) and (6.6) for an extremum - the extrema of (6.1a) are therefore,

$$R_*^{A,D}(t) = \mp J_e(t) = \pm[\gamma_c(t)-\gamma_s(t) \int_{-E}^{\infty} dE_i \int_{-D}^{-E} (P_f^{A,D}-P_i^{A,D})C_{if}dE_f \tag{7.8a}$$

the constant-in-energy current J_e past any level E_i in block E; $-J_e$ directed down the energy ladder for association and $+J_e$ upward for dissociation. The extremum to (7.1b) for association is therefore,

$$R_*^A(t) = \frac{\partial}{\partial t} \int_{-D}^{-S} n_i dE_i = [\gamma_c(t) - \gamma_s(t)] \int_{-D}^{-S} dE_i \int_{-D}^{\infty} P_f^D C_{if} dE_f$$

$$\equiv \alpha N_A(t) N_B(t) - k\, n_s(t) \tag{7.8b}$$

where

$$\alpha \tilde{N}_A \tilde{N}_B = \int_{-D}^{-S} dE_i \int_{-D}^{\infty} P_f^D C_{if} dE_f = k\tilde{n}_s$$

The extremum to (7.1c) for dissociation is

$$R_*^D(t) = \frac{\partial}{\partial t} \int_{0}^{\infty} n_i dE_i = -[\gamma_c(t) - \gamma_s(t)] \int_{0}^{\infty} dE_i \int_{-D}^{\infty} P_f^A C_{if} dE_f \tag{7.8c}$$

$$\equiv -\alpha N_A(t) N_B(t) + k n_s(t) \tag{7.8d}$$

where

$$\alpha \tilde{N}_A \tilde{N}_B = \int_{0}^{\infty} dE_i \int_{-D}^{\infty} P_f^A C_{if} dE_f = k\tilde{n}_s \tag{7.8e}$$

and where $P_i^{D,A}$ in block E are solutions of (7.7). The nature of the extrema is determined by performing independent variations δP_i^A to P_i^A for each bound level in block E under the constraint (6.3) of constant $P^{A,D}$ in blocks C and S. The resulting change to (7.1) is

$$\delta R^A = -\delta R^D = 2[\gamma_c(t) - \gamma_s(t)][\int_{-S}^{0} dE_i\ \delta P_i^A \int_{-D}^{\infty} (P_i^A - P_f^A)\ C_{if}\ dE_f$$

$$+ 1/4 \int_{-D}^{\infty} dE_i \int_{-D}^{\infty} (\delta P_i^A - \delta P_f^A)^2\ C_{if}\ dE_f] \qquad (7.9)$$

to second order in δP_i^A. Since δP_i^A are independent of one another, the change in R^A to first order in δP^A vanishes for an extremum and condition (7.7a) is recovered from (7.9), as expected. The change in R^A to second order is wholly determined by the sign of $(\gamma_c - \gamma_s)$. When $\gamma_c > \gamma_s$ and the overall direction according to (6.8) is association, then $R_*^A(t)$ is minimum - and $R_*^D(t)$ is maximum . When the overall direction is dissociation, then $\gamma_s > \gamma_c$ and $R_*^D(t)$ is maximum and $R_*^A(t)$ is minimum.

The proposed Variational Principle is such that the rate corresponding to the overall direction always adjusts itself therefore to a minimum i.e., there is a tendency to counteract the change and the evolution towards equilibrium is impeded.

Rather than solving the integral equations (7.7), an alternative procedure is therefore to explore the variation of $R^{A,D}$ with $P_i^{A,D}$ and to seek a minimum to that rate via (7.1b) for R^A and (7.1c) for R^D, whichever corresponds to the net direction of the process.

Expressions (7.1) pertain to association/dissociation under all conditions, including non-QSS (Quasi-Steady-State), while expressions (7.8) are valid only for QSS-conditions (7.7).

7.2 General Rate Expression and Application of Variational Principle

Since $\partial P_i^D/\partial E_i$ tends to zero as E_i tends both to zero and to -D ($\approx -\infty$), a possible trial function is,

$$\partial P^D(\lambda;\lambda_*)/\partial\lambda = a\lambda e^{-d\lambda} \; ; \; d = 1/\lambda_* \tag{7.10}$$

where a is a normalization parameter, where λ is the internal energy ($-E_i/k\Theta$) in units of $k\Theta$ of the gas M, and where d is the one variational parameter which can be expressed as $(1/\lambda_*)$, in terms of the location at $\lambda = \lambda_*$ of the minimum to (7.10).

Under the constraints that $P^D(\lambda=0)$ is unity and that $P^D(\lambda \to \infty)$ tends to zero then the normalization parameter a is $(-1/\lambda_*)$, and integration of (7.10) then yields,

$$P^D(\lambda;\lambda^*) = e^{-x}(1+x) \qquad , \; x = \lambda/\lambda_* \tag{7.11}$$

and

$$P^A(\lambda;\lambda^*) \equiv 1 - P^D = 1 - e^{-x}(1+x) \tag{7.12}$$

which are simple one-parameter variational functions for the dissociation/association probabilities $P^{D,A}(\lambda)$. The variational association rate (7.14) in terms of the time-independent rate α (cm^2s^{-1}) of association in (7.8b) and of $\Gamma(t)$ of (5.33) is

$$R^A(t) = \alpha N_A N_B[1-\Gamma(t)] = [\gamma_c(t)-\gamma_s(t)] \int_{-D}^{\infty} P_i^A dE_i \int_{-D}^{\infty} (P_i^A - P_f^A) C_{if} dE_f \tag{7.13}$$

$$= \frac{1}{2}\left[\gamma_c(t)-\gamma_s(t)\right] \int_{-D}^{\infty} dE_i \int_{-D}^{\infty} (P_i^A - P_f^A)^2 C_{if} a E_\gamma \qquad (7.13b)$$

Consider, as an example, ion-ion recombination ($X^+ + X^- + X \rightarrow X_2 + X$) between equal-mass species. The relevant one-way equilibrium collision kernels C_{if} to be used in (7.13) are given by expression (B39), (B40), (B44), (B51), (B52) and (B54) of Appendix B.

When (7.12) is inserted into (7.13) and when λ^* is varied, the long-dashed curve in Fig. 2 is obtained for the ratio $R(\lambda^*,t)/R_*^A(t)$. The exact rate $R_*^A(t)$ is determined by inserting the solution of the integral eqn. (7.7a), the QSS condition, in (7.13), so that it is simply the downward (E-constant) current, $-J_e$, given by

$$R_*^A(t) = -J_e(t) = \left[\gamma_c(t) - \gamma_s(t)\right] \int_{-E}^{\infty} dE_i \int_{-D}^{-E} (P_i^A - P_f^A) C_{if} a E_f \qquad (7.14)$$

which is of course identical to (5-34a-c) and to (7.8a). Not only does the variational parameter $\lambda_* = 1.25$ provide a minimum but it yields its exact result!

Introduction of a three-parameter (λ_*,b,c) trial function

$$\partial P^D(\lambda;\lambda_*,b,c)/\partial\lambda = a\lambda(1 + b\lambda + c\lambda^2)e^{-d\lambda} \qquad (7.15)$$

where d can be expressed in terms of the location at λ_* of the minimum to (7.15) by

$$\Lambda_* = 1/d = \lambda_*(1 + b\lambda_* + c\lambda_*^2)/(1+2b\lambda_* + 3c\lambda_*^2) \qquad (7.16)$$

Upon integration, the association probability is therefore,

$$P^A(\lambda;\lambda_*,b,c) = 1 - e^{-x}[1 + x + x^2\Lambda_*(b + 3c\Lambda_* + c\Lambda_* x)/(1+2b\Lambda_*+6c\Lambda_*^2)] \qquad (7.17)$$

where

$$x = \lambda/\Lambda_* \qquad (7.18)$$

and its derivative is,

$$dP^A(\lambda;\lambda_*,b,c)/\partial\lambda = e^{-x}(x+b\Lambda_* x^2+c\Lambda_*^2 x^3)/(1+2b\Lambda_*+6c\Lambda_*^2) \qquad (7.19)$$

Fig. 2 illustrates that a minimum at $\lambda_* \approx 1.25$ is again obtained for the combinations (b = 0.20, c = 0) and (b = 0.20, c = -0.006) and that this minimum is the exact QSS-result. Comparison of the corresponding probabilities for all three variational cases with the exact numerical solution of (7.7) is shown in Fig. 3. The agreement is excellent for such simple variational functions. A more sensitive test is provided in Fig. 4 by the corresponding comparison of the derivatives. All these curves including the exact solution display a maximum at the same location $\lambda = 1.25 = \lambda_*$ which is perhaps key to the overall success obtained.

In conclusion, the present Variational Principle appears to be very powerful. Also, when approximate probabilities are derived then (7.13) is the basic expression to be used for the association rates, rather than (7.14) which is approriate only for exact QSS-solutions in block *E*. Under exact QSS, (7.13) of course reduces to (7.14). If, for example, probabilities based on the diffusion equation are adopted, then (7.13) provides highly accurate rates.[28]

7.3 Tellegen's Theorem and the Principle of Least Dissipation

The set of equations (6.1b) for $\partial n_i/\partial t$ for the blocks C, E and S involves the energy E_i as a continuous variable since the spacing between the bound levels are much smaller than the thermal energy $k\Theta$ of the gas. The discrete representation of (6.1b) can be written as

$$I_i \equiv \frac{\partial n_i}{\partial t} = \sum_f \frac{\partial n_{if}}{\partial t} \equiv \sum_f I_{if} \tag{7.20}$$

where

$$\frac{\partial}{\partial t} n_{if} = [\gamma_f(t) - \gamma_i(t)]C_{if} \equiv (V_f - V_i)/R_{if} \equiv I_{if} \tag{7.21}$$

As Bates[29] has pointed out, the formal structure of (7.20) is identical to an electrical network where the current I_{if} in the line segment e_{if} (edges, element) between nodes (vertices), i and f, of the network is equivalent to the voltage drop V_{fi} ($= V_f - V_i \equiv \gamma_f - \gamma_i$) times the conductivity C_{if} of the element e_{if} (with resistance R_{if}) i.e., (7.21) is simply Ohm's Law for each element.

The quasi-equilibrium condition ($\partial n_i/\partial t = 0$ in block E) is equivalent to Kirchhoff's Current Law (KCL),

$$I_i(t) = \sum_f I_{if}(t) = 0 \tag{7.22}$$

i.e., the net instantaneous current entering and leaving each node i in block E is zero, which expresses the conservation of current.

Since $\gamma_i(t)$ varies continuously and monotonically with E_i between γ_c (constant over all energies in block C) and γ_s (constant over all energies in

block S),

$$\oint_{e_{if}} V_{fi} = \oint [\gamma_f(t) - \gamma_i(t)] = 0 \tag{7.23}$$

where the sum is over each segment e_{if} within a closed loop ($C \gtrless E \gtrless S$). Eq. 7.23) is analogous to Kirchhoff's Voltage Law (KVL) i.e., the sum of voltage changes V_{fi} around a closed loop is zero, and expresses the uniqueness of potential or of γ_i.

Just as KCL and KVL deal with an equilibrium distribution of current and voltage, an equally powerful relationship for equilibrium of power in a network which satisfies Kirchhoff's Laws was first enunciated in 1952 by Tellegen.[30] Tellegen's Theorem (TT) for KCL and KVL network states that the sum of instantaneous powers p_i delivered to all elements e_{if} is zero[30-32] i.e.,

$$\sum_i p_i(t) = \sum_i \sum_{e_{if}} I_{if}(t)\, V_{if}(t) = -\sum_i^{E\ (C,E,S)} \sum_{e_{if}} [\gamma_f(t) - \gamma_i(t)]^2 C_{if} = 0 \tag{7.24}$$

for all elements e_{if} with all nodes i only in the block E which only obeys KCL (since $\partial n_i/\partial t = 0$) and KVL, and with nodes f in any of the blocks C, E and S. Since the equilibrium rate C_{if} is symmetric, the rate (7.1a) with (7.2) may be expressed as,

$$R^{A,D}(t) = \pm\, 1/2[\gamma_c(t) - \gamma_s(t)] \int_{-D}^{\infty} dE_i \int_{-D}^{\infty} (P_i^A - P_f^A)^2 C_{if}\, dE_f \tag{7.25}$$

where (+) and (-) are associated with R^A and R^D, respectively.

The contribution to (7.1) which originates from the block E is

$$R^{A,D}(E;t) = \frac{\partial}{\partial t} \int_{-S}^{0} P_i^{A,D}\, n_i(t) dE_i = 0 \tag{7.26}$$

under the quasi-equilibrium condition ($\partial n_i/\partial t = 0$ in block E). Hence

$$R^{A,D}(E,t) = \pm\, 1/2\, [\gamma_c(t) - \gamma_s(t)] \int_{-S}^{0} dE_i \int_{-D}^{\infty} (P_i^A - P_f^A)^2 C_{if}\, dE_f = 0 \qquad (7.27)$$

which is the continuum analogy of Tellegen's Network Theorem (7.24)

Since p_i is the time rate of change in total energy ($n_i E_i$) of all pairs n_i of energy E_i,

$$p_i(t) = \frac{\partial}{\partial t}\,(n_i E_i) \qquad (7.28)$$

then Tellegen's Theorem implies

$$\sum_i p_i(t) = \frac{\partial}{\partial t} \sum_i (n_i E_i) \equiv \frac{\partial}{\partial t} \left[\int_{-S}^{0} n_i E_i\, dE_i\right] = 0 \qquad (7.29)$$

such that the total energy of all pairs in block E therefore <u>remains constant in time</u> and total energy of all pairs in block E is then conserved. This is a remarkable result! But the principle of energy conservation is already inherent to Kirchhoff's Laws and therefore need not be separately stipulated as implied in (7.29) via TT. The three laws are equally powerful in that any two of KCL, KVL and TT imply the third. The greater significance of Tellegen's Theorem, however, lies not in the confirmation of this fundamental law to one network, which in itself is no surprise, but in its general application to two topologically equivalent networks which obey Kirchhoff's Laws via the basic result

$$\sum_i \sum_{e_{if}} I_{if}(t)\, v_{if}(t) = \sum_i \sum_{e_{if}} i_{if}(t)\, V_{if}(t) = 0 \qquad (7.30)$$

where (I_{if}, V_{if}) and (i_{if}, v_{if}) are associated with each of two equivalent networks respectively and satisfy Kirchhoff's Laws for each network.

The Voltage Minimax Theorem[31] i.e., the maximum and minimum potentials in nonlinear resistor networks are at external nodes (i.e., within the C and S blocks external to block E), is applicable here and can be deduced[31] from Tellegen's Theorem.

In the full electrical network composed of blocks C, E and S, KCL is of course not satisfied in the C and S blocks (since $\partial n_i/\partial t$ is non-zero except in the $t \to \infty$ limit of thermodynamic equilibrium), and neither is TT. With the aid of (7.24) and (7.25) the total power absorbed by the complete network (C, E and S),

$$\sum_{C,E,S} p_i(t) = \frac{\partial}{\partial t}\left[\int_{-D}^{\infty} E_i n_i(t) dE_i\right] = -[\gamma_c(t) - \gamma_s(t)]^2 \int_{-D}^{\infty} dE_i \int_{-D}^{\infty} (P_i^A - P_f^A)^2 C_{if}\, dE_f$$

$$= \begin{cases} -2[\gamma_c(t) - \gamma_s(t)]R^A(t) \leqslant 0 \\ +2[\gamma_c(t) - \gamma_s(t)]R^D(t) \leqslant 0 \end{cases} \qquad (7.31)$$

is always negative i.e., energy is always dissipated. The equality only holds at thermodynamic equilibrium when $\gamma_c \to \gamma_s \to 1$. When the net direction is association, $\gamma_c > \gamma_s$ and R^A is positive and minimum. The Variational Principle (§ 7.1) of minimum R^A then implies via (7.31) that the energy dissipated to the gas bath is least. When the net direction is dissociation, $\gamma_s > \gamma_c$, R^D is positive and minimum and the Variational Principle (§ 7.1) also implies via (7.31) least energy of dissipation. An alternative form of the present Variational Principle is that the probabilities are so distributed among the energy levels not only to yield extremum rates $R^{A,D}(t)$, as in § 7.1, but also to provide least rate (7.31) of energy dissipation. This Principle of Least Dissipation is of great significance

in many fields e.g., thermodynamics,[33] heat conduction, fluid mechanics, etc. Onsager,[15] for example, derived the Principle explicitly for heat conduction. Joule's Law for a net current entering into a KVL and a KCL electrical network (block E) via all connecting elements in the block C and to all existing modes in the block S, states that the currents are so distributed within the network that the summed rate of dissipation of energy in the combined C, E and S blocks is a minimum. We have here derived the Principle explicitly from (7.22) via extrema (§7.1) to the rates of association/dissociation processes. Bates,[29] by analogy with Joule's Law, postulated that a measure S of the restoration rate of thermodynamic equilibrium by recombination for highly non-equilibrium systems (i.e., $\gamma_C >> \gamma_S$ such that explicit time-dependence can be ignored) be a minimum, a Principle which resulted[34] for recombination alone in the quasi-steady-state condition (7.6) of block E. From eq. (7.1) and (7.31) it follows that this unnormalized time-independent measure S can now be identified with the rate $2\alpha\tilde{N}_A\tilde{N}_B$. We have also generalized the situation by asserting that association/dissociation in general proceeds such that the rates $R^{A,D}(t)$ of (7.1) are extrema at all times such that $R^{A,D}(t\to\infty)$ tends naturally to zero when thermodynamic equilibrium is established (in contrast to S). The Principle of Least Dissipation is then satisfied, irrespective of the QSS-condition (7.6). Under the added constraints (7.3), the condition for extrema in $R^{A,D}$ yields the QSS-condition (7.5) quite naturally. We have also shown that the QSS-condition is equivalent to Tellengen's Theorem (7.29) such that the total power (7.31) in the Principle of Least Dissipation reduces to the sum of powers dissipated only in blocks C and S.

In conclusion, an alternative procedure to solution of coupled integro-differential equations derived in §4 is the direct search for extrema to the rates (7.1). These extrema are the actual rates of the process and the system satisfies the Principle of Least Dissipation. The procedure is, in general, irrespective of the quasi-steady-state condition (7.5) which necessarily follows only when the further constraints (7.3) are imposed. Direct application of the Variational Principle yields excellent results (cf Fig. 2-4).

8. Summary

Sets of transport-collisional Master Equations required for a comprehensive description of the two-particle non-equilibrium microscopic distribution n of subsystems (A-B) in a thermal gas bath M have been derived in §2 and §3 for various physical representations. Each set is appropriate to the variation of gas density N between its low and high density limits. Assumption of equilibrium in one or more of the dynamical physical quantities $(\underset{\sim}{R},E,L_i^2,T_i)$ in §4 helps reduce the complexity and dimensionality of the solution n for the corresponding Master Equation for the distribution of subsystems. Even in the limit of low gas density N, the procedure, not only of course yields the appropriate input-out Master Equation (4.12a), the subject of many previous studies[6-14], but also uncovers an additional eqn,(4.12b) or (4.17b) which helps complete the full description of association/dissociation processes at low N. The various Master Equations furnish complete details of n as N is varied.

In §5, expressions for association/dissociation rates $R^{A,D}(t)$ are formulated in terms of two-particle distribution function under conditions both of quasi-steady-state (QSS) of block E and of non-QSS, when the appropriate rates are given by (3.34) and by (5.36), respectively. By operating at a more basic microscopic level, the present approach has also exposed in §5.3 the key assumptions inherent to the Debye-Smoluchowski Equation used frequently for chemical reactions in condensed matter. The present treatment therefore provides a unified account of reactions in both gas and condensed matter phase.

In §6, the evolution from a non-equilibrium situation to full thermodynamic equilibrium with the gas M is provided by introduction of the probabilities $P_i^{A,D}$ for association or dissociation of level i of the A-B

pair. Here, the ansatz (6.7) permits separation of time t from the remaining physical variables as $(E_i, L_i^2, \underset{\sim}{R})$, and automatically permits the QSS-condition to be maintained at all times towards eventual equilibrium. The non-QSS rates $R^{A,D}(t)$ are now given by (7.1) and (7.13) and the QSS-rates by (7.8) or (7.14). The former expressions are valuable[28] when approximate probabilities $P_i^{A,D}$, such as those given by the diffusion approach,[28] are used, whereas the latter QSS-rates are inappropriate[28] when approximate $P_i^{A,D}$ are used.

A new Variational Principle for general association/dissociation rates $R^{A,D}(t)$ of eq. (7.1) is proposed in §7.1. The Principle asserts that the actual rates $R^{A,D}(t)$ are extrema at all times i.e. the rate $R^A(t)$ or $R^D(t)$, whichever corresponds to the overall direction of the process, always adjusts itself to a minimum. If conditions are such that the overall direction is association then, at all times t, $R^A(t)$ is minimum and $R^D(t)$ is maximum; and vice-versa when dissociation is the overall direction. There is therefore a tendency to counteract the change and evolution towards equilibrium is impeded. Provided P_i^A is zero and unity in blocks *C* and *S*, respectively, a consequence is the QSS-condition (7.6), or the integral eq. (7.7b), so that QSS-rates $R_*^{A,D}(t)$, which can now be derived directly from the current, are extrema, and are exact.

Direct application of the Principle in §7.2 shows that use of simple analytical variational functions for $P_i^{A,D}$ in the new general expressions (7.1) or (7.13) for $R^{A,D}(t)$ under non-QSS yields a minimum (for ion-ion recombination) which reproduces the exact QSS-rates.[10] The general expression (7.1) is valuable when approximate probabilities $P_i^{A,D}$ are used, in contrast to the QSS-expression (7.8).

In §7.3, contact is established between the present Principle and (a) with Tellegen's Theorem[30-32] for theory of electrical networks i.e. the

total energy in QSS-block E remains constant in time, and (b) with the Principle of Least Dissipation (of Onsager[15,33] for heat conduction) wherein the total energy dissipated by the (A-B) pairs in combined blocks C, E and S is always least and (c) with Bates' Postulate[29] for highly non-equilibrium systems ($\gamma_C >> \gamma_S$) that, by analogy with Joule's Law[29], an unnormalized measure S of the total rate of restoration of thermodynamic equilibrium is a minimum, which results[34] in the QSS-condition. The general principle here is that the net time-dependent rates $R^{A,D}(t)$ are extrema at all times t, and it naturally follows that $R^{A,D}(t \to \infty)$ tends to zero, as it should, when thermodynamic equilibrium is established.

Various components of the present theory e.g. reduction of the collisional terms via a Fokker-Planck analysis to obtain a diffusional treatment which is highly accurate for all systems and interactions, and the search for (exact) time-dependent analytical solutions of the Debye-Smoluchowski Equation (§5.4) for general interactions are considered in future papers.[27,28]

Acknowledgment

This research is supported by the U.S. Air Force Office of Scientific Research under Grant No. AFOSR-84-0233. The author acknowledges a disucssion with Dr. R. Fox concerning Tellegen's Theorem.

Appendix A: Equilibrium Distributions and Related Properties

Here we summarize and derive various classical equilibrium distributions and properties relevant to the present theory. Bates and McKibbin[35] have already discussed several important aspects of classical distribution functions. The probability distribution of AB pairs with internal separation $\underset{\sim}{R}$ and internal momentum $\underset{\sim}{p}$ in the phase interval $d\underset{\sim}{R}d\underset{\sim}{p}$ under thermodynamic equilibrium at temperature T with dissociated species A and B is[36]

$$n(\underset{\sim}{R},\underset{\sim}{p})d\underset{\sim}{R}d\underset{\sim}{p} \equiv \frac{n_{AB}(\underset{\sim}{R},\underset{\sim}{p})d\underset{\sim}{R}d\underset{\sim}{p}}{N_A N_B} = \frac{\omega_{AB}}{\omega_A \omega_B} \frac{h^3}{(2\pi mkT)^{3/2}} \left(\frac{d\underset{\sim}{p}d\underset{\sim}{R}}{h^3}\right) \exp(-E/kT) \qquad (A1)$$

where the combined electronic and nuclear degeneracy factors are ω_{AB} for the AB pair with phase density n_{AB}, with reduced mass m and internal energy $E \leq 0$, and are ω_A and ω_B for each of the dissociated species of equilibrium concentration (cm^{-3}) N_A and N_B, respectively. The ratio of the corresponding translational partition functions (number of quantum states available to "move" at temperature T) is $h^3/(2\pi mkT)^{3/2}$, and $d\underset{\sim}{p}d\underset{\sim}{R}/h^3$ is the number of internal AB states (relative energy E and angular momentum L) in the element $d\underset{\sim}{p}d\underset{\sim}{R}$ of phase space. The exponential term is the canonical distribution for the species of energy $E< 0$ interacting with a heat reservoir (gas) at temperature T. The equilibrium constant $K_{eq}(\underset{\sim}{R},\underset{\sim}{p})d\underset{\sim}{R}d\underset{\sim}{p} = (\alpha/k)d\underset{\sim}{R}d\underset{\sim}{p}$ for $A + B \underset{k}{\overset{\alpha}{\rightleftarrows}} AB$, with forward association rate $\alpha(cm^3\ s^{-1})$ and dissociation frequency $k(s^{-1})$, is also given by (A1) since $\alpha N_A N_B = k n_{AB}$.

Implicit to (A1), the internal energy,

$$E = T_i + V(R) = p^2/2m + V(R) \qquad (A2)$$

where V(R) is the potential energy between A and B at separation R and where T_i is the relative kinetic energy $p^2/2m$, and the internal angular momentum

squared of the AB pair,

$$L^2 = R^2\, p^2 \sin^2\theta \tag{A3}$$

where θ is the angle between $\hat{R}$ and $\hat{p}$, are both conserved in time. For structureless particles $\omega_{AB} = \omega_A\, \omega_B$.

The equilibrium distribution $n(R,p)$ is independent of the directions (θ,ϕ) and (θ_R, ϕ_R) of $\hat{p}$ and $\hat{R}$, respectively, and depends only on p and R via (A2) for E. Since $p^2\, dp\, d(\cos\theta) = (m\, p\, dE)dL^2/(2R^2p^2\cos\theta)$, then

$$n(R,E,\theta) = \frac{\exp(-E/kT)}{(2\pi mkT)^{3/2}} \quad (2\pi mp) \quad , \tag{A4}$$

the probability density (per unit $dRdEd(\cos\theta)$) of (R,E,θ) pairs is independent of θ. Since L^2 varies from $0 \to L^2_{max}(=R^2p^2) \to 0$ as θ varies from $0 \to \frac{\pi}{2} \to \pi$, then

$$n(R,E,L^2) = \frac{\exp(-E/kT)}{(2\pi mkT)^{3/2}} \left[\frac{2\pi m}{R^2(p^2-L^2/R^2)^{1/2}}\right] \tag{A5}$$

is the probability density (per unit $dR\ dE\ dL^2$) of pairs with (R,E,L^2). Also the probability density is

$$n(R,E) = \int_0^{R^2p^2} n(R,E,L^2)dL^2 = \frac{\exp(-E/kT)}{(2\pi mkT)^{3/2}} \left[4\pi mp\right] \tag{A6}$$

per unit $dRdE$ and is the Maxwell-Boltzmann distribution

$$n(R,T) = \frac{2}{\sqrt{\pi}} \frac{T_i^{1/2}\exp(-T_i/kT)}{(kT)^{3/2}} \exp(-V/kT) \tag{A7}$$

per unit $dRdT$. The distribution per unit $dE\ dL^2$ is

$$n(E,L^2) = \int_{R_1}^{R_2} n(\underset{\sim}{R},E,L^2)d\underset{\sim}{R} = \frac{\exp(-E/kT)}{(2\pi mkT)^{3/2}}\left[4\pi^2\tau_R(E,L^2)\right] \tag{A8}$$

where τ_R is the radial period i.e., time dR/v_R for completion of a round trip between the turning points $R_1(E,L^2) \rightarrow R_2(E,L^2) \rightarrow R_1(E,L^2)$ given by the zeros of the radial speed v_R i.e., of

$$\frac{1}{2}mv_R^2 = p^2/2m - L^2/2mR^2 = E-[V(R) + L^2/2mR^2] \tag{A9}$$

The probability that (E,L^2)-pairs have separation $\underset{\sim}{R}$ in the interval $d\underset{\sim}{R}$ about $\underset{\sim}{R}$ is then

$$\frac{n(\underset{\sim}{R},E,L^2)d\underset{\sim}{R}}{n(E,L^2)} = \frac{2dR}{\tau_R v_R} = \frac{dT}{T} \tag{A10}$$

where T is half the radial period. This is expected since L^2-conservation implies constant areal speed.

The radial period for a Coulomb field ($V = -e^2/R$) is

$$\left.\begin{aligned}\tau_R^{(c)}(E,L^2) &= (m/2|E|)^{1/2}\int_{R_1}^{R_2}\left[(R_2-R)(R-R_1)\right]^{-1/2}dR^2 \\ &= 2\pi(e^2/2|E|)^{3/2}(m/e^2)^{1/2} \equiv 2\pi a^{3/2}(m/e^2)^{1/2}\end{aligned}\right\} \tag{A11}$$

is independent of L^2, and is proportional to the cube-root of the semimajor axis a ($\equiv e^2/2|E|$) for elliptical motion (Kepler's Law). Since the radial and angular periods are the same for Coulomb attraction τ_R, is also the time τ_c for completion of the closed elliptical orbit,

$$R = 2R_1R_2[(R_1+R_2) + (R_2-R_1)\cos\theta]^{-1} \tag{A12}$$

which is the distance from the focus (force-center) and θ is measured from the eccentricity vector joining the focus to the periapsis.

For the three dimensional harmonic oscillator ($V = \frac{1}{2} k R^2$), the radial period is

$$\tau_R^{(0)}(E,L^2) = (m/k)^{1/2} \int_{R_1}^{R_2} \left[(R_2^2-R^2)(R^2-R_1^2)\right]^{-1/2} dR^2 = \pi(m/k)^{1/2} \equiv \pi/\omega = \frac{1}{2} \tau_c \qquad (A13)$$

is independent of both E and L^2, and is one half the angular period or the time $2\pi/\omega$ for completion of the associated closed elliptical orbit

$$R^2 = 2R_1^2R_2^2[(R_1^2+R_2^2) + (R_2^2-R_1^2)\cos 2\theta]^{-1} \qquad (A14)$$

with the force center at the center of the ellipse. While circular orbits are possible for certain combinations of E and L^2 for other interactions V, closed orbits for all $E < 0$ and L^2 are only possible for the above Coulombic (C) and oscillator (O) interactions which, in addition to conservation of E and L appropriate to all radial V(R), yield a futher (time) conserved quantity associated with a further dynamical symmetry; for C, the direction of the Runge-Lenz vector[37] which joins the foci and periapsis is constant in time; for O, each component energy E_x and E_y for individual motion in the X and Y directions of the orbit plane are conserved, as is $E = E_x + E_y$, the total energy.

The energy distribution for all states with L^2 in a specified range $0 \leq L^2 \leq L_x^2$ of L^2 is therefore with the aid of (A11) and (A13) in (A8) given by

$$n(E,L^2 \leq L_x^2) = \frac{\exp(-E/kT)}{(2\pi mkT)^{3/2}} \left[4\pi^2 \tau_R L_x^2\right] \qquad (A15)$$

for both Coulomb and Oscillator interactions. The probability density (per unit energy interval) of orbits with a given energy E which therefore intersect a sphere of radius R_x is given therefore by (A15) with $L_x^2 = p_x^2 R_x^2$

$= 2m\, R_x^2\, [E-V(R_x)]$ where p_x is the momentum at R_x associated with the orbit which just touches the R_x-sphere.

The distribution per unit dE is

$$n(E) = \int_o^{R_E} n(\underset{\sim}{R},E)d\underset{\sim}{R} = \int_o^{L_o^2} n\,(E,L^2)dL^2 \tag{A16}$$

where R_E is the classical turning point given by $|V(R_E) = |E|$ and where L_o is the maximum angular momentum associated with a given energy E.

For Coulombic attraction, $L_o^2 = 2m\, E\, a^2$ so that

$$n_c(E) = \frac{4\pi^2\, \exp(-E/kT)}{(2\pi mkT)^{3/2}}\, \tau_R(E) L_o^2 = \frac{\exp(-E/kT)}{(2\pi mkT)^{3/2}} \left[\frac{2^1/_2 m^{3/_2} \pi^3 e^6}{|E|^{5/_2}}\right] \tag{A17}$$

the Saha-Boltzmann formula for ionization equilibrium. For the three-dimensional oscillator, $L_o = (m/k)^{1/2}\, E = E/\omega$, the equilibrium energy distribution is,

$$n_o(E) = \frac{\exp(-E/kT)}{(2\pi mkT)^{3/2}} \left[4\pi^3 (m/k)^{3/2}\, E^2\right] \tag{A18}$$

The fraction of the total number of bound orbits of energy E which <u>cross</u> a sphere of radius R_x, i.e., those with $L^2 \leq L_x^2 = 2m\, R_x^2 [E-V(R_x)]$, is therefore,

$$f_x(E) = L_x^2/L_o^2 = \begin{cases} (R_x/a)^2 [E-V(R_x)]/|E| \ , & \text{Coulomb} \\ 2m(\omega R_x/E)^2 [E-V(R_x)], & \text{Oscillator} \end{cases} \tag{A19}$$

Thus $f_x(E)\, n(E)dE$ is the number of classical orbits with energy between E and E + dE that cross a sphere of radius R_x centered at the origin. As R_x increases from zero, the number of crossing Coulombic orbits increases as R_x, reaches a maximum at $R_x = a = e^2/2|E|$, and then decreases to zero as R_x tends to

$e^2/|E| = 2a$, the classical turning point for the L = 0 orbit; because high L-orbits fully encompass the R_x-sphere for small $R_x < a$ and are fully encompassed by the R_x-sphere when $a < R_x < 2a$.

The fractional contribution to the overall Coulombic density distribution (A17) that arises within the R_x-sphere is

$$g_x(E) = \frac{n(E,R\leq R_x)}{n(E)} = \frac{2}{\pi}\left[\theta_x - \frac{1}{4}\sin 2\theta_x - \frac{1}{4}\sin 4\theta_x + \frac{1}{12}\sin 6\theta_x\right] \qquad (A20)$$

where $\theta_x = \sin^{-1}(R_x/R_E)$ in terms of the turning point $R_E = e^2/|E|$ where $g_x \to 1$.

Thus $g_x(E)n(E)dE$ is the equilibrium number of pairs with internal separation $R \leq R_x$ and with internal energy between E and E + dE.

The density of bound AB-pairs with internal separation $\underset{\sim}{R}$ is

$$n(\underset{\sim}{R}) = \int_{-V(R)}^{o} n(\underset{\sim}{R},E)dE = \int_{o}^{T_o} n(\underset{\sim}{R},T_i)dT_i \qquad (A21)$$

where T_o is the maximum kinetic energy (-V) of relative motion at R. With respect to the distribution exp(-V/kT) over R of all levels (bound and continuous) the normalized fraction

$$f(R) = n(\underset{\sim}{R})/\exp(-V/kT) = [\mathrm{erf}(-V/kT)^{1/2} - \frac{2}{\sqrt{\pi}}|V/kT|^{1/2}\exp(V/kT)] \qquad (A22)$$

of bound levels varies from 0 to 1 as R decreases from infinity to zero. For Coulombic attraction, f is 0.20, 0.43, 0.73 and 0.996 at $R = 2R_e$, R_e, 0.5 R_e and 0.15 R_e, respectively, where R_e is the natural (Onsager) radius e^2/kT where V = kT.

The conditional equilibrium probability or the equilibrium constants $K_{eq} = \alpha/k$ per unit $d\Gamma_1\, d\Gamma_2 \ldots$ for $A + B \underset{k}{\overset{\alpha}{\rightleftarrows}} AB$ can in general be written as,

$$n(\Gamma_1,\Gamma_2,..,\Gamma_s) = \frac{h^3 \exp(-E/kT)}{(2\pi mkT)^{3/2}} \rho_c(\Gamma_1,\Gamma_2,..,\Gamma_s) \equiv K_{eq}(\Gamma_1,\Gamma_2,..,\Gamma_s) \qquad (A23)$$

where ρ_c is the classical density or statistical weights of internal states. The corresponding statistical volumes, $h^3\rho_c$ are given directly by the square-bracket terms in (A4) - (A8) for each of the five sets $(\underset{\sim}{R},E,\theta)$, $(\underset{\sim}{R},E,L^2)$, $(\underset{\sim}{R},E)$, $(\underset{\sim}{R},T)$ and (E,L^2) of variables and in (A17) and (A18) for the particular energy distributions appropriate to Coulombic and oscillator attractions.

Finally, it is worth noting that equilibrium with respect to a given variable Γ_j alone implies that the fractional distribution $n(\Gamma_1,\Gamma_2, \ldots, \Gamma_s)/\int n\, d\Gamma_j$ is given simply by the corresponding equilibrium fraction.

Classical-Quantal Correspondences. Since the three-dimensional Coulomb (C) and oscillator (O) interactions are unique in having closed bounded orbits for all values of $E < 0$ and L^2, new and interesting classical-quantal correspondences may be derived. Under appropriate quantization, $n_\phi h$ and $(n_{R,\theta}+1/2)h$ when $n_{R,\theta,\phi} = 0, 1, \ldots$, of the actions associated with (ϕ) and libration (R,θ) generalized coordinates, and generalized momenta (p_R,p_θ,p_ϕ) respectively, the full classical action for Coulombic attraction

$$J = \oint p_R dR + \oint p_\phi d\phi + \oint p_\theta d\theta = (2m)^{1/2}\, \pi e^2\, |E|^{-1/2} = (n_r + n_\theta + n_\phi + 1)h \qquad (A24)$$

being quantized to integral $(n \geq 1)h$, yields, as is well known, the exact quantal energies. For the isotropic oscillator, the quantized classical action

$$J = \oint p_x dx + \int p_y dy + \int p_z dz = 2\pi(m/k)^{1/2}\, E = (n+3/2)h \quad , \quad n = 0, 1, \ldots \qquad (A25)$$

yields the correct quantal energies[38]

$$E_n = (n + 3/2)\hbar\omega \quad ; \quad \omega = (k/m)^{1/2} \tag{A26}$$

with degeneracy $\frac{1}{2}(n+1)(n+2)$. The number of internal states $\rho_Q(E)$ per unit energy interval dE is therefore given by

$$\rho_Q(E)dE = \tfrac{1}{2}(n+1)(n+2)dn = \tfrac{1}{2}(n+1)(n+2)dE_n/\hbar\omega \tag{A27}$$

which in the limit of high $n >> 1$ agrees with the classical density $\rho_c(E) = 4\pi^3 E^2/(h^3\omega^3)$ obtained from (A18) and (A23). Since even ℓ are associated with even n, and odd ℓ are associated with odd n, then in the classical limit of continuous ℓ,

$$\rho_Q(E,L^2)dE_n\, dL^2 = \tfrac{1}{2}(2\ell+1)dn\, d\ell = \tfrac{1}{2}\, dE_n\, dL^2/\hbar^3\omega \tag{A28}$$

with $L^2 = \ell(\ell+1)\hbar^2$. This quantal density ρ_Q agrees exactly with the classical density $\rho_c(E,L^2) = 4\pi^2\tau_R/h^3$ obtained from (A8) and (A13). Corresponding identities

$$\rho_Q(E,L^2) = n^3/(me^4) = 4\pi^2\tau_c/h^3 = \rho_c(E,L^2) \tag{A29}$$

and

$$\rho_Q(E) = n^5/(e^2/a_o) = 4\pi^2\tau L_o^2/h^3 = \rho_c(E) \tag{A30}$$

for Coulombic attraction have already been shown.[35] These identities support the use of classical distributions for these interactions in heavy-particle systems.

The classical average of R^s for bound orbits with $E < 0$ and all accessible L^2, is

$$\langle R^s(E)\rangle = \int_0^{R_E} R^s\, n(\underset{\sim}{R},E)d\underset{\sim}{R} \Big/ \int_0^{R_E} n(\underset{\sim}{R},E)d\underset{\sim}{R} \tag{A31}$$

which, for the Coulomb case, yields

$$\langle R^s(E)\rangle = R_E{}^s\, B(\tfrac{3}{2}, \tfrac{5}{2} + s)/B(\tfrac{3}{2}, \tfrac{5}{2}) \tag{A32}$$

where R_E is the turning point $e^2/|E|$ and where the Beta function $B(x,y)$ is $\Gamma(x)\,\Gamma(y)/\Gamma(x+y)$ in terms of the Gamma function Γ. Hence,

$$\langle R(E_n)\rangle = \left(\frac{5}{4}\right) a \qquad ; \qquad a = e^2/2|E_n| \equiv n^2 a_o \tag{A33}$$

whch agrees at high $n >> 1$ with the quantal expectation value[39]

$$\langle R_n\rangle = \frac{1}{n^2} \sum_{\ell=0}^{n-1} (2\ell+1)\langle R_{n\ell}\rangle = \frac{5}{4}\,(1 + 1/5n^2)n^2 a_o \tag{A34}$$

Moreover, the classical average of R over a given bound (E,L^2)-orbit is

$$\begin{aligned}\langle R(E,L^2)\rangle &= \int_{R_1}^{R_2} R\, n(\underset{\sim}{R},E,L^2)d\underset{\sim}{R} \Big/ \int_{R_1}^{R_2} n(\underset{\sim}{R},E,L^2)d\underset{\sim}{R} \\ &= \frac{3}{2}\, a - L^2/2me^2\end{aligned} \tag{A35}$$

and agrees exactly with the quantal value $\frac{1}{2}\, a_o[3n^2 - \ell(\ell+1)]$.[39] If the ℓ-summation in (A34) is replaced by L^2-integration between 0 and $L^2_{max} = 2m|E|a^2$, then the quantal result (A34) yields the classical result (A33) exactly.

The averaged value of R for these orbits of energy E that cross a sphere of radius R_x is therefore

$$\langle R(E,L_x^2)\rangle = \int_0^{L_x^2} dL^2 \int_{R_1}^{R_2} R\, n(\underset{\sim}{R},E,L^2)d\underset{\sim}{R} \Big/ \int_0^{L_x^2} dL^2 \int_{R_1}^{R_2} n(\underset{\sim}{R},E,L^2)d\underset{\sim}{R}$$

$$= \frac{3}{2}a - L_x^2/4me^2 \qquad \text{(A36)}$$

$$= \frac{3}{2}a - \frac{1}{2e^2}R_x^2[E - V(R_x)] \qquad \text{(A37)}$$

which for Coulomb attraction tends to $\frac{3}{2}a$ in the limit of small radii $R_x << a$ when only the L = 0 orbit crosses. When R_x equals a, all L^2-orbits cross and (A37) tends to $\left(\frac{5}{4}\right)a$, in agreement with (A33).

Apart from the intrinsic interest and considerable insight gained from noting that the classical equilibrium probability distribution and the quantal probability $|\psi_{n\ell m}|^2$ have much in common, all of the distributions (A4)-(A8), (A15)-(A22) over physical variables $(\underset{\sim}{R},E,L^2)$ and their associated properties (A32)-(A37), are directly relevant towards implementation of the theory and solution of the Master Equations developed in the main text for association/ dissociation processes in dense gases.

Appendix B: Equilibrium Energy-Change Collisional Rates for Various Subsystem AB-Bath M Interactions.

Theoretical Equilibrium Rates: In this section the collisional term (2.1b) of the "Boltzmann" equation (2.1) is transformed so as to yield equilibrium rates $C_{if}(R)$ for $i \to f$ transitions in the internal energy E_i of the AB pair with internal separation R via collision with the Maxwellian bath of gas particles M. Explicit expressions for C_{if} appropriate to various interactions (Coulomb, Polarization, Hard-Sphere, Charge-Transfer) of A and B with M are summarized for use as a comprehensive package in the theory provided in the main text.

Denote A, B and M by i = 1, 2 and 3, respectively, their masses and reduced masses by M_i and M_{ij}, respectively, and their pre- and post-collision velocities and momenta by $\underset{\sim}{v}_i$, $\underset{\sim}{p}_i$ and $\underset{\sim}{v}_i'$, $\underset{\sim}{p}_i'$ taken all relative to the (1-2) center of mass before the (1-3) collision. The (1-3) relative velocities before and after the collision are $\underset{\sim}{g}$ and $\underset{\sim}{g}'$ with orientation (ψ,ϕ) with respect to polar axis along $\hat{\underset{\sim}{g}}$. The changes $\varepsilon(\equiv E_f-E_i)$ and $\underset{\sim}{P}$ in the internal energy and internal momentum of the pair AB are $\frac{1}{2} M_{12}[(\underset{\sim}{v}'-\underset{\sim}{v}_2)^2 - (\underset{\sim}{v}_1-\underset{\sim}{v}_2)]^2$ and $M_{12}\ (\underset{\sim}{g}'-\underset{\sim}{g})$, respectively.

The rate C_{if} is the sum $C_{if}^{(1)} + C_{if}^{(2)}$ of the individual contributions $C_{if}^{(j)}$ arising from (j-3) scattering alone. Expressions for the averaged rates

$$k_{if}(E_i,E_f) = \int F(u)\ k_{if}(u)du \tag{B1}$$

arising from elastic (j-3) scattering by general,[7] hard-sphere[11] and polarization[8] interactions and from charge-transfer collisions[10] for general masses have been determined previously[7,11] by integrating the partial rates $k_{if}(u)$ for a fixed (1-2) relative speed u over the normalized speed

distribution F(u). Since the emphasis here is on the non-equilibrium R distributions of Boltzmann's equation at higher gas densities, the more relevant quantity is the energy change kernel $C_{if}(R)$ which is related to the previous quantity (B1) via

$$k_{if}(E_i,E_f) = [\tilde{n}_i(E_i)]^{-1} \int_0^{R_{if}} \tilde{n}_i(\underset{\sim}{R},E_i)\, k_{if}(R)d\underset{\sim}{R} \equiv [\tilde{n}_i(E_i)]^{-1} \int_0^{R_{if}} C_{if}(R)d\underset{\sim}{R} \qquad (B2)$$

where R_{if} is the minimum of the outermost turning points R_i and R_f associated with E_i and E_f respectively. The isolated kernels $C_{if}(R)$ for the various interactions are extracted from the previous work[7,8,10,11] as follows.

The Jacobians J in the following transformations

$$d\hat{\underset{\sim}{g}}'(\psi,\phi)\; d\hat{\underset{\sim}{p}}_3(\theta_3\phi_3) \equiv J_2\; d\varepsilon\, d(\cos\psi)dg\; d\phi_3 = J_3\; d\varepsilon\, dP\; dg\; d\phi_3 \qquad (B3)$$

valuable to the collisional term in Boltzmann's Equation (2.1b) have already been determined[7,9,40-42] as has[42] also J_5 in

$$d\underset{\sim}{p}_1'\; d\hat{\underset{\sim}{p}}_3' = J_5\; d\varepsilon\, dP\; d\underset{\sim}{p}_1 \qquad (B4)$$

valuable to transformation between quantal and semiquantal treatments[42]. The orientation (θ_3,ϕ_3) of $\hat{\underset{\sim}{p}}_3$ is taken with respect to the polar axis along $\hat{\underset{\sim}{p}}_1$. Evaluation of J_2 in (B3) yields (from ref. 7 for elastic A-M collisions and refs. 41 and 42 for inelastic A-M collisions),

$$\frac{1}{2}\, d(\cos\theta_3)d\phi\; d(\cos\psi) \equiv \frac{g\; dg}{v_1 v_3} \frac{d\varepsilon}{gS(v_1,v_3,g)} \frac{d(\cos\psi)}{[(\cos\psi^+ - \cos\psi)(\cos\psi - \cos\psi^-)]^{1/2}} \qquad (B5)$$

where

$$S(v_1,v_3,g) = \frac{M_{13}}{(1+a)}\ [(1+a)(v_1^2+av_3^2) - ag^2]^{1/2} = S(v_1',v_3',g') \qquad (B6)$$

is symmetric with respect to pre- and post-speeds. The limits[7,41,42] $\psi^{\pm}(v_1,v_3,g;\ )$ in (B5) to the scattering angle ψ for fixed v_1, v_3, g and ε need not be reproduced here. The limits $g^{\pm}(v_1,v_3;\varepsilon)$ to the relative speed g in (B5) are[7,41,42]

$$\left.\begin{aligned} g^-(v_1,v_3;\varepsilon) &= \max[|v_1-v_3|\ ,\ |v_1'-v_3'|] \\ g^+(v_1,v_3;\varepsilon) &= \min[v_1+v_3,\ v_1'+v_3'] \end{aligned}\right\} \qquad (B7)$$

and $g^+ \geq g^-$.

Determination of J_3 in (B3) yields[9,40-42] the alternative expression,

$$\frac{1}{2}\, d(\cos\theta_3)d\phi\ d(\cos\psi) \equiv \frac{g\ dg}{v_1 v_3}\ \frac{2g\ d\varepsilon}{P[(g_+^2-g^2)(g^2-g_-^2)]^{1/2}}\ \frac{P\ dP}{M_{13}^2 g^2} \qquad (B8)$$

where the limits $g_{\pm}(v_1,v_3;P,\varepsilon)$ to the relative speed g for fixed v_1, v_3, P and ε also need not be reproduced here. The limits $P^{\pm}(v_1,v_3;\varepsilon)$ to the momentum change P are

$$\left.\begin{aligned} P^-(v_1,v_3;\varepsilon) &= \max[M|v_1'-v_1|,\ M_s|v_3'-v_3|] \\ P^+(v_1,v_3;\ ) &= \min[M(v_1'+v_1)\ ,\ M_s(v_3'+v_3)] \end{aligned}\right\} \qquad (B9)$$

where

$$M = M_1(1 + M_1/M_2) \qquad (B10)$$

the effective mass of the AB pair in the (1-3) collision, and where

$$M_s = (M_1+M_2)M_3/(M_1+M_1+M_3) = aM = (1+a)M_{13} \quad , \tag{B11}$$

the reduced mass of the full pair-gas system, can be expressed in terms of a mass-ratio parameter[7]

$$a = M_2M_3/M_1(M_1+M_2+M_3) \tag{B12}$$

for (1-3) collisions.

Under thermodynamic equilibrium at temperature T,

$$\frac{\tilde{n}_i(\underset{\sim}{R},E_i)}{\tilde{N}_A\tilde{N}_B} = \frac{\exp(-E_i/kT)}{(2\pi M_{12}kT)^{3/2}} \; 4\pi M_{12}(M_1v_1) \tag{B13}$$

then the equilibrium rate for energy-change collisions at frequency ν_{if} is

$$C_{if}(R)dE_f = \tilde{n}_i(\underset{\sim}{R},E_i)\nu_{if}(R)\; dE_f \tag{B14a}$$

$$\equiv \tilde{n}_i(\underset{\sim}{R},E_i)dE_f \int \; N_o(\underset{\sim}{p}_3)d\underset{\sim}{p}_3 g\sigma(g,\psi)\; d(\cos\psi)(d\phi/d\varepsilon) \tag{B14b}$$

which is, in general, a four-dimensional integral. The transformation (B5) is appropriate to the cases of general differential cross sections $\sigma(g,\psi)$ or of isotropic cross sections $\sigma(g)$, and (B8) is appropriate for $\sigma(P,g)$ or $\sigma(P)$. For isotropic gas distributions $N_o(P_3)$, $C_{if}(R)$ is therefore a triple integral for general scattering of the AB pairs by M. Considerable reduction to a double or single integral or to an algebraic expression occurs for the following specific interactions.

CASE (1), $\sigma(P)$: For Coulombic attraction $(-e^2/R)$ between 1 and 3, the differential cross section per unit solid angle is

$$\sigma(P) = 4\, e^4\, M_{13}{}^2/P^4 \tag{B15}$$

a function only of momentum-change P. With (B8) in (B14b), the g-integration involves the integral $\int_{x^-}^{x^+}(x^+-x)(x-x^-)^{-1/2}\,dx = \pi$ so that the equilibrium rate is (B14a) with the frequency (per unit dE_f) given by

$$\nu_{if}^{(1)}(R) = (\pi/M_{13}^2 v_1)N \int_{v_o}^{\infty} v_3^{-1}\, G(v_3)dv_3 \int_{P^-}^{P^+} \sigma(P)dP \tag{B16}$$

for general $\sigma(P)$. The limit v_o arises from reality of $P^{\pm}$ in (B8) and satisfies $\frac{1}{2} M_s\, v_o{}^2 = \max(0, E_f - E_i)$, which asserts that the kinetic energy of AB-M relative motion be sufficient for excitation ($E_f > E_i$) or be at least zero for de-excitation ($E_f < E_i$). The R-dependence of ν_{if} at fixed E_i occurs via v_1 in $E_i = \frac{1}{2} M\, v_1^2 + V(R)$. The distribution G in speeds v_3 of the bath particles 3 of density N (cm^{-3}) is orientation independent and may for example be taken as the Maxwellian

$$\int_{4\pi} N_o(\underset{\sim}{p}_3)d\underset{\sim}{p}_3 = N\, G(v_3)dv_3 = \frac{2N}{\sqrt{\pi}} (\tfrac{1}{2} M_s\, v_3{}^2/kT)^{1/2}$$

$$\exp(-\tfrac{1}{2} M_s\, v_3{}^2/kT)d(\tfrac{1}{2} M_s\, v_3{}^2/kT) \tag{B17}$$

appropriate to thermodynamic equilibrium between 3 and the (1-2) center-of-mass. Hence,

$$\exp(-E_i/kT)v_3^{-1}\, G(v_3)dv_3 = \frac{2}{\sqrt{\pi}} (\tfrac{1}{2} M_s/kT)^{1/2} \exp(-E/kT)d(E/kT) \tag{B18}$$

where the total (conserved) energy of the system is

$$E = \tfrac{1}{2} M_s v_3^2 + E_i = \tfrac{1}{2} M_s v_3'^2 + E_f \qquad (B19)$$

From (B13) and (B15),

$$\frac{\tilde{n}_i(\underset{\sim}{R},E_i)}{\tilde{N}_A \tilde{N}_B} \frac{G(v_3)dv_3}{v_1 v_3} = \frac{2}{\pi} \frac{a^{1/2} M}{(kT)^2} \exp(-E/kT)\, d(E/kT) \qquad (B20)$$

so that the equilibrium collisional ($E_i \rightarrow E_f$) rate (B14) for general $\sigma(P)$ is

$$C_{if}^{(1)}(R) = \frac{2a^{1/2} MN}{M_{13}^2 (kT)^2} \int_{E_o}^{\infty} \exp(-E/kT)\, d(E/kT) \int_{P^-}^{P^+} \sigma(P) dp \qquad (B21)$$

where E_o is $\max(E_i,E_f)$. Since $P_\pm$ of (B9) is symmetric with respect to pre and post collision speeds, C_{if} is also symmetric thereby satisfying required detailed balance. For hard-sphere scattering, $\sigma(P) = \sigma_o/4\pi$, and the inner integral in (B21) is simply $(P^+ - P^-)\sigma_o/4\pi$; and (B21) then agrees with Eq. (32) of ref. (11), for Coulomb scattering (B15), the inner integrand of (B21) is $\frac{4}{3} e^4 M_{13}^2 (P^{-3} - P^{-3})$.

The frequencies ν_{if} and rates C_{if} are pure functions only of the initial and final kinetic energies $T_i = \frac{1}{2} M v_1^2$ and $T_f = \frac{1}{2} M v_1'^2$; and the R-dependence in (B21) arises via the (1-2) interaction $V(R)$ in $T_i = E_i - V(R)$ and $T_f = E_f - V(R)$ for fixed E_i and E_f.

CASE (2); $\sigma(g)$: When the (1-3) differential cross section is taken as the orbiting cross section,

$$\sigma(g) = (\alpha e^2/4M_{13} g^2)^{1/2} \equiv B/g \qquad (B22)$$

appropriate to polarization attraction ($-\alpha e^2/2R^4$) followed by core repulsion then, on integrating (B5) over ψ,

$$\nu_{if}^{(2)}(R) = (\pi/v_1)N \int_{v_o}^{\infty} v^{-1}\, G(v_3)dv_3 \int_{g^-}^{g^+} g\sigma(g)dg/S(v_1,v_3,g) \qquad (B23)$$

for isotropic (1-3) cross sections $\sigma(g)$, in general.

On adopting the Maxwellian distribution (B17) for G, the equilibrium collisional rate (B14) for this second case is therefore

$$C^{(2)}(R) = [2a^{1/2}MN/(kT)^2] \int_{E_o}^{\infty} \exp(-E/kT)d(E/kT) \int_{g^-}^{g^+} g\sigma(g)dg/S(v_1,v_3,g) \qquad (B24)$$

For polarization attraction (B22), the inner integral yields

$$B \int_{g^-}^{g^+} dg/S = \frac{B(1+a)}{M_{13}a^{1/2}} \left[\sin^{-1}(g^+/A) - \sin^{-1}(g^-/A)\right] \qquad (B25)$$

where

$$A^2(v_1,v_3) = (1+a)(v_1^2+av_3^2)/a \qquad (B26)$$

Since

$$2\sin^{-1} x^{1/2} = \tfrac{1}{2}\pi - \sin^{-1}(1-2x), \qquad (B27)$$

the result of Bates and Mendaš[8] for k_{if}, the averaged energy-change rate (B2) per AB-pair, is recovered.

CASE (3); Charge-Transfer: On assuming that the cross section σ^X for symmetrical resonance charge transfer

$$X^+ + X \rightarrow X + X^+ \qquad (B28)$$

is independent of the speed g of relative motion as at low energies, then the angular integrations of (B14) yield simply,

$$\frac{d(\cos\theta_3)}{4\pi} \int_{(\psi,\phi,\phi_3)} [g\sigma^X(g,\psi)d(\cos\psi)d\phi]d\phi_3 = \frac{1}{2}\,(v_1^2+v_3^2-2v_1v_3\cos\theta_3)^{1/2}\,Q^X d(\cos\theta_3)$$

$$= \left(\frac{1+c}{c}\right)^{3/2}[v_3^2-(v_1^2+2\varepsilon/M_1)]^{1/2}\,Q^X dE_f/(2M_1v_1v_3) \qquad (B29)$$

where Q^X is the integral cross section for charge transfer, where

$$c = M_1/M_2 \qquad (B30)$$

for (1-3) collisions and where $\varepsilon = E_f - E_i$ is the energy change. The frequency of $i \rightarrow f$ collisional transitions at (1-2) separation $\underset{\sim}{R}$ is therefore,

$$\nu_{if}^{(3)}(R) = \left(\frac{1+c}{c}\right)^{3/2}\left(\frac{NQ^X}{2M_1v_1}\right)\int_{v^-}^{v^+} v_3^{-1}\,G(v_3)\,[v_3^2-(v_1^2+2\varepsilon/M_1)]^{1/2} \qquad (B31)$$

where the limits to v_3 for a specified energy change ε at given speed v_1 are[10]

$$v^{\pm}(v_1;\varepsilon) = (1+c)\,[v_1 + 2\,/M_1(1+c)]^{1/2} \;\pm\; c\,v_1 \qquad (B32)$$

and originate from the assumption that the (1-3) collision (B28) simply interchanges $\underset{\sim}{v}_1$ and $\underset{\sim}{v}_3$. On adopting the Maxwellian distribution, (B31) can be rewritten as

$$\nu_{if}^{(3)}(R) = \left(\frac{1+c}{c}\right)^{3/2}\left(\frac{NQ^X}{2M_1v_1}\right)\exp(E_i/kT)\;I_{if}(v_1;E_i,E_f) \qquad (B33)$$

where

$$I_{if}(v_1;E_i,E_f) = \left[\exp -\left(\frac{1+c}{1+2c}\right)\left(\frac{E_i+E_f}{kT}\right)\right] \exp\left[-V(R)/(2c+1)kT\right] \int_{E^-}^{E^+} G(E)dE \qquad (B34)$$

is symmetrical in E_i and E_f. The fraction of Maxwell particles with energies E in the range $E^- \leq E \leq E^+$ is

$$G(E)dE = \left[\mathrm{erf}(E/kT)^{1/2} - \frac{2}{\sqrt{\pi}} (E/kT)^{1/2} \exp(-E/kT)\right]_{E_-}^{E+} \qquad (B35)$$

where for this case,

$$E^{\pm} = [c(1+c)/(1+2c)][\{E_i - V(R)\}^{1/2} \pm \{E_f - V(R)\}^{1/2}]^2 \qquad (B36)$$

Hence the equilibrium rate for i → f charge-transfer collisional transitions is

$$C_{if}^{x}(R) = \frac{[(1+c)/c]^{3/2}}{(2\pi M_{12})^{1/2}} \frac{N Q^x}{(kT)^{3/2}} I_{if}(v_1;E_i,E_f) \qquad (B37)$$

an algebraic expression which satisfies detailed balance and which yields the rate (in ref. 9) for k_{if}, the averaged rate (B2) per AB-pair.

Computational Equilibrium Rates: All of these equilibrium rates for the above three cases may be conveniently expressed for computational purposes in terms of dimensionless units,

$$\lambda = - E_i/kT, \quad \mu = - E_f/kT, \quad v(r) = - V(R)/kT$$
$$r = R/R_e, \quad R_e = e^2/kT \qquad (B38)$$

as

as

$$4\pi\, C_{if}(R)R^2 dR|dE_i||dE_f| = \Gamma \alpha_T\, F(\lambda,\mu;r) r^2\, dr\, d\lambda du,\ (cm^3\ s^{-1}) \qquad (B39)$$

in terms of specified mass factors Γ and the Thomson (low density) rates (see, for example, ref. 10).

$$\alpha_T = \frac{4}{3}\,\pi(R_e/\beta)^3(3kT/M_{12})^{1/2}\,\sigma_o N\ , \qquad \beta = 3/2 \qquad (B40)$$

where σ_o is the integral cross section for (1-3) collisions at relative energy $\frac{3}{2}$ kT. The appropriate mass factors Γ in (B39) and cross sections σ_o in (B40) are

$$\Gamma^H = \left(\frac{3}{2}\right)^{1/2}\left(\frac{\beta^3}{\pi}\right)\ \frac{(1+a)^2}{a^{3/2}}\ \left(\frac{M_{12}}{M_1}\right)\ ;\quad \sigma_o = \sigma_o^H \qquad (B41)$$

for hard-sphere (1-3) collisions with integral cross section σ_o^H,

$$\Gamma^C = \frac{3a}{\pi(1+a)}\ \Gamma^H\ ;\quad \sigma_o = \sigma_o^C = \frac{1}{9}\,\pi R_e^2 \qquad (B42)$$

for Coulomb (1-3) collisions with integral cross section $\sigma_o{}^C$ which corresponds to Coulomb scattering by angles $\psi \geq \pi/2$, and to energy transfers $\epsilon \gtrsim (3/2)kT$ for equal mass species. For (1-3) polarization attraction/core repulsion;

$$\Gamma^P = \left(\frac{3}{2}\right)\left(\frac{\beta^3}{\pi}\right)\ \frac{(1+a)^{5/2}}{a^{3/2}}\left(\frac{M_{12}}{M_1}\right)\ ;\quad \sigma_o = \sigma_o^P = 2\pi(\alpha R_e/3)^{1/2} \qquad (B43)$$

and $\sigma_o{}^P$ adopted in Thomson's rate (B40) is the corresponding integral (elastic or momentum transfer) collisional cross section at (3/2)kT relative energy. For (1-3) charge-transfer collisions,

$$\Gamma^X = \left(\frac{3}{2}\right)^{1/2}\left(\frac{\beta^3}{\pi}\right)\left(\frac{1+c}{c}\right)^{3/2}\ ;\quad \sigma_o = 2Q^X \qquad (B44)$$

where σ_o in (B46) is the corresponding momentum-transfer cross section, taken as twice the cross section Q^X for charge transfer.[43]

The corresponding dimensionless functions F in (B39) are symmetric in λ and μ and are

$$F^H(\lambda,\mu;r) = \int_{Y_o}^{\infty} \exp(-Y)dY\ [\tilde{P}_+ - \tilde{P}_-];\quad Y_o = \max(-\lambda,-\mu) \tag{B45}$$

for hard-sphere (1-3) collisions with (dimensionless) momentum-change limits $\tilde{P}_+ \geq \tilde{P}_-$, given by

$$\tilde{P}_-(\lambda,\mu;r) = \max\left[[v(r) - \lambda]^{1/2} - [v(r)-\mu]^{1/2}\ ;\ a^{1/2}[(Y+\lambda)^{1/2}-(Y+\mu)^{1/2}]\right]$$
and (B46)
$$\tilde{P}_+(\lambda,\mu;r) = \min\left[[v(r) - \lambda]^{1/2} + [v(r)-\mu]^{1/2}\ ;\ a^{1/2}\ [(Y+\lambda)^{1/2} + (Y+\mu)^{1/2}]\right]$$

Also

$$F^c(\lambda,\mu;r) = \int_{Y_o}^{\infty} \exp(-Y)dY\ [\tilde{P}_-^{-3} - \tilde{P}_+^{-3}] \tag{B47}$$

for Coulomb (1-3) collisions.

For polarization (1-3) collisions,

$$F^P(\lambda,\mu;r) = \int_{Y_o}^{\infty} \exp(-Y)dY\ [\sin^{-1}(G_2/A) - \sin^{-1}(G_1/A)] \tag{B48}$$

where

$$G_1(\lambda,\mu;r) = \max\left[\left|(Y+\lambda)^{1/2} - a^{1/2}[v(r)-\lambda]^{1/2}\right|;\left|(Y+\mu)^{1/2} - a^{1/2}[v(r)-\mu]^{1/2}\right|\right]$$
(B49)
$$G_2(\lambda,\mu;r) = \min\left[(Y+\lambda)^{1/2} + a^{1/2}[v(r)-\lambda]^{1/2};\ (Y+\mu)^{1/2} + a^{1/2}[v(r)-\mu]^{1/2}\right]$$

and

$$A = (1+a)^{1/2} \left[v(r) + Y\right]^{1/2} \tag{B50}$$

For charge-transfer (1-3) collisions

$$F^{x}(\lambda,\mu;r) = \exp\left(\frac{1+c}{1+2c}\right)(\lambda+\mu)\left[\frac{\sqrt{\pi}}{2}\,\mathrm{erf}\; g - g\exp(-g^2)\right]_{g_-}^{g_+} \tag{B51}$$

where

$$g_{\pm}^2(\lambda,\mu;r) = \frac{c(1+c)}{(1+2c)}\left[\left[v(r)-\lambda\right]^{1/2} \pm \left[v(r)-\mu\right]^{1/2}\right]^2 \tag{B52}$$

The universal expression (B39) is also valuable in that the one-way equilibrium rate across an arbitrary bound level $\nu = -E/kT$ is simply

$$\alpha_{eq} = \Gamma\,\alpha_T \int_{-\infty}^{\nu} d\lambda \int_{\nu}^{\omega} F(\lambda,\mu)\,d\mu \tag{B53}$$

where $\omega = -D/kT$ is the maximum binding energy in units of (kT) and where

$$F(\lambda,\mu) = \int_{o}^{r_m} F(\lambda,\mu;r)\,r^2\,dr\;,\quad r_m = 1/\max(\lambda,\mu) \tag{B54}$$

This equilibrium collisional rate displays[10,11] a minimum at $\nu^* = (1\text{-}3)kT$, the location of a bottleneck.[28]

Moreover, the non-equilibrium association/dissociation rate (6.3) reduces simply to

$$\alpha_A = \Gamma\,\alpha_T \int_{-\infty}^{\nu} d\lambda \int_{\nu}^{\omega} \left[P^D(\lambda) - P^D(\mu)\right] F(\lambda,\mu)\,d\mu \tag{B55}$$

where $P^D(\lambda)$ is the net probability of collisional dissociation of pairs with energy $(-\lambda kT)$. Eq. (B55) with $\nu = 0$ provides the loss rate (6.17) from the continuum (Block C); and provides, with $\nu = -S/kT = \varepsilon$, the growth rate (6.15) of block S, and with arbitrary ν in the block E, $(0 < \nu < \varepsilon)$, provides the association rate (6.23) under quasi-steady-state conditions in block E.

Also various energy-change monents,

$$D_i^{(m)}(E_i) = \frac{1}{m!} \int_{-D}^{\infty} (E_f - E_i)^m C_{if} dE_f \tag{B56}$$

useful in a Fokker-Planck analysis[43] of the collision term (2.1b) of the main text and expressed simply as

$$D_i^m(E_i) = r\alpha(kT)^{m-1}(-1)^m \mathcal{D}_i^{(m)}(\lambda) \tag{B57}$$

where the dimensionless moments

$$\mathcal{D}_i^{(m)}(\lambda) = \frac{1}{m!} \int_{-\infty}^{\omega} (\mu-\lambda)^m F(\lambda,\mu) d\mu \tag{B58}$$

are easily determined[28] on using the relevant expression, (B45), (B47), (B48) or (B51), appropriate to the chosen interaction between AB and the gas species.

References

1. M. R. Flannery, Philos. Trans. Roy, Soc. London, Ser. A 304, 447 (1982).

2. M. R. Flannery, in Applied Atomic Collision Physics: Vol. 3, Gas Lasers, edited by E. W. McDaniel and W. L. Nighan (Academic, New York, 1982), Chap. 5.

3. M. R. Flannery, Int. J. Quantum Chem.: Quant. Chem. Symp. 13, 501 (1979).

4. M. T. O'Connor and G. J. Diebold, J. Chem. Phys. 81, 812 (1984).

5. M. R. Flannery, in Swarms of Ions and Electrons in Gases, edited by W. Lindinger, T. D. Mark and F. Howorka (Springer-Verlag, Wien, New York, 1984), p. 103.

6. D. R. Bates and R. J. Moffett, Proc. Roy. Soc. London, Ser. A 291, 1 (1966).

7. D. R. Bates and M. R. Flannery, Proc. Roy. Soc. London, Ser. A 302, 367 (1968).

8. D. R. Bates and I. Mendaš, J. Phys. B 15, 1949 (1982).

9. M. R. Flannery in Case Studies in Atomic Collision Physics, Vol. 2, edited by E. W. McDaniel and M. R. C. McDowell (North Holland, Amsterdam, 1972), p. 1.

10. M. R. Flannery, J. Phys. B 13, 3649 (1980); M_1 in eqs. (25) and (32) and a in eq. (47) should be replaced by $M_1^{1/2}$ and c, respectively.

11. M. R. Flannery, J. Phys. B. 14, 915 (1981).

12. D. R. Bates and C. S. McKibbin, Proc. Roy. Soc. London, Ser. A 339, 13 (1974).

13. J. C. Keck and G. Carrier, J. Chem. Phys. 43, 2284 (1965); J. C. Keck, in Adv. Atom. Mol. Phys., Vol. 8, edited by D. R. Bates and I. Estermann (Academic, New York, 1972), p. 39.

14. K. Andersen and K. E. Shuler, J. Chem. Phys. 40, 633 (1964); E. W. Montroll and K. E. Shuler, Adv. Chem. Phys. 1, 361 (1958).

15. L. Onsager, Phys. Rev. 37, 405 (1931).

16. D. R. Bates, in Case Studies in Atomic Physics, Vol. 4, edited by M. R. C. McDowell and E. W. McDaniel (North Holland, Amsterdam, 1974), p. 59.

17. D. R. Bates, A. E. Kingston and R. W. P. McWhirter, Proc. Roy. Soc. London, Ser. A 267, 297 (1962).

18. D. R. Bates and A. E. Kingston, Proc. Roy. Soc. London, Ser. A 279, 10 and 32 (1964).

19. D. R. Bates and S. P. Khare, Proc. Phys. Soc. 85, 231 (1965).

20. D. R. Bates, V. Malaviya and N. A. Young, Proc. Roy. Soc. London, Ser. A 320, 437 (1971).

21. M. R. Flannery and E. J. Mansky, Philo. Trans. Roy. Soc. London, Ser. A (in preparation).

22. See, for example, G. Arfken, Mathematical methods for Physicists, (Third Edition, Academic, New York, 1985), p. 478, p. 865, p. 937.

23. D. R. Bates and I. Mendaš, Proc. Roy. Soc. London, Ser. A 359, 275 (1978).

24. M. R. Flannery, Phys. Rev. Letts. 47, 163 (1981).

25. M. R. Flannery, Phys. Rev. A. 25,3403 (1982).

26. M. R. Flannery, Phys. Rev. Letts. 49, 1681 (1982).

27. M. R. Flannery and E. J. Mansky, Phys. Rev. A (accompanying paper).

28. M. E. Flannery, Phys. Rev. A (accompanying paper).

29. D. R. Bates, Proc. Roy. Soc. London, Ser. A 337, 15 (1974).

30. B. D. Tellegen, Philips Res. Rep. 7, 259 (1952).

31. P. Penfield, R. Spence and S. Drinker, Tellegen's Theorem and Electrical Networks (MIT Press, Cambridge, Mass., 1970).

32. N. Balabanian and T. A. Bickart, Linear Network Theory (Matrix, Beaverton, oregon, 1981), Chap. 9.

33. J. Keizer, Biosystems 8, 219 (1977).

34. I. Mendaš, J. Phys. B. 12, L209 (1979).

35. D. R. Bates and C. S. McKibbin, J. Phys. B 6, 2485 (1973).

36. R. H. Fowler, Statistical Mechanics (Second Edition, Cambridge University Press, London, 1955), p. 161.

37. H. Goldstein, Classical Mechanics (Second Edition, Addison-Wesley, 1981), p. 102.

38. C. Cohen-Tannoudji, B. Din and F. Laloe, Quantum Mechanics, Vol. 1 (Wiley, New York, 1977), p. 814.

39. H. A. Bethe and E. E. Salpeter, Quantum Mechanics of One- and Two-Electron Systems (Plenum, New York, 1977), p. 17.

40. D. R. Bates and W. R. McDonough, J. Phys. B 3, L83 (1970).

41. M. R. Flannery, Annals of Physics, N. Y. 61, 465 (1970); 79, 480 (1983).

42. M. R. Flannery, Phys. Rev. A 22, 2408 (1980).

43. A. Dalgarno, Phil. Trans. Roy. Soc. London, Ser. A 250, 426 (1958).

Figure Captions

Fig. 1. Assignment of the fully dissociated block C of free A + B pairs, of the fully-associated block S of bound (A-B) pairs and the block E of pairs in highly excited bound levels.

Fig. 2. Ratio of the association rate $R^A(\lambda^*,b,c)$, eq. (7.13) to the exact QSS-rate, eq. (7.14) over variational parameters λ^*, b and c.

Fig. 3. Association and Dissociation Probabilities $P^{A,D}(\lambda)$ as a function of depth into the energy well. For $E_i \sim 10\ k\Theta$, where Θ is gas temperature, P^A is almost unity and P^D is negligible. ——— EXACT QSS; — — — —, ----, ... Variational Functions with $\lambda_* = 1.25$ and with the set (b,c) equal to (0,0), (0.20,0) and (0.20,-0.006) respectively.

Fig. 4. First Derivative $(dP^A/d\lambda)$ of association probabilities, corresponding to curves of Fig. 3. The minima of the exact QSS and Variational functions result in identical locations.

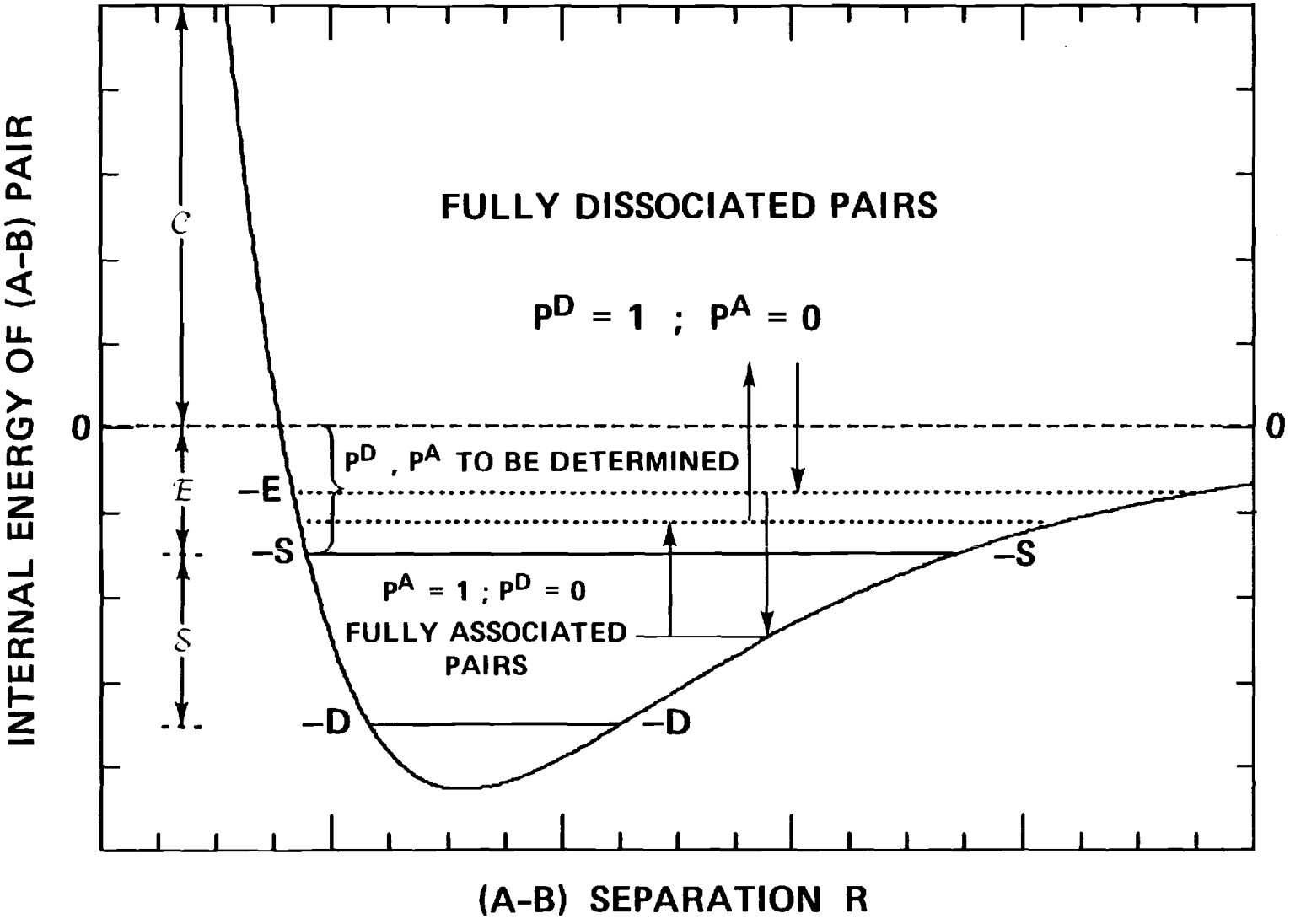
INTERNAL ENERGY OF (A-B) PAIR
FULLY DISSOCIATED PAIRS
$P^D = 1$; $P^A = 0$
C
0
0
E
-E
P^D , P^A TO BE DETERMINED
-S
-S
S
$P^A = 1$; $P^D = 0$
FULLY ASSOCIATED PAIRS
-D
-D
(A-B) SEPARATION R

Figure 1

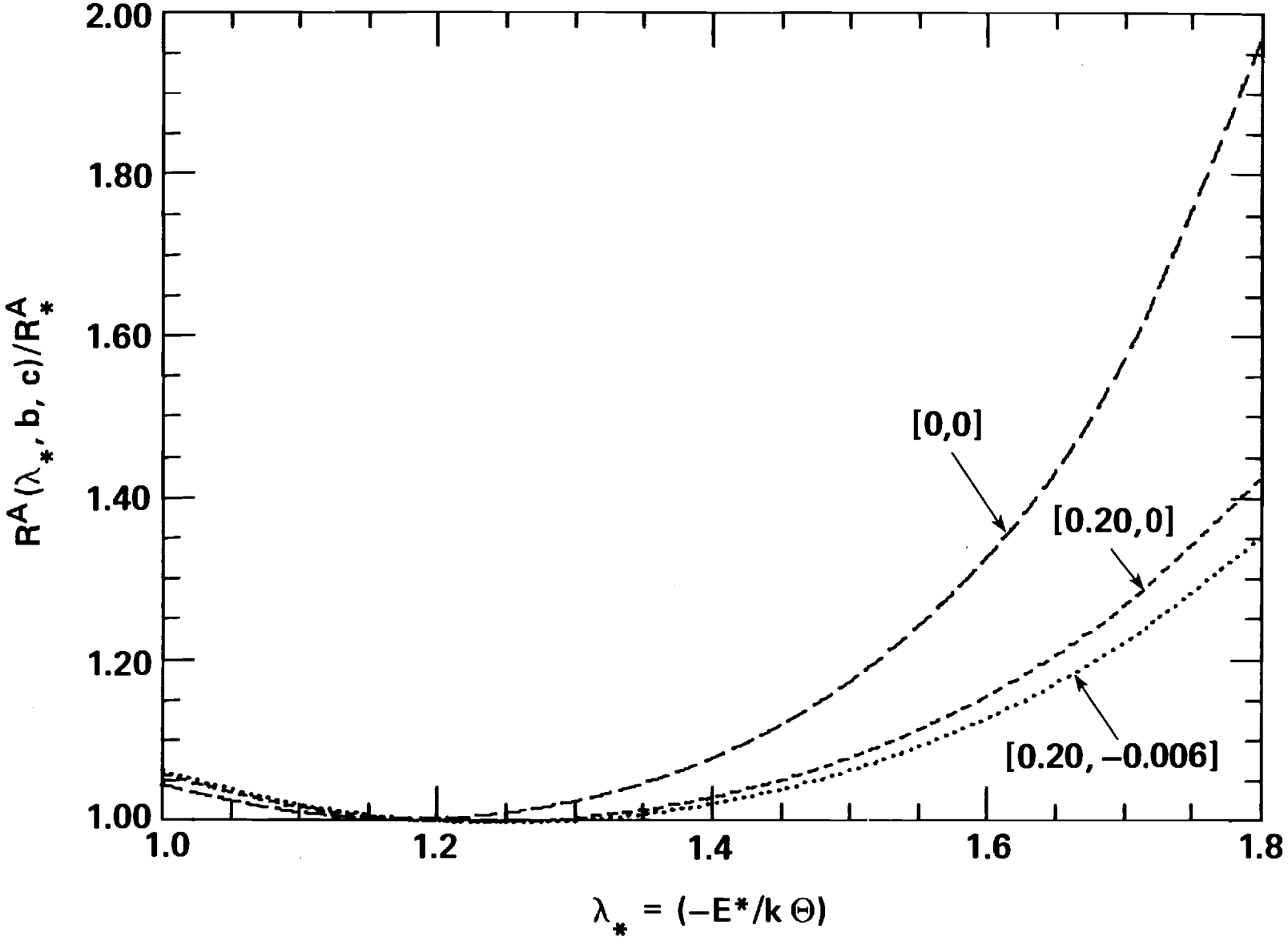
2.00
1.80
1.60
1.40
1.20
1.00
1.0
1.2
1.4
1.6
1.8
$R^A(\lambda_*, b, c)/R^A_*$
$\lambda_* = (-E^*/k\,\Theta)$
[0,0]
[0.20,0]
[0.20, −0.006]

Figure 2

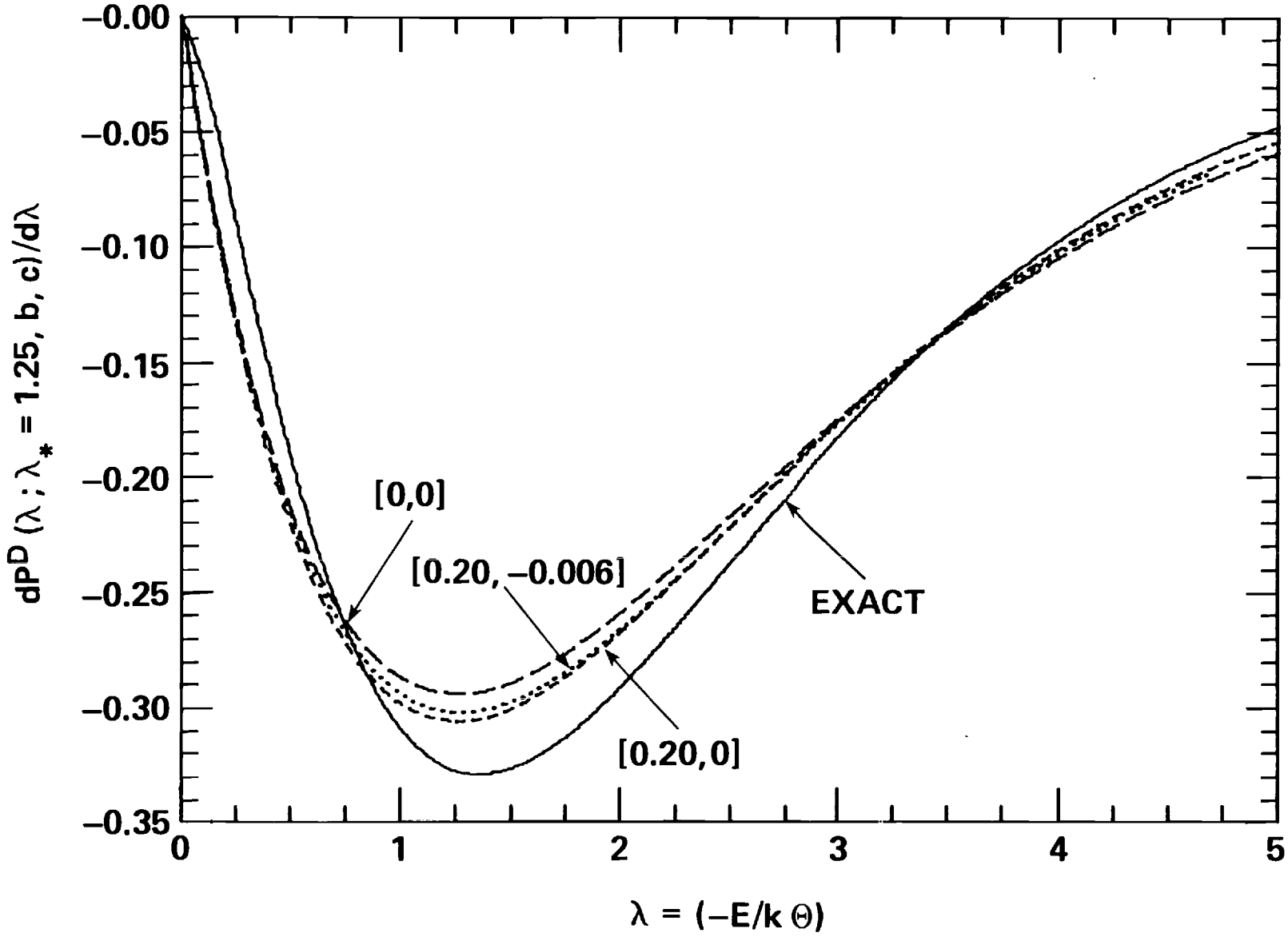
−0.00
−0.05
−0.10
−0.15
−0.20
−0.25
−0.30
−0.35
0
1
2
3
4
5
dP^D (λ ; λ* = 1.25, b, c)/dλ
λ = (−E/k Θ)
[0,0]
[0.20, −0.006]
[0.20,0]
EXACT

Figure 3

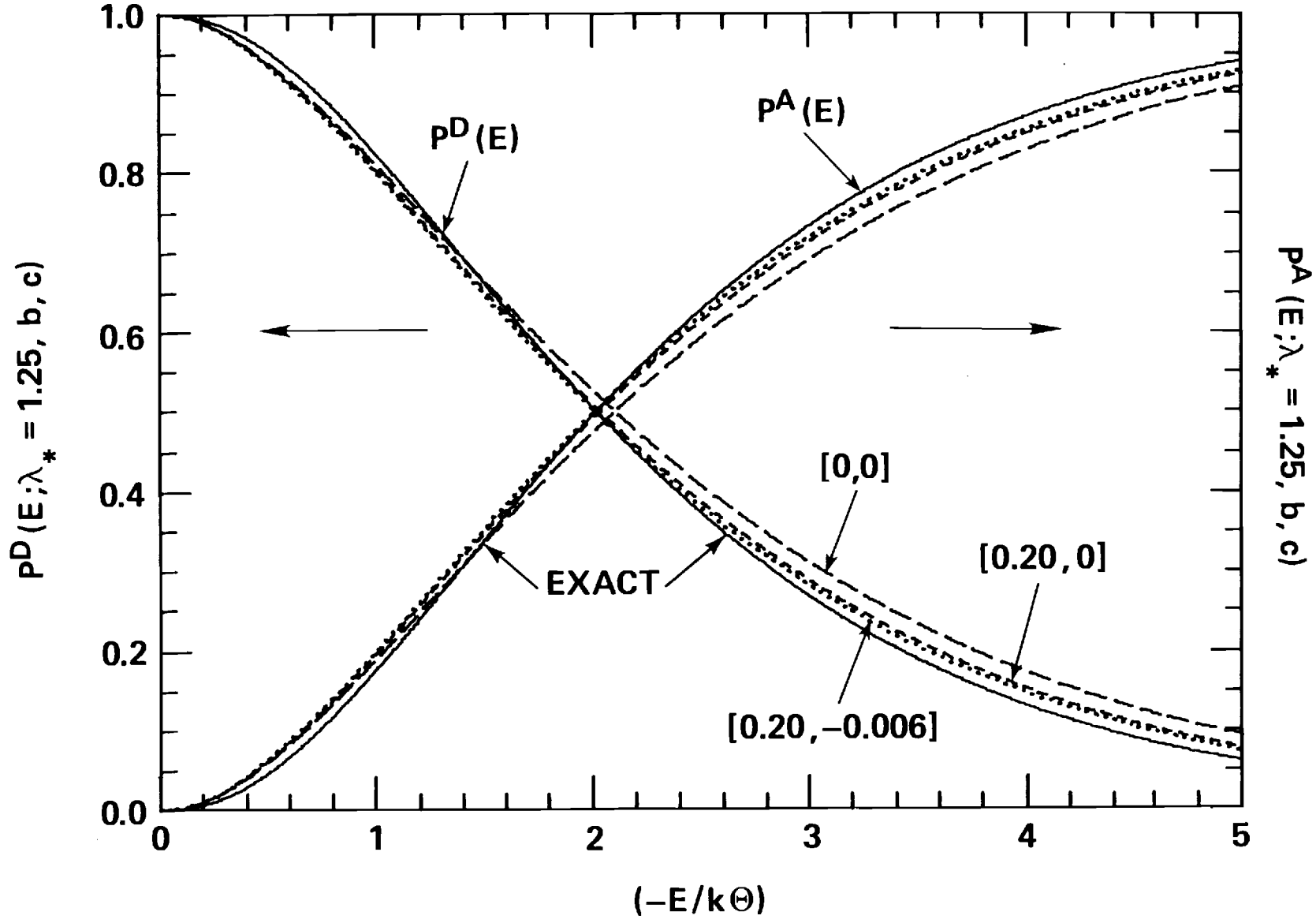
1.0
0.8
0.6
0.4
0.2
0.0
0
1
2
3
4
5
$P^D(E)$
$P^A(E)$
[0,0]
[0.20, 0]
EXACT
[0.20, –0.006]
$P^D(E;\lambda_* = 1.25, b, c)$
$P^A(E;\lambda_* = 1.25, b, c)$
(–E/kΘ)

Figure 4

Appendix B

Diffusional Theory of Association/Dissociation

Non-Equilibrium Processes for General Systems

Diffusional Theory of Association/Dissociation Non-Equilibrium Processes for General Systems

M. R. Flannery,
School of Physics,
Georgia Institute of Technology
Atlanta, Georgia, 30332, U.S.A.

Abstract: Upon re-examination of the foundations of the diffusional treatment of association/dissociation processes involving a non-equilibrium distribution of (A-B) pairs in a gas M, it is shown that highly accurate results may be obtained for general mass systems provided a new and more basic expression for the time-dependent association/dissociation rates $R^{A,D}(t)$ is introduced. These rates $R^{A,D}(t)$ are derived here in terms of the probability $P_i^{A,D}(E_i)$ that (A-B) pairs with internal energy E_i has associative/dissociative character and are obtained without appeal to the quasi-steady-state (QSS) condition for highly excited levels E_i. Then association and dissociation can be treated in a unified way and evolution towards equilibrium with the gas is naturally achieved. Comparison is made between the exact probabilities $P_i^{A,D}$ obtained from the QSS-condition to the Exact input-output Master Equation and those obtained from the derived diffusional equation. $R^{A,D}(t)$ reduces to the constant-in-energy current $J(t)$ through the excited levels only for exact QSS of the Master Equation. When approximate probabilities are adopted, identificiation of $R^{A,D}(t)$ with $J(t)$ is not justified. The basic expression introduced here for $R^{A,D}(t)$ is appropriate for both exact and approximate (diffusional) probabilities and yields excellent results for ion-ion recombination in a dilute gas over the full range of masses of the species involved and over various classes of ion-neutral interaction (polarization, hard-sphere and charge-transfer).

PACS: 34.10X, 34.50.Lf., 82.20.Mj.

Contents

1. Introduction

The picture of recombination and of association/dissociation processes involving subsystems (A-B) in a thermal bath of dilute gas M as occurring via diffusion in energy-space has stimulated[1-7] a great deal of interest, in principle valuable to elucidation of many examples of laser-induced plasmas, decay, of reaction processes in flames, of shock wave propagation etc. In a classic paper, Pitaevskii[1] derived a rather elegant analytical result, which because of its inherent simplicity over more sophisticated and therefore time-consuming procedures based on a collisional input-output Master Equation[8-10], has been applied to situations[3-5], other than to electron-ion recombination[1,7] for which it was originally intended. Bates[11] has pointed out that of the several different classical diffusion models of electron-ion recombination, the correct model is that of Pitaevskii.[1] Moreover, the formula of Pitaevskii can be reproduced[12] exactly by Thomson-style arguments. In spite of its attractive features, the diffusion picture as formulated[1-6] achieved remarkably disappointing results for heavy-particle ion-ion recombination[3-6], or for any atom-atom association process, in a gas.

Apart from recognition that diffusion methods (based on a Fokker-Planck reduction of the input-output collisional integral) are likely to be valid only when the collisional energy changes are small, the basic intrinsic defect for application of the Pitaevskii expression to general mass systems remains undetected. Moreover, that a much less sophisticated "bottleneck" model[13] achieved much closer agreement[10] with the exact results of the Master Equation[8-10] for ion-ion recombination presents a puzzle.

On examination in this paper of the foundation of the diffusion approach in a new light, the basic defect in the treatment becomes apparent. In §2, probabilities $P_i^{A,D}$ for association/dissociation of pairs (A-B) with internal

energy E_i are introduced and an expression for the time-dependent current $J_i(E_i,t)$ is developed. In §3.1, a Fokker-Planck (FP) analysis of the collision integral and current J_i is performed consistently to fourth-order and useful relationships between the various energy-change moments are established. In §3.2, the diffusion approach, based on a second-order FP-analysis, is shown to provide accurate probabilities $P_i^{A,D}$ for general systems but inaccurate heavy-particle currents from which previous rates were obtained.[2-6] A new expression for the time-dependent rates $R^{A,D}(t)$ under all conditions is developed in §4 in terms of $P_i^{A,D}$. These rates obtained with diffusional $P_i^{A,D}$ will then be compared with exact rates[10,15] for the benchmark case of ion-ion recombination in a gas for various masses and ion-gas interactions.

As initiated in ref (14), the analysis here so describes the time evolution from a non-equilibrium distribution of (A-B) pairs with a thermal bath of gas M towards full thermodynamic equilibrium that association and dissociation are treated in a unified way and that general expressions for the rates of association/dissociation are obtained without appeal to the quasi-steady-state condition[1-10] for highly excited levels of the (A-B) pair.

2. Master Equation and Quasi-Steady-State Rates

The collisional input-output Master Equation[2,4,8-10] that governs the distribution $n_i(E_i,t)dE_i$ for the density (cm^{-3}) of subsystems AB with internal energy E_i in the interval dE_i about E_i can be written as,[14]

$$\frac{\partial}{\partial t} n_i(E_i,t) = - \int_{-D}^{\infty} S_{if}(t)dE_f \equiv - \frac{\partial}{\partial E_i} J_i(E_i,t) \qquad (2.1)$$

where the net two level input-output collisional rate of depletion of energy level E_i is

$$S_{if}(t) = n_i(E_i,t)\nu_{if}(E_i,E_f) - n_f(E_f,t)\nu_{fi}(E_f,E_i) = -S_{fi}(t) \qquad (2.2)$$

in terms of $\nu_{if}dE_f$, the frequency (s^{-1}) for i → f transitions which change the energy E_i to between E_f and $E_f + dE_f$ by collision of the (A-B) pair with the gas M. The energy of the lowest bound level of the AB pair is -D with respect to the dissociation limit, taken as zero energy. The separation between the energy levels of AB is sufficiently small in comparison to the thermal energy (kT) of the bath species M that the levels form a quasi-continuum. Thus J_i in (2.1) is the net upward current (in energy space) past energy level E_i. Since J_i vanishes as $E_i \to \infty$ and -D, it is therefore determined either by the integral expression,

$$J_i(E_i,t) = \int_{E_i}^{\infty} dE_i \int_{-D}^{\infty} S_{fi}(t)dE_f = \int_{E_i}^{\infty} dE_i \int_{-D}^{E_i} S_{fi}(t)dE_f \qquad (2.3)$$

with the aid of the null effect, $S_{if} + S_{fi} = 0$, of collisions, or by the equivalent expression,

$$J_i(E_i,t) = \int_{-D}^{E_i} dE_i \int_{-D}^{\infty} S_{if}(t)dE_f = \int_{-D}^{E_i} dE_i \int_{E_i}^{\infty} S_{if}(t)dE_f \qquad (2.4)$$

since the currents past the end points (-D, ∞) vanish.

Subdivide the range (-D → ∞) of internal energy into three blocks[14]; the continuum block C in which the pairs (A+B) are fully dissociated, the intermediate block $\bar{E}$ of highly excited bound levels of (A-B) between the dissociation limit at zero energy and a lower bound level -S, and the lowest (sink) block S composed of tightly bound levels between -S and -D where the pairs AB are fully associated. The level -S is sufficiently deep that the net

probability of direct dissociation by collision with the thermal bath is negligible. In practice, level -S arises quite naturally from the collisional mechanics via the cut-off effect of the Maxwellian distribution of the gas bath at temperature T and generally lies ~ 10 kT below the dissociation limit (cf. Fig 3 of §3).

The net rate of depletion of dissociated species (A+B) with density (cm^{-3}),

$$n_C(t) = \int_0^\infty n_i(E_i,t)dE_i \tag{2.5}$$

in block C ($0 \leq E_i \leq \infty$) is simply

$$R_C(t) = -\frac{\partial n_C}{\partial t}(t) = -J(0,t) = \int_0^\infty dE_i \int_{-D}^{0} S_{if}(t)dE_f \tag{2.6}$$

the downward current past the dissociation neck. The net rate of increase in the density (cm^{-3})

$$n_S(t) = \int_{-D}^{-S} n_i(E_i,t)dE_i \tag{2.7}$$

of pairs considered to be fully associated in block S with energy E_i in the range, $-S \leq E_i \leq -D$ is

$$R_S(t) = \frac{\partial n_S(t)}{\partial t} = -J(-S,t) = \int_{-S}^{\infty} dE_{if} \int_{-D}^{\infty} S_{if}(t)dE_f \tag{2.8}$$

the net downward current past level -S.

Since the system is considered to be closed

$$R_c(t) = R_s(t) + \int_{-S}^{o} \left(\frac{\partial n_i}{\partial t}\right) dE_i \qquad (2.9)$$

Introduce, as in ref. 14, the time-independent probability $P_i^A(E_i)$ that (A-B) pairs with energy E_i are considered as associated, then the overall rate for association is

$$R^A(t) = \int_{-D}^{\infty} P_i^A(E_i)\left(\frac{\partial n_i}{\partial t}\right) dE_i = R_s(t) + \int_{-S}^{o} P_i^A \left(\frac{\partial n_i}{\partial t}\right) dE_i \qquad (2.10)$$

since P_i^A is unity in block S and is zero in block C. The overall rate for dissociation is similarly,

$$R^D(t) = \int_{-D}^{\infty} P_i^D(E_i)\left(\frac{\partial n_i}{\partial t}\right) dE_i = - R_c(t) + \int_{-S}^{o} P_i^D\left(\frac{\partial n_i}{\partial t}\right) dE_i \qquad (2.11)$$

where $P_i^D(E_i)$, the probability that (A-B) pairs with energy E_i are considered as dissociated, is unity in block C and zero in block S.

In terms of the one-way equilibrium rate

$$C_{if} = \tilde{n}_i \nu_{if} = C_{fi} \qquad (2.12)$$

where $\tilde{n}_i dE_i$ is the (time independent) equilibrium number density of AB pairs in the energy interval dE_i about E_i, and of the normalized distribution,

$$\gamma_i(E_i,t) = n_i(E_i,t)/\tilde{n}_i(E_i) \qquad (2.13)$$

then (2.2) yields

$$S_{if}(t) = [\gamma_i(t) - \gamma_f(t)]C_{if} = -S_{fi}(t) \qquad (2.14)$$

with the aid of detailed balance (2.12). The Master Equation (2.1) is then

$$\frac{\partial n_i}{\partial t} = \int_{-D}^{\infty} [\gamma_f(t) - \gamma_i(t)]C_{if}dE_f = -\frac{\partial J_i}{\partial E_i} \tag{2.15}$$

Assume that the energy distribution of pairs in the Continuum block C and the Sink block S is Maxwellian i.e.

$$\gamma_i(E_i,t) = \begin{cases} \gamma_C(t) & , E_i > 0 \\ \gamma_S(t) & , -S > E_i > -D \end{cases} \tag{2.16}$$

are pure functions of time t which tend to unity as $t \to \infty$.

The non-equilibrium energy distribution of pairs in the intermediate block E of excited levels is therefore separable in energy and time according to the ansatz[14],

$$\gamma_i(E_i,t) = P_i^D(E_i)\gamma_C(t) + P_i^A(E_i)\gamma_S(t) \xrightarrow{t \to \infty} 1 \tag{2.17}$$

where P_i^D is the probability that state i is coupled to the continuum i.e. P_i^D is the probability of dissociation, and where P_i^A is the probability that state i is coupled to the sink i.e. P_i^A is the probability of association. Thus $(P_i^A + P_i^D)$ is unity at all times since $\gamma_{C,S}(t \to \infty)$ and $\gamma_i(t \to \infty)$ all tend to unity when full thermodynamic equlibrium with the gas M is established. Hence (2.15) can be conveniently separated in E_i and t according to

$$\frac{\partial n_i(E_i,t)}{\partial t} = -[\gamma_C(t) - \gamma_S(t)] \int_{-D}^{\infty} (P_f^A - P_i^A)C_{if}dE_f \tag{2.18a}$$

$$= [\gamma_C(t) - \gamma_S(t)] \int_{-D}^{\infty} (P_f^D - P_i^D)C_{if}dE_f \tag{2.18b}$$

and the time-dependent current (2.3) or (2.4) separates as

$$J_i(E_i,t) = [\gamma_c(t) - \gamma_s(t)]j_i(E_i) \tag{2.19}$$

where the time-independent fraction of the current down the energy ladder is

$$-j_i(E_i) = \int_{E_i}^{\infty} dE_i \int_{-D}^{E_i} (P_f^A - P_i^A)C_{if}dE_f = \int_{-D}^{E_i} dE_i \int_{E_i}^{\infty} (P_f^D - P_i^D)C_{if}dE_f \tag{2.20}$$

Hence

$$\frac{\partial n_i}{\partial t} = [\gamma_c(t) - \gamma_s(t)](\frac{\partial j_i}{\partial E_i}) \tag{2.21}$$

2.1 Quasi-steady-state (QSS) Rates

As has previously been shown[14], the association/dissociation rates $R^{A,D}(t)$ achieve extrema $R_*^{A,D}(t)$ when the number densities n_i in block E are in quasi-steady-state (QSS) i.e. $\partial n_i/\partial t \approx 0$ in E. The rate R_*^A is a minimum[14] when the net direction is association (as in relaxation of a fully dissociated plasma). The minimum association rate in terms of the effective two-body (constant) rate α (cm^3s^{-1}) for association between A and B with densities $N_{A,B}(t)$ at time t and of the frequency $k(s^{-1})$ of dissociation of S-pairs with density $n_s(t)$ is

$$R_*^A(t) = \alpha N_A(t)N_B(t) - kn_s(t) = R_s(t) = R_c(t) \tag{2.22}$$

which, by (2.10), is therefore equal to the rate $R_s(t)$ for production of S-pairs or the rate $R_c(t)$ for loss of C-pairs. Hence the required coefficient α is determined from either

$$\alpha N_A(t)N_B(t)[1-\Gamma(t)] = \int_{-S}^{\infty} dE_i \int_{-D}^{-S} S_{if}(t)dE_f = -J(-S,t) \tag{2.23a}$$

with the aid of (2.3), or from

$$\alpha N_A(t)N_B(t)[1-r(t)] = \int_0^\infty dE_i \int_{-D}^{0} S_{if}(t)dE_f = -J(0,t) \tag{2.23b}$$

where a measure of the departure of the densities $N_{A,B}$ and n_s from their corresponding values $\tilde{N}_{A,B}$ and $\tilde{n}_s$ for full thermodynamic equilibrium with the gas M is provided by the factor,

$$r(t) = [\tilde{N}_A\tilde{N}_B/N_A(t)N_B(t)][n_s(t)/\tilde{n}_s] \tag{2.24}$$

The dissociation frequency constant k in (2.22) automatically satisfies the detailed balance relation

$$k\tilde{n}_s = \alpha\tilde{N}_A\tilde{N}_B \tag{2.25}$$

which satisfies (2.22) when equilibrium ($r = 1$) is established so that the net rate $R^A_\star(t)$ vanishes.

Under the ansatz (2.17), (2.23) and (2.25) with the aid of (2.20) yield the constants

$$\alpha\tilde{N}_A\tilde{N}_B = [\int_0^0 dE_i \int_{-D}^{0} P^A_f C_{if}dE_f] = - j(0) \tag{2.26}$$

which uniquely identifies P^A_f as the association probability, and

$$k\tilde{n}_s = [\int_{-D}^{-S} dE_i \int_{-S}^{\infty} P^D_f C_{if}dE_f] = - j(-S) \tag{2.27}$$

which similarly identifies P^D_f as the dissociation probability. Under QSS for

level E_i in block E, (2.21) shows that

$$\alpha\tilde{N}_A\tilde{N}_B = - j(0) = - j_i(E_i) = -j(-S) = k\tilde{n}_s \qquad (2.28)$$

so that the constants α and k are simply determined by the current (2.20) past arbitary level E_i in block E. Under QSS of block E, the probabilities $P_i^{A,D}$ in the currents (2.20), (2.26) and (2.27) must satisfy the integral equation

$$P_i^{A,D} \int_{-D}^{\infty} C_{if}dE_f = \int_{-S}^{\infty} P_f^{A,D}C_{if}dE_f \ , \qquad (2.29)$$

the QSS-condition, obtained from (2.18) and solved subject to the constraints that P_i^A is zero in block C ($0 < E_i < \infty$), and is unity in block S ($-S > E_i > -D$). Also P_i^D is unity and zero in C and S, respectively.

It is now the aim to find simple analytical <u>approximate</u> expressions for both $P_i^{A,D}$ and j_i by converting in §3 from an integral representation as (2.1) or (2.18) to a differential representation, and then to raise and resolve the question (in §4) whether or not (2.28) is the correct expression which has always been assumed[1-6] when <u>approximate</u> probabilities $P_i^{A,D}$ are involved, rather than the exact solutions of the integral equation (2.29) - the exact QSS condition which yields (2.28) exactly.

3. <u>Fokker-Planck Reduction</u>

The conversion of the integral operator in (2.18) into a differential operator is achieved by a Fokker-Planck analysis[1] useful when the collision kernel C_{if} favors small energy changes. Here the current J_i in (2.18) is determined to fourth-order, rather than to the customary second order[2].

3.1 Fokker-Planck Current to Fourth-Order in Enery-Change Moments

On introduction of an arbitary but well-behaved function $\Phi_i(E_i)$ whose derivatives vanish at the end-points $[\infty, -D]$, then, with the aid of (2.18),

$$\int_{-D}^{\infty} \Phi_i \frac{\partial n_i}{\partial t} dE_i = \int_{-D}^{\infty} \gamma_i dE_i \int_{-D}^{\infty} (\Phi_f - \Phi_i) C_{if} dE_f \tag{3.1}$$

On expanding the difference

$$\Phi_f - \Phi_i = \sum_{n=1}^{\infty} \frac{1}{n!} (E_f - E_i)^n \left[\frac{\partial^n \Phi_i}{\partial E_i^n}\right] \tag{3.2}$$

as a function of energy change $(E_f - E_i)$, assumed small, and upon integration by parts under the explicit recognition that $(\partial^n \Phi_i / \Phi E_i^n) \to 0$ for $n > 1$ as $E_i \to [\infty, -D]$, then (3.1) can be expressed as

$$\int_{-D}^{\infty} \Phi_i \frac{\partial n_i}{\partial t} dE_i = [J_i \Phi_i]_{-D}^{\infty} - \int_{-D}^{\infty} \Phi_i \frac{\partial J_i}{\partial E_i} dE_i \tag{3.3}$$

to give the following expression for the current,

$$J_i(E_i, t) = \sum_{n=0}^{\infty} (-1)^n \frac{\partial^n (\gamma_i D_i^{(n+1)})}{\partial E_i^n} \tag{3.4}$$

where the energy change moments[2-4] of the collision kernel C_{if} for one-way $(i \to f)$ equilibrium collision rates (2.2) are

$$D_i^{(m)}(E_i) = \frac{1}{m!} \int_{-D}^{\infty} (E_f - E_i)^m C_{if} dE_f \tag{3.5}$$

Evaluation of these moments can be facilitated by adopting the expressions for C_{if} which corresponds to various A-M and B-M binary interactions (symmetrical resonance charge-transfer[8-10], hard-sphere[10], polarization[15], coulombic[14]) which are presented in universal form in Appendix B of ref. 14. These moments are normalized[14] to the quantity $(-1)^m \Gamma \alpha_T (kT)^{m-1}$ where α_T is the Thomson rate[14], where Γ is a mass factor[14] which depends on the interaction involved (see Appendix B, ref. 14), and where T is the temperature of the gas bath.

The frequency of all collisions for an equilibrium distribution of E_i-pairs is $D_i^{(0)}$; $D_i^{(1)}/D_i^{(0)}$ and $2D_i^{(2)}/D_i^{(0)}$ are respectively the averaged energy-change $\langle \Delta E_i \rangle$ and the average energy change squared $\langle \Delta E_i^2 \rangle$ per collision with the gas. Figs. 1(a,b) illustrate the general trend of these moments calculated here for the specific case[8,10] where internal-energy changes in an ion pair (X^+-X^-) are due to symmetrical resonance charge-transfer (X^+-X) collisions. In this case, the velocity vectors of the (fast) ion X^+ and the (thermal) neutral X are interchanged. Large transfers of energy are therefore involved, as is confirmed by $D_i^{(2)}$, the averaged energy-change squared $\langle \Delta E_i^2 \rangle$ per second shown in Fig. 1(a). This case will therefore provide a most stringent test for the weak-collision (diffusion) procedures studied here.

As the binding $\lambda = -E_i/kT$, in units of the thermal energy kT of the gas, increases from the dissociation limit (at zero), the equilibrium number[10] ($\sim \lambda^{-5/2} \exp \lambda d\lambda$) of levels in the range $d\lambda$ about λ decreases from a large value, reaches a minimum at $\lambda^* = 2.5$ and then increases exponentially. Since the energy change frequency ν_{if} for each pair decreases rapidly with increase of binding, the overall shapes of the equilibrium moments $D_i^{(m)}$ in Figs. 1a,b can therefore be explained. Note that the equilibrium collisional frequency $D_i^{(0)}$ is relatively constant in the range (1.8-4) kT of binding. Also the

frequency $D_i^{(0)}$ of energy-change is negative for binding energies $\lambda = (-E_i/kT) < 1.4 = \lambda^*$, i.e. these pairs become less tightly bound upon collision and pairs with binding $\lambda > 1.4$ kT become more tightly bound upon collision (when $D_i^{(1)} > 0$). This critical binding energy specifies the location at λ^* of a bottleneck, which separates the region $\lambda < \lambda^*$ where excitation dominates from the region $\lambda > \lambda^*$ where de-excitation is prevalent. Note also that the even moments $D_i^{(m)}$ display minima which become sharper with increase of m, as expected, and that the minimum in $D_i^{(2)}$ coincides with the zero of $D_i^{(1)}$ at λ^*, as clearly shown in Fig. 1b. As we go deeper into the well, D_1/D_o, the averaged energy-change per collision and D_2/D_o, the averaged energy-change squared per collision tend to increase linearly with energy depth (Fig. 1b). These features are quite general for the various ion-neutral interactions and can be exploited here.

Figs. (2a,b) illustrate the variation of inverses of the even moments $D_i^{(2)}$ and $D_i^{(4)}$ for different interactions[14] of A and B with M (charge-transfer CX, hard-spahere HS, and polarization POL). The bottleneck to $D_i^{(2)}$ occurs roughly in the same location ($\sim$ 1.25 kT) for all the interactions, and the energy-change squared per sec is greatest for the charge-transfer interaction and weakest for the polarization attraction, as expected. The moment $D_i^{(4)}$ exhibits similar but more amplified behavior.

Since C_{if} is symmetrical in i and f - the detailed-balance relation (2.12) - then C_{if}, when expressed as a function of the energy-mean $\bar{E} = \frac{1}{2}(E_f + E_i)$ and the energy-change $\Delta = E_f - E_i$, is such that[2] $C_{if} = C_{if}(\bar{E}, |\Delta|)$. On expanding C_{if} about E_i in terms of the expansion parameter Δ, which is assumed small, then

$$C_{if}(\bar{E} = E_i + \tfrac{1}{2}\Delta, |\Delta|) = \sum_{n=0}^{\infty} \frac{1}{n!} (\tfrac{\Delta}{2})^n \left(\frac{\partial^n C_i}{\partial E_i{}^n}\right) \qquad (3.6)$$

where C_i is $C_{if}(\tilde{E} = E_i, |\Delta|)$. The moments (3.5) are therefore determined from,

$$m!D_i^{(m)}(E_i) = \sum_{n=1,3,5,}^{odd} (2^n n!)^{-1}\left[\frac{\partial^n F_i^{(m+n)}}{\partial E_i^n}\right] \; ; \; m \text{ odd}, \tag{3.7a}$$

$$= \sum_{n=0,2,4,}^{even} (2^n n!)^{-1}\left[\frac{\partial^n F_i^{(m+n)}}{\partial E_i^n}\right] \; ; \; m \text{ even}, \tag{3.7b}$$

which involves only the terms

$$F_i^{(s)}(E_i) = \int_{-D}^{\infty} \Delta^s C_i(E_i, |\Delta|)dE_f \tag{3.8}$$

with s-even, since -D is effectively infinite (~ 5 eV) for the excited states i in the range $0 \geq E_i \geq$ (10-20)kT of interest (cf. Fig. 3a, below).

In equilibrium, γ_i in (3.4) is unity and the current can then be expressed, with the aid of (3.7), as

$$\mathcal{J}_i = \sum_{n=0}^{\infty} (-1)^n\left[\frac{\partial^n D_i^{(n+1)}}{\partial E_i^n}\right] = \sum_{n=0,2,}^{even} \sum_{j=0,2}^{even} (n-2j)[2^{j+1}(n+2)!(j+1)!]^{-1}$$

$$\frac{\partial^{j+n+1} F_i^{(j+n+2)}}{\partial_i E^{j+n+1}} \tag{3.9}$$

This new form clearly shows that the coefficient of its first term $\partial F_i^{(2)}/\partial E_i$, which arises from the leading term of the expansion (3.7) for both

$D_i^{(1)}$ and $\partial D_i^{(2)}/\partial E_i$, is identically zero. The coefficient of the second term $\partial^3 F_i^{(4)}/\partial E_i^3$, which is the net balance of the second term in the expansion (3.7) for both $D_i^{(1)}$ and $\partial D_i^{(2)}/\partial E_i$ and of the leading term in the expansion (3.7) for both $\partial^2 D_i^{(3)}/\partial E_i^2$ and $\partial^3 D_i^{(4)}/\partial E_i^3$, is also zero. The leading non-vanishing contribution to (3.9) is $[-\frac{1}{576}\partial^5 F_i^{(6)}/\partial E_i^5]$ which is the net balance of the third terms in the expansion (3.7) for both $D_i^{(1)}$ and $\partial D_i^{(2)}/\partial E_i$ and of the second terms in the expansion (3.7) for both $\partial^2 D_i^{(3)}/\partial E_i^2$ and $\partial^3 D_i^{(4)}/\partial E_i^4$. The consistent neglect of $\partial^4 D_i^{(5)}/\partial E_i^4 \sim \partial^5 F_i^{(6)}/\partial E_i^5$ and higher-order derivatives demands both the neglect in (3.4) of terms with $n > 4$ and the neglect in (3.7a) and (3.7b) of terms with $n > 5$ and $n > 4$, respectively. Hence, the equilibrium current

$$\mathcal{J}_i \approx D_i^{(1)} - \partial D_i^{(2)}/\partial E_i + \partial^2 D_i^{(3)}/\partial E_i^2 - \partial D_i^{(4)}/\partial E_i^3 \equiv 0 \qquad (3.10)$$

is exact to fourth-order in the moments and is identically zero! Relationships between even and odd moments can be obtained from (3.7) by neglecting $F_i^{(6)}$ and higher terms, i.e. $D_i^{(5)}$ and higher moments, to give

$$D_i^{(1)} = \frac{\partial}{\partial E_i}\left[D_i^{(2)} - \frac{\partial^2 D_i^{(4)}}{\partial E_i^2}\right] \qquad (3.11a)$$

$$D_i^{(3)} = 2\frac{\partial}{\partial E_i} D_i^{(4)} \qquad (3.11b)$$

which also ensure zero equilibrium current. In view of (3.11) note that equilibrium ($\mathcal{J}_i = 0$) is obtained only when the current (3.4) is expanded to even order.

With the aid of (3.10), the non-equilibrium current (3.4) to fourth order in moments $D_i^{(m)}$ is

$$J_i^{(4)}(E_i,t) = -\left[D_i^{(2)} - 2\frac{\partial D_i^{(3)}}{\partial E_i} + 3\frac{\partial^2 D_i^{(4)}}{\partial E_i^2}\right]\left(\frac{\partial \gamma_i}{\partial E_i}\right) + \left[D_i^{(3)} - 3\frac{\partial D_i^{(4)}}{\partial E_i}\right]\left(\frac{\partial^2 \gamma_i}{\partial E_i^2}\right) - D_i^{(4)}\left(\frac{\partial^3 \gamma_i}{\partial E_i^3}\right) \quad (3.12)$$

which is the differential representation (up to and including the fourth-order moment $D_i^{(4)}$) of the double integral

$$J_i(E_i,t) = \int_{E_i}^{\infty} dE_i \int_{-D}^{E_i} [\gamma_f(t) - \gamma_i(t)]C_{if}dE_f \quad (3.13)$$

for the exact current (2.3). The differential form (3.12) can be called the Fokker-Planck current to fourth-order since the general Fokker-Planck expansion can be employed for any variable whose changes are small in comparison with averaged characteristic values e.g. the collisional energy change Δ here is assumed small relative to the thermal energy kT of the gas bath. Changes in vector momentum $\underset{\sim}{p}$ are in general very large here so that the usual Fokker-Planck analysis[1] in vector $\underset{\sim}{p}$-space would not be valid.

Upon use of the approximations (3.11), which are internally consistent to neglect of moments higher than $D_i^{(4)}$, (3.12) reduces to

$$J_i^{(4)}(E_i,t) = -\left[D_i^{(2)} - \frac{\partial^2 D_i^{(4)}}{\partial E_i^2}\right]\left(\frac{\partial \gamma_i}{\partial E_i}\right) - \frac{1}{2}D_i^{(3)}\left(\frac{\partial^2 \gamma_i}{\partial E_i^2}\right) - D_i^{(4)}\left(\frac{\partial^3 \gamma_i}{\partial E_i^3}\right) \quad (3.14)$$

Inserting the ansatz (2.17) in (3.12), then (2.15) with (3.12) yields

$$\frac{\partial n_i(E_i,t)}{\partial t} = -[\gamma_c(t) - \gamma_s(t)]\frac{\partial j_i}{\partial E_i}(E_i) \quad (3.15)$$

where in terms of the probability P_i^D for dissociation, the time independent

current to fourth-order is,

$$j_i^{(4)}(E_i) = -\left[D_i^{(2)} - 2\frac{\partial D_i^{(3)}}{\partial E_i} + 3\frac{\partial^2 D_i^{(4)}}{\partial E_i^2}\right]\left(\frac{\partial P_i^D}{\partial E_i}\right)$$
$$+\left[D_i^{(3)} - 3\frac{\partial D_i^{(4)}}{\partial E_i}\right]\left(\frac{\partial^2 P_i^D}{\partial E_i^2}\right) - D_i^{(4)}\left(\frac{\partial^3 P_i^D}{\partial E_i^3}\right) + \ldots \qquad (3.16)$$

For quasi-steady-state (QSS) in block , j_i is constant. When third-order and higher derivatives of P_i^D, are ignored, a straightforward exercise in the solution of the resulting second-order differential equation can be performed to provide analytical expressions for P_i^D, if required.

3.2 Diffusion Equation and Current

On ignoring in (3.16) moments $D_i^{(3)}$ and higher, the (diffusional) current is,

$$j_d(E_i) = -D_i^{(2)}\frac{\partial P_i^D}{\partial E_i} = D_i^{(2)}\frac{\partial P_i^A}{\partial E_i} \qquad (3.17)$$

so that (3.15) reduces to

$$\frac{\partial n_i(E_i,t)}{\partial t} = [\gamma_c(t) - \gamma_s(t)]\frac{\partial}{\partial E_i}\left[D_i^{(2)}\frac{\partial P_i^D}{\partial E_i}\right] \qquad (3.18)$$

which is a diffusion equation in energy space. The frequency $D_i^{(2)}$ at which the averaged energy-transferred squared changes under thermodynamic equilibrium conditions is the diffusion coefficient (energy^{2}s^{-1}) in energy space. This kind of streaming equation has been previously derived via other techniques by Pitaevskii[1] for electron-ion recombination under highly non-equilibrium conditions when $\gamma_c >> \gamma_s$ so that $\gamma_i = P_i^D\gamma_c$ in (2.20), and by Keck and Carrier[2] for heavy-particle association/dissociation. It has been studied

by Landon and Keck[3], by Mahan[5] and by Bates and Zundi[6] for highly non-equilibrium ($\gamma_c >> \gamma_o$) ion-ion recombination. By explicitly including here the factor ($\gamma_c - \gamma_s$) via the ansatz (2.17), eqs. (3.15) and (3.18) for all $\gamma_{c,s}$ help to emphasize the complete evolution towards thermodynamic equilibrium attained when $\gamma_c \to \gamma_s \to 1$.

Another advantage of the ansatz (2.17) is that the intermediate block of highly excited levels can be taken to be in quasi-steady-state (QSS) i.e. $\partial n_i/\partial t \approx 0$ in either (2.18) or (3.18) <u>for all times</u>. The QSS-diffusional curent (3.17) is constant over E, so that the solution of (3.17) subject to condition

$$P_i^D(-S) = 0, \quad P_i^A(-S) = 1 \tag{3.19}$$

is

$$P_d^D(E_i) = - j_d \left[\int_{-S}^{E_i} dE/D^{(2)}(E) \right] = 1 - P_d^A(E_i) \tag{3.20}$$

where the subscript d denotes quantities associated with the diffusion equation (3.18). Various levels of approximate schemes readily follow.

(A) Since

$$P_i^D(0) = 1, \quad P_i^A(0) = 1 \tag{3.21}$$

then (3.20) yields

$$-j_d^{(p)} = \left[\int_{-S}^{0} dE/D^{(2)}(E) \right] = \alpha_p \tilde{N}_A \tilde{N}_B \tag{3.22}$$

for the downward diffusional current which, when compared with (2.28) provides the recombination rate α_p of Pitaevskii[1] used for ion-ion recombination by

Landon and Keck[3] and by Mahan.[5] Note that the current (3.22) is proportional to the area under the curves in Fig. 2a, and that the association and dissociation probabilities $P_i^{A,D}$ at energy E_i are proportional to the areas which correspond to the energy-ranges $(0 \to E_i)$ and $(E_i \to -S)$ respectively.

(B) Rather than requiring (3.21), j_d in (3.20) can be fixed by inserting (3.20) into (2.26) for $j(0)$ to give

$$-j(0) = \int_{-D}^{0} C_f dE_f + j_d \int_{-D}^{0} dE_f C_f \left[\int_{-S}^{E_f} dE_i / D_i^{(2)} \right] \tag{3.23}$$

where

$$C_f(E_f) = \int_{0}^{\infty} C_{if}(E_i, E_f) dE_i \tag{3.24}$$

is the total one-way equilibrium rate for collisional population of a bound level E_f from the continuum C. On equating the exact current $j(0)$ in (3.23) with the diffusional current j_d, then

$$-j_d^{(k)} = \left[\int_{-D}^{0} C_f dE_f \right] \left\{ 1 + \int_{-D}^{0} dE_f C_f \left[\int_{-S}^{E_f} dE / D^{(2)}(E) \right] \right\}^{-1} = \alpha_K \tilde{N}_A \tilde{N}_B \tag{3.25}$$

which yields the expression of Keck[4] for α_k. The term in braces, $\{-\}^{-1}$ is simply the ratio of the downward diffusional current to the one-way equilibrium current across the dissociation neck.

(C) Another possibility in similar vein to (B) is to insert (3.20) into (2.27) for $j(-S)$ to give

$$j_d(-S) = \left[\int_{0}^{\infty} D_f dE_f \right] \left\{ 1 + \int_{-S}^{0} dE_f D_f \left[\int_{-S}^{E_f} dE / D^{(2)}(E) \right] \right\}^{-1} = \alpha \tilde{N}_A \tilde{N}_B \tag{3.27}$$

where

$$D_f(E_f) = \int_{-D}^{-S} C_{if}(E_i, E_f) dE_i \tag{3.28}$$

is the total one way equilibrium rate for collisional excitation out of block S to any level f in blocks E and C. The term in braces, $\{-\}^{-1}$ is simply the ratio of the upward diffusional current across -S to the one-way equilibrium current across -S.

The feature common to all the above procedures (A)-(C) is that the required current (3.17) depends on the accuracy of the gradient (dP_i^D/dE_i) which, due to the neglect of higher derivatives in (3.16), is described by the diffusion equation (3.18) less precisely than are the actual diffusion QSS-solutions i.e. (3.18) may furnish accurate P_i^D but relatively inaccurate derivatives. More importantly however is that (2.28), which is valid only under exact QSS-condition (2.29) of the exact Master Equation, (2.1) or (2.18), has been invoked for the diffusional currents $j_d^{(P)}$ of (3.22) and $j_d^{(k)}$ of (3.23) which result from the QSS-condition of the different Master (diffusional) Equation (3.18).

The QSS-solution of (3.18) subject to constraints (3.19) and (3.21) is

$$P_d^A(E_i) = \{\int_{E_i}^{0} dE/D^{(2)}(E)\}\{\int_{-S}^{0} dE/D^{(2)}(E)\}^{-1} \tag{3.29}$$

for the probability that any level E_i in block E, once accessed by collision, has "associative" character. The probability that level E_i has "dissociative" character is the complementary function

$$P_d^D(E_i) = \{\int_{-S}^{E_i} dE/D^{(2)}(E)\}\{\int_{-S}^{0} dE/D^{(2)}(E)\}^{-1} \tag{3.30}$$

Thus both functions are constrained to vary monotonically between zero and unity as does the exact numerical solution to the integral equation (2.29) so that, when compared with the exact numerical values, will involve less error than their corresponding derivatives

$$\frac{\partial P_i^{A,D}}{\partial E_i} = \mp \{D_i^{(2)}(E_i)\}^{-1} j_d^{(p),(k)} \tag{3.31}$$

appropriate to currents (3.22) and (3.25) in schemes (A) and (B) above.

3.3 Calculations

The ion-ion (termolecular) recombination process

$$X^+ + Y^- + M \rightarrow XY + M \tag{3.32}$$

is taken as a benchmark case. The recombination coefficient α has previously been represented[9,16] very accurately by the sum

$$\alpha = \alpha_1 + \alpha_2 \tag{3.33}$$

of coefficients α_i obtained by considering separate contributions from (X^+ -Z) and (Y^--Z) binary collisions (i = 1 and 2, respectively). The exact numerical rates α_i are obtained from (2.28) by inserting the exact numerical solution of the integral equation (2.29), the QSS-condition into (2.20) for the current $j_i(E_i)$. The rates α_i have been tabulated[9,10,15] as a function of the mass-ratio parameter,

$$a_i = M_j M_3 / M_i (M_1 + M_2 + M_3) \tag{3.34}$$

where M_i are the masses of species X^+, Y^- and M, i = 1,2 and 3 respectively and where the set (i,j) is equal to (1,2) or (2,1) depending (1-3) or (2-3) collisions, respectively.

Based on previous analysis[8-10], universal expressions have been presented in Appendix B of ref 14 for the equilibrium rate C_{if} appropriate to the three classes - polarization[15], charge-transfer[8,10] and hard-sphere[10] - of ion-neutral interactions, calculations have been performed here for the exact QSS-rates α_E that rise from (1-3) collisions and for the corresponding diffusional rates, (3.22) for α_P and (3.25) for α_K of Pitaevskii[1] and Keck[4] respectively. The exact rates α_E reproduce the previous calculations[10,15], and there is little discernable difference between α_P and α_K which now be simply called the diffusional rates α_D obtained when the diffusional current (3.17) is inserted in (2.28).

Table I provides present values of the ratio α_D/α_E for the various interactions over the full range of mass parameter a, eq. (3.34) with i=1 and 2. Small $a \approx 10^{-3}$ corresponds to collisional recombination of heavy ions ($M_1 \approx M_2 >> M_3$) in a much lighter (electron) gas, intermediate a(= 1/3 for $M_1 = M_2 = M_3$) corresponds to species of equal mass, and large $a \approx 10^3$ for $M_1 << M_2 \approx M_3$ corresponds to electron-ion recombination in an ambient gas. The cases of small and large a involve energy transfers which are very much less than the energy kT of the gas so that the diffusional (weak collision) approach is likely to be valid.

As Table I shows, the diffusional rates are reliable, as expected, only for recombination in a vanishingly light gas ($a \approx 10^{-3}$) or for electron-ion recombination ($a \approx 10^3$) in a general gas, the case for which Pitaevskii[1] designed his diffusional treatment. The diffusional rates are higher by

between a factor of 3-6 for intermediate a ~ 1. As the ion-neutral interaction varies from polarization attraction, to hard-sphere repulsion and to charge-transfer interaction, the energy-change in the ion-neutral collision becomes progressively larger (see Fig. 2a,b) so that the diffusional rates (based on weak collisions) become less accurate, as shown directly by the variation of entries in Table 1 for a specified mass parameter a.

Since (3.17) predicts zero current in both the fully dissociated and fully associated blocks, C and S respectively, the diffusional current (3.17) is therefore discontinuous, zero in C, j_d in E and zero in S. The diffusion rates (3.22) of Pitaevskii and (3.25) of Keck are therefore expected to be valid only in the limit of vanishingly small rates α of association. This is true only for the limiting cases in Table 1 of small and large a. Then the actual rates α_E for electron-ion collisional recombination in a gas and for electron-ion recombination in a gas are[7] $\sim 10^{-9}$ cm^3 s^{-1} at STP, which are three orders of magnitude less that the rate[17] $\alpha_E \sim 10^{-6}$cm^{3}s^{-1} at STP for ion-ion recombination in an equal mass gas.

Another reason for failure of the diffusion approach as previously applied to general-mass cases is also apparent. As Figs. 3(a,b) show, the diffusion equation (3.18) in general furnishes fairly accurate probabilities $P_i^{A,D}$, (3.29) and (3.30), but less reliable gradients $dP_i^{A,D}/dE_i$.

In an effort to distinguish between the requirements of accurate distributions $P_i^{A,D}$ and the integral/differential forms of the collision integral of the Master Equation, assume that the intermediate block E between blocks C and S is absent i.e.,

$$P_i^D(E_i) = \begin{cases} 1, & -E < E_i < \infty \\ 0, & -D < E_i < -E \end{cases} \tag{3.35}$$

where -E is some bound energy level. The current (2.25) then reduces to

$$-j_{BN}(-E) = \int_{-E}^{\infty} dE_i \int_{-D}^{-E} C_{if} dE_f = \alpha_{BN}(E)\tilde{N}_A\tilde{N}_B \qquad (3.36)$$

which is the one-way equilibrium downward current across level -E. As -E is varied, this current achieves a minimum[10] at energy -E* (≈ -2kT) which therefore acts as a "bottleneck"[13] to the recombination which proceeds at rate $\alpha_{BN}(E^*)$. The ratio of α_{BN} at the bottleneck E* to the exact numerical rate α_E is displayed in Table I for the "intermediate" hard-sphere case[10]. The bottleneck method fails quite markedly for small and large mass parameters a, where by contrast the diffusion current is successful, and becomes much more reliable than the diffusion approach at intemediate a (≈ 1). Since (3.36) assumes the least possible knowledge of the probabilities $P_i^{A,D}$ (subject to the constraints) but an integral form to the input-output collision dynamics, it follows that accurate distributions are essential at small and large a where the collision dynamics is weak, so that the discontinuous integral form (2.25) does reduce indeed to the continuous streaming form (3.17). For intermediate a when the energy-changes are certainly not weak, inclusion of the integral form (2.25) is apparently more important than the use of accurate distributions (which are constrained to vary between unity and zero at the boundaries of block E).

The closeness exhibited in Fig. 3(a) between the diffusional probabilities, (3.29) and (3.30), and the exact numerical probabilities may be exploited in two ways. First, an interative procedure

$$P^{(n+1)}(E_i) \int_{-D}^{\infty} C_{if} dE_f = \int_{-S}^{\infty} P^{(n)}(E_f) C_{if} dE_f \qquad (3.37)$$

to the solution of the integral equation (2.29) can be developed by using the diffusional analytical probabilities as the starting (n=0) solution. It is found here that convergence to within 1% of the exact solution can be in general achieved after five iterations, so that accurate rates can then be determined from (2.28) and (2.20) since the QSS-condition (2.29) is satisfied.

Since the diffusional probabilities (3.29) and (3.30) are reasonably accurate, a second possibility is to insert them directly into (2.20) to yield the rate α from (2.28). This procedure, at first sight attractive, is however inconsistent, in that the diffusional probabilities while satisfying quasi-steady-state (QSS) of the diffusional equation (3.18) in block E, do not satisfy the condition (2.29) for QSS of the Master Equation (2.18). The resulting current (2.20) will therefore not be a constant in block E. This is demonstrated by Fig. 4 which compares the exact downward current $-j_E(E_i)$ past level E_i obtained from the solution of (2.29) in (2.20) with the approximate downward current $-j_A(E_i)$ obtained by inserting (3.29) in (2.20). Not only is the approximate current past the bound levels far from being constant, but assignment of a bound level E_i for determination of α from (2.28) is uncertain. Moreover the current j_i exhibits a very rapid variation in the neighborhood of the dissociation limit (at zero energy) that use of j(0) in (2.28) cannot be recommended. The exact value of j(0) is ~ 50% higher than the approximate j(0). Some defense can be made by adopting the value of j_A at the bottleneck energy of ~ 2 kT to (3.36). Then $j_A \approx j_E$, but the foundation is not firm.

The basic reason for the inconsistency of this second approach for j_A is not that the diffusional probabilities are not sufficiently accurate for useful application but that the current expression (2.28) for the association

rate is not valid when approximate probabilities, which do not satisfy the QSS-condition (2.29) to the exact Master Equation, are used. This dilemma is resolved in the following section.

4. Basic Expression for Rates and Results

The expression (2.9) for the time-dependent association (recombination) rate $R^A(t)$ is exact, while expressions for α in §2.1 hold only for QSS ($\partial n_i/\partial t = 0$) of the Master Equation (2.18) for block E. With the aid of (2.1) in (2.9), the rate

$$R^A(t) = \int_{-D}^{\infty} P_i^A dE_i \int_{-D}^{\infty} S_{fi}(t) dE_f \tag{4.1}$$

where S_{fi} is given by (2.2) is also exact. Under the basic ansatz (2.17), then

$$R^A(t) = [\gamma_c(t) - \gamma_s(t)] \int_{-D}^{\infty} P_i^A dE_i \int_{-D}^{\infty} (P_i^A - P_f^A) C_{if} dE_f \tag{4.2a}$$

$$= \frac{1}{2} [\gamma_c(t) - \gamma_s(t)] \int_{-D}^{\infty} dE_i \int_{-D}^{\infty} (P_i^A - P_f^A)^2 C_{if} dE_f \tag{4.2b}$$

$$\equiv \alpha N_A(t) N_B(t) - k n_s(t) \tag{4.3}$$

with the result that the time-independent rate constant α ($cm^3 s^{-1}$) of association is determined by

$$\alpha N_A N_B = \int_{-D}^{\infty} P_i^A dE_i \int_{-D}^{\infty} (P_i^A - P_f^A) C_{if} dE_f \tag{4.4}$$

When the exact QSS condition (2.29) is satisfied by the probabilities $P_i^{A,D}$, then (4.4) reduces to (2.28) with (2.20) for the current j_i. When

$P_i^{A,D}$ are determined via an approximate procedure, as by the diffusional treatment of §3.2, then (4.4) remains the appropriate expression for the rate α. The QSS-condition (2.29) corresponds to a minimum[14] in α and hence any approximate $P_i^{A,D}$ will yield higher rates α (cf. Table 1).

An alternative exact expression which emphasizes the role of the current J_i is obtained by using (2.1) and by integrating (2.10) and (2.11) by parts to give

$$R^{A,D}(t) = -\int_{-D}^{\infty} P_i^{A,D}(E_i)\left(\frac{\partial J_i}{\partial E_i}\right)dE_i = \int_{-S}^{\infty} J_i(E_i,t)\left(\partial P_i^{A,D}/\partial E_i\right)dE_i \qquad (4.5)$$

since J_i vanishes at the end points and since $P_i^{A,D}$ are both constants in blocks C and S. It is only when J_i, given exactly by (2.3) or (2.4) is constant-in-energy (QSS) over block E that it can be taken outside the integral sign to give the minimum

$$R_*^A(t) = R_*^D(t) = [\gamma_c(t)]-\gamma_s(t)]j_i(E_i) \qquad (4.6)$$

in terms of (2.20) for j_i and of P_i determined from the QSS-condition (2.29). Otherwise, the exact expression (4.5) is used.

The exact rates α_E obtained in §3.3 for the various ion-neutral interactions are normalized (cf ref. 10 and Appendix B, ref 14) to the corresponding Thomson rate[10]

$$\alpha_T = \frac{4}{3}\pi\,(R_e/\beta)^3(3kT/M_{12})^{1/2}\sigma_o N \quad , \quad \beta = 3/2 \qquad (4.7)$$

where R_e is the natural unit (e^2/kT) for Coulombic attraction between the ions 1 and 2. The integral cross section σ_o for (1-3) elastic collisions at

relative energy ($\frac{3}{2}$ kT) is taken in (4.5) to be $2Q^X$, $2\pi(pR_e/3)^{1/2}$ and σ_o^H respectively for symmetrical resonance charge-transfer collisions[11] with cross section Q^X, for polarization (orbiting) collisions in terms of the polarizability p of the gas M, and for hard-sphere collisions with cross section σ_o^H. Universal expressions for the normalized ratios (α_E/α_T) have already been presented[14] in a form suitable for direct computation.

Approximate rates α_A can now be determined by inserting the diffusional (approximate) probabilities (3.29) in (4.4). Fig. 5 displays a comparison of the corresponding ratios

$$R_T = (M_1/M_{12})(\alpha/\alpha_T) \tag{4.8}$$

where α is taken as the exact rate α_E or the approximate rate α_A, which arises from (1-3) collisions.

Excellent agreement is obtained over the full range of the mass parameter a, eq (3.34) with i = 1 and j =2 i.e. from $a \approx 10^{-3}$ for association of heavy ions in a light (electron) gas, to intermediate $a \approx 1/3$ for equal mass species and up to large $a \approx 10^3$ which corresponds to electron-recombination in a gas. As expected, greatest departures occur for the case of equal masses which involves the largest energy transfer so that the diffusional probabilities would also show their greatest departure from the exact probabilities as in Fig. 3a. For this case (a = 1/3), the diffusional result corresponding to hard-sphere collisions which in turn involve largest energy-transfers (cf. Fig. 2) exhibit the largest of small departures. The present diffusional treatment is also excellent for all of the various classes of (1-3) interaction considered.

5. Summary

On introduction of probabilities $P_i^{A,D}(E_i)$ that pairs (A-B) with internal energy E_i will tend to associate and dissociate in a thermal bath of gas M, and upon use of the ansatz (2.17) for their normalized energy distribution $\gamma_i(t)$ at time t, the basic Master Equation (2.1) and current (2.3) has been transformed into corresponding equations (2.18) and (2.19) which are separable in E_i and t. The diffusional equation (3.18), which is a derived approximation to the Master Equation (2.18), yields, for general systems, accurate probabilities $P_i^{A,D}$ (cf Fig 3) but very inaccurate currents (3.22) or (3.25), cf Table 1. Since previous expressions for association (recombination) rates α rely on a Quasi-Steady-State Condition (QSS) of (2.29) to the original Master Equation (2.18), they were therefore based on the currents (2.20), (2.26) and (2.27) via eq (2.28). Since the diffusional probabilities do not satisfy this original QSS-condition, the corresponding diffusional current is, in general, not appropriate for determination of the rates α. The resulting diffusional rates (3.22), or (3.25), are therefore not reliable[2-6] (Table 1), except for those cases in which the current is relatively small i.e. for collision electron-ion recombination[1] in a gas and for ion-ion recombination in a vanishingly light gas.

A new expression (4.2), derived for the rates, is the correct and more basic expression for use under general conditions, as when QSS is not satisfied. When QSS is satisfied, (4.2) reduces to (2.28) based on the current (2.20) and the QSS-rates are minimum.[14] The rate (4.2) is required for use of approximate probabilities, such as those (3.29) provided either by the diffusional treatment, as here, or by simple analytical variational functions for $P_i^{A,D}$, which do not satisfy the basic QSS-condition (2.29).

The diffusional probabilities can be used in an iterative solution of (2.29) to give highly accurate probabilities (to within 1%) after a few iterations and hence accurate rates (2.28). They can also be used in the basic formula (4.2) to yield excellent agreement with the exact numerical QSS-results for various classes of ion-neutral interactions over the full range of mass parameters for general systems.

In conclusion, application of the diffusional equation (3.18) to general systems is an accurate procedure provided the solutions $P_i^{A,D}$ are inserted in the appropriate and more basic expression (4.2) for the rate, rather than into the derived expressions (3.17) or (2.20) for the diffusional or exact currents, which only follow from the QSS-condition (2.29) to the exact input-output Master Equation (2.18).

Acknowledgment

This research is supported by U.S.AFOSR under grant No. AFOSR-84-0233.

References

1. L. P. Pitaevskii, Soviet Physics - JETP **15**, 919 (1962); E. M. Lifshitz and L. P. Pitaevskii, in Physical Kinetics (Pergamon, Oxford, 1981) Chap 2, p 89, p 102.

2. J. C. Keck and G. Carrier, J. Chem. Phys. **43**, 2284 (1965).

3. S. A. Landon and J. C. Keck, J. Chem. Phys. **48**, 374 (1968).

4. J. C. Keck, in Advances in Atomic and Molecular Physics, Vol. 8, edited by D. R. Bates and I. Estermann (Academic, New York, 1972) p 39.

5. B. H. Mahan, J. Chem. Phys. **48**, 2629 (1968).

6. D. R. Bates and Z. Jundi, J. Phys. B 1, 1145 (1968).

7. D. R. Bates and S. P. Khare, Proc. Phys. Soc. **85**, 231 (1965).

8. D. R. Bates and R. J. Moffett, Proc. Roy. Soc. London, Ser. A**291**, 1 (1966).

9. D. R. Bates and M. R. Flannery, Proc. Roy. Soc. London, Ser. A**302**, 367 (1968).

10. M. R. Flannery, J. Phys. B **13**, 3649 (1980); **14**, 915 (1981).

11. D. R. Bates, J. Phys. B 13, 2587 (1980).

12. M. R. Flannery, Phys. Rev. A (submitted).

13. S. B. Byron, R. C. Stabler and P. I. Bortz, Phys. Rev. Letts. 8, 376 (1962).

14. M. R. Flannery, Phys. Rev. A (submitted).

15. D. R. Bates and I. Mendaš, J. Phys. B **15**, 1949 (1982).

16. M. R. Flannery and T. P. Yang, J. Chem. Phys. 73, 3239 (1980).

17. M. R. Flannery, in Applied Atomic Collision Physics, Vol 3, Gas Lasers, edited by E. W. McDaniel and W. L. Nighan (Academic, New York, 1982) p 167.

Table 1: Variation of the ratio (α_D/α_E) and (α_{BN}/α_E) with mass-ratio parameter a for (1-3) collisions and with the various (1-3) interactions: polarization (POL), hard-sphere (HS) and symmetrical resonance charge-transfer (CX). The exact, diffusional and bottleneck rates are α_E, α_D and α_{BN}, respectively.

	α_D/α_E			α_{BN}/α_E
a	POL	HS	CX*	HS
0.001	0.955	0.969	0.997	50.51
0.01	1.159	1.205	1.295	7.692
0.1	2.000	2.410	2.985	2.950
1/3	2.924	3.891	5.051	2.227
1.0	3.413	4.854	6.329	2.020
10.0	2.000	2.941	-	2.674
100.0	1.156	1.403	-	6.452
1000.0	0.955	1.053	-	32.26

*Here small a implies $M_2 \ll M_1 = M_3$ and a = 1 implies $M_2 \gg M_1 = M_3$.

Figure Captions

Fig. 1 (a) Normalized energy-change frequency moments $D^{(m)}$ (energy^m s^{-1}), m = 0-4, as a function of internal energy $E_i = -\lambda(kT)$ of the bound ion-pair. (b) Ratios $D^{(m)}/D^{(o)}$ (energy^m per collision), m = 1 and 2, and comparison of $D_i^{(1)}$ with $\partial D_i^{(2)}/\partial\lambda$ which shows that the minimum of $D_i^{(2)}$ has same location as the zero in $D_i^{(1)}$. Equal-mass species and charge-transfer ion-neutral collisions are assumed and moments are normalized to the quantity $(-1)^m \Gamma\alpha_T (kT)^{m-1}$ given in ref. 14.

Fig. 2 Inverses of moments (a) $D^{(2)}(\lambda)$ and (b)$D^{(4)}(\lambda)$ as a function of internal energy $E_i = -\lambda kT$ of the ion-pair for various ion-neutral interactions: POL (polarization), HS (hard-sphere), CX (charge-transfer). Equal-mass species are assumed.

Fig. 3(a). Probabilities $P^{A,D}$ for association and dissociation of an ion-pair bound with energy $E_i = -\lambda kT$. Equal-mass species and charge-transfer ion-neutral collisions are assumed. ——: Exact QSS-solution of eq. (2.29). ----: Diffusional Approximation, eq. (3.29) and (3.30).

Fig. 3(b) Derivatives $(dP^A/d\lambda)$ of probability P^A of Fig. (3a) for association. QSS: from solution of eq (2.29). D: diffusional approximation, eq (3.31).

Fig. 4. Comparison of currents, eq (2.20), past energy level $E_i = -\lambda kT$, obtained (——) from exact solution of eq (2.29) and from (---) diffusion probabilities eq (3.29). Equal-mass species and charge-transfer ion-neutral collisions are assumed. The current is normalized to $(2\alpha_T \tilde{N}_A \tilde{N}_B)$ where α_T is the Thomson rate, eq (4.5).

Fig. 5. Normalized rates R_T, eq (4.6), for ion-ion recombination in a dilute gas as a function of mass parameter a, eq (3.34) for various ion-neutral interactions: HS (hard-sphere), CX (charge-transfer) and POL (polarization). ——: exact rates. □, ○, △: rates obtained with diffusional probabilities, eq (3.29), in basic eq (4.4) for HS, CX and POL interactions.

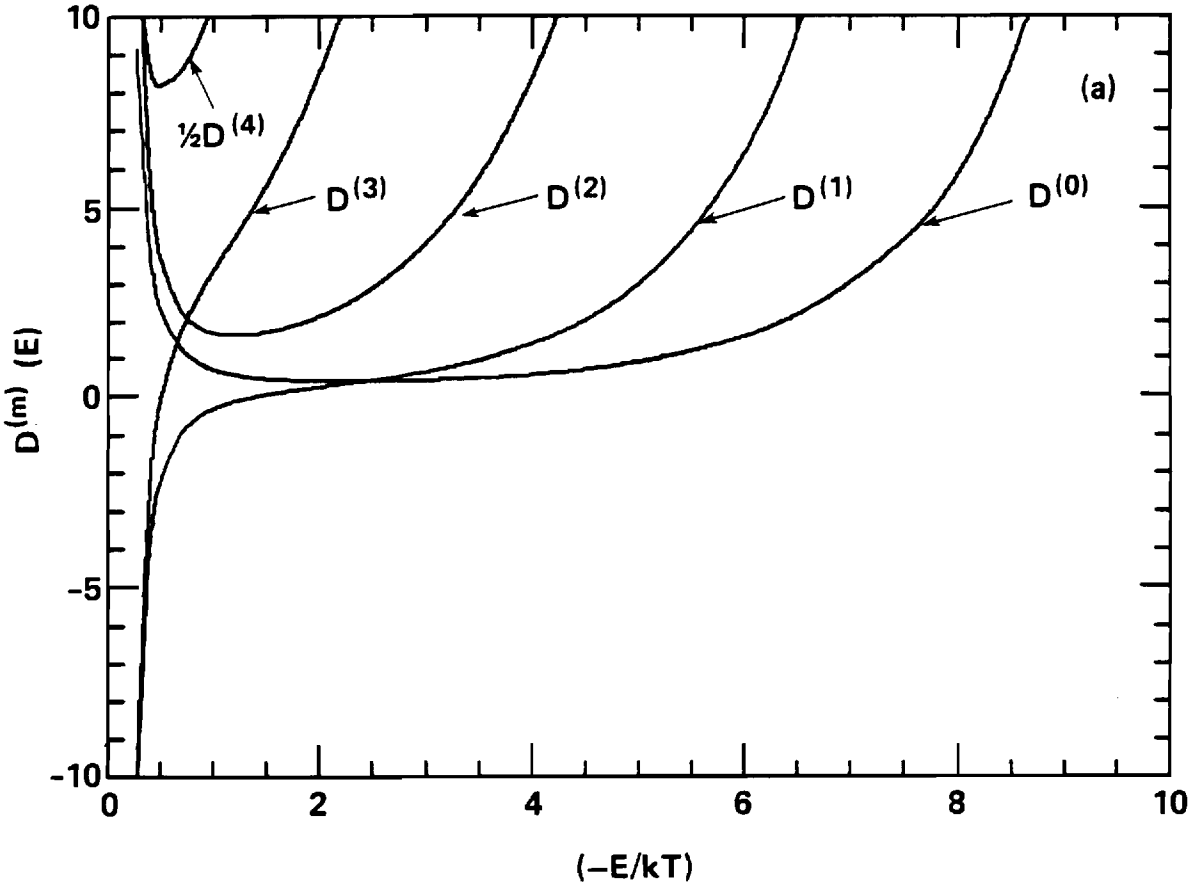
10
5
0
-5
-10
0
2
4
6
8
10
(a)
½D(4)
D(3)
D(2)
D(1)
D(0)
D(m) (E)
(–E/kT)

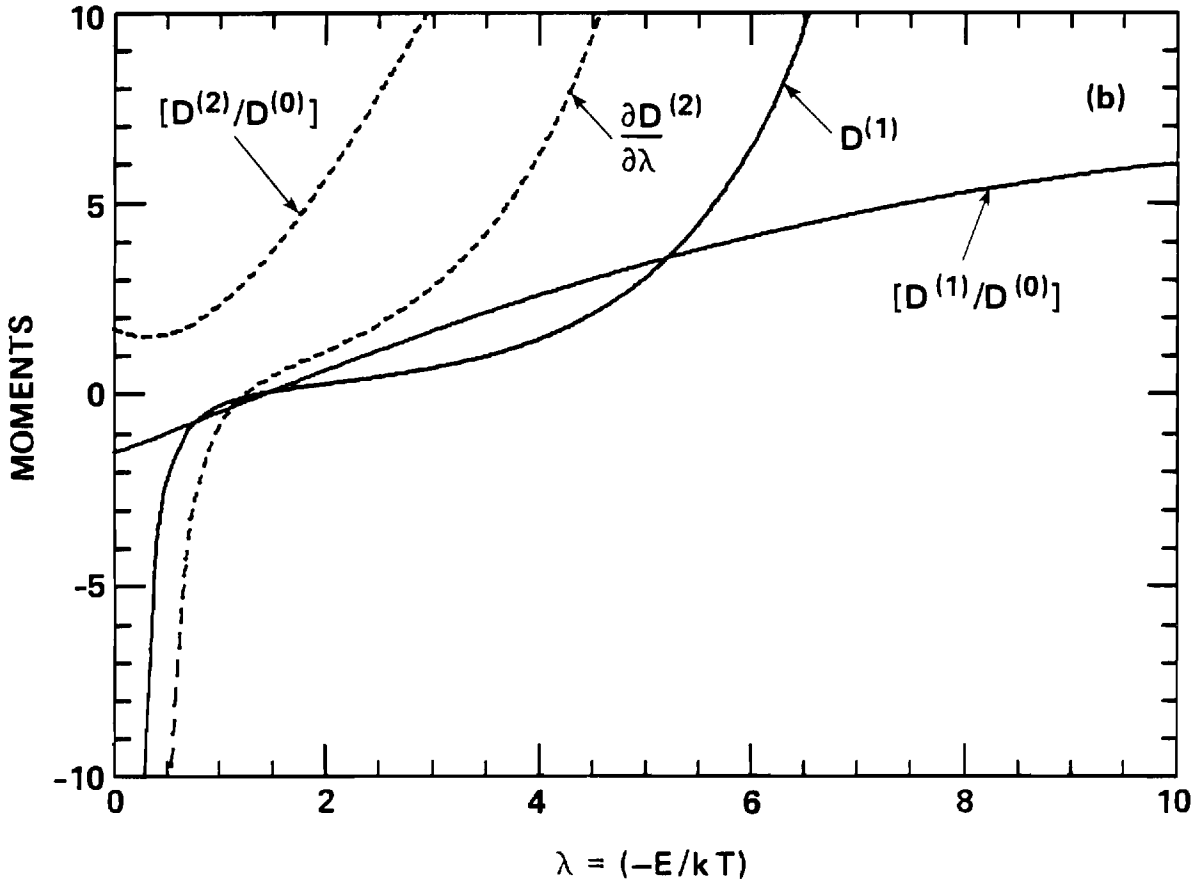
10
5
0
-5
-10
0
2
4
6
8
10
(b)
[D(2)/D(0)]
∂D(2)/∂λ
D(1)
[D(1)/D(0)]
MOMENTS
λ = (–E/kT)

Figure 1

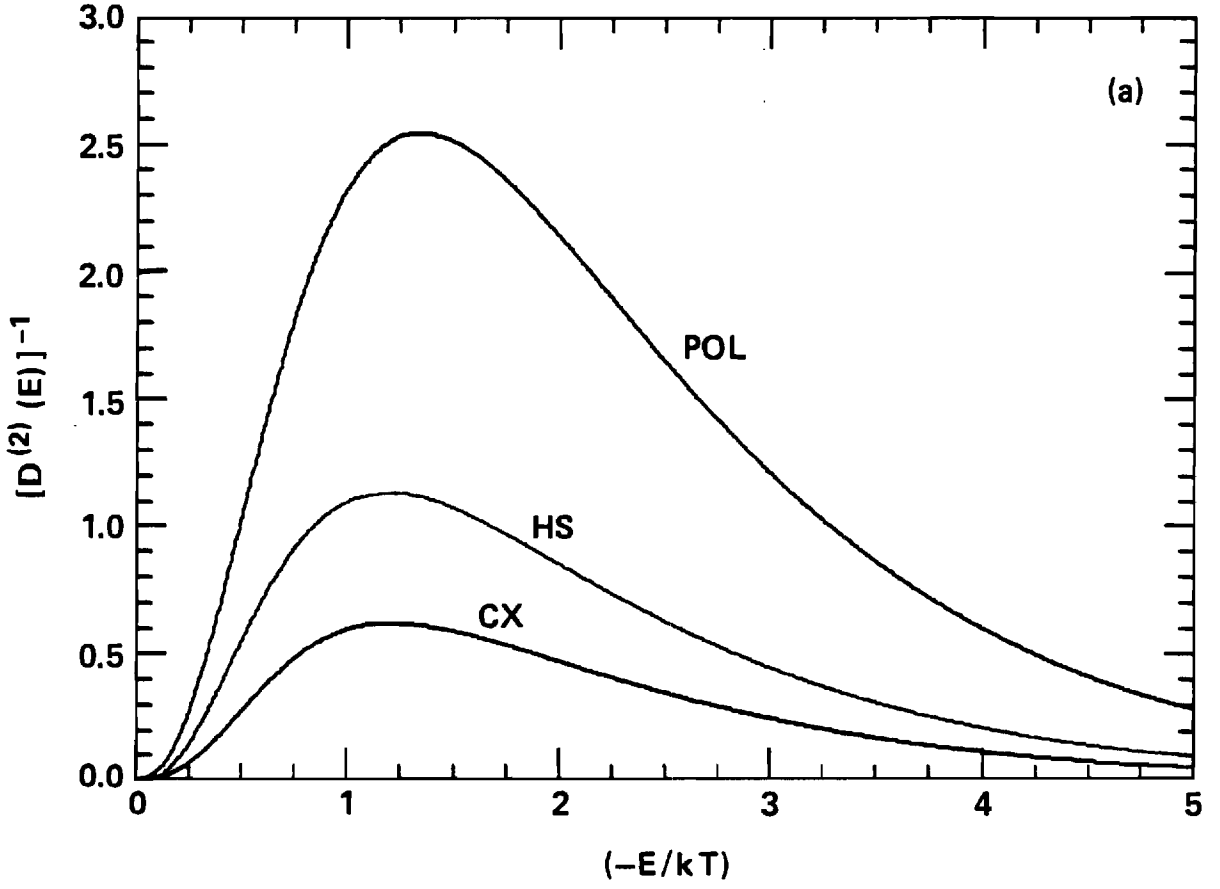
(a)
POL
HS
CX
$[D^{(2)}(E)]^{-1}$
(−E/kT)
0.0
0.5
1.0
1.5
2.0
2.5
3.0
0
1
2
3
4
5

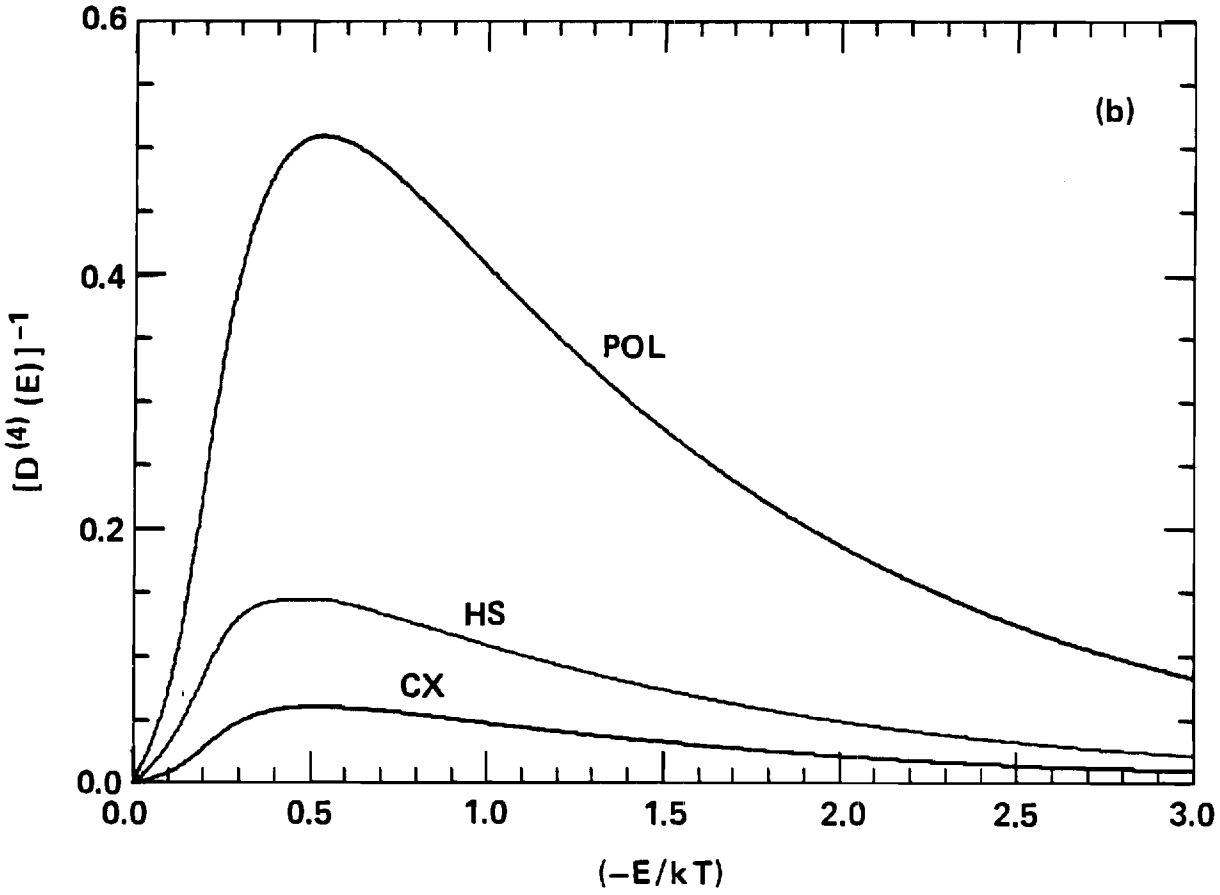
(b)
POL
HS
CX
$[D^{(4)}(E)]^{-1}$
(−E/kT)
0.0
0.2
0.4
0.6
0.0
0.5
1.0
1.5
2.0
2.5
3.0

Figure 2

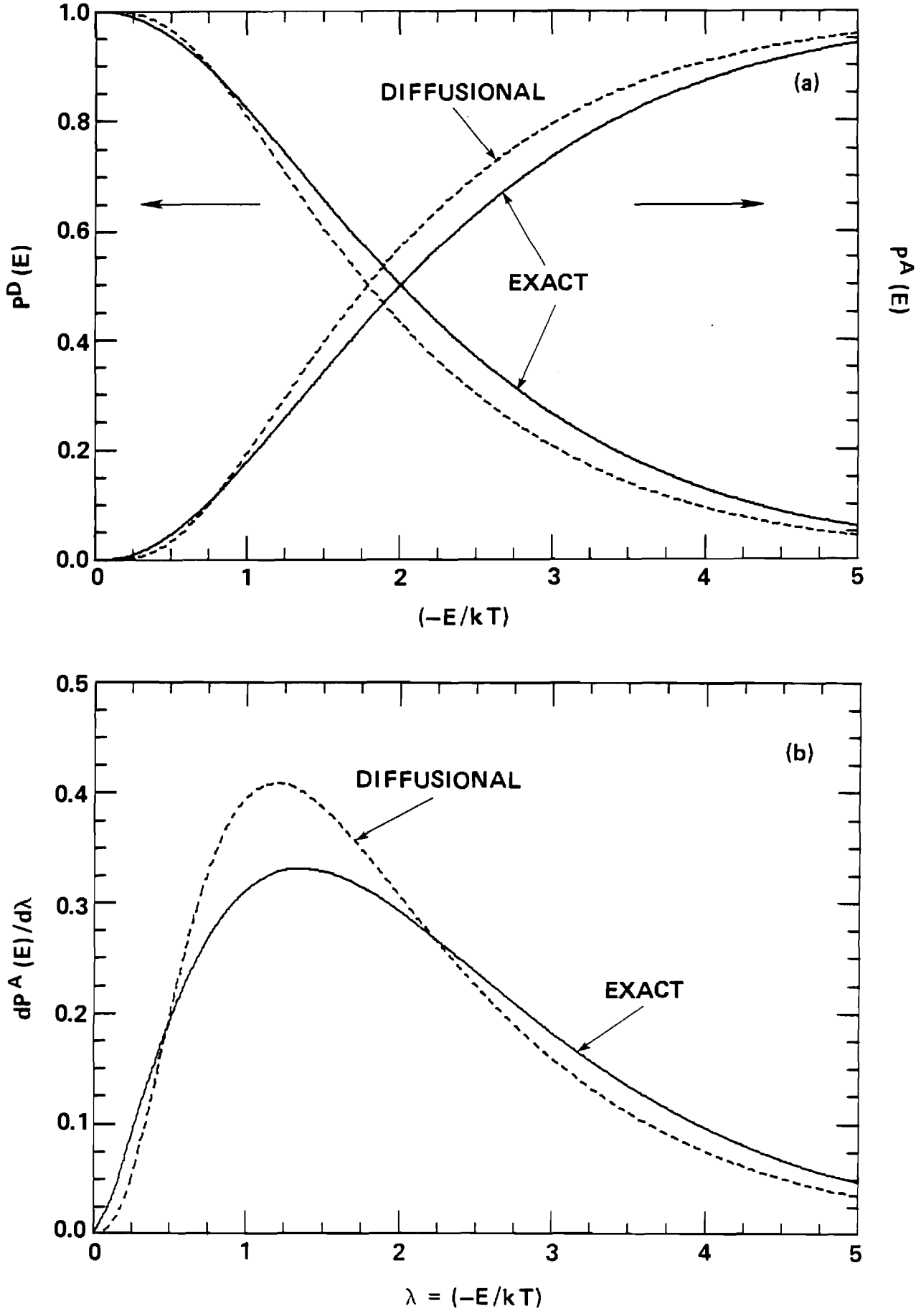
1.0
0.8
0.6
0.4
0.2
0.0
0
1
2
3
4
5
DIFFUSIONAL
EXACT
(a)
$P^D(E)$
$P^A(E)$
(−E/kT)
0.5
0.4
0.3
0.2
0.1
0.0
(b)
DIFFUSIONAL
EXACT
$dP^A(E)/d\lambda$
λ = (−E/kT)

Figure 3

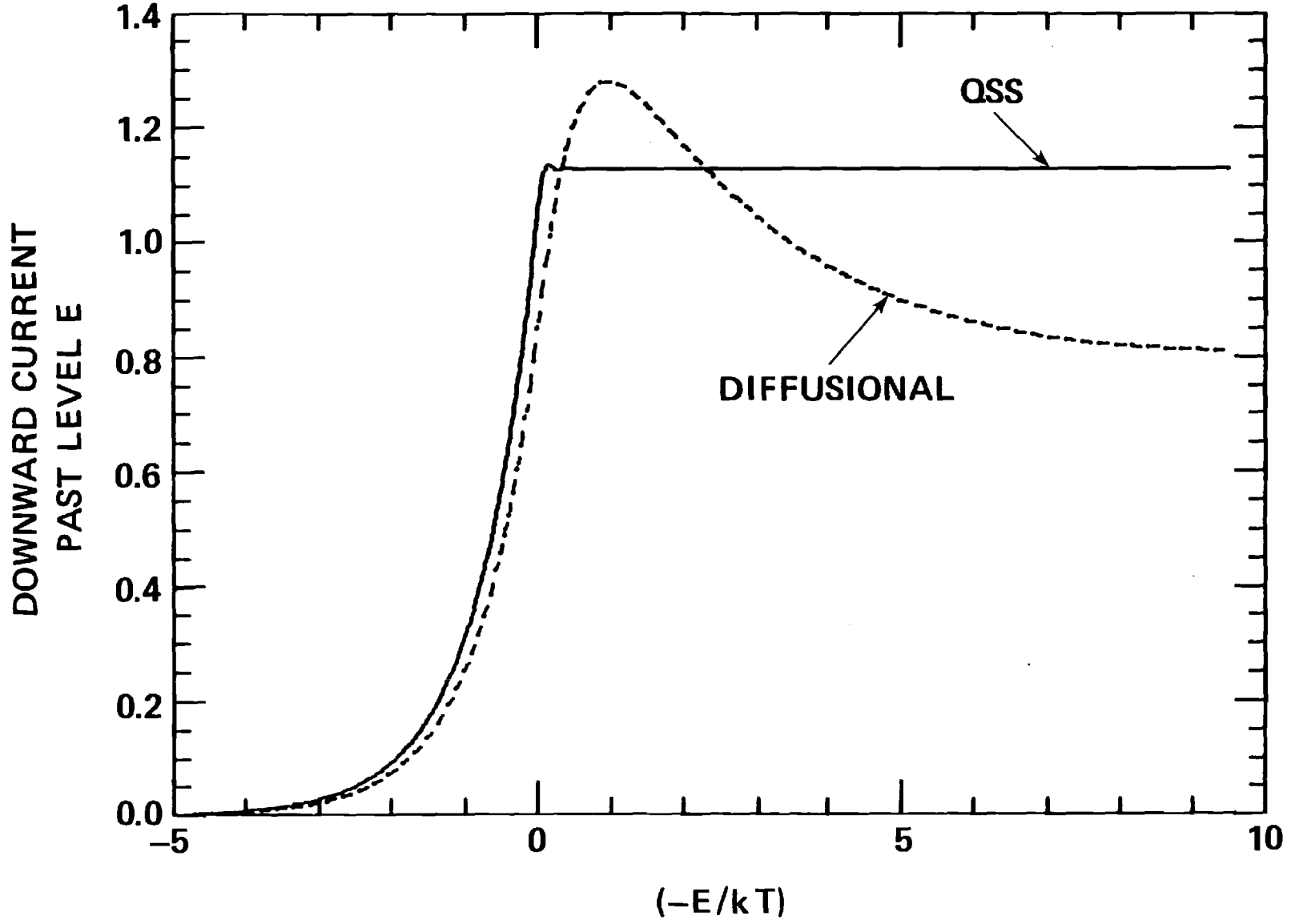
1.4
1.2
1.0
0.8
0.6
0.4
0.2
0.0
DOWNWARD CURRENT
PAST LEVEL E
QSS
DIFFUSIONAL
–5
0
5
10
(–E/kT)

Figure 4

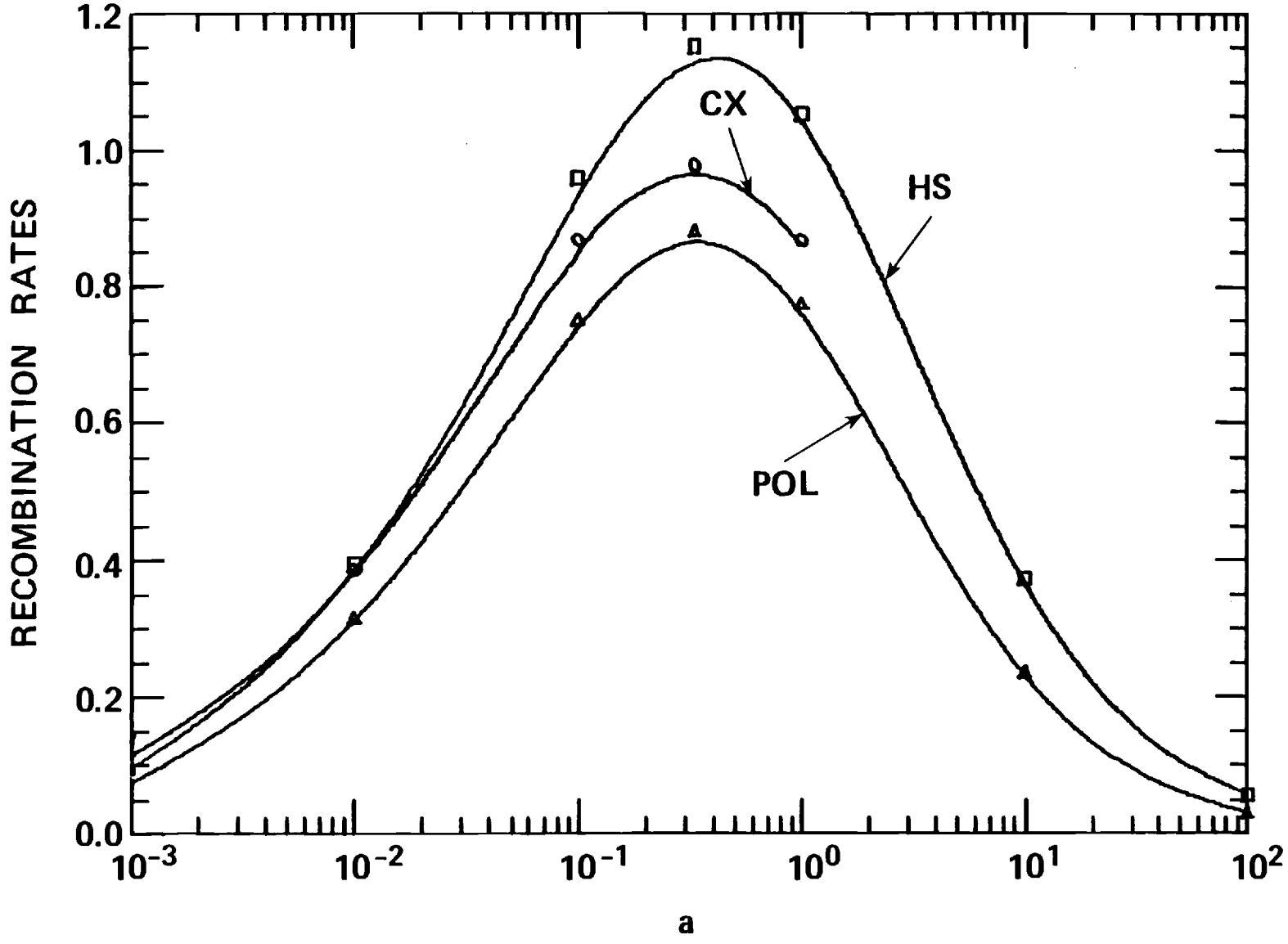
RECOMBINATION RATES
1.2
1.0
0.8
0.6
0.4
0.2
0.0
CX
HS
POL
10^{-3}
10^{-2}
10^{-1}
10^{0}
10^{1}
10^{2}
a

Figure 5

Appendix C

Microscopic Basis and Analytical and Numerical Solutions of the Debye-Smoluchowski Equation

Microscopic Basis and Analytical and Numerical Solutions of the Debye-Smoluchowski Equation

M. R. Flannery and E. J. Mansky

School of Physics

Georgia Institute of Technology

Atlanta, Georgia 30332

By explicitly including collisions and by operating at a level more basic than the macroscopic Debye-Smoluchowski Equation (DSE), various assumptions within the DSE-treatment of transport influenced reactions of A and B in a dense medium M become naturally exposed. The appropriate modification of DSE to description of the kinetics within the region of the sink is provided.

Analytical expressions for probability densities and rates are derived which are exact solutions of DSE (a) at all times t and large internal separations R of the pair (A-B), (b) at long times t and all R and (c) at short times t and all R. Not only are the transient rates $\alpha_S(t)$ and $\alpha_L(t)$ exact at short and long times, respectively, but they are naturally bounded for all times with $\alpha_S(t\to\infty)$ and $\alpha_L(t\to 0)$ tending to the correct limit, albeit with an incorrect transience. Comparison with exact numerical solutions of DSE illustrates the effectiveness of a proposed solution over the full range of time.

PACS: 34.10.+x, 51.10.+y, 66.10.+x.

Contents

1. Introduction

In chemical kinetics of reactions in the condensed phase or in solution and of coagulation of colloids, the Debye-Smoluchowski Equation (DSE)[1-3] has received widespread application. It involves solution of the continuity equation

$$\partial n(\underset{\sim}{R},t)/\partial t + \underset{\sim}{\nabla}\cdot\underset{\sim}{J}^{d}(\underset{\sim}{R},t) = 0 \quad , \quad R \geq R_s \tag{1.1}$$

subject to the radiation boundary condition

$$4\pi R_s^2 \, J^d(R_s,t) = -\alpha_3 \, n(R_s,t) \quad , \tag{1.2}$$

which equates (as in heat-conduction problems) the frequency of transport with the frequency of absorption, assumed to proceed at a local rate $\alpha_3(cm^3\ s^{-1})$ at the boundary of a spherical sink of radius R_s. The number density of pairs AB with internal separation $\underset{\sim}{R}$ between $\underset{\sim}{R}$ and $\underset{\sim}{R} + d\underset{\sim}{R}$ is $n(\underset{\sim}{R})d\underset{\sim}{R}$ and $J^d(R)d\underset{\sim}{R}$ is the intramolecular net current within pairs which are in the state of internal expansion across interval $d\underset{\sim}{R}$ about $\underset{\sim}{R}$ within some medium M. In the absence of any sources, the rate of disappearance of pairs with $R \geq R_s$ is,

$$(\partial/\partial t) \int_{R_s}^{\infty} n(\underset{\sim}{R},t)d\underset{\sim}{R} = 4\pi R_s^2 \, J^d(R_s,t) = -\alpha(t)N_A N_B \tag{1.3}$$

where α is the overall rate of association of species A and B with averaged number densities $N_{A,B}$ at time t. Hence the rate,

$$\alpha(t) = \alpha_3 \, n(R_s,t)/N_A N_B \tag{1.4}$$

relies only on the macroscopic density $n(R_s,t)$ at the sink boundary provided the local rate α_3 is regarded as a pre-assigned parameter. The net current $\underset{\sim}{J}^d$ in (1.1) can be related to the total density n via[2-4]

$$\underset{\sim}{J}^d(R,t) = -D \underset{\sim}{\nabla} n(\underset{\sim}{R},t) + (K/e)(\underset{\sim}{\nabla}V)\, n(\underset{\sim}{R},t) \qquad (1.5)$$

where V(R) is the energy of interaction between A and B. In terms of the diffusion and mobility coefficients $D_{A,B}$ and $K_{A,B}$, respectively, for the isolated species A and B in the medium M, the coefficients in (1.5) for relative diffusion and relative mobility are $D = D_A + D_B$ and $K = K_A + K_B$. Hence the rate $\alpha(t)$ can be determined from the solution of (1.1) at the sink via (1.4) and the overall problem is reduced to one of transport alone.

Although the DSE-method has been applied to reactions in solution, its de-facto generalization to lower densities of the medium (as a gas) is not immediately obvious, nor are the assumptions intrinsic to validity of DSE transparent. The effective decoupling of reaction from transport as in (1.2) and in (1.4) is likely to be valid in the limit of high gas densities when reaction proceeds much faster than transport which is then the rate-limiting step. As the density is reduced, reaction and transport are coupled, and address is required at a microscopic level[4] more basic than (1.1)-(1.5). In §2, this microscopic basis[5] of DSE is summarized so that the validity requirements of DSE are naturally exposed. It is shown that the DSE-method when applied to transport-influenced reactions in a gas retains its usefulness for evaluation of time dependent rates $\alpha(t)$ via determination of that particular time-dependent combination of the individual transport and reaction rates α_{TR} and α_{RN}, respectively, which are time-independent and which are regarded as being independent parameters, externally assigned.

Although DSE can be solved exactly for the field-free case ($V = 0$), no simple exact analytical solution yet exists for general interaction $V(R)$ between A and B. For the pure Coulomb case, DSE has been solved[6] in terms of Mathieu functions, which can be expressed as infinite series of products of modified Bessel functions but which are as complicated to evaluate as the exact numerical solution. For approximate solution of (1.1) with general $V(R)$ a large body of literature (see ref. 7) exists on various schemes based on Green's function,[8] "prescribed" diffusion[9] and "matched perturbation"[10] techniques.

Here (in § 3 and §4), highly accurate analytical solutions for general $V(R)$ are proposed, and are then tested (in § 5) explicitly for pure Coulombic attraction. Exact analytical expressions for the densities $n(\underset{\sim}{R},t)$ and the rates $\alpha(t)$ are derived (a) for short times and all R, (b) for long times and all R, and (c) for all times t and large R. The only simple analytical expression available up to now has been that derived[11] from the method of "matched perturbation solutions"[10] for the exact asymptotic transient ($t \to \infty$) . The present long-time solution,(b) above,not only yields this exact asymptotic transient but provides an analytical solution which is exact down to much shorter times. Some preliminary reports of these analytical expressions have already been presented.[12-14] Finally, an approximate and highly accurate combination of short-time and long-time solutions is proposed in § 6 for the rates $\alpha(t)$ at all times t.

The aim of the present paper is therefore to examine the foundation and validity requirements of DSE within a modern perspective and, then to present analytical solutions of DSE under a general interaction $V(R)$ between the species A and B reacting in a thermal gas bath M. The microscopic theory used in this paper has been developed earlier[5].

2. Microscopic Basis of the Debye-Smoluchowski Equation

For the closed system,

$$A + B + M \rightleftarrows AB + M \tag{2.1}$$

with no external sources or sinks as discussed previously,[5] the continuity equation

$$\frac{\partial}{\partial t} n^s(\underset{\sim}{R},t) + \underset{\sim}{\nabla}\cdot\underset{\sim}{J}^d(\underset{\sim}{R},t) = 0 \tag{2.2}$$

holds for the integrated macroscopic distribution

$$n^s(\underset{\sim}{R},t) = \int_{-V(R)}^{\infty} n_i{}^s(\underset{\sim}{R},E_i,t)dE_i \tag{2.3}$$

in number density (cm^{-3}) of AB pairs. The microscopic distribution n_i^s is such that $n_i^s d\underset{\sim}{R}dE_i$ is the number density of pairs with internal separation $\underset{\sim}{R}$ and internal energy E_i within the interval $d\underset{\sim}{R}dE_i$ about $(\underset{\sim}{R},E_i)$ and $n^s d\underset{\sim}{R}$ is then the number density within interval $d\underset{\sim}{R}$ of pairs with all possible internal energies between the lowest bound level $-V(R)$ consistent with a fixed R and the far continuum. The interaction between A and B is V(R). The net $\underset{\sim}{R}$-macroscopic current vector

$$\underset{\sim}{J}^d(\underset{\sim}{R},t) = \int_{-V}^{\infty} \underset{\sim}{J}_i{}^d(\underset{\sim}{R},E_i,t)dE_i \tag{2.4}$$

is the energy-integration of the $(\underset{\sim}{R},E_i)$-microscopic net current $\underset{\sim}{J}_i^d$ in

$$\underset{\sim}{J}_i^{s,d}(\underset{\sim}{R},E_i,t) = \int_{(+)} n_i(\underset{\sim}{R},E_i,\hat{\underset{\sim}{v}}_i;t)\underset{\sim}{v}_i\, d\hat{\underset{\sim}{v}}_i \pm \int_{(-)} n_i(\underset{\sim}{R},E_i,\hat{\underset{\sim}{v}}_i;t)\underset{\sim}{v}_i\, d\hat{\underset{\sim}{v}}_i \tag{2.5}$$
$$\equiv \underset{\sim}{J}_i{}^+(\underset{\sim}{R},E_i,t) \pm \underset{\sim}{J}_i{}^-(\underset{\sim}{R},E_i,t)$$

where the conditional pair distribution $n_i(\underset{\sim}{R},E_i,\hat{\underset{\sim}{v}}_i;t)$ is such that the number density of pairs AB with internal separation $\underset{\sim}{R}$, internal energy E_i and with the direction $\hat{\underset{\sim}{v}}_i$ of the internal relative velocity $\underset{\sim}{v}_i$ in interval $d\underset{\sim}{R}\, dE_i\, d\hat{\underset{\sim}{v}}_i$ about $(\underset{\sim}{R},E_i,\hat{\underset{\sim}{v}}_i)$ is $n_i(\underset{\sim}{R},E_i,\hat{\underset{\sim}{v}}_i;t)d\underset{\sim}{R}dE_i d\hat{\underset{\sim}{v}}_i$ at time t. Corresponding to (2.5) define the sum (s) and difference (d) of microscopic densities by

$$n_i^{s,d}(\underset{\sim}{R},t) = n_i^{s,d}(\underset{\sim}{R},E_i,t) = \int_{(+)} n_i(\underset{\sim}{R},E_i,\hat{\underset{\sim}{v}}_i;t)d\hat{\underset{\sim}{v}}_i \pm \int_{(-)} n_i(\underset{\sim}{R},E_i,\hat{\underset{\sim}{v}}_i;t)d\hat{\underset{\sim}{v}}_i \qquad (2.6)$$

$$\equiv n_i^{+} \pm n_i^{-}$$

The integrations in (2.5) and (2.6) are over the positive (+) region where $\underset{\sim}{R}\cdot\underset{\sim}{v}_i \geq 0$, and the negative (-) region where $\underset{\sim}{R}\cdot\underset{\sim}{v}_i \leq 0$, such that the net current J_i^{d} and the net density n_i^{d} of pairs which are in the states of internal expansion (+) or contraction (-) are $(J_i^{+} - J_i^{-})$ and $(n_i^{+} - n_i^{-})$ respectively. Also n_i^{s} and J_i^{s} are the respective sums $(n_i^{+} + n_i^{-})$ and $(J_i^{+} + J_i^{-})$ of densities and currents of internally expanding (+) and contracting (-) pairs.

The continuity equation corresponding to (2.2) but for the microscopic distribution $n_i^{s}(\underset{\sim}{R},t)$ has already been derived[5] from a Boltzmann-type equation for the two-particle correlation function $n(\underset{\sim}{R},\underset{\sim}{v},t)$ and is[5]

$$\frac{\partial}{\partial t} n_i^{s}(\underset{\sim}{R},E_i,t) + \underset{\sim}{\nabla}\cdot\underset{\sim}{J}_i^{d}(\underset{\sim}{R},E_i,t) = \int_{-V(R)}^{\infty} S_{fi}^{s}(R,t)dE_f \qquad (2.7)$$

where the net frequency of collisional transitions $(i \to f)$ is S_{fi}^{s} given in

$$S_{if}^{s,d}(R,t) = n_i^{s,d}(\underset{\sim}{R},t)\, \nu_{if}(R) - n_f^{s,d}(\underset{\sim}{R},t)\, \nu_{fi}(R) = -S_{fi}^{s,d}(R,t) \qquad (2.8)$$

in terms of the frequency $\nu_{if}\, dE_f$ of AB-M collisions, which change the internal energy of a pair AB from E_i to between E_f and $E + dE_f$ at a fixed

nuclear separation $\underset{\sim}{R}$ of A and B. Thus, the net rate at time t of collisional production of (R,E_i)-pairs from all levels f within the accessible energy range $[-V \to \infty]$ is the RHS of (2.7). On integration of (2.7) over the full energy range of E_i, the macroscopic continuity equation (2.2) for the closed system is recovered since the overall effect of collisions $\int_{-V}^{\infty} dE_i \int_{-V}^{\infty} dE_f \, S^s_{fi}$ is null. Although the macroscopic net current $J^d(\underset{\sim}{R},t)$ can be related[4] to the summed densities $n^s(\underset{\sim}{R},t)$ via the excellent approximation,[4]

$$\underset{\sim}{J}^d(\underset{\sim}{R},t) = -D \underset{\sim}{\nabla} n^s(\underset{\sim}{R},t) + (\frac{K}{e}) \, (\underset{\sim}{\nabla}V) \, n^s(\underset{\sim}{R},t) \qquad (2.9)$$

in term of the macroscopic coefficients D and K for relative diffusion and relative mobility of A and B in medium M, no similar relation has yet been derived for the corresponding microscopic current $J_i^d(\underset{\sim}{R},E_i,t)$. As has previously[5] been shown, (2.7) must then be coupled to the following equation

$$\frac{\partial}{\partial t} n_i^d(\underset{\sim}{R},E_i,t) + \underset{\sim}{\nabla}\cdot\underset{\sim}{J}_i^s(\underset{\sim}{R},E_i,t) - \left[\frac{2}{R} - (E_i-V)^{-1} \frac{\partial V}{\partial R}\right] n_i^{\pm}(\underset{\sim}{R},E_i,\hat{\underset{\sim}{R}}\cdot\hat{\underset{\sim}{v}}_i = \tfrac{\pi}{2};t)v_i \qquad (2.10)$$

$$= \int_{-V}^{\infty} S_{fi}^d(R,t)dE_f$$

in terms of the quantities J_i^s, n_i^d and S_{fi}^d defined in (2.5), (2.6) and (2.8) respectively. When equilibrium is established in the internal angular momentum L of the pair (A-B), n_i is then independent[5] of v_i so that $J_i^{s,d}$ in (2.7) and (2.10) are simply $\frac{1}{2} n_i^{s,d} v_i$. Also $n_i^{\pm}$ in (2.10) is then given by[5] $n_i^- = \frac{1}{2}(n_i^s - n_i^d)$ for all R and $E_i \geq 0$, and for bound levels $E_i \leq 0$ by $n_i^+ = \frac{1}{2}(n_i^S + n_i^D)$ for $R \leq A$ or by $n_i^- = \frac{1}{2}(n_i^s - n_i^d)$ for $A \leq R \leq B$. Here A is the radius of the bound circular orbit (associated with maximum angular momentum L), and B is the radius of the outermost turning point of the orbit with L = 0 where $|E_i| = V(B)$. Under

conditions of thermodynamic equilibrium in L, $J_i^{s,d} = \frac{1}{2} n_i^{s,d} v_i$ in (2.7) and (2.10) which are therefore coupled in n_i^s and n_i^d; in contrast to the direct use of (2.9) in (2.2) for the macroscopic densities $n^s(\underset{\sim}{R},t)$. Operation at a level more basic than (2.2) therefore necessitates solution of coupled time-dependent equations, rather than the single equation (2.2). It is therefore advantageous to explore the conditions for which a macroscopic treatment based on (2.2) can be invoked.

2.1 Macroscopic Transport-Collisional Equations

For a given R, subdivide the energy range into three blocks: a block of strongly bound levels between levels -V(R) and -S within which the pairs are considered to be fully associated, a block *S* of excited levels between -S and the dissociation limit taken at zero energy within which the pairs are in the process of associating or dissociating, and a continuum block *C* which describes fully dissociated pairs. The sum of the distributions n_c and n_e of pairs in blocks *C* and *E* respectively,

$$n(\underset{\sim}{R},t) = \int_{-S}^{\infty} n_i^s(\underset{\sim}{R},E_i;t)dE_i \equiv n_c(\underset{\sim}{R},t) + n_e(\underset{\sim}{R},t) \tag{2.11}$$

and the corresponding net current

$$J(\underset{\sim}{R},t) = \int_{-S}^{\infty} J_i^d(\underset{\sim}{R},E_i;t)dE_i \equiv J_c(\underset{\sim}{R},t) + J_e(\underset{\sim}{R},t) \tag{2.12}$$

then satisfy, with the aid of (2.7), the equation

$$\frac{\partial}{\partial t} n(\underset{\sim}{R},t) + \underset{\sim}{\nabla}\cdot\underset{\sim}{J} = -\int_{-S}^{\infty} dE_i \int_{-V}^{-S} S_{if}(R,t)dE_f \quad ; \quad R \lesssim R_s \tag{2.13}$$

for $R \lesssim R_s$, the outermost turning point associated with level -S. In (2.13) and in what follows S_{if}^{s} is written simply as S_{if}. For $R \gtrsim R_s$, block S does not exist so that

$$\frac{\partial}{\partial t} n(\underset{\sim}{R},t) + \underset{\sim}{\nabla}\cdot\underset{\sim}{J} = 0 \quad ; \quad R \gtrsim R_s \tag{2.14}$$

Integration of (2.13) yields,

$$\frac{\partial}{\partial t} \int_0^{R_s} n(\underset{\sim}{R},t)d\underset{\sim}{R} + 4\pi R_s^{\,2}\, J(\underset{\sim}{R}_s,t) = - \int_0^{R_s} dR \int_{-S}^{\infty} dE_i \int_{-V}^{-S} S_{if}(R,t)dE_f \tag{2.15}$$

On introducing

$$S_{if}(t) = \int_0^{R_{if}} S_{if}(R,t)d\underset{\sim}{R} = - S_{fi}(t) \tag{2.16}$$

the net frequency per unit $dE_i dE_f$ of collisional transitions between levels E_i and E_f, where R_{if} is the lesser of R_i and R_f, the turning points associated with levels E_i and E_f, integration of (2.7) over all accessible R-space yields

$$\frac{\partial}{\partial t} n_i(E_i,t) = - \int_0^{R_i} d\underset{\sim}{R} \int_{-V}^{\infty} S_{if}(R,t)dE_f = - \int_{-D}^{\infty} S_{if}(t)dE_f \tag{2.17}$$

Eq. (2.15) is then

$$\frac{\partial}{\partial t} \int_0^{R_s} n(\underset{\sim}{R},t)d\underset{\sim}{R} + 4\pi R_s^{\,2}\, J(\underset{\sim}{R}_s,t) = - \int_{-S}^{\infty} dE_i \int_{-D}^{-S} S_{if}(t)dE_f = - \partial n_s(t)/\partial t \tag{2.18}$$

where the density of pairs in block S is

$$n_s(t) = \int_0^{R_s} n_s(\underset{\sim}{R},t)d\underset{\sim}{R} = \int_0^{R_s} d\underset{\sim}{R} \int_{-V}^{-S} n_i^{\,s}(\underset{\sim}{R},E_i;t)dE_i = \int_{-D}^{-S} n_i(E_i,t)dE_i \tag{2.19}$$

Eq. (2.18) states that the flux, $-4\pi R_s^2 J$, entering the (reaction) sphere of radius R_s equals the net collisional rate of production of S-pairs plus the rate of increase of the contribution from the reaction volume to the density (2.11) of C and S pairs. On assuming no net flux at infinite separation R, integration of (2.14) yields

$$\frac{\partial}{\partial t} \int_{R_s}^{\infty} n(\underset{\sim}{R},t) d\underset{\sim}{R} = 4\pi R_s^2 J(R_s,t) \tag{2.20}$$

which, when added to (2.18), provides

$$\frac{\partial}{\partial t} \int_{o}^{\infty} n(\underset{\sim}{R},t) d\underset{\sim}{R} + \frac{\partial}{\partial t} n_s(t) = 0 \tag{2.21}$$

the conservation equation as expected for this closed system. On defining the averaged local rate α_3 ($cm^3\ s^{-1}$) for production of block S via collisional absorption from blocks C and S by

$$\alpha_3\, n(R_s,t) = \int_{-S}^{\infty} dE_i \int_{-D}^{-S} S_{if}(t) dE_f = \partial n_s(t)/\partial t \tag{2.22}$$

The effective two body rate α ($cm^3\ s^{-1}$) for association of dissociated species A and B with densities $N_{A,B}(t)$ (cm^{-3}) and the frequency k (s^{-1}) for dissociation of S-pairs AB with density $n_s(t)$ are related by[5]

$$\partial n_s(t)/\partial t = \alpha N_A(t) N_B(t) - k\, n_s(t) \tag{2.23}$$

when quasi-steady-state (QSS) conditions ($\partial n_i/\partial t$) are assumed for block E. On further assuming that those pairs within the reaction volume of blocks C and E are also in QSS i.e.,

$$\frac{\partial}{\partial t} \int_0^{R_s} n(\underset{\sim}{R}_s, t) d\underset{\sim}{R} = 0 \tag{2.24}$$

then (2.18) and (2.22) yield

$$\partial n_s(t)/\partial t = - 4\pi R_s^2 \, J(\underset{\sim}{R}_s, t) = - \alpha_3 \, n(R_s, t) \tag{2.25}$$

so that the effective two-body rate of association is

$$\alpha(t) = \alpha_3 [1 - \Gamma(t)]^{-1} \, n(R_s, t)/N_A(t) N_B(t) \tag{2.26}$$

where the quantity

$$\Gamma(t) = [\tilde{N}_A \tilde{N}_B / N_A(t) N_B(t)] \; [n_s(t)/\tilde{n}_s] \tag{2.27}$$

is a measure of the departure of the densities of the dissociated A,B and associated AB species from their corresponding time-dependent values $\tilde{N}_{A,B}$ and $\tilde{n}_s$ appropriate to full thermodynamic equilibrium ($\Gamma = 1$) with the gas bath M. Since

$$n_s(t) - n_s(0) = \alpha_3 \int_0^t n(R_s, t) dt, \tag{2.28}$$

$\Gamma(t)$ can therefore be determined given $N_{A,B}(t)$.

Provided the local rate α_3 in (2.22) is specified as some external parameter or else is obtained by other means, α is therefore determined via (2.26) solely by the transport equation (2.14),

$$\frac{\partial}{\partial t} n(\underset{\sim}{R}, t) + \underset{\sim}{\nabla} \cdot \underset{\sim}{J} = 0 \quad , \quad R \geq R_s \tag{2.29a}$$

solved subject to the radiation boundary condition

$$4\pi R_s^2 \, J(R_s,t) = \alpha_3 \, n(R_s,t) \qquad (2.29b)$$

at the sink. When (2.9) is used for J, this combination (2.29) represents the Debye-Smoluchowski Equation (DSE), familiar in kinetics of reactions in the condensed phase[1-3] and in solution[7-10] and to coagulation of colloids. It was obtained originally by applying the macroscopic continuity Eqn. (2.2) outside ($R \gtrsim R_s$) the sink region, and by equating the transport and absorption rates at $R = R_s$, as in (1.1) - (1.5). Since the reaction rate α_3 is considered as a pre-assigned parameter, DSE concentrated solely on solution of the transport portion $J^D(R \gtrsim R_s,t)$ of the problem, external to the sink.

2.2 Assumptions Intrinsic to DSE

By operating at a level more basic than DSE, the present treatment has exposed the two underlying criteria for validity of DSE

$$\left.\begin{aligned} &\frac{\partial}{\partial t} n_i(E_i,t) \approx 0 \qquad 0 \gtrsim E_i \gtrsim -S \\ &\frac{\partial}{\partial t} \int_0^{R_s} n(\underset{\sim}{R},t) d\underset{\sim}{R} \approx 0 \end{aligned}\right\} \qquad (2.30)$$

i.e., quasi-steady-state conditions are assumed for pairs in the intermediate block E of excited levels and for those pairs with internal separation $R \lesssim R_s$ and with internal energies in the E and the continuum block C.

The present treatment has also provided the logical transport equation (2.13) for description of the sink. It is also usual to consider a situation of high non-equilibrium ($\Gamma << 1$) so that the association rate is simply

$$\alpha(t) = \alpha_3 \, n(R_s,t)/N_A N_B \tag{2.31}$$

where $N_{A,B}$ is the averaged concentration of dissociated species A and B.

If however α_3 is not predetermined (as is the general case) then the complete microscopic treatment based on the solution of the coupled transport-collision equations (2.7) and (2.10) for the microscopic densities $n_i^{s,d}$ is required.

Since α_3 in (2.22) is also determined by the collisional frequency ν_{if} in S_{if} assignment and use within DSE as an external parameter can, however, provide very valuable insight to chemical kinetics in a dense medium. For example the steady state solution ($\partial n/\partial t = 0$) of (2.29) yields the steady-state rate[3-4] which can be written as,[4,12]

$$\alpha_\infty = \frac{\alpha_{RN} \, \alpha_{TR}}{(\alpha_{RN} + \alpha_{TR})} \tag{2.32}$$

in terms of the reaction rate, defined by

$$\alpha_{RN} = \alpha_3 \exp(-KV(R_s)/De) \tag{2.33}$$

and of the transport rate

$$\alpha_{TR} = 4\pi D \, \tilde{R}_s \tag{2.34}$$

where

$$\tilde{R} = [\int_R^\infty \exp(KV/De) R^{-2} \, dR]^{-1} \tag{2.35}$$

The steady state rate α_∞ is therefore controlled by the rate limiting step. However, there are at present no exact analytical solutions of DSE (2.29) - for general V(R), although a large body of literature[7-10] exists for

various types of approximations. For the pure Coulombic case, DSE can be solved formally[6] in terms of Mathieu functions, which in turn can be expressed as an infinite series of products of modified Bessel functions, the full evaluation of which is however as time consuming and as illuminating as the direct numerical solution of (2.29).

In the following section § 3, useful time-dependent analytical solutions for the rates $\alpha(t)$ and densities $n(R,t)$ of (2.24) for general $V(R)$ are proposed. The assumed initial ($t = 0$) condition and asymptotic ($R \to \infty$) boundary condition

$$n(R,t=0) = N_0 \exp(-KV/De) = n(R\to\infty,t) \tag{2.36}$$

are appropriate to association of (A-B) pairs with an initial Boltzmann distribution in internal separation R, and to a continuous source at infinity which maintains the Boltzmann distribution only at asymptotic R.

2.3 Field-Free Expressions

For reference purposes, the analytical solution[15] for the field-free case (V=0) of (2.29) subject to (2.36) can be written as[4]

$$n(R,t) = N_0\{1 + (\alpha_\infty/\alpha_d)(S/R)\ [\exp(\chi_0^2)\exp(2\chi_0\Omega_0)\ \mathrm{erfc}(\chi_0+\Omega_0) - \mathrm{erfc}\ \Omega_0]\} \tag{2.37}$$

in terms of the time-dependent pair (χ_0,Ω_0) of functions,[4]

$$\chi_0(t) = (\alpha_3/\alpha_\infty)(Dt/S^2)^{1/2}\ ;\ \Omega_0(R,t) = (R-S)/2(Dt)^{1/2}\ , \tag{2.38}$$

and of the steady-state (field-free) rate

$$\alpha_\infty^{(0)} = (\alpha_3\alpha_d)/(\alpha_3 + \alpha_d) \tag{2.39}$$

where α_3 is the pre-assigned rate of reaction at $R_s = S$, the sink-radius, and where

$$\alpha_d = 4\pi DS \tag{2.40}$$

is the rate of pure diffusion at S. The exact transient rate of association from (2.31) is therefore,

$$\alpha(t) = \alpha_3\{1 + (\alpha_\infty^{(0)}/\alpha_d)\,[\exp \chi_o^2 \operatorname{erfc} \chi_o - 1\ ]\} \tag{2.41a}$$

$$\equiv \alpha_\infty\,[1 + (\alpha_3/\alpha_d)\exp \chi_o^2 \operatorname{erfc} \chi_o] \tag{2.41b}$$

which initially decreases from the finite reaction rate α_3 as

$$\alpha(t\to 0) = \alpha_3^{(0)}[1 - (2/\pi^{1/2})(\alpha_3/\alpha_d)(Dt/S^2)^{1/2}]\ , \tag{2.42}$$

and approaches the steady-state rate $\alpha_\infty^{(0)}$ via the asymptotic transient

$$\alpha(t\to\infty) = \alpha_\infty^{(0)}[1 + (\alpha_\infty^{(0)}/\alpha_d)(S^2/\pi Dt)^{1/2}] \tag{2.43}$$

In the diffusion limited region $\alpha_\infty^{(0)} \to \alpha_d << \alpha_3$, then (2.41b) reduces exactly to (2.43). It is worth noting that the only exact analytical expression[11] yet available (to the author's knowledge) for the rate $\alpha(t)$ under general V(R) is the asymptotic transient which may be rewritten[12] compactly as,

$$\alpha(t\to\infty) = \alpha_\infty[1+ (\alpha_\infty/\alpha_{TR})\ (\tilde{S}^2/\pi Dt)^{1/2}] \tag{2.44}$$

which corresponds to the same level of approximation as (2.43) but with α_3, α_d, $\alpha_\infty^{(0)}$ and S all replaced by α_{RN}, α_{TR}, α_∞ and $\tilde{S}$ of (2.32) - (2.35), respectively. The basic expression had been earlier obtained[11] from a straightforward application of the method[10] of "matched perturbation solutions". An expression which covers a time range considerably broader than the asymptotic transient (2.44) is derived in the following section, together with a corresponding short-time solution which tends to the initial transient

$$\alpha(t\to 0) = \alpha_{RN}\,[1-(2/\pi^{1/2})(\alpha_{RN}/\alpha_{TR})(\tilde{dR}/dR)_S\,(Dt/\tilde{S}^2)^{1/2}]\ , \qquad (2.45)$$

This transient is the appropriate generalization of (2.42) to arbitrary interaction V(R), but with inclusion of the additional factor

$$(\tilde{dR}/dR) = (\tilde{R}/R)^2\,\exp(KV/De) \qquad (2.46)$$

which is absent in the corresponding generalization (2.44) of the asymptotic transient (2.43).

3. Exact Analytical Solutions (a) for All Times and Large R, (b) for Long Times and All R, and (c) for Short Times and All R.

Under the nonlinear transformation[4,12,16]

$$\tilde{R} = [\int_{R}^{\infty} \exp(KV/De)\, R^{-2}\, dR]^{-1} \tag{3.1}$$

the Debye-Smoluchowski Equation (1.1) for general interaction V(R) has been shown to reduce to[12]

$$\partial\rho(\tilde{R},t)/\partial t = D(d\tilde{R}/dR)^2\, \nabla^2_{\tilde{R}}\, \rho(\tilde{R},t) \tag{3.2}$$

where the fractional departure from Boltzmann equilibrium is

$$\rho(R,t) = n(R,t)/[N_o \exp(-KV/De)] \tag{3.3}$$

At temperature T of the gas, the Einstein relation De = K(kT) holds for weak fields so that the argument of the exponent in (3.1) and (3.3) is (V/kT).

In this 'tilda' space[12], the total flux

$$4\pi R^2\, J(R,t) = 4\pi\tilde{R}^2\, \tilde{J}(\tilde{R},t) \tag{3.4}$$

remains invariant, with the current vector in this $\tilde{R}$-space being defined as

$$\tilde{J} = -DN_o\, \nabla_{\tilde{R}}\rho \tag{3.5}$$

which is formally equivalent to the current due to field-free diffusion in $\tilde{R}$-space but with n(R,t) replaced by $N_o\, \rho(R,t)$.

In terms of this solution ρ of (3.2) and of the rates α_{RN} and α_{TR} in (2.33) and (2.34) for reaction and transport under interaction V(R), the association rate $\alpha(t)$ of (1.4) and the "radiation" boundary condition RBC of (1.2) yields

$$\alpha(t) = \alpha_{RN}\, \rho(\tilde{S},t) = \alpha_{TR}\, \tilde{S}[\partial\rho/\partial\tilde{R}]_{\tilde{S}} \tag{3.6}$$

which shows that $\rho(\tilde{S},t) \to 0$ when $\alpha_{TR} << \alpha_{RN}$, as in the limit of high gas densities N, and that $(\partial\rho/\partial\tilde{R}) \to 0$ (which implies the Boltzmann distribution, $\rho = 1$) when $\alpha_{TR} >> \alpha_{RN}$, as in the limit of vanishing N. At each of these respective limits, α_∞, the steady-state rate (2.32) tends to the rate limiting step of transport or of reaction, respectively.

Introduce the dimensionless variables,

$$\tilde{r} = \tilde{R}/\tilde{S} - 1, \quad \tau = Dt/S^2, \quad \phi = (\tilde{R}/\tilde{S})\rho = (\tilde{r}+1)\rho \tag{3.7}$$

so that (3.2) reduces to

$$\partial\phi(\tilde{r},\tau)/\partial\tau = (d\tilde{r}/dr)^2\, (\partial^2\phi/\partial\tilde{r}^2) \tag{3.8}$$

subject to the initial and asymptotic boundary conditions (2.36), rewritten as

$$\phi(\tilde{r},\tau = 0) = (\tilde{r}+1) = \phi(\tilde{r}\to\infty,\tau) \tag{3.9a}$$

and to RBC in (3.6), rewritten as

$$\alpha(\tau) = \alpha_{RN}\, \phi(0,\tau) = \alpha_\infty[\partial\phi(\tilde{r}\to 0,\tau)/\partial\tilde{r}] \tag{3.9b}$$

since the sink is located at $\tilde{r} = 0$.

Under Laplace transformation,

$$\tilde{\phi}(\tilde{r},s) = \int_0^\infty \phi(\tilde{r},\tau)\, \exp(-s\tau)d\tau \tag{3.10}$$

then, with the initial condition (3.9a) incorporated, (3.8) yields

$$(\partial^2\tilde{\phi}/\partial\tilde{r}^2) = (dr/d\tilde{r})^2\, s[\tilde{\phi} - (\tilde{r}+1)/s], \tag{3.11}$$

with formal solution,

$$\tilde{\phi}(\tilde{r},s) = A(s)\, \exp[-\gamma(\tilde{r},s)s^{1/2}] + (\tilde{r}+1)/s, \tag{3.12}$$

in terms of unknown functions $A(s)$ and $\gamma(r,s)$. The asymptotic boundary condition (3.9a) specifies that $\gamma(\tilde{r}\to\infty,s) \to \infty$. On setting

$$k = (dr/d\tilde{r}) \equiv (\tilde{S}/S)(dR/d\tilde{R}) \quad , \tag{3.13}$$

then (3.12) in (3.11) yields the differential equation

$$s^{-1/2}(dy/d\tilde{r}) = y^2(\tilde{r},s) - k^2(\tilde{r}) \tag{3.14a}$$

to be solved for y and hence γ in

$$y(\tilde{r},s) = d\gamma(\tilde{r},s)/d\tilde{r} \tag{3.14b}$$

With knowledge of y and γ, and with RBC in (3.9b) used to

determine A(s) in (3.12), the Laplace transform $\tilde{\rho}$ of the departure function ρ, (3.3), is therefore

$$\tilde{\rho}(\tilde{r},s) = \tilde{\phi}(\tilde{r},s)/(\tilde{r}+1) = \left\{\frac{1}{s} - \left(\frac{\alpha_{RN}}{\alpha_{TR}}\right) \frac{\exp-[\gamma(\tilde{r},s)-\gamma(o,s)]s^{1/2}}{(\tilde{r}+1)s[y(o,s)s^{1/2}+\alpha_{RN}/\alpha_{\infty}]}\right\} \tag{3.15}$$

The corresponding Laplace transform $\tilde{\alpha}$ of the transient association rate $\alpha(t)$, (3.6), is therefore

$$\tilde{\alpha}(s) = \alpha_{RN}\,\tilde{\rho}(0,s) = \alpha_{RN}\left\{1/s - (\alpha_{RN}/\alpha_{TR})[s\{y(o,s)s^{1/2} + \alpha_{RN}/\alpha_{\infty}\}]^{-1}\right\}, \tag{3.16}$$

Progress in the search for simple analytical formulae is now limited by the availability or determination of closed expressions for the inverse Laplace transforms of the overall s-functional dependence in (3.15) and (3.16), which are mainly governed by the form of $\gamma(\tilde{r},s)$ and its derivative $y = (d\gamma/d\tilde{r})$.

For attractive interactions of the general form $(V/kT) = -(R_e/R)^n$, where R_e is the natural unit of length characterized by $V(R_e) = kT$, integration of (3.1) then yields,

$$\tilde{x} = (\tilde{R}/R_e) = n\,\gamma[(1/n),\, x^n] \quad ; \; x = R/R_e \tag{3.17}$$

where the incomplete Gamma function is

$$\gamma(1/n,x^{-n}) = \frac{n}{x}\left[1 + \sum_{m=0}^{\infty} \frac{(-1)^m}{m!}\,\frac{x^{mn}}{(mn+1)}\right] \tag{3.18}$$

In the limit of small x, $R << R_e$, and $\gamma \to \Gamma(1/n)$, the complete Gamma function, so that

$$\tilde{x} \to n\,\Gamma^{-1}(1/n) = x_o, \qquad x = R/R_e << 1 \tag{3.19}$$

a constant; 1 (n = 1), 1.1284 (n = 2), 1.1200 (n = 3), 1.1032 (n = 4) and 1.0779 (n = 6) for the Coulombic (n = 1), Dipole (n = 2), Quadrupole (n = 3), Polarization (n = 4) and Van der Waals (n = 6) attractions, respectively.

For large $R >> R_e$ then

$$\tilde{x} = x\left[1 + \frac{1}{(n+1)}\,x^{-n} + \left\{\frac{1}{(n+1)^2} - \frac{1}{2(2n+1)}\right\} x^{-2n} + \left\{\frac{1}{(n+1)^3} - \frac{1}{(n+1)(2n+1)} + \frac{1}{6(3n+1)}\right\} x^{-3n} + \ldots\right] \tag{3.20}$$

to give

$$\tilde{x} = x + 1/2 + (1/12x) + 0\,(x^{-3}) \qquad , (n = 1)$$

$$= x + (1/3x) + (1/90x^3) - (11/1890x^5) + .. \qquad , (n = 2)$$

$$= x + (1/5x^3) - (7/450x^7) + \ldots \qquad , (n = 4)$$

$$= x + (1/7x^5) - (23/1274x^{11}) + \ldots \qquad , (n = 6)$$

for the various attractions, respectively. The derivative which appears in the basic expression (3.2) is

$$(d\tilde{R}/dR) = (\tilde{x}/x)^2 \exp(-x^{-n}) \xrightarrow{x<<1} (x_o/x)^2 \exp(-x^{-n}) \tag{3.21}$$

so that

$$(d\tilde{R}/dR) = \left\{1 - \left|\frac{n-1}{n+1}\right| x^{-n} + \left[\frac{1}{2} - \frac{1}{(2n+1)} - \frac{(2n-1)}{(n+1)^2}\right] x^{-2n} + \ldots\right\} \qquad (3.22)$$

As illustrated in Fig. 1a for the various attractions, $(dR/d\tilde{R})$ increases rapidly from zero at $\tilde{x} = x_o$ to its unit asymptote at large $x \gtrsim 1$. Note that the coefficient of x^{-1} in $(d\tilde{R}/dR)$ and of x^{-2} in $\tilde{x} = (\tilde{R}/R_e)$ vanishes for Coulombic attraction, so that $(d\tilde{R}/dR)$ tends to its unit asymptote as $[-(1/12)x^{-2} + O(x^{-4})$ which is somewhat faster than that $[-(1/3)\ x^{-2} + O(x^{-4})]$ for the pure dipole case.

Particular values of the nonlinear function

$$(\tilde{R}/R_e) = \tilde{x} = [1 - \exp(-1/x)]^{-1} \qquad (3.23)$$

for Coulomb attraction and of its derivative

$$(d\tilde{R}/dR) = (d\tilde{x}/dx) = \tilde{x}^2(1 - \tilde{x}^{-1})\ \ell n^2(1 - \tilde{x}^{-1}) \qquad (3.24)$$

are displayed in Table 1 which shows that the derivative attains its unit asymptotic value

$$(d\tilde{x}/dx) \to 1 - \frac{1}{12}[\tilde{x}^{-2} + \tilde{x}^{-3} + (13/15)\ \tilde{x}^{-4} + \ldots]$$

very rapidly. This variation is also amplified in Fig. (1b) over the important range $0 \leq \tilde{R} \leq 1.5$ of $\tilde{R}$.

(a) On this basis, the solution at large $\tilde{R}$ ($\gtrsim$ 1.5 n.u.) is therefore obtained by replacing $(d\tilde{R}/dR)$ in (3.13) by unity so that the solutions of y and γ of (3.14) are,

$$\left.\begin{aligned} y(\tilde{r},s) &= \tilde{S}/S \quad , \\ \gamma(\tilde{r},s) &= \tilde{S}\,\tilde{r}/S = (\tilde{R}-\tilde{S})/S \end{aligned}\right\} \tag{3.25}$$

which are all independent of s.

(b) At long times (when $s \to o$), y in (3.14a) is therefore constant for all $\tilde{r}$, so that

$$\left.\begin{aligned} y(\tilde{r},s \to o) &= \tilde{S}/S \equiv y_{\ell} \quad , \\ \gamma(\tilde{r},s \to o) &= \tilde{S}\tilde{r}/S \equiv \gamma_{\ell} \end{aligned}\right\} \tag{3.26a}$$

which are all identical with (3.25). The criterion for validity of (3.26) is that

$$s^{1/2}[(\tilde{S}/S)^2 - (dr/d\tilde{r})^2] \to 0 \tag{3.26b}$$

which holds, not only for long times and all R as in (b), but also for large R and all times as in (a), so that the solutions <u>at long times for all R</u> and <u>at all times for large R</u> are identical. The closer that $(dr/d\tilde{r})$ is to $(\tilde{S}/S)$. the greater will be the range of t over which (3.26) is valid. The variation of $(d\tilde{r}/dr)$ with r for various values of S is illustrated in Fig. 1(c) which shows quite clearly that the key function $(d\tilde{r}/dr)$ in (3.8) may be considered constant $(S/\tilde{S})$ over a large range of $\tilde{r}$ and S.

(c) At short times when $s \to \infty$, the solutions of (3.14) are,

$$\left.\begin{aligned} y(\tilde{r},s >> s_{min}) &= k(\tilde{r}) \equiv y_{\delta}(\tilde{r}) \quad , \\ \gamma(\tilde{r},s) &= r \equiv \gamma_{\delta}(\tilde{r}) \end{aligned}\right\} \tag{3.27}$$

In this approximation, (3.14a) yields

$$(y/k) = 1 - s^{-1/2}\left\{\left|\frac{d^2r}{d\tilde{r}^2}\right|\Big/\left|\frac{dr}{d\tilde{r}}\right|^2\right\} \qquad (3.28a)$$

so that the above approximation (3.27) is valid provided

$$s^{1/2} >> (d^2r/d\tilde{r})^2/(dr/d\tilde{r})^2 = s_{min}^{1/2} \qquad (3.28b)$$

a condition which is more rigorous and less restrictive than the requirement of infinite s.

For $\tilde{r} \gtrsim 0.25$ in Fig. (1c), $k = (dr/d\tilde{r})$ tends to the constant $(\tilde{S}/S)$ so that the key validity criterion $s >> s_{min}$ can be satisfied for longer times. Also (3.27) for y_δ at "short" times and all $\tilde{r}$ tends at large $\tilde{r}$ to (3.25) for y at all times and large $\tilde{r}$, so that the range of validity of the above short-time solution (3.27) can extend into longer times by increase of $\tilde{r}$.

All of the above three solutions, (3.25) - (3.27), are s-independent so that the inverse Laplace transform of (3.18) can be readily performed to yield the same formal expression

$$\rho(R,t) = n(R,t)/N_0 \exp(-KV/De) = \phi(\tilde{r},t)/(\tilde{r}+1)$$

$$= \{1 + (\alpha_\infty/\alpha_{TR})(\tilde{S}/\tilde{R})\,[\exp(2\Omega\chi)\,\exp\chi^2\,\mathrm{erfc}\,(\chi+\Omega) - \mathrm{erfc}\,\Omega\,]\} \qquad (3.29)$$

for each of the above cases (a) - (c) which are distinguished by the pair (χ,Ω) of functions,

$$\left.\begin{aligned} \chi_\ell(t) &= (\alpha_{RN}/\alpha_\infty y_\ell)\sqrt{\tau} \equiv (\alpha_{RN}/\alpha_\infty)(S/\tilde{S})\sqrt{\tau} \\ \Omega_\ell(R,t) &= \gamma_\ell(\tilde{r})/2\sqrt{\tau} \equiv (\tilde{R}-\tilde{S})/(2S\sqrt{\tau}) \equiv \tilde{r}(\tilde{S}/S)/2\sqrt{\tau} \end{aligned}\right\} \quad (3.30)$$

for cases (a) and (b) i.e., for long times and all R, or for all times and asymptotic $R \gtrsim 1$ n.u., (since (3.25) and (3.26) are identical); and by

$$\left.\begin{aligned} \chi_\delta(t) &= [\alpha_{RN}/\alpha_\infty\, y_\delta(0)]\sqrt{\tau} = (\alpha_{RN}/\alpha_\infty)(d\tilde{R}/dR)_S(S/\tilde{S})\sqrt{\tau} = (\alpha_{RN}/\alpha_\infty)(d\tilde{r}/dr)_o\sqrt{\tau} \\ \Omega_\delta(R,t) &= (R-S)/2S\sqrt{\tau} = r/2\sqrt{\tau} \end{aligned}\right\} \quad (3.31)$$

for case (c) for short times and all R. For large S note that $\chi_\delta \to \chi_\ell$ and that $\Omega_\delta \to \Omega_\ell$ for large R and S.

The corresponding transient recombination rates obtained from (3.16) or from (3.6) directly, are written in terms of the steady-state rates (2.26) - (2.28) and of the appropriate (χ,Ω) above as

$$\alpha(t) = \alpha_{RN}\,\rho(S,t) = \alpha_{RN}[1 + (\alpha_\infty/\alpha_{TR})\,\{\exp \chi^2 \operatorname{erfc} \chi - 1\}] \quad (3.32a)$$

$$= \alpha_\infty[1 + (\alpha_{RN}/\alpha_{TR})\exp \chi^2 \operatorname{erfc} \chi] \quad (3.32b)$$

Note that (3.29) and (3.32) are all formally identical (in the tilda representation) to the "field-free" expressions (2.31) and (2.35). By comparison, the overall effect of the general field V(R) is therefore to change the transport rate from α_d,(2.40),to α_{TR},(2.34), the reaction rate from α_3 to α_{RN},(2.33),and the pair of functions (χ_o,Ω_o) of (2.38) to either of the pairs (3.30) or (3.31) for long or short times, respectively.

Short-time and long-time expansions of (3.29) are facilitated with the aid of the corresponding expansions,

$$\exp \chi^2 \operatorname{erfc} \chi \to 1 - (2/\pi^{1/2})\chi + \chi^2 - (4/3\pi^{1/2})\chi^3 + \ldots; \quad \chi \to 0 \tag{3.33}$$

for small χ (at short times) and

$$\exp \chi^2 \operatorname{erfc} \chi \to (1/\chi\pi^{1/2})(1 - \tfrac{1}{2}\chi^{-2} + \tfrac{3}{4}\chi^{-4} - \ldots); \quad \chi \to \infty \tag{3.34}$$

for large χ (at long times).

Since the higher-order expansion terms above are alternatively positive and negative, the short time limits $\alpha_S^{(n)}$, where n denotes the order of χ included in (3.33), tend to (3.32a) from above or below according as n is even or odd, respectively. At short-times, therefore the rate $\alpha(t)$ initially decreases from α_{RN} as $t^{1/2}$ via

$$\begin{aligned}\alpha_S^{(1)}(t \to 0) &= \alpha_{RN}\{1 - (\alpha_\infty/\alpha_{TR})(2/\pi^{1/2})\chi_\delta\} \\ &= \alpha_{RN}\{1 - (\alpha_{RN}/\alpha_{TR})(d\tilde{R}/dR)_S\,(4Dt/\pi\tilde{S}^2)^{1/2}\}\end{aligned} \tag{3.35}$$

which tends to α_S from below. At longer times it decreases as $t^{-1/2}$ via

$$\begin{aligned}\alpha_L^{(1)}(t \to \infty) &= \alpha_\infty[1 + (\alpha_{RN}/\alpha_{TR})/\chi_\ell\pi^{1/2}] \\ &= \alpha_\infty[1 + (\alpha_\infty/\alpha_{TR})(\tilde{S}^2/\pi Dt)^{1/2}]\end{aligned} \tag{3.36}$$

which tends to α_L from above and then to the asymptotic steady-state limit α_∞.

This asymptotic transient (3.36) is identical to that previously derived[11] by the method[10] of "matched perturbation solutions". Thus (3.30) in (3.32b) provide the appropriate extension of (3.36) down to shorter times; and

(3.31) in (3.32a) extends the new short-time transient (3.35) up to longer times. Both the $t^{-1/2}$ long-time transient and the $t^{1/2}$ short-time transient become suppressed in the "reaction limited region" where $\alpha_{RN} << \alpha_{TR}$, and are fully amplified in the "transport limited region" where $\alpha_\infty = \alpha_{TR} << \alpha_{RN}$. The resulting formulae for α_S, $\alpha_S^{(1)}$, α_L and $\alpha_L^{(1)}$ appear to be the only simple analytical expressions apart from (3.36) for $\alpha_L^{(1)}$, yet derived for general interactions V(R).

Procedures for numerical solution (see § 5) of the basic eq. (3.2) for all times require initialization of ρ and $\partial\rho/\partial\tilde{r}$ either at short times when integrating forward in t, or at long times when integrating backwards in t. Direct differentiation of the basic solution,

$$\rho(\tilde{r},\tau) = 1 + (\alpha_\infty/\alpha_{TR})\,[\exp \chi^2 \exp(2\chi\Omega)\ \mathrm{erfc}(\chi+\Omega) - \mathrm{erfc}\ \Omega]/(\tilde{r}+1) \qquad (3.37)$$

where the sets $(\chi_\delta,\Omega_\delta)$ and (χ_ℓ,Ω_ℓ) distinguish short and long times, respectively, yields

$$(\partial\rho/\partial\tilde{r}) = (\alpha_{RN}/\alpha_{TR})\ C(\tilde{r})\mathrm{erfc}\,\Omega/(\tilde{r}+1) + (\alpha_{RN}/\alpha_\infty)[C(\tilde{r})-(\alpha_\infty/\alpha_{RN})/(\tilde{r}+1)](\rho-1) \qquad (3.38)$$

where

$$C_\delta(\tilde{r}) = (d\tilde{r}/dr)_0/(d\tilde{r}/dr)$$
$$C_\ell(\tilde{r}) = 1 \qquad (3.39)$$

for short (δ) and long (ℓ) times, respectively. The radiation boundary condition,

$$\alpha_{TR}(\partial\rho/\partial\tilde{r})_0 = \alpha_{RN}\,\rho(0,\tau) = \alpha_{RN}\ \{1 + (\alpha_\infty/\alpha_{TR})\ [\exp \chi^2\ \mathrm{erfc}\ \chi - 1\ ]\} \qquad (3.40)$$

is of course satisfied by (3.38) at the sink ($\tilde{r} = 0$) at all times. As $\tau \to 0$, $\rho \to 1 - O(\tau^{1/2})$, and $(\partial\rho/\partial\tilde{r})$ varies continuously with $\tilde{r}$ as,

$$(\partial\rho/\partial\tilde{r}) = \frac{(\alpha_{RN}/\alpha_{TR})}{(\tilde{r}+1)}\, C_\delta(\tilde{r})\ \mathrm{erfc}\ \Omega_s \to \begin{cases} (\alpha_{RN}/\alpha_{TR}) & ;\ \tilde{r} \to 0 \\ \dfrac{(\alpha_{RN}/\alpha_{TR})}{(\tilde{r}+1)}\,\dfrac{2C_\delta(\tilde{r})}{r}\left(\dfrac{\tau}{\pi}\right)^{1/2} \exp(-r^2/4\tau) & ;\ r \gg 2\sqrt{\tau} \end{cases} \qquad (3.41)$$

which indicates the dramatic decrease, with increase of r, of $(\partial\rho/\partial\tilde{r})$ at short times from a constant value $(\alpha_{RN}/\alpha_{TR})$ at the sink. Accurate numerical integration around initial times $\tau \sim 10^{-3}$ therefore demands intervals Δr in r as small as 10^{-3} so as to ensure dense coverage of the complementary error function

$$\mathrm{erfc}\ \Omega = \frac{2}{\sqrt{\pi}} \int_\Omega^\infty \exp(-\Omega^2)\, d\,\Omega \qquad (3.42)$$

between unity (at $r = 0$) and zero (at $r \gg 2\sqrt{\tau}$).

4. Extension for Intermediate Times and all R

In an effort to seek extensions of (3.29), with (3.30) for long times, down to intermediate times for all R, insert the expansion

$$y(\tilde{r},s) = y_\ell[1 + F_1(\tilde{r})s^{1/2} + F_2(\tilde{r})s + \ldots] \tag{4.1}$$

in powers of $s^{1/2}$ in (3.14a), and equate equal powers of s. Since the exact solution at large $\tilde{r}$ is y_ℓ, (3.26), then $F_i\ (\tilde{r} \to \infty) \to 0$. The expansion coefficients are therefore determined by

$$F_1(\tilde{r}) = S^{-1} \int_{\tilde{R}}^{\infty} \left[\left(\frac{dR}{d\tilde{R}} \right)^2 - 1 \right] d\tilde{R} \quad ,$$

which for Coulomb attraction tends at large $\tilde{R}$ to

$$F_1(\tilde{r}) = (R_e/S) \left[\frac{1}{6}(R_e/R) + \frac{1}{12}(R_e/R)^2 + \ldots \right] \tag{4.2}$$

and by

$$F_2(r) = -2S^{-1} \int_{\tilde{R}}^{\infty} F_1(\tilde{r}) d\tilde{R}. \tag{4.3}$$

On retaining only the F_1-term in (4.1), the rate, obtained directly from the inverse Laplace Transform of (3.16), is

$$\alpha_{LS}(t) = \alpha_\infty[1 + (\alpha_{RN}/\alpha_{TR}) \{a_+ \exp \chi_-^2 \ \text{erfc}\ \chi_- - a_- \exp \chi_+^2 \ \text{erfc}\ \chi_+\} / (a_+ - a_-)] \tag{4.4}$$

for long → short times and is restricted to cases for which

$$\chi_{\pm}/\sqrt{\tau} = a_{\pm} = \{1 \pm [1 - 4(\alpha_{RN}/\alpha_{\infty})\tilde{S} F_1(0)/S]^{1/2}\} /2F_1(0) \qquad (4.5)$$

remain real i.e., when $F_1(0) \lesssim \frac{1}{4}(\alpha_{\infty}/\alpha_{RN})(S/\tilde{S})$. The range of application of (4.4) is therefore rather limited.

The corresponding extension from shorter ($s \to \infty$) to longer times may be accomplished by expanding y in terms of $s^{-1/2}$ so that, on equating equal powers of $s^{-1/2}$,

$$y(\tilde{r},\tilde{s}) = k(\tilde{r}) + [k'(\tilde{r})/2k(\tilde{r})]s^{-1/2} \; ; \; k = (dr/d\tilde{r}) \; , \qquad (4.6)$$

where k' is $(dk/d\tilde{r})$. The condition for validity of the short-time solution $y = k(\tilde{r})$ is therefore $s^{1/2} >> (d^2r/d\tilde{r}^2)/(dr/d\tilde{r})^2$, as before. The required rate, for short→ long times and for all assigned parameters is

$$\alpha_{SL}(t) = \alpha_{RN}[1 + (\alpha_{\infty}/\alpha_{TR})\{1 + (k'_o/2k_o)(\alpha_{\infty}/\alpha_{RN})\}^{-1}\{\exp \chi_{SL}^2 \operatorname{erfc} \chi_{SL} - 1\}] \qquad (4.7a)$$

$$= \alpha_{\infty}\{1 + (k'_o/2k_o)(\alpha_{\infty}/\alpha_{RN})\}^{-1}[1 + (k'_o/2k_o) + (\alpha_{RN}/\alpha_{TR}) \exp\chi_{SL}^2 \operatorname{erfc}\chi_{SL}] \qquad (4.7b)$$

where k'_o is $k'(\tilde{r}=0)$ and where

$$\chi_{SL} = [(\alpha_{RN}/\alpha_{\infty}) + (k'_o/2k_o)]\sqrt{\tau}/k_o \qquad (4.8)$$

Although (4.7a) has been designed as an extension of the short time result α_S to longer times, it does not, however, tend to the correct

asymptotic ($t \to \infty$) limit, α_∞, as does α_S, (3.31) in (3.32b). Because it is automatically constrained to vary monotonically between α_{RN} (as $t \to 0$) and (as $t \to \infty$), α_S may indeed yield a better approximation than α_{SL} except perhaps in some intermediate-time range. Although α_S tends to the correct asymptotic limit α_∞, its asymptotic transience (i.e., the rate at which α_S approaches α_∞) will <u>not</u> be correct since it is characterized by χ_δ rather than by the correct χ_ℓ to give

$$\alpha_S(t \to \infty) = \alpha_\infty[1 + (\alpha_\infty/\alpha_{TR})(dR/d\tilde{R})_S\ (\tilde{S}^2/\pi Dt)^{1/2}] \tag{4.9}$$

which agrees with the exact transient (3.36) only for large sink radii S when $(dR/d\tilde{R})_S \to 1$ (cf. Fig. 1b).

Analogous considerations also apply to the comparison of α_{LS} of (4.4) with α_L of (3.29) and (3.27). The rate α_L decreases monotonically from α_{RN} to α_∞ as τ increases, in contrast to α_{LS} which does not tend to α_{RN} as $\tau \to 0$. The long-time solution α_L yields, however, the incorrect short-time transience

$$\alpha_L(t \to 0) = \alpha_{RN}[1 - (\alpha_{RN}/\alpha_{TR})(4Dt/\pi\tilde{S}^2)^{1/2}] \tag{4.10}$$

which agrees with the exact short-time transience (3.35) only for large S when $(d\tilde{R}/dR)_S \to 1$.

5. Numerical Solutions

The basic equation (3.2) in tilda-space for the fractional departure (3.3) from Boltzmann equilibrium, is

$$\frac{\partial \rho}{\partial \tau} = \left(\frac{d\tilde{r}}{dr}\right)^2 \left[\frac{\partial^2 \rho}{\partial \tilde{r}^2} + \frac{2}{(\tilde{r}+1)} \frac{\partial \rho}{\partial \tilde{r}}\right] \tag{5.1}$$

in dimensionless units (3.7). In numerical algorithms, the assigned initial condition

$$\rho(\tilde{r},0) = 1 \tag{5.2}$$

must be supplemented by an additional initial condition for $(\partial\rho/\partial\tilde{r})$. Eqs. (3.37) and (3.38) with (3.31) for $(\chi_\delta,\Omega_\delta)$ are used to facilitate forward integration in τ from 10^{-3} when small intervals Δr in r are required. The boundary conditions at the sink ($\tilde{r} = 0$) and at asymptotic $\tilde{r}$ are

$$\left.\begin{aligned} (\partial\rho(\tilde{r},\tau)/\partial\tilde{r})_0 &= (\alpha_{RN}/\alpha_{TR})\ \rho(0,\tau), \\ \rho(r\to\infty,\tau) &= 1 \end{aligned}\right\} \tag{5.3}$$

at all times τ. Eq. (5.1) is a linear partial differential equation with nonlinear coefficients and is of the general form

$$\partial f(x,t)/\partial t = F(x,t,f(x,t),\ \partial f/\partial x,\ \partial^2 f/\partial x^2) \tag{5.4}$$

which can be solved by standard numerical procedures[17] subject to the initial conditions,

$$f(x,t=0) = f_o(x) \quad ; \quad \partial f(x,0)/\partial x = \partial f_o/\partial x \tag{5.5}$$

and the boundary ($x \to 0,\infty$) conditions

$$\alpha f(x,t) + \beta\, \partial f(x,t)/\partial x = \gamma(t) \; ; \; (x \to 0,\infty) \tag{5.6}$$

where α and β are constants independent of (x,t). In the numerical method adopted,[17] the boundary conditions are imposed indirectly via the differential equation

$$\alpha\, \partial f(x,t)/\partial t + \beta\, \partial^2 f(x,t)/\partial t \partial x = \partial\gamma/\partial t \tag{5.7}$$

such that $\gamma(t)$ in (5.6) must be either constant or a continuous function of t. The selected algorithm[18] DPDES designed primarily for parabolic problems (as is the case here) solves a system of equations of type (5.4) by a method of lines, wherein the solution is expanded in a series of cubic Hermite basis functions of x. The t-dependent undetermined coefficients are evaluated from a collocation procedure[17] at each t i.e., from the differential equations obtained by imposing the boundary conditions (5.7) at the endpoints (x_o, x_N) and by requiring that the differential equation (5.4) is satisfied at two Gaussian quadrature points between adjacent points x_p, x_{p+1} in the x-discretization: $x_0 \leq x_p \leq x_N$; $x_p = x_0 + ph$ ($p = 0, 1, 2, \ldots, N$).

Eq. (5.1) was therefore solved numerically in equal intervals $\Delta r = 10^{-3}$, 10^{-2} and $5\ 10^{-2}$ over the respective ranges ($0 - 10^{-2}$), ($10^{-2} - 5\ 10^{-2}$) and ($5\ 10^{-2} - 30$) in r; at equal intervals $\Delta\tau = 10^{-3}$, 10^{-2} and $5\ 10^{-2}$ over the respective τ-ranges, ($10^{-3} - 10^{-2}$), ($10^{-2} - 1$) and ($1 - 100$). At short times

$\tau \sim 10^{-3} - 10^{-2}$, small intervals $\Delta r \sim 10^{-3}$ in r are required (see § 3) for accurate initialization via (3.37) and (3.38). All calculations were performed on a CDC 7600 computer with a typical execution time of 14 minutes (with a relative error of 10^{-6} in the t-discretization) for a given sink radius S and ratio $(\alpha_\infty/\alpha_{TR})$.

As a test, the numerical results reproduced the exact analytical solutions (2.37) and rates (2.41) for the field-free (V = 0) case.

Figure 2 illustrates for a representative case ($S = \frac{1}{2}$ n.u., $\alpha_\infty/\alpha_{TR} = 1/2$) of Coulombic attraction, the collapse with scaled time $\tau (\equiv Dt/S^2)$ of the exact fractional departure $\rho(\tilde{r},\tau) = n(R,t)/\exp(-KV/De)$ of the probability density n from its initial Boltzmann distribution, $\rho(\tilde{r},0) = 1$, onto the steady-state $(\partial\rho/\partial\tau \to 0$ as $\tau \to \infty)$ distribution

$$\rho_\infty(\tilde{r},\tau\to\infty) = 1 - (\alpha_\infty/\alpha_{TR})(\tilde{S}/\tilde{R}) \tag{5.8}$$

as a function of $\tilde{r} = (\tilde{R}/\tilde{S}) - 1$. With increase of the parameter $(\alpha_\infty/\alpha_{TR})$ to its limiting value of unity (characteristic of full transport controlled processes), the steady-state ρ_∞ is approached much more rapidly than those for smaller $(\alpha_\infty/\alpha_{TR})$, and deeper holes in the distribution appear in the neighborhood of the sink at $\tilde{r} = 0$ where a highly non-equilibrium distribution has developed. As the sink radius S decreases, the curves in Fig. 2 for given $(\alpha_\infty/\alpha_{TR})$ collapse onto ρ_∞ over all r much more slowly i.e., it takes longer to attain steady-state, as expected.

The above asymptote ρ_∞ in Fig. 2 is rendered universal for all $(\alpha_\infty/\alpha_{TR})$ by simply relabelling the ρ-axis from the vertex at $(1 - \alpha_\infty/\alpha_{TR})$ in general, rather than at 0.5, in equal intervals to unity.

The variation with τ of the intercept $\rho(0,\tau)$ provides directly the τ-

variation of the recombination rate,

$$\alpha(\tau) = \alpha_{RN}\, \rho(0,\tau) = \alpha_{TR}\, [\partial\rho(\tilde{r}\to 0,\tau)/\partial\tilde{r}]_0 \qquad (5.9)$$

Since the accuracy of the various schemes (§ 3,4) of analytical approximation improves at all τ for larger r, detailed comparison between the exact numerical intercept $\rho_E(0,\tau)$ and the derived analytical intercepts

$$\rho(0,\tau) = 1 + (\alpha_\infty/\alpha_{TR})\, [\exp \chi^2\, \mathrm{erfc}\, \chi - 1] = \alpha(\tau)/\alpha_{RN}, \qquad (5.10)$$

or between the corresponding association rates $\alpha(\tau)$, provide the most stringent test of the accuracy of the various approximations for $\rho(\tilde{r},\tilde{\tau})$ and its derivative $(\partial\rho/\partial\tilde{r})$.

5.1 Comparison with Analytical Expressions

As indicated by (3.35) and (3.36), the transience, $\alpha(\tau)$ versus $\tau[\equiv (Dt/S^2)$, in units of (S^2/D) a characteristic time scale for diffusion across a distance S], becomes amplified for larger χ i.e., for transport controlled regions, when $\alpha_{RN} >> \alpha_\infty$ (i.e., when $\alpha_\infty/\alpha_{TR} \to 1$), and/or for large sink radii S which result in larger $(d\tilde{r}/dr)_0$ for χ_δ (cf. Fig. 1c) and in smaller $(\tilde{S}/S)$ for χ_ℓ (cf. Table 1).

Figs. 3(a-h) - 5(a-h) illustrate comparison with the exact numerical solution α_E of the various short-time solutions α_S and α_{SL}, as in (a-d), and of the various long-time solutions α_L and α_{LS}, as in (e-h), over externally assigned values of both the sink radius (S = 1, 0.75, 0.5, 0.25 n.u.) and of the ratio $\alpha_\infty/\alpha_{TR}$ (= 0.1, 0.5, 0.9). Since the transition from steady-state reaction

controlled processes to transport controlled processes is characterized by increase from small $\alpha_\infty/\alpha_{TR}$ (where $\alpha_{RN} << \alpha_{TR}$) to unit $\alpha_\infty/\alpha_{TR}$ (where $\alpha_{RN} >> \alpha_{TR}$) as in (2.32), the selected range (0.1 - 0.9) of $\alpha_\infty/\alpha_{TR}$ therefore corresponds to increase in gas density. Since $\alpha(t)$ tends to α_{RN} as $t \to 0$ and to α_∞ as $t \to \infty$, all of the short-time curves (a) - (d) for $\alpha(\tau)/\alpha_{RN}$, and all of the long-time curves (e) - (h) for $\alpha(\tau)/\alpha_\infty$ are normalized so as to tend to unity at their respective short-time and long-time limits. As $t \to \infty$, $\alpha(\tau)/\alpha_{RN}$ in (a) - (d) tends to $[1 - (\alpha_\infty/\alpha_{TR})]$, which gives 0.9, 0.5 and 0.1 for each respective value of $(\alpha_\infty/\alpha_{TR})$; and $\alpha(\tau)/\alpha_\infty$ in (e)-(h) tends as $t \to 0$ to $[1 - (\alpha_\infty/\alpha_{TR})]^{-1}$ i.e., to 1.11, 2, and 10 for each respective case.

Figs. 3(a) - 3(d) for the small ratio $(\alpha_\infty/\alpha_{TR}) = 0.1$ i.e., for $(\alpha_\infty/\alpha_{RN}) = 0.9$ which imply a reduction in $\alpha(\tau)$ of 10% from α_{RN} over the full time range, show that α_S, (3.22a) with (3.31), and α_{SL}, (4.7a) with (4.5), both reproduce the exact numerical results α_E at short times over the given range (1 - 0.25 n.u.) of S. As S increases both α_S and α_{SL} agree with α_E over longer periods of time, as expected from validity criteria (3.28b). They also represent substantial improvements over the short-time transients, $\alpha_S^{(1)}$ and $\alpha_S^{(3)}$ which are the expansions of α_S, (3.32) up to and including terms in $t^{1/2}$ and $t^{3/2}$, respectively. As $t \to 0$ both $\alpha_S^{(1)}$ and $\alpha_S^{(3)}$ eventually converge (from below) to α_S, as expected, and then to α_E. For the larger S, the suggested more rapid variation in all of the rates from α_{RN} is apparent.

As expected, α_{SL} shows some improvement over α_S for longer times up to $\tau \gtrsim 1$, particularly at larger $(\alpha_\infty/\alpha_{TR})$ and smaller S, as is apparent in Figs. 3-5. For longer times $\tau >> 1$, α_{SL} eventually diverges since it is not automatically constrained, as is α_S, to tend to the limiting asymptote α_∞. This is the essential reason that the short-time expression for α_S exhibits in general a better overall agreement with the exact α_E over the full range of τ. Even for the most extreme case, S = 0.25 n.u. in Figs. (3-5)d, for which

$(d\tilde{R}/dR)$ is small (cf. Fig. 1b) so that the basic analytical approximation for all times tends to lose validity, α_S departs from α_E at intermediate $\tau \sim 1$ but then eventually approaches α_∞ albeit with an <u>incorrect</u> transience, as $t \to \infty$, in direct contrast to α_{SL}. Note that an overall effect of increase in $(\alpha_\infty/\alpha_{TR})$ in Figs. 3-5 is to effectively shift the amplification from short times (Fig. 3), to intermediate times (Fig. 4) and longer times (Fig. 5).

The exact long time rates α_L, (3.30) in (3.32b), the long-short approximation α_{LS} of (4.4), and $\alpha_L^{(1)}$ the asymptotic transient (3.36) to α_L, are all compared in Figures 3(e-h) - 5(e-h) with the exact numerical results α_E. Both α_L and α_{LS} yield considerable improvement over $\alpha_L^{(1)}$ which up to now has been the "best" simple analytical long-time expression yet proposed[11] (via the method of matched perturbation solutions[10]). This result $\alpha_L^{(1)}$ eventually tends to the present analytical result α_L which then tends to α_E (see in particular Fig. 4(h) and Fig. 5(g), 5(h)).

Although α_{LS}, (which, in order to ensure real $a_\pm$ in (4.5), is restricted only to cases (e) of Figs. 3 and 4 and to case (f) of Fig. 3), is designed to extend α_L into the shorter-time regime, it only partially succeeds, but it does not, in general, represent an overall improvement to α_L. The rate α_L is, of course, automatically constrained to vary from the exact asymptotic $(t \to \infty)$ limit with the correct long-time transience to the exact $(t \to 0)$ limit α_{RN}, with, however, the incorrect short-time transience. In contrast α_{LS} does increase with the correct long-time transience from α_∞, but reaches a maximum and then tends as $t \to 0$ to the incorrect limit α_∞.

Corresponding sets of curves are displayed in Fig. 4 for the ratio $\alpha_\infty/\alpha_{TR} = 0.5$ which is appropriate to atmospheric gas pressures and which represents equal rates of transport and reaction. A 50% decrease in $\alpha(t)$ from α_{RN} to will therefore occur as t develops. Both α_S and α_{SL} again represent a

considerable improvement over their short-time limits $\alpha_S^{(1)}$ and $\alpha_S^{(3)}$; and α_L is significantly more accurate than the previous standard result $\alpha_L^{(1)}$. Note, for this larger ratio of $\alpha_\infty/\alpha_{TR}$, that the extensive range $[10^{-2} - 10^2]$ in time does not include the short-time limits when $\alpha/\alpha_{RN} \to 1$, as in Fig. 3, but emphasizes rather the intermediate-time and long-time regimes. Fig. 3 illustrates very clearly, even for the worst case (h) with S = 0.25 n.u., the dividend that accrues from the built-in variation of α_L between α_{RN} at short times and α_∞ at long times. At intermediate times, $\alpha_S > \alpha_E$, $\alpha_L < \alpha_E$ and $\alpha_L^{(1)} > \alpha_E$. Since $\alpha_L^{(1)}$ tends to α_L more rapidly than α_L tends to α_E, $\alpha_L^{(1)}$ must therefore cross α_E so that somewhat closer but accidental agreement is exhibited,as in Figs. (4h) and (5h).

The general picture which is therefore emerging is that both α_S and α_L are highly accurate analytical solutions which are, in general, better than their corresponding extensions α_{SL} and α_{LS}, respectively, into the intermediate-time regime, mainly because the basic expression (3.32) automatically varies between the correct limits α_{RN} and α_∞; α_S is the exact short-time transience and α_L is the exact long-time transience. No short-time approximation as α_S, $\alpha_S^{(1)}$, $\alpha_S^{(3)}$, α_{SL} has been previously proposed and the present long-time result α_L is quite superior to $\alpha_L^{(1)}$ which has been the only analytical expression previously reported.[11]

This underlying order has become further clarified in Figure 5 which is appropriate to transport-controlled processes at high gas pressures ($\sim$ tens of atmospheres). This case with $(\alpha_\infty/\alpha_{TR}) = 0.9$, involves a 90% reduction in $\alpha(\tau)$ from α_{RN} to α_∞ as τ develops. The τ-range $[10^{-2} - 10^2]$ emphasizes intermediate $\to$ long times. Figs. 5c,d exhibit quite clearly, for the first time, the marked departure of α_S from α_E at intermediate times τ = 1 - 10 followed by the eventual return of α_S to α_E in the limit of long-times. Also

the convergence of $\alpha_L^{(1)}$ to α_L is quite apparent in Fig. 5h. Even for this most extreme case S = 0.25 n.u. where the validity criteria (3.26b) and (3.28b) is being stretched for all times, the present expressions for α_S and α_L are quite superior to $\alpha_S^{(1)}$, $\alpha_S^{(3)}$ and to $\alpha_L^{(1)}$, respectively.

Since the various terms in the expansion (3.33) for α_S of (3.32a), are alternatively negative and positive, $\alpha_S^{(n)}$ tends to α_S from above or below depending on whether the number n of time-dependent terms included in (3.33) is even or odd, respectively. Since α_L is less than α_E and since α_S is greater than α_E at intermediate times, some time-dependent combination of α_S and α_L is suggested (see § 6).

The long-time curves (e) - (h) in Figs. 3-5 show directly that $\alpha_{E,L,S}$ achieve their steady-state value α_∞ more rapidly for transport-controlled recombination, i.e., for $(\alpha_\infty/\alpha_{TR}) \lesssim 1$, than for reaction-controlled recombination, $(\alpha_\infty/\alpha_{TR}) << 1$, which is characterized by a much slower rate of decrease to a higher relative value α_∞.

Even with its incorrect short-time transience, α_L is somewhat better than α_S over all time τ for the reaction dominated recombination, (Fig. 3), and α_S, in spite of its incorrect long-time transience, is somewhat better than α_L over all τ for transport dominated recombination (Fig. 5).

6. Validity Criteria and Improved Transient Result

Although the long-time and short-time expressions obtained by inserting (3.30) and (3.31) respectively in (3.29) for $n(R,t)$ and in (3.32) for $\alpha(t)$, have now been shown to be highly accurate, they have been derived from the Laplace-transform technique such that neither do the actual equations satisfied by the derived analytical formulae or do rigorous validity criteria apart from (3.26b) and (3.28b) naturally materialize. The basic equation

$$\left(\frac{\partial\phi}{\partial\tau}\right)_{\tilde{r}} = \left(\frac{d\tilde{r}}{dr}\right)^2 \left(\frac{\partial^2\phi}{\partial\tilde{r}^2}\right)_{\tau} \tag{6.1}$$

for $\phi(\tilde{r},t) = (\tilde{r}+1)\,\rho(\tilde{r},t)$, as in (3.7) and (3.8), where ρ is the fractional departure $n(R,t)/N_0 \exp(-KV/De)$ of the probability density $n(R,t)$ from Boltzmann equilibrium, may be expressed in alternative forms as

$$\left(\frac{\partial\phi}{\partial\tau}\right)_{\tilde{r}} = \frac{\partial^2\phi}{\partial r^2} + \left\{\left(\frac{d\tilde{r}}{dr}\right)^2\left(\frac{d^2r}{d\tilde{r}^2}\right)\right\}\left(\frac{\partial\phi}{\partial r}\right) \tag{6.2a}$$

$$= \frac{\partial^2\phi}{\partial r^2} - \left(\frac{d^2\tilde{r}}{dr^2}\right)\left(\frac{\partial\phi}{\partial\tilde{r}}\right) \tag{6.2b}$$

used to discuss the short-time solution, or as

$$\left(\frac{\partial\phi}{\partial\tau}\right)_{\tilde{r}} = \left(\frac{S}{\tilde{S}}\right)^2 \left(\frac{\partial^2\phi}{\partial\tilde{r}^2}\right)_{\tau} + \left[\left(\frac{d\tilde{r}}{dr}\right)^2 - \left(\frac{S}{\tilde{S}}\right)^2\right]\left(\frac{d\tilde{r}}{dr}\right)^{-2}\left(\frac{\partial\phi}{\partial\tau}\right)_{\tilde{r}} \tag{6.2c}$$

used to discuss the solutions at large r.

The recombination rate is simply

$$\alpha(\tau) = \alpha_{RN}\,\rho(0,\tau) = \alpha_{TR}\,[\partial\rho(\tilde{r}\to 0,\tau)/\partial\tilde{r}] \tag{6.3a}$$

or, equivalently,

$$\alpha(\tau) = \alpha_{RN}\ \phi(0,\tau) = \alpha_{\infty}\ [\partial\phi(\tilde{r}\to 0,\tau)/\partial\tilde{r}] \tag{6.3b}$$

in which RBC, the radiation boundary condition (3.6) or (3.9b) between the function and its derivative, is explicitly used.

Provided

$$|\partial\phi/\partial\tau| >> (d^2\tilde{r}/dr^2)\left[(\partial\phi/\partial\tilde{r}) - 1\right] \tag{6.4}$$

as for all r and small τ (but not for large r and all τ), (6.2b) reduces to

$$\frac{\partial\phi_{\delta}}{\partial\tau} = \frac{\partial^2\phi_{\delta}}{\partial r^2} - \frac{d^2\tilde{r}}{dr^2} \tag{6.5}$$

which, apart from the term $d^2\tilde{r}/dr^2$, is formally identical to field-free diffusion in (r,τ)-space. Provided,

$$\left[\left(\frac{d\tilde{r}}{dr}\right)^2 - \left(\frac{S}{\tilde{S}}\right)^2\right]\left(\frac{d\tilde{r}}{dr}\right)^{-2} = \left[1 - \left(\frac{dR}{d\tilde{R}}\right)^2\right] << 1 \tag{6.6}$$

as at large r and all τ, then (6.2c) reduces to

$$\frac{\partial\phi_{\ell}}{\partial\tilde{\tau}} = \frac{\partial^2\phi_{\ell}}{\partial\tilde{r}^2} \qquad ; \qquad \tilde{\tau} = (S/\tilde{S})^2\ \tau \tag{6.7}$$

which is formally identical with field-free diffusion in $(\tilde{r},\tilde{\tau})$-space.

The exact solutions of (6.5) and (6.7) appropriate to the above initial and boundary conditions (3.9) in $(\tilde{r},\tilde{\tau})$ space are then

$$\phi(\tilde{r},\tau) = (\tilde{r}+1) + (\alpha_{\infty}/\alpha_{TR})\ [\exp(2\Omega\chi)\ \exp\chi^2\ \mathrm{erfc}(\chi+\Omega) - \mathrm{erfc}\ \Omega]\ , \tag{6.8}$$

where the pair (χ,Ω) of functions are defined as

$$\left.\begin{aligned} \chi_{\delta,\ell}(\tau) &= a_{\delta,\ell}\sqrt{\tau} \quad ; a_{\delta} = (\alpha_{RN}/\alpha_{\infty})(d\tilde{r}/dr)_0; \; a_{\ell} = (\alpha_{RN}/\alpha_{\infty})(S/\tilde{S}) \\ \Omega_{\delta}(r,\tau) &= r/2\sqrt{\tau}; \; \Omega_{\ell}(\tilde{r},\tau) = \tilde{r}/2\sqrt{\tau} \end{aligned}\right\} \qquad (6.9)$$

with subscript δ appropriate to the exact solution ϕ_s at short times and all r, and with subscript ℓ appropriate to the exact solution ϕ_ℓ for all times and large r.

These approximate solutions $\phi_{\delta,\ell}$ of the basic eq. (6.1) are exactly those (3.29) - (3.31) previously derived via the Laplace Transform technique which procedure is however required to show that the solution ϕ_ℓ for large r and all τ is identical with that for all r and long τ. Direct differentiation of (6.8) yields

$$(\partial\phi_{\delta}/\partial\tilde{r}) = 1 + (\alpha_{RN}/\alpha_{\infty})\,\frac{(d\tilde{r}/dr)_0}{(d\tilde{r}/dr)}\,[\phi_{\delta} - (\tilde{r}+1) + (\alpha_{\infty}/\alpha_{TR})\,\mathrm{erfc}\,\Omega_s] \qquad (6.10a)$$

and

$$(\partial\phi_{\ell}/\partial\tilde{r}) = 1 + (\alpha_{RN}/\alpha_{\infty})\,[\phi_{\ell} - (\tilde{r}+1) + (\alpha_{\infty}/\alpha_{TR})\,\mathrm{erfc}\,\Omega_{\ell}] \qquad (6.10b)$$

which assume their largest values $[\alpha_{\delta,\ell}(\tau)/\alpha_{\infty}]$ at the sink (cf. Fig. 2) where RBC, Eq. (6.3b) is of course satisfied. Also, differentiation of (6.8) yields

$$(\partial\phi_{\delta,\ell}(r,\tau)/\partial\tau) = a^2_{\delta,\ell}\left[\phi_{\delta,\ell} - (\tilde{r}+1) + (\alpha_{\infty}/\alpha_{TR})\{\mathrm{erfc}\,\Omega_{\delta,\ell} - \exp(-\Omega^2_{\delta,\ell})/(\sqrt{\pi}\chi_{\delta,\ell})\}\right] \qquad (6.11)$$

which can be used to provide $\partial^2\phi_{\delta}/\partial r^2$ or $\partial^2\phi_{\ell}/\partial\tilde{r}^2$ via (6.5) or (6.7), respectively.

Fig. 1c, which illustrates the variation for Coulomb attraction of $(d\tilde{r}/dr)$ with $\tilde{r}$ for various sink radii shows that the terms of (6.2b) and (6.2c) which are omitted in (6.5) and (6.7), respectively, are largest at the sink. At the sink,

$$\phi_{\delta,\ell}(0,\tau) = 1 + (\alpha_\infty/\alpha_{TR})\,[\exp\chi^2\ \mathrm{erfc}\ \chi - 1] \tag{6.12a}$$

$$= (\alpha_\infty/\alpha_{RN})[\partial\phi_{\delta,\ell}(0,\tau)/\partial\tilde{r}] = \alpha_{S,L}(\tau)/\alpha_{RN}$$

and

$$\partial\phi_{\delta,\ell}(0,\tau)/\partial\tau = (a^2_{\delta,\ell}/\alpha_{RN})\,[\alpha_{S,L}(\tau) - \alpha_{S,L}(\tau\to\infty)] \tag{6.12b}$$

where $\alpha_{S,L}(\tau\to\infty)$ are the long-time asymptotic transients,

$$\alpha_{S,L}(\tau\to\infty) = \alpha_\infty\,[1 + (\alpha_{RN}/\alpha_{TR})/\chi_{\delta,\ell}\sqrt{\pi}] \tag{6.13}$$

of the basic rates,

$$\alpha_{S,L}(\tau) = \alpha_{RN}\{1 + (\alpha_\infty/\alpha_{TR})\,[\exp\chi^2_{\delta,\ell}\ \mathrm{erfc}\ \chi_{\delta,\ell} - 1]\} \tag{6.14a}$$

$$= \alpha_\infty\,[1 + (\alpha_{RN}/\alpha_{TR})\ \exp\chi^2_{\delta,\ell}\ \mathrm{erfc}\ \chi_{\delta,\ell}] \tag{6.14b}$$

At long times,

$$\phi_{\delta,\ell}(\tilde{r},\tau\to\infty) = (\tilde{r}+1) - (\alpha_\infty/\alpha_{TR});\ (\partial\phi_{\delta,\ell}/\partial\tau) \to 0 \tag{6.15}$$

and at short times,

$$\phi(\tilde{r},\tau\to 0) = (\tilde{r}+1); \quad (\partial\phi_{\delta,\ell}/\partial\tau) \to -(\alpha_{RN}/\alpha_{TR})(d\tilde{r}/dr)_0 \exp(-r^2/4\tau)/\sqrt{\pi\tau} \qquad (6.16)$$

With the aid of (6.10a) and (6.11), the key criteria (6.4) for validity of the short-time solution ϕ_δ for all r is,

$$(\alpha_{RN}/\alpha_\infty)\left|\phi_\delta - (\tilde{r}+1) + (\alpha_\infty/\alpha_{TR})[\text{erfc}\ \Omega_\delta - \exp(-\Omega_\delta{}^2)/\chi_\delta\sqrt{\pi}\ ]\right|$$

$$>> \frac{(d^2\tilde{r}/dr^2)}{(d\tilde{r}/dr)_0(d\tilde{r}/dr)}\left|\phi_\delta - (\tilde{r}+1) + (\alpha_\infty/\alpha_{TR})\ \text{erfc}\ \Omega_\delta\right| \qquad (6.17a)$$

which specifically excludes long times ($\tau\to\infty$) since then $\Omega_\delta \to 0$ and both sides vanish, with the aid of (6.15). This condition becomes more transparent at the sink where (6.4) reduces, with the aid of (6.12a,b) to,

$$(\alpha_{RN}/\alpha_\infty)(d\tilde{r}/dr)_0{}^2\ [\alpha_S(\tau) - \alpha_S(\tau\to\infty)] >> (d^2\tilde{r}^2/dr^2)_0\ [\alpha_S(\tau) - \alpha_\infty\ ] \qquad (6.17b)$$

which also specifically excludes long times since α_S tends to $\alpha_S(\tau\to\infty)$, the long-time transient, faster than α_S tends to α_∞, the steady-state asymptote. Moreover the validity of this "short time" solution extends into longer times both for the transport controlled regime when $(\alpha_{RN}/\alpha_\infty)$ >> 1, and for larger sinks when $(d\tilde{r}/dr)_0$ becomes larger so that $(d^2\tilde{r}^2/dr^2)_0$ becomes smaller (cf. Fig. 1c). This systematic trend is indeed confirmed by Figs. 3-5.

The key criteria (6.6) for validity of the solution ϕ_ℓ of (6.7) is satisfied for large R (cf. Fig. 1 and Table 1) at all times. As shown by the Laplace Transform method ϕ_ℓ is also the exact solution for all R at long times.

6.1 Effective Transient

Although $\alpha_{S,L}(\tau)$ yield the exact transients at the respective short (S) and long (L) times, $\alpha_S(\tau\to\infty)$ does not tend to the correct long-time transient $\alpha_L^{(1)}(\tau)$ of (3.36), and $\alpha_L(\tau\to 0)$ does not tend to the correct short-time transient $\alpha_S^{(1)}$ of (3.35) since, a_δ and a_ℓ in (6.9) are not equal, except at large sink radii (cf. Figs. 3(a) - 5(a)) when $(d\tilde{r}/dr) \to (S/\tilde{S})$. The appropriate asymptotic limits α_{RN} at zero t and α_∞ at infinite t are however reproduced by both α_S and α_L via the functional dependence (6.14), an asset worth exploitation.

Expand the solution,

$$\phi_A(\tilde{r},\tau) = \phi_\delta(\tilde{r},\tau)\ \exp - \sigma(\tau) + \phi_\ell(\tilde{r},\tau)\ [1 - \exp -\sigma(\tau)]\ , \qquad (6.18)$$

of the basic Eq. (6.1) in terms of the known functions $\phi_{\delta,\ell}$. The exact short-time and long-time transients are ensured by insisting that the unknown function $\sigma(\tau)$ is such that $\sigma(\tau \to 0) \to 0$ and $\sigma(\tau \to \infty) \to \infty$. Also $\phi_A(\tilde{r}\to\infty,\tau) \to (\tilde{r}+1)$, irrespective of $\sigma(\tau)$. The radiation boundary condition in (6.3b) is satisfied provided σ is a function <u>only</u> of τ. This restriction precludes (6.18) from tending to the exact solution $\phi_\ell(\tilde{r},\tau)$ at large r. The combination (6.18) is therefore expected to provide an improved transient in the vicinity of the sink where the transient rates $\alpha(\tau) = \alpha_{RN}\ \phi(0,\tau)$ are determined.

According to Figs. 3-5, α_S departs most from the exact rate at intermediate times $\tau \gtrsim 10$, and α_L departs most at short times $\tau \lesssim 1$. Plausible combinations consistent with (6.18) are therefore

$$\alpha^{(-)}(\tau) = \alpha_L(\tau)\ \exp(-\tau^{-1/2}) + \alpha_S(\tau)\ [1 - \exp(-\tau^{-1/2})] \qquad (6.19)$$

and

$$\alpha^{(+)}(\tau) = \alpha_L(\tau)\,[1 - \exp(-\tau^{1/2}] + \alpha_S(\tau)\,\exp(-\tau^{1/2}) \qquad (6.20)$$

In Table 2 are displayed the maximum percentage errors

$$\Delta = 100\,(\alpha - \alpha_E)/\alpha_E \qquad (6.21)$$

between the exact numerical rates α_E and the analytical rates $\alpha = \alpha_S$, α_L and $\alpha^{(\pm)}$ over all τ. The above combinations for $\alpha^{(\pm)}$ provide considerable improvement over the individual $\alpha_{S,L}$ particularly in the transport limited regime $\alpha_\infty \to \alpha_{TR}$ for the extreme case of smaller $S \sim 0.25$. The combination (6.20) provides rates within 7% lower than the exact rates over the full τ-range. Other trial combinations involving $\tau^{\pm 1}$ instead of $\tau^{\pm 1/2}$ in (6.20) and (6.19) were adopted with similar but somewhat less accurate results. As Cols. 2 and 3 of Table 2 show, the greatest error occurs for those cases with the largest differences between a_ℓ and a_δ in (6.9). Also α_L involves less error in general than α_S over the full τ-range.

Another possibility is retention of the basic functional forms,(6.8) for ϕ and (6.14) for α, but to allow $\chi\tau^{-1/2}$ to vary continuously from a_δ, the exact short-time value (6.9) to a_ℓ, the exact long-time value (6.9). The forms (6.8) and (6.14) ensure automatic satisfaction of both boundary conditions (radiation and asymptotic) for well behaved (χ, Ω) and provide the correct limits α_{RN} and α_∞ at zero and infinite times, respectively. Since maximum error in the previous analytical expression for α's occurred for those cases with the largest constants $(\chi_\ell - \chi_\delta)\,\tau^{-1/2}$, direct approximation to χ, under the constraints that $\chi \to \chi_\delta$ as $\tau \to 0$ and $\chi \to \chi_\ell$ as $\tau \to \infty$, is therefore indicated.

Figs. 6(a) - 6(c) illustrate the variation of $\chi_{1,2}^{(-)}\,\tau^{-1/2}$, where

$$\chi_n^{(-)}(\tau) = \exp(-\tau^{-n/2})\chi_\ell + [1 - \exp(-\tau^{-n/2})]\,\chi_\delta \quad ; \; n = 1, 2 \qquad (6.22)$$

between the exact short-time and long-time constant limits, as compared with the numerical solution χ_E of (3.32) with α taken as the exact numerical rates α_E. Since $\chi_\delta \leq \chi_E \leq \chi_\ell$, then $\alpha_\delta \leq \alpha_E \leq \alpha_\ell$, as illustrated already by Figs. 3-5. The more gradual variation of $\chi_1^{(-)}$ is much closer to χ_E than is the more abrupt variation of $\chi_2^{(-)}$, even for those transport limited cases which involved the largest difference $(\chi_\ell - \chi_\delta)$.

Figs. 7(a) - 7(c) demonstrate the close agreement of the resulting rates $\alpha[\chi_1^{(-)}]$ with the exact numerical rate over the full range of τ for the worst cases (transport-limited and small sinks). Although the percentage errors (Table 2) associated with α_L and α_S are here as large as -33% and 68%, respectively, use of $\chi_1^{(-)}$ in (6.14) involves errors less than 4%, as indicated in Column 9 of Table 2. Inspection of Figs. 6 and 7 shows that α is not too sensitive to variation in χ e.g., a 10% variation in χ in Fig. 6 results in little variation of α. Also the fact that χ_1^- intersects χ_E twice ($\chi_1^- < \chi_E$ at short times, $\chi_1^- > \chi_E$ at intermediate times, $\chi_1^- < \bar{\chi}_E$ at long times) results in a corresponding but less of a variation in α.

7. Summary and Conclusions

By operating at a level more basic than the macroscopic Debye-Smoluchowski Equation (DSE), the present treatment (§ 2), has exposed the following assumptions intrinsic to DSE: (1) the densities n and associated net current J in eq. (1) refer to pairs in the combined blocks *C* (of fully dissociated states) and *E* (at highly excited states) as in eq. (2.11); (2) steady-state conditions for all pairs in each energy level of block *E* and (3) steady-state for all pairs with $R \leq R_s$ and all energies in blocks *C* and *E* as in eq. (2.30). Also (4) DSE is mainly limited to cases of high non-equilibrium.

In addition, the microscopic treatment has also provided the appropriate modification (2.14) of DSE, which was applicable only to regions $R \geq R_s$ external to the sink, to description of the kinetics within ($R \leq R_s$) the sink.

The microscopic treatment has also indicated that the actual rate (2.20) is determined by the self-consistent solution[5] of the two simultaneous equations (2.7) and (2.10) each of which couple transport and collisions.

The local rate α_3 of reaction in (2.23) thus remains an integral and internal part of the treatment by being determined from the self consistent solutions.

This local rate α_3 (or α_{RN}) is externally assigned in DSE which therefore describes via (2.9) in (2.24a), the transport portion of the problem consistent with this external choice for α_3. Under the provisor that the transport and reaction rates α_{TR} and α_{RN} are fully uncoupled, the DSE-prescription is valuable for investigation of that particular time-dependent combination of α_{RN} and α_{TR} involved in the process as time evolves.

In § 3, a nonlinear transformation[12] into tilda-space $\tilde{R}(R)$, has

facilitated the search for simple analytical time-dependent solutions of DSE for general interactions V(R). Expressions have been obtained for the time dependent probability density n(R,t), that the pair AB has separation R, and for reaction rates $\alpha(t)$ which are exact (a) at all times and large R, (b) at long times and all R and (c) at short times and all R. In particular, the solutions for cases (a) and (b) are identical. The transformation technique is, in itself, quite general and can be applied to a variety of problems. For example, Cukier[19] by following previous reports[12] of this strategy, recently used this tilda space representation to successfully study concentration dependent fluorescent quenching.

By comparison in § 5.1 with exact numerical transient rates α_E of § 5, the rates $\alpha_S(t)$ and $\alpha_L(t)$, (3.32) with (3.31) and (3.30), are the exact DSE transients at short and long times, and are, respectively, higher and lower than α_E at intermediate times. Over the full time-range, $\alpha_L(t)$ is, in general, closer to α_E than is α_S. Retention of only the first $t^{-1/2}$-term in the $t^{-1/2}$-expansion of $\alpha_L(t)$ provides $\alpha_L^{(1)}(t)$ in (3.36), which is identical with the asymptotic transient derived[11] previously from a perturbation-type method.[10] The present expression (3.32) with (3.30), for $\alpha_L(t)$ provides considerable improvement over $\alpha_L^{(1)}$ which, up to now, has been (to the author's knowledge) the only simple analytical rate available. Similar expansions (3.35) for short times are also provided.

Not only is α_S the exact transient at short times but α_S tends to the correct steady state asymptote α_∞ at long times, albeit with an incorrect transience; and α_L, not only is the exact long time transient but tends (with an incorrect transience) at short times to the correct rate α_{RN} at $t = 0$. The varations of both $\alpha_{L,S}(t)$ with t are therefore bounded, unlike the previous rate $\alpha_L^{(1)}$. This asset is the essential reason that extensions of $\alpha_{L,S}$

proposed in § 4 to cover intermediate times are not as effective over the full time-range.

By exploitation of this asset, which is based on the unique functional dependence of $\alpha(t)$ in (3.32) on $\chi(t)$, a time-dependent combination of $\chi_\delta(t)$ and $\chi_\ell(t)$ for $\chi(t)$ provides, in § 6.1, rates highly accurate (to within 4% for the worst case) over several decades of time!

Acknowledgement

This research is supported by the U. S. Air Force Office of Scientific Research under Grant No. AFOSR-84-0233.

References

1. M. von Smoluchowski, Phys. Z 17, 557, 585 (1916); Z Phys. Chem. 92, 127 (1917).
2. P. Debye, Trans. Electrochem. Soc. 82, 265 (1942).
3. R. M. Noyes, Prog. React. Kinet. 1, 129 (1961).
4. M. R. Flannery, Phil. Trans. Roy. Soc. A 304, 447 (1982).
5. M. R. Flannery, Phys. Rev. A (preceding paper).
6. K. M. Hong and J. Noolandi, J. Chem. Phys. 68, 5163 (1978).
7. S. A. Rice, P. R. Butler, M. J. Pilling and J. K. Baird, J. Chem. Phys. 70, 4001 (1
8. S. A. Rice and J. K. Baird, J. Chem. Phys. 69, 1989 (1978) and references therein.
9. A. Mozumder, J. Chem. Phys. 61, 780 (1974) and references therein.
10. J. L. Magee and A. B. Tayler, J. Chem. Phys. 56, 3061 (1972).
11. K. M. Hong and J. Noolandi, J. Chem. Phys. 68, 5172 (1978).
12. M. R. Flannery, Phys. Rev. Letts. 47, 163 (1981); 48, 1573(E) (1982).
13. M. R. Flannery, Phys. Rev. Letts. 49, 1681 (1982).
14. M. R. Flannery, Phys. Rev. A 25, 3403 (1982).
15. A. T. Reid, Arch. Biochem. Biophys. 43, 416 (1952).
16. M. R. Flannery, in Applied Collision Physics, edited by H. S. W. Massey, B. Bederson and E. W. McDaniel (Academic, New York, 1982) vol. 3, chap. 5.
17. L. Collatz, The Numerical Treatment of Differential Equations (Third Edition) (Springer-Verlag, Wien, 1960), Chap. V, 4.
18. IMSL Library (Edn. 9, 1982).
19. R. I. Cukier, J. Chem. Phys. 82, 5457 (1985).

Table 1. Values of R and $\tilde{R}$, in natural units ($R_e = e^2/kT$), and of $(d\tilde{R}/dR)$ for Coulombic Attraction.

R	$\tilde{R}$	$(d\tilde{R}/dR)$
0	1	0
0.25	1.0187	0.3041
0.5	1.1565	0.7241
0.75	1.3580	0.8642
1.0	1.5820	0.9207
1.5	2.0552	0.9638
2.0	2.5415	0.9794
3.0	3.5277	0.9908
6.0	6.5139	0.9977
10	10.5083	0.9992
.	.	.
.	.	.
.	.	.
R	R+0.5	1.0

Table 2: Largest Percentage Errors $\Delta = 100(\alpha - \alpha_E)/\alpha_E$ associated with various levels of approximation.

$(\alpha_\infty/\alpha_{TR})$	S	$a_s^\dagger$	$a_\ell^\dagger$	Δ					
				α_S	$-\alpha_L$	$\alpha^{(-)}$	$-\alpha^{(+)}$	$\alpha[\chi_1^{(-)}]$	$-\alpha[\chi_2^{(-)}]$
0.1	1	0.647	0.702	0.15	0.13	0.03	0.04	0.03	0.06
0.1	0.75	0.530	0.614	0.29	0.22	0.05	0.08	0.05	0.09
0.1	0.50	0.348	0.480	0.69	0.45	0.07	0.21	0.07	0.16
0.1	0.25	0.083	0.273	2.98	1.24	-0.24	0.93	-0.43	0.85
0.5	1	1.164	1.264	0.93	0.96	0.26	0.21	0.26	0.45
0.5	0.75	0.955	1.105	1.75	1.62	0.42	0.41	0.39	0.72
0.5	0.50	0.626	0.865	4.33	3.24	0.68	1.09	0.61	1.25
0.	0.25	0.149	0.491	20.63	8.92	1.33	5.67	-2.64	-5.43
0.9	1	5.820	6.322	2.25	3.63	1.23	0.17	1.20	1.77
0.9	0.75	4.773	5.523	4.32	6.14	2.17	0.33	2.05	3.16
0.9	0.50	3.130	4.323	11.24	12.32	4.62	0.87	3.88	6.69
0.9	0.25	0.746	2.454	68.29	32.70	15.06	6.43	3.65	11.24

$\alpha_{S,L}(\tau)$: Eq. (3.32) with (3.31) or (3.30); $\alpha[\chi_{1,2}^{(-)}]$: Eq. (3.32) with (6.22) for $\chi_{1,2}^-$.

$$\alpha^{(-)}(\tau) = \exp(-\tau^{-1/2})\alpha_L + [1 - \exp(-\tau^{-1/2})]\alpha_S;$$

$$\alpha^{(+)}(\tau) = \exp(-\tau^{1/2})\alpha_S + [1 - \exp(-\tau^{1/2})]\alpha_L;$$

$$^\dagger a_{s,\ell} = \chi_{s,\ell}\, \tau^{-1/2}$$

Figure Captions

Fig. 1. Variation of $(d\tilde{R}/dR)$ with $\tilde{R}$(n.u.) for (a) the attractive interactions $V(R) = -(R_e/R)^n$, n = 1, 2, 4 and 6. $\tilde{R}$ is in units of R_e, the natural unit (n.u.). The variation for pure Coulomb attraction (n = 1, $R_e = e^2/kT$) is amplified in (b) where (X) denote the values selected as sink radii S.(c) Variation of scaled derivative $(d\tilde{r}/dr)$ with scaled distance $\tilde{r}$ for the selected sink radii (S = 1, 0.75, 0.5 and 0.25 n.u.).

Fig. 2. Exact numerical solutions for the fractional departure $\rho = n/N_o \exp(-V/kT)$ of the probability density n from Boltzmann equilibrium as a function of reduced distance $\tilde{r} = (\tilde{R}/\tilde{S})-1$ at scaled sequential times $\tau = (Dt/S^2) = 0.05, 0.5, 1, 2, 5, 10, 20, 30, 100, 200, 500$ up to infinity (∞). Assigned parameters: $\alpha_\infty/\alpha_{TR} = 0.5$, S = 0.5 (n.u.).

Fig. 3. Comparison with exact numerical rates of various short-time (a)-(d) and of various long-time (e)-(h) analytical rates over several decades of scaled time $\tau = Dt/S^2$, for various sink radii S(n.u.). Assigned parameter: $\alpha_\infty/\alpha_{TR} = 0.1$.

Fig. 4. As in Fig. 3, but with $\alpha_\infty/\alpha_{TR} = 0.5$.

Fig. 5. As in Fig. 3, but with $\alpha_\infty/\alpha_{TR} = 0.9$.

Fig. 6. Variation of $\chi(\tau)\ \tau^{-1/2}$ with scaled time $\tau = (Dt/S^2)$ for extreme case of small sink radius S = 0.25 n.u. and for $\alpha_\infty/\alpha_{TR}$ taken as (a) 0.1, (b) 0.5 and (c) 0.9. Curve E is obtained from exact solution of eq. (3.22) for exact numerical rate, and curves 1 and 2 are obtained from eq. (6.22) of text with n = 1 and 2, respectively. Long-time and short-time exact limits $\chi_{\ell,s}(\tau)\ \tau^{-1/2}$ are illustrated.

Fig. 7. Comparison over scaled time $\tau = (Dt/S^2)$ between exact numerical rate α_E and various analytical rates: $\alpha[\chi_1^{(-)}]$ obtained from eq. (6.22) for χ_1^- in eq. (3.22) for α. The exact long-time and short-time transients are α_L and α_S, respectively. Assigned Parameters: $(\alpha_\infty/\alpha_{TR})$ = (a) 0.1, (b) 0.5, (c) 0.9; and S = 0.25 n.u. an extreme case for validity of basic assumptions.

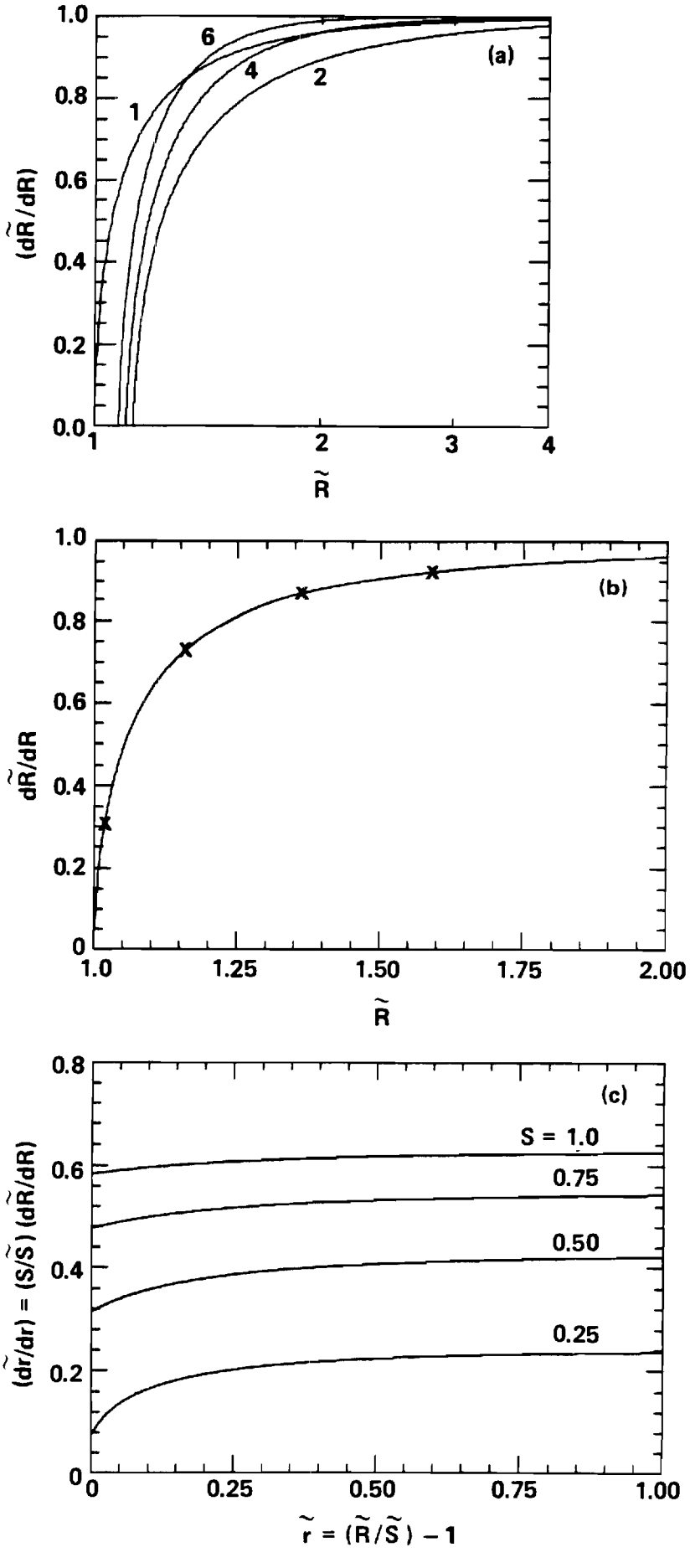
(a)
6
4
2
1
$(d\tilde{R}/dR)$
$\tilde{R}$
(b)
$d\tilde{R}/dR$
$\tilde{R}$
(c)
S = 1.0
0.75
0.50
0.25
$(d\tilde{r}/dr) = (\tilde{S}/S)\,(d\tilde{R}/dR)$
$\tilde{r} = (\tilde{R}/\tilde{S}) - 1$

Figure 1

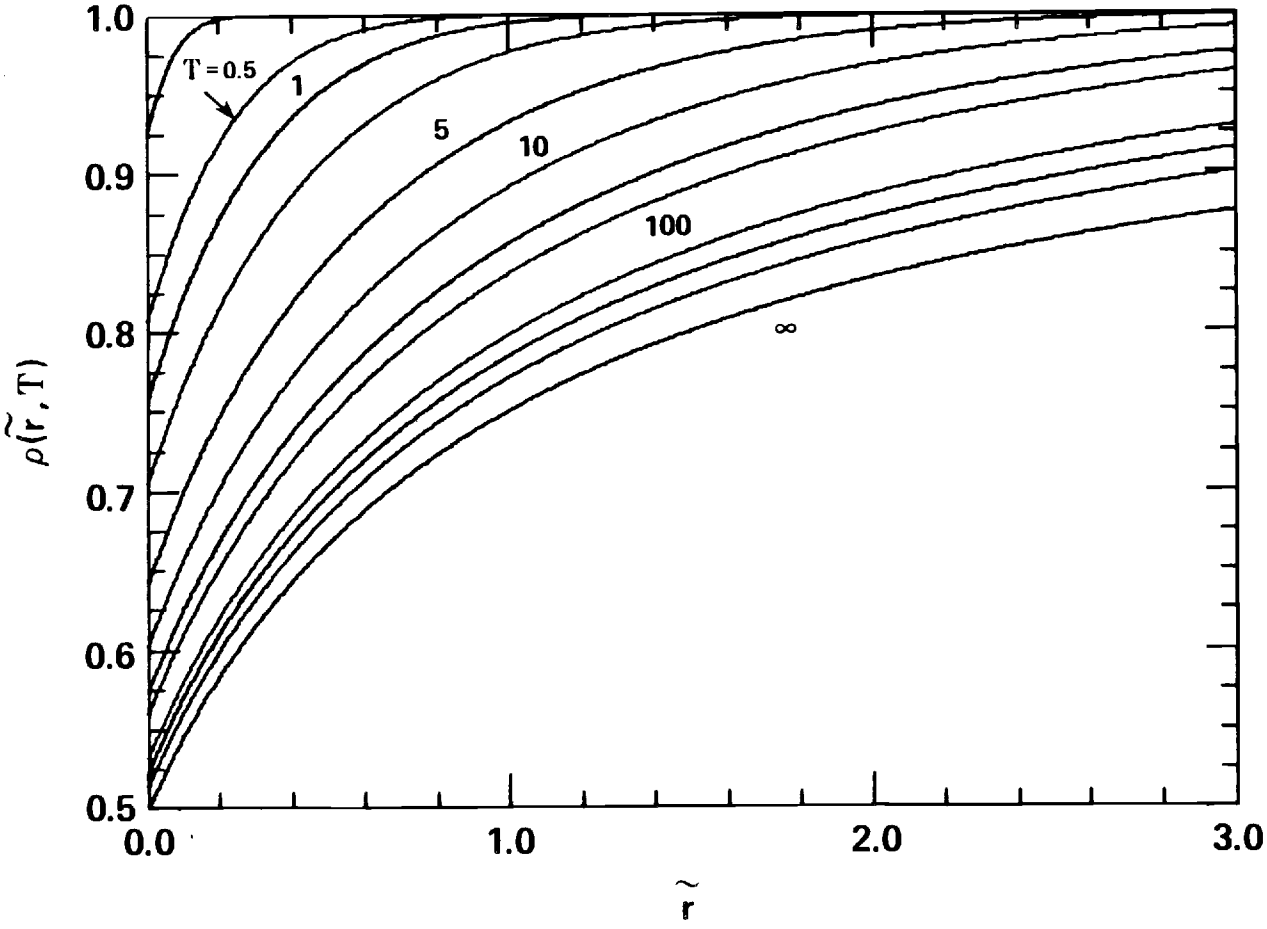

Figure 2

Figure 3

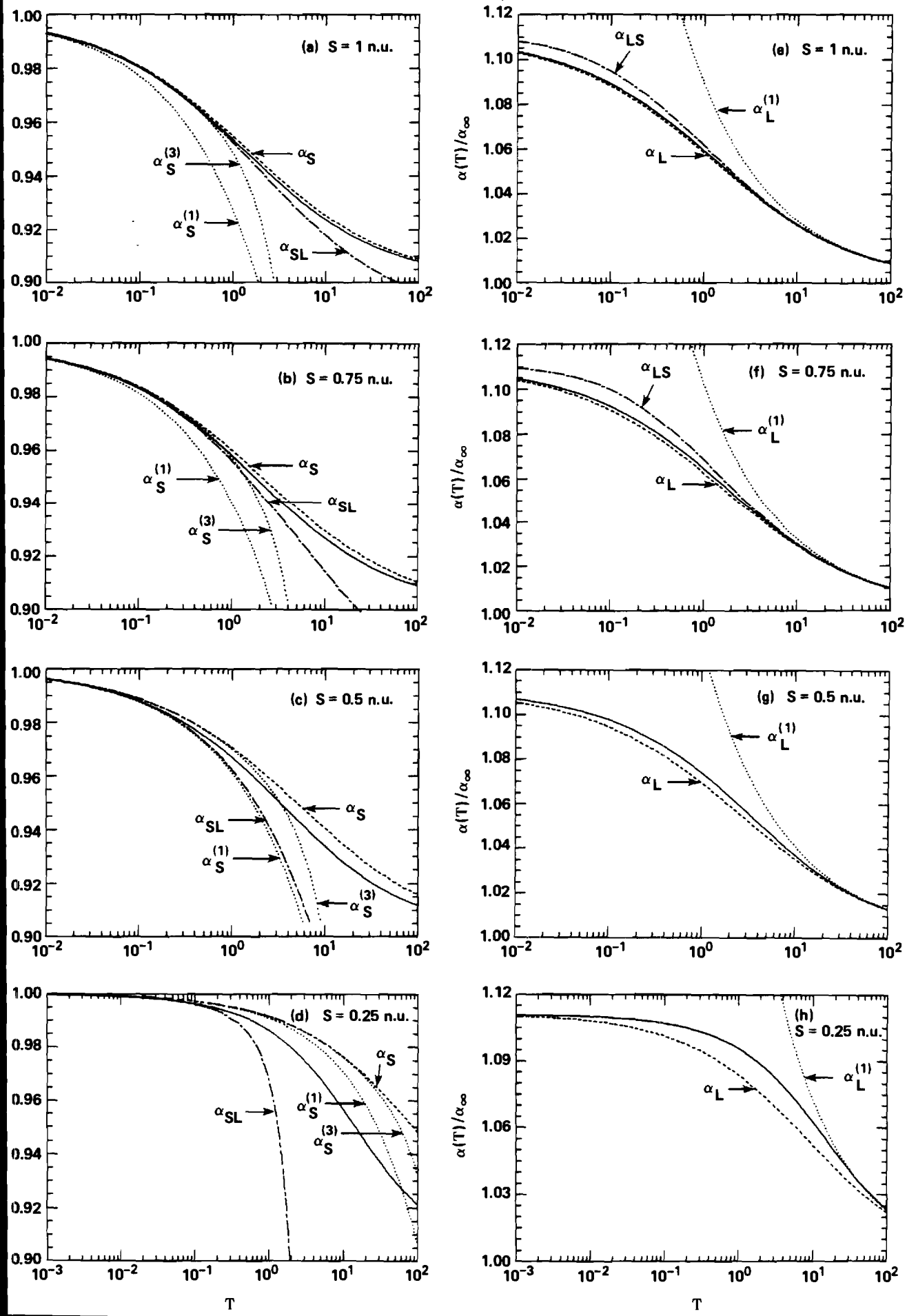
(a) S = 1 n.u.
(b) S = 0.75 n.u.
(c) S = 0.5 n.u.
(d) S = 0.25 n.u.
(e) S = 1 n.u.
(f) S = 0.75 n.u.
(g) S = 0.5 n.u.
(h) S = 0.25 n.u.
α(T)/α∞
T

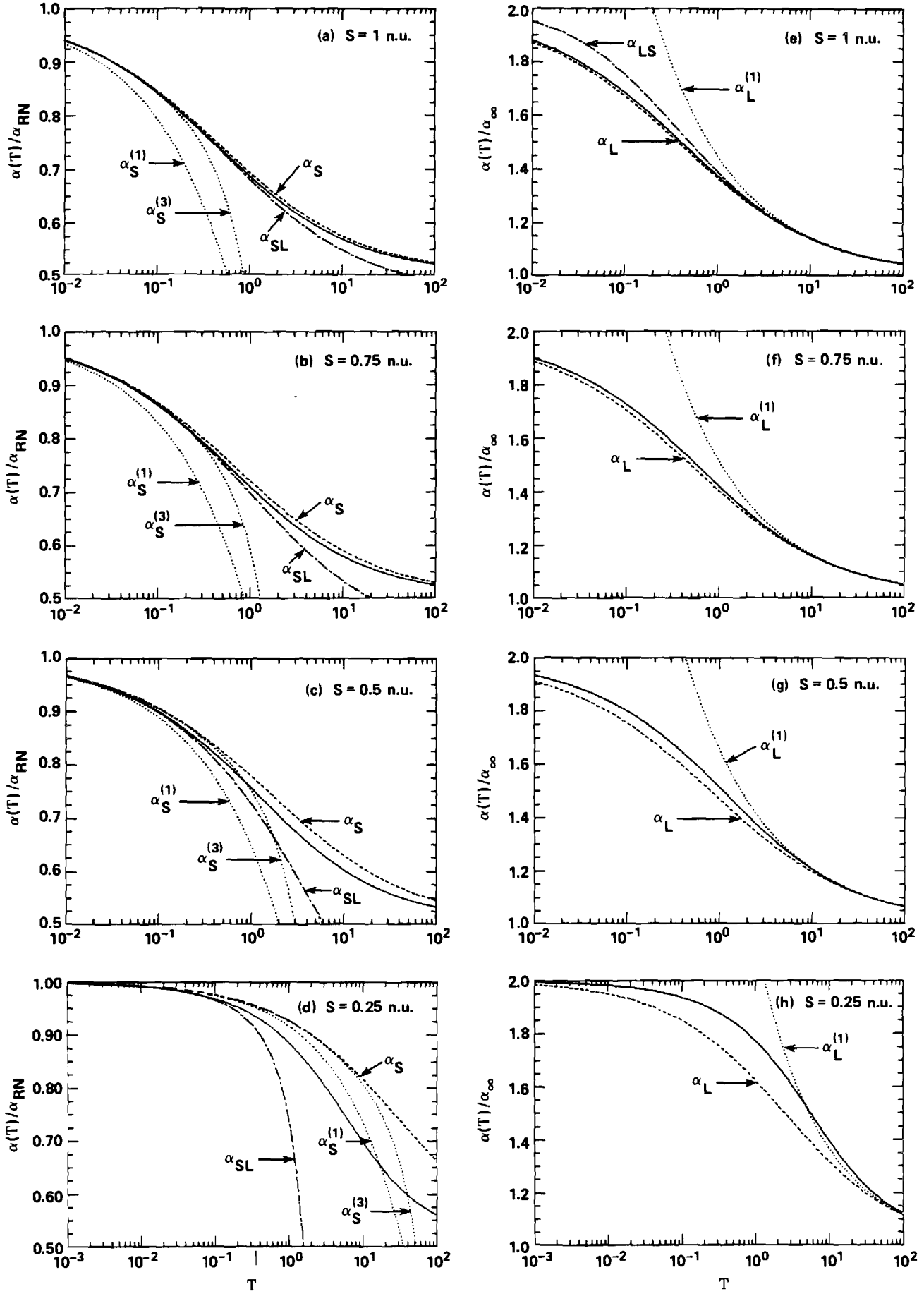
(a) S = 1 n.u.
(b) S = 0.75 n.u.
(c) S = 0.5 n.u.
(d) S = 0.25 n.u.
(e) S = 1 n.u.
(f) S = 0.75 n.u.
(g) S = 0.5 n.u.
(h) S = 0.25 n.u.
α(T)/α_RN
α(T)/α_∞
α_S
α_S^(1)
α_S^(3)
α_SL
α_LS
α_L
α_L^(1)
T

Figure 4

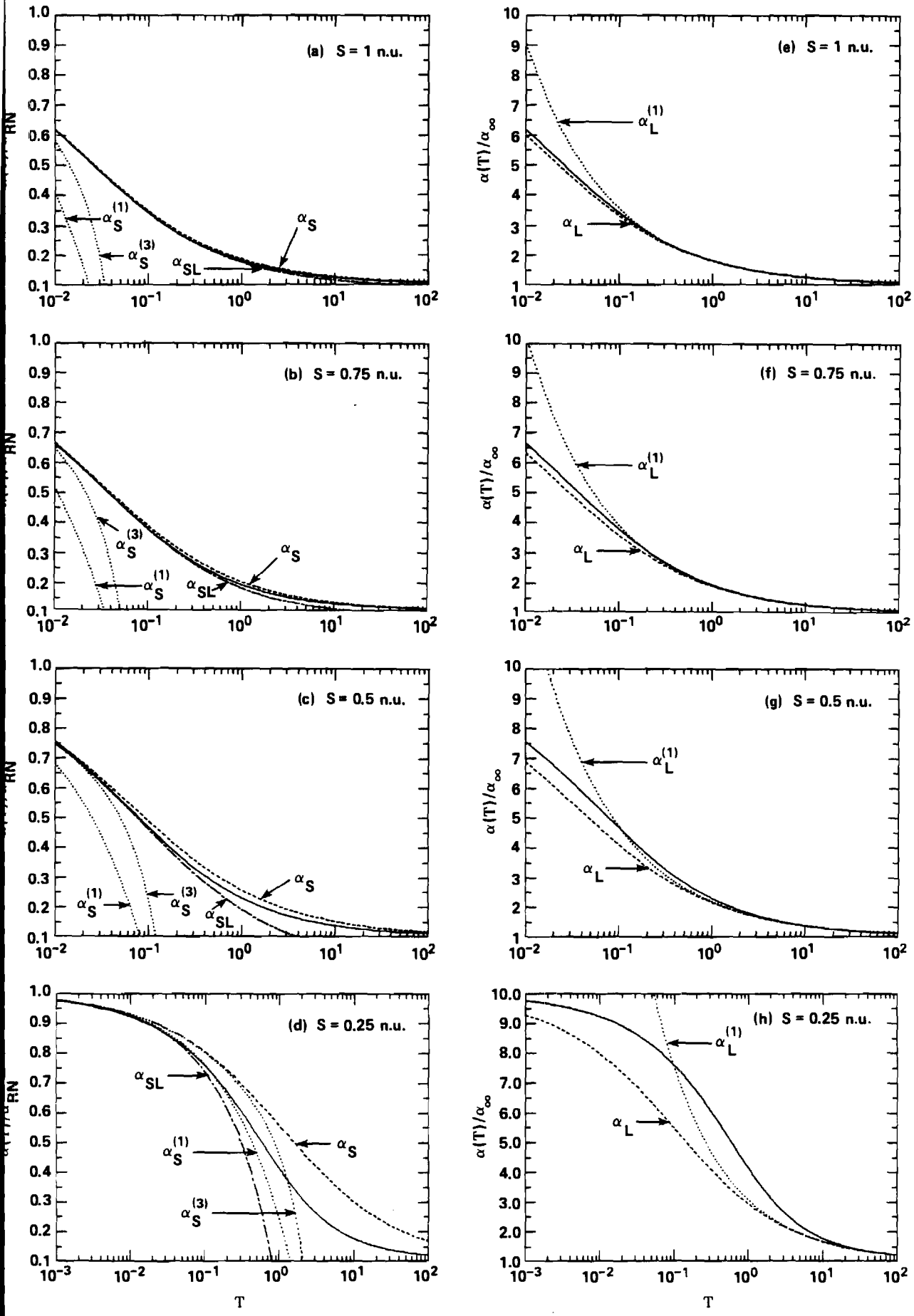
(a) S = 1 n.u.
(b) S = 0.75 n.u.
(c) S = 0.5 n.u.
(d) S = 0.25 n.u.
(e) S = 1 n.u.
(f) S = 0.75 n.u.
(g) S = 0.5 n.u.
(h) S = 0.25 n.u.
α_S
$\alpha_S^{(1)}$
$\alpha_S^{(3)}$
α_{SL}
α_L
$\alpha_L^{(1)}$
$\alpha(T)/\alpha_\infty$
T

Figure 5

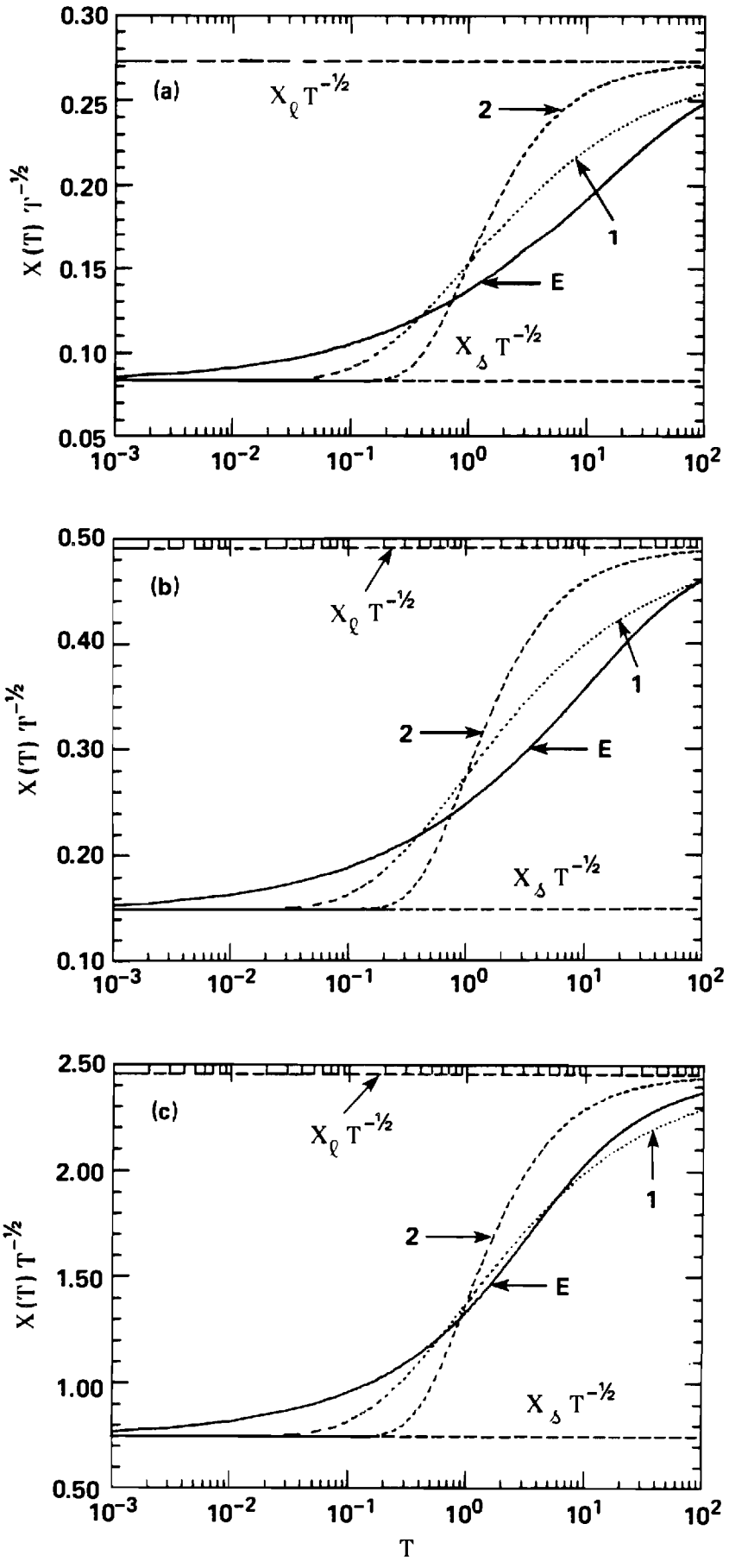
(a)
$X_\ell T^{-1/2}$
2
1
E
$X_\delta T^{-1/2}$
0.30
0.25
0.20
0.15
0.10
0.05
10^{-3}
10^{-2}
10^{-1}
10^{0}
10^{1}
10^{2}
$X(T)\,T^{-1/2}$
(b)
$X_\ell T^{-1/2}$
2
1
E
$X_\delta T^{-1/2}$
0.50
0.40
0.30
0.20
0.10
(c)
$X_\ell T^{-1/2}$
2
1
E
$X_\delta T^{-1/2}$
2.50
2.00
1.50
1.00
0.50
T

Figure 6

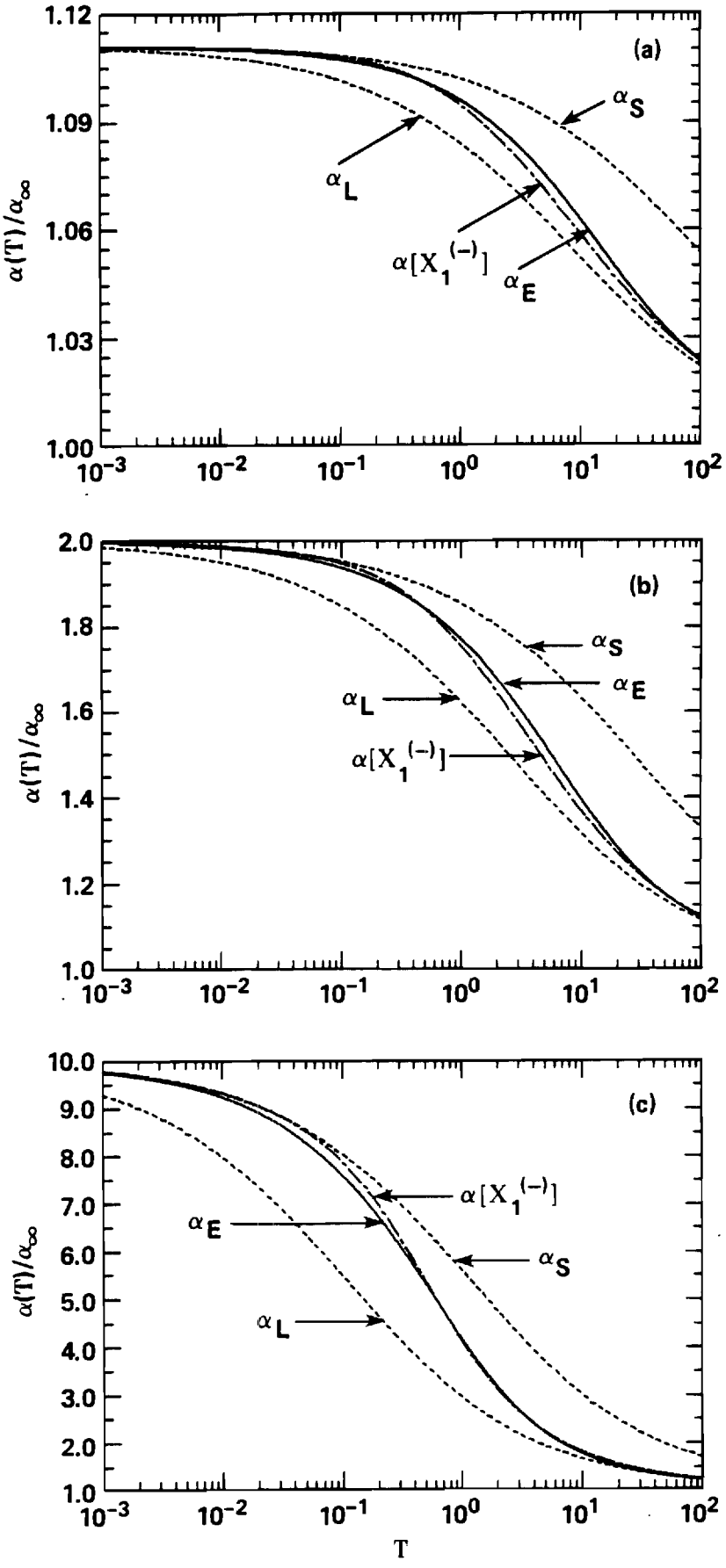

Figure 7

Appendix D

Ion-Ion Recombination at High Ion Density

Ion-Ion Recombination at High Ion Density

M. R. Flannery

School of Physics

Georgia Institute of Technology

Atlanta, Georgia 30332, U.S.A.

Abstract. By appeal to a Thomson-type treatment of recombination, it is shown that the rate for recombination of ions generated with uniform frequency within a reaction volume is a factor of (9/4) times greater than the rate for recombination of ions which approach each other from infinite separation. A valuable relationship connecting the two problems is uncovered. The analysis is pertinent to recombination involving dilute and high degrees of ionization.

Physics Abstracts Classification Numbers: 3410, 3450L, 8220, 8240

For (X^+-Y^-) ion-ion recombination in an ambient gas Z (neutral or ion), the following important distinctions between the cases of low and high ion densities $N^{\pm}$ are evident:

(A) For dilute ionization with ion densities $N^{\pm} \lesssim 10^8$ cm^{-3}, recombination can be based on consideration of the flow of positive ions X^+ (say) towards a central stationary negative ion Y^-. Steady-state conditions are then maintained by a source of ionization at infinity. For high ionization with $N^{\pm} \gtrsim 2 \times 10^{14}\ (T/300)^{3/2}$ cm^{-3}, when the Debye-Huckel shielding distance $R_s \lesssim R_e$, the natural unit (e^2/kT) of length characteristic of ion-ion recombination in a low density gas at temperature T, the positive ions X^+ already exist in a pre-assigned configuration with respect to Y^-, and the steady-state source is then distributed uniformly throughout the volume (Bates 1981).

(B) Recombination results not only from ion-neutral gas collisions but also from ion-ion (X^+-X^+), (Y^-Y^-), (X^+-Y^-) collisions which tend to increase the rate (Bates 1982).

(C) The interaction between the ions may no longer be considered as pure Coulomb at low gas densities N but will involve some appropriate measure of screening as determined by the self-consistent Poisson-Boltzmann treatment (Flannery 1981, 1982a,b).

(D) There are no longer isolated sinks, as for low $N^{\pm}$, but cooperative and competitive effects can arise between the closely spaced sinks distributed throughout the region.

Bates (1981) has reasoned that screening (C) does <u>not</u> affect the recombination at high gas densities N, on the basis that ions which are initial nearest neighbours remain nearest neighbours, and drift towards one

another until recombination occurs, with the result that the usual Langevin-Harper rate at high N is not affected by increase of ion-densities $N^{\pm}$. Flannery (1981, 1982a) has shown that the recombination rate α is, in general, determined as a function of N and $N^{\pm}$ by the self-consistent solution of the Boltzmann equation for the two particle distribution function and of Poisson's equation for the interaction between the ions. Calculation (Flannery 1981) indicates that increase in ion density up to 10^{14} cm^{-3} causes some reduction to α only at low and intermediate N. A molecular dynamics simulation (Morgan et al 1982) which incorporates this self-consistent idea (Flannery 1981) illustrates that the reduction can become quite significant when higher densities $N^{\pm} \gtrsim 10^{15}$ at gas pressures $\lesssim$ 1 atm are reached. Bates (1982) demonstrated that the effect of ion-ion collisions in (B) then tends to oppose the decrease resulting from (C) particularly at lower temperatures T and $N^{\pm} \gtrsim 10^{15}$ cm^{-3}. The isolated effects of (A) and (D) have not yet been addressed.

The present goal is to investigate the effect of distinction (A) above, in isolation from (C) and (D). Since a detailed treatment based on microscopic principles (Flannery 1982a) would couple (A)-(D), and would therefore tend to obscure the key issue, it is worthwhile to illustrate the general trend by appeal to a Thomson-style treatment (constant speed, full absorption upon suitable collision). In so doing, a valuable connection between two distinct problems becomes apparent.

In the following analysis, diffusional drift which influences the approach of the ions at intermediate gas densities N is ignored so that the present treatment is appropriate to low $N \lesssim 10^{17} - 10^{18}$ cm^{-3}. At higher $N \gtrsim 10^{20} - 10^{21}$ cm^{-3}, the distinction A loses its significance since the radius R_T of the reaction sphere, within which recombination occurs, becomes

very small in comparison with both the Debye-Hückel radius R_s and the natural unit R_e, so that ions are generated well outside the reaction volume.

Let the positive ions X^+ be born isotropically with frequency F_r at a point $\underset{\sim}{r}$ from the central negative ion Y^-. The flux (number of ions per sec) which escapes in all directions $\underset{\sim}{\Omega}_E$ through a convex surface of area S enclosing a volume V (Figure 1a) is

$$F_E(\underset{\sim}{r}) = (F_r/4\pi) \int_S R^{-2}\exp(-R/\lambda)(\underset{\sim}{\Omega}_E \cdot \underset{\sim}{n})dS = (F_r/4\pi) \int_{\Omega_E} \exp(-R/\lambda)d\Omega_E \qquad (1)$$

where R is the length from the internal point source $\underset{\sim}{r}$ to the exit point on S in the direction $\underset{\sim}{\Omega}_E$, where λ is the mean free path of the ion X^+ in the gas, and where $d\Omega_E$ is the solid angle $(\underset{\sim}{\Omega}_E \cdot \underset{\sim}{n})dS/R^2$ subtended at $\underset{\sim}{r}$ by elemental area dS with outward normal $\underset{\sim}{n}$. The probability for escape through S of ions born at $\underset{\sim}{r}$ is therefore

$$P_E(\underset{\sim}{r}) = F_E(\underset{\sim}{r})/F_r = (1/4\pi) \int_{\Omega_E} \exp(-R/\lambda)d\Omega_E \qquad (2)$$

and provided the production frequency F_r is the same constant at all points $\underset{\sim}{r}$ within V, the averaged probability for escape is

$$\langle P_E \rangle = \frac{1}{V} \int_V P_E(\underset{\sim}{r})d\underset{\sim}{r} = (1/4\pi V) \int_V dV \int_{\Omega_E} \exp(-R/\lambda)d\Omega_E \qquad (3)$$

Subdivide V into tubes with axes directed along $\underset{\sim}{\Omega}_E$, as in Figure 1(b), such that the elemental volume at $\underset{\sim}{r}$ is,

$$dV = (\underset{\sim}{n}_i \cdot \underset{\sim}{\Omega}_E)dSdR \qquad (4)$$

where R is the distance along $\underset{\sim}{\Omega}_E$ of $\underset{\sim}{r}$ from elemental area dS with normal $\underset{\sim}{n}_i$ pointing inward. On integration over R between zero and the maximum chord length $R_m(\underset{\sim}{\Omega}_E, \underset{\sim}{n}_i)$ consistent with the specified directions $\underset{\sim}{\Omega}_E$ and $\underset{\sim}{n}_i$, the averaged escape-probability is

$$\langle P_E \rangle = \frac{1}{4\pi} (\lambda/V) \int_S dS \int_{\Omega_E} d\Omega_E (\underset{\sim}{\Omega}_E \cdot \underset{\sim}{n}_i)[1-\exp(-R_m/\lambda)] \tag{5}$$

where the region of integration is such that $\underset{\sim}{\Omega}_E \cdot \underset{\sim}{n}_i > 0$.

The averaged probability for absorption within V is therefore

$$\langle P_A \rangle = 1 = \langle P_E \rangle \tag{6}$$

so that, the rate α_V ($cm^3 s^{-1}$) of volume recombination (absorption) within V is,

$$\alpha_V = \langle P_A \rangle Sv \tag{7}$$

where v is speed of the ions across surface S. This rate holds for ions generated with constant frequency F_r at all points within any volume V enclosed by any convex surface of area S. Under steady-state conditions, the source frequency is

$$F_r = \alpha_V \langle \rho \rangle \tag{8}$$

where $\langle \rho \rangle$ is the averaged density $(1/V)\int_V \rho(\underset{\sim}{r}) d\underset{\sim}{r}$ within volume V in terms of the density distribution $\rho(\underset{\sim}{r})$ of ions within V.

For a sphere of radius R_T, in particular, R_m is $2(\underset{\sim}{\Omega}_E \cdot \underset{\sim}{n}_i)R_T$, so that the absorption probability obtained via (6) is

$$\langle P_A \rangle = 1 - (3\lambda/4R_T)W(R_T/\lambda) \tag{9}$$

where

$$W(X) = 1 - (1/2X^2)[1 - (1 + 2X)\exp(-2X)] \tag{10}$$

$$\rightarrow (\tfrac{4}{3}X)[1 - \tfrac{3}{4}X + \tfrac{2}{5}X^2 - \tfrac{1}{6}X^3 + \ldots], \qquad X \rightarrow 0$$

$$\rightarrow 1 - (1/2X^2) \qquad , \qquad X \rightarrow \infty$$

is the well-known Thomson probability (Thomson 1924, Loeb 1955), the relevance of which to the present problem will become apparent below. The recombination rate (8) for ions distributed with uniform frequency within the reaction sphere is therefore,

$$\alpha_V = 4\pi R_T^2 v[1 - (3\lambda/4R_T)W(R_T/\lambda)] \tag{11}$$

which tends at low gas densities (where $\lambda >> R_T$) to

$$\alpha_V = (\tfrac{9}{4})(\tfrac{4}{3}\pi R_T^3)(v/\lambda) \tag{12}$$

which is a factor of (9/4) higher than the corresponding Thomson rate for recombination of ions approaching from infinite separation (Thomson 1924, Loeb,1955), rather than from the pre-assigned configuration.

For dilute ionization, the number of ions per sec which travel (still in the absence of diffusional drift) from infinity and enter the volume V through S from all directions $\underset{\sim}{\Omega}_0$ is

$$\frac{dN_{EN}}{dt} = -(\rho_\infty v/4\pi)\int_S dS \int_{\Omega_0} (\underset{\sim}{\Omega}_0 \cdot \underset{\sim}{n}) d\Omega_0 = \frac{1}{4}\rho_\infty v S \tag{13}$$

where $\underset{\sim}{n}$ is the outward-pointing normal to surface area dS. The density within V is

$$\rho(\underset{\sim}{r}) = \int \rho(\underset{\sim}{r},\underset{\sim}{\Omega})d\Omega \tag{14}$$

where the angular density at the internal point $\underset{\sim}{r}$ in direction $\underset{\sim}{\Omega}$ is

$$\rho(\underset{\sim}{r},\underset{\sim}{\Omega}) = -(\rho_\infty v/4\pi)\int dS \int K(\underset{\sim}{r},\underset{\sim}{\Omega};\underset{\sim}{r}_0,\underset{\sim}{\Omega}_0)(\underset{\sim}{\Omega}_0\cdot\underset{\sim}{n})d\Omega_0 \tag{15}$$

in terms of $K(\underset{\sim}{r},\underset{\sim}{\Omega};\underset{\sim}{r}_0,\underset{\sim}{\Omega}_0)$ which is the angular density of ions at $\underset{\sim}{r}$ travelling in direction $\underset{\sim}{\Omega}$ which originate from a source radiating with a unit (flux) rate at $\underset{\sim}{r}_0$ in direction $\underset{\sim}{\Omega}_0$ at surface S. This propagator satisfies the principle of microreversibility,

$$K(\underset{\sim}{r},\underset{\sim}{\Omega};\underset{\sim}{r}_0,\underset{\sim}{\Omega}_0) = K(\underset{\sim}{r}_0,-\underset{\sim}{\Omega}_0;\underset{\sim}{r},-\underset{\sim}{\Omega}) \tag{16}$$

which is such that the angular density at $\underset{\sim}{r}$ in direction $\underset{\sim}{\Omega}$ which originates from a unit source radiating at $\underset{\sim}{r}_0$ in direction Ω_0, is equivalent to the angular density generated at $\underset{\sim}{r}_0$ in direction $-\Omega_0$ by a unit source radiating at $\underset{\sim}{r}$ in direction $-\underset{\sim}{\Omega}$. In terms of this propagator, the probability of escape of ions born at $\underset{\sim}{r}$ is, by definition,

$$P_E(\underset{\sim}{r}) = (v/4\pi)\int dS \int K(\underset{\sim}{r}_0,\underset{\sim}{\Omega}_0;\underset{\sim}{r},\underset{\sim}{\Omega})(\underset{\sim}{\Omega}_0\cdot\underset{\sim}{n})d\Omega_0 \tag{17}$$

the ratio (2) of the frequency at which ions emerge (with $\underset{\sim}{\Omega}_0\cdot\underset{\sim}{n} > 0$) through surface S in directions $\underset{\sim}{\Omega}_0$ to the frequency of their internal production at $\underset{\sim}{r}$. Upon use of (16) in (15), and upon reversal of signs of $\underset{\sim}{\Omega}_0$ and $\underset{\sim}{\Omega}$ in

the resulting expression for (14), the internal density (14) is simply

$$\rho(\underset{\sim}{r}) = P_E(\underset{\sim}{r})\rho_\infty \quad . \tag{18}$$

The average escape probability is then

$$\langle P_E \rangle = \frac{1}{V}\left[\int_V \rho(\underset{\sim}{r})d\underset{\sim}{r}\right]/\rho_\infty = \langle\rho\rangle/\rho_\infty \tag{19}$$

for any surface geometry.

This expression (19) therefore provides the unique link common to the two distinct problems addressed here i.e., between the escape probability for ions generated isotropically at constant frequency within a confined volume V and the averaged density of ions injected into V from an external bath extending to infinity.

Since the rate of ion entry into V from the bath is given by (13), and since the number of ions which exit per second from V back into the bath is

$$\frac{dN_{EX}}{dt} = (\rho_\infty v/4\pi)\int dS\int \exp(-R_m/\lambda)(\underset{\sim}{\Omega}_o\cdot\underset{\sim}{n})d\Omega_o \tag{20}$$

the number of ions which are absorbed per second within V is

$$\frac{dN_A}{dt} = \frac{d}{dt}(N_{EN} - N_{EX}) = (\rho_\infty v/4\pi)\int dS\int (\underset{\sim}{\Omega}_o\cdot\underset{\sim}{n})[1-\exp(-R_m/\lambda)]d\Omega_o = \alpha_\infty\rho_\infty \tag{21}$$

where $\alpha_\infty\rho_\infty$ is the frequency of generation of ions at infinity.

The treatment assumes that absorption (recombination) occurs following collision at constant speed v so that the absorption frequency is also

$$\frac{dN_A}{dt} = (N\sigma v) \int_V \rho(\underset{\sim}{r})dV = (\frac{v}{\lambda})<\rho>V \qquad (22)$$

where σ is the cross section for collisions with the third bodies Z of density N. With the equivalence of (21) and (22) in (19), the escape probability (19) is then

$$<P_E> = <\rho>/\rho_\infty = \frac{1}{4\pi}(\lambda/V) \int_S dS \int_{\Omega_o} d\Omega_o(\underset{\sim}{\Omega}_o \cdot \underset{\sim}{n})[1-\exp(-R_m/\lambda)] \qquad (23)$$

which is precisely the relation (6) previously derived ab-initio without the connection (19). The fraction of ions that are absorbed within V is

$$f = (dN_A/dN_{EN}) = (4V/S\lambda)<P_E> \qquad (24)$$

which, for a sphere of radius R_T, reduces to

$$f = (4R_T/3\lambda)<P_E> \equiv W(R_T/\lambda) \qquad (25)$$

which is, as expected, simply the Thomson probability (10) for collision, within the trapping sphere, of ions which enter the sphere from an external bath.

The connection of $<P_E>$ to the rates of both problems is demonstrated by comparison of the rate

$$\alpha_\infty = \frac{<\rho>}{\rho_\infty} V(\frac{v}{\lambda}) = <P_E>V(\frac{v}{\lambda}) = \frac{1}{4} fSv \qquad (26)$$

obtained from (21) and (22) for recombination of ions entering S from infinity with the rate (7),

$$\alpha_V = [1-\langle P_E \rangle]Sv = [1-(\frac{4V}{S\lambda})f]Sv \qquad (27)$$

for recombination of ions generated isotropically within V at a uniform frequency. The appearance of f (≡ the Thomson probability W for a sphere) in both problems is now evident.

Moreover, the averaged density $\langle\rho\rangle$ within the reaction volume follows from (19) directly or from (26) where the frequency $\alpha_\infty\rho_\infty$ of ion production at infinity is set equal to the frequency $(v/\lambda)\langle\rho\rangle V$ of absorption within V to give

$$\langle\rho\rangle = \alpha_\infty\rho_\infty(\lambda/vV) \qquad (28)$$

irrespective of the mode of transport from inifinity to S. When α_∞ is controlled by reaction alone (i.e. α_∞ is $\frac{1}{4}$ fSv), then, for a spherical volume

$$\langle\rho\rangle = [(3/4x)W(x)]\rho_\infty \qquad (29)$$

which tends at low gas densities N (where $X = R_T/\lambda << 1$) to $\rho_\infty[1-3R_T/\lambda +...]$. The linear dependance on $N(\sim 1/\lambda)$ of α_∞ in (28) therefore arises from the constant term ρ_∞ in this expansion of $\langle\rho\rangle$ so that the recombination rate at low N follows directly by taking either $\langle\rho\rangle = \rho_\infty$ in (28) or $\langle P_E \rangle = 1$ in (26) to give

$$\alpha_\infty \xrightarrow{\lambda >> R_T} V(v/\lambda) = (4/3)\pi R_T^3(v/\lambda) \qquad (30)$$

thereby providing a one-line derivation (from (28)) of the Thomson N-linear

rate at low N. Nonlinear variation of α_∞ with N arises from the departure of $\langle P_E \rangle$ from unity.

In the presence of diffusional drift, the above Thomson rates (26) and (27) can be regarded as reaction rates (Flannery 1982a,b). As the gas density N increases then, for a sphere, the ratio (α_V/α_∞) increases from 2.25 to 4 when $\lambda \ll R_T$. The factor 4 is simply the relative measure of flux for both problems. This enhancement will favor an earlier onset with N of diffusional-drift which will eventually become the rate limiting step.

In summary, the partial recombination rate arising from $(X^+\text{-}Z)$ collisions for the (dilute-ionization) case of $(X^+\text{-}Y^-)$ approach from infinite separation at speed v_{12} is the Thomson rate,

$$\alpha_T = \pi R_T^2 v_{12} W(R_T/\lambda) \xrightarrow{\lambda>>R_T} (\tfrac{4}{3}\pi R_e^3)\beta^{-3}(v_{12}/\lambda) \; ; \qquad \beta=3/2 \; , \qquad (31)$$

(which incidentally identifies R_e as the natural unit (e^2/kT) for volume recombination). This is to be compared with the corresponding rate

$$\alpha_V = 4\pi R_T^2 v_{12}[1 - (3\lambda/4R_T)W(R_T/\lambda)] \qquad (32)$$

$$\xrightarrow{\lambda>>R_T} \frac{9}{4}(\tfrac{4}{3}\pi R_e^3)\beta^{-3}(v_{12}/\lambda) = \frac{9}{4}\alpha_T$$

for the present (dense ionization) case where a steady-state distribution of ions X^+ is maintained by constant-frequency isotopic sources (8) distributed uniformly within the reactive sphere centered at Y^-. The full rate is the sum of the partial rates based on X^+-Z and Y^--Z collisions. So as to account for the inefficiency of energy transfer between dissimilar masses, the Thomson-rate (31) can be multiplied by a mass-dependent efficiency factor designed to

reproduce the highly accurate rates (cf Flannery 1982b) obtained from solution of the conventional collisional input-output Master Equation at low gas densities. This overall normalization should not affect the basic connection between (31) and (32), or the basic prediction that the effect of the distinction (A) between the cases of dilute and high degrees of ionization is to increase the recombination rate (by a factor ~ 9/4).

The effect of ion-ion collisions (B) can now be incorporated directly within (32) by regarding (Bates 1982) third bodies Z as ions X^+(or Y^-). Thomson- recombination between ions of separation $R < R_T = (2/3)e^2/kT$ occurs upon any collision which is assumed to transfer energy $\Delta E > (3/2)kT$. For ion-ion Coulomb scattering between equal masses at relative energy (3/2)kT, this energy is transferred provided the (CM) scattering angle is greater than $(\pi/2)$. The cross section for such collisions, after a straightforward exercise, is

$$\sigma = (1/9)\pi R_e^{\ 2} \tag{33}$$

In a gas of electrons of mass m and density N^-, (33) in (31) yields

$$\alpha_T^{(e)} = (4\pi^2/27\beta^3)(8kT/\pi m)^{1/2} R_e^{\ 5} N^- \tag{34}$$

$$\equiv 3.5\ 10^{-9} T^{-4.5} N^- \ (cm^3 s^{-1})$$

for the rate of electron-ion collisional recombination which, remarkably, is 92% of the identical collisional rates (Mansbach and Keck 1967, Stevefelt et al. 1975) based on the detailed Master Equation. Generalization of (34) to cover ion-ion recombination in an ion gas may be deduced as in Bates (1982). Incorporation of ion-ion collisions within (32) will also increase the

recombination rate, particularly for ion-densities $N^{\pm} \gtrsim 10^{15}$ cm^{-3} and lower temperatures (Bates 1982).

In conclusion, the rate for recombination of ions distributed uniformly within a reaction volume V has been shown to be a factor of (9/4) greater than the rate for ions which approach the reaction sphere from infinity. These two situations are respectively appropriate to the present examination of the effect of distinctions A and B (in isolation from C and D) on the cases of high and dilute ionization, respectively. In so doing, a valuable relationship (19) which connects the two distinct problems of approach from infinity and of escape from a confined volume of generation has been uncovered.

Acknowledgment.

This research is supported by the U. S. Air Force Office of Scientific Research under Grant No. AFOSR-84-02333.

References

Bates D R 1981 J. Phys. B:At. Mol. Phys. **14** L115-9

Bates D R 1982 J. Phys. B:At. Mol. Phys. **15** L755-8

Flannery M R 1981 Chem. Phys. Lett. **80** 531-6

Flannery M R 1982a Phil. Trans. Roy. Soc. A **304** 447-97

Flannery M R 1982b Applied Atomic Collision Physics. Vol. 3:Gas Laser ed H S W Massey, B Bederson and E W McDaniel (New York:Academic) Chap 5

Loeb L B 1955 Basic Processes of Gaseous Electronics (Berkeley:University of California Press) Chap. 6

Mansbach P and Keck J 1969 J. Chem. Phys. **181** 275-89

Morgan W L, Bardsley J N, Lin J and Whitten B L 1982 Phys. Rev., A **26** 1696-1703

Stevefelt J, Boulmer J and Delpech J-F 1975 Phys. Rev. A 12 1246

Thomson, J J 1924 Phil. Mag. 47 337-378.

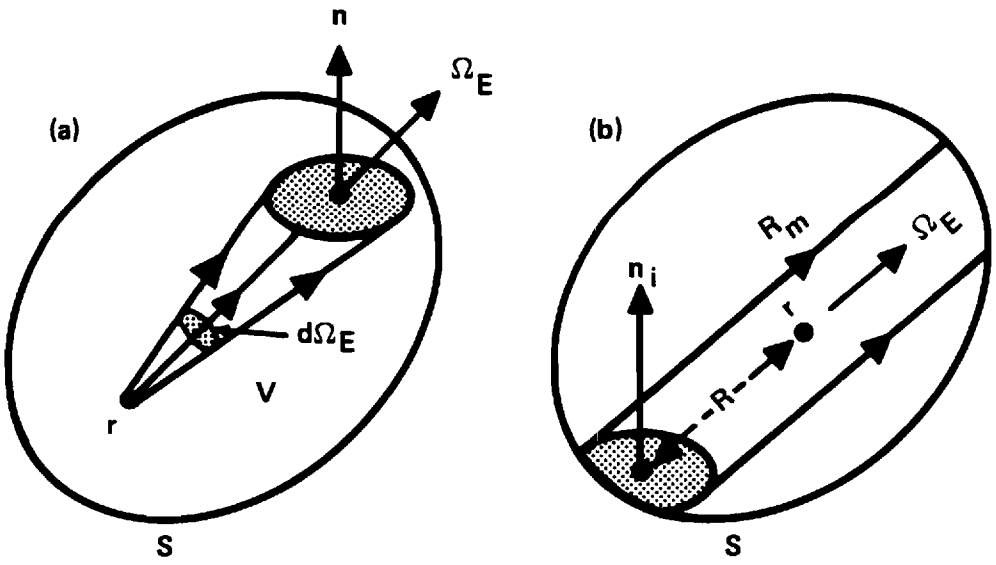

Figure 1: (a) Ions borns at point $\underset{\sim}{r}$ within volume V enclosed by surface S escape within solid angle $d\underset{\sim}{\Omega}_E$ through elemental area with outward normal $\underset{\sim}{n}$. (b) Elemental volume $dV = (\underset{\sim}{\Omega}_E \cdot \underset{\sim}{n}_i)dSdR$ of tubes with axis along $\underset{\sim}{\Omega}_E$ at angle to inward normal $\underset{\sim}{n}_i$ of surface element dS. R_m is maximum chord length for specified directions $\underset{\sim}{n}_i$ and $\underset{\sim}{\Omega}_E$.

REPORT DOCUMENTATION PAGE

1a. REPORT SECURITY CLASSIFICATION UNCLASSIFIED	1b. RESTRICTIVE MARKINGS
2a. SECURITY CLASSIFICATION AUTHORITY	3. DISTRIBUTION/AVAILABILITY OF REPORT Approved for public release; distribution unlimited.
2b. DECLASSIFICATION/DOWNGRADING SCHEDULE	
4. PERFORMING ORGANIZATION REPORT NUMBER(S) GIT-85-008	5. MONITORING ORGANIZATION REPORT NUMBER(S) N/A
6a. NAME OF PERFORMING ORGANIZATION Georgia Institute of Technology 6b. OFFICE SYMBOL (If applicable)	7a. NAME OF MONITORING ORGANIZATION Air Force Office of Scientific Research (AFOSR) Directorate of Physical and Geophysical Science
6c. ADDRESS (City, State and ZIP Code) School of Physics Georgia Institute of Technology Atlanta, Georgia 30332	7b. ADDRESS (City, State and ZIP Code) AFOSR/NP Bolling Air Force Base, Bldg. 410 Washington, D. C. 20332-6448
8a. NAME OF FUNDING/SPONSORING ORGANIZATION AFOSR 8b. OFFICE SYMBOL (If applicable) NP	9. PROCUREMENT INSTRUMENT IDENTIFICATION NUMBER AFOSR-84-0233
8c. ADDRESS (City, State and ZIP Code) Building 410 Bolling AFB, D.C. 20332-6448	10. SOURCE OF FUNDING NOS. PROGRAM ELEMENT NO. 61102F; PROJECT NO. 2301; TASK NO. A4; WORK UNIT NO. N/A
11. TITLE (Include Security Classification) Termolecular Association (UNCL)	
12. PERSONAL AUTHOR(S) M. R. Flannery	
13a. TYPE OF REPORT Annual Technical Report 13b. TIME COVERED FROM 7/1/85 TO 6/30/86	14. DATE OF REPORT (Yr., Mo., Day) 1/21/87 15. PAGE COUNT
16. SUPPLEMENTARY NOTATION	

17. COSATI CODES			18. SUBJECT TERMS (Continue on reverse if necessary and identify by block number)
FIELD	GROUP	SUB. GR.	Termolecular, Association, Atomic Collisions, Electron-Atom.
N/A	N/A	N/A	

19. ABSTRACT (Continue on reverse if necessary and identify by block number)

Research has been initiated and conducted (a) on Termolecular Association in Gases and (b) on electron-excited atom collisions.

A microscopic theory of ion-atom association in a gas was formulated. Connection with previous macroscopic treatments was established, and various dilemmas with previous macroscopic formula were noted and resolved. The present theory yields a much more accurate representation of the variation of the termolecular rate with gas density.

A ten-channel eikonal treatment of electron-helium collisions was performed for a basis set of (1^1S, 2^1S, 2^1P, 3^1S, 3^1P, 3^1D) target states to yield the first theoretical results for the very basic orientation and alignment parameters for the 3^1D level of helium. Good agreement with recent measurements of the coincidence rate between the electron scattered inelastically in a given direction and the ($2^1P \rightarrow 1^1S$) photon emitted in the cascade transition $3^1D \rightarrow 2^1P \rightarrow 1^1S$ was obtained.

20. DISTRIBUTION/AVAILABILITY OF ABSTRACT UNCLASSIFIED/UNLIMITED ☒ SAME AS RPT. ☐ DTIC USERS ☐	21. ABSTRACT SECURITY CLASSIFICATION UNCLASSIFIED
22a. NAME OF RESPONSIBLE INDIVIDUAL Dr. Ralph E. Kelley	22b. TELEPHONE NUMBER (Include Area Code) (202) 767-4908 22c. OFFICE SYMBOL NP

Contents

Abstract

During this second year of the grant, research has been initiated and conducted (a) on Termolecular Association in Gases and (b) on electron-excited atom collisions.

A microscopic theory of ion-atom association in a gas was formulated. Connection with previous macroscopic treatments was established, and various dilemmas with previous macroscopic formula were noted and resolved. The present theory yields a much more accurate representation of the variation of the termolecular rate with gas density.

A ten-channel eikonal treatment of electron-helium collisions was performed for a basis set of (1^1S, 2^1S, 2^1P, 3^1S, 3^1P, 3^1D) target states to yield the first theoretical results for the very basic orientation and alignment parameters for the 3^1D level of helium. Good agreement with recent measurements of the coincidence rate between the electron scattered inelastically in a given direction and the ($2^1P \rightarrow 1^1S$) photon emitted in the cascade transition $3^1D \rightarrow 2^1P \rightarrow 1^1S$ was obtained.

1. Research Initiated and Completed

1.1 List of Topics

During the second year (7/1/85 - 6/30/86) of the Grant, theoretical research on the following topics was initiated, completed and written up for publication in scientific journals.

(A) The Rate for Transport-Influenced Reactions

(B) Basic Expression for the Rates of Termolecular Recombination and Dissociation

(C) Connection between Microscopic and Thomson theories of Recombination

(D) Orientation and Alignment Parameters for e-He($1^1S \rightarrow 3^1D$) Collisions

(E) Macroscopic and Microscopic Perspectives of Termolecular Reactions in Physics of Atoms and Molecules

1.2 Summary of Topics

A summary of each of the above topics (A)-(E) now follows. Full details of each topic are presented in Appendices (A)-(E) of this report.

Topic (A): The Rate for Transport-Influenced Reactions

The termolecular rate α_{∞} for transport-influenced reactions between species A and B in a gas M is expressed in terms of the averaged probability (P_E) of escape of pairs from the reaction zone. This procedure permits rigorous identification of the local (reaction) rate α_3 at the edge of the reaction zone, which is left unassigned by the Debye-Smoluchowski treatment.

Topic (B): Basic Expression for the Rates of Termolecular Recombination and Dissociation

It is noted that the usual identification of the rate $R^A(t)$ for termolecular recombination at time t with the downward current past a bound energy level is appropriate to cases which involve energy distributions that

satisfy the quasi-steady-state (QSS) condition to the exact master equation. A general expression for $R^A(t)$ is derived which is valid for both QSS and non-QSS distributions, such as those non-QSS distributions obtained from both the diffusional and variational methods or from numerical approximation to the exact QSS condition.

Topic (C): Connection Between Microscopic and Thomson Theories of Termolecular Recombination

By making certain key assumptions in the microscopic theory of termolecular ion-ion recombination in a gas, a firm connection with the Thomson treatment is established.

Topic (D): Orientation and Alignment Parameters for e-He($1^1S \rightarrow 3^1D$) Collisions

A ten channel eikonal treatment of electron-helium collisions is performed for a basis set of (1^1S, 2^1S, 2^1P, 3^1S, 3^1P and 3^1D) target states to yield the first theoretical results for the orientation and alignment parameters for the 3^1D level of helium. Good agreement with recent measurements is obtained.

Topic (E): Macroscopic and Microscopic Perspectives of Termolecular Reactions

A microscopic theory of termolecular association

$$A^+ + B + M \rightarrow AB^+ + M$$

of ion A^+ and atom B in a gas M was developed. Connection with previous macroscopic treatments was established and a hierarchy of relevant approximations was established.

1.3 Paper Presented at Scientific Meetings

The following paper

1. "Variational Principle for Association/Dissociation in Dense Gases", by M. R. Flannery was presented at the 38th Annual Gaseous Electronics Conference, October 15-18, 1985, at the Naval Postgraduate School, Monterey, California. The abstract is:

A new Variational Principle is presented for the rate $R^A(t)$ of evolution towards equilibrium of a non-equilibrium distribution of (A-B) pairs, either associated or dissociated, in a gas M. An expression for $R^A(t)$ is developed in terms of the probabilities P^A_i for association of pairs with internal energy E_i. With simple variational analytical functions for P^A_i, application of the Variational Principle yields minima which are in exact agreement with detailed numerical results of the more time-consuming Quasi-Steady-State Method which, in principle involves the solution of an integral equation for P^A_i and provides the minimum to $R^A(t)$. The new expression for R^A is also very valuable when approximate P^A_i, as those given by the diffusion treatment, are adopted. Results will be illustrated.

Appendix A

The Rate for Transport-Influenced Reactions

J. Phys. B: At. Mol. Phys. 18 (1985) L747-L749. Printed in Great Britain

LETTER TO THE EDITOR

The rate for transport-influenced reactions

M R Flannery

School of Physics, Georgia Institute of Technology, Atlanta, Georgia 30332, USA

Received 22 August 1985

Abstract. The termolecular rate α_∞ for transport-influenced reactions between species A and B in a gas M is expressed in terms of the averaged probability ($\mathcal{P}_E$) of escape of pairs from the reaction zone. This procedure permits rigorous identification of the local (reaction) rate α_3 at the edge of the reaction zone, which is left unassigned by the Debye-Smoluchowski treatment.

Consider the association (recombination) reaction between species A and B in a gas M by collisions between the pair (A-B) and M. The intramolecular current of A and B with relative diffusion coefficient D and relative mobility K in the gas M is (see, for example, recent reviews by Bates (1985) and by Flannery (1982))

$$J(R) = -D\nabla\rho(R) + (K/e)(\nabla V(R))\rho(R)$$
$$= -D\exp(-V/kT)\nabla[\rho(R)\exp(V/kT)] \tag{1}$$

where $\rho(R)\,d\boldsymbol{R}$ is the density of (A − B) pairs with internal separation $\boldsymbol{R}$ in the interval $d\boldsymbol{R}$ about $\boldsymbol{R}$, and where $V(R)$ is the internal interaction between A and B. An alternative picture (used here) is that J is the net outward current at R of particles A with density ρ from a fixed central species B. Reaction occurs within a (spherical) volume $\mathcal{V}$ with radius S centred at B. In the steady state the solution of the continuity equation

$$\nabla \cdot J = 0 \tag{2}$$

subject to the asymptotic boundary condition that $\rho \to \rho_\infty$ as $R \to \infty$, yields the constant flux

$$-4\pi R^2 J(R) = \alpha_\infty \rho_\infty \tag{3}$$

where α_∞ is the required termolecular association (recombination) rate. The solution of equation (3) with (1) then yields the density

$$\rho_s = \rho_\infty \exp(-V(S)/kT)(1 - \alpha_\infty/\alpha_{TR}) \tag{4}$$

at the edge S of the assumed reaction zone $R \leq S$ where the steady-state rate α_{TR} for transport from infinity is

$$\alpha_{TR} = 4\pi D\left(\int_S^\infty R^{-2}\exp(V/kT)\,dR\right)^{-1} \equiv 4\pi D\tilde{S}. \tag{5}$$

The key point here is that in the steady state

$$\alpha_\infty \rho_\infty = \langle\rho\rangle\mathcal{V}\left(\frac{v_A}{\lambda_A} + \frac{v_B}{\lambda_B}\right) \equiv \langle\rho\rangle\mathcal{V}(v/\lambda) \tag{6}$$

0022-3700/85/210747+03$02.25

where (v/λ) is the frequency of (A–B) collisions with the gas at relative speed v, and $\langle\rho\rangle$ is the average density of A *within* the reaction volume $\mathcal{V}$ centred at B. The mean free path of A with speed v_A or B with speed v_B in M is $\lambda_{A,B}$. It has already been shown (Flannery 1985) that $\langle\rho\rangle$ and ρ_s are related in a Thomson-style treatment (constant speed v, full absorption upon collision within $\mathcal{V}$) by the averaged probability

$$\langle\mathscr{P}_E\rangle = \langle\rho\rangle/\rho_s \tag{7}$$

of escape of pairs to outside the volume $\mathcal{V}$. Hence equation (6) yields

$$\alpha_\infty = \langle\mathscr{P}_E\rangle\mathcal{V}(v/\lambda)(\rho_s/\rho_\infty). \tag{8}$$

An expression for $\langle\mathscr{P}_E\rangle$ has been derived (Flannery 1985) but is not required here. With the aid of the diffusional-drift result (4), equation (8) can now be solved for α_∞ to give the conventional result (see e.g. Flannery 1982)

$$\alpha_\infty = \alpha_{RN}\alpha_{TR}/(\alpha_{RN}+\alpha_{TR}) \tag{9}$$

but with the rate of reaction within $\mathcal{V}$ defined by

$$\alpha_{RN} = \langle\mathscr{P}_E\rangle\mathcal{V}(v/\lambda)\exp(-V(S)/kT). \tag{10}$$

If $\mathcal{V}$ is a spherical volume of radius $S = R_T$, then for straight-line A–B motion the averaged probability reduces to (Flannery 1985)

$$\langle\mathscr{P}_E\rangle = (3\lambda/4R_T)W(R_T/\lambda) \tag{11}$$

where

$$W(X) = 1-(1/2X^2)[1-(1+2X)\exp(-2X)] \tag{12}$$

is the (Thomson) probability for an A–M collision with straight-line relative motion within the reaction volume $\mathcal{V}$. Hence the reaction rate (10) in this instance is

$$\alpha_{RN} = \pi R_T^2 W(R_T/\lambda)\exp(-V(R_T)/kT). \tag{13}$$

Although this analysis has reproduced the customary relation (9) for transport-influenced reactions, it has done so by addressing the important point of what happens *within* the sink region. In the conventional Debye–Smoluchowski model (Debye 1942, Smoluchowski 1917, Flannery 1982) reaction (absorption) is assumed to occur at the edge S of the sink at a local frequency $\alpha_3\rho_s$ such that solution of the continuity equation (2), subject to both the asymptotic condition ($\rho \to \rho_\infty$ as $R \to \infty$) and to the 'radiation' boundary condition

$$-4\pi S^2 J(S) = \alpha_3\rho_s \tag{14}$$

at the sink, yields (9) with

$$\alpha_{RN} = \alpha_3\exp(-V(S)/kT). \tag{15}$$

In the conventional treatment this local rate α_3 remains unassigned (since the physics of the sink's interior is left unspecified) whereas the present treatment has now explicitly identified α_3 as

$$\alpha_3 = \langle\mathscr{P}_E\rangle\mathcal{V}(v/\lambda) \tag{16}$$

where an expression for $\langle\mathscr{P}_E\rangle$ has already been provided (Flannery 1985) for any surface geometry enclosing the volume $\mathcal{V}$. This advance has been made possible by the valuable relationship (7) previously reported (Flannery 1985). It is worth noting

that the single-speed treatment here can be easily generalised to cover a distribution over speeds v; only the averaging procedure is affected.

Therefore, by equating the frequency (3) for diffusional drift to the frequency (6) of absorption *within* the sink, the expression (9) for the rate of transport-influenced reactions has been reproduced in terms of a reaction rate (10) expressed in terms of the averaged probability ($\mathscr{P}_E$) of escape from the reaction volume $\mathscr{V}$. In so doing the local rate α_3 in (14), which appears in models based on the premise that reaction occurs with frequency $\alpha_3\rho_s$ at the edge of the sink, has been clearly and rigorously identified by equation (16).

This research is supported by the US Air Force Office of Scientific Research under Grant No AFOSR-84-0233.

References

Bates D R 1985 *Advances in Atomic and Molecular Physics* vol 20, ed D R Bates and B Bederson (New York: Academic) ch 1

Debye P 1942 *Trans. Electrochem. Soc.* **82** 265-72

Flannery M R 1982 *Applied Atomic Collision Physics* vol 3 *Gas Lasers* ed H S W Massey, B Bederson and E W McDaniel (New York: Academic) ch 5

—— 1985 *J. Phys. B: At. Mol. Phys.* **18** L531-7

Smoluchowski M v 1917 *Z. Phys. Chem.* **92** 129-68

Appendix B

Basic Expression for the Rates of Termolecular Recombination and Dissociation

J. Phys. B: At. Mol. Phys. 18 (1985) L839–L844. Printed in Great Britain

LETTER TO THE EDITOR

Basic expression for the rates of termolecular recombination and dissociation

M R Flannery

School of Physics, Georgia Institute of Technology, Atlanta, Georgia 30332, USA

Received 17 September 1985

Abstract. It is noted that the usual identification of the rate $R^{A}(t)$ for termolecular recombination at time t with the downward current past a bound energy level is appropriate to cases which involve energy distributions that satisfy the quasi-steady-state (QSS) condition to the *exact* master equation. A general expression for $R^{A}(t)$ is derived which is valid for both QSS and non-QSS distributions, such as those non-QSS distributions obtained from both the diffusional and variational methods or from numerical approximation to the exact QSS condition.

The net rate $R^{A}(t)$ for recombination at time t via the termolecular process

$$A^{+} + B^{-} + M \underset{k}{\overset{\alpha}{\rightleftarrows}} AB + M \tag{1}$$

which proceeds in the forward direction with effective two-body rate $\alpha(\mathrm{cm^3\,s^{-1}})$ and in the reverse direction with frequency k $(\mathrm{s^{-1}})$ and which involves energy changing collisions between the pair $(A^{+}\text{-}B^{-})$ of ions and the constituents M of a thermal gas bath is given under quasi-steady-state conditions by

$$R^{A}(t) = -J_i(E_i, t) \tag{2}$$

the net downward current $(-J_i)$ in energy space of pairs past a bound energy level E_i of AB. The separation between the energy levels AB is sufficiently small in comparison with the thermal energy (kT) of the bath species M. The levels therefore form a quasi-continuum so that $n_i(E_i, t)\,\mathrm{d}E_i$ is the number density $(\mathrm{cm^{-3}})$ of AB pairs with internal energy E_i in the interval $\mathrm{d}E_i$ about E_i. There exists a block $\mathscr{S}$ of low-lying levels in the energy range $-S \geqslant E_i \geqslant -D$ of tightly bound AB pairs which are stable against *direct* dissociative collisions with the thermal M. The energy of the lowest bound level of AB is $-D$ with respect to the dissociation limit, taken as zero energy, and the energy level $-S$ arises quite naturally from the collisional dynamics via the cut-off effect of the Maxwellian distribution of the gas bath.

The reasons for the present letter are: (i) to note that equation (2) follows only when the energy distribution n_i of pairs in the highly-excited block $\mathscr{E}$ of levels lying between the dissociation limit and $-S$ is in exact quasi-steady-state (QSS) i.e.,

$$\partial n_i(E_i, t)/\partial t = 0 \qquad 0 \geqslant E_i \geqslant -S \tag{3}$$

as in the time-independent treatment of Bates and Moffett (1966) and of Bates and Flannery (1968), and (ii) to derive a general expression for the rate $R^{A}(t)$ pertinent

0022-3700/85/240839+06$02.25

to non-QSS situations and to cases which involve the use of approximate distributions n_i as provided, for example, by the diffusional equation (Pitaevskii 1962, Keck and Carrier 1965, Flannery 1986b), by variational techniques (Flannery 1986a) or by approximate (iterative) numerical procedures.

In the limit of low gas densities, the conventional input-output master equation that governs the distribution $n_i(E_i, t)\,\mathrm{d}E_i$ for the density (cm^{-3}) of subsystems AB with internal energy E_i in the interval $\mathrm{d}E_i$ about E_i can be written as (cf Flannery 1986a)

$$\frac{\partial}{\partial t} n_i(E_i, t) = -\int_{-D}^{\infty} S_{if}(t)\,\mathrm{d}E_f \equiv -\frac{\partial}{\partial E_i} J_i(E_i, t) \tag{4}$$

where the *net* two-level input-output collisional rate of depletion of energy level E_i at time t is

$$S_{if}(t) = n_i(E_i, t)\nu_{if}(E_i, E_f) - n_f(E_f, t)\nu_{fi}(E_f, E_i) = -S_{fi}(t) \tag{5}$$

in terms of $\nu_{if}\,\mathrm{d}E_f$, the frequency (s^{-1}) for $i \to f$ transitions which change the energy E_i to between E_f and $E_f + \mathrm{d}E_f$ by collision of the (A^+-B^-) pair with the gas M. The net upward current J_i in energy space past level E_i is therefore determined either by the integral expression,

$$J_i(E_i, t) = \int_{E_i}^{\infty} \mathrm{d}E_i \int_{-D}^{\infty} S_{fi}(t)\,\mathrm{d}E_f = \int_{E_i}^{\infty} \mathrm{d}E_i \int_{-D}^{E_i} S_{fi}(t)\,\mathrm{d}E_f \tag{6}$$

with the aid of the null effect, $S_{if} + S_{fi} = 0$, of collisions, or by the equivalent expression,

$$J_i(E_i, t) = \int_{-D}^{E_i} \mathrm{d}E_i \int_{-D}^{\infty} S_{if}(t)\,\mathrm{d}E_f = \int_{-D}^{E_i} \mathrm{d}E_i \int_{E_i}^{\infty} S_{if}(t)\,\mathrm{d}E_f \tag{7}$$

since the current past the end points $(-D, \infty)$ vanishes. The quasi-steady-state (QSS) treatment is therefore based on the solution of equations (3)-(5) so that the rate (2) is given by the current (6) or (7) which is constant over all energy levels E_i in block $\mathscr{E}$.

Although the system (1) is considered by equation (4) as closed, owing to the explicit neglect of mechanisms other than (A^+-B^-)-M collisions such as one-way mutual neutralisation $\mathrm{A}^+ + \mathrm{B}^- \to \mathrm{AB}^* \to \mathrm{A}^* + \mathrm{B}$, quantum tunnelling $\mathrm{AB} \to \mathrm{A} + \mathrm{B}$ and radiative transitions $\mathrm{AB}^* \to \mathrm{AB} + h\nu$, the above master equation (4) is easily modified to cover more general cases such as collisional-radiative recombination (Bates *et al* 1962) in a plasma. Integration over the quasi-continuum can also be replaced by a corresponding summation over discrete levels so that processes such as electron-ion recombination in a gas can be accurately described. These generalisations do not affect the following basic argument.

In general, the overall rate of association is (Flannery 1986a),

$$R^{\wedge}(t) = \int_{-D}^{\infty} P_i^{\wedge}(E_i)(\partial n_i/\partial t)\,\mathrm{d}E_i = \int_{-D}^{\infty} J_i(E_i, t)(\partial P_i^{\wedge}/\partial E_i)\,\mathrm{d}E_i \tag{8}$$

where $P_i^{\wedge}(E_i)$ is the probability that pairs with energy E_i are collisionally coupled to the fully associated block $\mathscr{S}$. Introduce the distribution,

$$\gamma_i(E_i, t) = n_i(E_i, t)/\tilde{n}_i(E_i) \xrightarrow{t \to \infty} 1 \tag{9}$$

normalised to the density $\tilde{n}_i$ appropriate to full thermodynamic equilibrium with the gas bath. Assume that the energy distributions of (fully dissociated) pairs ($\mathrm{A}^+ + \mathrm{B}^-$) in

the continuum block $\mathscr{C}$, $0 \leq E_i \leq \infty$, and of (fully associated) pairs AB in the lowest block $\mathscr{S}$, $-D \leq E_i \leq -S$, are in thermal equilibrium with M so that the corresponding normalised distributions,

$$\gamma_c(t) = \left(\int_0^\infty n_i(E_i, t)\,dE_i\right)\left(\int_0^\infty \tilde{n}_i(E_i)\,dE_i\right)^{-1} = (N_A(t)N_B(t))/\tilde{N}_A\tilde{N}_B \xrightarrow{t\to\infty} 1 \qquad (10a)$$

in block $\mathscr{C}$ and

$$\gamma_s(t) = n_s(t)/\tilde{n}_s = \left[\int_{-D}^{-S} n_i(E_i, t)\,dE_i\left(\int_{-D}^{-S} \tilde{n}_i(E_i)\,dE_i\right)^{-1}\right] \xrightarrow{t\to\infty} 1 \qquad (10b)$$

in block $\mathscr{S}$, are pure functions only of time t. The non-equilibrium distributions at time t are $N_{A,B}(t)$ and $n_s(t)$ for the fully dissociated and associated species, respectively, and the corresponding thermodynamic equilibrium values are $\tilde{N}_{A,B}$ and $\tilde{n}_s$, respectively. Since no internal one-way sources and sinks exist within the intermediate excited block $\mathscr{E}$, the normalised energy distribution of pairs in block $\mathscr{E}$ can then be expressed by the linear combination of time-dependent strengths of external sources and sinks as,

$$\gamma_i(E_i, t) = P_i^D(E_i)\gamma_c(t) + P_i^A(E_i)\gamma_s(t) \xrightarrow{t\to\infty} 1 \qquad (11)$$

which identifies P_i^D and P_i^A as the probabilities that pairs with internal energy E_i are collisionally coupled to the continuum (source) block $\mathscr{C}$ and to the (bound) sink block $\mathscr{S}$, respectively, i.e., $P_i^{A,D}$ are the probabilities of association (A) and dissociation (D) respectively, as implied in (8). Alternatively, $P_i^{A,D}$ are the probabilities for external stabilisation (A) or disruption (D) of pairs in bound level E_i by subsequent multi-collisions with M. Since the system is closed, the sum $(P_i^A + P_i^D)$ is unity so that the net rate of dissociation,

$$R^D(t) = \int_{-D}^{\infty} P_i^D(E_i)(\partial n_i/\partial E_i)\,dE_i \qquad (12)$$

when added to (8), the net rate of association, yields

$$R^A(t) + R^D(t) = \int_{-D}^{\infty} (\partial n_i/\partial t)\,dE_i = 0 \qquad (13)$$

zero, as expected.

In block $\mathscr{S}$, P_i^A is unity and P_i^D is zero, and in block $\mathscr{C}$, P_i^D is unity and P_i^A is zero, by definition, so that the ansatz (11) incorporates both (10*a*) and (10*b*). The master equation (4) then separates in E_i and t, under (11), as

$$(\partial n_i/\partial t) = -(\gamma_c(t) - \gamma_s(t))\left(\int_{-D}^{\infty} (P_f^A - P_i^A)C_{if}\,dE_f\right) \qquad (14)$$

and the current (7) separates as

$$J_i(E_i, t) = (\gamma_c(t) - \gamma_s(t))\left(\int_{E_i}^{\infty} dE_i \int_{-D}^{E_i} (P_f^A - P_i^A)C_{if}\,dE_f\right) \qquad (15a)$$

$$= (\gamma_c(t) - \gamma_s(t))j_i(E_i) \qquad (15b)$$

in terms of the background current j_i. The one-way equilibrium collisional rate

$$C_{if}(E_i, E_f) = \tilde{n}_i(E_i)\nu_{if}(E_i, E_f) = \tilde{n}_f(E_f)\nu_{fi}(E_f, E_i) = C_{fi}(E_f, E_i) \qquad (16)$$

between levels i and f satisfies detailed balance.

The net rate (8) similarly factors

$$R^{\wedge}(t) = (\gamma_c(t) - \gamma_s(t))\left(\int_{-D}^{\infty} P_i^{\wedge}\,dE_i \int_{-D}^{\infty} (P_i^{\wedge} - P_f^{\wedge})C_{if}\,dE_f\right) \tag{17a}$$

$$= \tfrac{1}{2}(\gamma_c(t) - \gamma_s(t))\left(\int_{-D}^{\infty} dE_i \int_{-D}^{\infty} (P_i^{\wedge} - P_f^{\wedge})^2 C_{if}\,dE_f\right). \tag{17b}$$

Since the effective two-body constant $\alpha(\mathrm{cm^3\,s^{-1}})$ for association and the frequency constant k $(\mathrm{s^{-1}})$ for dissociation in (1) are related to the overall rates $R^{\wedge}(t)$ by

$$R^{\wedge}(t) = \alpha N_A(t) N_B(t) - k n_s(t) = -R^{D}(t) \tag{18}$$

$$= \alpha \tilde{N}_A \tilde{N}_B(\gamma_c(t) - \gamma_s(t)) = -k\tilde{n}_s(\gamma_s(t) - \gamma_c(t)) \tag{19}$$

they are therefore determined by the time-independent part of (17) i.e., by

$$\alpha \tilde{N}_A \tilde{N}_B = \left(\int_{-D}^{\infty} P_i^{\wedge}\,dE_i \int_{-D}^{\infty} (P_i^{\wedge} - P_f^{\wedge})C_{if}\,dE_f\right) = k\tilde{n}_s \tag{20}$$

which is the present basic expression to be used whether or not the probabilities $P_i^{\wedge}$ are known exactly.

When one-way mutual neutralisation is assumed to depopulate the $\mathscr{S}$ block instantaneously in comparison with collisional vibrational relaxation then $\gamma_s(t)$ in the foregoing analysis vanishes.

A new rigorous variational principle (Flannery 1986a, c) for association/dissociation processes (1) or, in general, for chemical reactions in gases, asserts that the probabilities $P_i^{\wedge}$ are so distributed that the rate (8) at any time t is a minimum and that as a consequence of conditions (10*a*, *b*) the distribution $n_i(E_i, t)$ in the excited block $\mathscr{E}$ is in quasi-steady-state (see also Bates 1974, Mendaš 1979) i.e.,

$$[\partial n_i(E_i, t)/\partial t] = 0 = -[\partial J_i(E_i, t)/\partial E_i] \qquad 0 \geqslant E_i \geqslant -S \tag{21}$$

so that, with the aid of (14), the probabilities $P_i^{\wedge,D}$ then satisfy the integral equation,

$$P_i^{\wedge,D} \int_{-D}^{\infty} C_{if}\,dE_f = \int_{-D}^{\infty} P_f^{\wedge,D} C_{if}\,dE_f \tag{22}$$

which is analogous to the time-independent quasi-equilibrium method pioneered by Bates and associates (cf Bates 1985) for the highly non-equilibrium case $\gamma_c \gg \gamma_s$. Alternatively, the current $J_i(E_i, t)$ at a given time t is constant over all energies $-E$ of block $\mathscr{E}$. Since $P_i^{\wedge}$ is constant (zero in block $\mathscr{C}$ and unity in block $\mathscr{S}$), (8) directly yields the minimum rate to be the downward current,

$$R_*^{\wedge}(t) = \int_{-D}^{-S} (\partial n_i/\partial t)\,dE_i = -J(-E, t) \tag{23}$$

in accord with (2). With the aid of (19) and (15*b*) the minimum rate constants α_* and k_* are therefore determined from

$$\alpha_* \tilde{N}_A \tilde{N}_B = -j(-E) = \int_{-E}^{\infty} dE_i \int_{-D}^{-E} (P_f^{\wedge} - P_i^{\wedge})C_{if}\,dE_f = k_* \tilde{n}_s. \tag{24}$$

Upon recognition of the constant-current QSS condition (21) from the outset, (24) has been the fundamental expression (Bates and Moffett 1966, Bates and Flannery 1968, Bates 1985) based on the equivalence of the rates of disappearance of fully dissociated

pairs and the rate of appearance of fully associated pairs via a constant net current, $-j(E)$, of pairs past bound level $-E$ in the intermediate block $\mathscr{E}$. Equation (24) also follows from the direct use of the QSS condition (22) in the basic equation (20).

When, however, the probabilities $P_i^{A,D}$ can only be derived from some procedure other than from the exact numerical solution of the exact QSS condition (22) to the master equation (4), the exact current (15) is not constant through block $\mathscr{E}$ and the more basic expressions (17) for the time-dependent rate $R^A(t)$ and (20) for the rate constants α and k must therefore be used instead of the derived expressions (23) and (24) which only follow from (17) and (20) on invoking the exact QSS condition (21) or (22) to the exact master equation (4). Nor are the expressions (23) and (24) appropriate for *approximate* numerical solutions to (22), or when the following important diffusional and variational methods are used to evaluate $P_i^{A,D}$.

(i) *The diffusional treatment.* A Fokker–Planck analysis can be adopted to reduce the integral collisional (discontinuous) term on the right-hand side of the master equation (14) to a differential (streaming) form so that the diffusion-in-energy equation (Flannery 1986b)

$$\partial n_i/\partial t = -(\gamma_c(t) - \gamma_s(t))\frac{\partial}{\partial E_i}(D_i^{(2)}\,\partial P_i^A/\partial E_i) \tag{25}$$

$$= -(\gamma_c(t) - \gamma_s(t))(\mathrm{d}j_d/\mathrm{d}E_i)$$

is obtained (cf Pitaevskii 1962, Keck and Carrier 1965, Lifshitz and Pitaevskii 1981), where half the equilibrium energy change squared per second

$$D_i^{(2)}(E_i) = \tfrac{1}{2}\int_{-D\to-\infty}^{\infty}(E_f - E_i)^2 C_{if}\,\mathrm{d}E_f \tag{26}$$

or second-order moment of the energy change, is analogous to the conventional diffusion coefficient in configuration space. The QSS solution of this *approximate* master equation (25) subject to the appropriate boundary conditions ($P_i^A(0) = 0$, $P_i^A(-S) = 1$) is

$$P_i^A(E_i) = \left(\int_{E_i}^{0}\mathrm{d}E/D^{(2)}(E)\right)\left(\int_{-S}^{0}\mathrm{d}E/D^{(2)}(E)\right)^{-1} \tag{27}$$

so that the corresponding QSS downward (diffusional) time-independent part of the current is obtained from (25) to give

$$-j_d = \int_{-S}^{0}\mathrm{d}E_i/D^{(2)}(E) = \alpha_P\tilde{N}_A\tilde{N}_B \tag{28}$$

which, when identified with the association rate $\alpha\tilde{N}_A\tilde{N}_B$ as prescribed by the customary relation (24), yields α_P, the rate constant obtained by Pitaevskii (1962) and by Keck and Carrier (1965). Although this rate α_P has been shown (Flannery 1986b) to agree with that calculated from (22) and (24) *only* for collisional electron–ion recombination in a gas, the case for which it was originally designed (Pitaevskii 1962), it involves great error when applied to general systems, such as ion–ion recombination in a gas (Bates and Zundi 1968, Flannery 1986b). The basic reason for this inadequacy is not that (27) is, in general, grossly inaccurate; (27), in fact, provides a good working approximation (Flannery 1986b). Rather, identification of the overall rate of association with the downward current as in (24) and (28) is *not* in general appropriate since the exact current (15) with the approximate probabilities (27) is *not* constant over

block $\mathcal{E}$. When the diffusional probabilities (27) are used directly in (17) or alternatively in (20) then, when compared with exact QSS rates determined from solution of (22) in (24), highly accurate results (Flannery 1986b) for termolecular ion–ion recombination rates associated with general mass systems are obtained. Only for the particular case for electron–ion recombination in a heavy gas are the currents (24) and (28) equal, being about three orders of magnitude less than for the general case, and any numerical difference between the use of (27) in (20) and (24) disappears (Flannery 1986b).

(ii) *The variational treatment.* When trial analytical functions for $P_i^{A,D}$ are adopted in a search for the minimum of (8), the appropriate procedure is variation of the integral (17) or alternatively of (20), and not of (2) or (24). The minimum so obtained is then the required rate (Flannery 1986c).

In summary, identification of the association (recombination) rate $R^A(t)$ or α for termolecular processes with the downward current (23) or (24) is restricted only to those cases for which the density distribution $n_i(E_i, t)$ is obtained exactly from the exact quasi-steady-state (QSS) condition (22) of the exact master equation (4). Expressions (17) and (20) derived here for $R^A(t)$ and α, respectively, are appropriate when QSS and non-QSS distributions are used, including those derived from approximate numerical procedures and from the important diffusional and variational methods.

This research is supported by the US Air Force Office of Scientific Research under Grant No AFOSR-84-0233.

References

Bates D R 1974 *Proc. R. Soc.* A **337** 15–20
—— 1985 *Advances in Atomic and Molecular Physics* vol 20, ed D R Bates and B Bederson (New York: Academic) ch 1
Bates D R and Flannery M R 1968 *Proc. R. Soc.* A **302** 367–83
Bates D R, Kingston and McWhirter R W P 1962 *Proc. R. Soc.* A **267** 297–312
Bates D R and Moffett R J 1966 *Proc. R. Soc.* A **291** 1–8
Bates D R and Zundi Z 1968 *J. Phys. B: At. Mol. Phys.* **1** 1145–8
Flannery M R 1986a *Phys. Rev.* A at press
—— 1986b *Phys. Rev.* A at press
Keck J C and Carrier G 1965 *J. Chem. Phys.* **43** 2284–98
Lifshitz E M and Pitaevskii L P 1981 *Physical Kinetics* (Oxford: Pergamon) ch 2
Mendaš I 1979 *J. Phys. B: At. Mol. Phys.* **12** L209–11
Pitaevskii L P 1962 *Sov. Phys.-JETP* **15** 919–21

Appendix C

Connection Between Microscopic and Thomson Theories of Termolecular Recombination

J. Phys. B: At. Mol. Phys. 19 (1986) L227-L233. Printed in Great Britain

LETTER THE THE EDITOR

Connection between microscopic and Thomson theories of termolecular recombination

M R Flannery
School of Physics, Georgia Institute of Technology, Atlanta, Georgia 30332, USA

Received 20 January 1986

Abstract. By making certain key assumptions in the microscopic theory of termolecular ion-ion recombination in a gas, a firm connection with the Thomson treatment is established.

The Thomson rate (Thomson 1924)

$$\alpha_T = \pi R_T^2 (8kT/\pi m)^{1/2} W(R_T/\lambda) \tag{1}$$

serves as a useful baseline at low gas densities N for comparison between various linear N dependencies (cf Bates 1985, Flannery 1982a) of effective two-body rates α ($cm^3\,s^{-1}$) for termolecular recombination,

$$A^- + B^- + M \rightarrow AB + M \tag{2}$$

between various systems of positive and negative ions, A^+ and B^-, of reduced mass m, in a gas M at temperature T. As N is raised beyond the linear region, equation (1) predicts a non-linear increase with N in accordance with physical intuition. The connection between (1) and the basic microscopic theory (Flannery 1982b) for the variation of α with N has not, however, as yet been established, nor has the actual N variation which is contained in equation (1) within the probability W for collisions between M and those pairs (A-B) with internal separations $R \leq R_T$, where R_T is some pre-assigned trapping radius within which reaction occurs. This (macroscopic) probability is

$$W(R_T/\lambda) = w(R_T/\lambda_A) + w(R_T/\lambda_B) - w(R_T/\lambda_A)w(R_T/\lambda_B) \tag{3}$$

where λ_A and λ_B are the mean free paths of A^- and B^- in the gas and the probability of an individual ion-atom collision within the R_T sphere centred at the other ion is (Loeb 1955)

$$w(X) = 1 - (1/2X^2)[1 - \exp(-2X)(1+2X)] \rightarrow \begin{cases} \frac{4}{3}X(1 - \frac{3}{4}X + \ldots) & N \rightarrow 0 \\ 1 & N \rightarrow \infty \end{cases} \tag{4}$$

assuming rectilinear ion-ion relative motion. Since $\lambda_{A,B} \sim N^{-1}$, α_T varies correctly as N, at low N, but at high N displays its well known inadequacy by tending to a saturation limit rather than to the correct limiting rate (Langevin 1903, cf Bates 1985, Flannery 1982a) of diffusional drift, which is neglected in Thomson's result (1) and which varies as N^{-1}. Detailed microscopic theory has, as yet, been applied (Bates and Moffett 1966, Bates and Flannery 1968, Flannery 1980, 1981, Bates and Mendaš

0022-3700/86/070227+07$02.50

1982) only to the limit $N \to 0$, where α increases linearly with N and where energy relaxation is the rate-limiting step. When relaxation in internal separation R is also acknowledged at higher N some connection (Bates and Mendaš 1978, Flannery 1982a, b) with the N variation predicted by (1) has been obtained.

In order to acknowledge coupling with transport and to retain the attractive features intrinsic to (1), the rate

$$\alpha = \alpha_{RN}\alpha_{TR}/(\alpha_{RN} + \alpha_{TR}) \tag{5}$$

was suggested (Bates and Flannery 1969, Flannery 1982a, b) for all N. The reaction rate α_{RN} in (5) is taken as the Thomson rate (1), suitably normalised to reproduce the correct microscopic gradient as $N \to 0$, so that trapping radii R_T can be accurately specified for each ion-atom collision. The transport (diffusional drift) rate in (5) is α_{TR}. Such a procedure yields good agreement (Flannery 1982a, b) with Monte-Carlo simulations (cf Bates 1985) and experiment (cf Bates and Flannery 1969).

Although a detailed microscopic theory for the recombination in (2) has recently been formulated (Flannery 1982a) for all gas densities N, it has not yet been implemented, owing to the complexity of the coupled sets of master equations (Flannery 1986a) that are derived from the microscopic theory (Flannery 1982b). The implicit assumption that equation (1) for α_{RN}, albeit normalised to the microscopic results at low N, provides a correct variation with N has yet to be proven.

The purpose of this letter is to establish a firm connection between the microscopic treatment and (1), and thereby to expose the underlying key assumptions within (1).

The basic set of master equations satisfied by the distributions $n_i^{\pm}(\boldsymbol{R}, t) \equiv n_i^{\pm}(\boldsymbol{R}, E_i, L_i^2, t)$ per unit interval $\mathrm{d}\boldsymbol{R}\,\mathrm{d}E_i\,\mathrm{d}L_i^2$ of pairs (A-B) with internal energy E_i and internal angular momentum (squared) L_i^2, expanding (+) or contracting (−) with radial speed $|v_R|$ at internal separation R is (Flannery 1986a)

$$\frac{\mathrm{d}n_i^{\pm}}{\mathrm{d}t}(\boldsymbol{R}, E_i, L_i^2, t) = \frac{\partial n_i^{\pm}}{\partial t} \pm \frac{1}{R^2}\frac{\partial}{\partial R}(R^2 n_i^{\pm}(\boldsymbol{R}, E_i, L_i^2, t)|v_R|)_{E_i, L_i^2}$$

$$= \int_{-V_i(R)}^{\infty} \mathrm{d}E_f \int_0^{R^2 p_f^2} \mathrm{d}L_f^2 (n_f^{\pm}(\boldsymbol{R}, t)\nu_{fi}(R) - n_i^{\pm}(\boldsymbol{R}, t)\nu_{if}(R)) \tag{6}$$

where $\nu_{if}(R)$ is the frequency per unit interval $\mathrm{d}E_f\,\mathrm{d}L_f^2$ for $(E_i, L_i^2 \to E_f, L_f^2)$ transitions induced by collisions between M and the pair (A-B) with fixed internal separation R. The interaction between A and B with reduced mass m is $V(R)$, the relative momentum squared p_i^2 is $2m(E_i - V(R))$ and

$$V_i(R) = V(R) + L_i^2/2mR^2 \tag{7}$$

is the effective radial interaction, so that $-V_i(R)$ in (6) denotes the energy of the lowest vibrational level of AB consistent with fixed L_i and R, relative to the dissociation limit taken at zero energy. Equation (6) is the continuity equation for R streaming in the presence of input-output discontinuous collisions of (A-B) pairs in mutual trajectories of prescribed E_i and L_i^2, and can be derived (Flannery 1986a) from the Boltzmann equation (Flannery 1982b) for the two-particle distribution functions.

The fundamental rate of recombination is (Flannery 1986a)

$$R^{\wedge}(t) = \int_{-D}^{\infty} \mathrm{d}E_i \int_0^{R_i} \mathrm{d}\boldsymbol{R} \int_0^{R^2 p_i^2} P_i^{\wedge}(\boldsymbol{R}, E_i, L_i^2)(\mathrm{d}n_i/\mathrm{d}t)\,\mathrm{d}L_i^2 \tag{8}$$

where $P_i^{\wedge}$ is the probability that expanding and contracting $(\boldsymbol{R}, E_i, L_i^2)$ pairs with

distribution $n_i = (n_i^+ + n_i^-)$ are stabilised (or associated) by subsequent multiple collisions, R_i is the outermost turning point at which $|V(R_i)| = |E_i|$, and $-D$ is the lowest vibrational level of the AB pair.

On introduction of the averaged probability

$$P_f^{\wedge}(\boldsymbol{R}, E_f) = \left(\int_0^{R^2p_f^2} P_f^{\wedge}(\boldsymbol{R}, E_f, L_f^2) n_f(\boldsymbol{R}, E_f, L_f^2, t)\, \mathrm{d}L_f^2\right)\left(\int_0^{R^2p_f^2} n_f(\boldsymbol{R}, E_f, L_f^2, t)\, \mathrm{d}L_f^2\right)^{-1} \tag{9}$$

the rate (8) may be rearranged to give, with (6),

$$R^{\wedge}(t) = \int_{-D}^{\infty} \mathrm{d}E_i \int_{-D}^{\infty} \mathrm{d}E_f \int_0^{R_{if}} P_f^{\wedge}(\boldsymbol{R}, E_f) S_{if}(\boldsymbol{R}, E_i, E_f)\, \mathrm{d}\boldsymbol{R} \tag{10}$$

where R_{if} is the lesser of the turning points R_i and R_f and where

$$S_{if}(\boldsymbol{R}, E_i, E_f) = \int_0^{R^2p_i^2} \mathrm{d}L_i^2 \int_0^{R^2p_f^2} \mathrm{d}L_f^2 (n_i \nu_{if}(R) - n_f \nu_{fi}(R)) = -S_{fi}(\boldsymbol{R}, E_f, E_i) \tag{11}$$

is the net collisional rate per unit interval $\mathrm{d}E_i\, \mathrm{d}E_f$ for $(E_i \rightarrow E_f)$ transitions at fixed internal separation R of the associating pair.

The following three assumptions are now made.

(A) Assume that the probability for stabilisation of level E_f is

$$P_f^{\wedge}(R, E_f) = 1 \qquad R \leqslant R_T,\ E_f \leqslant 0 \tag{12}$$

and is zero otherwise ($E_f > 0$, all R; $E_f \leqslant 0$, $R \geqslant R_T$) in keeping with the concept that only bound pairs with internal separations R less than some trapping radius R_T can be collisionally stabilised. Hence (10) reduces to

$$R^{\wedge} = \int_0^{\infty} \mathrm{d}E_i \int_{-D}^{0} \mathrm{d}E_f \int_0^{R_f'} S_{if}(\boldsymbol{R}, E_i, E_f)\, \mathrm{d}\boldsymbol{R} = \int_0^{\infty} \mathrm{d}E_i \int_0^{R_T} \mathrm{d}\boldsymbol{R} \int_{-V(R)}^{0} S_{if}(\boldsymbol{R}, E_i, E_f)\, \mathrm{d}E_f \tag{13}$$

where R_f' is the lesser of R_T and R_f.

(B) Include in (6) only absorption by continuum-bound collisional transitions so that, for a steady-state distribution n_i^+ of pairs in the continuum,

$$\frac{\mathrm{d}n_i^+}{\mathrm{d}t}(\boldsymbol{R}, E_i, L_i^2, t) = \pm \frac{1}{R^2} \frac{\partial}{\partial R}(\boldsymbol{R}^2 n_i^+(\boldsymbol{R}, E_i, L_i^2, t)|v_R|)_{E_i, L_i^2}$$

$$= -n_i^+(\boldsymbol{R}, E_i, L_i^2, t)\nu_i(\boldsymbol{R}, E_i, L_i^2) \tag{14}$$

where the frequency for collisional formation of bound pairs is

$$\nu_i(\boldsymbol{R}, E_i, L_i^2) = \int_{-V_i(R)}^{0} \mathrm{d}E_f \int_0^{R^2p_i^2} \nu_{if}(\boldsymbol{R}, E_i, L_i^2, E_f, L_f^2)\, \mathrm{d}L_f^2. \tag{15}$$

(C) Assume that transport by diffusional drift can be neglected outside the trapping sphere, so that the incoming distribution $n_i^-(\boldsymbol{R}, E_i, L_i^2)$ at R_T is given by $\tilde{n}_i^-(\boldsymbol{R}, E_i, L_i^2)$, appropriate to thermodynamic equilibrium with the bath of thermal gas. The solution of (14) for contracting pairs with $R \leqslant R_T$ is therefore

$$n_i^-(R \leqslant R_T, E_i, L_i^2) = \tilde{n}_i^-(\boldsymbol{R}, E_i, L_i^2) \exp\left(-\int_R^{R_T} a_i(R)\, \mathrm{d}R\right) \tag{16}$$

where the number of (associative) collisions that occur during a time $\mathrm{d}t$ within the

element ds_{12} of the (E_i, L_i^2) trajectory for (A-B) relative motion at speed v_{12} is

$$a_i(\boldsymbol{R}, E_i, L_i^2)\,\mathrm{d}R = \nu_i\,\mathrm{d}R/|v_R| = \nu_i\,\mathrm{d}s_{12}/v_{12} \equiv \mathrm{d}s_{12}/\lambda_i \equiv \nu_i\,\mathrm{d}t \tag{17}$$

in terms of the free path length $\lambda_i (\equiv v_{12}/\nu_i)$ peculiar to the prescribed (E_i, L_i^2). In the solution of (14), use was made of the fact that the equilibrium radial flux

$$\tilde{F}_i^-(\boldsymbol{R}, E_i, L_i^2) = 4\pi R^2 \tilde{n}_i^-(\boldsymbol{R}, E_i, L_i^2)|v_R| = 4\pi^2(2\pi mkT)^{-3/2}\exp(-E_i/kT) \tag{18}$$

of contracting pairs is independent of R. Since n_i^- at the pericentre $R_1(E_i, L_i^2)$ of the open orbit equals $n_i^+(\boldsymbol{R}_1, E_i, L_i^2)$, the solution of (14) for expanding pairs with $R \geq R_1$ is

$$n_i^+(R > R_1, E_i, L_i^2) = \tilde{n}_i^-(\boldsymbol{R}, E_i, L_i^2)\exp\left(-\oint_{R_1}^{R_T} a_i\,\mathrm{d}R\right)\exp\left(\int_R^{R_T} a_i\,\mathrm{d}R\right) \tag{19}$$

where $\oint$ denotes the integral over that part ($R_T \to R_1 \to R_T$) of the (A-B) relative trajectory enclosed by the R_T sphere.

On changing the order of integration and setting $S_{if} = n_i\nu_i = (n_i^+ + n_i^-)\nu_i$ in accordance with (14), the rate (13) reduces to

$$R^A = \int_0^\infty \mathrm{d}E_i \int_0^{L_{max}^2} \mathrm{d}L_i^2 \int_{R_1}^{R_T} \mathrm{d}\boldsymbol{R}(\tilde{n}_i^-(\boldsymbol{R}, E_i, L_i^2)\nu_i(\boldsymbol{R}, E_i, L_i^2))\left[\exp\left(-\oint_R^{R_T} a_i\,\mathrm{d}R\right)\right.$$
$$\left. + \exp\left(-\oint_{R_1}^{R_T} a_i\,\mathrm{d}R\right)\exp\left(\int_R^{R_T} a_i\,\mathrm{d}R\right)\right] \tag{20}$$

where the maximum value of L_i^2 for the E_i orbit accessible to the R_T sphere is

$$L_{max}^2 = 2m(E_i - V(R_T))R_T^2 = (2mE_i)\rho_{max}^2 \tag{21}$$

in terms of the maximum impact parameter ρ_{max} of the E_i orbit that just touches the R_T sphere. Since

$$4\pi R^2\tilde{n}_i^-(\boldsymbol{R}, E_i, L_i^2)\nu_i(\boldsymbol{R}, E_i, L_i^2) = 4\pi^2 N_A N_B a_i(2\pi mkT)^{-3/2}\exp(-E_i/kT) \tag{22}$$

in terms of a_i defined by (17) and of the densities N_A, N_B of species A^- and B^- and since

$$\int_{R_1}^{R_-} a_i(R')\exp\left(\mp\int_R^{R_-} a_i\,\mathrm{d}R\right)\mathrm{d}R' = 1 \mp \exp\left(\mp\int_{R_1}^{R_T} a_i\,\mathrm{d}R\right) \tag{23}$$

the $\boldsymbol{R}$ integration in (20) can be performed to yield the recombination rate

$$R^A = 4\pi^2 N_A N_B(2\pi mkT)^{-3/2}\int_0^\infty \mathrm{d}E_i\exp(-E_i/kT)$$
$$\times \int_0^{L_{max}^2} \mathrm{d}L_i^2\left[1 - \exp\left(-2\int_{R_1(E_i, L_i^2)}^{R_T} \mathrm{d}s_{12}/\lambda_i\right)\right] \tag{24}$$

which is an exact result under the above assumptions (A)-(C), i.e. (12), (14) and the neglect of diffusional drift in (16) for $R \geq R_T$. The term in square brackets in (24) is simply the probability of collision of (E_i, L_i^2) pairs with separations R in the range $R_1 \leq R \leq R_T$. It tends to unity as the gas density $N \to \infty$, since $\lambda_i = (v_{12}/\nu_i) \sim N^{-1}$. The rate (24), therefore, initially increases linearly, and thereafter non-linearly, with N towards the eventual saturation limit

$$R^A = (\pi R_T^2)\int_0^\infty v_\infty(1 - V(R_T)/E_i)G(E_i)\,\mathrm{d}E_i \tag{25}$$

where

$$G(E_i)\,dE_i = (2/\sqrt{\pi})E_i^{1/2}(kT)^{-3/2}N_A N_B \exp(-E_i/kT)\,dE_i \tag{26}$$

is the Maxwell distribution of unbound pairs with energy $E_i = \frac{1}{2}mv_\infty^2$.

On introduction of the L_i^2-averaged probability

$$\bar{W}_i(E_i, R_T) = L_{max}^{-2}\int_0^{L_{max}^2} dL_i^2\left[1 - \exp\left(-2\int_{R_i}^{R_T} ds_{12}/\lambda_i\right)\right] \tag{27}$$

for collisions within the R_T sphere at a given energy, equation (24) can be rewritten as

$$R^A = \pi R_T^2 \int_0^\infty v_\infty(1 - V(R_T)/E_i)\,\bar{W}_i(E_i, R_T)G(E_i)\,dE_i. \tag{28}$$

When the binary separation of the energy-change frequency ν_i for (A-B)-M collisions is effected in terms of the frequencies ν_i^{AM} and ν_i^{BM} for individual A-M and B-M collisions via

$$\nu_i = \nu_i^{AM} + \nu_i^{BM} \tag{29}$$

then (27) separates according to

$$\bar{W}_i = w_i^{AM} + w_i^{BM} - w_i^{AM}w_i^{BM} \tag{30}$$

where w_i^{AM} is the probability for individual A-M collisions within a sphere of radius R_T centred at B, i.e. w_i^{AM} and w_i^{BM} are given by (27) with λ_i replaced by $\lambda_i^{AM} = v_{12}/\nu_i^{AM}$ and by $\lambda_i^{BM} = v_{12}/\nu_i^{BM}$ respectively. This result (30) is very gratifying in that the binary assumption (29) naturally leads to the inclusion in (30) of the probability $w_i^{AM}w_i^{BM}$ of simultaneous collision with M; otherwise $\bar{W}_i$ would, at high gas densities, tend (incorrectly) to two, rather than to unity.

On ignoring both the flux-focusing factor $(1 - V/E_i)$ and the dependence of the specific path λ_i on E_i and L_i^2, and on assuming a straight line (A-B) trajectory, the standard Thomson prescription (1) and (3) is recovered from (28) and (27).

With the aid of the analytical expression derived for the length $L = \oint ds_{12}$ of the hyperbolic Coulombic (E_i, L_i^2) orbit enclosed within the sphere of the radius R_T (Flannery 1986b), and under the assumption that the specific path λ_i is independent of E_i and L_i^2 and equal to the mean free path λ, equation (27) can be evaluated explicitly. Figure 1 compares (27), the hyperbolic result H, with (4), the straight-line probability S, as a function of ρ_{max}/λ. The maximum impact parameter ρ_{max} of the hyperbolic trajectory H, of energy $E_i = \frac{3}{2}kT$, that just touches the sphere of radius $R_T = \frac{1}{2}(e^2/kT)$ is $\sqrt{2}R_T$, from (21). For straight-line motion S, $\rho_{max} = R_T$. Figure 1 therefore illustrates that equation (4), with $X = \rho_{max}/\lambda$ provides a fairly accurate analytical representation of (27). This closeness is perhaps the key to the success (Flannery 1982a) enjoyed by expression (5) for the overall rate α as a function of gas density N.

When the analytical expression for L is again adopted in (27), it can be shown (Flannery 1986b) that the rate (28) for the *collisional* recombination

$$e + A^+ + M \rightarrow A + M \tag{31}$$

between electrons of mass m and density n_e and ions of density N^+ in a monatomic gas of mass M reduces, at low gas densities, to

$$R_e = \alpha n_e N^+ = 8\pi\left(\frac{m}{M}\right)\left(\frac{e^2}{kT}\right)^2\left(\frac{8kT}{\pi m}\right)^{1/2}\left(\frac{R_T}{\lambda}\right)n_e N^+ \tag{32}$$

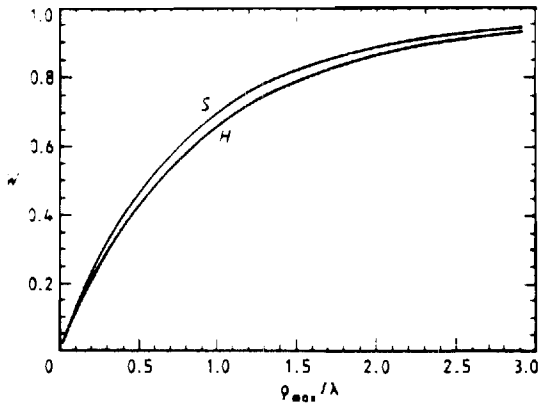

Figure 1. Comparison of the collisional probabilities obtained from equation (4) for (A-B) straight-line relative motion (S, $\rho_{max} = R_T$) and from (27) for a hyperbolic trajectory (H, $\rho_{max} = \sqrt{2}R_T$), as a function of (ρ_{max}/λ) at internal energy $E_i = \frac{3}{2}kT$ of the pair (A-B).

in exact agreement with the expression derived by Pitaevskii (1962) from a diffusional treatment. An averaging procedure (Bates 1980) differing from that of (27) yields a result that is two thirds that of Pitaevskii.

By recourse to the basic microscopic theory (Flannery 1982b, Flannery 1986a) of termolecular ion-ion recombination, the above assumptions (A)-(C) underlying the Thomson rate (1) and (3) as a function of N have been exposed. The analytical probability (3) derived (Loeb 1955) for rectilinear ion-ion trajectories has also been shown to be an accurate representation of the correct expression (27) with hyperbolic trajectories, provided that the specific path λ_i is identified with the mean free path λ and that X in (3) is given by ρ_{max}/λ rather than R_T/λ. The analytical expression of Pitaevskii (1962) for collisional electron-ion recombination at low N can also be reproduced.

This research is supported by the U'S Air Force Office of Scientific Research under Grant No AFOSR-84-0233.

References

Bates D R 1980 *J. Phys. B: At. Mol. Phys.* **13** 2587-99
—— 1985 *Advances in Atomic and Molecular Physics* vol 20, ed D R Bates and B Bederson (New York: Academic) ch 1
Bates D R and Flannery M R 1968 *Proc. R. Soc.* A **302** 367-83
—— 1969 *J. Phys. B: At. Mol. Phys.* **2** 184-90
Bates D R and Mendaš I 1978 *Proc. R. Soc.* A **359** 275-85
—— 1982 *J. Phys. B: At. Mol. Phys.* **15** 1949-56
Bates D R and Moffett R J 1966 *Proc. R. Soc.* A **291** 1-8
Flannery M R 1980 *J. Phys. B: At. Mol. Phys.* **13** 3649-64
—— 1981 *J. Phys. B: At. Mol. Phys.* **14** 915-34
—— 1982a *Applied Atomic Collision Physics* vol 3 ed E W McDaniel and W L Nighan (New York: Academic) ch 5
—— 1982b *Phil. Trans. R. Soc.* A **304** 447-97

—— 1986a *Phys. Rev.* A submitted
—— 1986b in preparation
Langevin 1903 *Ann. Chim. Phys.* **28** 433–530
Loeb L B 1955 *Basic Processes of Gaseous Electronics* (Berkeley: University of California) ch 6
Pitaevskii L P 1962 *Sov. Phys.-JETP* 919–21
Thomson J J 1924 *Phil. Mag.* **47** 337–78

Appendix D

Orientation and Alignment Parameters for $e\text{-}He(1\,^1S \rightarrow 3\,^1D)$ Collisions

Orientation and Alignment Parameters for e-He ($1^1S \rightarrow 3^1D$) Collisions

E. J. Mansky and M. R. Flannery

School of Physics

Georgia Institute of Technology

Atlanta, Georgia 30332 U.S.A.

Abstract: A ten channel eikonal treatment of electron-helium collisions is performed for a basis set of (1^1S, 2^1S, 2^1P, 3^1S, 3^1P and 3^1D) target states to yield the first theoretical results for the orientation and alignment parameters for the 3^1D level of helium. Good agreement with recent measurements is obtained.

Subject Index: 3450, 3480D.

In excitation by electrons of an atom from initial state i to some metastable state f, the photon emitted in the subsequent radiative transition $f \rightarrow n$ to an intermediate state n is correlated with the $(i \rightarrow f)$ inelastically scattered electron. As is well known, the rates for these measured electron-photon coincidences provide basic insight to the intrinsic dynamics of the scattering event, and characterization of the electron-photon correlation in terms of the coincidence rate furnishes a view of the collision process that is more exhaustive than that evident via measurement of integral and differential cross sections.

Measurements of electron-photon coincidences in e-He collisions have concentrated mainly on the excitation from the ground state and decay of the 2^1P and 3^1P levels of He (Eminyan et al. 1973, 1974; Standage and Kleinpoppen, 1976). Also, the delayed coincidence between the inelastically scattered electron, following the 1^1S-3^1D collisional excitation in He, and the subsequent emission of the 2^1P-1^1S photon resulting from the cascade transition $3^1D \rightarrow 2^1P \rightarrow 1^1S$ has been measured (van Linden van den Heuvell et al. 1981, 1983). No corresponding theoretical results as yet exist.

The purpose of this letter is to present the first theoretical treatment for the coincidence rate $N(\theta_\gamma,\phi_\gamma)$ between the scattered electron and the photon emitted in the direction $(\theta_\gamma,\phi_\gamma)$ from a final state f with angular momentum L=2. When the quantization axis of the target atom is chosen perpendicular to the scattering plane, the radiation pattern of the emitted photon is easier to detect and the position of the peak of the measured rate N occurs for an emission direction $(\theta_\gamma,\phi_\gamma)$ which is independent of the angle θ_e of the scattered electron. The composite differential cross section σ for the 1^1S-3^1D excitation is then $|f_0|^2+|f_2|^2+|f_{-2}|^2$ where f_m is the scattering amplitude for the 1^1S-3^1D_m transition. The basic parameters

$$\xi = |f_o|^2/\sigma \tag{1a}$$

$$\upsilon = |f_o f_2^* + f_{-2} f_o^*|/\sigma \tag{1b}$$

$$\zeta = \arg[(f_o f_2^* + f_{-2} f_o^*)/f_o] \tag{1c}$$

and

$$\omega = [\,|f_2|^2 - |f_{-2}|^2]/\sigma \tag{1d}$$

can then be deduced from the measured rates

$$N(\theta_\gamma, \phi_\gamma = \pi) \sim \sigma\,[\frac{3}{4} - \frac{1}{6}\xi - \frac{1}{2}\frac{\upsilon}{\sqrt{6}}\cos\zeta + (\frac{1}{4} - \frac{1}{2}\xi + \frac{1}{2}\frac{\upsilon}{\sqrt{6}}\cos\zeta)\cos 2\theta_\gamma] \tag{2a}$$

or

$$N(\theta_\gamma = \frac{\pi}{2}, \phi_\gamma) \sim \sigma\,[\frac{1}{2} + \frac{1}{3}\xi + \frac{\upsilon}{\sqrt{6}}\cos(2\phi_\gamma - \zeta)] \tag{2b}$$

for the respective cases when the photon detector is in the scattering plane ($\phi_\gamma = 0, \pi$) or in a plane ($\theta_\gamma = \pi/2$) perpendicular to the incident beam.

Since the present theoretical treatment adopts the quantization axis to be along the incident beam, the following parameters

$$\lambda = |f_o|^2/\sigma \tag{3a}$$

$$\mu = 2|f_1|^2/\sigma \tag{3b}$$

$$\chi = \arg(f_1/f_0) \tag{3c}$$

$$\psi = \arg(f_2/f_0) \ . \tag{3d}$$

are more appropriate to the characterization of the coincidence rate (cf. Nienhuis 1980, Andersen and Nielsen 1982). The differential cross section σ in (3) is then of course $|f_0|^2+2|f_1|^2+2|f_2|^2$. The appropriate transformation between the measured parameters (ξ,η,ζ,ω) of (1) and the calculated parameters (λ,μ,χ,ψ) of (3) has been worked out in detail elsewhere (Mansky 1985). The coincidence rate can now be expressed for the above two directions of the photon detector as,

$$N(\theta_1,\phi_1=\pi) \sim \sigma\ [2 - \frac{1}{4}\ (d_0-d_2) - \frac{1}{4}\ (3d_0+d_2)\ \cos 2\theta_1 + \frac{1}{2}\ d_1 \sin(2\theta_1)] \tag{4a}$$

and

$$N(\theta_1 = \frac{\pi}{2},\ \phi_1) \sim \sigma\ [2 + \frac{1}{2}\ d_0 + \frac{1}{2}\ d_2\ \cos(2\phi_1)] \tag{4b}$$

respectively, where, in terms of the present theoretical parameters (3),

$$d_0 = -\ 1 + 2\lambda + (3\mu/2) \tag{5a}$$

$$d_1 = -\ \sqrt{3\lambda\mu}\ \cos\chi - 3\sqrt{\mu(1-\lambda-\mu)}\ \cos\psi \tag{5b}$$

$$d_2 = 2\sqrt{3\lambda(1-\lambda-\mu)}\ \cos(\chi+\psi) - (3\mu/2) \tag{5c}$$

Note that a typographical error exists in equation (2.17) of van Linden van den Heuvell et al. (1981) and in equation (2.3) and (2.5) of van Linden van den Heuvell et al. (1983). The correct expressions are (4a) and (5c) and agree with those given in the review of Andersen and Nielsen (1982).

The present multichannel eikonal treatment was originally designed for electron-excited (metastable) atom collisions in mind (Flannery and McCann 1975a), since then electron-exchange can be explicitly neglected in the basis set expansion for spin allowed transitions and the assumption of a straight line trajectory becomes highly justified, the dominant contribution to the integral cross section resulting from scattering mainly in the forward direction $\theta_e \lesssim 40^o$. Comparison with other theoretical treatments and measurements reveals that it is also accurate for excitation in e-H(1s) and e-He(1^1S) collisions (Flannery and McCann 1974, 1975b, Mansky and Flannery 1987) at intermediate and high impact energies $E \gtrsim 25$ eV.

The present multichannel eikonal treatment DMET (Mansky and Flannery 1987) adopts the same wavefunctions for the ten (1^1S, 2^1S, 2^1P, 3^1S, 3^1P, 3^1D) target states as previously used (Flannery and McCann 1975a), solves the appropriate coupled equations more accurately over a much finer mesh, and contains a modification to acknowledge the effect of dipoles at large impact parameters $\rho \geq \rho_{max}$. The upper limit of the impact parameter range (0-ρ_{max}) within which the full set of ten closely-coupled equations (Flannery and McCann 1975a) were solved is ρ_{max}. Comparison between present results and measured values (van Linden van den Heuvell et al. 1983) for the parameters ξ, η and ζ as a function of impact energy E for an electron scattering angle θ of 35^o is displayed in Figs. 1(a-c). Good agreement is in general obtained bearing in mind the present experimental error bars which reflects the difficult nature of the experiment.

Since DMET becomes increasingly accurate for smaller scattering angles at

higher impact energies, measurements and other theoretical results for thisregion would be very desirable for comparison purposes.

Although the parameter ω in (1d) was not measured by van Linden van den Heuvell et al. 1983), the ratio of $\sigma(3^1D)/\sigma(3^1P)$ of the composite differential cross sections for the $1^1S \rightarrow 3^1P$ and $1^1S \rightarrow 3^1D$ excitations was measured at $\theta = 35^o$ for impact energies E = 28.5, 31.5, 34.6 and 45.6 eV. The present DMET results are compared in Fig. 2 with these measurements and with the only other available results; MET (Flannery and McCann, 1975b; FOMBT (first-order-many-body-theory of Chutjian and Thomas 1975); DW (the 9-state distorted wave theory of Winters et al. 1977). The present agreement with measurements is good. The large discrepancy with FOMBT is presumably due to the neglect in FOMBT of interchannel couplings. Neglect of the contribution of the 3^1D state has, as pointed out by van Linden van den Heuvell et al. (1983), a measurable effect on the experimental determination of the coincidence rate associated with the 3^1P level. The DW-variation with E is quite different to that exhibited by the present results.

In summary, the first theoretical results for the orientation and alignment parameters for the 3^1D level of helium have provided good agreement with measurements of the parameters ξ, ρ and ζ. Comparison with the measured values of the ratio $\sigma(3^1D)/\sigma(3^1P)$ indicates that accurate theoretical prediction of the differential cross sections σ requires that all interchannel couplings, within a multichannel basis, be directly included in the calculation.

Acknowledgement. This research is supported by the US Air Force Office of Scientific Research under Grant No. AFOSR-84-0233.

References

Andersen, N. and Nielsen, S. E., 1982, Adv. At. Mol. Phys. 18,, 265-308.

Chutjian, A. and Thomas, L. D., 1975, Phys. Rev. A 11, 1583-95.

Eminyan, M., MacAdam, K. B., Slevin, J., and Kleinpoppen, H., 1973, Phys. Rev. Lett. 31, 576-9.

Eminyan, M., MacAdam, K. B., Slevin, J., and Kleinpoppen, H., 1974, J. Phys. B At. Mol. Phys. 7, 1519-42.

Flannery, M. R. and McCann, K. J., 1975, J. Phys. B: Atm. Mol. Phys. 8, 1716-33.

Flannery, M. R. and McCann, K. J., 1974, J. Phys. B: Atom. Molec. Phys. 7, L522-27.

———————————— 1975a, Phys. Rev. A 12, 846-55.

———————————— 1975b, J. Phys. B: Atom. Molec. Phys. 8, 1716-33.

van Linden van den Heuvell, H. B., Nienhuis, G., van Eck, J., and Heideman, H. G. M., 1981, J. Phys. B: Atm. Mol. Phys. 14, 2667-76.

van Linden van den Heuvell, H. B., van Gasteren, E. M., van Eck, J., and Heideman, H. G. M., 1983, J. Phys. B. Atm. Mol. Phys. 16, 1619-31.

Mansky, E. J., 1985, Ph.D. Thesis (Chap. 4, Appendix A), Georgia Institute of Technology.

Mansky, E. J. and Flannery, M. R., 1987, in preparation.

Neinhuis, G., 1980, Coherence and Correlation in Atomic Collisions, ed. H. Kleinpoppen and J. F. Williams (Plenum Press, N.Y.) pp. 121-132.

Standage, M. C. and Kleinpoppen, H., 1976, Phys. Rev. Letts. 36, 577-80.

Winters, K. H., Issa, M., and Bransden, B. H., 1977, Can. J. Phys. 55, 1074-82.

Figure Captions

Figure 1 (a-c). Comparison of measurements of van Linden van den Hewell et al. 1983 with present ten-channel eikonal theoretical results for the parameters ξ, η and ζ as a function of electron impact energy E(eV) at a fixed electron scattering angle $\theta_e=35^o$.

Figure 2. Present ten-channel eikonal results (solid line) for the ratio $\sigma(3^1D)/\sigma(3^1P)$ of differential cross sections at electron scattering angle $\theta_e=35^o$ as a function of impact energy E(eV). Measurements: ⧗ Van Linden van den Heuvell et al. (1983). Previous theoretical results: --- (Flannery and McCann 1975b); □ (Chutjian and Thomas 1975); x (Winters et al. 1977).

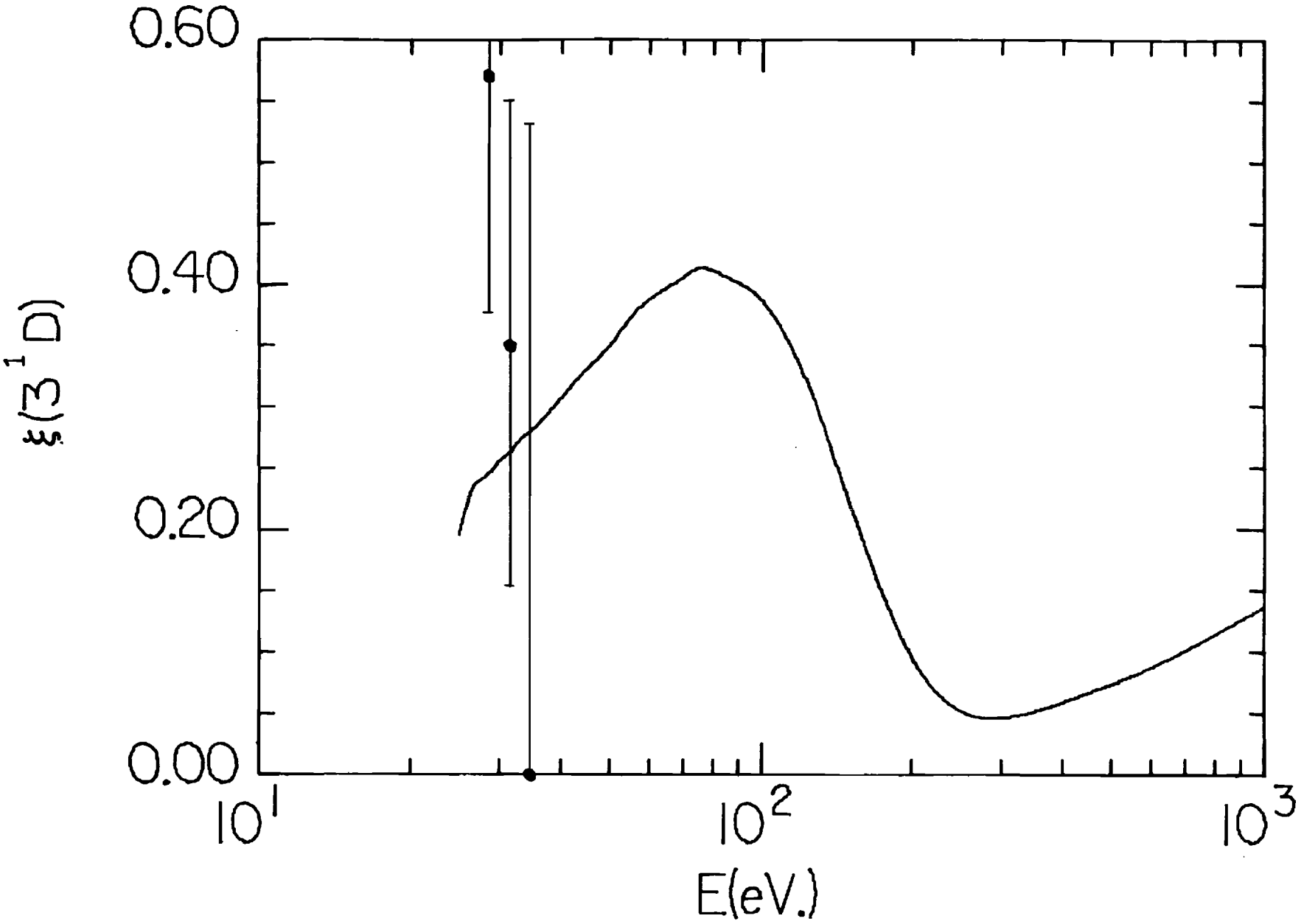

Figure 1(a).

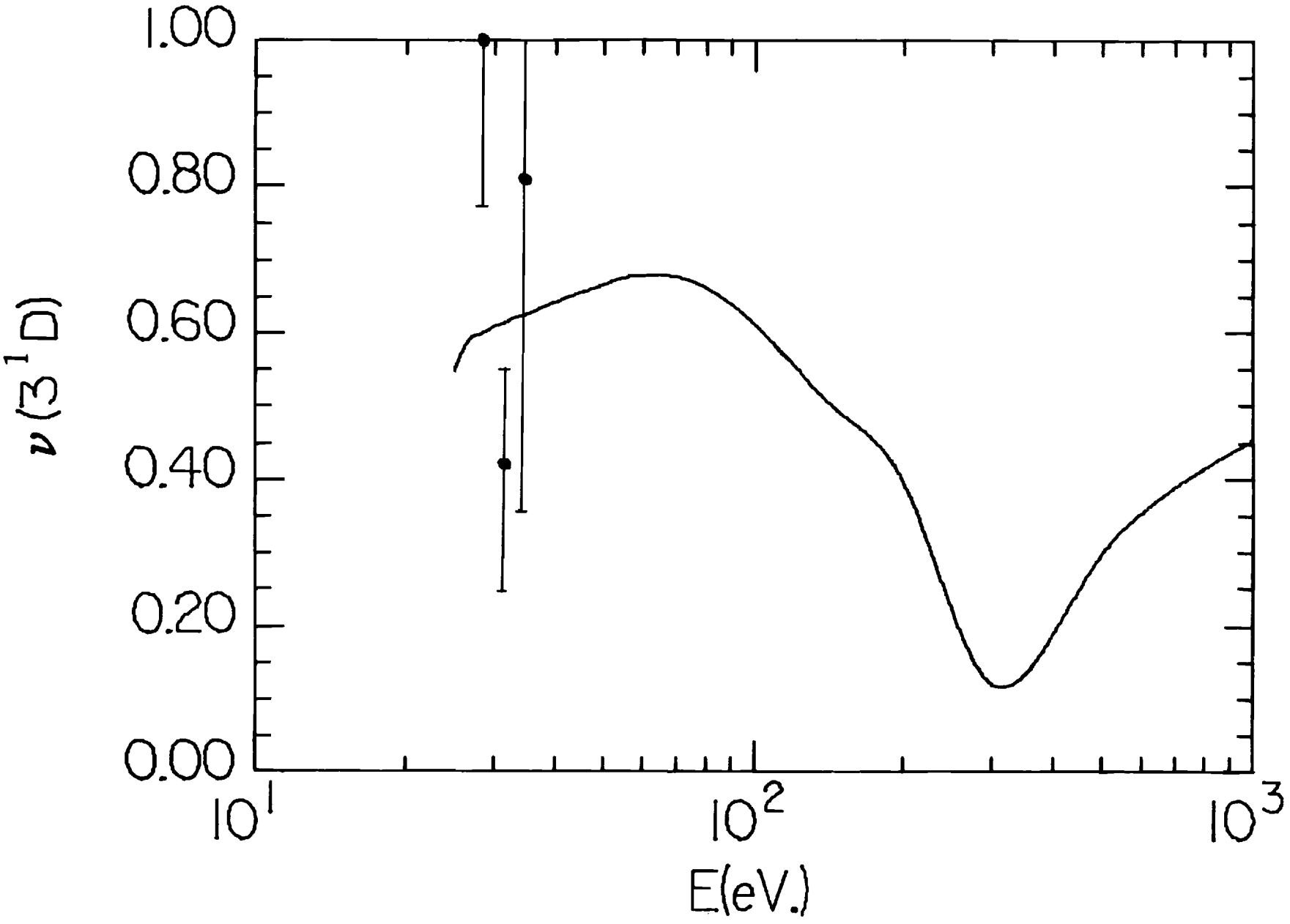

Figure 1(b).

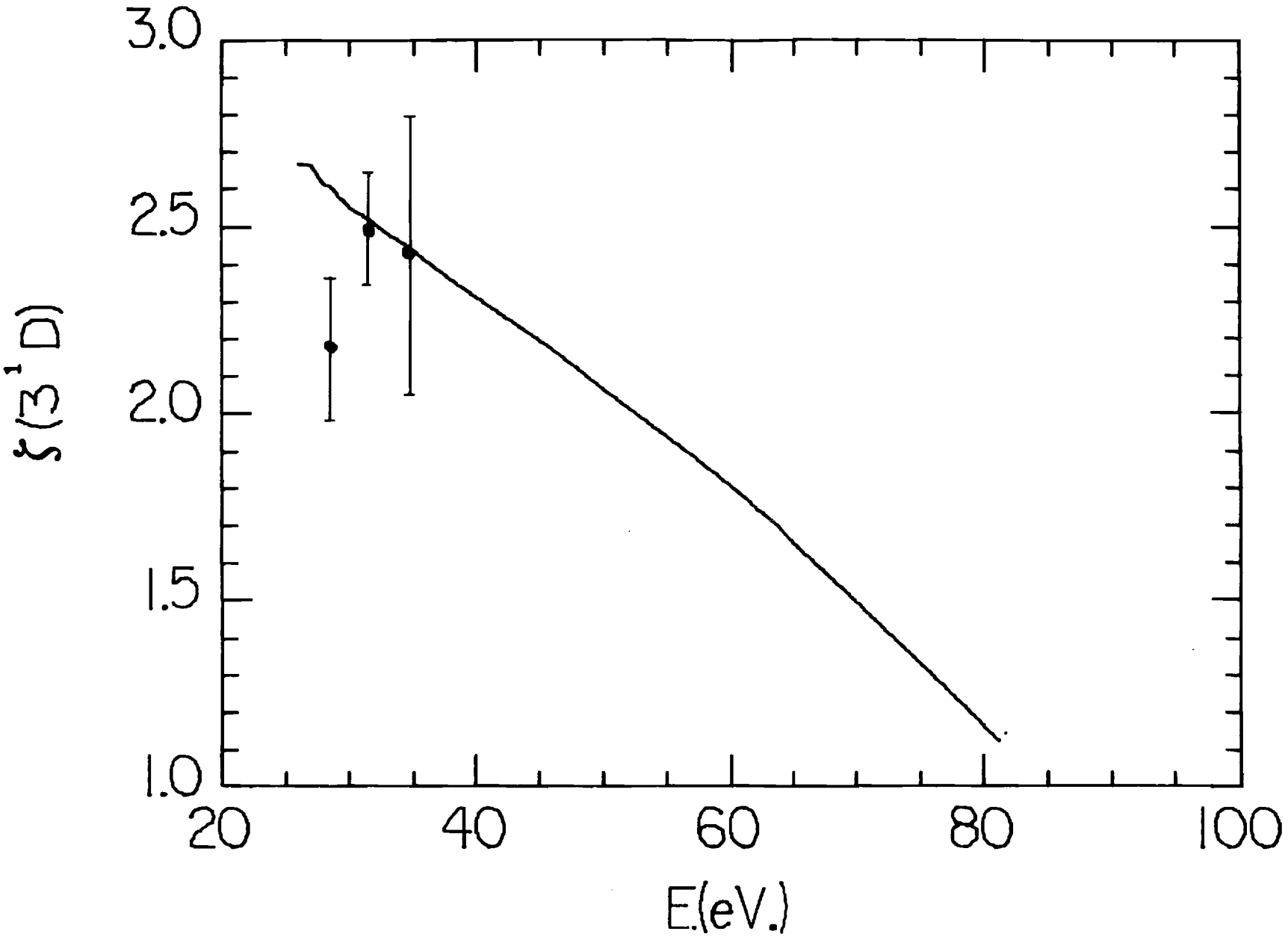

Figure 1(c).

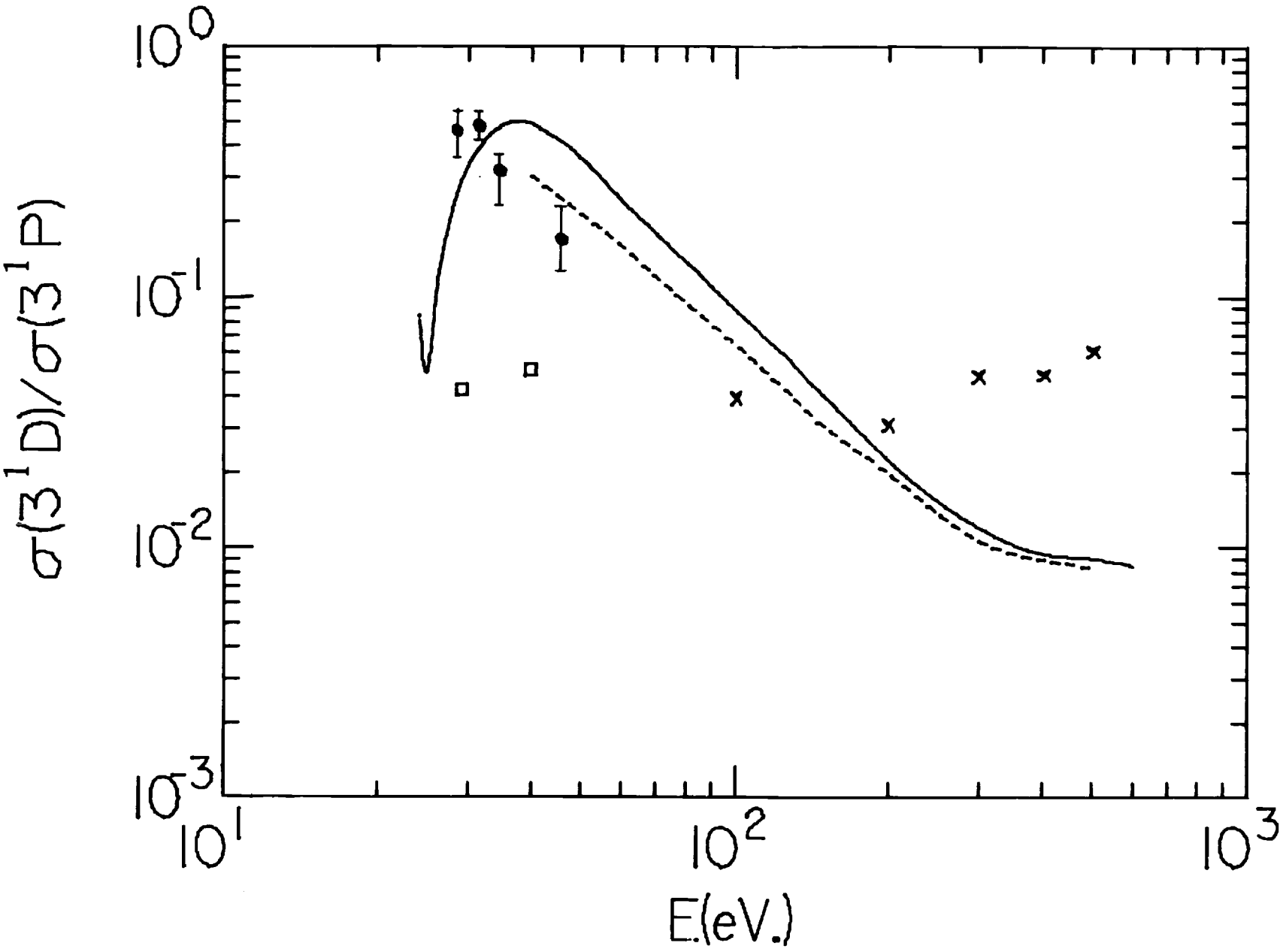

Figure 2.

Appendix E

Macroscopic and Microscopic Perspectives of Termolecular Reactions

MACROSCOPIC AND MICROSCOPIC PERSPECTIVES OF TERMOLECULAR REACTIONS

M. Raymond Flannery

School of Physics
Georgia Institute of Technology
Atlanta, Georgia 30332

1. MACROSCOPIC TREATMENT

The sequence normally invoked to explain the termolecular association process

$$A + B + M \rightarrow AB + M \tag{1.1}$$

where the associating pair (A-B) may be a positive ion-negative ion or a positive ion-neutral pair, is the *energy-transfer sequence* characterized in macroscopic terms as

$$A + B \underset{k_{-1}}{\overset{k_1}{\rightleftharpoons}} AB^* \quad (R \leq R_T) \tag{1.2a}$$

$$AB^*(R \leq R_T) + M \xrightarrow{k_s} AB + M \tag{1.2b}$$

wherein intermediate complexes AB^* formed with internal separations $R \leq R_T$ at rate k_1 ($cm^3\ s^{-1}$) can decompose naturally at frequency k_{-1} (s^{-1}) or can be stabilized at rate k_s ($cm^3\ s^{-1}$) via energy-changing collisions with the atomic or molecular species M of a thermal gas. The inverse of this sequence is known as the *Lindemann mechanism* (cf. Forst 1973) for collisional dissociation.

Process (1.1) may also proceed in parallel by the *chaperone mechanism*

$$A + M + (M) \underset{k_d}{\overset{k_c}{\rightleftharpoons}} AM^* + (M) \tag{1.3a}$$

$$AM^* + B \xrightarrow{k_r} AB + M \tag{1.3b}$$

wherein intermediate complexes AM^* which may include bound levels are

formed at rate k_c ($cm^3\ s^{-1}$) by two- or three-body collisions and then undergo rearrangement with B at rate k_r ($cm^3\ s^{-1}$). The function of the chaperone M is not to keep the reactants A and B apart but to promote their stable union. Since the dependence on gas density of the resulting rate laws for formation of AB are similar, distinction between the two parallel processes are not evident from measurements. The energy transfer sequence (1.2) is dominant for *termolecular ion-ion recombination* owing to the long-range Coulombic attraction and is normally invoked for *ion-molecule association*. The chaperone mechanism (1.3) can however become important for association, particularly at lower gas temperatures and higher gas densities, and in some instances can be dominant (Blades and Kebarle, 1983 for COH^+-CO and N_2H^+-N_2 association in H_2).

The effective two-body rate $\alpha(cm^3\ s^{-1})$ or the associated termolecular rate k_T ($cm^6\ s^{-1}$) for (1.1) via the sequence (1.2) is

$$\alpha n_A n_B = k_s n^*_{AB}\, N = k_T\, N \tag{1.4}$$

where the gas density is N, and where the density n^*_{AB} of complex AB^* pairs satisfies

$$dn^*_{AB}/dt = k_1\, n_A n_B - (k_{-1} + k_s N) n^*_{AB} \tag{1.5}$$

where n_A and n_B are the densities of the reactants A and B. In steady-state

$$n^*_{AB}/n_A n_B = k_1/(k_{-1}+k_s N) = k_1[K/(k_1+k_s KN)] \tag{1.6}$$

where the *reaction volume* under full equilibrium conditions is

$$K = \tilde{n}^*_{AB}/\tilde{n}_A \tilde{n}_B = k_1/k_{-1} \tag{1.7}$$

which is not an equilibrium constant in the usual sense since the complex AB^* does <u>not</u> include bound states. The overall rate

$$\alpha(N) = \frac{k_1(K\, k_s N)}{k_1+(Kk_s N)} \rightarrow \begin{cases} K\, k_s N = \alpha_o & ;\ N \rightarrow 0 \\ k_1 & ;\ N \rightarrow \omega \end{cases} \tag{1.8}$$

initially increases linearly with gas density N as $\alpha_o = (Kk_s N)$, characteristic of three-body kinetics, and eventually tends to a saturation value k_1 characteristic of two-body kinetics alone. Introduce the N-dependent probabilities,

$$P^S(N) = (k_s KN)/(k_1+k_s KN) \tag{1.9}$$

for collisional stabilization of the complex and

$$P^D(N) = k_1/(k_1+k_s KN) \tag{1.10}$$

for natural decomposition of the complex so that alternative expressions for the effective two-body rate are

$$\alpha = P^S(N)k_1 \tag{1.11}$$

$$= P^D(N)\ k_s KN \equiv P^D(N)\alpha_o \tag{1.12}$$

1.1. The Reaction Volume

By virtue of (1.8), K represents the reaction volume at low N and is in general given by (Forst 1973)

$$K(T) = \frac{h^3}{(2\pi mkT)^{3/2}}\ \frac{q(AB^*)}{q(A)q(B)}\ \frac{\omega_{AB}}{\omega_A\omega_B} \tag{1.13}$$

where q and ω denote the internal partition functions and electronic statistical weights associated with each reactant A and B and with the activated complex AB^*. While q(A) and q(B) are known, $q(AB^*)$ is such that it must include only those rotational-vibrational states of AB^* accessible at energies E above the dissociation threshold E_T in A-B collisions. It may also include conservation of total angular momentum which can be redistributed between the orbital angular momentum $\underset{\sim}{L}$ for relative (A-B) motion and the combined internal momentum $\underset{\sim}{J}_R$ of the individual reactants.

For structureless reactants A and B with relative separation $\underset{\sim}{R}$, relative energy $E \geq 0$ as measured above the threshold energy E_T for dissociation from the ground vibrational state of AB, relative momentum $\underset{\sim}{P}$ and angular momentum $L = \hbar J$, then

$$K(T) = h^3(2\pi mkT)^{-3/2} \int \exp(-E/kT)d\underset{\sim}{R}\ d\underset{\sim}{p}/h^3 \tag{1.14a}$$

$$= h^3(2\pi mkT)^{-3/2} \int_0^\infty dE \int_0^{J_{max}} \rho(E,J)\ \exp(-E/kT)dJ^2 \tag{1.14b}$$

The density of ro-vibrational states per unit interval $dE\ dJ^2$ produced from the relative (A-B) motion is

$$\rho(E,J) = \tau(E,J)/\hbar = 1/h\nu \tag{1.15}$$

in terms of the lifetime

$$\tau(E,\rho) = \int_{R_1}^{R_T} \frac{dR}{v_R} = \left(\frac{m}{2}\right)^{1/2} \int_{R_1}^{R_T} \left[E\left(1 - \frac{\rho^2}{R^2}\right) - V(R)\right]^{-1/2} dR \tag{1.16}$$

of the complex towards natural decomposition with radial speed v_R via an orbit with angular momentum L and impact parameter ρ which are related by

$$L = \hbar J = (2mE)^{1/2}\,\rho \qquad (1.17)$$

The maximum angular momentum L_{max} of those $(A^+\text{-}B)$ orbits which can overcome the centrifugal barriers for $L \leq L_{max}$ at fixed energy E is given by $(8m\alpha_B e E)^{1/4}$ for pure polarization attraction $V(R) = -\alpha_B e^2/2R^4$ where α_B is the polarizability of B. The associated reaction radius R_T is taken as the barrier location $(\alpha_B e^2/2E)^{1/4}$, the Langevin orbiting radius.

So as to obviate the necessity for numerical evaluation of the time (1.16) during which R is in the range $R_1 \leq R \leq R_T$ for realistic interactions V(R), a simplifying assumption is now invoked. Reactions which occur via intermediate complexes generally involve randomization of the internal energy in the complex. If this energy is statistically distributed within the various internal modes the reaction can be treated by statistical methods such that the (formidable) problems associated with application of molecular dynamics and classical trajectories to microscopic lifetimes of intermediate complexes are thereby avoided. The complex is therefore assumed to be in its most stable configuration which results from rapid energy transfer out of the external collision coordinates $\underset{\sim}{R}$ and $\underset{\sim}{p}$ into other internal coordinates so that, following large perturbations in $(A^+\text{-}B)$ close encounters, a quasi-equilibrium among excited states is obtained. Upon this key randomization assumption (which is viable provided the lifetime against stabilization collisions is long in comparison to the (A-B) collision time) the density (1.15) may therefore be replaced by the density

$$\rho_H(E,J) = 1/h\nu_H(E,J) \qquad (1.18)$$

of levels (one per energy-level spacing $h\nu_H$) of a harmonic oscillator of frequency ν_H. The number of levels within rotational spacing dJ of the free rotor complex remains as $dJ^2 = 2J\,dJ$. The difficult molecular-dynamics aspects of the complex have therefore been avoided and are replaced by the known structural properties of the complex. Eq. (1.14b) with (1.18) can be formally generalized to cover polyatomic reactants.

1.2 Temperature Dependence: Polyatomic Reactants

Temperature dependence of association reactions elucidate reaction pathways. Since the unimolecular dissociation rate k_{-1} increases with T, a T^{-n}-variation is expected. Current theories have mainly focused on the temperature dependence of the low density three body rate $k_T = Kk_s$. Accord with measurements is becoming somewhat acceptable (Bates 1985, Viggiano 1985, van Koppen et al. 1984). The rate k_s for stabilization of ion-molecule collision complexes may be taken as some fraction of the constant Langevin rate for spiraling collisions,

$$k_L = 2\pi e(\alpha_M/\mu)^{1/2} \qquad (1.19)$$

where α_M is the polarizability of M and where μ is the reduced mass of the $(AB^*\text{-}M)$ system. Since the partition functions q(A) and q(B) of the reactants are known, (e.g., q(A)q(B) for ground vibrational levels

$\sim T^{-(r/2)}$ where r is the sum (r_A+r_B) of the number of degrees of rotational freedom of the isolated reactants), the temperature dependence of k_T is therefore mainly controlled by the less well determined partition function $q(AB^*)$ in (1.13) of the activated complex. The different temperature dependences exhibited by similar systems, e.g., k_T for $(O_2^+-O_2)-O_2$ association decreases as $\sim T^{-2.9} - T^{-3.2}$ which is more rapid than $k_T \sim T^{-1.6} - T^{-1.85}$ for $(N_2^+-N_2) - N_2$ association, is simply a manifestation (Bates 1985) of the temperature characteristics of $q(AB^*)$.

Bates (1978) has outlined a scheme for the internal partition function $q(AB^*)$ which is the generalization of (1.14a) and of (1.15) to atomic-diatomic and to diatomic-diatomic ion-neutral reactants which are free to rotate and vibrate in the potential well. The states accessible in Langevin collisions are determined by conservation of energy and angular momentum. As with (1.14b), this *barrier model* of Bates in general involves time-consuming numerical calculation of the lifetime τ for A-B collisions. Upon invoking the randomization assumption, however, this lifetime may be replaced, as in (1.18), by known vibrational periods of the complex.

Apart from the long-range polarization (A^+-B) attraction and the resulting looseness of the activated complex $(AB^+)^*$, termolecular ion-molecule association as described by (1.2) is in principle the inverse of neutral unimolecular decomposition which is primarily concerned with calculation of the decomposition rate k_{-1}. The Rice-Ramsperger-Kassel-Marcus (RRKM) theory (cf. Forst 1973) for calculation of the internal partition function of the complex has been adapted for ion-neutral fragmentation. In his *thermal RRKM method* for ion-molecule association Herbst (1979) includes all ro-vibrational states above the dissociation limit at E_T. Following the *barrier model* of Bates (1979a,b) it was subsequently modified (Herbst 1980) to include only those levels above the centrifugal barrier. The *quasi-equilibrium theory* QET (Klots 1971) and *phase space theory* PST (Bass et al. 1979), in contrast to RRKM, rigorously conserve angular momentum of all states of the system including relative orbital and internal rotational angular momentum of the fragments and accounts for the centrifugal barrier. Marcus (1975) has modified "tight" transition state theory to cover the cases when the total angular momentum of the complex is transferred totally to orbital or totally to internal angular momenta of the products. The effect of internal angular momenta of ion-neutral reactants is however minor and can be ignored (Bates 1985) in association.

The generalization of (1.14b) to polyatomic reactants together with the appropriate generalization of the randomization assumption (1.18) yields the result of phase space theory (PST). By using PST and the practical expressions of Troe (1977), Bates (1986) provided a result which is identical with (1.14b) but with ρ therein replaced by

$$\rho(E,J) = \rho_v(E+E_T)\ F(E_T,J)/\sigma \qquad (1.20)$$

where σ is the (symmetry) number of indistinguishable ways of orienting the AB^*-complex. The density of vibrational states at energy E above the dissociation threshold $E_T = [E_o+(1/2)\sum_{i=1}^{s} h\nu_i] \equiv E_0+E_Z$ as measured from the minimum of the potential energy surface V(R) is,

$$\rho_v(E+E_T) = [(s-1)/(s-1.5)]^m \; (E+E_T)^{s-1}/[(s-1)! \prod_{i=1}^{s} h\nu_i] \qquad (1.21)$$

where ν_i are the frequencies of s harmonic oscillators in $(AB^+)^*$, and where m is the number of oscillators that disappear during dissociation. The first factor [ ] in (1.21) is an anharmonic correction, and for complexes with more than three atoms, $E_T = E_0 + aE_Z$ where a is the correction of Whitten and Rabinovitch (1963) designed to improve the semiclassical approximation involved with the zero point energy. The factor F in (1.20) is

$$F(E_T, J) = \gamma[1 - BJ^2/E_T]^{s-1} \qquad (1.22)$$

(γ = 1, and 2J for linear and symmetrical-top complexes, respectively) and acknowledges the effect that the averaged rotational energy BJ^2 of the complex has reduced the energy available to vibrational modes. For structureless reactants s is unity so that (1.21) reproduces the original result (1.14b) with (1.15).

1.3. Density Dependence

In contrast to the temperature dependence, the density dependence (1.8) or its microscopic equivalent (§ 2) has been tacitly accepted without any critical analysis. In order to isolate the key issue, express (1.14) in the equivalent form

$$K(T) = \int_0^\infty v_\infty \, G(E)dE \int_0^{\rho_{max}} \tau(E,\rho)(2\pi\rho d\rho) \qquad (1.23)$$

where the dynamical lifetime τ is given by (1.16), where $E = mv_\infty^2/2$ and where $\rho_{max} = R_T[1-V(R_T)/E_i]^{1/2}$ is the maximum impact parameter ρ of that orbit which just gains entry to the R_T-sphere. For polarization attraction $\pi\rho_{max}^2$ is $2\pi e(\alpha_B/m)^{1/2} \; v_\infty^{-1}$ such that the thermal approach rate $k_1 = \pi\rho_{max}^2 v_\infty$ is independent of T.

When the (A-B) interaction V(R) is neglected, τ is $2(R_T^2 - \rho^2)^{1/2}/v_\infty$, and (1.23) for K reduces naturally to the volume $4\pi R_T^3/3$ of the complex. For termolecular ion-ion recombination the stabilization frequency $\nu_s = k_s N$ can be separated as $\langle v\rangle(\lambda_A^{-1} + \lambda_B^{+1})$ where $\lambda_{A,B}$ are the path lengths for individual A-M and B-M binary collisions at average speed $\langle v\rangle$. The stabilization probability (1.9) for $\lambda_A = \lambda_B = \lambda$ is then

$$P_K^S(N) = \frac{(8X/3)}{1+(8X/3)} = (8X/3)\left[1 - (8X/3) + (8X/3)^2 - (8X/3)^3 \ldots\right], \qquad (1.24)$$

by the *partition-function method*, where X is R_T/λ.

The stabilization probability in (1.11) may also be identified as

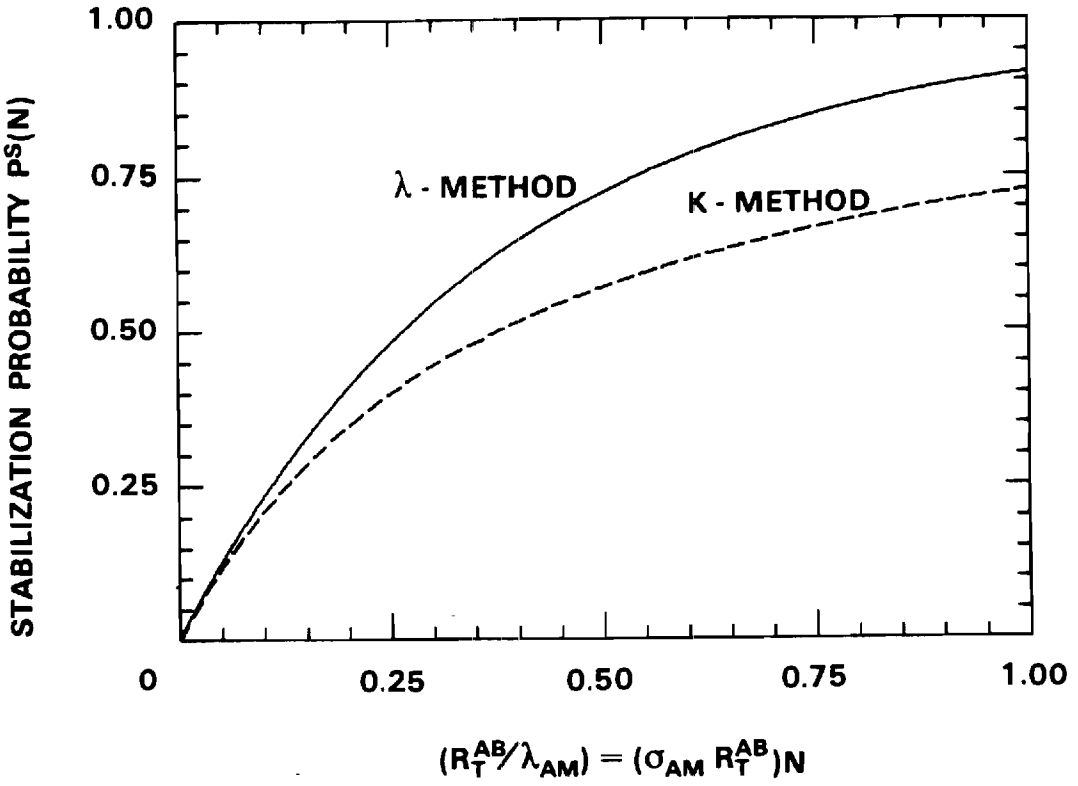

Fig. 1. $P^S(N)$ as determined by free-path (λ) and partition (K) methods.

$$P_T^S(N) = W(X_A) + W(X_B) - W(X_A)W(X_B) \qquad (1.25)$$

the combined probability for A-M and B-M collisions. The Thomson probability W for individual A-M collision for rectilinear (A-B) relative motion within the R_T-sphere is explicitly determined (Loeb 1955) as

$$W(X) = 1 - \frac{1}{2X^2}[1-\exp(-2X)(1+2X)] = \sum_{n=1}^{\infty} (-1)^{n+1} \frac{2^{n+1}X^n}{(n+1)!} \frac{(n+1)}{n+2} \qquad (1.26)$$

so that the total probability (1.25) for AB^* ($R \leq R_T$)-M stabilization encounters is

$$P_T^S(N) = (8X/3)\,[1 - (17X/12) + (7X^2/5) - (129X^3/120) + \ldots\,] \qquad (1.27)$$

Although (1.24) and (1.27) agree in the low and high density limits, there is significant departure at intermediate densities (Figure 1). For ion-atom association the appropriate comparison is between the single collision probability $W(X = R_T/\lambda_{AB})$ for AB^*-M collisions with free path λ_{AB} and $(4X/3)/(1+4X/3)$, the corresponding P_K^S, and is similar to that depicted in Fig. 1. For association note that M does not necessarily have to be within the R_T-sphere for collisions to occur.

Dilemma 1: Which of the above methods is more accurate? The outcome is certainly important in principle and may be important in practice since (1.8) is generally used to deduce third order rates α_o from measurements at various N (cf. Mahan and Person 1964 for recombination and Bates 1986 for association). For ion-ion recombination the Thomson radius (see §4) R_T is $(2/3)e^2/kT \sim 370\mathring{A}$ at 300 K, and for ion-atom association the Langevin radius R_L of the AB^+ complex is $(\alpha_B e^2/3kT)^{1/4} \sim (5\text{-}15)\mathring{A}$. Hence the range of X in Fig. 1 which corresponds to gas pressures up to (1/2) atm. (where $\lambda \sim 180\mathring{A}$ at STP) is $0 \rightarrow 1$ for recombination and $0 \rightarrow \sim 0.05$ for association. For most pressures of practical interest, therefore, variation of the association rate is given by either method (cf. Fig. 1). For recombination, there is a large difference. For higher pressures, however, diffusional drift (§4) ignored by both methods becomes important only for recombination.

Dilemma 2: Although the form of (1.8),

$$\alpha = (k_1\alpha_o)/(k_1+\alpha_o) \quad , \qquad \alpha_o = Kk_TN \tag{1.28}$$

is aesthetically pleasing in that it illustrates quite naturally that the overall rate is given by the rate limiting step, k_1 being the thermal rate as such does not acknowledge diffusional drift (§4) which arises from a non-equilibrium distribution in R outside the reaction sphere. As the gas density N is raised can we simply replace the thermal rate k_1 of approach by the rate α_{TR} of transport by diffusional drift to R_T?

In order to address these queries a microscopic treatment of the energy-transfer sequence (1.2) for structureless reactants in a chemically inert gas must first be developed (§ 2). Appropriate generalization to structured reactants, if required, appears straightforward.

2. MICROSCOPIC DEVELOPMENT

The set of Master Equations derived from the Boltzmann equation for the two-particle distribution function (Flannery 1982) for the (cm^{-3}) concentrations $n_i^{\pm}(\underset{\sim}{R},t) \equiv n_i^{\pm}(\underset{\sim}{R},E_i,L_i^2;t)$ per unit interval $d\underset{\sim}{R}\, dE_i\, dL_i^2$ of A-B pairs with internal energy E_i, and internal angular momentum (squared) L_i^2 that are internally expanding (+) and contracting (−) with radial speed $|v_R|$ at internal separation R is (Flannery 1986, 1987)

$$dn_i^{\pm}(\underset{\sim}{R},t)/dt = \partial n_i^{\pm}(\underset{\sim}{R},t)/\partial t \pm \frac{1}{R^2}\frac{\partial}{\partial R}\left[R^2\, n_i^{\pm}(\underset{\sim}{R},t)\,|v_R|\right]_{E_i,L_i^2}$$

$$= -\int_{V_i(R)}^{\infty} dE_f \int_0^{L_{mf}^2} S_{if}^{\pm}(\underset{\sim}{R})\, dL_f^2 \tag{2.1}$$

where the net collisional rate per unit intervals $dE_i dL_i^2$ and $dE_f dL_f^2$

about the initial and final states i and f respectively is

$$S_{if}^{\pm}(\underset{\sim}{R}) = n_i^{\pm}(\underset{\sim}{R})\ \upsilon_{if}(R) - n_f^{\pm}(\underset{\sim}{R})\ \upsilon_{fi}(R) = -S_{fi}^{\pm}(\underset{\sim}{R}) \tag{2.2}$$

in terms of the frequency $\upsilon_{if}(R)$ per unit interval $dE_f dL_f^2$ for transitions $i\ (E_i, L_i^2) \rightarrow f\ (E_f, L_f^2)$ induced by collisions between M and the pair (A-B). The relative interaction energy between A and B of reduced mass m is V(R) and the effective radial interaction is

$$V_i(R) = V(R) + L_i^2/2mR^2 \tag{2.3a}$$

For fixed E_i and R, the maximum value of L_i^2 is

$$L_{mi}^2(E_i, R) = 2m\,[E_i - V(R)]R^2 \tag{2.3b}$$

and, for fixed E_i alone, the maximum value of L_{mi}^2 with respect to R is $L_{oi}^2(E_i)$.

The basic expression for the rate ($cm^3\ s^{-1}$) of termolecular association processes (1.1) at time t is (Flannery 1985)

$$R^A(t) = \int_{-D}^{\infty} dE_i \int_0^{L_{oi}^2} P_i^A(E_i, L_i^2)\,dL_i^2 \int_{R_i^-}^{R_i^+} \left[\frac{dn_i(\underset{\sim}{R}, t)}{dt}\right] d\underset{\sim}{R} \tag{2.4}$$

where the summed distribution $n_i = n_i^+ + n_i^-$ of the expanding and contracting R-pairs in (2.1) satisfies (Flannery 1986)

$$dn_i(\underset{\sim}{R}, t)/dt = \partial n_i(\underset{\sim}{R}, t)/\partial t + \frac{1}{R^2}\frac{\partial}{\partial R}\left[R^2(n_i^+ - n_i^-)\,|v_R|\right]_{E_i, L_i^2}$$

$$= -\int_{V_i}^{\infty} dE_f \int_0^{L_{mf}^2} S_{if}(R, t)\,dL_f^2 \tag{2.5}$$

in which S_{if} is the sum $(S_{if}^+ + S_{if}^-)$ of collision rates defined in (2.2).

In (2.4), P_i^A is the probability that (E_i, L_i^2) -pairs are in the product (association) channel, R_i^- and R_i^+ are the perigee and apogee of the relative (E_i, L_i^2) motion, and -D is the lowest vibrational energy level of AB with respect to the dissociation limit taken as zero energy.

(A) Assume that pairs in the block $\mathcal{E}$ of highly excited bound AB levels, sandwiched between the continuum block $\mathcal{C}$ of fully dissociated states (where P_i^A is zero) and the sink block $\mathcal{S}$ of fully associated

stabilized levels between -D and some level -S (throughout which P_i^A is unity), are in quasi-steady-state (QSS). Hence

$$n_i(t) = \int_{R_i^-}^{R_i^+} n_i(\underset{\sim}{R}, t)\, d\underset{\sim}{R} \tag{2.6}$$

in block $\mathcal{E}$ satisfies

$$dn_i/dt = \partial n_i/\partial t = -\int_{R_i^-}^{R_i^+} d\underset{\sim}{R} \int_{V_i}^{\infty} dE_f \int_0^{L_{mf}^2} S_{if}(R)\, dL_f^2 \simeq 0 \tag{2.7}$$

since $n_i^+ = n_i^-$ at both turning points $R_i^{(+)}(E_i, L_i^2)$. Under the conservation requirement

$$\frac{\partial}{\partial t} \int_{-D}^{\infty} dE_i \int_0^{L_{oi}^2} n_i(t)\, dL_i^2 = 0 \tag{2.8}$$

for a complete steady-state system, (2.4) therefore reduces under QSS of block $\mathcal{E}$, to the following equivalent forms

$$R^A(t) = \int_{-D}^{-S} dE_i \int_0^{L_{oi}^2} dL_i^2 \int_{R_i^-}^{R_i^+} \left[\frac{dn_i}{dt}\right] d\underset{\sim}{R}\,, \tag{2.9a}$$

the $\mathcal{E} \to \mathcal{I}$ current, or

$$R^A(t) = \int_0^{\infty} dE_i \int_0^{L_{oi}^2} dL_i^2 \int_{R_i^-}^{R_i^+} \left[\frac{dn_i}{dt}\right] d\underset{\sim}{R} \tag{2.9b}$$

the $\mathcal{C} \to \mathcal{E}$ current, or

$$= \int_0^{\infty} dL_i^2 \int_{U_i}^{\infty} dE_i \int_{R_i^-}^{R_i^+} d\underset{\sim}{R} \int_{V_i}^{U_i} dE_f \int_0^{L_{mf}^2} S_{if}(R)\, dL_f^2 \tag{2.9c}$$

which is simply the net collisional current flowing downwards across the top U_i of the centrifugal barrier for (E_i, L_i^2)-motion.

The density (per unit interval $d\Gamma_i = dE_i dL_i^2$)

$$n_i^*(t) = \int_{R_i^-}^{R_T} n_i(\underset{\sim}{R}, t)\, d\underset{\sim}{R} \tag{2.10}$$

of (E_i, L_i^2)-pairs which form the activated complex with internal separation R in the range $R_i^- \leq R \leq R_T(E_i, L_i^2)$ satisfies

$$\partial n_i^*(t)/\partial t = 4\pi R_T^2 v_R(R_T) n_i^-(R_T)[1-P_i^d(R_T)] - \int_{R_i^-}^{R_T} d\underset{\sim}{R} \int S_{if}(R) d\Gamma_f \qquad (2.11a)$$

$$= 4\pi R_T^2 v_R(R_T) n_i^-(R_T) P_i^s(R_T) - \int_{R_i^-}^{R_T} d\underset{\sim}{R} \int S_{if}(R) d\Gamma_f \qquad (2.11b)$$

where the implied two-dimensional grid for Γ_f-integration is $0 \leq L_f^2 \leq L_{of}^2$ and $V_i \leq E_f \leq U_i$. The microscopic probabilities

$$P_i^d(R_T) = n_i^+(R_T)/n_i^-(R_T) \qquad (2.12)$$

for decomposition of the activated (E_i, L_i^2, R_T)-complex, and

$$P_i^s(R_T) = [n_i^-(R_T) - n_i^+(R_T)]/n_i^-(R_T) = 1 - P_i^d(R_T) \qquad (2.13)$$

for collisional stabilization of the complex, are introduced in (2.11).

The basic QSS-rate (2.9) in terms of the stabilization probability (2.13) is now

$$R^A(t) = \alpha n_A n_B = \int_o^\infty dL_i^2 \int_{U_i}^\infty dE_i \, [4\pi R_T^2 v_R(R_T) n_i^-(R_T)] P_i^s(R_T) \qquad (2.14)$$

in a form suitable for general $R_T(E_i, L_i^2)$. When R_T is constant, or is only a function of E_i, then the equivalent form

$$\alpha n_A n_B = \int_o^\infty dE_i \int_o^{L_{max}^2} dL_i^2 \, [4\pi R_T^2 v_R(R_T) n_i^-(R_T)] P_i^s(R_T) \qquad (2.15)$$

is also appropriate, where

$$L_{max}^2 = 2m E_i[1 - V(R_T)/E_i] R_T^2 = (2mE_i)\rho_{max}^2 \qquad (2.16)$$

is associated, as in §1, with that limiting orbit with impact parameter $\rho = \rho_{max}$ which just touches the R_T-sphere.

2.1 Treatment with Thermal Rate of Approach

When there is a thermal distribution of AB-pairs with internal separation $R \geq R_T$

$$n_i^-(R)/n_A n_B = \tilde{n}_i^-(R)/\tilde{n}_A\tilde{n}_B \tag{2.17}$$

where the tildas (~) signify thermodynamic equilibrium, then (2.14) yields,

$$\alpha = \int_0^\infty dL_i^2 \int_{U_i}^\infty dE_i\ k_i(R_T)P_i^s(R_T) \tag{2.18}$$

in which the one-way thermal equilibrium rate k_i for formation of R_T-pairs (per unit interval $dE_i dL_i^2$) may be written in the following variety of suggestive forms,

$$k_i = 4\pi R_T^2 v_R(R_T)\tilde{n}_i^-(R_T)/\tilde{n}_A\tilde{n}_B \tag{2.19a}$$

$$= 4\pi^2 \exp(-E_i/kT)/(2\pi mkT)^{3/2} \tag{2.19b}$$

$$= \pi R_T^2[1 - V(R_T)/E_i]v_\infty\ G(E_i)/L_{max}^2 \tag{2.19c}$$

$$= [\tilde{n}_i^*(E_i, L_i^2)/\tilde{n}_A\tilde{n}_B]/\tau_i^d \tag{2.19d}$$

$$= v_\infty\ G(E_i)\ 2\pi\ \rho(d\rho/dL_i^2) \tag{2.19e}$$

each being appropriate to application of (2.18) or (2.15) with (2.17). The Maxwellian distribution of relative energies $E_i = m\ v_\infty^2/2$ is

$$G(E_i)dE_i = 2(E_i/\pi kT)^{1/2} \exp(-E_i/kT)\ d(E_i/kT) \tag{2.20}$$

For the polarization (A^+-B) potential, use of (2.15) involves $R_T(E_i) = (\alpha_B e^2/2E_i)^{1/4}$ and $L_{max} = (8m\alpha_B eE_i)^{1/4}$, as in §1, and use of (2.18) involves $R_T(L_i) = (\alpha_B m)^{3/2}e/l_i$ and $U_i(R_T) = \alpha_B e^2/2R_T^4$, the barrier height.

The equilibrium microscopic concentration per unit interval dE_i of <u>all</u> pairs in the $R \leq R_T$ complex in (2.19d) is

$$\tilde{n}_i^*(E_i, L_i^2)dL_i^2 = dL_i^2 \int_{R_i}^{R_T} \tilde{n}_i(\underset{\sim}{R}, E_i, L_i^2)d\underset{\sim}{R} = \tilde{n}_A\tilde{n}_B[v_\infty G(E_i)][2\pi\rho d\rho]\tau_i^d \tag{2.21}$$

where the natural lifetime of the complex is

$$\tau_i^d(E_i, L_i^2) = \int_{R_i^-}^{R_T} dR/v_R = [\upsilon_i^d(E_i, L_i^2)]^{-1} \qquad (2.22)$$

Note that the reaction volume $K_i = \tilde{n}_i^*/\tilde{n}_A\tilde{n}_B$ per unit $dE_i dL_i^2$, the microscopic equivalent of (1.14), may be written in various forms as

$$K_i(E_i, L_i)dE_i dL_i^2 = h^3(2\pi mkT)^{-3/2}\, \rho_i(E_i, J_i)\, \exp(-E_i/kT)dE_i dJ_i^2 \qquad (2.23a)$$

$$= (\pi/2mE_i)[v_\infty G(E_i)dE_i]dL_i^2 \qquad (2.23b)$$

$$= [v_\infty G(E_i)dE_i][2\pi\rho d\rho]\tau_i^d(E_i, \rho) = k_i \tau_i^d\, dE_i dL_i^2 \qquad (2.23c)$$

where the density of states ρ_i is $(h\upsilon_i^d)^{-1}$, which is the microscopic generalization of (1.15).

Provided that the stabilization probability P_i^s can be determined, the rate α follows directly from (2.18). Common to the following two approximations for P_i^s is the *strong-collision assumption* that collisional absorption within the complex only occurs. Thus, for a steady state distribution of pairs in the complex, (2.1) is simplified to yield,

$$\pm \frac{1}{R^2}\frac{\partial}{\partial t}\,[R^2 n_i^{\pm}(R)|v_R|]_{E_i, L_i^2} = -\, n_i^{\pm}(\underset{\sim}{R})\upsilon_i(R) \qquad (2.24)$$

where the frequency for collisional formation of bound pairs with $R \leq R_T$ below the centrifugal barrier is

$$\upsilon_i(R) = \int_{V_i}^{U_i} dE_f \int_0^{L_{mf}^2} \upsilon_{if}(R)dL_f^2 \qquad (2.25)$$

2.2 Partition-Function Method

This first method is based on (2.11) which is the microscopic generalization of (1.5). On defining the one-way equilibrium microscopic rate of formation or thermal approach rate as in §2.1 by

$$k_i\, \tilde{n}_A\tilde{n}_B = 4\pi R_T^2 v_R(R_T)\tilde{n}_i^-(R_T) \quad , \qquad (2.26)$$

and the non-equilibrium rates for natural decomposition,

$$k_i^*\, n_i^* = 4\pi R_T^2 v_R(R_T) n_i^+(R_T) \quad , \qquad (2.27)$$

and for collisional stabilization

$$\upsilon_i^s\, n_i^* \equiv (k_i^s\, N) n_i^* = \int_{R_i}^{R_T} n_i(R)\upsilon_i(R)d\underset{\sim}{R} \tag{2.28}$$

of the complexes, then (2.11) can be expressed as

$$\partial n_i^*/\partial t = k_i n_A n_B - (k_i^* + k_i^s\, N) n_i^* \tag{2.29}$$

For a steady state distribution of complexes, the rate (2.18), with the aid of (2.25) - (2.29), is

$$R^A(t) = \int_o^\infty dL_i^{\,2} \int_{U_i}^\infty dE_i\, [n_i^*\, k_i^s\, N] \tag{2.30}$$

$$= \int_o^\infty dL_i^{\,2} \int_{U_i}^\infty dE_i \left[\frac{k_i(k_i^s K_i N)}{(k_i + k_i^s K_i N)}\right] \tag{2.31}$$

which is the microscopic generalization of (1.8). The reaction volume

$$K_i = \tilde{n}_i^*(E_i, L_i^{\,2})/\tilde{n}_A\tilde{n}_B = k_i/k_i^* \tag{2.32}$$

per unit $dE_i dL_i^2$ is given by any of the forms in (2.23), whichever proves most convenient. The integration order in (2.31) may be interchanged as in (2.15). The form of (2.31) is well known (Bass et al. 1979, Bates 1986).

With the aid of (2.23) the ratio

$$K_i/k_i = \tau_i^d = 1/k_i^* \tag{2.33}$$

is simply the lifetime of the (E_i, L_i^2)-complex towards natural decomposition. Hence,

$$\alpha = \int_o^\infty dL_i^{\,2} \int_{U_i}^\infty dE_i\, [k_i\, P_i^s(N)] = \int_o^\infty dL_i^{\,2} \int_{U_i}^\infty dE_i\, [k_i^s\, K_i N\, P_i^d(N)] \tag{2.34}$$

where k_i is given by (2.19), and where the probabilities for collisional stabilization and natural decomposition can be identified with the aid of (2.28), as

$$P_i^s(N) = k_i^s\, K_i N/(k_i + k_i^s K_i N)$$

$$= \upsilon_i^s \tau_i^d/(1 + \upsilon_i^s \tau_i^d) \quad \rightarrow \quad \begin{cases} \upsilon_i^s \tau_i^d & , N \rightarrow 0 \\ 1 - 1/\upsilon_i^s \tau_i^d & , N \rightarrow \infty \end{cases} \tag{2.35}$$

and as

$$P_i^d(N) = k_i/(k_i+k_i^s K_i N)$$

$$= 1/(1 + \nu_i^s \tau_i^d) \quad \rightarrow \quad \begin{cases} 1 & , N \rightarrow 0 \\ 1/\nu_i^s \tau_i^d & , N \rightarrow \infty \end{cases} \tag{2.36}$$

respectively. When R_T is constant or depends only on E_i, the order of integrations in (2.34) can be interchanged and performed over the range $0 \leq E_i \leq \infty$ and $0 \leq L_i^2 \leq L_{max}^2$. The above expressions are the appropriate microscopic generalizations of (1.8)-(1.10). At low densities N therefore

$$\alpha = \int_0^\infty dL_i^2 \int_{U_i}^\infty dE_i \; k_i(E_i, L_i^2) \; [\nu_i^s \tau_i^d] = \int_0^\infty dL_i^2 \int_{U_i}^\infty K_i(E_i, L_i^2) \nu_i^s \; dE_i \tag{2.37}$$

which is $(\nu_i^s \tau_i^d)$ averaged over k_i, the one-way equilibrium rate (2.19) for complex formation, or equivalently is ν_i^s, the stabilization frequency in (2.28) averaged over the reaction volume K_i. Note that α may be expressed as $k_1 \langle \tau^d \rangle (k_s N)$ only when the so-called average lifetime $\langle \tau^d \rangle$ is defined as above (see also Bates 1979a). The low-density rate (2.37) may also be expressed as,

$$\alpha \; \tilde{n}_A \tilde{n}_B = \int_0^\infty dL_i^2 \int_{U_i}^\infty dE_i \; \tilde{n}_i^*(E_i, L_i^2) \; \nu_i^s \tag{2.38}$$

which is the equilibrium version of (2.30). When the stabilization frequency ν_i^s does not depend on (E_i, L_i^2), and is taken as a constant β times the Langevin rate (1.19) then the low density rate is simply

$$\alpha \; \tilde{n}_A \tilde{n}_B = \beta (k_L N) \tilde{n}^* \tag{2.39}$$

where $\tilde{n}^*$ is the concentration of pairs above all the centrifugal barriers, in accord with (1.4).

2.3. Free-path Method

This method is based on the direct solution of (2.24) subject to the boundary conditions

$$\begin{aligned} n_i^-(R_T) &= \tilde{n}_i^-(R_T) \\ n_i^+(R_i^-) &= n_i^-(R_i^-) \end{aligned} \tag{2.40}$$

where $R_i(E_i,L_i^2)$ is, as before, the perigee of the (E_i,L_i^2)-orbit. Hence (Flannery 1985)

$$n_i^-(R_i^- \le R \le R_T, E_i, L_i^2) = \tilde{\tilde{n}}_i(R)\ \exp[-\int_R^{R_T} a_i(R)dR]$$

$$n_i^+(R_i^- \le R \le R_T, E_i, L_i^2) = \tilde{\tilde{n}}_i(R)\ \exp[-\int_R^{R_T} a_i(R)dR]\exp[\oint_{R_i^-}^{R_T} a_i(R)dR] \qquad (2.41)$$

are the (R,E_i,L_i^2)-distributions of individual AB pairs within the complex.

The number of stabilizations that occur in a time $dt = dR/v_R$ or within element ds of the (E_i,L_i^2) trajectory for (A-B) relative motion at relative speed v_i are

$$a_i(R,E_i,L_i^2)dR = \upsilon_i dt = \upsilon_i dR/v_R = \upsilon_i ds/v_i = ds/\lambda_i \qquad (2.42)$$

where λ_i is the free path length (v_i/υ_i) between collisions at frequency υ_i given by (2.25). The stabilization probability is therefore

$$P_i^s(R_T,E_i,L_i^2) = 1 - \exp(-2\int_{R_i^-}^{R_T} ds/\lambda_i) \qquad (2.43)$$

the microscopic probability of collision of (E_i,L_i^2)-pairs with separation R in the range $R_i^- \le R \le R_T(E_i,L_i^2)$. The association rate under the strong-collision assumption is then (2.34) with (2.43).

On defining, with the aid of the stabilization frequency in (2.28),

$$\upsilon_i^s\ \bar{\tau}_i^d = \oint_{R_i^-}^{R_T} \upsilon_i(R)dR/v_R = \oint ds/\lambda_i \qquad (2.44)$$

which equals $\upsilon_i^s\ \tau_i^d$ only if the collision frequency (2.25) in (2.28) is independent of R, then (2.43) is simply

$$P_i^s = 1 - \exp(-\upsilon_i^s\ \bar{\tau}_i^d) \qquad (2.45)$$

which has been obtained from the distribution (2.41) of individual pairs within the complex. This is to be compared with the customary form (2.35) obtained from the averaged distribution in (2.29).

For straight line trajectories at constant speed and with $\upsilon_i = \upsilon_i^s = \langle v\rangle\ (\lambda_A^{-1} + \lambda_B^{-1})$, then τ_i^d of (2.33) and $\bar{\tau}_i^d$ of (2.44) are each equal to

$2(R_T^2 - \rho^2)^{1/2}/\langle v\rangle$ so that the above free-path method for A-M and B-M collisions yields

$$P_{Ti}^S = 1 - \exp - [X_A(\rho) + X_B(\rho)] \quad , \; X_{A,B} = 2(R_T^2 - \rho^2)^{1/2}/\lambda_{A,B} \tag{2.46}$$

which is to be compared with the corresponding result

$$P_{Ki}^S = (X_A + X_B)/[1+(X_A+X_B)] \tag{2.47}$$

given by the partition-function method. The comparison for various impact parameters ρ illustrates discrepancies similar to that displayed in Fig. 1. It is worth noting that (2.15) with (2.43) for constant R_T and $\lambda_{A,B}$ and a straight line trajectory reduces to the rate (Flannery 1986)

$$\alpha = \pi R_T^2 \left[\int_0^\infty [1 - V(R_T)/E_i] \, v_\infty \, G(E_i) dE_i \right] P_T^S(N) \tag{2.48}$$

where the macroscopic probability P_T^S is given by (1.25). This rate is identical with (1.11) The first dilemma posed in §1 is therefore resolved. The free path method based on knowledge of individual R_T pairs within the complex represents a more basic procedure than does the partition method which is based only on knowledge of the averaged density n^* of all pairs with $R \leq R_T$. The stabilization probability (1.9) is not as accurate as (1.25) and (1.27).

3. TREATMENT WITH DIFFUSIONAL-DRIFT RATE OF ENTRY

Assume upon approach to the reaction R_T-sphere that the energy gained by the (A-B) pairs from their mutual field V(R) is lost upon collision with M so that their relative kinetic energy T_i is restored to their asymptotic equilibrium value E_i. Hence

$$T_i(R) = E_i + V(R+\lambda) - V(R) = E_i + \Delta V, \qquad R \geq R_T \tag{3.1}$$

where λ is the macroscopic mean free path and L_{max}^2 is $(2mT_i)R_T^2$. The microscopic velocity distribution at R is assumed Maxwellian i.e.,

$$n_i(R)dT_i = [(T_i/\pi kT)^{1/2} \exp(-T_i/kT) \, d(T_i/kT)]n(R) \tag{3.2}$$

outside the reaction sphere. The non-equilibrium density n(R) of all AB-pairs with $R \geq R_T$ satisfies the continuity equation $\nabla \cdot \underset{\sim}{J} = 0$, which follows from integration of (2.5) over all (E_i, L_i^2). The net outward radial current is

$$J = - \left[D \frac{dn}{dR} + \left[\frac{K}{e}\right]\left[\frac{dV}{dR}\right] n(R) \right]$$

$$= - D \exp(-V/kT) \; (d[n(R)\exp(V/kT)]/dR) \tag{3.3}$$

where D and K, the coefficients for relative diffusion and mobility in the gas, are related by De = KkT under equilibrium with the field.

The appropriate distribution for $R \geq R_T$ is therefore (cf. Flannery 1982a,b)

$$n(R_T) = \tilde{n}_A \tilde{n}_B \exp(-V/kT) \left[1 - \left(\frac{\alpha}{\alpha_{TR}}\right) \frac{\tilde{R}}{\tilde{R}_T}\right] \tag{3.4}$$

where

$$\alpha_{TR} = 4\pi D \tilde{R}_T \tag{3.5}$$

is the rate of formation by transport of pairs with separation $R \leq R_T$ and where

$$\tilde{R} = \left[\int_R^\infty \exp(KV/De) R^{-2} dR\right] \tag{3.6}$$

is a scaled length in presence of interaction V(R).

With this analysis, the rate (2.17) yields the standard result (cf. Flannery 1982a,b)

$$\alpha = \frac{\alpha_{RN}\, \alpha_{TR}}{\alpha_{RN}+\alpha_{TR}} \tag{3.7}$$

for termolecular processes in the presence of diffusional drift. The reaction rate therein is identified as

$$\alpha_{RN} = \int_o^\infty dE_i \int_o^{L^2_{max}} dL_i^2\, v_\infty [1+\Delta V(R_T)/E_i] \exp[-V(R_T+\lambda)/kT][G(E_i)/L^2_{max}] \times$$

$$P_i^s(R_T, E_i, L_i^2) \tag{3.8}$$

for general $R_T(E_i, L_i^2)$. As $\lambda \to \infty$ i.e., when diffusional-drift can be neglected outside the R_T-sphere (3.8) reduces to (2.18) with (2.19c) as expected.

Resolution of the dilemma posed in §1 is based on the recognition that (1.28), although similar in form to (3.7) is an approximation only to the reaction rate (3.8) and Expression (1.28) therefore does not contain the physics intrinsic to (3.7). The attractive form of (1.28) tends to mask its approximate character.

4. TERMOLECULAR RECOMBINATION AT LOW GAS DENSITIES

Simplifications to the full microscopic treatment as characterized by the appropriate solutions of (2.5) in (2.9c) can be therefore achieved by assuming (i) a *reaction radius* R_T - the location of the centrifugal barrier $U_i(L_i)$ for $(A^+\text{-}B)$ association or a constant $R_T \sim \frac{1}{2}(e^2/kT)$ for $(A^+\text{-}B^-)$ recombination - and (ii) a one-way downward collisional absorption or stabilization rate (2.25) and (2.28) which represents *the strong collision limit*. This rate is given either by the flux across the neck U_i of the effective potential $V_i(R, E_i, L_i^2)$ for $A^+\text{-}B$ association, or by the flux across the dissociation limit at $E_i = 0$ for ion-ion recombination since the

Coulombic attraction here cannot support an angular momentum barrier.

In order to assess the effectiveness of these two basic assumptions and of other alternative procedures (such as a weak-collision limit and a Variational procedure) which may be adopted, consider the well developed case of termolecular ion-ion recombination at low gas densities. At low N, equilibrium in coordinates R and L_i^2 is quickly established and relaxation in internal energy E_i is the rate limiting step. Integration of (2.5) over (R, L_i^2) yields the standard input-output Master equation

$$dn_i(E_i,t)/dt = \partial n_i(E_i,t)/\partial t = -[n_i(t)\int_{-D}^{\infty} \upsilon_{if}\, dE_f - \int_{-D}^{\infty} n_f(t)\, \upsilon_{fi}\, dE_f] \quad (4.1)$$

for the time-dependent pair distribution $n_i(E_i,t)$ per unit energy interval dE_i for bound ($E<0$) levels in block $\mathcal{E}$ in terms of the frequency υ_{if} per unit interval dE_f for $E_i \rightarrow E_f$ transitions via (AB-M) collisions. This distribution is now expanded as (Flannery 1985)

$$\frac{n_i(E_i,t)}{\tilde{n}_i(E_i)} = P_i^D(E_i)\left[\frac{n_A(t)n_B(t)}{\tilde{n}_A\tilde{n}_B}\right] + P_i^A(E_i)\left[\frac{n(\mathcal{S},t)}{\tilde{n}(\mathcal{S})}\right] \quad (4.2)$$

where $P_i^{A,D}(E_i)$ are the probabilities that E_i-pairs are in the reactive channels which result in association or dissociation respectively. Thus, $P_i^A(E_i \geq 0)$ is zero in the continuum block $\mathcal{C}$ and $P_i^A(-S \geq E_i \geq -D)$ is unity in the block $\mathcal{S}$ of stabilized levels with overall distribution $n(\mathcal{S},t)$. On inserting (4.2) into (4.1) and with the aid of (2.4), the basic expression

$$\alpha\, \tilde{n}_A\tilde{n}_B = \int_{-D}^{\infty} P_i^A\, dE_i \int_{-D}^{\infty} (P_i^A - P_f^A)C_{if}dE_f \quad (4.3)$$

can be derived (Flannery 1985). The one-way equilibrium collision rate for $E_i \rightarrow E_f$ transitions is

$$C_{if}(E_i,E_f) = \int_0^{R_{if}} C_{if}(R)d\underset{\sim}{R} = \int_0^{R_{if}} d\underset{\sim}{R} \int_0^{L_{mi}^2} \tilde{n}_i(R)dL_i^2 \int_0^{L_{mf}^2} \upsilon_{if}(R)dL_f^2 \quad (4.4)$$

where R_{if} is the lesser of the outermost classical turning points R_i^+ and R_f^+ associated with levels E_i and E_f respectively. For a quasi-steady state (QSS) distribution of pairs in excited block $\mathcal{E}$ ($0 \geq E_i \geq -S$), (4.3) reduces exactly to the net downward steady-state current (Flannery 1985)

$$\alpha_E\, \tilde{n}_A\tilde{n}_B = -\, j(-E) = \int_{-E}^{\infty} dE_i \int_{-D}^{-E} (P_f^A - P_i^A)C_{if}\, dE_f \quad (4.5)$$

across an arbitrary bound level -E in block $\mathcal{E}$. The probabilities in (4.5) satisfy the QSS-condition

$$P_i^A \int_{-D}^{\infty} C_{if}\, dE_f = \int_{-D}^{\infty} P_i^A\, C_{if}\, dE_f \qquad (4.6)$$

which must rigorously hold in order that α be identified as in (4.5) with a current j(-E) that is constant to variation of E within block $\mathcal{E}$. The equations (4.5) and (4.6) are essentially those as given by the standard QSS-method (Bates and Moffett, 1966; Bates and Flannery, 1968) for recombination under the condition $n_A(t)n_B(t)/\tilde{n}_A\tilde{n}_B >> n(\mathcal{V},t)/\tilde{n}(\mathcal{V})$. The rate (4.5) in practice reduces to a sum of rates each arising from A^+-M and B^--M collisions, respectively (Bates and Flannery, 1968; Flannery and Yang, 1980).

4.1. One-Way Equilibrium Rate: *Strong Collision Limit*

On ignoring upward transitions across E = 0 for $R \leq R_T$ and upon assuming full thermodynamic equilibrium (which entails equal upward and downward collisional rates at each R) for $R \geq R_T$ then (4.5) provides the one-way downward equilibrium flux across E = 0 as

$$\alpha_T\, \tilde{n}_A\tilde{n}_B = \int_o^{\infty} dE_i \int_o^{R_T} \frac{dR}{\sim} \int_{-D}^{o} C_{if}(R)dE_f \qquad (4.7)$$

which is the modern collisional equivalent of the low density treatment of Thomson (1924). Figure 2 displays the variation obtained by Flannery and Mansky (1987) of the ratio (α_T/α_E) with R_T for equal mass species A^+, B^- and M. Energy-changing collisions via various $(A^+$-M) interactions CX for symmetrical resonance charge transfer (Flannery 1980), HS for hard sphere encounters (Flannery 1981) and for polarization collisions (Bates and Mendas 1982) are considered. Equivalence between α_E and α_T occurs for $R_T \sim 0.5\ (e^2/kT)$, a value that can be assigned only after detailed calculations for α_E. Table 1 displays the assigned R_T for various values of the mass ratio parameters

$$a = M_B M/M_A(M_A+M_B+M) \qquad (4.8)$$

where $M_{A,B}$ and M are the masses of the ions and gas atoms respectively. The very small values of R_T for small $a \sim 10^{-3}$ are simply a manifestation that (4.7) becomes invalid for electron-ion recombination since then only a small fraction $\delta = (2m_e/M)$ of the electron's energy can be transferred in e-M collisions so that the upper limit of the E_i-integration in (4.7) is $\delta e^2/R_T$ rather than infinity (Bates, 1980).

The divergence of (4.7) illustrated in Fig. 2 as $R_T \to \infty$ results from the divergence in the equilibrium density $\tilde{n}(E_i)$ of Coulombic levels as $E \to 0$, and from the neglect in (4.7) of upward collisional transitions within

Table 1: Radius R_T (in units of e^2/kT) so assigned that the one-way equilibrium rate (4.7) reproduces the exact rate (4.5) for various mass parameters (4.8) and (A^+-M) interactions.

a	CX	HS	POL
0.001	0.1200	0.1655	0.0922
0.010	0.2277	0.2902	0.1801
0.100	0.3657	0.4510	0.3074
0.333	0.3992	0.5076	0.4861
1.000	0.5449	0.5187	0.3749
10.000	-	0.4211	0.4280
100.000	-	0.2444	0.2735
1000.000	-	0.1188	0.0922

the R_T-sphere, an assumption which is inappropriate as $R_T \to \infty$.

This divergence can be eliminated, not only by maintaining R_T finite, but also by considering the one-way equilibrium rate

$$\alpha_B(E)\ \tilde{n}_A \tilde{n}_B = \int_{-E}^{\infty} dE_i \int_{-D}^{-E} dE_f \int_0^{R_{if}} C_{if}(R) d\underset{\sim}{R} \qquad (4.9)$$

across any bound level $-E$ in block $\mathcal{E}$. The variation (Fig. 3) with $-E$ of this rate displays a minimum (Flannery 1980, 1981) at the bottleneck energy $E^* \underset{\sim}{\simeq} -2kT$. Thus $\alpha_B(E^*)$ is the least upper limit. This variational procedure is akin to the Wigner-Keck Variational phase-space treatment (Wigner, 1937; Keck, 1967). Table 2 provides (α_B/α_E) for various mass parameters a. The procedure is more reliable for a in the range $0.1 \leq a \leq 10$ where the collisional dynamics for larger energy-transfers are important.

4.2. Diffusion Method: *Weak-Collision Limit*

For small energy-transfers, the collision integral in (2.5) when integrated over R and L_i^2 can be represented in differential form, so that the diffusional net current in energy space is (cf. Flannery 1987)

$$j_D(E_i) = - D_i^2(E_i)\ (\partial P_i^D/\partial E_i) \qquad (4.10)$$

where the energy diffusion coefficient is

$$D_i^2(E_i) = \frac{1}{2} \int_{-D}^{\infty} (E_f - E_i)^2\ C_{if}\ dE_f \qquad (4.11)$$

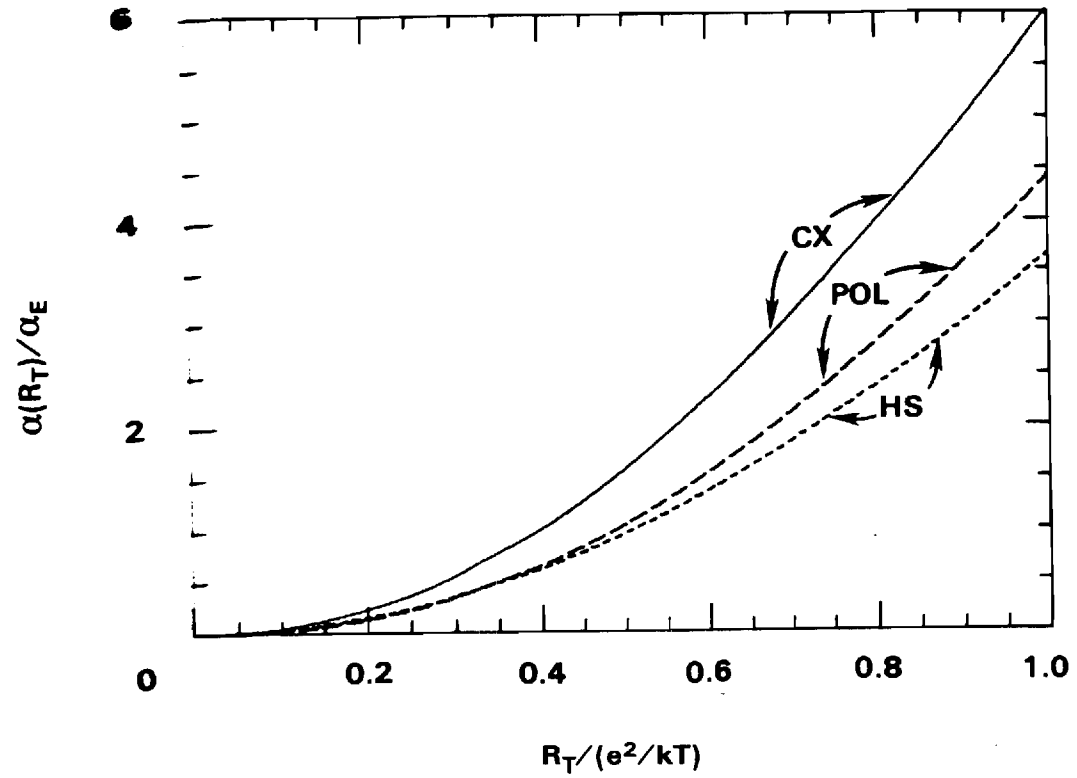

Fig. 2. Strong Collision Limit: Variation with R_T of the one-way equilibrium rate, (4.7) of text, across energy level E = 0.

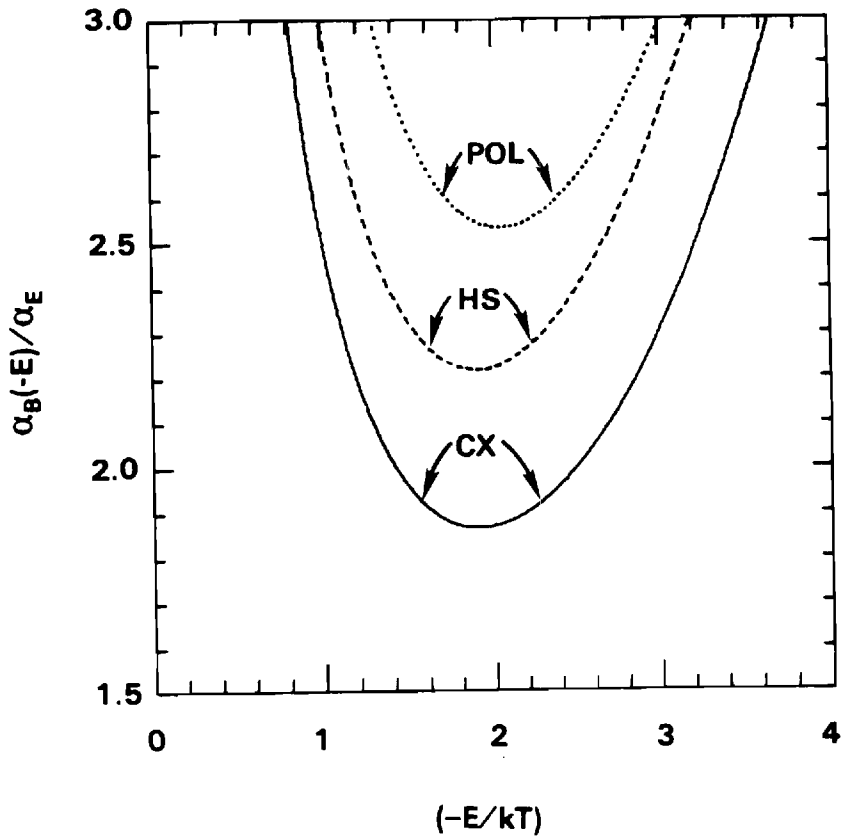

Fig. 3. Bottleneck Method: One-way equilibrium rates, (4.9) of text across excited levels with energy -E relative to the dissociation threshold.

Table 2: Ratio of α_P/α_E and α_B/α_E from (4.13), (4.9) and (4.5) for various mass ratios (4.8) and (A^+-M) interactions.

	α_P/α_E			α_B/α_E		
a	CX	HS	POL	CX	HS	POL
0.001	1.0275	1.0127	1.0008	16.9958	25.7816	32.4466
0.010	1.3040	1.2216	1.1634	5.5130	7.3362	8.3690
0.100	3.5223	2.7388	2.1306	2.3835	2.9386	3.3538
0.333	6.8404	4.9678	3.3611	1.8645	2.2155	2.5414
1.000	9.2715	6.6036	4.0598	1.7222	2.0152	2.3328
10.000	------	3.5103	2.1306	----	2.7464	3.3537
100.000	------	1.4550	1.1634	----	6.3015	8.3690
1000.000	------	1.0934	1.0008	----	20.2334	32.4466

Solution of (4.10) subject to steady state current j_D within block $\mathcal{E}$ and to the conditions to P_i^A at the boundaries to block $\mathcal{E}$ yield

$$P_D^A(E_i) = \left[\int_{E_i}^{0} dE/D_i^{(2)}(E) \right] \left[\int_{-S}^{0} dE/D_i^{(2)}(E) \right] \qquad (4.12)$$

so that the steady-state downward diffusional current across E = 0 is then

$$-j_D(0) = \alpha_P \tilde{n}_A \tilde{n}_B = \left[\int_{-S}^{0} dE/D_i^{(2)}(E) \right]^{-1} \qquad (4.13)$$

This is the original result of Pitaevskii (1962) who designed it only for electron-ion recombination in a gas. Table 2 shows that it is indeed correct in this collisional limit of large a. Its departure from α_E for general mass ratios arises from identification in (4.13) of α with a current based on (4.10) or (4.12), which does not satisfy the exact QSS-condition (4.6). When (4.12) is inserted in the basic rate (4.3) to give α_D, excellent agreement is apparent (Fig.4) for all mass ratios a and A^+-M interactions. The rates in Fig. 4 are normalized (Flannery 1980, 1981, 1987) to Thomson rates. In the limit of small energy transfers (small and large a) the current (4.13) is so small and agrees essentially (as in Table 2) with the result of (4.3).

4.3. *Variational Principle*

It has recently been proposed (Flannery 1987) that termolecular association proceeds in such a manner that the overall association rate (2.4) is a minimum at any given time. Under the separation (4.2) which is necessary for emergence of the QSS condition (4.6), a Variational Treatment of the QSS approximation can therefore be constructed by varying P_i in (4.5) so as to yield minimum rates α. With $\lambda = -E_i/kT$, the simplest one-parameter variational form

$$P_V^A(\lambda;\lambda_*) = 1 - (1+\chi)\exp(-\chi) \qquad \chi = \lambda/\lambda_* \qquad (4.14)$$

which tends to zero as $E_i \to 0$ and to unity as $E_i \to -\infty$ (rather than to unity as $E_i \to -S$), yields the exact QSS rate α_E of (4.5) for $\lambda^* \approx 1.2$. Fig. 5

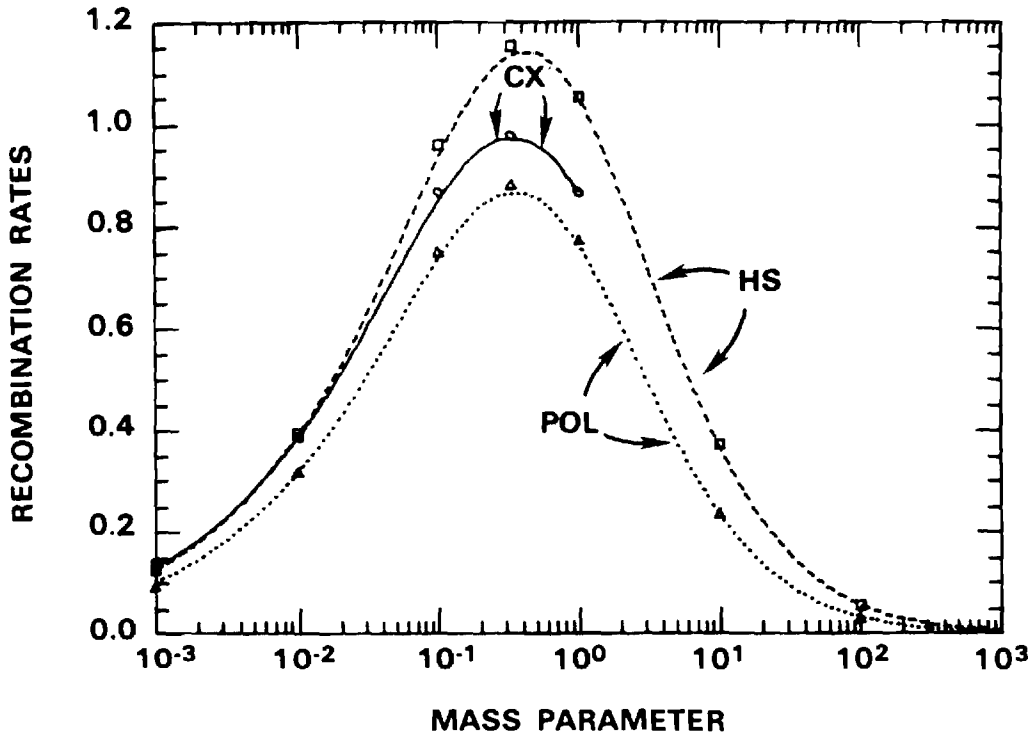

Fig. 4. Variation of QSS-rates (lines) and diffusion rates (symbols) with mass parameter a.

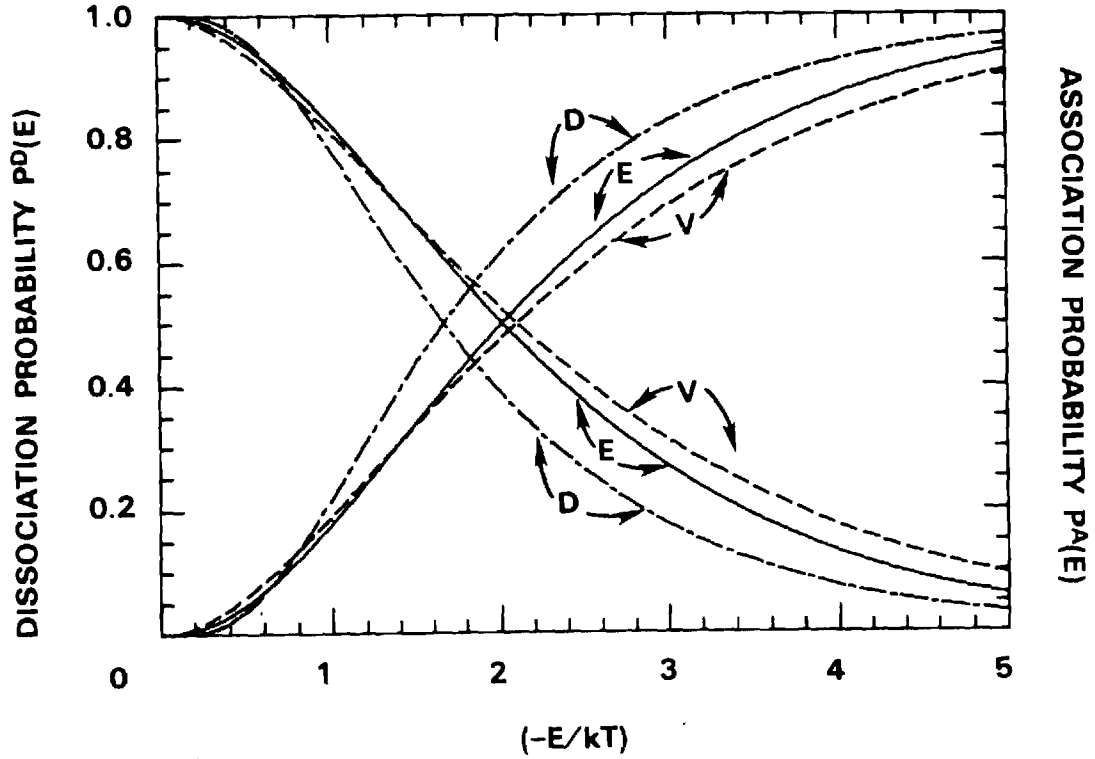

Fig. 5. Probabilities for dissociation and association of pairs with internal energy -E relative to the dissociation limit.

illustrates the comparison between $P_V^{A,D}$, $P_D^{A,D}$ and $P_E^{A,D}$ which are respectively the variational diffusional, and exact QSS probabilities for termolecular recombination of equal mass species under a polarization A^+-M attraction. More elaborate expressions with two and three variational parameters-yield probabilities closer to the exact $P_E^{A,D}$ (Flannery 1987). The overall rate α is however not sensitive to these changes as suggested by the close agreement between the diffusion and exact results of Figs. 4 and 5. All of the adopted variational expressions produces α_E exactly.

Acknowledgement: I would like to thank Dr. E. J. Mansky for help in preparation of the Tables and Figures. I also thank Audrey Ralston for her pioneering efforts in adapting the latest computer and laser technology to the overall production of the paper. This research is supported by the US Air Force Office of Scientific Research under Grant No. AFOSR-84-0233.

References

Bass, L., Chesnavich, W. J., and Bowers, M. T., 1979, J. Amer. Chem Soc., 103:5493
Bates, D. R., 1978, Proc. Roy. Soc. Lond. A., 360:1
Bates, D. R., 1979a, J. Phys. B. Atom. Molec. Phys., 12:4135
Bates, D. R., 1979b, J. Chem. Phys., 71:2318
Bates, D. R., 1980, J. Phys. B. Atom. Molec. Phys., 13:2587
Bates, D. R., 1986, J. Chem. Phys., 84:6233
Bates, D. R., 1985, J. Chem. Phys., 83:4448
Bates, D. R., and Flannery, M. R., 1968, Proc. Roy. Soc. Lond. A., 302:367
Bates, D. R., and Mendas, 1982, J. Phys. B. Atom. Molec. Phys., 15:1949
Bates, D. R., and Moffett, R. J., 1966, Proc. Roy. Soc. Lond. A., 291:1
Blades, A. T., and Kebarle, P., 1983, J. Chem. Phys., 78:783
Flannery, M.R., 1980, J. Phys. B. Atom. Molec. Phys., 13:3649
Flannery, M.R., 1981, J. Phys. B. Atom. Molec. Phys., 14:915
Flannery, M. R., 1982a, Ion-Ion Recombination in High Pressure Plasmas, in: "Applied Atomic Collision Physics, Vol. 3", E. W. McDaniel and W. L. Nighan, eds., Academic Press, New York.
Flannery, M. R., 1982b, Phil. Trans. Roy. Soc. Lond. A., 304:447
Flannery, M. R., 1985, J. Phys. B. Atom. Molec. Phys., 18:L839
Flannery, M. R., 1986, J. Phys. B. Atom. Molec. Phys., 19:L227
Flannery, M. R., 1987 (in preparation).
Flannery, M. R., and Mansky, E. J., 1987 (in preparation).
Flannery, M. R., and Yang, T. P., 1980, J. Chem. Phys. 73:3239.
Forst, W., 1973, Theory of Unimolecular Reactions, Academic Press, New York.
Herbst, E., 1979, J. Chem. Phys., 70:2201
Herbst, E., 1980, J. Chem. Phys., 72:5284
Keck, J. C., 1967, Adv. Chem. Phys., 13:85
Klots, C. E., 1971, J. Phys. Chem., 75:1526
Loeb, L. B., 1955, "Basic Processes of Gaseous Electronics", Ch. 6, Univ. of California, Berkeley.
Mahan, B. H., and Person, J. C., 1964, J. Chem. Phys., 40:392
Marcus, R. A., 1975, J. Chem. Phys., 62:1372
Pitaevskii, L. P., 1962, Soviet Physics-JETP 15:919
Thomson, J. J., 1924, Phil. Mag., 47:337
Troe, J., 1977, J. Chem. Phys., 66:4758
van Koppen, P. A. M., Jarrold, M. F., Bowers, M. T., Bass, L. M., and Jennings, K. R., 1984, J. Chem. Phys., 81:288
Viggiano, A. A., 1986, J. Chem. Phys., 84:244
Whitten, G. Z., and Rabinovitch, B. S., 1963, J. Chem. Phys., 38:2466
Wigner, E., 1937, J. Chem. Phys., 5:720

UNCLASSIFIED
SECURITY CLASSIFICATION OF THIS PAGE

REPORT DOCUMENTATION PAGE

1a. REPORT SECURITY CLASSIFICATION UNCLASSIFIED	1b. RESTRICTIVE MARKINGS
2a. SECURITY CLASSIFICATION AUTHORITY	3. DISTRIBUTION / AVAILABILITY OF REPORT Approved for public release; distribution unlimited.
2b. DECLASSIFICATION / DOWNGRADING SCHEDULE	
4. PERFORMING ORGANIZATION REPORT NUMBER(S) GIT-85-009	5. MONITORING ORGANIZATION REPORT NUMBER(S) N/A
6a. NAME OF PERFORMING ORGANIZATION Georgia Institute of Technology 6b. OFFICE SYMBOL (*If applicable*)	7a. NAME OF MONITORING ORGANIZATION Air Force Office of Scientific Research (AFOSR) Directorate of Physical and Geophysical Sciences
6c. ADDRESS (*City, State, and ZIP Code*) School of Physics Georgia Institute of Technology Atlanta, Georgia 30332	7b. ADDRESS (*City, State, and ZIP Code*) AFOSR/NP Bolling Air Force Base, Bldg. 410 Washington, D. C. 20332-6448
8a. NAME OF FUNDING / SPONSORING ORGANIZATION AFOSR 8b. OFFICE SYMBOL (*If applicable*) NP	9. PROCUREMENT INSTRUMENT IDENTIFICATION NUMBER AFOSR-84-0233
8c. ADDRESS (*City, State, and ZIP Code*) Building 410 Bolling AFB, D. C. 20332-6448	10. SOURCE OF FUNDING NUMBERS PROGRAM ELEMENT NO. 61102F; PROJECT NO. 2301; TASK NO. A4; WORK UNIT ACCESSION NO. N/A
11. TITLE (*Include Security Classification*) REPRESENTATIONS OF THE TRANSPORT EQUATION FOR REACTIVE PROCESSES	
12. PERSONAL AUTHOR(S) M. R. Flannery	
13a. TYPE OF REPORT Annual Technical Report	13b. TIME COVERED FROM 7/1/86 TO 6/30/87
14. DATE OF REPORT (*Year, Month, Day*) 8/28/87	15. PAGE COUNT 24
16. SUPPLEMENTARY NOTATION	

17. COSATI CODES		
FIELD	GROUP	SUB-GROUP
N/A	N/A	N/A

18. SUBJECT TERMS (*Continue on reverse if necessary and identify by block number*)
Termolecular, Association, Boltzmann, Transport, Reaction.

19. ABSTRACT (*Continue on reverse if necessary and identify by block number*)

Research has been initiated and conducted on Termolecular Association. Various representations of the Transport Equation for Reactive Processes were developed. The standard transport equation in the phase space $(\underset{\sim}{R},\underset{\sim}{p})$ representation with streaming in $\underset{\sim}{R}$-space at fixed momentum $\underset{\sim}{p}$ and streaming in p-space at fixed position $\underset{\sim}{R}$ is converted to a more compact and useful (field free) form which, in an energy E-angular momentum L representation yields quite naturally a basic microscopic equation of continuity valuable in general to the solution of the Boltzmann equation. The analysis is directly relevant to the theory of various energy-transfer processes in a gas. The appropriate set of transport-collisional equations governing termolecular ion-atom association and ion-ion recombination of atomic species in a gas then follow quite naturally.

20. DISTRIBUTION / AVAILABILITY OF ABSTRACT ☒ UNCLASSIFIED/UNLIMITED ☐ SAME AS RPT. ☐ DTIC USERS	21. ABSTRACT SECURITY CLASSIFICATION UNCLASSIFIED
22a. NAME OF RESPONSIBLE INDIVIDUAL Dr. Ralph E. Kelley	22b. TELEPHONE (*Include Area Code*) (202) 767-4980 22c. OFFICE SYMBOL NP

DD FORM 1473, 84 MAR 83 APR edition may be used until exhausted. All other editions are obsolete.

SECURITY CLASSIFICATION OF THIS PAGE
UNCLASSIFIED

Contents

Abstact

During this third year of the grant research has been conducted on Termolecular Association in Gaseous. Various representations on the Transport Equation for Reactive Processes were derived. The standard transport equation in the phase space ($\underset{\sim}{R},\underset{\sim}{p}$) representation with streaming in $\underset{\sim}{R}$-space at fixed momentum $\underset{\sim}{p}$ and streaming in $\underset{\sim}{p}$-space at fixed position $\underset{\sim}{R}$ is converted to a more compact and useful (field-free) form which, in an energy E-angular momentum L representation yields quite naturally a basic microscopic equation of continuity valuable in general to the solution of the Boltzmann equation. The analysis is directly relevant to the theory of various energy-transfer processes in a gas. The appropriate set of transport collisional equations governing termolecular ion-atom association and ion-ion recombination of atomic species in a gas then follow quite naturally.

1. Research Completed

The following paper included as Appendix D of the previous Annual Technical Report, GIT-85-008, for the period 7/1/85 - 6/30/85 has been published.

(A) "Orientation and Alignment Parameters for e-He(1^1S-3^1D) Collisions", by E. J. Mansky and M. R. Flannery, J. Phys. B: Atom. Molec. Phys. 20 (1987) 253. Six copies are attached as a separate report GIT-85-010.

The following research, included as Appendix E of the previous Annual Technical Report.

(B) "Macroscopic and Microscopic Perspectives of Termolecular Association of Atomic Reactants in A Gas",

is to be published as a Chapter in the Book: "Modern Atomic and Molecular Processes", Plenum Press, New York.

2. Research Initiated This Year and Completed

(C) "Representations of the Transport Equation for Reactive Processes", has been initiated this year, completed and submitted for publication. It is attached as an Appendix to this report.

3. Papers Presented at Scientific Meetings

3.1 A contributed paper entitled, "Microscopic Perspective to Termolecular Ion-Molecule Reactions", by M. R. Flannery was presented at the 39th Gaseous Electronics Conference, Madison, Wisconsin, October 7-10, 1986.

3.2 A contributed paper entitled, "Detailed Investigation of the Thomson Model of Termolecular Recombination", by E. J. Mansky and M. R. Flannery was presented at the 39th Gaseous Electronics Conference, Madison, Wisconsin, October 7-10, 1987.

3.3 An invited talk entitled, "Termolecular Association in Gases", by M. R. Flannery was presented at a Conference in Honor of Sir David Bate's 70th birthday at the Queen's University of Belfast, November 1986.

4. Abstracts of Papers Presented

BA-2 Microscopic Perspective to Termolecular Ion-Molecule Reactions,* M. R. FLANNERY, School of Physics, Georgia Tech--Current chemical kinetics of various ion-molecule reactions and of termolecular recombination, $A+B+M \rightleftarrows AB+M$, in a gas M invokes simplified macroscopic schemes so as to predict the general variation with gas density of such processes. In this paper a non-equilibrium microscopic treatment of the various energy-transfer and stabilization sequences is provided, and connection is established with the previous macroscopic treatments. Expressions for the three-body rate for stabilization of complexes AB^* by collision with M are derived. This rate is, in general, dependent on the gas density. For moderate-high gas densities, the effect of transport, while important for ion-ion recombination, is not important for termolecular ion-atom and atom-atom association at most gas densities of practical interest.

*Research supported by U. S. Air Force Office of Scientific Research under Grant No. AFOSR-84-0233.

LC-1 Detailed Investigation of the Thomson Model of Termolecular Recombination,* E. J. MANSKY and M. R. FLANNERY, School of Physics, Georgia Tech-- The quasi-steady-state rate of ion-ion recombination in a gas M is given by the net downward current in energy space across a band of highly excited bound energy levels of the ion pair (A^+-B^-), including the dissociation neck at zero energy. The contribution to the one-way equilibrium current across this neck that arises from the range [0-R] in internal separation R of the ion pair (A^+-B^-) exhibits a rapid monotonic increase with R, and diverges for large R. Calculations which illustrate this divergence are provided for various ion-gas interactions. Comparison with exact calculations of the net current illustrates the effectiveness of a modern Thomson-style model for equal-mass species.

*Research supported by U. S. Air Force Office of Scientific Research under Grant No. AFOSR-84-0233.

Appendix

Representations of the Transport Equation for Reactive Processes

M. R. Flannery
School of Physics
Georgia Institute of Technology
Atlanta, Georgia 30332, USA

Abstract: The standard transport equation in the phase space ($\underset{\sim}{R}$,$\underset{\sim}{p}$) representation with streaming in $\underset{\sim}{R}$-space at fixed momentum $\underset{\sim}{p}$ and streaming in $\underset{\sim}{p}$-space at fixed position $\underset{\sim}{R}$ is converted to a more compact and useful (field-free) form which, in an energy E-angular momentum L representation yields quite naturally a basic microscopic equation of continuity valuable in general to the solution of the Boltzmann equation. The analysis is directly relevant to the theory of various energy-transfer processes in a gas. The appropriate set of transport-collisional equations governing termolecular ion-atom association and ion-ion recombination of atomic species in a gas then follow quite naturally.

Subject Index: 3410, 5110, 8220R

1. Introduction

In termolecular ion-ion recombination and ion-atom association

$$A + B + M \rightarrow AB + M \tag{1}$$

which occurs via collisional transfer of internal energy and angular momenta of the (A-B) pair with gas species M, the two particle (phase-space) distribution $n(\underset{\sim}{R},\underset{\sim}{p},t)$ of (A-B) pairs over internal separation $\underset{\sim}{R}$ and internal relative momentum $\underset{\sim}{p} = m\underset{\sim}{v}$ is governed (Flannery 1982a,b) by the microscopic transport equation

$$\frac{d}{dt} n(\underset{\sim}{R},\underset{\sim}{p},t) = \frac{\partial n}{\partial t} + \underset{\sim}{v}\bullet\underset{\sim}{\nabla}_{\underset{\sim}{R}} n - \left[\frac{\partial V}{\partial R}\right] \hat{\underset{\sim}{R}}\bullet\underset{\sim}{\nabla}_{\underset{\sim}{p}} n \tag{2a}$$

$$= \frac{\partial n}{\partial t} + [\underset{\sim}{\nabla}_{\underset{\sim}{R}}\bullet(n\underset{\sim}{v})]_{\underset{\sim}{p}} - \left[\frac{\partial V}{\partial R}\right] [\nabla_{\underset{\sim}{p}}\bullet(n\hat{\underset{\sim}{R}})]_{\underset{\sim}{R}} \tag{2b}$$

where V(R) is the (symmetrical) interaction energy between A and B with reduced mass m. When the transport rate (2) is set equal to the net input-output rate for collisional population at fixed $\underset{\sim}{R}$ of state $\underset{\sim}{p}$ from all states $\underset{\sim}{p}'$ of the pair (A-B), a Boltzmann equation is obtained (Flannery 1982a,b) for $n(\underset{\sim}{R},\underset{\sim}{p},t)$ appropriate to the case of dilute concentration of reactants A and B in a gas bath M of general density N.

Integration of (2b) over all $\underset{\sim}{p}$ results in the familiar macroscopic continuity equation

$$\frac{dn(\underset{\sim}{R},t)}{dt} = \frac{\partial n}{\partial t} + \underset{\sim}{\nabla}\bullet\underset{\sim}{J}(\underset{\sim}{R},t) \tag{3}$$

linking the macroscopic distribution

$$n(\underset{\sim}{R},t) = \int n(\underset{\sim}{R},\underset{\sim}{p},t)d\underset{\sim}{p} \tag{4}$$

and its first moment

$$\underset{\sim}{J}(R,t) = \int n(\underset{\sim}{R},\underset{\sim}{p},t)\underset{\sim}{v}\, d\underset{\sim}{p} \tag{5}$$

which is the current across a sphere of radius R.

Analytical or numerical solution of the transport equation (2) set equal to an input-output collisional rate is common to many problems in atomic, molecular and plasma physics based on the Boltzmann equation. Solution for the phase-space distribution $n(\underset{\sim}{R},\underset{\sim}{p})$ in general involves complex mathematical analysis (cf. Chapman and Cowling 1970, McDaniel and Mason, 1973, Duderstadt and Martin 1979).

In this paper, (2) is expressed in a more compact form natural to consideration of (1) and amenable to direct solution. A microscopic continuity equation, similar in form to the macroscopic equation (3), is then obtained when n is expressed as a function of $\underset{\sim}{R}$, internal energy

$$E = p^2/2m - V(R) \tag{6}$$

and internal relative angular momentum

$$\underset{\sim}{L} = \underset{\sim}{R} \times \underset{\sim}{p} = (R\, p\, \sin\theta)\hat{\phi} \tag{7}$$

where θ and ϕ are the spherical polar and azimuthal coordinates of $\hat{\underset{\sim}{p}}$ with

respect to polar axis taken along $\hat{\underset{\sim}{R}}$. On rotating $\phi \leq \pi$ through π at fixed θ, the direction of $\underset{\sim}{L}$ becomes reversed as viewed from the X-axis from a clockwise orbital motion about the force center to a counterclockwise motion. Pairs which contract in R as they proceed towards the pericenter (or away from the apocenter) and pairs which expand in R as they leave the pericenter (or approach the apocenter) are specified by the respective ranges $0 \leq \theta < \pi/2$ and $\pi/2 < \theta \leq \pi$.

In the absence of collisions with the gas M note that the quantities E and $\underset{\sim}{L}$ above are conserved.

2. Analysis

With $\underset{\sim}{p}$ held fixed at angle θ to variable $\underset{\sim}{R}$, then after some analysis,

$$\underset{\sim}{p}\cdot\nabla_{\underset{\sim}{R}} n(\underset{\sim}{R},\underset{\sim}{p}) = \frac{1}{R^2}\frac{\partial}{\partial R}(R^2 n\cos\theta)_{p,\theta} + \frac{1}{R}\frac{\partial}{\partial(\cos\theta)}[np\sin^2\theta]_{p,R} \qquad (8)$$

$$+ \frac{\sin\theta}{R}\left[\cos\phi\left[\frac{\partial n}{\partial\theta_R}\right] + \frac{\sin\phi}{\sin\theta_R}\left[\frac{\partial n}{\partial\phi_R}\right] - \sin\phi\cot\theta_R\left[\frac{\partial n}{\partial\phi}\right]\right]$$

for general $n[\underset{\sim}{R}(R,\theta_R,\phi_R), \underset{\sim}{p}(p,\theta,\phi)]$, where (θ,ϕ) are the spherical coordinates of $\hat{\underset{\sim}{p}}$ with polar axis along $\hat{\underset{\sim}{R}}$ which, in turn, has spherical coordinates (θ_R,ϕ_R) with respect to a space-fixed reference frame. Since the interaction V(R) is radial, then the probability density n is a function only of R, p and θ, the angle between $\hat{\underset{\sim}{R}}$ and $\hat{\underset{\sim}{p}}$. Under azimuthal (ϕ,ϕ_R) symmetry, and with the aid of (8) together with the corresponding expression for $\hat{\underset{\sim}{R}}\cdot\nabla_{\underset{\sim}{p}} n$, the transport equation (2a) reduces to

$$\frac{d}{dt}\, n(\underset{\sim}{R},\underset{\sim}{p};t) = \frac{\partial n}{\partial t} + \frac{1}{R^2}\frac{\partial}{\partial R}\,(R^2\, n\, v\, \cos\theta)_{p,\theta} + \frac{1}{R}\frac{\partial}{\partial(\cos\theta)}\,[nv\,\sin^2\theta]_{p,\underset{\sim}{R}}$$

$$- \left[\frac{\partial V}{\partial R}\right]\left[\frac{1}{p^2}\frac{\partial}{\partial p}\,(p^2\, n\, \cos\theta)_{\underset{\sim}{R},\theta} + \frac{1}{p}\frac{\partial}{\partial(\cos\theta)}\,[n\,\sin^2\theta]_{p,\underset{\sim}{R}}\right] \qquad (9)$$

which is its conservative form in the $(\underset{\sim}{R},\underset{\sim}{p})$-representation, since the angular redistribution terms vanish when integrated over the full range $0 \leq \theta \leq \pi$ of the momentum direction $\hat{\underset{\sim}{p}}$ for fixed $\underset{\sim}{R}$. In what follows, the ϕ-integration (which is over all directions $\hat{\underset{\sim}{L}}$ of the angular momentum vector) of the various distributions is implied, and $\underset{\sim}{R}$ in $n(\underset{\sim}{R},\underset{\sim}{p})$, $n(\underset{\sim}{R},E,\theta)$ and $n(\underset{\sim}{R},E,L^2)$ signifies that n is the spherically symmetric distribution per unit element $4\pi R^2 dR$, in addition to unit elements $d\underset{\sim}{p}$, $dE\, d(\cos\theta)$, $dE\, dL^2$ respectively.

2.1 $(\underset{\sim}{R},E,\theta)$-Representation

Regrouping terms of (9) yields the alternative form,

$$\frac{d}{dt}\, n(\underset{\sim}{R},\underset{\sim}{p};t) = \frac{\partial n}{\partial t} + v\,\cos\,\theta\,\left[\left[\frac{\partial n}{\partial R}\right]_{p,\theta} - \frac{1}{v}\left[\frac{\partial V}{\partial R}\right]\left[\frac{\partial n}{\partial p}\right]_{R,\theta}\right] \qquad (10)$$

$$+ \frac{1}{2}\, v\, \sin^2\theta\,\left[\frac{2}{R} - \frac{1}{(E-V)}\frac{\partial V}{\partial R}\right]\left[\frac{\partial n}{\partial(\cos\theta)_{R,p}}\right]$$

Under the recognition that the one-dimensional $p \rightarrow E$ transformation implicit in

$$n(\underset{\sim}{R},E) = n(\underset{\sim}{R},p(R,E)) \qquad (11)$$

involves the identity

$$\left[\frac{\partial}{\partial R}\right]_E \equiv \left[\frac{\partial}{\partial R}\right]_p - \frac{1}{v}\left[\frac{\partial V}{\partial R}\right]\left[\frac{\partial}{\partial p}\right]_R \tag{12}$$

where the subscript specifies the particular quantity to be held fixed during the appropriate differentiation, then (10) is simply

$$\frac{d}{dt}\, n(\underset{\sim}{R},\underset{\sim}{p};t) = \frac{\partial n}{\partial t} + v\cos\theta\left[\frac{\partial n(\underset{\sim}{R},\underset{\sim}{p})}{\partial R}\right]_{E,\theta} + \frac{1}{2}\, v\sin^2\theta\left[\frac{2}{R} - \frac{1}{(E-V)}\,\frac{\partial V}{\partial R}\right]\left[\frac{\partial n}{\partial(\cos\theta)}\right]_{R,E} \tag{13}$$

Since the distributions per unit elements in the $(\underset{\sim}{R},\underset{\sim}{p})$ and $(\underset{\sim}{R},E,\theta)$-representations are related via

$$n(\underset{\sim}{R},\underset{\sim}{p})\; p^2\, dp = n_1(\underset{\sim}{R},E,\theta)dE \tag{14}$$

the transport equation for $n_1(\equiv mpn)$ is then

$$\frac{d}{dt}\, n_1(\underset{\sim}{R},E,\theta;t) = \frac{\partial n}{\partial t} + \left[\frac{1}{R^2}\,\frac{\partial}{\partial R}\,(R^2 n_1 v\cos\theta)_{E,\theta}\right.$$

$$\left. + \frac{1}{2}\, v\left\{\frac{2}{R} - \frac{1}{(E-V)}\,\frac{\partial V}{\partial R}\right\}\left[\frac{\partial(n_1\sin^2\theta}{\partial(\cos\theta)}\right]_{R,E}\right] \tag{15}$$

which is the conservative form of the transport equation (2) in the $(\underset{\sim}{R},E,\theta)$-representation.

The θ-integrated distributions

$$n^{+}(\underset{\sim}{R},E,t) = \int_{0}^{1} n_1(\underset{\sim}{R},E,\theta;t)\, d(\cos\theta) \tag{16a}$$

and

$$n^{-}(\underset{\sim}{R},E,t) = \int_{-1}^{0} n_1(\underset{\sim}{R},E,\theta;t)\, d(\cos\theta) \tag{16b}$$

for pairs with internal energy E which are expanding (+) outward or contracting (-) inward across a sphere of radius R therefore satisfy

$$\frac{d}{dt}\, n^{\pm}(\underset{\sim}{R},E,t) = \frac{\partial n^{\pm}}{\partial t} \pm \frac{1}{R^2}\frac{\partial}{\partial R}\left[R^2 j^{\pm}(R,E,t)\right]_E \mp \left[\frac{1}{2}\, n^{\pm}(R,E,\theta\to\pi/2\mp\epsilon,t)v\right]_E \frac{1}{R^2 p^2}\left[\frac{\partial}{\partial R}\,(R^2p^2)\right]_E \tag{17}$$

for <u>all</u> R and E where the corresponding currents of expanding (+) and contracting (-) pairs are

$$j^{+}(R,E,t) = \int_{0}^{1} n_1(\underset{\sim}{R},E,\theta;t)\; v\cos\theta\; d(\cos\theta) \tag{18a}$$

and

$$j^{-}(R,E,t) = \int_{-1}^{0} n_1(\underset{\sim}{R},E,\theta;t)\; v|\cos\theta|\, d(\cos\theta) \tag{18b}$$

respectively. In (17), the small positive quantity ϵ tends to zero.

Note that the maximum range of L^2 accessible for fixed E and R is $0 \leq L^2 \leq R^2p^2 = L^2_{max}$. As R increases, L_{max} for dissociated states continuously increases, but for bound states it reaches a maximum and then decreases. Contracting pairs with $L = L_{max}$ fail to enter the R-sphere since their orbit just touches the R-sphere externally at the pericenter. Expanding pairs with $L = L_{max}$ fail to exit from the R-sphere since their orbit touches the R-sphere internally at the apocenter. Eq. (17) for n^+ naturally contains the resulting compensation to the expanding flux at R by including either a source for n^+ at the pericenter (specified by $\theta = \pi/2$ and $[\partial(R^2p^2)/\partial R]_E > 0$), where contracting (-) pairs are converted at R by external reflection into expanding (+) pairs, or as a sink of n^+ at the apocenter (specified by $\theta = \pi/2$ and $[\partial(R^2p^2/\partial R]_E < 0$), where (+) pairs are reflected at R internally into (-) pairs. Eq. (17) for n^- contains the corresponding combination of a pericenter sink and an apocenter source for contracting pairs.

Fig. 1 illustrates variation with θ, or alternatively with angular momentum $L = Rp\sin\theta$, of the hyperbolic orbits for motion at fixed energy $E = \frac{3}{2}kT$ under pure Coulombic attraction $-e^2/R$. The spherically-symmetric distributions $n^+(R,E,\theta)$ and $n^-(R,\theta,\pi-\theta)$ which correspond to expanding and contracting pairs in the same $(E,\underset{\sim}{L})$-orbit are in general <u>not</u> equal since n^+ at a given R is the remnant of the contracting pairs after they pass through the R-sphere (within which collisional absorptions do occur). When R corresponds to the pericenter or apocenter of a given (E,L^2)-orbit then the precursors to n^+ at the pericenter and to n^- at the apocenter are n^- and n^+ respectively, so that, in (17),

$$n^{-}(R,E,\theta = \pi/2) \ , \ \partial(R^2p^2)/\partial R \geq 0$$

$$n^{\pm}(R,E,\theta = \pi/2\overline{+}\epsilon) \equiv n^{*}(R,E,\theta = \pi/2) = \tag{19}$$

$$n^{+}(R,E,\theta = \pi/2) \ , \ \partial(R^2p^2)/\partial R \leq 0$$

On integrating (15) over all θ, the distributions for the sum (s) and difference (d),

$$n^{s,d}(\underset{\sim}{R},E,t) = n^{+}(\underset{\sim}{R},E,t) \pm n^{-}(\underset{\sim}{R},E,t) \tag{20a}$$

and associated currents

$$j^{s,d}(R,E,t) = j^{+}(R,E,t) \pm j^{-}(R,E,t) \tag{20b}$$

then satisfy

$$\frac{d}{dt}\, n^{s}(\underset{\sim}{R},E,t) = \frac{\partial n^{s}}{\partial t} + \frac{1}{R^2}\frac{\partial}{\partial R}\,[R^2 j^{d}(R,E;t)]_{E} \tag{21a}$$

which is a <u>microscopic equation of continuity</u> in $(\underset{\sim}{R},E)$-space, a property which originates from the conservative form of (15) in the $(\underset{\sim}{R},E,\theta)$-representation, and

$$\frac{d}{dt}\, n^{d}(\underset{\sim}{R},E,t) = \frac{\partial n^{d}}{\partial t} + \frac{1}{R^2}\frac{\partial}{\partial R}\,[R^2 j^{s}(R,E;t)]_{E} - \left[\frac{n^{*}(\underset{\sim}{R},E,\pi/2)}{n^{\pm}(\underset{\sim}{R},E)}\right]\frac{1}{R^2}\frac{\partial}{\partial R}\,(R^2 \underset{\sim}{j}^{s})_{E} \tag{21b}$$

which contains the additional source-sink combination.

Since the phase space distribution $n(\underset{\sim}{R},\underset{\sim}{p})$ of pairs in full thermodynamic equilibrium at temperature T is

$$\underset{\sim}{n}(\underset{\sim}{R},\underset{\sim}{p}) = (2\pi mkT)^{-3/2}\exp(-E/kT) = \underset{\sim}{n}_{1}(\underset{\sim}{R},E,\theta,\phi)\ p^2(dp/dE) \tag{22}$$

then the equilibrium current $\underset{\sim}{j}^{s}$ in (21b) is

$$\tilde{j}^{s}(R,E) = \frac{1}{2}\,\tilde{n}(\underset{\sim}{R},E)\;v = (2\pi p^2)(2\pi mkT)^{-3/2}\exp(-E/kT) \tag{23}$$

on using (18) and (20) and $\tilde{n}^{\pm} = \frac{1}{2}\,\tilde{n}$. The above set (21) may also be recovered from (17) with the aid of (19).

When the different spherical distributions $n^{\pm}(\underset{\sim}{R},E,\theta)$ of contracting (-) and expanding (+) pairs which enter and exit the $\underset{\sim}{R}$-sphere are each independent of θ (which implies equilibrium in L^2) then (18)-(20) in this limit reduce to

$$j^{\pm}(R,E,t) = \frac{1}{2}\,n^{\pm}(\underset{\sim}{R},E,t)v \tag{24a}$$

$$j^{d,s}(R,E,t) = \frac{1}{2}\,n^{d,s}(\underset{\sim}{R},E,t)v \tag{24b}$$

$$n^{*}(\underset{\sim}{R},E,\pi/2,t) = n^{*}(\underset{\sim}{R},E,t) \tag{24c}$$

for use in (21) or (17). The set (17) under L^2-equilibrium reduce for <u>all</u> R and E to the set

$$\frac{d}{dt}\,n^{\pm}(\underset{\sim}{R},E,t) = \frac{\partial n^{\pm}}{\partial t} \pm \frac{1}{R^2}\frac{\partial}{\partial R}\left[\frac{1}{2}\,R^2\gamma^{\pm}(R,E,t)\tilde{j}^{s}(R,E)\right]_E$$

$$\mp\,\gamma^{*}(R,E,t)\,\frac{1}{R^2}\frac{\partial}{\partial R}\left[\frac{1}{2}\,R^2\tilde{j}^{s}(R,E)\right]_E \tag{25}$$

for the distribution

$$\gamma^{\pm}(R,E,t) = n^{\pm}(\underset{\sim}{R},E,t)/\tilde{n}^{\pm}(\underset{\sim}{R},E) \tag{26}$$

normalized to their thermodynamic equilibrium distribution

$$\tilde{n}^{\pm}(\underset{\sim}{R},E) = \frac{1}{2}\,\tilde{n}(\underset{\sim}{R},E) = (2\pi mp)(2\pi mkT)^{-3/2}\,\exp(-E/kT) \tag{27}$$

The distributions $\gamma^{\pm}$ are coupled in (25) by

$$\gamma^{*}(R,E,t) = \begin{cases} \gamma^{-}(R,E,t) & , \quad [\partial(R^2\underset{\sim}{j}^{s})/\partial R]_E \geq 0 \\ \gamma^{+}(R,E,t) & , \quad [\partial(R^2\underset{\sim}{j}^{s})/\partial R]_E \leq 0 \end{cases} \tag{28}$$

The set (25) for L^2-equilibrium is, as expected, identical to that obtained by Bates and Mendas (1978) from considerations of conservation in the interval $dE\, d\underset{\sim}{R}$.

2.2 The $(\underset{\sim}{R},E,L^2)$-Representation

The two-dimensional transformation $(p,\theta) \rightarrow (E,L^2)$ implicit in

$$n(\underset{\sim}{R},p,\theta) = n(\underset{\sim}{R},E(p,R),\, L^2(p,R,\theta)) \tag{29}$$

may be accomplished via use of the derived identities

$$\left[\frac{\partial n}{\partial R}\right]_{p,\theta} = \left[\frac{\partial n}{\partial R}\right]_{E,L^2} + \left[\frac{\partial n}{\partial E}\right]_{\underset{\sim}{R},L^2}\left[\frac{\partial E}{\partial R}\right]_{p} + \left[\frac{\partial n}{\partial L^2}\right]_{\underset{\sim}{R},E}\left[\frac{\partial L^2}{\partial R}\right]_{p,\theta} \tag{30a}$$

$$\left[\frac{\partial n}{\partial p}\right]_{\underset{\sim}{R},\theta} = \left[\frac{\partial n}{\partial E}\right]_{\underset{\sim}{R},L^2}\left[\frac{\partial E}{\partial p}\right]_{\underset{\sim}{R}} + \left[\frac{\partial n}{\partial L^2}\right]_{\underset{\sim}{R},E}\left[\frac{\partial L^2}{\partial p}\right]_{\underset{\sim}{R},\theta} \tag{30b}$$

and

$$\left[\frac{\partial n}{\partial(\cos\theta)}\right]_{\underset{\sim}{R},p} = \left[\frac{\partial n}{\partial L^2}\right]_{\underset{\sim}{R},E}\left[\frac{\partial L^2}{\partial(\cos\theta)}\right]_{\underset{\sim}{R},p} \tag{30c}$$

On inserting (30) into (9), the transport equation for the phase-space distribution is found to reduce to

$$\frac{d}{dt}\, n(\underset{\sim}{R},\underset{\sim}{p},t) = \frac{\partial n}{\partial t} + v\cos\theta \left[\frac{\partial}{\partial R}\, n(\underset{\sim}{R},\underset{\sim}{p},t)\right]_{E,L^2} \tag{31a}$$

$$= \frac{\partial n}{\partial t} + \underset{\sim}{v}\bullet\left[\underset{\sim}{\nabla}_{\underset{\sim}{R}}\, n(\underset{\sim}{R},\underset{\sim}{p},t)\right]_{E,L^2} \tag{31b}$$

in which the gradient operation is performed with the quantities (E,L^2), which remain conserved in the absence of collisions, held fixed. Eq. (31) represents a great formal simplification to the basic transport equation (2) or (9) and is based on the derived identity

$$\underset{\sim}{v}\bullet\left[\underset{\sim}{\nabla}_{\underset{\sim}{R}}\, n(\underset{\sim}{R},\underset{\sim}{p})\right]_{E,L^2} \equiv \underset{\sim}{v}\bullet\left[\underset{\sim}{\nabla}_{\underset{\sim}{R}}\, n(\underset{\sim}{R},\underset{\sim}{p})\right]_{\underset{\sim}{p}} - \left[\frac{\partial V}{\partial R}\right] \hat{\underset{\sim}{R}}\bullet\left[\underset{\sim}{\nabla}_{\underset{\sim}{R}}\, n(\underset{\sim}{R},\underset{\sim}{p})\right]_{\underset{\sim}{R}} \tag{32}$$

which, to the author's knowledge, has not been previously presented in spite of its apparent simple form. Eq. (32) is essentially the two-dimensional analogue of the one dimensional transformation (12). It, in effect, reduces the standard transport equation (2) to an equivalent field-free form. Although (32) is key to the further development of a comprehensive and tractable theoretical treatment (Flannery 1987) of termolecular atomic and molecular processes as a function of gas density N, it would appear to be quite valuable in general towards obtaining solutions of the Boltzmann equation for a variety of problems in transport theory (such as those in Duderstadt and Martin 1979).

It is also apparent from (32) that consideration alone of $\underset{\sim}{R}$-streaming for fixed (E,L^2) includes quite succintly both the usual streaming in $\underset{\sim}{R}$-space at fixed $\underset{\sim}{p}$ and streaming in $\underset{\sim}{p}$-space at fixed $\underset{\sim}{R}$ which separately gives rise to the effects of diffusion and drift, respectively.

The distributions in the phase-space $(\underset{\sim}{R},\underset{\sim}{p})$, $(\underset{\sim}{R},E,\theta)$ and $(\underset{\sim}{R},E,L^2)$ representations are related by

$$n(\underset{\sim}{R},\underset{\sim}{p})d\underset{\sim}{R}\ d\underset{\sim}{p} = n_1(\underset{\sim}{R},E,\theta,\phi)d\underset{\sim}{R}\ dE\ d(\cos\theta)\ d\phi = n_2(\underset{\sim}{R},E,L^2,\phi)d\underset{\sim}{R}\ dE\ dL^2\ d\phi, \quad (33)$$

where owing to azimuthal symmetry n is independent of the azimuthal angle ϕ of $\underset{\sim}{p}$ with respect to Z-axis along $\underset{\sim}{R}$. Hence

$$n(\underset{\sim}{R},\underset{\sim}{p}) = 2R^2\ n_2(\underset{\sim}{R},E,L^2,\phi)v\ \cos\theta = v\ n_1(\underset{\sim}{R},E,\theta,\phi)/p^2 \quad (34)$$

The transport equation (30) therefore yields

$$\frac{d}{dt}\ n(\underset{\sim}{R},E,L^2;t) = \frac{\partial n}{\partial t} + \frac{1}{R^2}\frac{\partial}{\partial R}\ [R^2 n(\underset{\sim}{R},E,L^2;t)v\ \cos\theta]_{E,L^2} \quad (35)$$

$$= \frac{\partial n}{\partial t} + [\underset{\sim}{\nabla}\bullet\underset{\sim}{j}(R,E,L^2;t)]_{E,L^2} \quad (36)$$

which is a <u>microscopic equation of continuity</u> for the distribution n_2 in the (E,L^2)- representation for which the outward radial current is

$$j(R,E,L^2;t) = n(\underset{\sim}{R},E,L^2;t)v\ \cos\theta \quad (37)$$

across a sphere of radius R. Such an equation is normally reserved as in (3) only for $\underset{\sim}{\rho}$-integrated distributions (4). The microscopic equation (36) is in accord with physical intuition since E and L^2 are naturally conserved in the absence of collisions with the gas.

The distributions $n^{\pm}(\underset{\sim}{R},E,L^2;t)$ of (E,L^2)-pairs which are expanding (+) into the angular range $0 \leq \theta \leq \frac{\pi}{2}$ or contracting (-) into the range $\frac{\pi}{2} \leq \theta \leq \pi$ across R, are therefore characterized by the transport equations

$$\frac{d}{dt} n^{\pm}(\underset{\sim}{R},E,L^2;t) = \frac{\partial n^{\pm}}{\partial t} \pm \frac{1}{R^2} \frac{\partial}{\partial R} [R^2 n^{\pm}(\underset{\sim}{R},E,L^2;t) v|\cos\theta|]_{E,L^2} \tag{38}$$

which also represent <u>microscopic continuity</u>.

The distributions

$$n^{s,d}(\underset{\sim}{R},E,L^2;t) = n^{+}(\underset{\sim}{R},E,L^2;t) \pm n^{-}(\underset{\sim}{R},E,L^2;t) \tag{39}$$

and associated summed and net currents

$$j^{s,d}(R,E,L^2;t) = n^{s,d}(\underset{\sim}{R},E,L^2;t) v|\cos\theta| \tag{40}$$

therefore satisfy the transport equations

$$\frac{d}{dt} n^{s}(\underset{\sim}{R},E,L^2;t) = \frac{\partial n^{s}}{\partial t} + \frac{1}{R^2} \frac{\partial}{\partial R} [R^2 j^{d}(R,E,L^2;t)]_{E,L^2} \tag{41a}$$

and

$$\frac{d}{dt} n^{d}(\underset{\sim}{R},E,L^2;t) = \frac{\partial n^{d}}{\partial t} + \frac{1}{R^2} \frac{\partial}{\partial R} [R^2 j^{s}(R,E,L^2;t)]_{E,L^2} \tag{41b}$$

of microscopic continuity.

On integrating (41) over the angular momentum range $0 \leq L^2 \leq R^2p^2$, and with the use of Leibnitz's rule

$$\int_0^{R^2p^2} \frac{1}{R^2} \frac{\partial}{\partial R} [R^2 j(R,E,L^2)]_{E,L^2} \, dL^2 = \frac{1}{R^2} \frac{\partial}{\partial R} [R^2 j(R,E)]_E$$

$$- j(R,E,R^2p^2) \frac{\partial}{\partial R} [R^2p^2]_E \qquad (42)$$

for differentiation with respect to R of an integral with variable R-limits, then, as a check, the set (21) for the general $(\underset{\sim}{R},E)$-distributions

$$n^{s,d}(\underset{\sim}{R},E,t) = \int_0^{R^2p^2} n^{s,d}(\underset{\sim}{R},E,L^2;t) dL^2 \qquad (43)$$

and currents

$$j^{s,d}(R,E,t) = \int_0^{R^2p^2} j^{s,d}(R,E,L^2;t) dL^2 \qquad (44)$$

is recovered, on remembering that $j^d(R,E,R^2p^2)$ at the turning points vanishes, and, with the aid of (34), that

$$j(R,E,L^2) = n_2(\underset{\sim}{R},E,L^2) \, v_R = \frac{1}{2} [n_1(\underset{\sim}{R},E,\theta)v]/R^2p^2 \qquad (45)$$

where the radial speed v_R is $v \cos\theta$.

3. Transport-Collisional Equations

Collisional rates may now be directly incorporated within the $(\underset{\sim}{R},E,L^2)$ and $(\underset{\sim}{R},E)$ representations (38) and (25). In termolecular ion-atom association (1), for example, the set of transport equations (38), is set equal to the net collisional-loss rate

$$\frac{d}{dt}\, n^{\pm}(\underset{\sim}{R},E_i,L_i^2,t) = -\int_{V_i(R)}^{\infty} dE_f \int_0^{L_{mf}^2} S_{if}^{\pm}(R)\,dL_f^2 \qquad (46)$$

for pairs in level (E_i,L_i^2), where, in terms of the frequency $\nu_{if}(R)$ per unit element $d\Gamma_f = dE_f dL_f^2$ for $i(E_i,L_i^2) \rightarrow f(E_f,L_f^2)$ transitions induced by collisions between M and the pair (A-B), the net input-output two level collisional rates $S_{if}^{\pm}(R)$ per unit interval $d\Gamma_i d\Gamma_f$ are

$$S_{if}^{\pm}(R) = n_i^{\pm}(\underset{\sim}{R},E_i,L_i^2)\,\nu_{if}(R) - n_f^{\pm}(\underset{\sim}{R},E_f,L_f^2)\nu_{fi}(R) = -S_{fi}^{\pm}(R) \qquad (47)$$

The effective radial interaction between A and B is

$$V_i(R) = V(R) + L_i^2/2mR^2 \qquad (48)$$

so that the energy of the lowest level of AB accessible by collision at a fixed L_i^2 and R can be denoted in (46) by $V_i(R)$. The maximum angular momentum in (46) accessible at fixed E_f and R is

$$L_{mf}^2(E_f,R) = p_f^2R^2 = 2m[E_f-V(R)]R^2 \qquad (49)$$

The equations in $n^{\pm}$ obtained from (38) and (46) are coupled via the condition

$$n_i^{+}(R_i^{\pm}) = n_i^{-}(R_i^{\pm}) \qquad (50)$$

at the pericenter R_i^- and apocenter R_i^+ of the (E_i, L_i^2)-orbit.

In termolecular ion-ion recombination where equilibrium in L^2 is established even at low N (Bates and Mendas 1975), the appropriate transport equation is then (25) set equal to the net collisional destruction rate,

$$\frac{d}{dt} n^{\pm}(\underset{\sim}{R}, E_i, t) = - \int_{-D}^{\omega} S_{if}^{\pm}(R) dE_f \tag{51}$$

of pairs in level E_i, where

$$S_{if}^{\pm}(R) = n_i^{\pm}(\underset{\sim}{R}, E_i)\, \upsilon_{if}(R) - n_f^{\pm}(\underset{\sim}{R}, E_f)\, \upsilon_{fi}(R) = -S_{fi}^{\pm}(R) \tag{52}$$

refers now to the net collisional rate per unit interval $dE_i dE_f$ for transitions $E_i \rightarrow E_f$. The L_i^2-averaged equations in $n^{\pm}$ are directly coupled in (25) via γ^* which originates from condition (50) at the turning points of (E_i, L_i^2)-orbits which in effect is incorporated within the E set equation (25).

The equivalent transport equations (2) and either (38) or (41) are each valuable in separate ranges of gas density N. At high N, the distribution n realizes equilibrium in $\underset{\sim}{\rho}$ but is highly non-equilibrium in $\underset{\sim}{R}$. It has already been illustrated (Flannery 1982a) that (2) for the phase-space distribution together with the first moment of Boltzmann equation, which provides an expression for the current (5) in terms of (4) and the coefficients D and K for relative diffusion and drift respectively, yield the familiar macroscopic equation of diffusional-drift which governs (cf. Bates 1985, Flannery 1982b) termolecular ion-ion recombination in the limit of high N. From low N, where collisional relaxation in (E, L^2) is the rate limiting step for termolecular ion-atom association and ion-ion recombination, to intermediate N, where the distribution is non-equilibrium in $\underset{\sim}{R}$, E and L^2, the (E, L^2) representation (38)

is more natural. In contrast to ion-ion recombination, diffusional-drift is negligible for ion-atom association at most densities N of practical interest. The (E,L^2)-representation (38) or (41) is then to be preferred for association at all gas densities. The general set (41) has been used to illustrate (Flannery 1987) how the rate α for termolecular association of atomic reactants increases with N towards a saturation value at high N, and also to illustrate the connection (Flannery 1986) of the microscopic theory with Thomson's treatment of termolecular recombination. The set (21) for L^2-equilibrium can also be used to illustrate this connection.

3. Conclusion

In summary therefore, the transport equation (2) with separate streaming in $\underset{\sim}{R}$ and $\underset{\sim}{p}$ has been converted into the more compact field-free form (31) based on $\underset{\sim}{R}$-streaming alone at constant E and L^2. The new form results quite naturally in valuable microscopic continuity equations (35), (38) and (41) when the distribution n for expanding and contracting pairs is expressed in the $(\underset{\sim}{R},E,L^2)$-representation. The derived equations (17) in the $(\underset{\sim}{R},E)$-representation contain source/sink contributions due to geometrical reflections at the pericenter and apocenter. The governing transport-collisional Master equations (48) with (46) and (25) with (51) for termolecular ion-atom association and ion-ion recombination between atomic reactants in gases then follow quite naturally.

This research is supported by the US Air Force Office of Scientific Research under Grant No. AFOSR-84-0233.

References

Bates, D. R., and Mendas, I., 1975, J. Phys. B: Atom. Molec. Phys. 8, 1770-1775.

_____, 1978, Proc. Roy. Soc. Lond. A 359, 275-85.

Bates, D. R., 1985, Advances in Atomic and Molecular Physics, Vol. 20, ed. D. R. Bates and B. Bederson (New York: Academic) Ch. 1.

McDaniel, E. W., and Mason, E. A., 1973, The Mobility and Diffusion of Ions in Gases (New York: Wiley).

Chapman, S., and Cowling, T. G., 1970, The Mathematical Theory of Non-Uniform Gases (Cambridge: University Press, 3rd edn.).

Duderstadt, J. J., and Martin, W. R., 1979, Transport Theory (New York: Wiley).

Flannery, M. R., 1982a, Phil. Trans. Roy. Soc. Lond. A 304, 447-97.

_____ 1982b, Applied Atomic Collision Physics, Vol. 3, ed. E. W. McDaniel and W. L. Nighan (New York: Academic), Ch. 5.

_____ 1986, J. Phys. B: Atom. Molec. Phys. 19, L227-L233.

_____ 1987, Modern Applications of Atomic and Molecular Processes, ed. A. E. Kingston (London: Plenum), Ch. xx, at press.

Figure Caption

Figure 1. Hyperbolic trajectories for motion in Cartesian XY-space with specified energy $E = \frac{3}{2} kT$ intersecting a sphere of radius $R_T = (2e^2/3kT)$ at angle θ under pure coulombic attraction $V(R) = -e^2/R$ for various angular momenta $L = Rp \sin\theta = (2mE)^{1/2}\rho$ or θ. Lengths are in units of R_T and the impact parameter ρ ranges from 0 to $\rho_{max} = \sqrt{2}\ R_T$. The distributions $n^+(R_T,E,\theta)$ and $n^-(R_T,E,\pi-\theta)$ of expanding and contracting pairs are in general unequal except at the pericenter $\theta = \pi/2$.

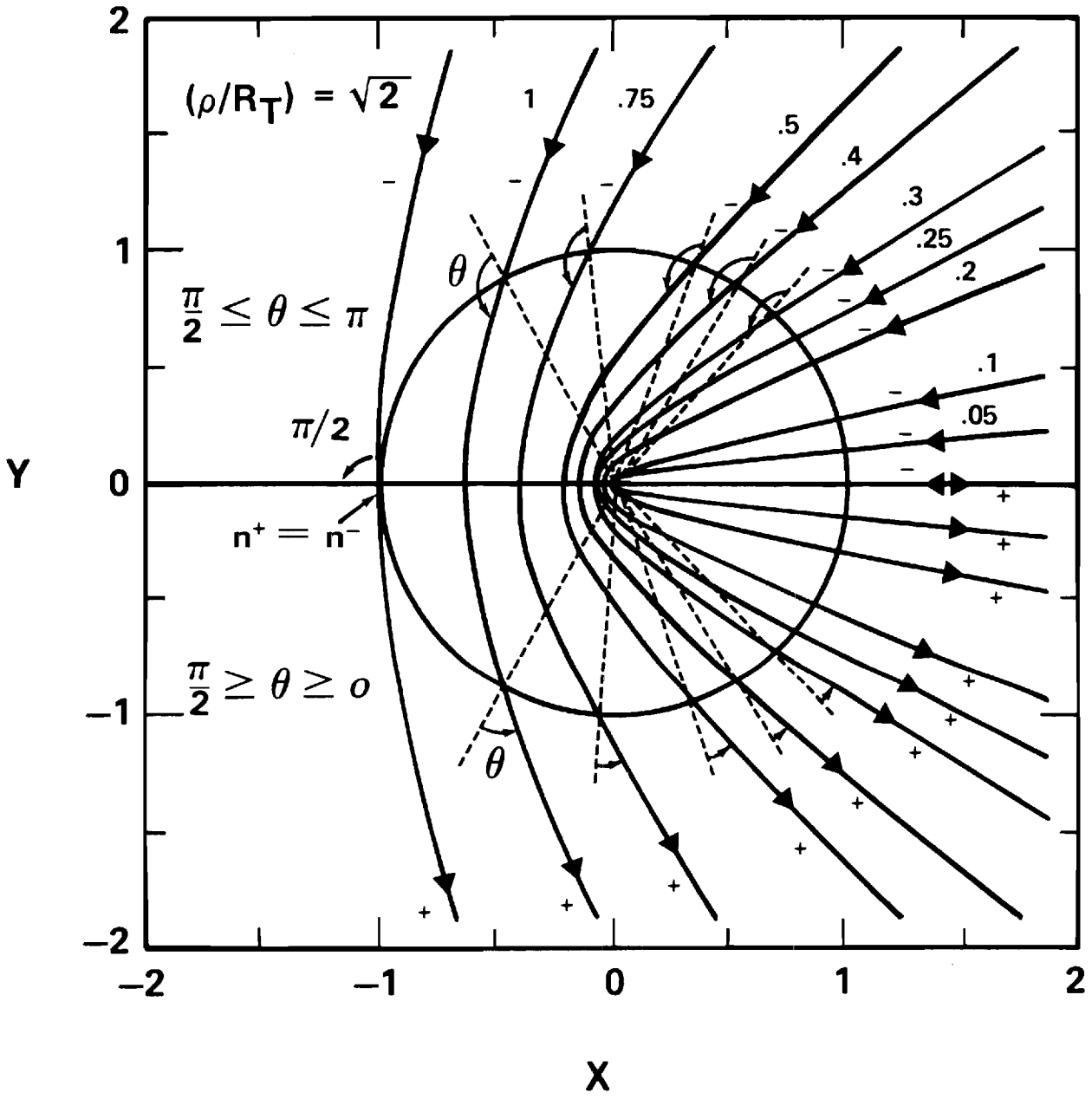
$(\rho/R_T) = \sqrt{2}$
1
.75
.5
.4
.3
.25
.2
.1
.05
θ
$\frac{\pi}{2} \leq \theta \leq \pi$
$\pi/2$
$n^+ = n^-$
$\frac{\pi}{2} \geq \theta \geq o$
θ
2
1
0
−1
−2
−2
−1
0
1
2
Y
X

UNCLASSIFIED

SECURITY CLASSIFICATION OF THIS PAGE

REPORT DOCUMENTATION PAGE

Form Approved OMB No. 0704-0188

1a. REPORT SECURITY CLASSIFICATION UNCLASSIFIED	1b. RESTRICTIVE MARKINGS
2a. SECURITY CLASSIFICATION AUTHORITY	3. DISTRIBUTION / AVAILABILITY OF REPORT Approved for public release; distribution unlimited.
2b. DECLASSIFICATION / DOWNGRADING SCHEDULE	
4. PERFORMING ORGANIZATION REPORT NUMBER(S) GIT-85-019	5. MONITORING ORGANIZATION REPORT NUMBER(S) N/A
6a. NAME OF PERFORMING ORGANIZATION Georgia Institute of Technology 6b. OFFICE SYMBOL (*If applicable*)	7a. NAME OF MONITORING ORGANIZATION Air Force Office of Scientific Research (AFOSR) Directorate of Physical & Geophysical Sciences
6c. ADDRESS (*City, State, and ZIP Code*) School of Physics Georgia Institute of Technology Atlanta, Georgia 30332	7b. ADDRESS (*City, State, and ZIP Code*) AFOSR/NP Bolling Air Force Base, Bldg. 410 Washington, D. C. 20332-6448
8a. NAME OF FUNDING / SPONSORING ORGANIZATION AFOSR 8b. OFFICE SYMBOL (*If applicable*) NP	9. PROCUREMENT INSTRUMENT IDENTIFICATION NUMBER AFOSR-84-0233
8c. ADDRESS (*City, State, and ZIP Code*) Building 410 Bolling AFB, D.C. 20332-6448	10. SOURCE OF FUNDING NUMBERS PROGRAM ELEMENT NO.: 61102F; PROJECT NO.: 2301; TASK NO.: A4; WORK UNIT ACCESSION NO.: N/A
11. TITLE (*Include Security Classification*) Termolecular Association of Ions in Gases, Recombination and Electron-Atom Collisions	
12. PERSONAL AUTHOR(S) M. R. Flannery	
13a. TYPE OF REPORT Final Report 13b. TIME COVERED FROM 7/1/84 TO 7/30/89	14. DATE OF REPORT (*Year, Month, Day*) 9/30/89 15. PAGE COUNT 171
16. SUPPLEMENTARY NOTATION	

17. COSATI CODES		
FIELD	GROUP	SUB-GROUP
N/A	N/A	N/A

18. SUBJECT TERMS (*Continue on reverse if necessary and identify by block number*)
Recombination, Master Equation, Variational Principle, Diffusional Method, Bottleneck Method, Strong-Collision, Coupled Nearest-Neighbor, Radiative, Dissociative

19. ABSTRACT (*Continue on reverse if necessary and identify by block number*)

A list of publications of the research performed during the period 7/1/84 - 7/30/89 of the Grant AFOSR - 84-0233 is provided. Theoretical research has been conducted on (a) Termolecular Association and Recombination (b) electron - (excited) atom collisions and on (c) analytical solutions of the Time-Dependent Debye-Smoluchowski equation for transport influenced reactions.Papers on all of the above topics have been written up and published as papers, with reprints sent to AFOSR at various times during the period. The exact Master Equation Method, a Variational Principle discovered during the course of this research, and various approximate treatments are presented is Special Highlights of this research. In addition, the Appendixes include a major review of Recombination Process in General.

20. DISTRIBUTION / AVAILABILITY OF ABSTRACT ☒ UNCLASSIFIED/UNLIMITED ☐ SAME AS RPT. ☐ DTIC USERS	21. ABSTRACT SECURITY CLASSIFICATION UNCLASSIFIED
22a. NAME OF RESPONSIBLE INDIVIDUAL Dr. Ralph E. Kelley	22b. TELEPHONE (*Include Area Code*) (202) 767-4904 22c. OFFICE SYMBOL NP

DD Form 1473, JUN 86 *Previous editions are obsolete.*

SECURITY CLASSIFICATION OF THIS PAGE

UNCLASSIFIED

CONTENTS

Abstract

A list of publications of the research performed during the period 7/1/84 - 7/30/89 of the Grant AFOSR-84-0233 is provided. Theoretical research has been conducted on (a) Termolecular Association and Recombination (b) electron-(excited) atom collisions and on (c) analytical solutions of the Time Dependent Debye-Smoluchowski equation for transport influenced reactions. Papers on all of the above topics have been written up and published as papers, with reprints sent to AFOSR at various times during the period. The Exact Master Equation Method, a Variational Principle discovered during the course of this research, and various approximate treatments are presented as Special Highlights of this research. In addition, the Appendices include a major review of Recombination Processes in General.

1. Accomplishments due to AFOSR Support

PRINCIPAL INVESTIGATOR: M. R. Flannery

School of Physics, Georgia Institute of Technology

Grant AFOSR-84-0233, Period 7/1/84 - 7/30/89

Program Element No. 61102F, Project No. 2301, Task No. A4

1.1 Research Objectives

There are two main objectives to this research program:

(1) Basic formulation and development of the theory of termolecular association processes

$$A^+ + B^- + M \rightarrow AB + M \qquad (1)$$

and

$$A^+ + B + M \rightarrow AB^+ + M \qquad (2)$$

(2) Development of scattering theories for the electron-(excited) atom collision process

$$e + A^* \rightarrow e + A^{**} \qquad (3)$$

It is important to conduct an exhaustive theoretical investigation of (1) since not only is (1) of great significance in its own right to many important applications (e.g., exciplex lasers, KrF^*, $XeCl^*$ etc.) but also it represents the simplest three-body chemical reaction. It can therefore be considered as serving as a prototype of three body processes in general.

During this grant period, this objective has been achieved for gases M at low densities. In addition to the Exact Master Equation Treatment of (1), a new Variational Principle has been discovered. This Variational Principle is applicable not only to ion-ion recombination (1) but to three-body processes

in general. It represents the first rigorous Variational Principle in Chemical Physics Collision Processes and is fully documented in §3.2.

Also various simpler but approximate treatments of (1) have been investigated - the Diffusion, Bottleneck, Strong Collision and Coupled Nearest-Neighbor Methods. These are discussed fully in §3.

The second main objective is the development of scattering theories for process (3). Now that some experimental activity is beginning to emerge it is important to develop theories for electron-(excited) atom collisions. This objective has been achieved and progress is detailed in Appendix B.

1.2 Full List of Refereed Publications in Scientific Journals (1984-1989)

1. "Ion-Ion Recombination at High Ion-Density", M. R. Flannery, J. Phys. B: Atom. Molec. Phys. 18, 5 (1985).

2. "Selected Bibliography on Atomic Collisions", M. R. Flannery, E. W. McDaniel and S. T. Manson, Atomic Data and Nuclear Data Tables 33, 1-148 (1985).

3. "The Rate for Transport-Influenced Reactions", M. R. Flannery, J. Phys. B: Atom. Molec. Phys. 18, L747-L749 (1985).

4. "Basic Expression for Termolecular Recombination and Dissociation", M. R. Flannery, J. Phys. B: Atom. Molec. Phys. 18, L839-L844 (1985).

5. "Connection Between Microscopic and Thomson Theories of Recombination", M. R. Flannery, J. Phys. B: Atom. Molec. Phys. 19, L227-L233 (1986).

6. "Orientation and Alignment Parameters for e-He($1\,^1S \rightarrow 3\,^1D$) Collisions", M. R. Flannery and E. J. Mansky, J. Phys. B: Atom. Molec. Phys. 20, L235-L239 (1987).

7. "Macroscopic and Microscopic Perspectives of Termolecular Association of Atomic Reactants in a Gas", M. R. Flannery, in Recent Studies in Atomic and Molecular Processes, ed. A. E. Kingston (Plenum Press, London, 1987), pages 167-191.

8. "Representations of the Transport Equation for Reactive Processes", M. R. Flannery, J. Phys. B: Atom. Molec. Phys. 20, 4929-4938 (1987).

9. "Diffusional Theory of Termolecular Recombination and Association of Atomic Species in A Gas", M. R. Flannery, J. Chem. Phys. 87, 6947-6956 (1987).

10. "Termolecular Recombination at Low Gas Density: Strong-Collision Bottleneck and Exact Treatments", M. R. Flannery and E. J. Mansky, J. Chem. Phys. 88, 4228-4241 (1988).

11. "Variational Principle for Termolecular Recombination in a Gas", M. R. Flannery, J. Chem. Phys. 89, 214-222 (1988).

12. "Termolecular Recombination: Nearest-Neighbor Limit and Uncoupled-Intermediate-Levels Limit", M. R. Flannery and E. J. Mansky, J. Chem. Phys. 89, 4086-4091 (1988).

13. "Analytical and Numerical Solutions of the Time-Dependent Debye-Smoluchowski Equation for Transport-Influenced Reactions", M. R. Flannery and E. J. Mansky, Chem. Phys. 132, 115-136 (1989).

14. "Recombination Processes", M. R. Flannery in Molecular Processes in Space: 'Physics of Atoms and Molecules' Series, edited by T. Watanabe, I. Shimamura, M. Shimizu and Y. Itikawa (Plenum Press, London, 1990).

Six reprints of each of the above publications were submitted to AFOSR as reprint reports with numbers GIT-85-002, 003, 006, 007, 004, 010, 012, 011, 015, 016 017 and 018, respectively.

1.3 Chapters in Books

1. "Macroscopic and Microscopic Perspectives of Termolecular Association of Atomic Reactants in a Gas", in Recent Studies in Atomic and Molecular Processes, ed. A. E. Kingston (Plenum Press, London, 1987) pages 167-191.

2. "Recombination Processes", in Molecular Processes in Space: 'Physics of Atoms and Molecules' Series, edited by T. Watanabe, I. Shimamura, M. Shimizu and Y. Itikawa (Plenum Press, London, 1990).

3. "The Numerical Solution of Partial Differential Equations in Atomic Scattering Theory", by E. J. Mansky in Proceedings of the Summer School of Computational Atomic and Nuclear Physics, edited by C. Bottcher, M. R. Strayer and J. B. McGrory (World Scientific, 1990).

4. "Iterative Solution of Large Linear Systems and Heavy Particle Collisions: Ion-Ion Recombination", by E. J. Mansky in Proceedings of the Summer School of Computational Atomic and Nuclear Physics, edited by C. Bottcher, M. R. Strayer and J. B. McGrory (World Scientific, 1990).

5. "Electron Collision Cross Sections Involving Excited States", by E. J. Mansky, in Proceedings of the NATO-Advanced Study Institute on "Non-Equilibrium Processes in Partially Ionized Gases", edited by M. Capitelli and J. N. Bardsley (Plenum Press, 1990).

Chapter #1 has been published. Six reprints have already been sent to AFOSR under Reprint Report GIT-85-012.

Chapters #2, 3, 4, 5 are in press. Reprints will be sent when available. These chapters are included as Appendices A, B, C and D of this report.

1.4 Annual Reports (7/1/84 - 7/30/88)

Full Annual Reports of the research performed during the previous twelve month period were prepared and submitted to AFOSR. The Performing Organization Report Numbers for the periods 7/1/84-6/30/85; 7/1/85-6/30/86; 7/1/86-6/30/87 and 7/1/87-7/30/88 were GIT-85-001, GIT-85-008, GIT-85-009 and GIT-85-014, respectively.

1.5 Funding History

Project AFOSR-84-0233:

7/1/84 - 6/30/85:	73,403
7/1/85 - 6/30/86:	70,188
7/1/86 - 6/30/87:	86,730
7/1/87 - 7/30/88:	92,845
8/1/88 - 7/30/89:	99,311
TOTAL:	$422,311

1.6 Personnel

1. Professor M. R. Flannery - Principal Investigator
2. Dr. E. J. Mansky - Research Scientist II
3. Mr. M. S. Keehan - Graduate Student
4. Mr. P. Smith - Graduate Student
5. Mr. A. Haffad - Graduate Student
6. Mr. A. Mekki - Graduate Student

2. Invited and Contributed Papers Presented at Professional Scientific Conferences (1984-1988)

1984: The following papers were presented at the 37th Annual Gaseous Electronics Conference, October 9-12, 1984 held at the University of Colorado. Abstracts were published in Bull. Amer. Phys. Soc. (1985) and in Annual Report GIT-85-001.

1. "Association/Dissociation in Dense Gases and Adsorption/Desorption on Surfaces", by M. R. Flannery.
2. "Analytical and Numerical Solutions of the Time Dependent Debye-Smoluchowski Equation", by M. R. Flannery and E. J. Mansky.
3. "Electron-Excited Hydrogen and Helium Collisions", by E. J. Mansky and M. R. Flannery.
4. "Symmetric Charge-Transfer Cross Sections in Rare Gas (Rg^+-Rg) Systems", by E. J. Mansky and M. R. Flannery.

1985: The following paper was presented at the 38th Annual Gaseous Electronics Conference, October 15-18, 1985, held at the Naval Postgraduate School, Monterey, California. The abstract was published in Bull. Amer. Phys. Soc. (1986) and in Annual Report GIT-85-008.

1. "Variational Principle for Association/Dissociation in Dense Gases", by M. R. Flannery, was presented at the 38th Annual Gaseous Electronics Conference, October 15-18, 1985, at the Naval Postgraduate School, Monterey, California.

1986: The following papers were presented at the 39th Annual Gaseous Electronics Conference, October 7-10, 1986, held at University of Wisconsin, Madison, Wisconsin. The abstracts were published in Bull. Amer. Phys. Soc. (1987) and in Annual Report GIT-85-009.

1. "Microscopic Perspective to Termolecular Ion-Molecule Reactions", by M. R. Flannery.
2. "Detailed Investigation of the Thomson Model of Termolecular Recombination", by E. J. Mansky and M. R. Flannery.

An invited lecture entitled:

3. "Termolecular Association in Gases", by M. R. Flannery was presented at a Conference held in Honor of Sir David Bates' 70th Birthday at Queen's University, Belfast, November 17 and 18, 1986.

The lecture was published as a Chapter in the book "Recent Studies in Atomic and Molecular Processes", edited by A. E. Kingston (Plenum Press, New York, 1987).

1987: Invited and Contributed Papers

1. An invited paper entitled "Termolecular Recombination", by M. R. Flannery, was presented at the 40th Annual Gaseous Electronics Conference, Atlanta, held at Georgia Institute of Technology, Georgia, Oct. 13-16, 1987. It is published in Bull. Amer. Phys. Soc. 33, $2 (1988) p. 122.
2. A contributed paper entitled "Orientation and Alignment Parameters for $e + He\ (2^{1,3}S) \rightarrow e + He\ (3^{1,3}P,\ 3^{1,3}D)$ Collisions", by E. J. Mansky and M. R. Flannery, was presented at the 40th Annual Gaseous Electronics Conference, Atlanta, held at Georgia Institute of Technology, Georgia, Oct. 13-16, 1987. It is published in Bull. Amer. Phys. Soc. 33, $2 (1988) p. 141.
3. A contributed paper entitled "Termolecular Recombination and Electrical Networks", by M. R. Flannery and E. J. Mansky was presented at the 1988 Spring Meeting of the American Physical Society (APS) in conjunction with the Annual Meeting of the APS Division of Atomic and Molecular and Optical Physics held at Baltimore, Maryland, April 18-21 (1988).

The abstracts were included in the Annual Report GIT-85-014.

1988:

(a) A long paper entitled "Multichannel Eikonal Theory of Electron-(Excited) Atom Collisions", by M. R. Flannery and a contributed paper entitled "Integral and Differential Cross Sections for e-He ($2^{1,3}S$) Collisions", by E. J. Mansky and M. R. Flannery were presented at the 41st Annual Gaseous Electronics Conference held at University of Minnesota, Minneapolis, Minnesota, Oct. 18-21, 1988. The abstracts are published in Bull. Amer. Phys. Soc. 34, #2 (1989) p. 302 and p. 315.

(b) Two contributed papers entitled "The Poincare Sphere for the 2^1P, 3^1P and 3^1D States of Helium", by E. J. Mansky and M. R. Flannery and "Orientation and Alignment Parameters for e-H(1s→3p,3d) Collisions", by E. J. Mansky were presented at the 20th Annual Meeting of the (APS) Division of Atomic, Molecular and Optical Physics held at the University of Windsor, Windsor, Ontario, May 17-19, 1989. The abstracts are published in Bull. Amer. Phys. Soc. 34, #5 (1989) p. 1371 and p. 1407.

(c) An invited paper entitled "Electron Cross Sections Involving Excited States", by E. J. Mansky was presented to the NATO-Advanced Study Institute, "Non-Equilibrium Processes in Partially Ionized Gases" held at Maratea, Italy, June 4-17, 1987. It is published as a Chapter in the Book, listed in §1.2.

(d) Two invited papers entitled "The Numerical Solution of Partial Differential Equations in Atomic Scattering Theory", and "Iterative Solutions in Large Linear Systems and Heavy Particle Collisions", by E. J. Mansky were presented to the Summer School of Computational Atomic and Nuclear Physics held at University of the South, Sewanee, Tennessee, June 16-July 7, 1989. They are published as Chapters in the Book, listed in

§1.3.

(e) A contributed paper entitled "Stokes Parameter Analysis of the 3^1D State of Helium", by E. J. Mansky and M. R. Flannery was delivered to 16th International Conference on the Physics of Electronic and Atomic Collisions held at New York, July 26 - Aug. 1, 1989.

3. Special Highlights

In a series of papers, #9 - #12 of the list in § 1.1, the Termolecular Recombination Process

$$A^+ + B^- + M \rightarrow AB + M \qquad (1)$$

was explored in depth. Exact treatments based on a Master Equation and on a New Variational Principle discovered by M. R. Flannery were developed and applied. Various approximate treatments as (a) The Diffusional Theory (b) Strong Collision and Bottleneck Models and (c) a Coupled Nearest-Neighbor Limit and Uncoupled Intermediate Levels Limits were also provided and compared with experiment. In order to explain the research fully, the resulting publications in J. Chem. Phys. are reproduced in the following Sections 3.1 - 3.4.

In §3.1, the Exact Treatment is discussed together with the Strong Collision and Bottleneck Methods.

In §3.2, the New Variational Principle is developed and applied.

In §3.3, the Diffusional Treatment is presented.

In §3.4, methods of Coupled Nearest-Neighbor and Uncoupled Intermediate Levels are presented and applied.

Since the Termolecular Process (1) is the simplest type of three-body Chemical Process, it is essential to understand it in required depth, not only because of its great significance in general applications but also because it serves as a prototype for three-body reactions. In the following sections, attempt is made to provide an exhaustive understanding.

Also a major review of Recombination Processes in General is included in Appendix A.

3.1 Exact Treatment, Strong Collision and Bottleneck Treatments.

Termolecular recombination at low gas density: Strong collision, bottleneck, and exact treatments

M. R. Flannery and E. J. Mansky
School of Physics, Georgia Institute of Technology, Atlanta, Georgia 30332

(Received 23 November 1987; accepted 24 December 1987)

On introducing the probabilities for association as a function of internal separation R and internal energy E of the associating (A–B) species the strong collision model is thoroughly investigated and compared, as a case study, with the exact treatment of termolcular ion–ion recombination at low gas densities. A bottleneck model is also investigated. Analytical expressions for the one way equilibrium energy-change rates at fixed R are provided in the Appendix.

I. INTRODUCTION

The theory of termolecular ion–ion recombination,

$$A + B + M \underset{k}{\overset{a}{\rightleftarrows}} AB + M \tag{1.1}$$

between positive and negative atomic ions A and B in a low density gas thermal M is now well established.[1–5] The distribution $n_l(E_l,t)$ per unit interval dE_l of recombining pairs AB with internal energy E_l a time t is governed by the collisional input–output Master equation[1–5]:

$$\frac{d}{dt}n_l(E_l,t) = \frac{\partial n_l}{\partial t} - F_l$$
$$= -\int_{-D}^{\infty}[n_l\nu_{lf} - n_f\nu_{fl}]\,dE_f$$
$$= -\frac{\partial}{\partial E_l}J_l(E_l,t), \tag{1.2}$$

where ν_{lf} is the frequency per unit interval dE_f for $E_l \to E_f$ transitions by collisions between AB and M, where J_l is the upward current in energy space past level E_l and where $-D$ is the energy of the lowest vibrational level of AB relative to the dissociation limit taken as zero energy. For dissociated pairs with $E_l > 0$, F_l is the net flux per unit interval dE_l of (contracting) AB pairs generated with energy E_l at infinite internal separation R. For bound pairs with $E_l < 0$, F_l is zero. The net rate for association is[4]

$$R^A(t) = \int_{-D}^{\infty} P_l^S\left(\frac{dn_l}{dt}\right)dE_l$$
$$= \alpha N_A(t)N_B(t) - kn_s(t), \tag{1.3}$$

where P_l^S is the probability that E_l pairs are collisionally connected to the product channel, i.e., have been stabilized against dissociative collisions with thermal M. The effective two-body rate constant for the association of A and B with (cm^{-3}) concentrations $N_A(t)$ and $N_B(t)$ is α ($cm^3\,s^{-1}$), and k (s^{-1}) is the frequency for dissociation of those tightly bound pairs of concentration $n_s(t)$, which are considered to be fully associated with energies E_l within a block $\mathscr{S}$ of low lying fully stabilized levels in a range $-S \geqslant E_l \geqslant -D$ within which the stabilization probability P_l^S is calculated to be unity. When the quasi-steady-state (QSS) condition $dn_l/dt = 0$ is satisfied for pairs in a block $\mathscr{E}$ of highly excited levels in the energy range $0 \geqslant E \geqslant -S$ between the dissociation limit at zero energy and level $-S$ the rate (1.3) reduces to[4]

$$R^A(t) = \int_{-D}^{-S}\left(\frac{dn_l}{dt}\right)dE_l$$
$$= \int_0^{\infty} F_l\,dE_l = -\int_{-E}^{\infty}\left(\frac{dn_l}{dt}\right)dE_l$$
$$= -J(-E,t) \tag{1.4}$$

for a steady-state ($\partial n_l/\partial t = 0$) distribution of pairs in the block $\mathscr{E}$ of fully dissociated states in the energy range $0 < E < \infty$, over which the stabilization probability P_l^S vanishes. The rate (1.3) therefore reduces[4] under QSS to the downward current $-J(-E,t)$ of pairs past energy level $-E$ in bound block $\mathscr{B}$.

At low gas densities the expansion[4]

$$\gamma_l(t) = \frac{n_l(E_l,t)}{\tilde{n}_l(E_l)} = P_l^D(E_l)\left[\frac{N_A(t)N_B(t)}{\tilde{N}_A\tilde{N}_B}\right]$$
$$+ P_l^S(E_l)\left[\frac{n_s(t)}{\tilde{n}_s}\right] \tag{1.5a}$$
$$\equiv P_l^D(E_l)\gamma_c(t) + P_l^S(E_l)\gamma_s(t) \tag{1.5b}$$

permits separation of variables E_l and t in the collisional part of Eq. (1.2). Here γ_l, γ_c, and γ_s are the various time-dependent distributions of states in blocks $\mathscr{B}$, $\mathscr{C}$, and $\mathscr{S}$ normalized to their respective equilibrium values $\tilde{n}_l, \tilde{N}_{A,B}$, and $\tilde{n}_s$. For $\mathscr{B}$ states, P_i^S and $P_i^D = 1 - P_i^S$ are the probabilities that state i is collisionally connected to the sink $\mathscr{S}$ and to the source $\mathscr{C}$. For $\mathscr{C}$ states at low gas densities P_i^D, the collision survival probability is unity when equilibrium conditions in E_i and R can be assumed in the collision part of Eq. (1.2). When Eq. (1.5) is inserted the collisional part of Eq. (1.2), then Eqs. (1.4) and (1.3) yield the expressions[4]

$$\alpha\tilde{N}_A\tilde{N}_B = -j(-E) = k\tilde{n}_s$$
$$= \int_{-E}^{\infty}dE_i\int_{-D}^{-E}(P_f^S - P_i^S)C_{if}\,dE_f \tag{1.6}$$

for the rate coefficients α and k in Eq. (1.1). The collision kernel C_{if} is the collisional rate $\tilde{n}_i\nu_{if}$ ($cm^3\,s^{-1}$) per unit element $dE_i\,dE_f$ for $E_i \to E_f$ transitions and varies linearly with the gas density N. At low N, α is linear in N so that $P_i^{S,D}$ are required only to zero order in N. The net downward time-dependent collisional current across arbitrary level $-E$ in block $\mathscr{B}$ separates as

 0021-9606/88/074228-14$02.10

$$-J(-E,t) = -j(-E)\left[N_A(t)N_{B(t)}/\tilde{N}_A\tilde{N}_B - n_s(t)/\tilde{n}_s\right] \quad (1.7)$$

which under conditions of full thermodynamic equlibrium tends therefore to zero.

The multicollisional stochastic aspect of the theory becomes apparent by correctly identifying the (time-independent and density-independent) stabilization probability as

$$P_i^S(E_i) = \left[\int_{-D}^{0} (n_i \nu_{if})\, P_f^S\, dE_f\right] \Big/ \left[\int_{-D}^{\infty} n_i \nu_{if}\, dE_f\right] \quad (1.8a)$$

which is the fraction of all collisions which result in association. Equation (1.8a) is consistent with the concept of a Markov element chain, and when rewritten in the form of an integral equation

$$P_i^S \int_{-D}^{\infty} C_{if}\, dE_f = \int_{-D}^{0} C_{if} P_f^S\, dE_f \quad (1.8b)$$

is seen, after substituting Eq. (1.5b) in Eq. (1.2), to be equivalent to the assumption of a quasi-steady-state (QSS) E_i distribution of pairs with energy within the highly excited block $\mathscr{E}$.

The rate (1.6) holds for $E=0$ and $E=S$ to give, respectively,

$$\alpha\tilde{N}_A\tilde{N}_B = -j(0) = \int_0^{\infty} dE_i \int_{-D}^{0} C_{if} P_f^S\, dE_f = k\tilde{n}_s \quad (1.9)$$

as the collisional rate from the fully dissociated states i to bound states f which are then collisionally stabilized with probability P_f^S, and

$$\alpha\tilde{N}_A\tilde{N}_B = j(-S) = \int_{-D}^{-S} dE_i \int_{-S}^{\infty} C_{if} P_f^D\, dE_f = k\tilde{n}_s \quad (1.10)$$

as the collisional rate from the fully associated states i to levels f which are then collisionally disrupted with probability P_f^D. Note that Eq. (1.9) or Eq. (1.6) is the QSS rate for association of a full equilibrium concentration $\tilde{N}_A\tilde{N}_B$ of dissociated pairs into a perfectly absorbing sink $\mathscr{S}$ maintained at zero population, i.e., $\gamma_c = 1$ and $\gamma_s = 0$ in Eq. (1.5b). Similarly Eq. (1.10) is the QSS rate for dissociation which would result from an equilibrium population $\tilde{n}_s$ of associated $\mathscr{S}$ pairs being dissociated into states $\mathscr{C}$ maintained at zero population, i.e., $\gamma_c = 0$ and $\gamma_s = 1$ in Eq. (1.5b).

In this paper two simplifications to the above exact treatment at low gas densities N are investigated in detail. In the strong collision and bottleneck models, the probabilities P_i^S are preassigned without recourse to Eq. (1.8). The first model assumes that P_i^S for all bound pairs with internal separation R is unity for R within the range $0 \leqslant R \leqslant R_T$, where R_T is some preassigned radius, outside which P_i^S is zero. In this strong collision (or Thomson-style[7]) model, bound pairs with $R \leqslant R_T$ are therefore considered to be fully associated and those with $R \geqslant R_T$ cannot be stabilized. In the bottleneck model, P_i^S for bound pairs at all accessible R is unity for $E_i < E^*$, and is zero for $E > E^*$ and E^* is a (bound) energy level within $\sim 2kT$ below the dissociation limit and past which the one-way equilibrium rate is a minimum which therefore acts as a bottleneck to the current. The level E^* is, in effect, a transition state. Each model therefore subdivides the two dimensional (R,E) space into regions of some physical signficance. The Thomson model has previously been addressed via a Monte Carlo simulation method[8] and indirectly by an analytical approach[9] based on collisional deactivation of dissociated pairs to levels lower than various bound levels. A more exhaustive and detailed investigation is undertaken here. The bottleneck model has also received some previous consideration.[1,2]

Not only will these models elucidate interesting dynamics underlying the recombination mechanism (1.1) at low gas densities N, but subsequent modification to cover higher gas densities proves quite valuable towards a study (in progress) of the variation of the recombination rate α with gas density N.

II. THEORY

The detailed investigation of the strong-collision model requires the generalization of the Master equation (1.2) to $(\mathbf{R},E)$ space and use of the frequencies $\nu_{if}(R)$ for $E_i \rightarrow$ transitions per unit interval $d\mathbf{R}\, dE_f$ by collisions between and the pair AB *at fixed internal separation* R. The appropriate input–output Master equation satisfied by the distribution $n_i(\mathbf{R})$ of (A–B) pairs per unit interval $d\mathbf{R}\, dE_i$ has been shown[10] to be the continuity equation

$$\frac{d}{dt} n_i(\mathbf{R},t) = \frac{\partial n_i}{\partial t} + \frac{1}{R^2}\frac{\partial}{\partial R}\left[R^2 j_i^d(R)\right]_{E_i}$$

$$= -\int_{V(R)}^{\infty} \left[n_i(\mathbf{R})\nu_{if}(R) - n_f(\mathbf{R})\nu_{fi}(R)\right] dE_f$$

$$\equiv -\int_{V(R)}^{\infty} S_{if}(R)\, dE_f, \quad (2$$

where $j_i^d(R)$ is the net outward transport current of pairs expanding at R, where S_{if} is the net two level collision absorption rate, and where $V(R)$ is the energy of interaction between A and B. Integration of Eq. (2.1) over all accessible R yields the customary Master equation (1.2) for dissociated and bound states.

A. Rates and stabilization probabilities

The steady-state rate (1.4), with the aid of Eq. (2.1

$$R^A(t) = -\int_0^{\infty} \lim_{R_T \to \infty} \left[4\pi R_T^2 j_i^d(R_T)\right] dE_i$$

$$= \int_0^{\infty} dE_i \int_0^{\infty} d\mathbf{R} \int_{V(R)}^{0} S_{if}(R)\, dE_f \quad (

which either is the net inward flux of dissociated pairs extracting by transport across a sphere of infinite radius R is the net collisional downflow across the dissociation at $E_i = 0$.

Now assume (a) that there is a finite radius R for which all E_i pairs with $R \geqslant R_T$ are in energy equilibrium each R, i.e.,

$$\frac{n_i(\mathbf{R})}{n(\mathbf{R})} = \frac{\tilde{n}_i(\mathbf{R})}{\tilde{n}(\mathbf{R})}, \quad R \geqslant R_T, \quad (

where

$$n(\mathbf{R}) = \int_{V(R)}^{\infty} n_i(\mathbf{R}) dE \tag{2.3b}$$

is the concentration per unit interval $d\mathbf{R}$ of all pairs with separation R. Thus S_{if} in Eq. (2.2) vanishes for $R \geqslant R_T$ to yield

$$R^A(t) = \int_0^{\infty} dE_i \int_0^{R_T} d\mathbf{R} \int_{V(R)}^{0} S_{if}(R) dE_f \tag{2.4}$$

which is the steady-state rate of association of dissociated pairs with $R \leqslant R_T$.

Association of R_T complex: At low gas densities N, the distribution $n_i(\mathbf{R})$ is independent of N so that the collision term S_{if} remains linear in N. On the right-hand side of Eq. (2.1) $n_i(R)$ is equilibrium with respect to $\mathbf{R}$, so that

$$\frac{n_i(\mathbf{R},E_i)}{n_i(E_i)} = \frac{\tilde{n}_i(\mathbf{R},E_i)}{\tilde{n}_i(E_i)}, \tag{2.5a}$$

where the distribution per unit interval dE_i is

$$n_i(E_i) = \int_0^{R_i} n_i(\mathbf{R}) d\mathbf{R} \tag{2.5b}$$

and R_i is the classical turning point of E_i motion. The separation (1.5) is then valid so that Eq. (2.4) yields

$$\alpha \tilde{N}_A \tilde{N}_B = \int_0^{\infty} dE_i \int_0^{R_T} d\mathbf{R} \int_{V(R)}^{0} C_{if}(R) P_f^S dE_f = k_s \tilde{n}_s \tag{2.6}$$

for the rate of association of dissociated pairs in the complex of radius R_T. The required one-way equilibrium rate

$$C_{if}(R) = \tilde{n}_i(R) v_{if}(R) = C_{fi}(R) \tag{2.7}$$

at each R is related to the $\mathbf{R}$-averaged rate C_{if} previously used[1-3] in Eq. (1.6) by

$$C_{if} = \tilde{n}_i v_{if} = \int_0^{R_{if}} \tilde{n}_i(\mathbf{R}) v_{if}(R) d\mathbf{R} = \int_0^{R_{if}} C_{if}(R) d\mathbf{R}, \tag{2.8}$$

where R_{if} is the lesser of the two outermost turning points R_i and R_f associated with levels E_i and E_f, of which one at least is bound. Detailed expressions for $C_{if}(R)$ are presented in the Appendix.

Strong collision rate: In addition to Eq. (2.3a), assume (b) that all bound states f with $R \leqslant R_T$ are fully stabilized, i.e.,

$$P_f^S = 1, \quad R \leqslant R_T, \; E_f \leqslant 0 \tag{2.9}$$

so that the required strong collision rate is

$$\alpha(R_T) \tilde{N}_A \tilde{N}_B = \int_0^{\infty} dE_i \int_0^{R_T} d\mathbf{R} \int_{V(R)}^{0} C_{if}(R) dE_f \tag{2.10}$$

which is the one-way equilibrium rate that dissociated pairs with $R \leqslant R_T$ are collisionally deexcited across the dissociation limit. The "complex" assumption (2.3a) is equivalent either to assigning in Eq. (2.2) zero probability $P_f^S = 0$ for $R \geqslant R_T$ and $E_f \leqslant 0$, i.e., to the overall neglect of association or to inclusion in Eq. (2.4) of upward equilibrating transitions past $E_i = 0$ for $R \geqslant R_T$. The *strong-collision* assumption (2.9) is equivalent to the neglect in Eq. (2.4) of the rate $\int_V^0 n_f(R) v_{fi}(R) dE_f$ for upward redissociation of pairs with $R \leqslant R_T$.

The physical basis to the two assumptions (2.3) and (2.9) can be illustrated by Fig. 1. Bound states at large R arise from highly elliptical Coulomb orbits with low angular momenta where the possible velocity vectors for relative (A–B) motion lie within a narrowly focused region. Upon collision with the gas, the velocity vector is mainly deflected into directions outside this region so that the post-collision velocity vector cannot be consistent with bound states at large R. Collisional dissociation of these highly excited levels at large R is therefore most likely to occur,[8] and stabilization of bound levels f is not viable so that $P_f^S (R \geqslant R_T) = 0$ in keeping with assumption (2.3) underlying complex formation for association to proceed.

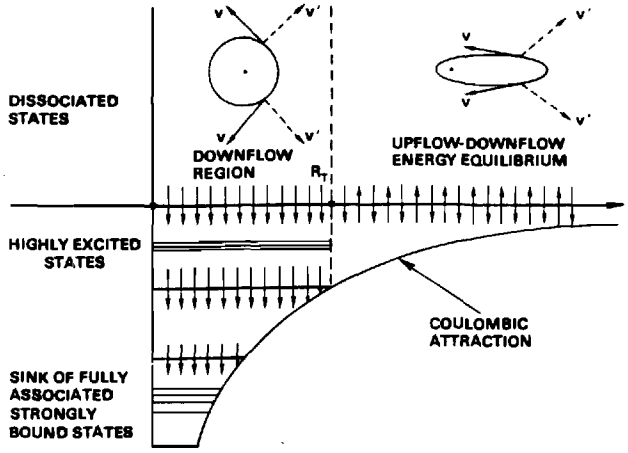

FIG. 1. Schematic basis for strong collisions within an assumed complex of radius R_T. A–B relative motion in circular and highly elliptical (large R) orbits with speeds v and v' before and after ion–neutral collision.

For intermediate R, however, the post-collision velocity can be accomodated by many angular-momentum bound orbits, more final angular momentum levels are accessible at these $R \simeq e^2/2|E_i|$, the radius of the circular orbit, and the number of accessible orbits at a given R increase with increasing binding. Collisional deexcitation of highly excited levels at smaller R therefore tends to occur and pairs with $R \leqslant R_T$ in all bound levels can be fully stabilized, in keeping with the strong-collision assumption (2.9).

The averaged kernels (2.8) have been previously derived for symmetrical resonance charge transfer,[1] hard-sphere,[2] and polarization[3] binary collisions between either ion A or B and the gas M. The R-dependent one-way equilibrium kernels $C_{if}(R)$ are not only required for this sudy but also for ongoing investigations of the nonlinear variation of α with gas density N. They are provided in the Appendix as a comprehensive package for present and future use and reference.

The exact low density rate (1.6) and the strong-collision rate (2.10) reduce to a sum[9,11] of rates α_A and α_B, each arising from A–M and B–M binary collisions, respectively, and α_A can be presented[1-3,5,9] as a universal function [cf. Eq. (A55)] of the mass parameter

$$a = \frac{M_B M_g}{M_A (M_A + M_B + M_g)}, \tag{2.11}$$

where M_A, M_B, and M_g are the masses of the reacting atomic ions and gas atoms, respectively.

Calculation of Eq. (1.6), the exact low density rate α_E,

and of the variation of the strong collision rate (2.10) with R_T can now be performed. For the exact rate (1.6), highly accurate converged solutions P_i^S of the integral equation (1.6), discretized as in Ref. 3 into an equivalent set of 100 algebraic equations, have been obtained. Previous results[1-3] were based on 36 coupled equations at most. Convergence of α_E to within 0.5% is found to be much more rapid for intermediate mass parameters a ($\sim 1/3$) than for small and large a which required 100 coupled equations for convergent rates.[5]

In contrast to ion–atom association where the radius R_T may, with some justification, be identified with the location of the centrifugal barrier, no such assignment for ion–ion recombination (without any centrifugal barrier) exists, although Thomson[7] suggested $R_T = 2e^2/3kT$ where the relative kinetic energy ($\frac{3}{2}kT + e^2/R$) is reduced to $\frac{3}{2}kT$ upon collision. Hence bound pairs with $E_f = e^2(1/R_T - 1/R) < 0$ can be formed within $R < R_T$.

The variation with R_T of the ratio $\alpha(R_T)/\alpha_E$ for the recombination of *equal-mass* ions via symmetrical resonance charge-transfer (CX), polarization (POL), and hard-sphere (HS) collisions with an *equal-mass* gas ($a = 1/3$) is displayed in Fig. 2. The ratio is unity for R_T in the range (0.48–0.55) (e^2/kT), in good agreement with Thomson's suggestion. The neglect in Eq. (2.6) of a positive contribution to association from possible collisional stabilization of those bound levels with $R > R_T \simeq 0.5$ (e^2/kT) is effectively offset by the neglect in Eq. (2.10) via Eq. (2.9) of a negative contribution arising from redissociation of those bound states with $R < R_T$.

The strong collision model is therefore capable of high accuracy *provided* R_T can be preassigned; realistic assignment to R_T for recombination being only feasible[9] after the exact treatment is performed! The radius R_T, once assigned, may however be adopted in models under development for variation of α with gas density N.

As R_T becomes large the rate (2.10) however tends rapidly to

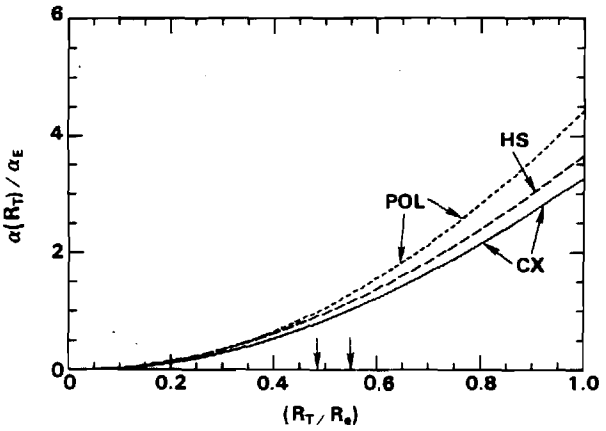

FIG. 2. R_T variation of $\alpha(R_T)$, the strong-collision rate (2.10) normalized to α_E, the exact rate (1.6), for equal-mass components and model ion–neutral interactions (POL: polarization; HS: hard sphere; CX: symmetrical resonance charge transfer). Arrows indicate where $\alpha(R_T) = \alpha_E$ for POL and CX in units of $R = e^2/kT$.

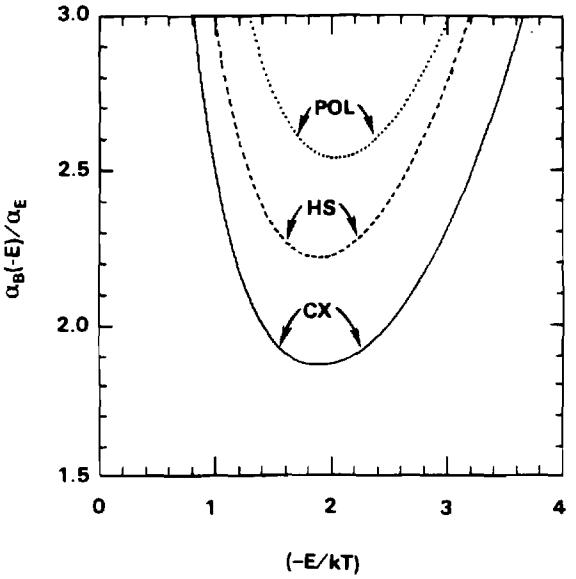

FIG. 3. One-way equilibrium rates $\alpha_{BN}(-E)$, Eq. (2.13), normalized α_E, the exact rate (1.6), across energy level $-E$ for model ion–neutr interactions POL, HS, and CX.

$$\alpha(R_T \to \infty)\tilde{N}_A\tilde{N}_B = \int_0^\infty dE_i \int_{-D}^0 C_{if}\, dE_f \qquad (2.1$$

which is of course infinite owing to the divergence, as $E_i \to$ of the equilibrium density $\tilde{n}_i(E_i) \sim |E_i|^{-5/2}\exp(-E_i/k$ of Coulomb bound states per unit interval dE_i. As $R_T \to$ the physical basis for adopting the one-way equilibrium ra (2.10) becomes untenable since bound states with large R are more readily redissociated (cf. Fig. 1). Upward co sions past the dissociation limit must therefore be includ for large R_T. The strong collision assumption is therefore longer justified for large R_T.

This divergence can be eliminated not only by mainta ing R_T finite but also by considering the one-way equilib um rate

$$\alpha_{BN}(-E)\tilde{N}_A\tilde{N}_B = \int_{-E}^\infty dE_i \int_{-D}^{-E} C_{if}\, dE_f \qquad (2.1$$

across any bound level $-E$ in block $\mathscr{E}$. Figure 3 illustra that this rate decreases from the infinite limit (2.12) $E = 0$ to a pronounced minimum at an energy $E^* = 2$ below the dissociation limit. Since Eq. (2.13) is an up limit to the exact rate by taking $P_i^S(E_i > -E)$ $P_f^S(E_f < -E)$ within Eq. (1.6) to be zero and unity, resp tively, then its minimum value $\alpha_{BN}(-E^*)$ is the least per limit and is the one-way rate past the effective bottlen to the curent at $-E^*$ which, in effect, is a transition st Although this bottleneck model (2.13) is physically dif ent from the previous strong collision model (2.10), worth noting that $E^* = 2kT$ corresponds to a turning p R_T of $\frac{1}{2}(e^2/kT)$ for which the strong collision model is ef tively exact (cf. Fig. 2). Figure 3 shows that the bottlen result is however a factor of 1.9–2.5 times larger than exact rate α_E. In contrast to the strong-collision m (2.10), Eq. (2.13) is always an upper limit since in orde obtain the bottleneck result (2.13) from Eq. (1.6), the

glected terms cannot cancel since they always remain negative. This search for the least upper limit to the one-way equilibrium rate across transition state E^* is identical in principle to the variational phase-space theory of Keck[13] as applied to termolecular ion–ion recombination. The strong collision (Fig. 2) and bottleneck pictures (Fig. 3) have been previously displayed in a recent review[12]; the present CX results in Fig. 2 correct those in Ref. 12.

B. Association probabilities

To obtain these, the low density rate (2.6) for association of dissociated pairs in the R_T complex may also be expressed with the aid of Eq. (2.2) as

$$\alpha(R_T)\tilde{N}_A\tilde{N}_B = \int_0^\infty [4\pi R_T^2 \bar{j}_i^-(R_T)]P_i^A(R_T)dE_i, \tag{2.14}$$

the net inward transport rate across the R_T sphere where

$$P_i^A(R_T) = [\bar{n}_i^-(R_T) - n_i^+(R_T)]/\bar{n}_i^-(R_T) \tag{2.15}$$

now specifies the desired probability that fully dissociated E_i pairs which are originally contracting at R_T will associate within the spherical complex of radius R_T. The distribution of dissociated pairs contracting at R_T is $\bar{n}_i^-(\mathbf{R}_T)$, the equilibrium value characteristic of low gas densities N, and is a nonequilibrium value $n_i^+(\mathbf{R}_T)$ for pairs expanding at R_T. The one-way incident current at temperature T and pertinent to low N is the one-way equilibrium current

$$\tilde{j}_i^-(R)dE_i = \tfrac{1}{2}\bar{n}_i^-(\mathbf{R})v_i(R)dE_i = \tfrac{1}{4}\bar{n}_i(R)v_i(R)dE_i \tag{2.16}$$

$$= \frac{1}{4}\left(\frac{8kT}{\pi M_{AB}}\right)^{1/2}\tilde{N}_A\tilde{N}_B[1 - V(R)/E_i]$$

$$\times (E_i/kT)\exp(-E_i/kT)d(E_i/kT), \tag{2.17}$$

where M_{AB} is the reduced mass of the pair (A–B) and where $\bar{n}_i$ is $\bar{n}_i^+ + \bar{n}_i^-$. By direct comparison of Eqs. (2.14) and (2.16) the exact association probability of fully dissociated pairs within $R \lesssim R_T$ at low gas densities is

$$P_i^{AE}(E_i \gtrsim 0, R_T) = [\pi R_T^2 \bar{n}_i(R_T)v_i(R_T)]^{-1}$$

$$\times \int_0^{R_T} d\mathbf{R}\int_{V(R)}^0 C_{if}(R)P_f^S(R)dE_f \tag{2.18}$$

which increases linearly with gas density N via C_{if}. The stabilization probabilities P_f^S which are solutions of Eq. (1.8) do not vary with N. As $R_T \to \infty$, Eq. (2.18) in Eq. (2.14) yields

$$\alpha_i(E_i \gtrsim 0, R_T) = \pi R_T^2 \bar{n}_i(R_T)v_i(R_T)P_i^{AE}(E_i \gtrsim 0, R_T), \tag{2.19}$$

the rate per unit interval dE_i for association of dissociated E_i pairs with $R \lesssim R_T$. As $R_T \to \infty$, Eq. (2.19) saturates to the exact partial rate.

The association rate per unit dE_i for the highly excited bound E_i pairs in block $\mathscr{E}$ of the complex of radius R_T is

$$\alpha_i(E_i < 0, R_T) = [\pi R_T^2 \bar{n}_i(R_T)v_i(R_T)]P_i^A(E_i < 0, R_T)$$

$$= \int_0^{R_T} d\mathbf{R}\left[\int_{V(R)}^0 C_{if}(R)P_f^S dE_f\right.$$

$$\left. - P_i^S\int_{V(R)}^\infty C_{if}(R)dE_f\right]. \tag{2.20}$$

As $R_T \to R_i$, the outermost turning point of E_i motion where $|E_i| = |V(R_i)|$, this rate (2.20) vanishes owing to the QSS requirement (1.8) of zero net gain of all E_i pairs with $R \lesssim R_i$ in block $\mathscr{E}$, a condition on which calculation of the stabilization probabilities P_i^S is based.

Strong collision and Thomson probabilities: The corresponding strong-collision association probability P_i^{ST} is given by Eq. (2.18) with $P_f^S = 1$, i.e., by the probability

$$P_i^{ST}(E_i \gtrsim 0, R_T) = [\pi R_T^2 \bar{n}_i(R_T)v_i(R_T)]^{-1}$$

$$\times \int_0^{R_T} d\mathbf{R}\int_{V(R)}^0 C_{if}(R)dE_f \tag{2.21}$$

for direct collisional formation of bound levels from a dissociated state of energy E_i. It overestimates the exact association probability by

$$P_i^{RD} \equiv P_i^{ST}(R_T) - P_i^{AE}(R_T)$$

$$= [\pi R_T^2 \bar{n}_i(R_T)v_i(R_T)]^{-1}$$

$$\times \int_0^{R_T} d\mathbf{R}\int_{V(R)}^0 C_{if}(R)P_f^D dE_f \tag{2.22}$$

which in fact is the probability P_i^{RD} for subsequent redissociation of bound pairs formed with $R \lesssim R_T$ and which is inherently neglected by the strong-collision model. On defining the free path length[4] $\lambda_i(R)$ for continuum–bound transitions in A–M collisions during the (A–B) trajectory by

$$\lambda_i^{-1}(R) \equiv [\nu_i(R)/v_i]$$

$$= \left[\int_{V(R)}^0 C_{if}(R)dE_f\right]/[\bar{n}_i(R)v_i(R)] \tag{2.23}$$

then the strong-collision probability (2.21) is redefined as in

$$\pi R_T^2[1 - V(R_T)/E_i]P_i^{ST}(R_T)$$

$$= \int_0^{R_T}[1 - V(R)/E_i]d\mathbf{R}/\lambda_i(R). \tag{2.24}$$

The corresponding strong collision rate (2.14) is now

$$\alpha_T(R_T) = \int_0^\infty G(E_i)dE_i$$

$$\times \int_0^{R_T} v_i[1 - V(R)/E_i)]^{1/2}d\mathbf{R}/\lambda_i(R), \tag{2.25}$$

where the (Boltzmann) distribution of internal energies $(E_i \gtrsim 0)$ is

$$G(E_i)dE_i = \frac{2}{\sqrt{\pi}}(E_i/kT)^{1/2}\exp(-E_i/kT)d(E_i/kT). \tag{2.26}$$

When λ_i is assumed to be λ, independent of R and E_i, as for hard-sphere collisions, and when $V(R)$ is neglected, Eq. (2.24) yields

$$P_T^A(R_T) = \tfrac{4}{3}R_T/\lambda \tag{2.27}$$

the Thomson probability[7] for (A–M) collisions during recti-

linear A–B relative motion within $R \leqslant R_T$. Also Eq. (2.25) yields

$$\alpha_T(R_T) = \tfrac{4}{3}\pi R_T^3(\bar{v}/\lambda) \tag{2.28}$$

the Thomson rate[7] in terms of $\bar{v}$, the mean (A–B) relative speed $(8kT/\pi M_{AB}^*)^{1/2}$. All of the rates calculated here and previously[1-3] are however normalized (cf. Appendix) to

$$\tilde{\alpha}_T = \frac{4}{3}\frac{\pi}{\lambda}\left(\frac{2}{3}\frac{e^2}{kT}\right)^3\left(\frac{3kT}{M_{AB}}\right)^{1/2}, \tag{2.29}$$

where the root-mean-square speed rather than $\bar{v}$ has been customarily used, and where $\frac{1}{3}(e^2/kT)$ is assigned for R_T. Unless otherwise noted, all of the following calculations in the following sections (II C–II E) refer to symmetrical resonance charge-transfer ion–neutral collisions involving equal-mass species $M_A = M_B$ in an equal mass gas.

C. Calculated stabilization and disruption probabilities, and partial rates

The stabilization and disruption probabilities P_f^S and $P_f^D = 1 - P_f^S$ are the stochastic probabilities that (A–B) pairs initially in a bound level E_f of block $\mathscr{E}$, will either become fully associated or disrupted by multicollisions with the thermal gas. For a quasi-steady-state distribution of bound pairs in block $\mathscr{E}$, P_f^S are numerical solutions of the integral equation (1.8) and are illustrated in Fig. 4. The probabilities P_f^S increase from zero at the dissociation limit to near unity for binding energy $|E_f| > 5kT$. Note that $P_f^S \approx 1/2 \approx P_f^D$ for $E_f \sim -2kT$, the bottleneck energy E^* (cf. Fig. 3) based on the assumption in Eq. (2.13) that P_f^S is zero for $E > E^*$ and unity for $E_i < -E^*$. The probabilities $P_f^D = (1 - P_f^S)$ for multistep collisional disruption of these pairs decrease fairly rapidly with binding energy $|E|$ and are negligible for binding $|E| > 5\,kT$. Since block $\mathscr{S}$ of fully stabilized levels is characterized by unit P_f^S, Fig. 4 suggests that the block $\mathscr{S}$ is composed of all levels with binding $\gtrsim 10kT$. Since the deexcitation frequency ν_{if} from the continuum directly to the strongly bound levels with $E_f \lesssim -10kT$ of block $\mathscr{S}$ is vanishingly small, association given by Eq. (1.9) therefore occurs primarily via multistep transitions to the block $\mathscr{E}$ of levels E_f within the range $0 > E_f > -10kT$, which are then connected stochastically with probability P_f^S to the fully associated block $\mathscr{S}$ via a Markov-element chain.[6]

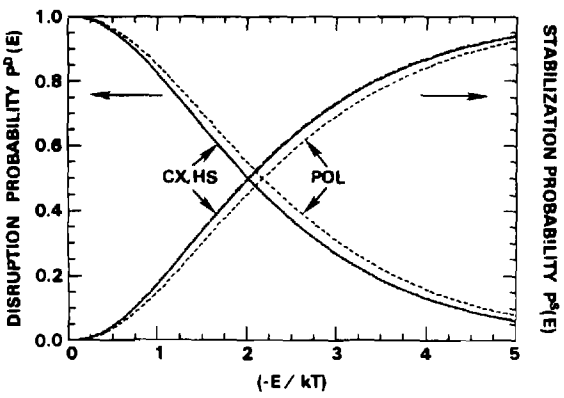

FIG. 4. Stabilization and disruption probabilities, solutions of Eq. (1.8) for equal mass components.

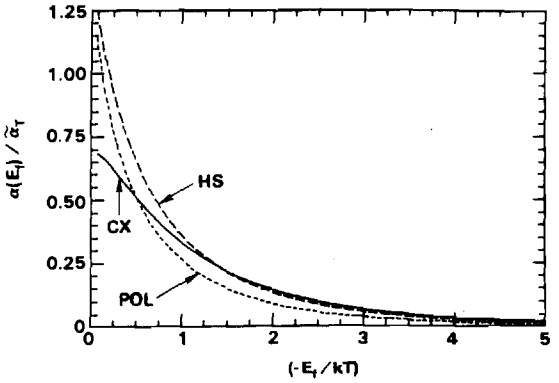

FIG. 5. Partial rates (2.30a) per final bound level $-E_f$ normalized to $\tilde{\alpha}_T$ the Thomson rate (2.29).

Figure 5 for the partial rate

$$\alpha(E_f)\tilde{N}_A\tilde{N}_B = \left(\int_0^\infty C_{if}\,dE_i\right)P_f^S(E_f) \equiv C_f P_f^S \quad (2.30a$$

normalized to $\tilde{\alpha}_T$, which is the contribution per unit norma ized interval (dE_f/kT) from level E_f to the full associati rate of all dissociated pairs, illustrates that levels in gene within kT of the dissociation limit, are mainly responsib for the association process. This is less so however for C since deactivation by symmetrical resonance charge trans involves larger energy reductions[1-3] than for the case of p larization and hard-sphere collisions. The very rapid crease of $\alpha(E_f)$ from zero at $E_f = 0$, not shown in Fig. and subsequent decrease arises from the combination of t monotonic increase from zero of the stabilization probab ties P_f^S and the rapid decrease from infinity of C_f, the co sional rate from the continuum to a bound level f.

Figure 6 for the E_i-partial contribution

$$\alpha(E_i)\tilde{N}_A\tilde{N}_B = \int_{-D}^{0} C_{if}P_f^S\,dE_f \quad (2.30$$

to the exact rate for association of dissociated E_i pairs unit interval (dE_i/kT) illustrates a monotonic increase $E_i > 0$ approaches the dissociated limit at zero energy. T

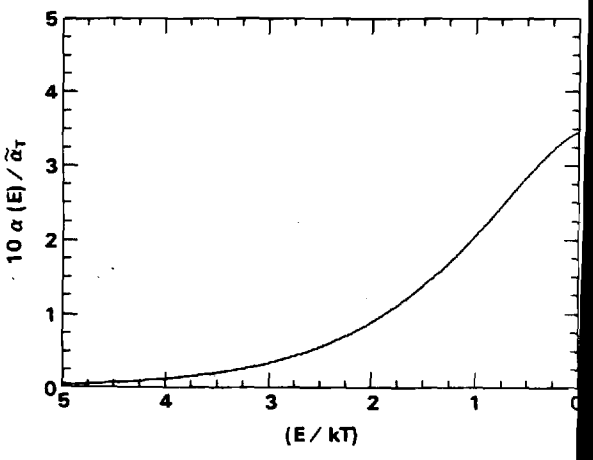

FIG. 6. Partial rate (2.30b) per initial continuum state E_i, normali $\tilde{\alpha}_T$, the Thomson rate (2.29).

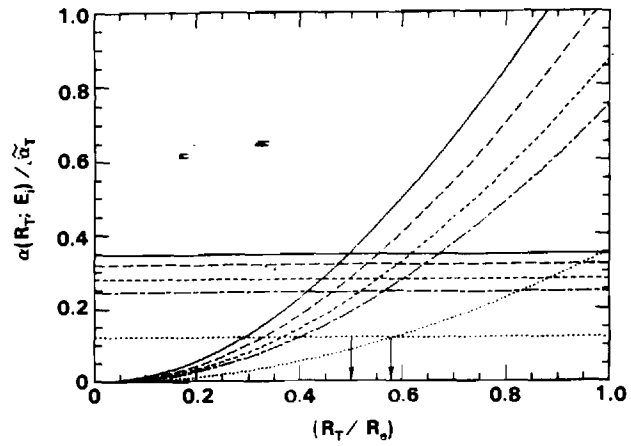

FIG. 7. Partial strong continuum rate $\alpha(R_T;E_i)$, Eq. (2.31), per initial continuum state E_i, normalized to $\tilde{\alpha}_T$, the Thomson rate (2.29). Exact normalized partial rates are indicated by straight lines. $E_i/kT = 0,0.26$, 0.529, 0.734, and 1.646 ordered sequentially from top to bottom.

is expected since C_{if} for a given bound level E_f increases quite rapidly as the energy difference $(E_i - E_f)$ is reduced. The full rate (1.9) is the E_i-integrated area of Fig. 6.

Variations of the partial E_i contributions

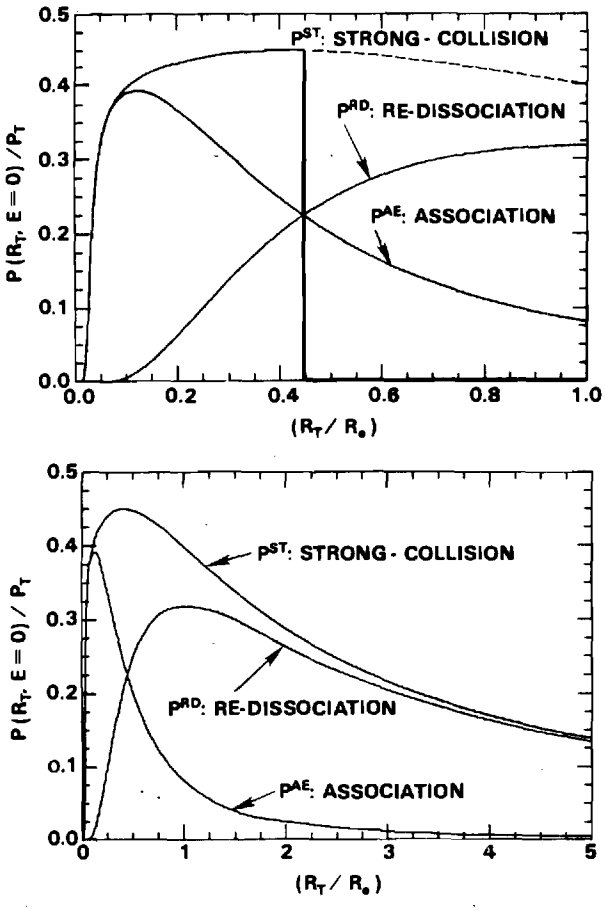

FIG. 8. (a),(b) Probabilities P^{ST}, P^{AE}, and P^{RD} for strong collisions (2.21), association (2.18), and redissociation (2.22) of (A–B) pairs with energy $E = 0$. Probabilities are normalized to the Thomson probability P_T, Eq. (2.27) and are presented as a function of R_T (normalized to $R_e = e^2/kT$).

$$\alpha(R_T;E_i)\tilde{N}_A\tilde{N}_B = \int_0^{R_T} d\mathbf{R} \int_{V(R)}^{0} C_{if}(R)dE_f \quad (2.31)$$

to the strong-collision rate (2.10) with R_T are displayed in Fig. 7. They intersect the corresponding exact partial rates (2.31a), represented as straight lines at R_T, in the range $0.5R_e < R_T < 0.6R$, a result consistent with the E_i-integrated rates of Fig. 2 where $R_T \sim 0.55R_e$.

D. R variation of calculated probabilities for multistep association

Figure 8 illustrates variation with R_T of P_i^{AE}, the exact probability (2.18) for multistep association via bound levels of $E_i = 0$ pairs with $R < R_T$, and of P_i^{ST}, the corresponding strong-collision probability (2.21). The probabilities are normalized to P_T, the Thomson probability (2.27). Also shown [Fig. 8(a)] is P_i^{RD}/P_T, the normalized probability (2.22) for redissociation of the bound pairs so formed with $R < R_T$. Figure 8(a) emphasizes that association dominates redissociation within smaller $R_T \ll (e^2/kt) \equiv R_e$ so that the exact and strong probabilities P_i^{AE} and P_i^{ST}, respectively, are equal. Figure 8(b) emphasizes that pairs within larger $R_T \gg R_e$ are mainly redissociated. The strong-collision probability P_i^{ST} accurately represents either P_i^{AE}, the association probability at small R_T, or P_i^{RD}, the redissociation probability at larger R_T, thereby providing the actual physical basis for Fig. 1.

Within radius $R_T \sim 0.45R_e$, there is as much association as redissociation [Fig. 8(a)] so that the strong rate is twice the exact rate for association of pairs with $R < 0.45R_e$. The contribution of pairs with $R > 0.45R_e$ to the exact rate is however equal to the contribution from $R < 0.45R_e$, so that the exact rate form all R and the strong rate from $R < 0.45R_e$ are fortuitously equal. This balance is the essential basis for agreement with the strong-collision model as previously illustrated by Figs. 2 and 7. Figure 8(a) also suggests that the R_T variation of the strong collision probability (2.21) is represented fairly well by P_T^A, the Thomson result (2.27), over the region $R < R_e$ important to association, although the magnitude is overestimated by a factor of $\lesssim 2.5$.

As the energy E_i of the dissociated pairs increases from

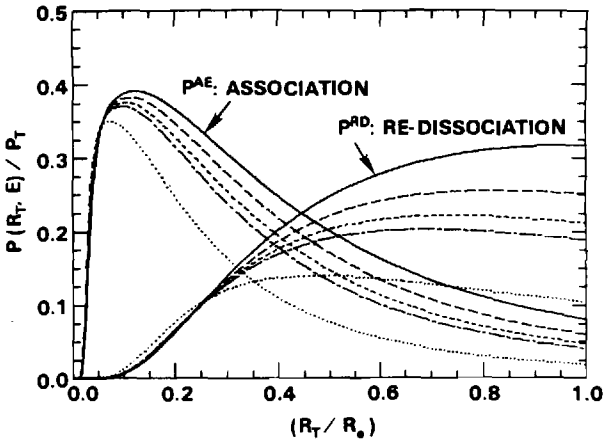

FIG. 9. As in Fig. 8 but for various continuum energies ($E/kT = 0$, 0.529, 1.09, 1.56, and 4.7 ordered sequentially from top to bottom).

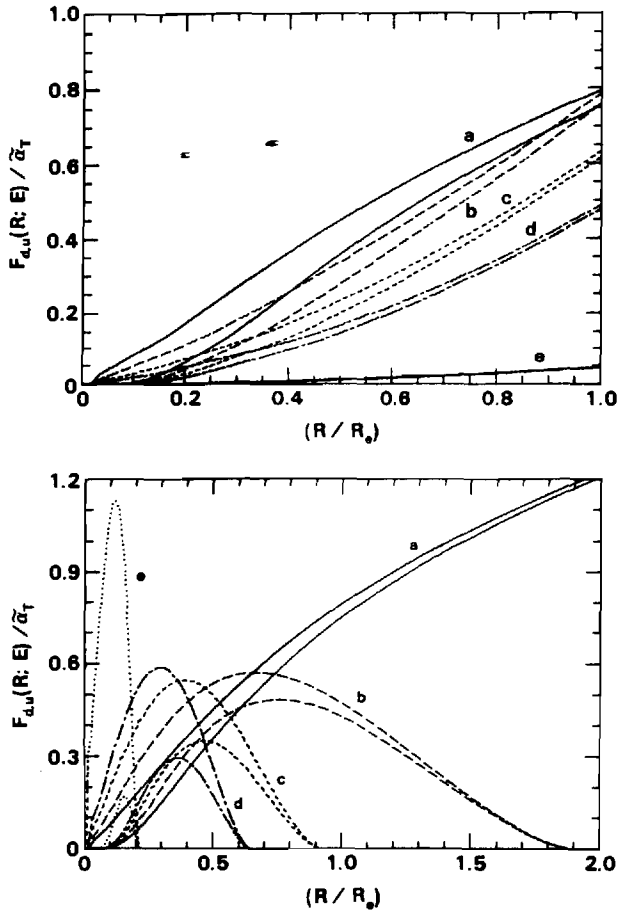

FIG. 10. R dependence of downward F_d and upward F_u normalized flux, Eqs. (2.32) and (2.33), upper and lower curves of each set, across various continuum energies [$E/kT = 0$, 0.529, 1.09, 1.56, and 4.7, (a)–(e), respectively] and across various bound energies [$-E/kT = 0$, 0.529, 1.09, 1.56, and 4.7, (a)–(e), respectively] in (b).

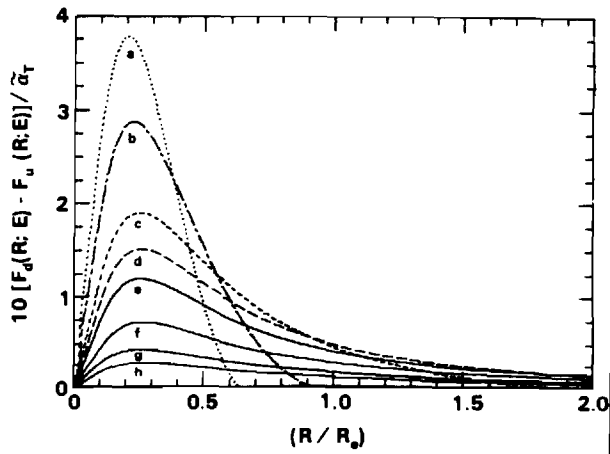

FIG. 11. R dependence of the net flux ($F_d - F_u$) downward across vario continuum [$E/kT = 0$, 0.529, 1.09, 1.56; (e)–(h), respectively] and bou [$-E/kT = 0.26$, 0.529, 1.09, 1.56; (d)–(a), respectively] energy leve

zero, Fig. 9 shows that the probabilities for association of these pairs and for subsequent redissociation decreases monotonically with E_i and that the R_T region over which association exceeds redissociation becomes somewhat smaller. As before, the strong collision probability P_i^{ST}, the sum ($P_i^{AE} + P_i^{RD}$) of each pair of curves, tends to P_i^{AE} at small R_T, to P_i^{RD} at large R_T. The sum is fairly constant for the range $0.2R_e \leqslant R_T \leqslant R_e$, as in Fig. 8(a).

E. (R,E) variation of calculated flux and rates

In Figs. 10(a) and 10(b) are shown the variation with R of the downward differential flux ($dF = FdR$),

$$F_d(R;E) = 4\pi R^2 \int_E^\infty (1 - P_i^S) dE_i \int_{V(R)}^E C_{if}(R) dE_f \tag{2.32}$$

per unit interval dR across various continuum [Fig. 10(a)] and bound [Fig. 10(b)] energy levels E, and of the corresponding upward flux

$$F_u(R;E) = 4\pi R^2 \int_E^\infty dE_i \int_{V(R)}^E (1 - P_f^S) C_{fi}(R) dE_f \tag{2.33}$$

with both normalized to the Thomson rate (2.29). For sma $R \leqslant 0.3R_e$, F_d increases more rapidly from zero and remai greater for all R than F_u which eventually tends at large R F_d from below. This limiting behavior at small and large also elucidate the physical basis for the separate R regions Fig. 1. For bound levels [Fig. 10(b)], both F_d and F_u acro state (R,E) increase from zero to a maximum and then d crease as expected to zero at the turning points associat with energy E.

Variation with R in Fig. 11 of $F(R)$, the *net* different flux ($F_d - F_u$) across both bound and continuum ener levels E exhibits a peak at roughly the same $R \sim (0.2\text{–}0.3)$ for all E. As E decreases through the continuum the fl and R-integrated flux, $\int_0^\infty F(R)dR$, increases. For bound the net flux increases and then decreases to zero at the clas cal turning points $R_i = e^2/|E|$. The net R-integrated f across the highly excited bound levels remains constant, i the area under each of the bound curves remains constant accord with the QSS condition [$dn_i(t)/dt = 0$] in block so that the flux becomes constricted into more restricted space as E decreases through the bound levels. The result increase exhibited in Fig. 11 of the net differential flux a decreases is therefore expected. The E variation of the n malized R-integrated net flux

$$F(E) = \begin{cases} \int_0^\infty [F_d(R;E) - F_u(R;E)]\,dR, & E \geqslant 0 \\ \int_0^{R_t} [F_d(R;E) - F_u(R;E)]\,dR, & E \leqslant 0 \end{cases} \tag{2.}$$

is illustrated in Fig. 12. That $F(E \leqslant 0)$ is constant sim reflects the QSS condition or constant flux through the hi ly excited block $\mathscr{B}$.

Figure 13 illustrates the variation with R_T of α_i exact partial rates (2.19) and (2.20) for the associatio dissociated pairs ($E_i \geqslant 0$) and of highly excited bound p ($E_i < 0$), respectively, within the sphere of radius R_T. former rate increases with R_T and saturates fairly rapidl large R_T to the exact rate for association which, in orde

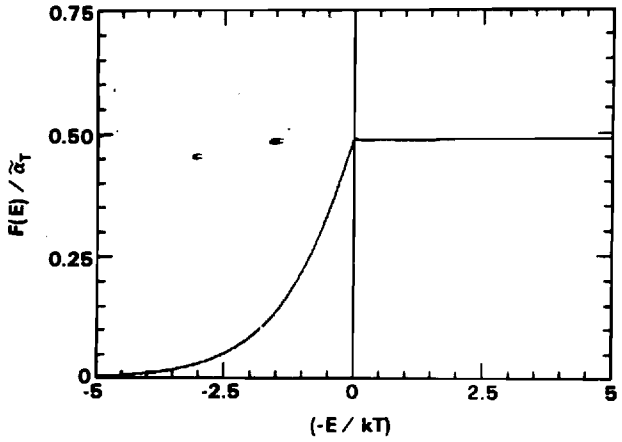

FIG. 12. Energy dependence of exact current, Eq. (2.34), normalized to $\tilde{\alpha}_T$, for the association of equal mass species under charge–transfer ion–neutral collisions. Exact rate is the constant current across bound levels.

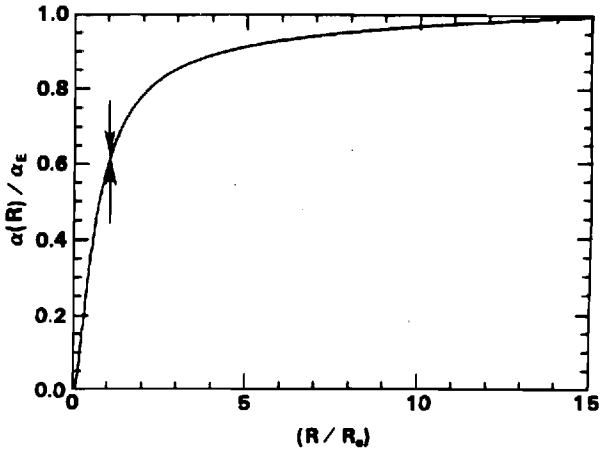

FIG. 14. Rate that fully dissociated pairs (with a Maxwellian energy distribution) recombine within a sphere of radius R. The exact rate is α_E.

maintain a steady-state $\mathscr{C}$ block, is the rate of generation of net inward E_l pairs with infinite separation.

The rates that bound E_i pairs are lost also increase with R_T due to continual downwards output, but reach a maximum when the upward input from other levels becomes competitive, and then decrease as a result to zero at the classical point R_i of classical motion. There is a net loss of bound E_l pairs with small R and a net gain of pairs with larger $R<R_i$ so that the R-integrated distribution (2.5b) remains constant in time. The zero rate at the apocenter R_l in Fig. 13 reflects the QSS condition (1.8) in Eq. (2.20) for no net loss or gain of R-integrated bound E_i pairs in block $\mathscr{E}$.

The rate $\alpha(R)$ of volume recombination within a sphere of radius R, the rates of Fig. 13 integrated over $E>0$ is given in Fig. 14 as a function of R. It is worth noting that 60% of the exact rate $\alpha_E = \alpha(R\to\infty)$ is achieved within the sphere of the natural (Onsager) radius $R_e = e^2/kT$ as designated by the arrows.

III. MASS EFFECT IN STRONG-COLLISION MODEL

Figures 2 and 7 illustrate the ratio of the strong collision result (2.10) to the exact result α_E for equal mass species recombining in an equal mass gas, i.e., a, the mass parameter (2.11), is (1/3). In Fig. 15 is displayed variation of the same ratio over the full range of a. Small $a\approx 10^{-3}$ implies heavy particle recombination in a vanishingly light gas, while electron–ion recombination in a normal gas is characterized by large $a\approx 10^3$. It is noted that the radius R_T^*, where $\alpha(R_T) = \alpha_E$ increases from $\sim 0.1R_e$ to $\sim 0.5R_e$ as the parameter a increases to unity, and then decreases back again as the parameter a further increases. For greatly mismatched species, i.e., in the limits of small and large a the energy-change collision dynamics is weak, and vanishingly small energy changes are involved particularly for deactivating transitions across the dissociation limit at $E_l = 0$. The stabilization probability P_f^S in Eq. (2.6) and Fig. 4 is therefore of prime significance. To invoke the strong-collision assumption (2.9) for these bound levels close to the dissociation limit and important at small and large a is therefore without validity. Although some physical significance can be attached to R_T^*, where $\alpha(R_T)$ and α_E are equal, for intermediate $a\sim 1$, as previously discussed in Sec. II, no such significance exists in the limits of small and large a. The essential reason why $R_T^*\sim 0.1R_e$ becomes unacceptably small at

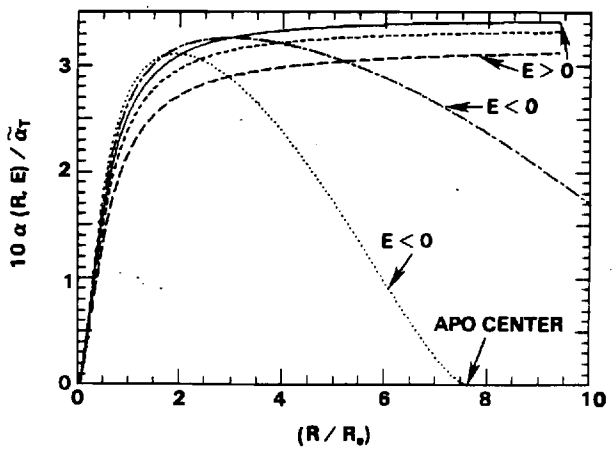

FIG. 13. Normalized rate equations (2.19) and (2.20) that pairs in continuum and bound energy levels E recombine within a sphere of radius R.

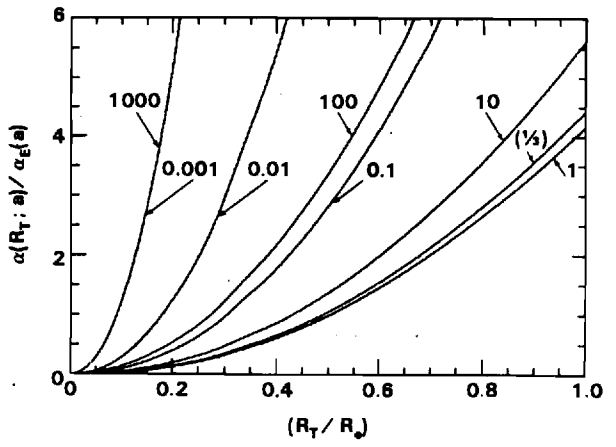

FIG. 15. Mass effect in strong-collision model: R_T variation of the strong-collision rate (2.31) normalized to the exact rate α_E, Eq. (1.6), for recombination of systems with various mass parameters a, Eq. (2.11).

these limits is that small R_f^* effectively (numerically) offsets the large addition to the inner integral of Eq. (2.10) entailed by the strong collision assumption ($P_f^S = 1$) in Eq. (2.6). The smaller exact values of P_f^S (cf. Fig. 4) are more appropriate to the important levels in the vicinity of the dissociation limit for large and small a.

IV. RECOMMENDED LOW-DENSITY TERMOLECULAR RATES

Due to the long-range Coulombic attraction and to the use of shorter-range ion–neutral interactions [charge–transfer (CX), polarization (POL), and hard sphere (HS)], rates for the termolecular ion–ion recombination,

$$A^+ + B^- + M \rightarrow AB + M \qquad (4.1)$$

between general atomic species in a general atomic gas may be characterized[9] by a universal function of the mass parameter (2.11) and of the gas temperature T [cf. Eqs. (A40)–(A55)]. This universality does not extend to ion–atom association which, due to the closer interactions involves, demands individual calculations for specific systems. As previously mentioned, rates (1.6) or (1.9) or (1.10) have been obtained numerically from Eq. (A55) via the highly accurate numerical solutions P_f^S to the integral equation (1.8) for the stabilization probabilities. Converged probabilities for small and large mass parameters a in particular were o tained only when the integral equation (1.8b) was disc tized into 100 algebraic equations via the efficient proced of Ref. 3. Previous results[1–3] adopted 36 equations at mo

Recommended values of the ratio[1–3]

$$\mathcal{R}(a) = (M_A/M_{AB})\,[\alpha_E^{(A)}(a,T)/\tilde{\alpha}_T(T)], \qquad (4$$

where $\alpha_E^{(i)}$ is the exact numerical rate (A55a) originat from $(i - M)$ collisions alone, are presented at clos spaced a in Table I. The exact low density rate can be rep sented to a high degree of accuracy by[9]

$$\alpha = \alpha_E^{(A)} + \alpha_E^{(B)}. \qquad (4$$

Although the partial rates $\alpha_E^{(i)}$ are tabulated here to f significant figures, the recombination rule (4.3) as previ ly tested was then shown to be accurate to three figure best or two figures at worst. The test however relies on accuracy of the solutions to the integral equations (1 with C_{if} taken as $C_{if}^{(A)}, C_{if}^{(B)}$ and $[C_{if}^{(A)} + C_{if}^{(B)}]$ w $C_{if}^{(A),(B)}$ is the one-way equlibrium rate which results f individual A–M and B–M collisions, respectively. Sinc present converged probabilities P_l^S have been determine a numerical procedure[3] more accurate and efficient that[9] previously used for the test, the accuracy of rule (is being updated.

TABLE I. Normalized partial rates 10 $(M_A/M_{AB})(\alpha_E^{\wedge}/\tilde{\alpha}_T)$ for termolecular recombination $A^+ + B^- + M \rightarrow AB + M$ as a function of mass parameter $a = M_A M_B/M_A (M_A + M_B + M_g)$ for various interactions (CX: symmetrical resonance charge transfer; HS: hard sphere; POL: polarization attraction) in collision between A and gas atoms of mass M_g.

a	CX[a]	HS[b]	POL[b]	a	HS[b]	POL[b]
0.0010	1.291	1.278	1.029	1.5000	9.452	6.751
0.0020	1.816	1.818	1.472	2.0000	8.593	6.044
0.0030	2.208	2.221	1.800	2.5000	7.877	5.472
0.0040	2.530	2.554	2.071	3.0000	7.276	5.003
0.0050	2.807	2.841	2.304	3.5000	6.766	4.611
0.0060	3.053	3.098	2.512	4.0000	6.328	4.280
0.0070	3.274	3.329	2.699	4.5000	5.947	3.994
0.0080	3.476	3.542	2.870	5.0000	5.613	3.746
0.0090	3.662	3.739	3.029	5.5000	5.317	3.529
0.0100	3.835	3.923	3.177	6.0000	5.053	3.336
0.0200	5.115	5.313	4.288	6.5000	4.815	3.164
0.0300	5.959	6.264	5.039	7.0000	4.601	3.010
0.0400	6.581	6.986	5.603	7.5000	4.406	2.871
0.0500	7.066	7.565	6.049	8.0000	4.228	2.744
0.0600	7.456	8.042	6.414	8.5000	4.065	2.629
0.0700	7.778	8.444	6.719	9.0000	3.914	2.523
0.0800	8.047	8.789	6.976	9.5000	3.775	2.426
0.0900	8.276	9.086	7.197	10.0000	3.646	2.336
0.1000	8.471	9.347	7.387	12.0000	3.212	2.036
0.2000	9.459	1.078, + 1	8.377	14.0000	2.875	1.806
0.3000	9.709	1.127, + 1	8.644	16.0000	2.604	1.624
0.3333	9.727	1.134, + 1	8.666	18.0000	2.382	1.476
0.4000	9.709	1.140, + 1	8.652	20.0000	2.196	1.353
0.5000	9.600	1.136, + 1	8.547	50.0000	1.029	6.064, − 1
0.6000	9.446	1.124, + 1	8.389	100.0000	5.535, − 1	3.177, − 1
0.7000	9.269	1.107, + 1	8.206	500.0000	1.195, − 1	6.582, − 2
0.8000	9.045	1.087, + 1	8.013	1000.0000	6.029, − 2	3.253, − 2
0.9000	8.860	1.067, + 1	7.818			
1.0000	8.678[c]	1.046, + 1	7.625			

[a] In CX small a implies $M_B \ll M_A = M_g$; $a = 1$ implies $M_B \gg M_A = M_g$.

[b] In HS and POL small a implies recombination in a vanishingly light gas and large a ($\simeq 10^3$) implies electron–ion recombination in a normal mass gas.

[c] For CX, the maximum value of a is 0.998.

The partial rates (4.2) are very insensitive to a realistic choice of either the level $-S(\lesssim -10kT)$, below which the stabilization probability P_i^S is calculated as unity, or the lowest level $-D$ since the one-way coupling C_{if} connecting the dissociated states i to any bound level f decreases extremely rapidly and is quite negligible for states with binding energies D as low as 30 kT, which is much smaller, in general, than dissociation energies of normal molecules.

The temperature dependence of $\alpha_E^{(j)}$ follows that of $\tilde{\alpha}_T$, the Thomson rate (A40) with Eqs. (A41)–(A44). Results of a recent diffusional treatment[5] are in close agreement with those of Table I.

In conclusion, via an exhaustive investigation of the strong-collision and bottleneck methods of the termolecular process (4.1), interesting underlying physics and dynamics of the basic process have been uncovered and studied. Highly accurate rates have been presented (Table I) for future use.

ACKNOWLEDGMENT

This research is supported by the U.S. Air Force of Scientific Research under Grant No. AFOSR-84-0233.

APPENDIX: ONE-WAY EQUILIBRIUM COLLISION KERNELS $C_{if}(R)$

The one-way equilibrium rate per unit interval $d\mathbf{R}\,dE_i\,dE_f$ for $E_i \to E_f$ transitions in the microscopic process,

$$(\text{A–B})_{E_i,R} + \text{M} \to (\text{A–B})_{E_f,R} + \text{M} \tag{A1}$$

at specified internal separation R of the pair AB is

$$C_{if}(R) = \tilde{n}_i(\mathbf{R})\nu_{if}(R) = \tilde{n}_i\left[\nu_{if}^{(1)}(R) + \nu_{if}^{(2)}(R)\right]. \tag{A2}$$

The equilibrium distribution $\tilde{n}_i(R)$ per unit interval $d\mathbf{R}$ of (A–B) pairs with internal energy E_i, internal kinetic energy T_{12}, and reduced mass M_{12} is

$$\frac{\tilde{n}_i(\mathbf{R})dE_i}{\tilde{N}_\text{A}\tilde{N}_\text{B}} = \frac{2}{\pi^{1/2}}\left(\frac{T_{12}}{kT}\right)^{1/2}\exp(-E_i/kT)d(T_{12}/kT) \tag{A3}$$

at temperature T. The frequency ν_{if} per unit interval dE_f for $E_i \to E_f$ transitions is assumed in Eq. (A2) to be the sum $\nu_{if}^{(1)} + \nu_{if}^{(2)}$ of the separate contributions $\nu_{if}^{(j)}$ that arise from (A–M), $j=1$, and (B–M), $j=2$, binary collisions at fixed $\mathbf{R}$. The species A, B, and M denoted by indices 1, 2, and 3, respectively, have masses M_i, reduced masses M_{ij} and velocities $\mathbf{v}_i$ and $\mathbf{v}_i'$ before and after the (1–3) elastic collision with differential cross section $\sigma(g,\psi)$ which changes the (1–3) relative velocity from $\mathbf{g}$ along the polar axis to $\mathbf{g}'(\psi,\phi)$. Hence the (1–3) energy-change collision frequency is

$$\nu_{if}^{(1)}(R)dE_f = \left[\int N_0(\mathbf{v}_3)d\mathbf{v}_3\int_{\psi^-}^{\psi^+} g\sigma(g,\psi)d(\cos\psi)\right]d\phi, \tag{A4}$$

where the integration is over the $(\mathbf{v}_3,\psi)$ region of velocity space accessible to $E_i \to E_f$ transitions. The velocity distribution of gas species with concentration N (cm^{-3}) over the kinetic energy

$$T_3 = \tfrac{1}{2}M_s v_3^2 \tag{A5}$$

of AB–M relative motion is the Maxwellian

$$N_0(\mathbf{v}_3)d\mathbf{v}_3 = NG(T_3)dT_3\left[\frac{1}{4\pi}d(\cos\theta_3)d\phi_3\right], \tag{A6}$$

where the distribution

$$G(T_3)dT_3 = \frac{2}{\sqrt{\pi}}(T_3/kT)^{1/2}\exp(-T_3/kT)d(T_3/kT) \tag{A7}$$

represents thermodynamic equilibrium at temperature T between 3 and the (1–2) center of mass.[14] The reduced mass of the AB–M system is

$$M_s = (M_1+M_2)M_3/(M_1+M_2+M_3) = aM = (1+a)M_{13}, \tag{A8}$$

where a convenient mass parameter[9] for (1–3) collisions is

$$a = M_2M_3/M_1(M_1+M_2+M_3). \tag{A9}$$

The (1–2) center of mass is at rest before the (1–3) collision which changes both the kinetic energy

$$T_{12} = \tfrac{1}{2}M_{12}(\mathbf{v}_1-\mathbf{v}_2)^2 = \tfrac{1}{2}M v_1^2;\quad M = M_1(1+M_1/M_2) \tag{A10}$$

of (1–2) relative motion to T_{12}' and the internal energy

$$E_i = \tfrac{1}{2}Mv_1^2 + V(R) \tag{A11}$$

at a fixed R by

$$\epsilon = T_{12}' - T_{12} = \tfrac{1}{2}M_{12}\left[(\mathbf{v}_1'-\mathbf{v}_2)^2 - (\mathbf{v}_1-\mathbf{v}_2)^2\right]. \tag{A12}$$

The (1–3) relative momentum is changed by

$$\mathbf{P} = M_{13}(\mathbf{g}'-\mathbf{g}) = M_1(\mathbf{v}_1'-\mathbf{v}_1) = M_3(\mathbf{v}_3-\mathbf{v}_3') \tag{A13}$$

and the (1–3) relative energy T_{13} remains $\frac{1}{2}M_{13}g^2$. On following from analysis in Ref. 15 it can be shown that the Jacobian J_2 in the angle-kinetic energy transformation

$$d(\cos\theta_3)d\phi = J_2\,dT_{13}\,dT_{12}' \tag{A14}$$

is given by

$$J_2(\psi,T_{13},T_3;\epsilon) = \frac{(1+a)^2}{2a}\left[(T_{12}T_3T_{13})\times(T_{12}+T_3-T_{13})(\mu^+-\mu)(\mu-\mu^-)\right]^{-1/2}. \tag{A15}$$

The scattering ψ region accessible at fixed T_{13}, T_3, and ϵ is the range $\mu^- \leqslant \cos\psi \leqslant \mu^+$, with limits

$$\mu^\pm = (1-\Gamma_i^2)^{1/2}(1-\Gamma_f^2)^{1/2} \pm \Gamma_i\Gamma_f, \tag{A16}$$

where

$$\Gamma_i^2 = \left[(T_{13}^+ - T_{13})(T_{13}-T_{13}^-)\right]/[4T_{13}(T_{12}+T_3-T_{13})] \tag{A17a}$$

and

$$\Gamma_f^2 = [(\tilde{T}_{13}^{+} - T_{13})(T_{13} - \tilde{T}_{13}^{-})]/ [4T_{13}(T_{12} + T_3 - T_{13})]. \quad \text{(A17b)}$$

The accessible T_{13} region accessible for fixed T_3 and ϵ is the range

$$T^- = \max(T_{13}^-, \tilde{T}_{13}^-) \leqslant T_{13} \leqslant \min(T_{13}^+, \tilde{T}_{13}^+) = T^+ \quad \text{(A18)}$$

which ensures real $\mu^{\pm}$, where

$$T_{13}^{\mp}(T_3;T_{12}) = (T_3^{1/2} \mp a^{1/2}T_{12}^{1/2})^2/(1+a) \quad \text{(A19a)}$$

is a function of the initial kinetic energies, and where

$$\tilde{T}_{13}^{\mp}(T_3';T_{12}') = (T_3'^{1/2} \mp a^{1/2}T_{12}'^{1/2})^2/(1+a) \quad \text{(A19b)}$$

is the same function of the final (1–2) and 3 kinetic energies

$$T_{12}' = T_{12} + \epsilon, \quad \text{(A20)}$$

$$T_3' = T_3 - \epsilon. \quad \text{(A21)}$$

Since

$$\frac{\tilde{n}_i(\mathbf{R})}{T_{12}^{1/2}} \frac{N_0(T_3)dT_3}{T_3^{1/2}} = \frac{4}{\pi} \frac{(\tilde{N}_A \tilde{N}_B)}{(kT)^2} \exp - (E/kT)d(E/kT), \quad \text{(A22)}$$

where

$$E = E_i + T_3 = (T_{12} + T_3) + V(R) = \tilde{T} + V(R) \quad \text{(A23)}$$

then the contribution to the one-way equilibrium rate (A2) from (1–3) collisions is

$$C_{if}^{(1)}(R) = \tilde{n}_i(\mathbf{R})\nu_{if}^{(1)}(R) = \frac{(1+a)^2}{a}\left(\frac{2}{M_{13}}\right)^{1/2} \times \frac{(\tilde{N}_A \tilde{N}_B N)}{\pi(kT)^2} \int_{E_0}^{\infty} \exp(-E/kT)d(E/kT) \times \int_{T^-}^{T^+} (\tilde{T} - T_{13})^{-1/2} dT_{13} \int_{\mu^-}^{\mu^+} \sigma(T_{13},\mu) \times [(\mu^+ - \mu)(\mu - \mu^-)]^{-1/2} d\mu, \quad \text{(A24)}$$

where T is $E - V(R)$, as defined in Eq. (A23), and where

$$E_0 = \min(E_i, E_f) \quad \text{(A25)}$$

ensures real T_3 and T_3' in Eq. (A18).

Case I: When the differential cross section σ is a function only of T_{13} as for spiralling ion–neutral collisions under pure polarization attraction when

$$\sigma(T_{13},\psi) = \left(\frac{\alpha_M e^2}{8T_{13}}\right)^{1/2}, \quad \text{(A26)}$$

where α_M is the polarizability of M, then

$$C_{if}^{(1)}(R) = \left(\frac{\alpha_M e^2}{M_{13}}\right)^{1/2} \times \frac{(1+a)^2(\tilde{N}_A \tilde{N}_B N)}{a(kT)^2} \int_{E_0}^{\infty} \exp(-E/kT) \times \left[\sin^{-1}\left(\frac{T^+}{\tilde{T}}\right)^{1/2} - \sin^{-1}\left(\frac{T^-}{\tilde{T}}\right)^{1/2}\right] \times d(E/kT), \quad \text{(A27)}$$

where $\tilde{T}$ is $T_{12} + T_3$ as in Eq. (A23). Integration over ψ yields an expression identical to that of Bates and Mendaš.

Case II: For hard sphere collisions when

$$\sigma(T_{13},\psi) = \frac{\sigma_0}{4\pi} \quad \text{(A28)}$$

then[2]

$$C_{if}^{(1)}(R) = \frac{\sigma_0}{\pi} \frac{(\tilde{N}_A \tilde{N}_B N)}{(2M_{13})^{1/2}(kT)^2} \int_{E_0}^{\infty} \exp(-E/kT) \times [(\tilde{T} - T^-)^{1/2} - (\tilde{T} - T^+)^{1/2}]d(E/kT). \quad \text{(A29)}$$

Case III. When $\sigma(T_{13},\psi)$ is a function only of momentum change P as for the Born approximation or for pure Coulombic attraction when

$$\sigma(T_{13},\psi) = 4e^4M_{13}^2/P^4 = \sigma(P) \quad \text{(A30)}$$

and by finding the Jacobean J_3 in

$$d(\cos\theta_3)\, d\phi\, d(\cos\psi) = J_3\, dT_{12}'\, dP\, dT_{13} \quad \text{(A31)}$$

then from previous analysis,[15] it can be shown that

$$C_{if}^{(1)}(R) = \frac{2^{1/2}(1+a)}{a^{1/2}M_{13}} \frac{(\tilde{N}_A \tilde{N}_B N)}{(kT)^2} \times \int_{E_0}^{\infty} \exp(-E/kT)d(E/kT) \int_{P^-}^{P^+} \sigma(P)dP \quad \text{(A32)}$$

where the limits to the momentum change P for specific $v_1^{(1)}$, $v_3^{(1)}$, and ϵ are

$$P^-(v_1,v_3;\epsilon) = \max[M|v_1' - v_1|, M_s|v_3' - v_3|] \quad \text{(A33)}$$

and

$$P^+(v_1,v_3;\epsilon) = \min[M(v_1' + v_1), M_s(v_3' + v_3)]. \quad \text{(A34)}$$

Case IV. Symmetrical resonance charge–transfer (1) collisions

$$X^+ + X \rightarrow X + X^+ \quad \text{(A35)}$$

between an ion and its parent gas simply interchange $\mathbf{v}_1$ and $\mathbf{v}_3$. At thermal energies the integral cross section σ^x is essentially independent of relative speed g. It can then be shown that[1]

$$C_{if}^{(1)}(R) = \frac{[(1+c)/c]^{3/2}}{(2\pi M_{12})^{1/2}} \frac{(\tilde{N}_A \tilde{N}_B N)\sigma^x}{(kT)^{3/2}} \times \exp\left[-\frac{(1+c)}{(1+2c)} \frac{(E_i + E_f)}{kT}\right] \times \exp\left[-\frac{V(R)/kT}{(2c+1)}\right] \int_{E^-}^{E^+} G(E)dE, \quad \text{(A36)}$$

where

$$c = M_1/M_2$$

and where the fraction of Maxwell particles with energy in the range $E^- \leqslant E \leqslant E^+$ with limits

$$E^{\pm} = [c(1+c)/(1+2c)][T_{12}^{1/2} \pm T_{12}'^{1/2}]^2 \quad \text{(A37)}$$

is

$$\int_{E^-}^{E^+} G(E)dE = \left[\text{erfc}(E/kT)^{1/2} - \frac{2}{\sqrt{\pi}}(E/kT)^{1/2}\exp(-E/kT)\right]_{E^-}^{E^+}. \quad \text{(A37)}$$

The above rates (A24), (A27), (A29), (A32), and (A35) satisfy the detailed balance relation $C_{if}(R) = C_{fi}(R)$, and **R** integration of Eqs. (A27), (A29), and (A35) yields previous expressions.[1-3]

Computational equilibrium rates: C_{if} may be conveniently expressed for computational purposes in terms of dimensionless units,

$$\lambda = -E_i/kT, \quad \mu = -E_f/kT, \quad v(r) = -V(R)/kT, \quad r = R/R_e, \quad R_e = e^2/kT \quad \text{(A38)}$$

by

$$4\pi C_{if}(R)R^2\,dR\,|dE_i|dE_f| = \Gamma\tilde{\alpha}_T F(\lambda,\mu;r)r^2\,dr\,d\lambda\,du \ \ (\text{cm}^3\,\text{s}^{-1}) \quad \text{(A39)}$$

in terms of specified mass factors Γ and the Thomson (low density) rates,

$$\tilde{\alpha}_T = \tfrac{4}{3}\pi(R_e/\beta)^3(3kT/M_{12})^{1/2}\sigma_0 N, \ \beta = 3/2, \quad \text{(A40)}$$

where σ_0 is the integral cross section for (1–3) collisions are relative energy $\frac{1}{2}kT$. The appropriate mass factors Γ in Eq. (A39) and cross section σ_0 in Eq. (A40) are

$$\Gamma^H = \left(\frac{3}{2}\right)^{1/2}\left(\frac{\beta^3}{\pi}\right)\frac{(1+a)^2}{a^{3/2}}\left(\frac{M_{12}}{M_1}\right); \quad \sigma_0 = \sigma_0^H \quad \text{(A41)}$$

for hard-sphere (1–3) collisions with integral cross section σ_0^H,

$$\Gamma^C = \frac{3a}{\pi(1+a)}\Gamma^H; \quad \sigma_0 = \sigma_0^c = \frac{1}{9}\pi R_e^2 \quad \text{(A42)}$$

for Coulomb (1–3) collisions with integral cross section σ_0^c which corresponds to Coulomb scattering by angles $\psi \geq \pi/2$, and to energy transfers $\epsilon \geq (3/2)kT$ for equal mass species. For (1–3) polarization attraction/core repulsion for collisions within the orbiting radius,

$$\Gamma^P = \left(\frac{3}{2}\right)\left(\frac{\beta^3}{\pi}\right)\frac{(1+a)^{5/2}}{a^{3/2}}\left(\frac{M_{12}}{M_1}\right); \quad \sigma_0 = \sigma_0^p = 2\pi(\alpha_M R_e/3)^{1/2} \quad \text{(A43)}$$

and σ_0^p adopted in Thomson's rate (A40) is the corresponding integral (elastic or momentum transfer) collisional cross section at $(3/2)kT$ relative energy. For (1–3) charge–transfer collisions,

$$\Gamma^X = \left(\frac{3}{2}\right)^{1/2}\left(\frac{\beta^3}{\pi}\right)\left(\frac{1+c}{c}\right)^{3/2}; \quad \sigma_0 = 2\sigma^X, \quad \text{(A44)}$$

where σ_0 in Eq. (A44) is the corresponding momentum-transfer cross section, taken as twice the cross section σ^X for charge transfer.[1]

The corresponding dimensionless functions F in Eq. (A39) are symmetric in λ and μ and are

$$F^H(\lambda,\mu;r) = \int_{Y_0}^{\infty}\exp(-Y)dY[\tilde{P}_+ - \tilde{P}_-]; \quad Y_0 = \max(-\lambda,-\mu) \quad \text{(A45)}$$

for hard-sphere (1–3) collisions with (dimensionless) momentum-change limits $\tilde{P}_+ \geq \tilde{P}_-$, given by

$$\tilde{P}_-(\lambda,\mu;r) = \max\{[v(r)-\lambda\,]^{1/2} - [v(r)-\mu]^{1/2}; a^{1/2}[(Y+\lambda)^{1/2} - (Y+\mu)^{1/2}]\} \quad \text{(A46a)}$$

and

$$\tilde{P}_+(\lambda,\mu;r) = \min\{[v(r)-\lambda\,]^{1/2} + [v(r)-\mu]^{1/2}; a^{1/2}[(Y+\lambda)^{1/2} + (Y+\mu)^{1/2}]\}. \quad \text{(A46b)}$$

For Coulomb (1–3) collisions,

$$F^C(\lambda,\mu;r) = \int_{Y_0}^{\infty}\exp(-Y)dY[\tilde{P}_-^{-3} - \tilde{P}_+^{-3}]. \quad \text{(A47)}$$

For polarization (1–3) collisions,

$$F^P(\lambda,\mu;r) = \int_{Y_0}^{\infty}\exp(-Y)dY \times[\sin^{-1}(G_2/A) - \sin^{-1}(G_1/A)], \quad \text{(A48)}$$

where

$$G_1(\lambda,\mu;r) = \max[|(Y+\lambda)^{1/2} - a^{1/2}[v(r)-\lambda\,]^{1/2}|; |(Y+\mu)^{1/2} - a^{1/2}[v(r)-\mu]^{1/2}|], \quad \text{(A49)}$$

$$G_2(\lambda,\mu;r) = \min[(Y+\lambda)^{1/2} - a^{1/2}[v(r)-\lambda\,]^{1/2}; (Y+\mu)^{1/2} - a^{1/2}[v(r)-\mu]^{1/2}],$$

and

$$A = (1+a)^{1/2}[v(r)+Y]^{1/2}. \quad \text{(A50)}$$

For charge–transfer (1–3) collisions

$$F^X(\lambda,\mu;r) = \exp\left[\left(\frac{1+c}{1+2c}\right)(\lambda+\mu)\right] \times\exp[-1/(1+2c)r] \times\left[\frac{\sqrt{\pi}}{2}\,\text{erf}\,g - g\exp(-g^2)\right]_{g_-}^{g_+}, \quad \text{(A51)}$$

where

$$g_\pm^2(\lambda,\mu;r) = \frac{c(1+c)}{(1+2c)}\{[v(r)-\lambda\,]^{1/2} \pm [v(r)-\mu]^{1/2}\}^2. \quad \text{(A52)}$$

The universal expression (A39) is also valuable in that the one-way equilibrium current (rate) across an arbitrary bound level $\nu = -E/kT$ is simply

$$\alpha_{eq} = \Gamma\tilde{\alpha}_T\int_{-\infty}^{\nu}d\lambda\int_{\nu}^{\omega}F(\lambda,\mu)d\mu, \quad \text{(A53)}$$

where $\omega = -D/kT$ is the maximum binding energy in units of (kT) and where

$$F(\lambda,\mu) = \int_0^{r_m}F(\lambda,\mu;r)r^2\,dr, \quad r_m = 1/\max(\lambda,\mu). \quad \text{(A54)}$$

This equilibrium collisional rate displays a minimum at $\nu^* = (1\text{–}3)kT$, the location of a bottleneck (see Fig. 3). The QSS rates (1.9), (1.10), and (1.6) reduce simply to

$$\alpha = \Gamma\tilde{\alpha}_T \int_{-\infty}^{0} d\lambda \int_{0}^{\omega} F(\lambda,\mu) P^{S}(\mu) d\mu, \tag{A55a}$$

$$\alpha = \Gamma\tilde{\alpha}_T \int_{\epsilon}^{\omega} d\lambda \int_{-\infty}^{\epsilon} F(\lambda,\mu) P^{D}(\mu) d\mu, \tag{A55b}$$

$$= \Gamma\tilde{\alpha}_T \int_{-\infty}^{\nu} d\lambda \int_{\nu}^{\omega} [P^{S}(\mu) - P^{S}(\lambda)] F(\lambda,\mu) d\mu, \tag{A55c}$$

where $\epsilon = -S/kT$.

Also various energy-change moments,

$$D_i^{(m)}(E_i) = \frac{1}{m!} \int_{-D}^{\infty} (E_f - E_i)^m C_{if}\, dE_f \tag{A56}$$

are useful[5] in a Fokker–Planck reduction of the collision term (1.2). These can be expressed simply as

$$D_i^m(E_i) = \Gamma\tilde{\alpha}_T \tilde{N}_A \tilde{N}_B (kT)^{m-1} (-1)^m \mathscr{D}_i^{(m)}(\lambda), \tag{A57}$$

where the dimensionless moments

$$\mathscr{D}_i^{(m)}(\lambda) = \frac{1}{m!} \int_{-\infty}^{\omega} (\mu - \lambda)^m F(\lambda,\mu) d\mu \tag{A58}$$

are easily determined[5] on using one of the relevant expressions, (A45), (A47), (A48), or (A51), pertinent to the chosen binary A–M and B–M interactions of A and B with the gas M.

[1] M. R. Flannery, J. Phys. B **13**, 3649 (1980).
[2] M. R. Flannery, J. Phys. B **14**, 915 (1981).
[3] D. R. Bates and I. Mendaš, J. Phys. B **15**, 1949 (1982).
[4] M. R. Flannery, J. Phys. B **18**, L839 (1985).
[5] M. R. Flannery, J. Chem. Phys. **87**, 6947 (1987).
[6] M. R. Flannery, Ann. Phys. (N.Y.) **67**, 376 (1971).
[7] J. J. Thomson, Philos. Mag. **47**, 337 (1924).
[8] P. J. Feibelman, J. Chem. Phys. **42**, 2462 (1965).
[9] D. R. Bates and M. R. Flannery, Proc. R. Soc. London Ser. A **302**, (1968).
[10] M. R. Flannery, J. Phys. B. **20**, 4929 (1987).
[11] M. R. Flannery and T. P. Yang, J. Chem. Phys. **73**, 3239 (1980).
[12] M. R. Flannery, *Recent Studies of Atomic and Molecular Processes*, ed by A. E. Kingston (Plenum, New York, 1987).
[13] J. C. Keck, in *Advances in Atomic and Molecular Physics*, edited by D Bates and I. Estermann (Academic, New York, 1972), Vol. 8; A Chem. Phys. **13**, 83 (1967).
[14] D. R. Bates, P. B. Hays, and D. Sprevak, J. Phys. B **4**, 962 (1971).
[15] M. R. Flannery, Phys. Rev. A **22**, 2408 (1980).

3.2 Variational Treatment.

Variational principle for termolecular recombination in a gas

M. R. Flannery
School of Physics, Georgia Institute of Technology, Atlanta, Georgia 30332-0430

(Received 29 February 1988; accepted 22 March 1988)

A variational principle for the rates of termolecular processes is proposed and then applied to recombination between atomic ions with excellent results. The variational expression when minimized with respect to stabilization probabilities is capable of providing rates identical to those determined from the quasi-steady-state solution of the full Master equation. Connection is made with electrical networks and with the principle of least dissipation.

I. INTRODUCTION

An important objective in chemical physics is the formulation of a variational theory of chemical reactions which is exact in the sense that the deduced variational expression will yield, upon variation of relevant parameters, the distributions n_i and rate constants which are identical with those obtained by direct solution of the exact Master equation for the particular process. The variational procedure of Wigner[1] and Keck[2] is "variational" in the sense that it yields a least upper bound to the rate of a chemical reaction as determined from a Master equation. The reaction is represented by the motion of a point $(\mathbf{p},\mathbf{q})$ in multidimensional phase space across a trial surface S which separates a block $\mathscr{C}$ of initial reactant states i from a block $\mathscr{S}$ of final product states f. The one-way rate R that representative phase points flow (downward) across S—or flux of trajectories—is an upper limit to the actual rate since (a) upward reexcitation to states i above S is ignored and since (b) a representative point which passes through S more than once is repeatedly included at each pass. The additional use of an equilbrium density $\tilde{n}_i$ for the reacting states then provides a rigorous upper bound R_e to the reaction rate. A minimum—the least upper bound—to R_e is then obtained by variation of the trial surface S.

In termolecular electron-ion or ion-ion collisional recombination

$$A^+ + B^- + M \rightarrow AB + M \qquad (1.1)$$

at low gas densities, for example, the "surface", can be taken as some bound energy level $-E$ of the pair AB so that an upper bound to the two-body rate constant $\alpha(\mathrm{cm^3\,s^{-1}})$ for recombination (1.1) is

$$R_e(-E) = \int_{-E}^{\infty} dE_i \int_{-D}^{-E} C_{if}\, dE_f > \alpha \tilde{N}_A \tilde{N}_B\,, \qquad (1.2)$$

where $\tilde{N}_A$ and $\tilde{N}_B$ are the equilibrium concentrations of A^+ and B^- and where C_{if} is the one-way equilibrium collisional rate per unit interval $dE_i\, dE_f$ for transitions between energy levels E_i and E_f of AB pairs. The level $-E$ separates the "reactant" block $\mathscr{C}$ of states i with energies E_i in the range $-E<E_i<\infty$ from the "product" block $\mathscr{S}$ of states f with energies E_f in the range $-E>E_f>-D$, where $-D$ is the lowest energy level of the AB pair relative to a dissociation limit at zero energy. A minimum to R_e occurs at $-E=-E^*$ which therefore acts as a bottleneck or transition state. States above $-E^*$ are more likely to be excited by collision and hence are unstable with respect to association, while those below $-E^*$ tend to be deexcited and are therefore considered as stable. For this one-dimensional surface, the Wigner–Keck treatment is then identical with the bottleneck method proposed by Byron *et al.*[3] for three-body electron–ion recombination.[4] For termolecular recombination of arbitrary mass ions in a gas, this variational treatment yields rates[5] which are higher by factors of 2 to 8 than the exact rates[6] obtained from a Master equation.

What is desirable is a variational method which will yield a rate identical to that determined from solution of the full Master equation. This search requires the addition, as illustrated by Fig. 1, of a block $\mathscr{E}$ of highly excited states i for which the reaction can go either way. The block is characterized by the overall probability P_i^S for stabilization via downward ($\mathscr{E}\rightarrow\mathscr{S}$) transitions or by the overall probability $P_i^D=(1-P_i^S)$ for disruption via upward ($\mathscr{E}\rightarrow\mathscr{C}$) transitions. This block $\mathscr{E}$ lies intermediate between the reactant and product blocks $\mathscr{C}$ and $\mathscr{S}$ which are separately characterized by $P_i^S=0$ and $P_i^S=1$, respectively.

In this paper such a method is proposed and is then applied as a case study to the well-developed example[6] of termolecular ion–ion recombination (1.1) in a low density gas M. Connection is then made with the principle of least

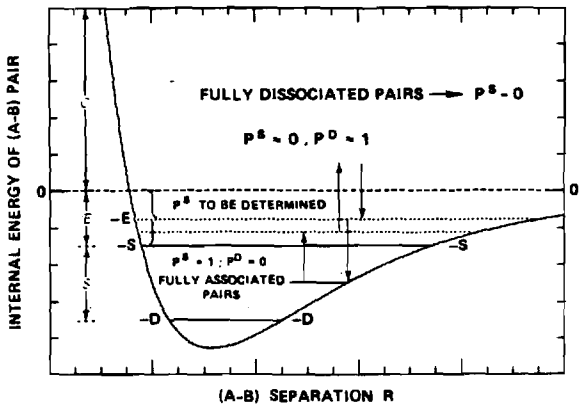

FIG. 1. Schematic diagram of energy blocks $\mathscr{C}$, $\mathscr{E}$, and $\mathscr{S}$ pertinent to recombination at low gas densities.

 0021-9606/88/130214-09$02.10

dissipation, well known in heat-conduction problems and in electrical networks. By analogy with this principle for a network of resistors, Bates[7] very perceptively postulated that a minimum would exist, with respect to variation in the normalized time-independent distributions $\gamma_i(E_i) = n_i/\tilde{n}_i$, in the time-independent measure:

$$\mathscr{M} = \int_{-D}^{\infty} dE_i \int_{-D}^{\infty} (\gamma_f - \gamma_i)^2 C_{if}\, dE_f \tag{1.3}$$

of the total rate of restoration to thermal equilibrium. Mendaš[8] then noted that minimum $\mathscr{M}$ is obtained for a quasi-steady-state distribution of excited levels determined by

$$\gamma_i \int_{-D}^{\infty} C_{if}\, dE_f = \int_{-D}^{\infty} \gamma_f\, C_{if}\, dE_f\,. \tag{1.4}$$

The present formulation permits the identification of this $\mathscr{M}$ so minimized with twice the actual (quasi-steady-state) rate constant

$$\alpha \tilde{N}_A\, \tilde{N}_B = \int_{-E}^{\infty} dE_i \int_{-D}^{-E} (\gamma_i - \gamma_f) C_{if}\, dE_f \tag{1.5}$$

which is the net downward constant energy-space current across any level $-E$, in the block $\mathscr{E}$ of excited levels in quasi-steady-state. A supplementary calculation of Eq. (1.5) with the variational result of Eq. (1.3) is then not required. Note that the upper bound [Eq. (1.2)] is recovered upon eliminating block $\mathscr{E}$ by assigning $\gamma_i(-E \le E_i < \infty) = 1$ and $\gamma_f(-E \ge E_f \ge -D) = 0$ in either Eq. (1.3) or Eq. (1.5).

II. VARIATIONAL PRINCIPLE

The net rate for termolecular association

$$A + B + M \underset{k}{\overset{\alpha}{\rightleftarrows}} AB + M \tag{2.1}$$

between A and B in a gas M is[9]

$$R^A(t) = \int_{-D}^{\infty} P_i^S \left(\frac{dn_i}{dt}\right) dE_i \tag{2.2}$$

$$= \alpha N_A(t) N_B(t) - k\, n_s(t)\,, \tag{2.3}$$

where P_i^S is the stochastic probability that a pair AB with internal relative energy E_i is connected via a series of energy (state)-changing collisions to a sink $\mathscr{S}$ of fully associated AB pairs. The concentration $n_i(t)$ of AB pairs with internal energy E_i of relative motion in unit interval dE_i about E_i develops in time t according to the standard Master equation[9]

$$\frac{dn_i}{dt} = -\int_{-D}^{\infty} [n_i(t)\nu_{if} - n_f(t)\nu_{fi}]\, dE_f = -\frac{\partial J_i}{\partial E_i}, \tag{2.4}$$

where $-D$ is the energy of the lowest vibrational level of AB relative to the dissociation limit taken as zero energy.

The frequency per unit interval dE_f for $E_i \to E_f$ transitions in AB by collision with gas species M is ν_{if} which is linear in gas density N. At low gas densities, R^A is linear in N so that P_i^S is then only required to zero order in N. Over the range $0 \le E_i < \infty$ which defines the $\mathscr{E}$ block of fully dissociated reactant states, n_i at low N can then be taken in the collisional part of Eq. (2.4) as its thermodynamic equilibrium value $\tilde{n}_i$, so that $P_i^S \approx 0$ for block $\mathscr{E}$. The effective two-body rate constant for the association of A and B with (cm^{-3} concentrations $N_A(t)$ and $N_B(t)$ at time t is α (cm^3 s^{-1}). The constant k(s^{-1}) is the frequency for dissociation of the tightly bound pairs in the product block $\mathscr{S}$ of levels with energies E_i in the range $-S \ge E_i \ge -D$, within which the stabilization probability P_i^S is unity. In the intermediate block $\mathscr{E}$ of "reacting" states with $0 \ge E_i \ge -S$ in Fig. 1, the probabilities P_i^S must be determined. The net rate for termolecular dissociation in the closed system is

$$R^D(t) = \int_{-D}^{\infty} P_i^D \left(\frac{dn_i}{dt}\right) dE_i = -R^A(t)\,, \tag{2.}$$

where $P_i^D = 1 - P_i^S$ is the probability that state i is collisionally connected to fully dissociated channels (at infinite A-separation).

The proposed variational principle now asserts that the probabilities $P_i^{S,D}$ and densities n_i have energy distributions which ensure that $R^{A,D}(t)$ of Eqs. (2.2) and (2.5) are extrema at time t.

A. The quasi-steady-state deduction

Rewrite Eq. (2.2) as

$$R^A(t) = -\int_{-D}^{\infty} P_i^S \left(\frac{\partial J_i}{\partial E_i}\right) dE_i \tag{2.}$$

in terms of the net downward collisional current

$$-J(E,t) = \int_{E}^{\infty} dE_i \int_{-D}^{E} [n_i(t)\nu_{if} - n_f(t)\nu_{fi}]\, dE_f \tag{2.}$$

past level E. Since J_i vanishes as E_i tends to both $-D$ and ∞, the rate is then

$$R^A(t) = \int_{-D}^{\infty} J_i(E,t) \left(\frac{dP_i^S}{dE_i}\right) dE_i\,. \tag{2.}$$

Since P_i^S is constant (0 and 1 in blocks $\mathscr{E}$ and $\mathscr{S}$, respectively), Eq. (2.8) further reduces to

$$R^A(t) = \int_{-S}^{0} J_i(E,t) \left(\frac{dP_i^S}{dE_i}\right) dE_i\,. \tag{2.}$$

A necessary condition for the integral

$$I = \int_{x_1}^{x_2} F[\mathbf{y}(x), \dot{\mathbf{y}}(x); x]\, dx, \quad \dot{\mathbf{y}} = d\mathbf{y}/dx \tag{2.}$$

to exhibit an extremum is given in the calculus of variations by the Euler–Lagrange equation[10]

$$\frac{d}{dx}\left(\frac{\partial F}{\partial \dot{y}_i}\right) - \frac{\partial F}{\partial y_i} = 0, \quad i = 1,2,\ldots,N, \tag{2.}$$

the solution of which determines $\mathbf{y}(x) \equiv [y_i(x)]$ over a fixed range $x_1 \le x \le x_2$. Write $x \equiv E_i$, $y_i \equiv P_i^S$, $F(\dot{y}(x); x) \equiv J(E_i)\,(dP_i^S/dE_i)$. The integral (2.9) is then an extremum provided

$$\frac{\partial J_i}{\partial E_i} = 0 = -\frac{dn_i}{dt}, \quad 0 \ge E_i \ge -S \tag{2.}$$

for each level i within block $\mathscr{E}$. This is the quasi-steady-state (QSS) condition for pairs in block $\mathscr{E}$ with $n_i(t)$ distributed so that J, the current (2.7), is constant over all energies $(-E)$ of block $\mathscr{E}$. The extremum rate, obtained from Eq. (2.12) in Eq. (2.9), is then the net downward current across bound level $-E$ of block $\mathscr{E}$:

$$R_*^A(t) = -J(-E,t) = \int_{-E}^{\infty} dE_i \times \int_{-D}^{-E} [n_i(t)\nu_{if} - n_f(t)\nu_{fi}]\, dE_f , \quad (2.13)$$

which depends on the probabilities P_i^S only implicitly via n_i. As E tends from above to the dissociation limit at $E=0$, $-J(E,t)$ increases monotonically to this rate.[5]

B. Analysis

From Eq. (2.4) the distribution

$$\gamma_i(t) = n_i(E_i,t)/\tilde{n}_i(E_i) \quad (2.14)$$

normalized to the distribution $\tilde{n}_i$ for full thermodynamic equilibrium satisfies

$$\frac{dn_i}{dt} = \tilde{n}_i \frac{d\gamma_i}{dt} = -\int_{-D}^{\infty} [\gamma_i(t) - \gamma_f(t)]\, C_{if}\, dE_f , \quad (2.15)$$

where the one-way equilibrium rate

$$C_{if} = \tilde{n}_i\, \nu_{if} = \tilde{n}_f\, \nu_{fi} = C_{fi} \quad (2.16)$$

satisfies detailed balance and is linear in gas density N. On introducing the implicit dependence of n_i on the probabilities $P_i^{S,D}$ via the separation[9]

$$\gamma_i(t) = P_i^D \gamma_c(t) + P_i^S \gamma_s(t) , \quad (2.17)$$

where

$$\gamma_c(t) = n_c(t)/\tilde{n}_c = N_A(t) N_B(t)/\tilde{N}_A\, \tilde{N}_B \quad (2.18a)$$

and

$$\gamma_s(t) = n_s(t)/\tilde{n}_s \quad (2.18b)$$

are the respective concentrations $n_c(t)$ and $n_s(t)$ of fully dissociated pairs with energies E_i in the range $0 \leqslant E_i \leqslant \infty$ of block $\mathscr{C}$ and of fully associated pairs of block $\mathscr{S}$ normalized to their respective equilibrium concentrations $\tilde{n}_c$ and $\tilde{n}_s$, then Eq. (2.15) separates as[9]

$$\frac{dn_i}{dt} = [\gamma_c(t) - \gamma_s(t)] \times \int_{-D}^{\infty} (P_i^S - P_f^S) C_{if}\, dE_f = -\frac{\partial J_i}{\partial E_i} . \quad (2.19)$$

Hence the macroscopic rate (2.3) is now

$$R^A(t) = \alpha \tilde{N}_A\, \tilde{N}_B\, [\gamma_c(t) - \gamma_s(t)] = -R^D(t) , \quad (2.20)$$

where the association rate in units of the time-dependent difference $(\gamma_c - \gamma_s)$ is the rate constant

$$\alpha \tilde{N}_A\, \tilde{N}_B = k\tilde{n}_s , \quad (2.21a)$$

$$= \int_{-D}^{\infty} P_i^S\, dE_i \int_{-D}^{\infty} (P_i^S - P_f^S)\, C_{if}\, dE_f , \quad (2.21b)$$

$$= \frac{1}{2} \int_{-D}^{\infty} dE_i \int_{-D}^{\infty} (P_i^S - P_f^S)^2\, C_{if}\, dE_f \quad (2.21c)$$

which is now time independent and is always positive. The upward current J past energy E in Eq. (2.19) separates similarly as[9]

$$J(E,t) = [\gamma_c(t) - \gamma_s(t)]\, j(E) , \quad (2.22)$$

where

$$j(E) = \int_E^{\infty} dE_i \int_{-D}^{E} (P_i^S - P_f^S)\, C_{if}\, dE_f . \quad (2.23)$$

Since Eq. (2.20) is an extremum provided the QSS condition (2.12) holds, i.e., Eq. (2.19) vanishes in block $\mathscr{E}$ where Eq. (2.23) is constant, then the probabilities P_i^S satisfy the standard integral equation[9]

$$P_i^S \int_{-D}^{\infty} C_{if}\, dE_f = \int_{-D}^{\infty} C_{if}\, P_f^S\, dE_f . \quad (2.24)$$

When inserted in Eq. (2.21) the solutions P_i^S yield after some reduction the extremum rate constant,

$$R_* = \alpha_* \tilde{N}_A\, \tilde{N}_B = \int_{-E}^{\infty} dE_i \int_{-D}^{-E} (P_f^S - P_i^S)\, C_{if}\, dE_f , \quad (2.25a)$$

$$= \int_0^{\infty} dE_i \int_{-D}^{0} C_{if}\, P_f^S\, dE_f , \quad (2.25b)$$

$$= \int_{-S}^{\infty} dE_f \int_{-D}^{S} C_{if}\, P_f^D\, dE_i , \quad (2.25c)$$

where $-E$ is any level in block $\mathscr{E}$, including the $\mathscr{C}$–$\mathscr{E}$ and $\mathscr{E}$–$\mathscr{S}$ boundaries at 0 and $-S$, respectively. This extremum simply confirms the identification in Eq. (2.13) of rate with current. The nature (maximum or minimum) of the extremum becomes apparent on performing independent variations δP_i^S to P_i^S for each level in block $\mathscr{E}$ subject to the constraints

$$P_i^S = 0; \quad 0 < E_i < \infty , \quad (2.26)$$
$$= 1; \quad -D < E_i < -S ,$$

associated with blocks $\mathscr{C}$ and $\mathscr{S}$, respectively. The resulting change in Eq. (2.20) is

$$\delta R^A(t) = 2[\gamma_c(t) - \gamma_s(t)] \times \left[\int_{-S}^{0} dE_i\, \delta P_i^S \left\{ \int_{-D}^{\infty} (P_i^S - P_f^S)\, C_{if}\, dE_f \right\} + \frac{1}{4} \int_{-D}^{\infty} dE_i \int_{-D}^{\infty} (\delta P_i^S - \delta P_f^S)^2\, C_{if}\, dE_f \right] \quad (2.27)$$

to second order in δP_i^S. For an extremum the change δR^A to first order in δP_i^S vanishes so that Eq. (2.24) is recovered from Eq. (2.27). The change to second order in δP_i^S is determined by the sign of $(\gamma_c - \gamma_s)$. When $\gamma_c(t) > \gamma_s(t)$ so that the overall direction, according to Eq. (2.20), is association, then the extremum to R^A is a minimum; and the dissociation rate R^D in Eq. (2.20) is a negative maximum. When $\gamma_s(t) > \gamma_c(t)$ so that the overall direction is dissociation, then R^A is a negative maximum; and R^D is a minimum. The proposed variational principle governing Eqs. (2.2) and (2.5) thus asserts that the rate R^A or R^D, whichever corresponds to the overall direction, always adjusts itself to a min-

imum, i.e., the probabilities P_i^S are so distributed that they tend to counteract the change so as to impede the progress towards full equilibrium (when $\gamma_c \to \gamma_s \to 1$). The rate R_* in Eq. (2.25) is a minimum to Eq. (2.21).

Rather than inserting the numerical solution of the QSS integral equation (2.23) in Eq. (2.25a) for the rate constant, an alternative procedure is therefore a direct search of a minimum in the rate (2.21) with respect to variation of P_i^S, a procedure similar to that noted by Mendaš with respect to variation of Eq. (1.3) with respect to γ_i. The present variational principle however provides a variational expression (2.21) for the actual QSS rate (2.25) obtained otherwise from the Master equation.

Although the present analysis has been developed with termolecular ion–ion recombination (1.1) in mind, it may be easily generalized to include ion–atom association

$$A^+ + B + M \to AB^+ + M \tag{2.28}$$

between atomic species in a low density gas M. Here quasi-bound levels (E_i, L_i^2) of AB^+ can be formed with $E_i > 0$ within the centrifugal barrier associated with internal relative angular momentum (squared) L_i^2. By adopting the ansatz [Eq. (5.2) of Ref. 5] for the distribution $n_i(E_i, L_i^2)$ of AB^+ pairs in terms of the stabilization probability $P_i^S(E_i, L_i^2)$ then expression (2.21), generalized to include relevant integrations over L_i^2 and L_f^2, is varied with respect to $P_i^S(E_i, L_i^2)$ so as to provide a minimum which is then the required QSS rate.

C. Application to termolecular recombination

Since dP_i^S/dE_i tends to zero as $E_i \to 0$ and as $E_i \to -S$ (taken now to be $-\infty$), the simplest one-parameter (λ^*) trial function is provided by

$$\frac{dP^S(\lambda;\lambda^*)}{d\lambda} = A\lambda\, e^{-(\lambda/\lambda^*)}, \tag{2.29}$$

where $\lambda = -E_i/kT$ is the binding energy in units of kT, the mean energy of the gas M, and where the variational parameter λ^* is the location of the maximum at $\lambda = \lambda^*$ of Eq. (2.29). Since $P(\infty)-P(0)$ is unity, then integration yields the normalization parameter A to be $(1/\lambda^*)^2$ and

$$P^S(\lambda;\lambda^*) = 1-(1+x)\exp(-x); x = \lambda/\lambda^*. \tag{2.30}$$

Consider, as a case study, the well-developed example of termolecular ion–ion recombination[6]

$$X^+ + X^- + X \to X_2 + X \tag{2.31}$$

between equal mass species. Necessary integrations of Eq. (2.21) and solution[6] of the integral equation (2.24) are performed by choosing 72 pivots each in blocks $\mathscr{C}$ and $\mathscr{B}$ according to the procedure outlined in Ref. 11. When Eq. (2.30) is inserted into Eq. (2.21) and when λ^* is varied, the long-dashed curve in Fig. 2 is obtained for the ratio

$$r = R(\lambda = \lambda^*)/R_*, \tag{2.32}$$

where R_* is the exact QSS rate (2.25) determined from the direct solution[6] of Eq. (2.24). Not only does the single parameter $\lambda^* = 1.1624$ provide a minimum to R but it also yields the exact result to 1% accuracy with $r = 1.011$. Introduction of a more sophisticated three parameter ($\lambda^*, a,$ trial function

$$dP^S(\lambda;\lambda^*,a,b)/d\lambda = A\lambda(1 + a\lambda + b\lambda^2)e^{-\lambda/\Lambda_*}, \tag{2.3}$$

where, in terms of the location at λ^* of the maximum to E (2.33), Λ_* is the function

$$\Lambda(\lambda,a,b) = \lambda(1 + a\lambda + b\lambda^2)/(1 + 2a\lambda + 3b\lambda^2) \tag{2.3}$$

evaluated at $\lambda = \lambda^*$.

Integration of Eq. (2.33) subject to the constraints E (2.26) determines the normalization factor A and yields

$$P^S(\lambda;\lambda^*,a,b) = 1 - [1 + x + x^2 g(x)^2]\exp(-x);$$
$$x = \lambda/\Lambda_*, \tag{2.3}$$

where

$$g(x;\Lambda_*,a,b) = \Lambda_*(a + 3b\Lambda_* + b\Lambda_* x)/$$
$$(1 + 2a\Lambda_* + 6b\Lambda_*^2). \tag{2.3}$$

The derivative is

$$\frac{dP^S(\lambda;\Lambda_*,a,b)}{d\lambda} = [(x + a\Lambda_* x^2 + b\Lambda_*^2 x^3)/$$
$$(1 + 2a\Lambda_* + 6b\Lambda_*^2)]\exp(-x). \tag{2.3}$$

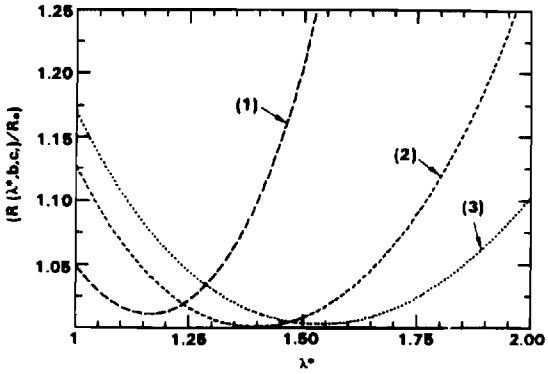

FIG. 2. Ratio of the variational rate (2.21) to the exact QSS rate (2.25) as function of variational parameter λ^*. (1): One parameter function (2.30 (2) and (3): Two- and three-parameter functions (2.35) with $a = 1$, $b =$ and $a = 1$, $b = 0.7$, respectively.

Figure 2 illustrates that minima $r = 1.0008$ a $r = 1.0029$ are obtained for two-parameter ($\lambda^* = 1.39$ $a = 1.0, b = 0$) and three-parameter ($\lambda^* = 1.5348, a =$ $b = 0.7$) trial functions, respectively, and that these mini agree with the calculation of the exact QSS rate (2.2 Comparison of the corresponding probabilities for all th variational cases with the exact QSS solution[6] of Eq. (2.2 is given in Fig. 3(a). The two-parameter function is grap cally indistinguishable from the numerical QSS solution Fig. 3(a). The agreement is in general very good for su simple variational functions, and could be easily improved larger λ by insisting that $P_i^S \to 1$ as $E_i \to -S \approx -(10$– kT rather than as $E_i \to -\infty$ in Eq. (2.35). Although two-parameter function provides a slightly better repres tation we note from Fig. 2 that the rate (2.21) is not ove sensitive to the small deviations in the probabilities.

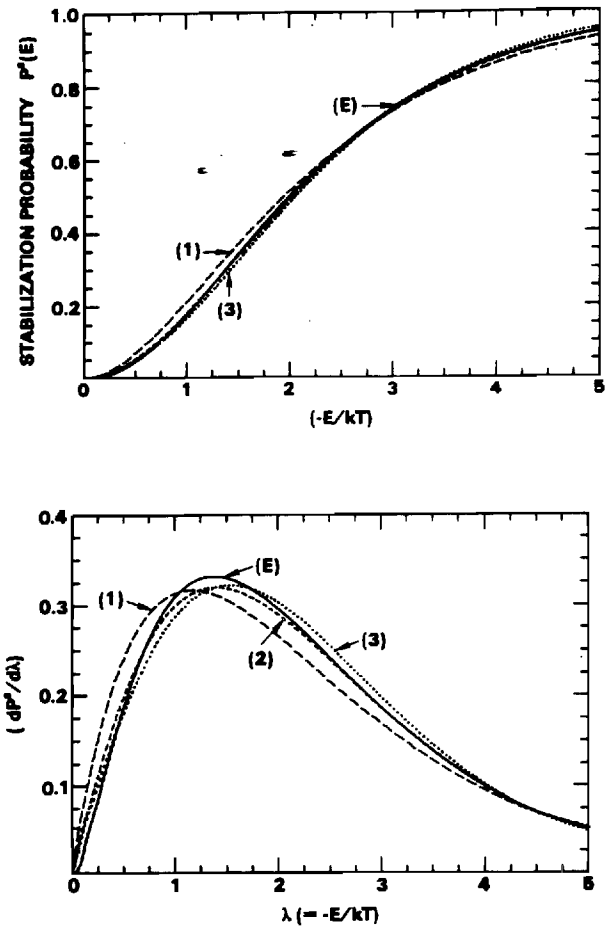

FIG. 3. (a) Variational probabilities (2.35), (1), (2), and (3) as a function of normalized bound energy $(-E/kT)$. Parameters (λ^*,a,b) given by (1.1624,0,0), (1.3962,1,0), and (1.5348,1,0.7), respectively. Exact QSS probability (2.24):(E). (b) Corresponding derivatives.

A more sensitive test[5] is provided in Fig. 3(b) which displays the corresponding comparison of the derivatives. All of these variational curves and the direct QSS solution of Eq. (2.24) display maxima almost equal and located in the same neighborhood. This location has physical significance and is perhaps key to the overall success obtained. This is most easily illustrated by expanding

$$P_f^S = P_i^S + (E_f - E_i)\left[\frac{dP_i^S}{dE_i}\right] + \tfrac{1}{2}(E_f - E_i)^2\left[\frac{d^2P_i^S}{dE_i^2}\right] + \cdots \quad (2.38)$$

in powers of the energy difference $(E_f - E_i)$ so that Eq. (2.19) yields

$$-[\gamma_c(t) - \gamma_s(t)]^{-1}\frac{dn_i}{dt} = D_i^{(1)}\left[\frac{dP_i^S}{dE_i}\right] + D_i^{(2)}\left[\frac{d^2P_i^S}{dE_i^2}\right] \quad (2.39)$$

to second order in the energy-change moments[5]

$$D_i^{(m)}(E_i) = \frac{1}{m!}\int_{-D}^{\infty}(E_f - E_i)^m C_{if}\,dE_f . \quad (2.40)$$

For QSS of block $\mathscr{E}$,

$$\left(\frac{d^2P_i^S}{dE_i^2}\right)\Big/\left(\frac{dP_i^S}{dE_i}\right) = -D_i^{(1)}/D_i^{(2)} \equiv -\chi_i(E_i) \quad (2.41)$$

so that (dP_i^S/dE_i) exhibits a maximum where $D_i^{(1)}$, the average energy increase per second, passes through zero, which in general occurs[5] at $E_i^* = -(1\text{–}2)\,kT$. The above trial expressions (2.29) and (2.33) therefore implicitly acknowledge the physical tendency for collisions to excite those pairs with $E > E_i^*$ and to degrade those with $E < E_i^*$. Once λ_i^* has been variationally determined by the present procedure, it will only coincide with the actual location of the zero in $D_i^{(1)}$ to the extent that approximation (2.39) is valid. If so the expressions then imply that the ratio (kT) $D_i^{(1)}/D_i^{(2)}$ may be represented quite accurately either by the simple form $(1/\lambda - 1/\lambda^*)$ or by the more complicated form $(1/\Lambda - 1/\Lambda_*$, respectively. Both forms yield zero at $\lambda = \lambda^*$. Interestingly enough, the zero of $D_i^{(1)}$ for symmetrical resonance charge transfer collisions occur at $\lambda_i^* = 1.329$ in close agreement with the two-parameter variational and exact calculations [cf. Fig. 3(b)].

The solution of Eq. (2.41) subject to Eq. (2.26) is

$$P^S(-E) = \left[\int_{-E}^{0} dE_f \exp\left\{\int_{-E_f}^{0}\chi_i\,dE_i\right\}\right] \times\left[\int_{-S}^{0} dE_f \exp\left\{\int_{-E_f}^{0}\chi_i\,dE_i\right\}\right]^{-1} \quad (2.42)$$

in block $\mathscr{E}$. When the approximation[5]

$$D_i^{(1)} = \frac{dD_i^{(2)}}{dE_i} \quad (2.43)$$

between moments $D_i^{(1)}$ and $D_i^{(2)}$ can be invoked, then

$$\exp\left[\int_{-E_f}^{0}\chi_i\,dE_i\right] = D^{(2)}(0)/D^{(2)}(-E_f) \quad (2.44)$$

so that Eq. (2.42) reduces to

$$P_d^S(-E_i) = \left[\int_{-E}^{0} dE_f/D^{(2)}(-E_f)\right] \times\left[\int_{-S}^{0} dE_f/D^{(2)}(-E_f)\right]^{-1} . \quad (2.45)$$

This expression (2.45) has been used in Eq. (2.21c) to provide accurate rates α_D in a previous diffusional treatment.[5] The more basic expression (2.42) is currently being tested.[12]

There are now two accurate treatments which provide accurate *analytical* representations of the collisional stabilization and disruption probabilities—the previous diffusional method[5] and the present (two-parameter) variational method. These results D from Eq. (2.45) and V from Eq. (2.35) are compared in Fig. 4 with the exact numerical solution E of Eq. (2.24). Due to a more accurate evaluation of $D_i^{(1)}$, the present diffusional results differ somewhat from those previously reported.[5] The resulting rates

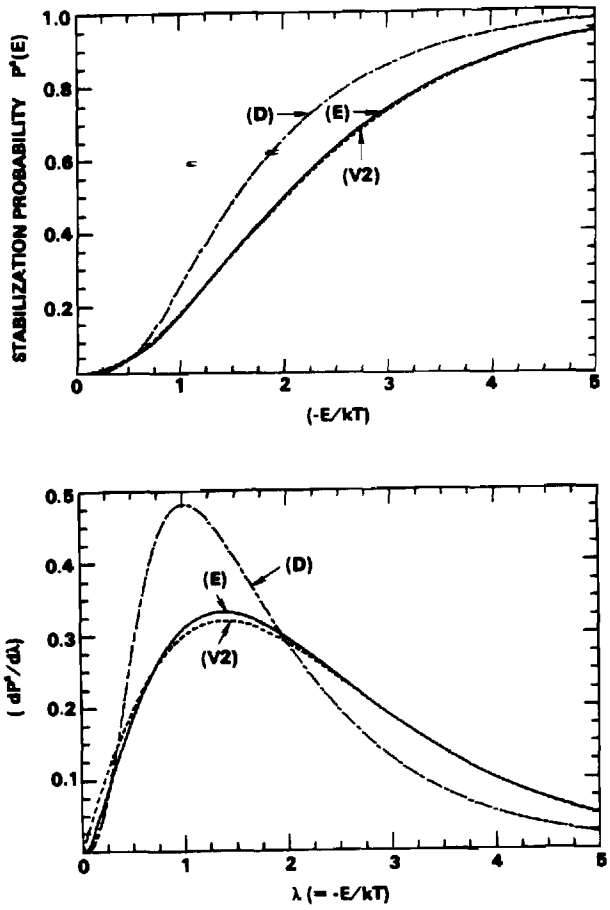

FIG. 4. (a) Probabilities and (b) corresponding derivatives in exact QSS (E), two-parameter ($\lambda^* = 1.3962$, $a = 1$) variational ($V2$), and diffusional (D) treatments, as a function of normalized bound energy ($-E/kT$).

($\alpha_D/\alpha_E = 1.08$, $\alpha_V/\alpha_E = 1$) are not that sensitive, as before, to the larger discrepancies in P_i^S resulting from the diffusional and variational treatments.

III. ANALOGY WITH (R,C) ELECTRICAL CIRCUIT AND WITH PRINCIPLE OF LEAST DISSIPATION

Bates[7] has already provided the interesting analogy with a network of resistors for the case when $\gamma_c(t) = 1 \gg \gamma_s(t)$ so that time dependencies can be omitted,[5] and has introduced the variational function $\mathscr{M}$, Eq. (1.3), as a measure of the restoration rate to thermodynamic equilibrium. Here capacitors are introduced (Sec. III A) so as to explicitly acknowledge time-dependent currents and voltages. The present approach allows us to identify (Sec. III B) the time-independent function $\mathscr{M}$ with $2\alpha\tilde{N}_A\tilde{N}_B$.

The Master equation (2.15) involves the internal energy E_f of relative (A–B) motion as a continuous variable since the spacing between bound levels are much smaller than the thermal energy (kT) of the thermal gas bath M. The discrete representation of Eq. (2.15) gives the net electrical current flowing outward from node i of a multimode system as

$$I_i(t) = -\frac{dn_i}{dt} = \sum_{f=-D}^{\infty} I_{if}(t)\,, \tag{3.1}$$

where the current in the $i \to f$ segment is

$$I_{if}(t) = [\gamma_i(t) - \gamma_f(t)]\, C_{if}\,. \tag{3.2}$$

This reduces under Eq. (2.16) to

$$I_{if}(t) = [\gamma_c(t) - \gamma_s(t)]\,(P_f^S - P_i^S)\, C_{if} \tag{3.3}$$

$$\equiv [\gamma_c(t) - \gamma_s(t)]\, i_{if}\,.$$

The formal structure of Eqs. (3.1) and (3.2) is identical[7] to an electrical network where the current I_{if} along the line element e_{if} from junction i to junction f in the network is equivalent to the time-dependent voltage drop

$$V_{if}(t) = [\gamma_i(t) - \gamma_f(t)] \tag{3.4}$$

$$= [\gamma_c(t) - \gamma_s(t)]\,(P_i^D - P_f^D) \tag{3.5}$$

times the conductivity $C_{if} = R_{if}^{-1}$ of the line element of resistance R_{if}.

Since, Eq. (3.2) is Ohm's law ($V_{if}(t) = I_{if}(t)\, R_{if}$)[7], a time-dependent potential

$$V_i(t) = \gamma_i(t) \tag{3.6}$$

can be associated with any level i. All states within the source block $\mathscr{C}$ are at equipotential $\gamma_c(t)$ and all levels within sink block $\mathscr{S}$ are at equipotential $\gamma_s(t)$. The potential γ_i of each $\mathscr{E}$ level i is below γ_c by an amount

$$V_{ci} = \gamma_c(t) - \gamma_i(t) = P_i^S\,[\gamma_c(t) - \gamma_s(t)] \tag{3.7}$$

or is above γ_s by an amount

$$V_{is} = \gamma_i(t) - \gamma_s(t) = P_i^D\,[\gamma_c(t) - \gamma_s(t)]\,. \tag{3.8}$$

Hence in units of $(\gamma_c - \gamma_s)$, P_i^S is the potential drop from $\mathscr{C}$ to i, P_i^D is the potential height of i above $\mathscr{S}$, and I_{if} the current Eq. (3.3) along segment e_{if}. Since P_i^D within increases with E_i continuously and monotonically from zero within $\mathscr{S}$ to unity within $\mathscr{C}$ then

$$\sum_{e_{if}} V_{if} = [\gamma_c(t) - \gamma_s(t)] \oint_{E_1}^{E_2} \left[\frac{dP_i^D}{dE_i}\right] dE_i = 0\,, \tag{3.9}$$

where the sum is over each segment e_{if} within any closed loop ($E_1 \to E_2 \to E_1$). Equation (3.9) as already noted,[7] is Kirchoff's voltage law (KVL) which is based on the uniqueness of the potential $\gamma_i(t)$ at a given time and which expresses *energy conservation* for any closed loop within the entire ($\mathscr{C}$, $\mathscr{E}$, $\mathscr{S}$) circuit at time t.

A. QSS simplification: (R,C) circuit

The QSS condition (2.12) for each level i of block $\mathscr{E}$ ($0 \geqslant E_i \geqslant -S$) is equivalent to

$$I_i(t) = \sum_{f=-D}^{\infty} I_{if}(t) = \sum_{f=-D}^{\infty} [\gamma_i(t) - \gamma_f(t)]\, C_{if} \tag{3.10}$$

$$\equiv [\gamma_c(t) - \gamma_s(t)] \int_{-D}^{\infty} (P_f^S - P_i^S)\, C_{if}\, dE_f \tag{3.11}$$

$$= 0, \quad i = 1, 2, N \tag{3.12}$$

which[7] is Kirchoff's current law (KCL). The balance of currents I_{if} which exits and enters any junction i within block

$\mathscr{B}$ ($1<i<N$) to all junctions ($f=N+1, N+2,..\infty$, in block $\mathscr{C}$, $f=1,2,...,N$ in block $\mathscr{B}$ and $f=0,-1,..,-D$ in block $\mathscr{S}$) of the network is zero. This expresses *charge conservation* at junction i where there is no net buildup of density (charge) n_i. The ansatz (2.17) which enables the QSS condition (2.12) to be satisfied by a specified distribution P_i^S at all times provides the separation in Eqs. (3.3), (3.5), and (3.10b).

Under KCL or QSS, the voltages P_i^S satisfy

$$P_i^S \int_{-D}^{\infty} C_{if}\, dE_f = \int_{-D}^{0} C_{if}\, P_f^S\, dE_f . \tag{3.11}$$

The time-dependent $\mathscr{C}$ and $\mathscr{S}$ blocks of states are analogous to capacitors connected in parallel with their positive plates charged to

$$Q_1(t) = n_c(t) = \int_0^{\infty} n_i(t) dE_i \tag{3.12}$$

and

$$Q_2(t) = n_s(t) = \int_{-D}^{-S} n_i(t) dE_i , \tag{3.13}$$

at time t and held at voltages

$$V_1(t) = \gamma_c(t) \tag{3.14}$$

and

$$V_2(t) = \gamma_s(t) \tag{3.15}$$

above their negative plates. Since $Q = C/V$, their capacitances

$$C_1 = \tilde{n}_c = \int_0^{\infty} \tilde{n}_i\, dE_i \tag{3.16}$$

and

$$C_2 = \tilde{n}_s = \int_{-D}^{-S} \tilde{n}_i\, dE_i \tag{3.17}$$

are constant. The external capacitor $C_1 \equiv \mathscr{C}$ is connected to internal KCL node f (or energy level) by equivalent resis-

$$\frac{1}{R_{Cf}} = \sum_{i=N+1}^{\infty} \frac{1}{R_{if}} \equiv \int_0^{\infty} C_{if}\, dE_i = C_{Cf} \tag{3.18}$$

and directly to the external capacitor $C_2 \equiv \mathscr{S}$ by a resistance R_{CS} given by

$$\frac{1}{R_{CS}} = \sum_{i=N+1}^{\infty} \sum_{f=-D}^{0} \frac{1}{R_{if}}$$

$$\equiv \int_0^{\infty} dE_i \int_{-D}^{-S} C_{if}\, dE_f = C_{CS} . \tag{3.19}$$

Each internal KCL node i of block $\mathscr{B}$ is coupled to internal node f by R_{if} and externally coupled to C_2 via R_{iS} given by

$$\frac{1}{R_{iS}} = \sum_{f=-D}^{0} \frac{1}{R_{if}} \equiv \int_{-D}^{-S} C_{if}\, dE_f = C_{iS} . \tag{3.20}$$

The above resistances R_{Cf}, R_{iS}, and R_{CS} are equivalent to a parallel network of resistances R_{if} connecting, respectively, all states $C(i=N+1,...,\infty)$ of block $\mathscr{C}$ to the specified $\mathscr{B}$-block state f, each $\mathscr{B}$-block state i to all states $S(f=0,-1,...,-D)$ of block $\mathscr{S}$ and all states C to all states S, respectively. The electrical network which corresponds to the Master equation (3.10) for association is illustrated by Fig. 5. A time-varying current $I(t)$ from capacitor C_1 with initial charge $Q_1(0) = n_c(0)$ is subdivided along mainline channels R_{Cn} to enter a KCL network with N nodes, composed entirely of resistors R_{nj} and internal currents $I_{nj}(t)$, and is then reconstituted at C_2 via mainline exit channels R_{fS}.

B. Principle of least dissipation

The network of resistances R_{CS}, R_{Cf}, R_{iS}, and R_{if} may now be replaced by an equivalent resistance R with throughput current $I(t)$ determined from the power loss

$$I(t)^2 R = [\gamma_c(t) - \gamma_s(t)] I(t) \tag{3.21}$$

$$= \sum_{n=-D}^{\infty} \sum_{f>n}^{\infty} I_{nf}^2 R_{nf} \tag{3.22}$$

to be

$$I(t) \equiv \frac{1}{2} [\gamma_c(t) - \gamma_s(t)]$$

$$\times \int_{-D}^{\infty} dE_i \int_{-D}^{\infty} (P_i^S - P_f^S)^2\, C_{if}\, dE_f . \tag{3.23}$$

The summations include external junctions $C(n=N+1,N+2,...,\infty)$ and $S(n=-D,-D+1,...,0)$ at the source and sink capacitors and the internal junctions ($n=1,2,...,N$). By comparison with Eq. (2.20), the association rate $R^A(t)$ may now be identified with the electrical current $I(t)$ of Eq. (3.23), and the rate constant identified with

$$\alpha \tilde{N}_A \tilde{N}_B = \frac{1}{2} \int_{-D}^{\infty} dE_i \int_{-D}^{\infty} (P_i^S - P_f^S)^2\, C_{if}\, dE_f , \tag{3.24}$$

the effective conductivity R^{-1} of the network, or with the time-dependent electrical current $I(t)$, Eq. (3.23), per unit

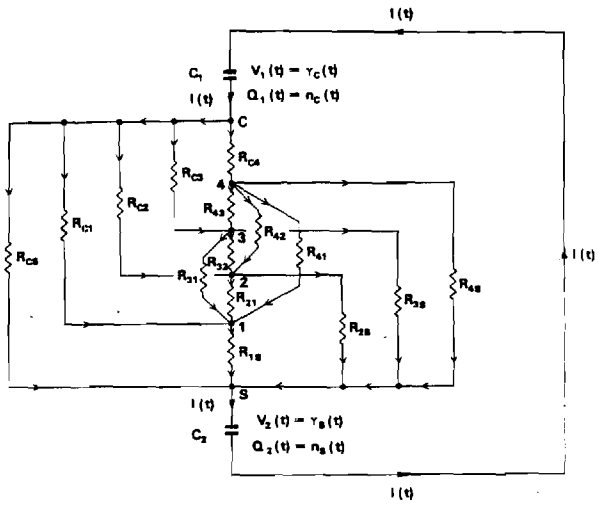

FIG. 5. (R,C) electrical diagram analogous to termolecular recombination.

voltage drop $[\gamma_c(t)-\gamma_s(t)]$. When the KCL condition (3.11) is used directly in Eq. (3.24) then the previous results (2.25) are obtained.

The power loss

$$I^2(t)R=[\gamma_c(t)-\gamma_s(t)]\,R^{A}(t)\geqslant 0 \tag{3.25}$$

is always positive. The present variational principle (VP) asserts that P_i^S, the voltage drop in units of $(\gamma_c-\gamma_s)$, are so distributed that the rate $R^A(t)$—the electrical current $I(t)$—is a minimum. When $\gamma_c(t)>\gamma_s(t)$, i.e., association occurs at positive rate $R^A(t)$, then VP implies that the power (3.25) dissipated by (A–B) and absorbed by the gas M is least. When R^A is negative, the net direction is dissociation which occurs at rate $R^D(t)=-R^A(t)$ when $\gamma_c<\gamma_s$, then VP implies that the power provided to AB *by* the gas M is least.

This principle of least dissipation is basic in many fields, e.g., thermodynamics, heat conduction, fluid mechanics. The principle for heat conduction was derived explicitly by Onsager.[13] For a current I entering a KVL and a KCL electrical network via R_{Cn} and exiting via R_{nS}, the currents within the KCL network are so distributed that the summed rate of dissipation of energy in the R_{Cn}, R_{nj}, and R_{nS} resistors is a minimum—Joule's law. With this law, Bates[7] postulated that a minimum would exist in the measure $\mathscr{M}$, Eq. (1.3) of the restoration rate of thermodynamic equilibrium by recombination in highly nonequilibrium systems [when $\gamma_c\gg\gamma_s$ and $\gamma_i=P_i^D$ in Eq. (2.17) so that explicit time dependences can be ignored[5]]. Mendaš[8] then noted that the distributions n_i associated with this minimum satisfy the QSS condition (1.4). From Eq. (3.23) it follows that this unnormalized time-independent measure $\mathscr{M}$ may now be uniquely identified as the rate $2\alpha\tilde{N}_A\tilde{N}_B$ so that the minimum of $\mathscr{M}$ yields the minimum rate (2.25a) directly, without the further need for substituting the final variational function $P_i^D=1-P_i^S$ in expression (2.23) for the current (2.25a) or in Eq. (1.5).

The present assertion that the rates (2.2) and (2.5) are extremum implies a principle of least dissipation for chemical reactions. The rates $R^{A,D}(t\to\infty)$ tend naturally to zero when thermodynamic equilibrium is obtained for the complete system. This is analogous to the electrical current I decaying to zero when the voltages across the capacitors C_1 and C_2 connected in series across R become equal.

C. Use of diagram

Various QSS results may be deduced rather readily from consideration of the electrical diagram (Fig. 5).

Result I: The mainline entrance current along R_{Cn} and entering KCL node n is

$$i_n^-=P_n^S\,C_{Cn} \tag{3.26}$$

in units of $(\gamma_c-\gamma_s)$. The total mainline current which enters all N nodes of KCL block $\mathscr{C}$ and node $n=0$ of block $\mathscr{S}$ from block $\mathscr{C}$ is

$$\alpha\tilde{N}_A\tilde{N}_B=\sum_{n=0}^{N}i_n^-\equiv\int_{-D}^{0}C_{Cf}\,P_f^S\,dE_f \tag{3.27}$$

which is the association rate $R^A(t)$ in units of $[\gamma_c(t)-\gamma_s(t)]$ in agreement with Eq. (2.25b).

Result II: The current which exits KCL node n along the internal resistors R_{nf} and external resistors R_{nS} of Fig is

$$i_n^+=\sum_{f=0}^{N}(P_n^S-P_f^S)\,C_{nf}. \tag{3.2}$$

The total current exiting from all N-KCL nodes is then

$$\sum_{n=1}^{N}i_n^+=\sum_{n=1}^{N}(1-P_n^S)\,C_{ns}\equiv\int_{-S}^{0}C_{Sf}\,P_f^D\,dE_f \tag{3.2}$$

which when combined with the $\mathscr{C}$–$\mathscr{S}$ direct curre $i_0=C_{CS}$ yields

$$k\,\tilde{n}_s=\int_{-S}^{\infty}C_{Sf}\,P_f^D\,dE_f \tag{3.3}$$

in agreement with Eq. (2.25c). The KCL l $I_n=i_n^+-i_n^-=0$, Eq. (3.10) applied to nodes $n=1,2,...$ not only confirms the QSS condition (2.25) but also mands equality of Eqs. (3.27) and (3.30), which provi macroscopic detailed balance.

Result III: From Fig. 5, the total mainline entrance c rent to nodes below a designated KCL node N^*:

$$i_*^-(<N^*)=\sum_{n=0}^{N^*}i_n^-\equiv\int_{-D}^{-E}C_{Cf}\,P_f^S\,dE_f, \tag{3.3}$$

where the junction N^* is associated with energy level — The internal and mainline exit currents from nodes above sum to

$$i_*^+\ (>N^*)=\sum_{n=N^*}^{N}i_n^+=\sum_{n=N^*}^{N}\sum_{f=0}^{N}(P_n^S-P_f^S)\,C_{nf} \tag{3.}$$

$$\equiv\int_{-E}^{0}dE_i\int_{-D}^{0}(P_f^S-P_i^S)\,C_{if}\,dE_f \tag{3.}$$

which reduces to

$$i_*^+=\int_{-E}^{0}dE_i\int_{-D}^{-E}(P_f^S-P_i^S)\,C_{if}\,dE_f. \tag{3.}$$

Since $i_n^+=i_n^-$ for each KCL node the total cur $(i_*^++i_*^-)$ in units of $[\gamma_c(t)-\gamma_s(t)]$ is

$$\alpha\tilde{N}_A\tilde{N}_B=\int_{-E}^{0}dE_i\int_{-D}^{-E}(P_f^S-P_i^S)\,C_{if}\,dE_f \tag{3.}$$

in agreement with Eqs. (2.23) and (2.25).

Result IV: When C_1 with charge $Q_1(t)$ gains a cha dQ_1 and C_2 with charge $Q_2(t)$ gains a charge dQ_2 on t positive plates within time dt, the sum of the total elec static energy $(V_1dQ_1+V_2dQ_2)$ gained by the capacitors the thermal energy (3.21) radiated must be zero. Since charge

$$q_i=n_i(t)=n_i(0),\quad i=1,2,...,N \tag{3.}$$

at each junction i of the N junction KCL network rem constant then the total charge distributed among the cap tors of initial charges Q_{10} and Q_{20} is

$$Q_1(t)+Q_2(t)=Q_{10}+Q_{20} \tag{3.}$$

and the discharging/charging current is

$$I=-\frac{dQ_1(t)}{dt}=\frac{dQ_2(t)}{dt}. \tag{3.}$$

Hence the power equation is

$$(V_1 - V_2)\left[\frac{dQ_1}{dt}\right] + I^2R = 0 \tag{3.39}$$

which also follows from application of KVL, Eq. (3.9), to the (C_1,R,C_2) circuit at time t. Hence

$$R^{\mathcal{A}}(t) = -\frac{dQ_1(t)}{dt} = \frac{dQ_2(t)}{dt}$$

$$= \frac{1}{R}\left[Q_1(t)/C_1 - Q_2(t)/C_2\right] \tag{3.40}$$

which is the analog of Eq. (2.20) with $R^{-1} = \alpha\tilde{N}_{\mathrm{A}}\,\tilde{N}_{\mathrm{B}}$, $\gamma_c = Q_1(t)/C_1$, and $\gamma_s = Q_2(t)/C_2$. The equation is linear (rather than quadratic) in Q_1 since Eq. (2.7) renders the basic equation (2.2) linear in the (pair) distribution (3.12) of dissociated species AB. The solution of Eq. (3.40) subject to C_1 being initially uncharged ($Q_{10} = 0$) is

$$Q_1(t) = Q_{20}(C/C_2)\left[1 - \exp - t/RC\right]$$

$$\overset{t\to\infty}{\to} \frac{C_1}{(C_1 + C_2)}\,Q_{20} \tag{3.41}$$

and

$$Q_2(t) = Q_{20}\left[1 - (C/C_2)(1 - \exp - t/RC)\right]$$

$$\overset{t\to\infty}{\to} \frac{C_2}{(C_1 + C_2)}\,Q_{20}\,, \tag{3.42}$$

where C is $C_1C_2/(C_1 + C_2)$. As $t\to\infty$, the voltages across each pair of plates, $\gamma_c = Q_1/C_1$ and $\gamma_s = Q_2/C_2$ are equal (and opposite), no current flows and charging is complete (corresponding to thermodynamic equilibrium). When C_1 has infinite capacity for absorbing charge, i.e., when $C_1 \gg C_2$ then $C\to C_2$ so that

$$Q_1(t)\to Q_{20}(1 - \exp - t/RC_2) \tag{3.43}$$

and

$$Q_2(t)\to Q_{20}\exp - t/RC_2\,, \tag{3.44}$$

so that the dissociation frequency k can be related to the time constant for discharging of C_2 and charging of C_1 by

$$k = 1/RC_2 \tag{3.45}$$

as expected (since $C_2 = \bar{n}_s$ and $1/R = \alpha\tilde{N}_{\mathrm{A}}\,\tilde{N}_{\mathrm{B}} = k\bar{n}_s$). This rate constant governs only the rate of approach to, but not the magnitude of, the asymptotic limits.

In summary, appeal to the network (Fig. 5) provides results (3.27), (3.30), and (3.35) which are exact under KCL condition (3.11). For voltages which do not satisfy this KCL condition, then Eq. (3.24) is used for the electrical current in units of $(\gamma_c - \gamma_s)$.

IV. SUMMARY

A variational principle based on the search for a minimum to the net rate $R^{\mathcal{A}}(t)$ for association with respect to variation of the stabilization probabilities P_i^S has been proposed. It is capable (Sec. II B) of providing probabilities P_i^S and rate coefficients α identical with those determined from direct QSS solutions of the Master equation. In this sense the developed expression (2.21) provides a variational expression for the QSS approximation. Good trial representations (Sec. II B) for P_i^S exhibit a maximum in $|dP_i^S/dE_i|$ near the location E_i^* of a physical bottleneck.

By introduction of the additional block $\mathscr{E}$ of highly excited levels i sandwiched between the reactant and product zones $\mathscr{C}$ and $\mathscr{S}$, respectively, and characterized by forward and reverse (variational) probabilities P_i^S and P_i^D, respectively, the present variational method is more detailed and complete than the least-upper-bound variational method of Wigner[1] and Keck[2] which ignores this block.

The minimum with respect to variation in n_i of function (1.3) postulated by Bates[7] via analogy with an electrical network is identified here with $2\alpha\tilde{N}_{\mathrm{A}}\,\tilde{N}_{\mathrm{B}}$ so that the supplementary explicit calculation of the rate (1.5) is not required. Electrical diagrams (as Fig. 5) may be utilized very effectively not only to analyze (Sec. III C) the detailed dynamics of termolecular processes but also to facilitate the ready construction of various simplified approximate schemes.[14]

ACKNOWLEDGMENT

This research is supported by the U. S. Air Force Office of Scientific Research under Grant No. AFOSR-84-0233.

[1]E. P. Wigner, J. Chem. Phys. **5**, 720 (1937).
[2]J. C. Keck, J. Chem. Phys. **32**, 1035 (1960).
[3]S. Byron, R. C. Stabler, and P. I. Bortz, Phys. Rev. Lett. **8**, 376 (1962).
[4]B. Makin and J. C. Keck, Phys. Rev. Lett. **11**, 281 (1963).
[5]M. R. Flannery, J. Chem. Phys. **87**, 6947 (1987).
[6]M. R. Flannery and E. J. Mansky, J. Chem. Phys. **88**, 4228 (1988), and Refs. 1–3 therein.
[7]D. R. Bates, Proc. R. Soc. London. Ser. A **337**, 15 (1974).
[8]I. Mendaš, J. Phys. B **12**, L209 (1979).
[9]M. R. Flannery, J. Phys. B **18**, L839 (1985).
[10]See, for example, G. Arfken, *Mathematical Methods for Physicists*, 3rd ed. (Academic, New York, 1985), p. 937.
[11]D. R. Bates and I. Mendaš, J. Phys. B **15**, 1949 (1982).
[12]M. R. Flannery and E. J. Mansky (work in progress).
[13]L. Onsager, Phys. Rev. **37**, 405 (1931).
[14]M. R. Flannery and E. J. Mansky, J. Chem. Phys. (to be published).

3.3. Diffusional Treatment.

Diffusional theory of termolecular recombination and association of atomic species in a gas

M. R. Flannery
School of Physics, Georgia Institute of Technology, Atlanta, Georgia 30332

(Received 10 June 1987; accepted 10 September 1987)

A diffusional treatment of termolecular association of atomic species A and B in a low density gas is presented and applied to positive ion–negative ion recombination over the full range of masses of reactants for various classes of ion–neutral interactions. In contrast to rates given by the diffusional current, excellent results are obtained for general mass species *provided* a more basic expression for the association rate is introduced.

I. INTRODUCTION

The picture of electron–ion recombination, of termolecular positive ion–negative ion recombination, and of termolecular ion–atom association:

$$\mathrm{A} + \mathrm{B} + \mathrm{M} \underset{k}{\overset{\alpha}{\rightleftarrows}} \mathrm{AB} + \mathrm{M}, \tag{1.1}$$

involving subsystems (A–B) associating in a thermal bath of dilute gas M as proceeding via diffusion in energy space has stimulated[1–7] a great deal of interest, in principle, valuable to elucidation of the dynamics of association processes and to many examples of decay of laser-produced plasmas, of reaction processes in flames, of shock wave propagation, etc. In a classic paper on electron–ion recombination, Pitaevskii[1] derived a rather elegant analytical expression for the two-body rate coefficient α ($\mathrm{cm}^3\,\mathrm{s}^{-1}$) in Eq. (1.1). Because of its inherent simplicity over more sophisticated and therefore time consuming procedures based on a collisional input–output Master equation,[8–12] the result has been applied to heavy-particle recombination[3–5] which proceeds three orders of magnitude faster than collisional electron–ion recombination[1,7] for which the result was originally intended. In spite of its attractive features, the diffusion picture as formulated[1–6] achieved remarkably disappointing results for heavy-particle termolecular ion–ion recombination.[3–6]

Apart from recognition that diffusion methods (based on a Fokker–Planck reduction of the input–output collision integral) are likely to be valid only when the collisional changes in energy are small, the basic intrinsic defect for application of the Pitaevskii expression to general mass sytems remains as yet undetected. Moreover, that a much less sophisticated "bottleneck" model[13] originally designed also for electron–ion recombination achieved much closer agreement[10] with the exact results of the Master equation[8–10] for ion–ion recombination presents a puzzle.

In this paper, the foundation of the diffusion approach as applied to processes (1.1) will be examined and the basic defect in previous applications will become apparent. The proposed theory is valid for termolecular ion–ion recombination[8–11] and ion–atom association[14] at low gas densities and as a case study will be applied here to ion–ion recombination. Association at rate coefficient α ($\mathrm{cm}^3\,\mathrm{s}^{-1}$) and dissociation at frequency k (s^{-1}) in Eq. (1.1) are treated in a unified way so that equilibrium can eventually be established.

II. RATES AND CURRENT

The distribution $n_i(E_i,t)$ per unit interval dE_i of pairs AB with internal energy E_i at time t is governed by the collisional input–output Master equation[2,8–11,15]

$$\frac{d}{dt} n_i(E_i,t) = -\int_{-D}^{\infty} S_{if}\, dE_f = -\int_{-D}^{\infty} [n_i(t)\nu_{if} - n_f(t)\nu_{fi}]\, dE_f, \tag{2.1}$$

where $-D$ is the energy of the lowest vibrational level of AB relative to the dissociation limit taken as zero energy, and where ν_{if} is the frequency per unit interval dE_f for $E_i \to E_f$ transitions by collisions between AB and M. For bound states $dn_i/dt = \partial n_i/\partial t$, and for dissociated states $dn_i/dt = (\partial n_i/\partial t + F_i)$ where F_i is the net flux of contracting E_i pairs created with infinite separation. A basic expression for the rate $R^A(t)$ of association has already been derived.[16] In the interests of elucidation and completeness of the present discussion (in Secs. III C and IV) and of direct comparison with the diffusional quasi-steady-state approach, the key steps therein are provided below. The first step involves writing the net rate for association as[16]

$$R^A(t) = \int_{-D}^{\infty} P_i^S \left(\frac{dn_i}{dt}\right) dE_i = \alpha N_A(t) N_B(t) - k n_s(t), \tag{2.2}$$

where P_i^S is the probability of stabilization of E_i pairs by subsequent multicollisions with M. The effective two-body rate constant for the association of A and B with (cm^{-3}) concentrations $N_A(t)$ and $N_B(t)$ is α ($\mathrm{cm}^3\,\mathrm{s}^{-1}$), and k (s^{-1}) is the frequency for dissociation of those tightly bound pairs of concentration $n_s(t)$ which are considered to be fully associated with energies E_i within a block of $\mathscr{S}$ of low lying levels in a range $-S > E_i > -D$ within which the stabilization probability P_i^S is calculated to be unity.

The separation between the energy levels of AB is sufficiently small compared to the thermal energy (kT) of the gas bath so that the levels form a quasicontinuum. Thus,

$$\frac{d}{dt} n_i(E_i,t) = -\frac{\partial}{\partial E_i} J(E_i,t), \tag{2.3}$$

so that the upward current past level E at time t is

$$J(E,t) = \int_E^{\infty} dE_i \int_{-D}^{E} S_{fi}(t) dE_f, \tag{2.4}$$

since J vanishes at the end points $(-D,\infty)$ and since $S_{if} + S_{fi} = 0$.

On introducing the normalized distribution

$$\gamma_i(t) = n_i(E_i,t)/\tilde{n}_i(E_i), \tag{2.5}$$

where $\tilde{n}_i$ is the pair distribution under full thermodynamic equilibrium with the gas, the Master equation (2.1) is

$$\frac{d}{dt} n_i(E_i,t) = -\int_D^{\infty} [\gamma_i(t) - \gamma_f(t)] C_{if}\, dE_f$$

$$= -\frac{\partial}{\partial E_i} J_i(E_i,t), \tag{2.6}$$

where the one-way equilibrium collisional rate

$$C_{if} = \tilde{n}_i \nu_{if} = \tilde{n}_f \nu_{fi} = C_{fi} \tag{2.7}$$

satisfied detailed balance. The second step is to introduce the ansatz[16]

$$\gamma_i(t) = P_i^D \left[\frac{N_A(t) N_B(t)}{\tilde{N}_A \tilde{N}_B}\right] + P_i^S \left[\frac{n_s(t)}{\tilde{n}_s}\right]$$

$$\equiv P_i^D \gamma_c(t) + P_i^S \gamma_s(t) \overset{t\to\infty}{\to} 1, \tag{2.8}$$

which holds at low gas densities. The equilibrium concentrations of A and B are $\tilde{N}_A$ and $\tilde{N}_B$. The probability that state i is a stabilized state, or is a destabilized state with respect to association is P_i^S or $P_i^D = 1 - P_i^S$, respectively, and γ_c and γ_s are the normalized distribution of pairs in the fully dissociated (source) block $\mathscr{C}$, $0 \leqslant E_i < \infty$, where P_i^D is unity, and in the fully associated (sink) block $\mathscr{S}$, $-S > E_i > -D$, where P_i^S is unity. Hence, the Master equation (2.6), current (2.4), and rate (2.2) separate as[16]

$$\frac{dn_i}{dt} = [\gamma_c(t) - \gamma_s(t)]$$

$$\times \int_{-D}^{\infty} (P_i^S - P_f^S) C_{if}\, dE_f = -\frac{\partial J_i}{\partial E_i}, \tag{2.9}$$

$$J(-E,t) = [\gamma_c(t) - \gamma_s(t)]$$

$$\times \int_{-E}^{\infty} dE_i \int_{-D}^{-E} (P_f^S - P_i^S) C_{if}\, dE_f, \tag{2.10}$$

and

$$R^A(t) = [\gamma_c(t) - \gamma_s(t)]$$

$$\times \int_{-D}^{\infty} P_i^S\, dE_i \int_{-D}^{\infty} (P_i^S - P_f^S) C_{if}\, dE_f. \tag{2.11}$$

From Eq. (2.9), the loss rates of fully dissociated and of fully associated species of energy E_i are, respectively,

$$-\frac{dn_i}{dt} = [\gamma_c(t) - \gamma_s(t)]$$

$$\times \int_{-D}^{0} C_{if} P_f^S\, dE_f, \quad E_i > 0 \tag{2.12}$$

and

$$-\frac{dn_i}{dt} = [\gamma_s(t) - \gamma_c(t)]$$

$$\times \int_{-S}^{\infty} C_{if} P_f^D\, dE_f, \quad -S > E_i > -D, \tag{2.1}$$

which illustrate quite effectively the significance of both stabilization and disruption probabilities P_f^S and P_f^D.

From Eqs. (2.9) and (2.10),

$$\frac{dn_i}{dt} = -[\gamma_c(t) - \gamma_s(t)] \left(\frac{\partial j_i}{\partial E_i}\right), \tag{2.}$$

where the time-independent background current downw across E is

$$-j(-E) = \int_{-E}^{\infty} dE_i \int_{-D}^{-E} (P_f^S - P_i^S) C_{if}\, dE_f. \tag{2.}$$

From Eq. (2.11) the time-independent macroscopic co cients α and k for association and dissociation in Eq. (are, therefore, given by the basic expression,

$$\alpha \tilde{N}_A \tilde{N}_B = \int_{-D}^{\infty} P_i^S\, dE_i \int_{-D}^{\infty} (P_i^S - P_f^S) C_{if}\, dE_f = \tag{2}$$

and satisfy (macroscopic) detailed balance.

The expressions (2.10) and (2.11), or equivalently (2.15) and (2.16) for the current j and rate coefficient α in general not identical unless the following additiona quirement is satisfied.

A. Quasi-steady-state (QSS)

As Eqs. (2.12) and (2.13) illustrate, the distributio pairs in blocks $\mathscr{C}$ and $\mathscr{S}$ are time dependent, until full t modynamic equilibrium is established when $\gamma_{c,s} \to 1$ f above and below, respectively. Since $dn_i/dt = \partial n_i/\partial t$ the intermediate block $\mathscr{E}$ of highly excited levels with en E_i in the range $0 > E > -S$ then quasi-steady-state (QS block $\mathscr{E}$ requires

$$\frac{dn_i}{dt} = 0, \quad 0 > E_i > -S \tag{2}$$

so that the stabilization probabilities in Eq. (2.9) then r ously satisfy the integral equation

$$P_i^S \int_{-D}^{\infty} C_{if}\, dE_f = \int_{-D}^{0} C_{if} P_f^S\, dE_f; \quad 0 > E_i > -S. \tag{2}$$

The stochastic probability for stabilization P_i^S of s is therefore the fraction of all collisions which event result in association. Under this circumstance it readil lows that the rate (2.11) reduces to

$$R^A(t) = -J(-E,t), \tag{2}$$

the downward current (2.10), and that the rate coeff (2.16) is given by

$$\alpha \tilde{N}_A \tilde{N}_B = -j(-E), \tag{2}$$

where E is an arbitrary energy level in bloc $(0 > E > -S)$.

The rate of association (2.16) may be identified wi

current (2.15) only when the QSS-condition (2.17) for the probabilities is satisfied.[16] Use of Eq. (2.17) from the outset in Eq. (2.2) also illustrates this relation,

$$R^{A}(t) = \int_{-D}^{-S} \left(\frac{dn_i}{dt}\right) dE_i$$
$$= -J(-S,t) = -J(-E,t), \tag{2.21}$$

although the basic expression (2.16) for α cannot then be deduced. An exact expression which emphasizes the role of the current J is obtained from Eqs. (2.2) and (2.3) to give

$$R^{A}(t) = -\int_{-D}^{\infty} P_i^S \left(\frac{\partial J_i(t)}{\partial E_i}\right) dE_i$$
$$= \int_{-S}^{0} J_i(t) \left(\frac{\partial P_i^S}{\partial E_i}\right) dE_i, \tag{2.22}$$

since J_i vanishes as $E_i \to -D$ and ∞, and since P_i^S is constant (0 and 1 within blocks $\mathscr{C}$ and $\mathscr{S}$, respectively). Only when Eq. (2.10) for J is constant over block $\mathscr{E}$, i.e., when QSS Eq. (2.18) is satisfied, does Eq. (2.22) reduce to Eq. (2.19). It may be shown (work in progress) that the QSS-condition (2.18) corresponds to a minimum[18] in Eq. (2.16) for α. Any approximate P_i^S which does not rigorously satisfy Eq. (2.18) will therefore yield higher rates α.

The QSS (minimum) rate coefficients are therefore given by

$$\alpha_* \bar{N}_A \bar{N}_B$$
$$= \int_{-E}^{\infty} dE_i \int_{-D}^{-E} (P_f^S - P_i^S) C_{if}\, dE_f = -j(-E) \tag{2.23}$$
$$= \int_{0}^{\infty} dE_i \int_{-D}^{0} C_{if} P_f^S\, dE_f = -j(0) \tag{2.24}$$
$$= \int_{-D}^{-S} dE_i \int_{-S}^{\infty} C_{if} P_f^D\, dE_f = -j(-S) = k_* \tilde{n}_s, \tag{2.25}$$

which are, in general, different from Eq. (2.16) *unless* the probabilities P_f^S *exactly* satisfy[16] the QSS-condition (2.18). Note that Eq. (2.24) is the QSS rate for association that would result from the full equilibrium concentration $\tilde{N}_A \tilde{N}_B$ of dissociated pairs and zero population of fully associated $\mathscr{S}$ pairs i.e., $\gamma_c = 1$ and $\gamma_s = 0$ in Eq. (2.8). Similarly, Eq. (2.25) is the QSS rate for dissociation which would result from an equilibrium population $\tilde{n}_s$ of associated $\mathscr{S}$ pairs and zero population of dissociated pairs, i.e., $\gamma_c = 0$ and $\gamma_s = 1$ in Eq. (2.8).

The aim is now to derive a simple analytic but approximate expression for $j(-E)$ by converting Eq. (2.15) from an integral representation to a differential representation so that approximate expressions for the probabilities P_i^S may be derived, in contrast to the exact numerical solutions of Eq. (2.18).

III. FOKKER–PLANCK REDUCTION FOR ION–ION RECOMBINATION AT LOW GAS DENSITIES

The conversion of the integral operator in Eq. (2.13) into a differential operator achieved by a Fokker–Planck analysis[1,2] is useful when the collision kernel C_{if} favors small changes in energy. Here the current J_i in Eq. (2.6) can be determined to fourth order, rather than to the customary second order.[2]

A. Fokker–Planck current to fourth order in energy-change moments

On introduction of an arbitrary but well-behaved function $\Phi_i(E_i)$ whose derivatives vanish at the end points $[\infty, -D]$, then, with the aid of Eq. (2.6),

$$\int_{-D}^{\infty} \Phi_i \frac{dn_i}{dt} dE_i$$
$$= \int_{-D}^{\infty} \gamma_i\, dE_i \int_{-D}^{\infty} (\Phi_f - \Phi_i) C_{if}\, dE_f. \tag{3.1}$$

On expanding the difference

$$\Phi_f - \Phi_i = \sum_{n=1}^{\infty} \frac{1}{n!} (E_f - E_i)^n \left[\frac{\partial^n \Phi_i}{\partial E_i^n}\right] \tag{3.2}$$

as a Taylor series in energy change $(E_f - E_i)$, assumed small, and on integration by parts with the explicit recognition that $(\partial^n \Phi_i / \partial E_i^n) \to 0$ for $n \geq 1$ as $E_i \to [\infty, -D]$, then Eq. (3.1) can be expressed as

$$\int_{-D}^{\infty} \Phi_i \frac{dn_i}{dt} dE_i = [J_i \Phi_i]_{-D}^{\infty} - \int_{-D}^{\infty} \Phi_i \frac{\partial J_i}{\partial E_i} dE_i, \tag{3.3}$$

where the current is

$$J_i(E_i,t) = \sum_{n=0}^{\infty} (-1)^n \frac{\partial^n [\gamma_i D_i^{(n+1)}]}{\partial E_i^n} \tag{3.4}$$

in terms of the normalized distributions γ_i and the energy change moments[2-4]

$$D_i^{(m)}(E_i) = \frac{1}{m!} \int_{-D}^{\infty} (E_f - E_i)^m C_{if}\, dE_f, \tag{3.5}$$

with respect to the one-way equilibrium rate for $E_i \to E_f$ transitions. The number per second of all collisions with an equilibrium distribution of E_i pairs in unit interval dE_i and unit volume is $D_i^{(0)}$; and $D_i^{(1)}$ and $2D_i^{(2)}$ are the average energy change and average energy change squared *per second*, $d\langle \Delta E \rangle / dt$ and $d\langle \Delta E^2 \rangle / dt$, respectively. The ratios $D_i^{(1)}/D_i^{(0)}$ and $2D_i^{(2)}/D_i^{(0)}$ specify $\langle \Delta E_i \rangle$ and $\langle \Delta E_i^2 \rangle$ *per collision*, respectively.

Evaluation of these moments can be facilitated by adopting the expressions for C_{if} which correspond to various A–M and B–M binary interactions (symmetrical resonance charge–transfer,[8-10] hard-sphere,[10] polarization[11]). They can be collected under a universal form (work in progress). These moments are normalized[10] to the quantity $(-1)^m \Gamma \alpha_T (kT)^{m-1} \tilde{N}_A \tilde{N}_B$ where α_T is the Thomson rate [Eq. (4.1) below], where Γ is a dimensionless mass factor[10] and where T is the temperature of the gas bath.

Figures 1(a) and 1(b) illustrate the general trend of these moments calculated here for the specific case[8,10] where internal-energy changes in an ion pair (X^+–X^-) are due to symmetrical resonance charge–transfer ($X^{\pm}$–X) collisions with a parent gas X. In this case, the velocity vectors of the

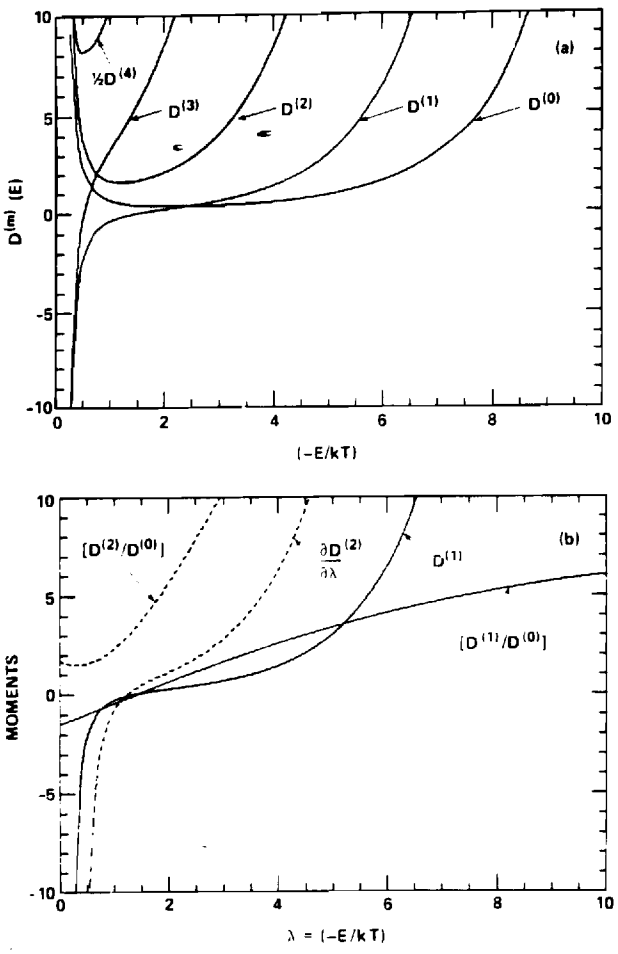

FIG. 1. (a) Normalized moments $D^{(m)}$ of energy change rate (energy^m s^{-1}), $m = 0$–4, as a function of internal energy $E_i = -\lambda(kT)$ of the bound ion pair. (b) Averaged energy change and energy-change squared $D^{(m)}/D^{(0)}$ per collision, $D^{(1)}$ and derivative of $D^{(2)}$. Equal-mass species and charge-transfer ion–neutral collisions are assumed and moments are normalized to the quantity $(-1)^m \Gamma \alpha_T (kT)^{m-1} \bar{N}_A \bar{N}_B$.

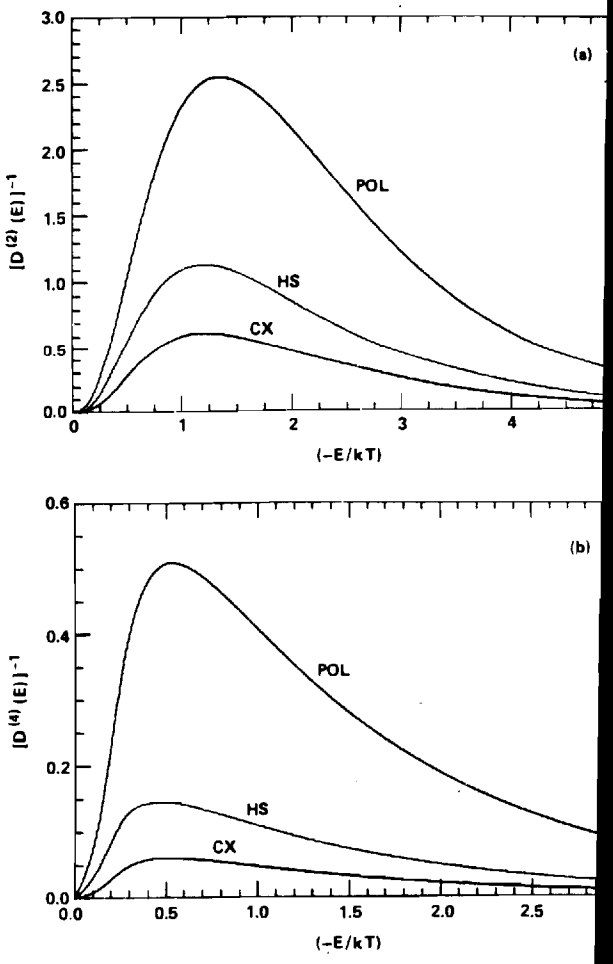

FIG. 2. Inverses of moments (a) $D^{(2)}(\lambda)$ and (b) $D^{(4)}(\lambda)$ as a functi internal energy $E_i = -\lambda kT$ of the ion pair for various ion–neutral int tions: POL (polarization), HS (hard-sphere), CX (charge–trans Equal mass species are assumed.

(fast) ion X^+ and the (thermal) neutral X are interchanged.[8] Large transfers of energy are therefore involved, as is confirmed by $D_i^{(2)}$, the averaged energy change squared $\langle \Delta E_i^2 \rangle$ *per second* shown in Fig. 1(a). This case will therefore provide a most stringent test of the weak-collision (diffusion) procedure adopted here.

As the binding energy $-E_i$ decreases from the dissociation limit (at zero energy), the equilibrium density $\bar{n}(E_i) \sim |E_i|^{-5/2} \exp(-E_i/kT)$ per unit interval dE_i decreases from infinity, reaches a minimum at $E_i = -2.5kT$ and then increases exponentially.[10] Since the energy change frequency ν_{if} for each pair decreases rapidly with increase of binding, the overall shapes of the equilibrium moments $D_i^{(m)}$ in Figs. 1(a) and 1(b) reflect the variation of the product $\bar{n}_i \nu_{if}$. Note that the equilibrium collisional rate $D_i^{(0)}$ is relatively constant in the range (1.8–4)kT of binding. Also $D_i^{(1)} \approx d/dt \langle \Delta E \rangle$ is positive for $E_i > -1.4kT = E^*$, so that these pairs on average become less tightly bound upon collision. Pairs with $E_i < -1.4kT$ become more tightly bound upon collision (since $D_i^{(1)} < 0$). This critical energy speci the location of E^* of a bottleneck where the averaged ene change vanishes and where the region $E_i > E^*$ where exc tion is greater is separated from the region $E_i < E^*$ wh deexcitation is greater. Note also that the even mom $D_i^{(m)}$ display minima which become sharper with increas m, as expected, and that the minimum in $D_i^{(2)} \approx$ $dt \langle \Delta E_i^2 \rangle$ coincides with the zero of $D_i^{(1)} \sim d/dt \langle \Delta E_i$ E^*, as is clearly shown in Fig. 1(b). These features are q general for the various ion–neutral interactions and are lized below.

Figures 2(a) and 2(b) illustrate the variation $[D_i^{(2)}]^{-1}$ and $[D_i^{(4)}]^{-1}$ for different interactions of A B with M (charge-transfer CX, hard-sphere HS, and po ization POL). The bottleneck to $D_i^{(2)}$ occurs where $\langle \Delta E_i^2 \rangle$ rate is least and in roughly in the same location $\sim 1.25kT$) for all the interactions. The $\langle \Delta E_i^2 \rangle$ rate is g est for the charge-transfer interaction and weakest fo polarization attraction, as expected. The moment $D_i^{(4}$ hibits similar but more rapidly varying behavior.

Since C_{if} is symmetrical in i and f—the detailed-ba

relation (2.7)—then C_{if}, when expressed as a function of the energy-mean $\overline{E} = \frac{1}{2}(E_f + E_i)$ and the energy change $\Delta = E_f - E_i$, is such that $C_{if} = C_{if}(\overline{E}, |\Delta|)$ as previously noted by Keck and Carrier.[2] On expanding C_{if} about E_i in terms of the expansion parameter Δ, which is assumed small, then

$$C_{if}(\overline{E} = E_i + \tfrac{1}{2}\Delta, |\Delta|) = \sum_{n=0}^{\infty} \frac{\Delta^n}{n!}\left(\frac{1}{2}\right)^n \left(\frac{\partial^n C_i}{\partial E_i^n}\right), \tag{3.6}$$

where C_i is $C_{if}(\overline{E} = E_i, |\Delta|)$. The general moments (3.5) are therefore determined from

$$m! D_i^{(m)}(E_i) = \sum_{n=1,3,5}^{\text{odd}} (2^n n!)^{-1} \left[\frac{\partial^n F_i^{(m+n)}}{\partial E_i^n}\right]; \quad m \text{ odd}, \tag{3.7a}$$

$$= \sum_{n=0,2,4}^{\text{even}} (2^n n!)^{-1} \left[\frac{\partial^n F_i^{(m+n)}}{\partial E_i^n}\right]; \quad m \text{ even}, \tag{3.7b}$$

which involves only the terms

$$F_i^{(s)}(E_i) \doteq \int_{-D}^{\infty} \Delta^s C_i(E_i, |\Delta|) dE_f, \tag{3.8}$$

with s even. Terms with s odd vanish since D is effectively infinite (~ 5 eV).

For equilibrium, γ_i in Eq. (3.4) is unity and the equilibrium current can then be expressed, with the aid of Eq. (3.7) as

$$\tilde{J}_i = \sum_{n=0}^{\infty} (-1)^n \left[\frac{\partial^n D_i^{(n+1)}}{\partial E_i^n}\right] = \sum_{n=0,2}^{\text{even}} \sum_{j=0,2}^{\text{even}} (n-2j)[2^{j+1}(n+2)!(j+1)!]^{-1} \times \frac{\partial^{j+n+1} F_i^{(j+n+2)}}{\partial E_i^{j+n+1}}. \tag{3.9}$$

This new form clearly shows that the coefficient of its first term $\partial F_i^{(2)}/\partial E_i$, which arises from the leading term of the expansion (3.7) for both $D_i^{(1)}$ and $\partial D_i^{(2)}/\partial E_i$, is identically zero. The coefficient of the second term $\partial^3 F_i^{(4)}/\partial E_i^3$, which is the net balance of the second term in the expansion (3.7) for both $D_i^{(1)}$ and $\partial D_i^{(2)}/\partial E_i$ and of the leading term in the expansion (3.7) for both $\partial^2 D_i^{(3)}/\partial E_i^2$ and $\partial^3 D_i^{(4)}/\partial E_i^3$, is also zero. The leading nonvanishing contribution to Eq. (3.9) is $[-\frac{1}{576}\partial^5 F_i^{(6)}/\partial E_i^5]$ which is the net balance of the third terms in the expansion (3.7) for both $D_i^{(1)}$ and $\partial D_i^{(2)}/\partial E_i$ and of the second terms in the expansion (3.7) for both $\partial^2 D_i^{(3)}/\partial E_i^2$ and $\partial^3 D_i^{(4)}/\partial E_i^3$. The consistent neglect of $\partial^4 D_i^{(5)}/\partial E_i^4 \sim \partial^5 F_i^{(6)}/\partial E_i^5$ and higher-order derivatives demands both the neglect in Eq. (3.4) of terms with $n > 4$ and the neglect in Eqs. (3.7a) and (3.7b) of terms with $n > 5$ and $n > 4$, respectively. Hence, the equilibrium current

$$\tilde{J}_i \approx D_i^{(1)} - \frac{\partial D_i^{(2)}}{\partial E_i} + \frac{\partial^2 D_i^{(3)}}{\partial E_i^2} - \frac{\partial^3 D_i^{(4)}}{\partial E_i^3} \equiv 0 \tag{3.10}$$

is exact to fourth order in the moments and is identically zero! Relationships between even and odd moments can be obtained from Eq. (3.7) by neglecting $F_i^{(6)}$ and higher terms, i.e., $D_i^{(5)}$ and higher moments, to give

$$D_i^{(1)} = \frac{\partial}{\partial E_i}\left[D_i^{(2)} - \frac{\partial^2 D_i^{(4)}}{\partial E_i^2}\right] \tag{3.11a}$$

and

$$D_i^{(3)} = 2\frac{\partial}{\partial E_i} D_i^{(4)}, \tag{3.11b}$$

which also ensure zero equilibrium current. In view of Eq. (3.11) note that equilibrium ($\tilde{J}_i = 0$) is obtained only when the current (3.4) is expanded to even order.

With the aid of Eq. (3.10), the nonequilibrium current (3.4) to fourth order in moments $D_i^{(m)}$ is

$$J_i^{(4)}(E_i,t) = -\left[D_i^{(2)} - 2\frac{\partial D_i^{(3)}}{\partial E_i} + 3\frac{\partial^2 D_i^{(4)}}{\partial E_i^2}\right]\left[\frac{\partial \gamma_i}{\partial E_i}\right] + \left[D_i^{(3)} - 3\frac{\partial D_i^{(4)}}{\partial E_i}\right]\left[\frac{\partial^2 \gamma_i}{\partial E_i^2}\right] - D_i^{(4)}\left[\frac{\partial^3 \gamma_i}{\partial E_i^3}\right] \tag{3.12}$$

which is the differential representation (up to and including the fourth-order moment $D_i^{(4)}$) of the double integral

$$J(E,t) = \int_E^{\infty} dE_i \int_{-D}^{E} [\gamma_f(t) - \gamma_i(t)] C_{if}\, dE_f \tag{3.13}$$

for the exact current (2.4). The differential form (3.12) is the Fokker–Planck current to fourth order since the general Fokker–Planck expansion can be employed for any variable whose changes are small in comparison with averaged characteristic values, e.g., the collisional energy change Δ here is assumed small relative to the thermal energy kT of the gas bath.

Upon use of the approximations (3.11), which are internally consistent to neglect of moments higher than $D_i^{(4)}$, Eq. (3.12) reduces to

$$J_i^{(4)}(E_i,t) = -\left[D_i^{(2)} - \frac{\partial^2 D_i^{(4)}}{\partial E_i^2}\right]\left[\frac{\partial \gamma_i}{\partial E_i}\right] - \frac{1}{2} D_i^{(3)}\left[\frac{\partial^2 \gamma_i}{\partial E_i^2}\right] - D_i^{(4)}\left[\frac{\partial^3 \gamma_i}{\partial E_i^3}\right]. \tag{3.14}$$

Inserting the ansatz (2.8) in Eq. (3.12), then Eq. (2.6) with Eq. (3.12) yields

$$\frac{dn_i(E_i,t)}{dt} = -[\gamma_c(t) - \gamma_s(t)]\frac{\partial j_i(E_i)}{\partial E_i}, \tag{3.15}$$

where in terms of the stochastic probability P_i^D that state i dissociates, the time-independent background current to fourth order is

$$j_i^{(4)}(E_i) = -\left[D_i^{(2)} - 2\frac{\partial D_i^{(3)}}{\partial E_i} + 3\frac{\partial^2 D_i^{(4)}}{\partial E_i^2}\right]\left[\frac{\partial^3 P_i^D}{\partial E_i}\right] + \left[D_i^{(3)} - 3\frac{\partial D_i^{(4)}}{\partial E_i}\right]\left[\frac{\partial^2 P_i^D}{\partial E_i^2}\right] - D_i^{(4)}\left[\frac{\partial^3 P_i^D}{\partial E_i^3}\right]. \tag{3.16}$$

B. Diffusion equation and current for termolecular recombination

On ignoring moments $D_i^{(3)}$ and higher, the (diffusional) current (3.16) is

$$j_d(E_i) = -D_i^{(2)} \frac{\partial \bar{P}_i^D}{\partial E_i} = D_i^{(2)} \frac{\partial P_i^S}{\partial E_i}, \tag{3.17}$$

so that Eq. (3.15) is

$$\frac{dn_i(E_i,t)}{dt} = [\gamma_c(t) - \gamma_s(t)] \frac{\partial}{\partial E_i}\left[D_i^{(2)} \frac{\partial P_i^D}{\partial E_i}\right], \tag{3.18}$$

which is a diffusion equation in energy space. The moment $D_i^{(2)} = \frac{1}{2}d/dt \ \langle \Delta E_i^2 \rangle$ is the diffusion coefficient (energy^2 s^{-1}) in energy space. This type of streaming equation has been previously derived via other techniques by Pitaevskii[1] for electron–ion recombination under highly nonequilibrium conditions when $\gamma_c \gg \gamma_s$ so that $\gamma_i = P_i^D \gamma_c$ in Eq. (2.6), and by Keck and Carrier[2] for heavy-particle association/dissociation. It has been investigated by Landon and Keck,[3] by Mahan[5], and by Bates and Zundi[6] for highly nonequilibrium ($\gamma_c \gg \gamma_s$) termolecular ion–ion recombination. By explicitly including here the factor $(\gamma_c - \gamma_s)$ via the ansatz (2.8), Eqs. (3.15) and (3.18) for all $\gamma_{c,s}$ help to emphasize the evolution via termolecular recombination and dissociation (into ion products) of the subsystems (A–B) towards thermodynamic equilibrium with the gas M, attained when $\gamma_c \to \gamma_s \to 1$.

Another advantage of the ansatz (2.8) is that the intermediate block of highly excited levels can be taken to be in quasi-steady-state (QSS), i.e., $\partial n_i/\partial t \approx 0$ in either Eq. (2.9) or (3.18), *for all times*. The QSS-diffusional current (3.17) is constant over $\mathscr{E}$, so that the solution of Eq. (3.17) subject to conditions,

$$P_i^D(-S) = 0, \quad P_i^S(-S) = 1 \tag{3.19}$$

is

$$P_d^D(E_i) = -j_d\left[\int_{-S}^{E_i} dE/D^{(2)}(E)\right] = 1 - P_d^S(E_i), \tag{3.20}$$

where the subscript d denotes quantities associated with the diffusion equation (3.18). Various levels of approximation readily follow:

(a) Since

$$P_i^D(0) = 1, \quad P_i^S(0) = 0, \tag{3.21}$$

then Eq. (3.20) yields

$$-j_d^{(P)} = \left[\int_{-S}^{0} dE/D^{(2)}(E)\right]^{-1} = \alpha_P \tilde{N}_A \tilde{N}_B \tag{3.22}$$

for the downward diffusional current which, when compared with Eq. (2.20) provides the recombination rate α_P of Pitaevskii,[1] adopted for ion–ion recombination by Landon and Keck[3] and by Mahan.[5] Note that the current (3.22) is the inverse of the area under the curves in Fig. 2(a), and that Eq. (3.20) for the stabilization and disruption probabilities $P_i^{S,D}$ at energy E_i are the respective ratios of the areas which correspond to the energy ranges $(0 \to E_i)$ and $(E_i \to -S)$ to the total area.

(b) Rather than requiring Eq. (3.21) for the probabil ties, j_d in Eq. (3.20) can be fixed by inserting Eq. (3.20 directly into Eq. (2.24) for $j(0)$ to give

$$-j(0) = \int_0^\infty dE_i \int_{-D}^{0} C_{if}\, dE_f + j_d \int_0^\infty dE_i \times \int_{-D}^{0} C_{if}\, dE_f \left\{\int_{-S}^{E_f} dE/D^2(E)\right\}. \tag{3.23}$$

On equating the exact current $j(0)$ in Eq. (3.23) with th diffusional current j_d, then

$$-j_d^{(k)}(0) = \left[\int_0^\infty dE_i \int_{-D}^{0} C_{if}\, dE_f\right]\left\{1 + \int_0^\infty dE_i \times \int_{-D}^{0} C_{if}\, dE_f \int_{-S}^{E_f} dE/D^{(2)}(E)\right\}^{-1} = \alpha_K \tilde{N}_A \tilde{N}_B, \tag{3.24}$$

which yields the expression of Keck[4] for α. The term braces, $\{\ \}^{-1}$ is simply the ratio of the downward diff sional current to the one-way equilibrium current across t dissociation neck.

(c) Another possibility in similar vein to (b) is to inse Eq. (3.20) directly into Eq. (2.25) for $j(-S)$ to give

$$j_d(-S) = \left[\int_{-D}^{-S} dE_i \int_{-S}^{\infty} C_{if}\, dE_f\right] \times \left\{1 + \int_{-D}^{-S} dE_i \int_{-S}^{0} C_{if}\, dE_f \times \int_{-S}^{E_f} dE/D^2(E)\right\}^{-1} = \alpha_K \tilde{N}_A \tilde{N}_B, \tag{3.2}$$

where the term in braces, $\{\ \}^{-1}$, is simply the ratio of upward diffusional current across $-S$ to the one-way eq librium current upward across $-S$.

The feature common to all the above procedures ((c) is that the required current (3.17) depends upon accuracy of the gradient (dP_i^D/dE_i) which, due to the glect of higher derivatives in Eq. (3.16), is described by diffusion equation (3.18) less precisely than are the act diffusion QSS solutions, i.e., Eq. (3.18) may furnish ac rate P_i^D but relatively inaccurate derivatives. More imp tantly, however, is that Eq. (2.20), which is valid only un exact QSS-condition (2.18) of the exact Master equat (2.19) has been invoked for the diffusional currents $j_d^{(P)}$ Eq. (3.22) and $j_d^{(k)}$ of Eq. (3.24) which are QSS solution the different and approximate diffusional equation (3.18

The QSS solution of Eq. (3.18) subject to both c straints (3.19) and (3.21) is

$$P_d^S(E_i) = \left\{\int_{E_i}^{0} dE/D^{(2)}(E)\right\}\left\{\int_{-S}^{0} dE/D^{(2)}(E)\right\}^{-} \tag{3.}$$

for the probability that any level E_i in block $\mathscr{E}$, once cessed by collision, has "associative" character. The pr bility that level E_i has "dissociative" character is the c plementary function

$$P_d^D(E_i) = \left\{\int_{-S}^{E_i} dE/D^{(2)}(E)\right\}\left\{\int_{-S}^{0} dE/D^{(2)}(E)\right\} \tag{3}$$

Thus, both functions are constrained to vary monotonically between zero and unity as does the exact numerical solution to the integral equation (2.18) so that, when compared with the exact numerical values, will involve less error than their corresponding derivatives

$$\frac{\partial P_i^{A,D}}{\partial E_i} = \mp \{D_i^{(2)}(E_i)\}^{-1} j_d^{(p),k} \tag{3.29}$$

appropriate to currents (3.22) and (3.24) in schemes (a) and (b) above.

C. Calculations for termolecular recombination at low N

The well developed case[8-12] of termolecular ion–ion recombination

$$A^+ + B^- + M \rightarrow AB + M \tag{3.30}$$

serves as a case study for assessing the accuracy of the diffusion approaches of Secs. III A and III B. The recombination coefficient α has previously been represented[9,17] very accurately by the sum

$$\alpha = \alpha_1 + \alpha_2 \tag{3.31}$$

of coefficients α_i obtained by considering separate contributions from (A^+–M) and (B^-–M) *binary* collisions ($i = 1$ and 2, respectively). The exact numerical rates α_i are obtained by inserting the exact numerical solution of the integral equation (2.18), the QSS condition into Eq. (2.32) for the current $j(-E_i)$. The rates α_i have been tabulated[9-11] as a function of the mass-ratio parameter:

$$a_i = M_j M_3 / M_i (M_1 + M_2 + M_3), \tag{3.32}$$

where M_i are the masses of species A^+, B^-, and M, $i = 1, 2$, and 3, respectively and where the set (i, j) is equal to (1,2) or (2,1) for $(1-3)$ or $(2-3)$ collisions, respectively.

Expressions for the equilibrium rate C_{if} appropriate to the three classes—polarization,[11] charge–transfer,[8,10] and hard-sphere[10]—of ion–neutral interactions have been previously derived.[9-11] Calculations have been performed here for the exact QSS-rates α_E that rise from 1–3 collisions and for the corresponding diffusional rates, (3.22) for α_P and (3.24) for α_K of Pitaevskii[1] and Keck,[4] respectively. Little discernable difference was found between α_P and α_K which may now be simply called the diffusional rates α_D obtained when the diffusional current (3.17) is inserted in Eq. (2.20). Previous results[9-11] were based on the solution of, at most, 36 coupled algebraic equations, the discretized equivalent representation of Eq. (2.18). Present calculations solve 100 coupled equations required for convergence in α for small and large mass parameters (3.32).

Table I provides present values of the ratio α_D/α_E for the various interactions over the full range of mass parameter a_1. Small $a \approx 10^{-3}$ corresponds to collisional recombination of heavy ions ($M_1 \approx M_2 \gg M_3$) in a much lighter (electron) gas, intermediate $a(=1/3$ for $M_1 = M_2 = M_3)$ corresponds to normal mass components, and large $a = 10^3$ for $M_1 \ll M_2 \approx M_3$ corresponds to electron–ion recombination in an ambient gas. The cases of small and large a involve energy transfers which are very much less than the energy kT of the gas so that the diffusional (weak collision) approach is likely then to be valid.

As Table I shows, the diffusional rates are reliable, as expected, only for recombination in a vanishingly light gas ($a \approx 10^{-3}$) or for electron–ion recombination ($a \approx 10^3$) in a general gas, the case for which Pitaevskii[1] designed his diffusional treatment. The diffusional rates are higher by between a factor of 3–9 for intermediate $a \sim 1$. As the ion–neutral interaction varies from polarization attraction to hard-sphere repulsion and then to charge–transfer interaction, the energy change in the ion–neutral collision becomes progressively larger [see Fig. 2(a) and 2(b)] so that the diffusional rates (based on weak collisions) become less accurate, as shown directly by the variation of entries in Table I for a specified mass parameter a.

Since Eq. (3.17) predicts zero current in both the fully dissociated and fully associated blocks, $\mathscr{C}$ and $\mathscr{S}$, respectively, the diffusional current (3.17) is therefore discontinuous, zero in $\mathscr{C}$, j_d in $\mathscr{E}$ and zero in $\mathscr{S}$. The diffusion rates (3.22) of Pitaevskii and (3.24) of Keck are therefore expected to be valid only in the limit of vanishingly small currents and rates α of recombination. This is confirmed in Table I for

TABLE I. Variation of the ratio (α_D/α_E) and (α_{BN}/α_E) with mass-ratio parameter a for 1–3 collisions and with the various 1–3 interactions: polarization (POL), hard-sphere (HS), and symmetrical resonance charge–transfer (CX). The exact, diffusional, and bottleneck rates are α_E, α_D, and α_{BN}, respectively.

	α_D/α_E			α_{BN}/α_E		
a	POL[a]	HS[a]	CX[b]	POL	HS	CX
0.001	1.001	1.013	1.030	32.447	25.782	16.996
0.01	1.163	1.222	1.321	8.369	7.336	5.513
0.1	2.131	2.739	3.522	3.354	2.939	2.384
1/3	3.360	4.967	6.840	2.541	2.215	1.865
1.0	4.060	6.604	9.272	2.333	2.015	1.722
10.0	2.131	3.510	⋯	3.354	2.746	⋯
100.0	1.163	1.455	⋯	8.369	6.302	⋯
1000.0	1.001	1.093	⋯	32.447	20.233	⋯

[a] In POL and HS, small a implies ion–ion recombination in a vanishingly light gas and large a ($\sim 10^3$) implies electron–ion recombination in a normal-mass gas.

[b] In CX small a implies $M_2 \ll M_1 = M_3$ and $a = 1$ implies $M_2 \gg M_1 = M_3$.

the limiting cases of small and large a. Then the actual rate for electron–ion collisional recombination in a gas is[7] $\alpha_E \sim 10^{-9}\,\mathrm{cm^3\,s^{-1}}$ at STP, which is three orders of magnitude less than the rate $\alpha_E \sim 10^{-6}\,\mathrm{cm^3\,s^{-1}}$ at STP (cf. Ref. 19) for ion–ion recombination a similar mass gas.

Another reason for the inadequacy of the diffusion approach as previously applied to general-mass cases is also apparent. As Figs. 3(a) and 3(b) show, the diffusion equation (3.18) in general furnishes fairly accurate probabilities $P_i^{A,D}$, Eqs. (3.29) and (3.30), but less reliable gradients $dP_i^{A,D}/dE_i$.

In an effort to assess the relative importance between using relatively accurate distributions P_i^S within the integral (2.23) or differential (3.17) forms of the collision integral of the Master equation, assume that the intermediate block $\mathscr{B}$ between blocks $\mathscr{C}$ and $\mathscr{S}$ is absent, i.e.,

$$P^S(E_i) = \begin{cases} 0, & -E < E_i < \infty \\ 1, & -D < E_i < -E \end{cases}, \tag{3.33}$$

where $-E$ is some bound energy level. The current (2.15) then reduces to

$$-j_{\mathrm{BN}}(-E) = \int_{-E}^{\infty} dE_i \int_{-D}^{-E} C_{if}\, dE_f = \alpha_{\mathrm{BN}}(E)\tilde{N}_{\mathrm{A}}\tilde{N}_{\mathrm{B}}, \tag{3.34}$$

which is the one-way equilibrium downward current across level $-E$. As $-E$ is varied, this current achieves a minimum[10] at energy $-E^*$ ($\approx -2kT$) which therefore acts as a bottleneck[13] to the recombination which proceeds at rate $\alpha_{\mathrm{BN}}(E^*)$. The ratio of α_{BN} at the bottleneck E^* to the exact numerical rate α_E is displayed in Table I for the various interactions. The bottleneck method fails quite markedly for small and large mass parameters a, where the diffusion current is by contrast successful, and becomes much more reliable than the diffusion approach at intermediate $a(\approx 1)$. For a given a, less error is involved for stronger collisions in harmony with Eq. (3.34) being a strong collision approximation. Since Eq. (3.33) assumes the least possible knowledge of the probabilities P_i^S (subject to the constraints) but an integral form (3.34) to the collision rate, it follows that fairly accurate distributions are required at small and large a where the collision rate and dynamics are weak, so that the discontinuous integral form (2.23) does reduce indeed to the continuous streaming form (3.17). For intermediate a when the energy changes are certainly not weak, inclusion of the integral form (2.22) is apparently more important than the use of fairly accurate distributions (which in any event are constrained to vary between unity and zero at the boundaries of block $\mathscr{B}$). Note also that the diffusional and bottleneck results are always greater than the exact QSS rates, in accord with predictions of the variational principle recently proposed.[18] The bottleneck method provides the *least* of the one-way equilibrium rates—the least upper limit—across a bound level. The diffusion method incorporates the effect of the net downward–upward collisional transitions.

The closeness exhibited in Fig. 3(a) between the diffusional probabilities, (3.27) and (3.28), and the exact numerical probabilities may be utilized in two ways. First, an

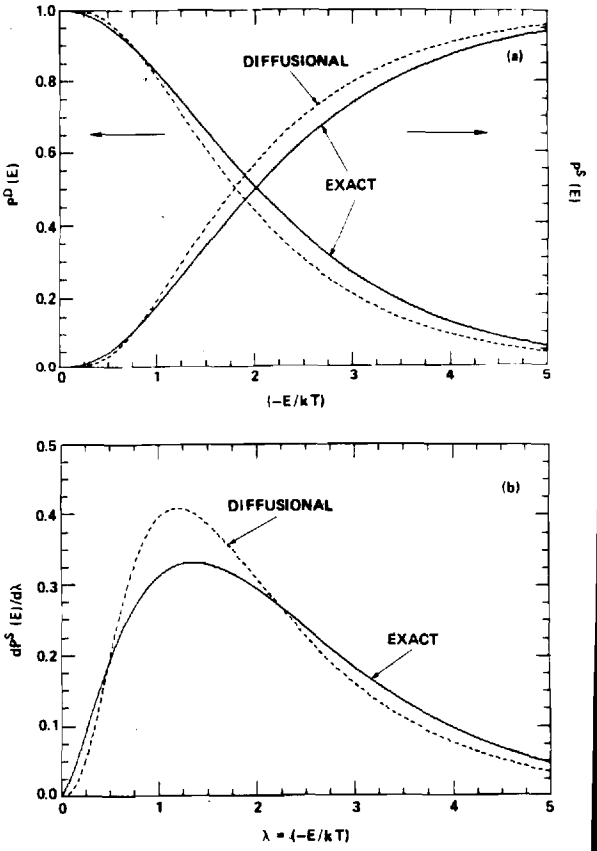

FIG. 3. (a) Probabilities $P^{S,D}$ for stabilization and dissociation of an pair bound with energy $E_i = -\lambda kT$. Equal-mass species and cha transfer ion–neutral collisions are assumed. —: Exact QSS solution o (2.18). - - -: Diffusional approximation, Eqs. (3.27) and (3.28). (b) rivatives ($dP^S/d\lambda$) of stabilization probability P^S. From numerical tion of Eq. (2.18) and from diffusional approximation, Eq. (3.29).

iterative procedure[4]

$$P^{(n+1)}(E_i)\int_{-D}^{\infty} C_{if}\, dE_f = \int_{-D}^{\infty} P^{(n)}(E_f) C_{if}\, dE_f \tag{3.}$$

to the solution of the integral equation (2.18) can be de oped by using the diffusional analytical probabilities (3. as the starting ($n = 0$) solution. It is found here that con gence to within 1% of the exact solution can be in gen achieved after five iterations, so that accurate rates can t be determined from Eqs. (2.23)–(2.25) since the QSS-c dition (2.18) is satisfied.

Since the diffusional probabilities (3.27) and (3.28) reasonably accurate, a second possibility is to insert t directly into the current (2.23). This procedure, at first s attractive, is however inconsistent, in that the diffusi probabilities while satisfying quasi-steady-state (QSS the diffusional equation (3.18) in block $\mathscr{B}$, *do not* satisf condition (2.18) for QSS of the Master equation (2.9 which Eq. (2.23) relies. The resulting current (2.15) therefore not be a constant in block $\mathscr{B}$. This is demonst by Fig. 4 which compares the exact downward cu $-j_E(E_i)$ past level E_i obtained from the solution o

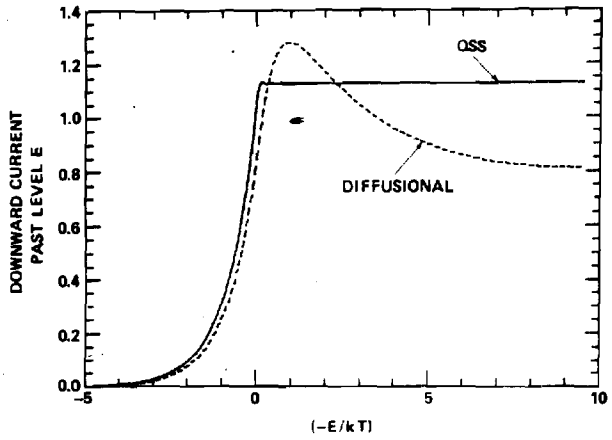

FIG. 4. Comparison of currents, Eq. (2.15), past energy level $-E=-\lambda kT$, obtained (—) from exact solution of Eq. (2.18) and from (- - -) diffusion probabilities Eq. (3.27). Equal-mass species and hard-sphere ion–neutral collisions are assumed. The current is normalized to $(2\alpha_T \tilde{N}_A \tilde{N}_B)$ where α_T is the Thomson rate, Eq. (4.1).

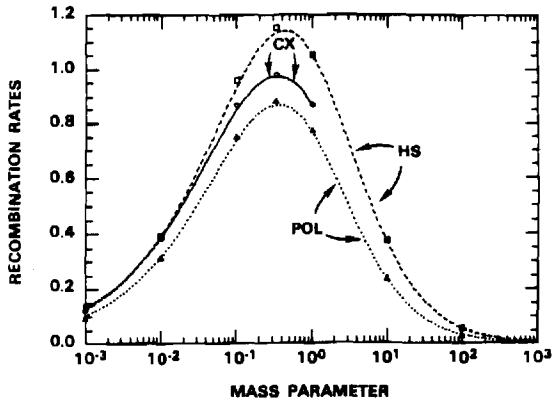

FIG. 5. Normalized rates R_T, Eq. (4.2), for ion–ion recombination in a dilute gas as a function of mass parameter a, Eq. (3.32) for various ion–neutral interactions: HS (hard-sphere), CX (charge–transfer) and POL (polarization). —: exact rates. □, ○, △: rates obtained with diffusional probabilities, Eq. (3.27), in basic Eq. (2.16) for HS, CX, and POL interactions.

(2.18) in Eq. (2.23) with the approximate downward current $-j_A(E_l)$ obtained by inserting Eq. (3.27) in Eq. (2.23). The diffusional current through the bound levels is far from constant over the block $\mathscr{E}$ of highly excited levels and hence, Eq. (2.20) cannot be used for steady-state rates. The figure also shows that assignment of a bound level E_l for determination of α from Eq. (2.23) is uncertain. Since the current $j(-E)$ exhibits a very rapid variation in the neighborhood of the dissociation limit (at zero energy), use of Eq. (2.24) for $j(0)$ is therefore a risky procedure, the exact value of $j(0)$ being $\sim 50\%$ higher than the approximate $j(0)$. Some defense can be made by calculating Eq. (2.23) at the bottleneck energy $E^* \sim -2kT$ where the diffusional and exact currents agree. This adoption is however not firmly based.

The basic reason for the inconsistency of using the diffusional probabilities (3.27) in Eq. (2.23) is not that the diffusional probabilities are not sufficiently accurate for useful application, but is that the expression (2.23) based on identifying the association rate with the current is not appropriate for the use of approximate probabilities, which do not satisfy the basic condition (2.18) for such identification.

IV. BASIC RATE WITH DIFFUSIONAL PROBABILITIES

The exact rates α_E obtained in Sec. III C from Eq. (2.18) in Eq. (2.23) for the various ion–neutral interactions are normalized[10,11] to the corresponding Thomson rate

$$\alpha_T = \tfrac{4}{3}\pi(R_e/\beta)^3(3kT/M_{12})^{1/2}\sigma_0 N, \quad \beta = 3/2, \quad (4.1)$$

where R_e is the natural unit (e^2/kT) for Coulombic attraction between the ions 1 and 2. The integral cross section σ_0 for 1–3 elastic collisions at relative energy $(\frac{3}{2}kT)$ is taken in Eq. (4.1) to be $2\sigma^X$, $2\pi(pR_e/3)^{1/2}$, and σ_0^H, respectively for symmetrical resonance charge–transfer collisions with cross section σ^X, for polarization (orbiting) collisions in terms of the polarizability p of the gas M, and for hard-sphere collisions with cross section σ_0^H.

Approximate rates α_A may now be determined by inserting P_l^S, the diffusional (approximate) probabilities (3.27) into the basic expression (2.16) which does not rely on the use of exact (QSS) P_l^S. Figure 5 displays a comparison of the corresponding ratios,

$$R_T = (M_1/M_{12})(\alpha/\alpha_T), \quad (4.2)$$

where α is taken as the exact rate α_E or the approximate rate α_A, which arises from 1–3 collisions. The exact rates reproduce those previously presented.[10,11] The present study adopts a 100-point quadrature throughout, rather than 36 and 18 used in Refs. 10 and 11, respectively, in order to obtain convergence at small and large a.

Excellent agreement between α_E and α_A is obtained over the full range of the mass parameter a, Eq. (3.32) for a_1 all the way, from $a \approx 10^{-3}$ for association of heavy ions in a light (electron) gas, to intermediate $a \approx 1/3$ for equal mass species and up to large $a \approx 10^3$ which corresponds to electron–ion recombination in a gas. As expected, greatest departures occur for the case of equal mass which involves the largest energy transfer so that the diffusional probabilities would also show their greatest departure from the exact probabilities as in Fig. 3(a). For this case $(a = 1/3)$, the diffusional result corresponding to hard-sphere collisions, which in turn involve largest energy transfers (cf. Fig. 2), exhibit the largest of small departures. The present diffusional treatment is also excellent over all of the various classes of 1–3 interaction considered.

V. ION–ATOM ASSOCIATION AT LOW GAS DENSITIES

The above theory may now be suitably modified to cover ion–atom association

$$A^+ + B + M \underset{k}{\overset{\alpha}{\rightleftarrows}} AB^+ + M \quad (5.1)$$

of atomic species A^+ and B in a low density gas M. In contrast to ion–ion recombination (3.30) where an equilibrium distribution over internal angular momentum L_i is established[12] the A^+–B attraction can support centrifugal barriers so that nonequilibrium distributions $n_l(E_l, L_l^2; t)$ over

both E_i and L_i^2 must be acknowledged. Thus, the ansatz (2.8) is replaced by

$$\gamma_i(E_i,L_i^2;t) = \frac{n_i(E_i,L_i^2;t)}{\bar{n}_i(E_i,L_i^2)} = P_i^D(E_i,L_i^2)\gamma_c(t) + P_i^S(E_i,L_i^2)\gamma_s(t) \xrightarrow{t\to\infty} 1, \quad (5.2)$$

where $P_i^S = 1 - P_i^D$, the probability of stabilization of (E_i,L_i^2) pairs by subsequent multicollisions, is zero for dissociated pairs and unity for fully associated pairs.

Bates and McKibbin[14] found that a delta function approximation $\delta(L_i^2 - L_f^2)$ for $(E_i,L_i^2 \to E_f,L_f^2)$ transitions was quite satisfactory. The above analysis in Secs. III A and III B for energy change alone can then be immediately modified to yield corresponding results for the stabilization probabilities $P_i^S(E_i,L_i^2)$ for quasibound and bound states. Thus, the diffusion approximation for the bound and quasibound level yields

$$P_d^S(E_i,L_i^2) = \left[\int_{E_i}^{U_i} dE/D^{(2)}(E,L_i^2)\right] \times \left[\int_{-S}^{U_i} dE/D^{(2)}(E,L_i^2)\right]^{-1}, \quad (5.3)$$

where $U_i(L_i^2)$ is the energy at the top of the centrifugal barrier of the effective interaction

$$V_i(R) = V(R) + L_i^2/2mR^2. \quad (5.4)$$

In terms of C_{if} the one way equilibrium rate per unit $dE_i\,dL_i^2\,dE_f\,dL_f^2$ for $(E_i,L_i^2 \to E_f,L_f^2)$ collisional transitions, the diffusion coefficient is

$$D^{(2)}(E_i,L_i^2) = \frac{1}{2}\int_{-D}^{\infty}(E_f - E_i)^2\,dE_f \times \int_0^{L_{0f}^2} C_{if}(E_i,L_i^2;E_f,L_f^2)\,dL_f^2, \quad (5.5)$$

where L_{0f} is the maximum angular momentum for fixed E_f. For dissociated levels P_d^S is zero. The association rate corresponding to the basic rate (2.16) is then given by

$$\alpha\tilde{N}_A\tilde{N}_B = \int_{-D}^{\infty} dE_i \int_0^{L_{0i}^2} P_i^S\,dL_i^2 \int_{-D}^{\infty} dE_f \times \int_0^{L_{0f}^2} (P_i^S - P_f^S)\,C_{if}\,dL_f^2, \quad (5.6)$$

where the stabilization probabilities P_i^S are given by Eq. (5.3).

VI. SUMMARY

On introduction of stochastic probabilities $P_i^{S,D}(E_i)$ that ion pairs A–B with internal energy E_i will be stabilized or disrupted by collisions with a thermal bath of gas M, and upon the use of the ansatz (2.8) for their normalized distributions $\gamma_i(t)$ at time t, the basic Master equation (2.1), rate (2.2) and current (2.4) has been transformed into corresponding equations (2.9)–(2.11) which are separable in E_i and t. The diffusional equation (3.18), yields, for systems of general mass, accurate probabilities $P_i^{S,D}$ but very inaccurate currents (3.22)–(3.25) (cf. Fig. 3 and Table I). Identification as in Eq. (2.20) of association rates α with current, is valid only under QSS quasi-steady-state condition (2.18), appropriate to the original Master equation (2.9). Since th diffusional probabilities do not satisfy this condition, the di fusional current in general, may not be identified with th rate α. As Table I shows, the resulting diffusional rat (3.22)–(3.25), are therefore not reliable[2–6] except for tho cases in which the current is relatively small, i.e., for coll sion electron–ion recombination[1] in a gas and for ion–io recombination in a vanishingly light gas.

A new expression (2.11) or (2.16) derived[16] for th rates, is more appropriate for use under general condition as when QSS is not satisfied. When QSS is satisfied, E (2.16) reduces to the current (2.23). The QSS rates are mi imum (Ref. 18 and work in progress). The rate (2.16) required when approximate probabilities are used, as here

The diffusional probabilities can also be used in an itera tive solution[4] of the QSS-condition (2.18) to provide high accurate probabilities (to within 1%) after a few iteratio and hence accurate QSS-rates (2.23)–(2.25).

Application of the diffusional equation (3.18) to ge eral systems represents an accurate procedure provided t solutions $P_i^{S,D}$ are inserted in the appropriate and more bas expression (2.16) for the rate, rather than into the deriv expressions (3.17) or (2.13) for the diffusional or exact cu rents. Excellent agreement with the exact numerical Q results for various classes of ion–neutral interactions ov the full range of mass parameters for general systems h been obtained.

Finally, generalization (Sec. V) of the above analy Secs. II and III to cover the distributions $n(E_i,L_i^2,t)$ of A pairs over their internal energy E_i and angular momentu L_i is straightforward. The resulting equations are appro ate to consideration of ion–atom association of atomic s cies in a gas.

ACKNOWLEDGMENT

This research is supported by the U.S. Air Force of S entific Research under Grant No. AFOSR-84-0233.

[1] L. P. Pitaevskii, Sov. Phys.–DETP **15**, 919 (1962); E. M. Lifshitz and P. Pitaevskii, in *Physical Kinetics* (Pergamon, Oxford, 1981), Chap. 2, 89 and 102.
[2] J. C. Keck and G. Carrier, J. Chem. Phys. **43**, 2284 (1965).
[3] S. A. Landon and J. C. Keck, J. Chem. Phys. **48**, 374 (1968).
[4] J. C. Keck, in *Advances in Atomic and Molecular Physics*, edited by D. Bates and I. Estermann (Academic, New York, 1972) Vol. 8, p. 39.
[5] B. H. Mahan, J. Chem. Phys. **48**, 2629 (1968).
[6] D. R. Bates and Z. Jundi, J. Phys. B **1**, 1145 (1968).
[7] D. R. Bates and S. P. Khare, Proc. Phys. Soc. **85**, 231 (1965).
[8] D. R. Bates and R. J. Moffett, Proc. Soc. London Ser. A **291**, 1 (1966
[9] D. R. Bates and M. R. Flannery, Proc. Soc. London Ser. A **302**, (1968).
[10] M. R. Flannery, J. Phys. B **13**, 3649 (1980); **14**, 915 (1981).
[11] D. R. Bates and I. Mendaš, J. Phys. B **15**, 1949 (1982).
[12] D. R. Bates and I. Mendaš, J. Phys. B **8**, 1770 (1975).
[13] S. B. Byron, R. C. Stabler, and P. I. Bortz, Phys. Rev. Lett. **8**, 376 (196
[14] D. R. Bates and C. S. McKibbin, Proc. R. Soc. London Ser. A **339** (1974).
[15] M. R. Flannery, J. Phys. B **20**, 4929 (1987).
[16] M. R. Flannery, J. Phys. B **18**, L 839 (1985).
[17] M. R. Flannery and T. P. Yang, J. Chem. Phys. **73**, 3239 (1980).
[18] M. R. Flannery, in *Recent Studies in Atomic and Molecular Proce* edited by A. E. Kingston (Plenum, New York, 1987), p. 167.
[19] M. R. Flannery, in *Applied Atomic Collision Physics*, edited by E McDaniel and W. L. Nighan (Academic, New York, 1982), Vol. 141.

3.4 Coupled Nearest-Neighbor and Uncoupled Intermediate Level Methods.

Termolecular recombination: Coupled nearest-neighbor limit and uncoupled intermediate levels limit

M. R. Flannery and E. J. Mansky
School of Physics, Georgia Institute of Technology, Atlanta, Georgia 30332

(Received 18 April 1988; accepted 15 June 1988)

Two extreme limits of collisional coupling in termolecular recombination are investigated. The coupled nearest neighbor (CNN) limit includes only couplings between neighboring excited energy levels of the associating species AB*, while the uncoupled intermediate levels (UIL) limit includes only couplings between the fully dissociated reactants A^+ and B^- and each of the (assumed uncoupled) excited levels of AB*, which are then coupled to the fully associated products AB. Comparison is made with results of previous exact and diffusion treatments.

I. INTRODUCTION

Analogy with a mathematically equivalent electrical network provides an effective framework whereby not only can the complicated multilevel collisional dynamics intrinsic to a master equation treatment of termolecular recombination

$$A^+ + B^- + M \rightarrow AB + M \qquad (1.1)$$

between atomic species A^+ and B^- in a gas M be analyzed in a different light[1,2] but also physically appealing models may be readily constructed. In previous reports,[2-4] the (exact) quasi-steady-state (QSS) master equation method,[3] the corresponding variational method,[2] and an approximate diffusional method[4] were considered. In this paper, two simple models prompted by considering the analogous electrical diagram (Fig. 1)are investigated. So as to emphasize the importance of collisional couplings between many excited levels in a realistic treatment of process (1.1), two extreme limits will be tested. The *coupled nearest-neighbor limit* includes only the coupling of a given excited level n with its lower neighboring level $n-1$. The limit of *uncoupled intermediate levels* includes only couplings from the (external) source block $\mathscr{C}$ of fully dissociated states of the reactants A^+ and B^- to each of the excited levels n assumed to be *uncoupled* within the (internal) block $\mathscr{E}$ and then the coupling from each of these uncoupled n to the (external) sink block $\mathscr{S}$ of fully associated levels of the products AB (cf. Fig. 1). The "*intermediate*" levels comprise block $\mathscr{E}$ which is *intermediate* between blocks $\mathscr{C}$ and $\mathscr{S}$.

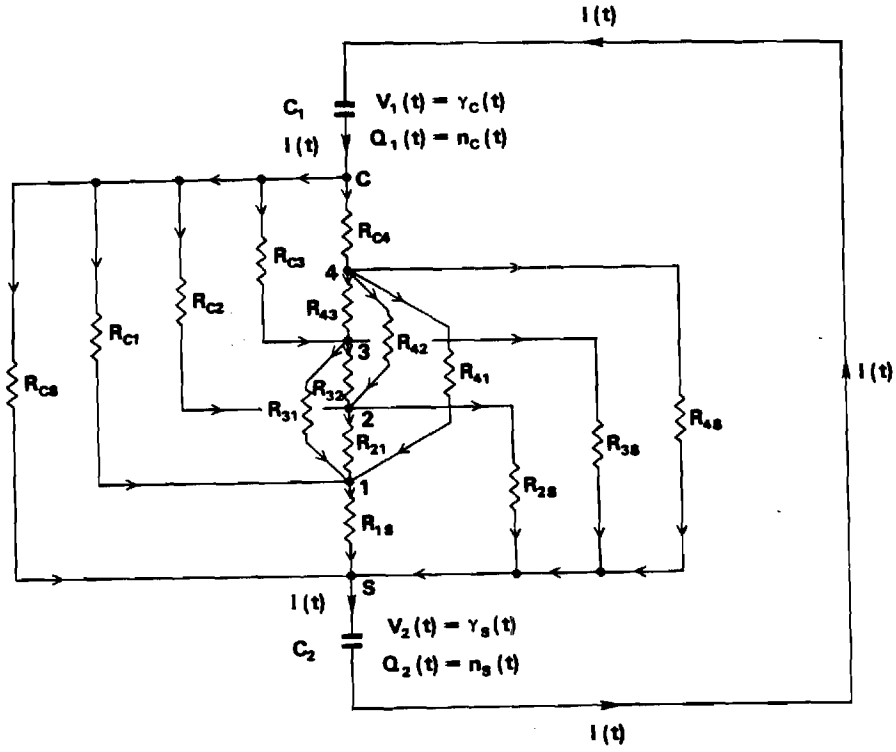

FIG. 1. (R, C) Electrical diagram (Ref. 2) appropriate to analysis of termolecular recombination, involving as an example, four excited levels ($n = 1,2,3,4$).

 0021-9606/88/194086-06$02.10

II. CONSTRUCTION

Termolecular recombination (1.1) may be described[4] via a *time-independent* treatment wherein equilibrium concentrations $\tilde{N}_A$ and $\tilde{N}_B$ of the fully dissociated atomic species A and B with relative energies E_i in the range $0 \leqslant E_i \leqslant \infty$, the reactant $\mathscr{C}$ block, are associated (a) by direct collisions into the product block $\mathscr{S}$ of fully associated molecular levels in the range $-S \geqslant E_i \geqslant -D$ maintained at zero population and (b) by a series of indirect transitions via the intermediate energy block $\mathscr{I}$ $(0 \geqslant E_i \geqslant -S)$ of highly excited levels. The indirect mechanism $\mathscr{C} \rightarrow \mathscr{I} \rightarrow \mathscr{S}$ is the most important[2-4] at thermal energies since the rate of the large energy transfers involved with direct $\mathscr{C} \rightarrow \mathscr{S}$ transitions is vanishingly small, by comparison. The lowest energy level of AB is $-D$, relative to the dissociated limit at zero energy, and $-S$ is a bound level below which the probability P_i^S of collisional stabilization of pairs in level E_i is by definition unity. The two key quantities are P_i^S which is unknown and the one-way equilibrium rate C_{if} which is given[3] in terms of the equilibrium number density of $\tilde{n}_i$ of levels of energy E_i per unit interval dE_i and the frequency ν_{if} for $E_i \rightarrow E_f$ transitions per unit interval dE_f by $\tilde{n}_i\, \nu_{if}$.

A hierarchy of approximate schemes are apparent via consideration[2] of process (1.1) in terms of the analogous electrical diagram displayed in Fig. 1. Here N discrete junctions ($\mathscr{I}$-block levels) n are at time-independent potentials P_n^S *below* the $\mathscr{C}$ block junctions C, all maintained at unit equipotential (due to the assumed equilibrium concentrations of A and B), or equivalently are at potentials $P_n^D = 1 - P_n^S$ *above* the zero potential of the $\mathscr{S}$ block junctions S (due to assumed zero concentration of AB). In terms of these voltages and of the conductances $C_{if} = R_{if}^{-1}$ of each element of resistance R_{if}, the rate constant deduced[2] from the power equation is then the effective conductance R^{-1} of the mathematically equivalent network. It follows from consideration of the power loss in the circuit that[2]

$$\alpha \tilde{N}_A \tilde{N}_B = \frac{1}{2} \int_{-D}^{\infty} dE_i \int_{-D}^{\infty} (P_i^S - P_f^S)^2 C_{if}\, dE_f \equiv R^{-1} . \tag{2.1}$$

Since the overall voltage drop is unity in the time-independent treatment, Eq. (2.1) is also the throughput electrical current. Only when the N nodes i in block $\mathscr{I}$ obey the Kirchoff current law, (KCL), or the following quasi-steady-state (QSS) equivalent condition for excited pairs:

$$P_i^S \int_{-D}^{\infty} C_{if}\, dE_f = \int_{-D}^{0} C_{if} P_f^S\, dE_f \tag{2.2}$$

does Eq. (2.1) reduce to $-j(0)$, the energy-space current

$$\alpha(0) \tilde{N}_A \tilde{N}_B = \int_0^{\infty} dE_i \int_{-D}^{0} C_{if} P_f^S\, dE_f = -j(0) \tag{2.3a}$$

across the dissociation limit at zero internal energy, or in general to

$$\alpha(-E) \tilde{N}_A \tilde{N}_B = \int_{-E}^{\infty} dE_i \int_{-D}^{-E} (P_f^S - P_i^S) C_{if}\, dE_f = -j(-E) , \tag{2.3b}$$

the constant energy-space downward current $-j(-E)$, across any arbitrary level of energy $-E$ in block $\mathscr{I}$. T extreme limits may now be constructed.

(A) *Uncoupled intermediate levels (UIL) limit*: Wh the mainline entrance and exit channels of resistances R and R_{nS} defined in terms of collisional couplings by

$$R_{Cn}^{-1} = \int_0^{\infty} C_{in}\, dE_i \equiv C_{Cn} \tag{2}$$

and

$$R_{nS}^{-1} = \int_{-D}^{-S} C_{nf}\, dE_f \equiv C_{nS} , \tag{2}$$

respectively, are only included in the network for indir passage between the reactant and product blocks $\mathscr{C}$ and via junction n, the current I_n flowing past any of the unc pled junctions n is given by

$$I_n [R_{Cn} + R_{nS}] = 1 , \tag{2}$$

since the voltage drop ($\mathscr{C} \rightarrow \mathscr{S}$) is unity and since n is coupled to any other junction n' of intermediate block The direct ($\mathscr{C} \rightarrow \mathscr{S}$) current

$$I_0 = R_{CS}^{-1} = \int_0^{\infty} dE_i \int_{-D}^{-S} C_{if}\, dE_f \tag{2}$$

is normally negligible but can be given by expression (since R_{fS} vanish for all nodes f in block $\mathscr{S}$. The voltage d between junctions C and each isolated n is then

$$P_n^S = I_n R_{Cn} = \frac{C_{nS}}{C_{Cn} + C_{nS}} , \tag{}$$

to be used in the basic power expression (2.1) for the constant.

Although expression (2.8) violates the KCL condi (2.2) required for reduction of Eq. (2.1) to Eq. (2.3) QSS rate (2.3a) nonetheless provides the rate

$$\alpha_1(0) \tilde{N}_A \tilde{N}_B = \int_{-D}^{0} \left[\frac{C_{Cf} C_{fS}}{(C_{Cf} + C_{fS})} \right] dE_f = \left[\int_{-D}^{0} \alpha_f\, dE_f \right] \tilde{N}_A \tilde{N}_B \tag{2}$$

which has several exemplary features. This rate is also effective conductance obtained from the total electrical rent $\Sigma_{n=0}^{N} I_n$ flowing between nodes C and S maintain unit potential difference. Although invalid when comp to Eq. (2.8) in Eq. (2.1), expression (2.9) illustrates effectively (a) that the partial rate α_f of a reaction w proceeds via the series sequence $\mathscr{C} \rightarrow f$ and $f \rightarrow \mathscr{S}$ of tr tions is given by the conductance

$$C_f = R_f^{-1} = [R_{Cf} + R_{fS}]^{-1} = \frac{C_{Cf} C_{fS}}{C_{Cf} + C_{fS}} \tag{2}$$

due to resistances R_{Cf} and R_{fS} connected in series and that the overall rate α_1 of the reaction which proceeds v parallel sequence involving each f is given by the co tance

$$C = R^{-1} = \sum_{f=0}^{N} R_f^{-1} = \sum_{f=0}^{N} C_f \tag{}$$

of the effective network with resistances R_f ($f = 1,2,$ connected in parallel. The resistance, $R_0 = R_{CS}$, of th

$\mathscr{S}$ direct connection is included in Eq. (2.11). Expressions (2.9) provide illustrations of the theorem due to Bates.[1] The approximate QSS rate $\alpha_1(-E)$ as a function of $\mathscr{E}$ block energy $-E$ is obtained by inserting Eq. (2.8) in Eq. (2.3b). The first rate under test is given by the probability (2.8) inserted in the power expression (2.1).

(*B*) *Coupled nearest-neighbor (CNN) limit*: When resistors $R_{n,n-1}$ are only included in block $\mathscr{E}$, the throughput current I is given by

$$I=\left[R_{\mathrm{CN}}+\sum_{n=1}^{N} R_{n,n-1}\right]^{-1}, \tag{2.12}$$

where junctions in block $\mathscr{S}$ are again denoted by $n=0$. As the highest excited bound level $N\to\infty$, R_{CN} vanishes, and the voltage drop between junctions C and f is then

$$P_f^S = I\sum_{n=f+1}^{\infty} R_{n,n-1} = \left[\sum_{n=f+1}^{\infty} C_{n,n-1}^{-1}\right]\left[\sum_{n=1}^{\infty} C_{n,n-1}^{-1}\right]^{-1}, \tag{2.13}$$

which, when inserted in the power equation (2.1) yields the second rate under investigation. A simplified rate given by the effective conductance (or electrical current) in Eq. (2.12) is

$$\alpha_2\tilde{N}_A\tilde{N}_B = R^{-1} = \left[\sum_{n=1}^{\infty} C_{n,n-1}^{-1}\right]^{-1}, \tag{2.14}$$

which again illustrates the reaction-in-series principle of Bates.[1] The approximation (2.14) has been previously obtained for $(e\text{-}A^+)+e$ recombination.[5] In contrast to Eq. (2.9), the result (2.14) cannot be obtained from the energy-space current (2.3a) since connections between C and the various n are ignored.

Note that the key approximations CNN, Eq. (2.13), and UIL, Eq. (2.8), satisfy the correct boundary conditions

$$P_l^S(E_l=0)=0,$$
$$P_l^S(E_l=-S)=1 \tag{2.15}$$

for the probability P_l^S.

III. RESULTS

As a test of the above approximations the case of termolecular ion–ion recombination (1.1) is adopted since the association (exact) rate α_E has been well studied (cf. Ref. 3) over full variation of the mass parameter

$$a=\frac{M_B M_g}{M_A(M_A+M_B+M_g)} \tag{3.1}$$

pertinent to A^+–M collisions and over the following model (A^+–M) interactions: symmetrical resonance charge transfer (CX), polarization attraction (POL), and hard-sphere repulsion (HS). The masses of A^+, B^-, and M are M_A, M_B, and M_g, respectively.

The approximate probabilities labeled UIL and CNN are calculated from the limit (2.8) for uncoupled-intermediate levels and the limit (2.13) for coupled-nearest-neighbor, respectively. They are compared in Fig. 2(a) with the exact quasi-steady-state (QSS) solution of Eq. (2.2). The results, which pertain to termolecular recombination of equal mass species ($a=\frac{1}{3}$) for A^+–M collisions under polarization attraction (POL), are quite representative of other cases. Closer agreement of CNN with the exact results indicates that association tends to proceed via a sequence of small energy-changing transitions down the ladder of intermediate levels n, as expected, rather than via the indirect ($\mathscr{E}\to n\to\mathscr{S}$) larger energy-changing transitions of UIL, which involves each intermediate level n presumed uncoupled from one another. Moreover, both approximations appear robust with respect both to the number N ($=36$ and 72) of intermediate levels n adopted in block $\mathscr{E}$ and to the consequent decrease in spacing between the levels. The N pivots and spacings are selected by the highly accurate method prescribed in Ref. 6.

Since both approximations CNN and UIL are seen to satisfy the correct constraints (2.15), the overall agreement in Fig. 2(a) may however mask certain deficiencies. A more sensitive quantity of greater significance to recombination is the gradient (dP_l/dE_l), since, in the limit of small energy transfers, the energy-space current (2.3b) across $\mathscr{E}$ block level $-E$ reduces[4] to the diffusional current

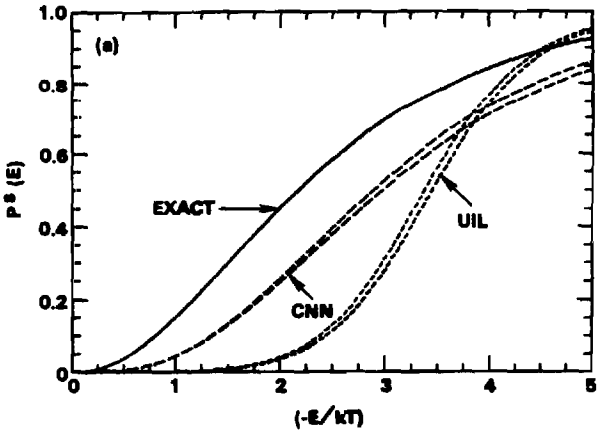

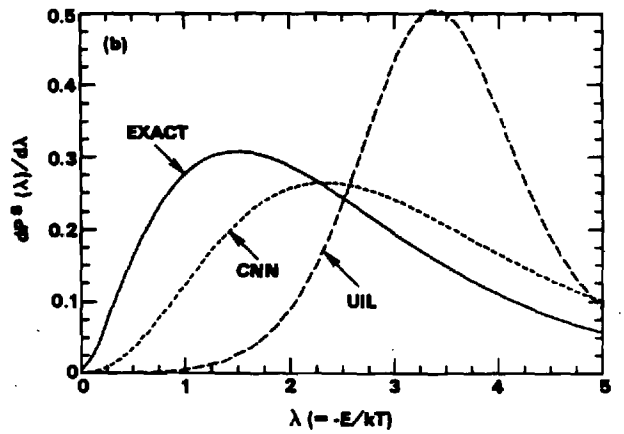

FIG. 2. (a) Stabilization probabilities (voltage drops) as a function of binding energy ($-E/kT$): EXACT [Eq. (2.2)]; CNN [Eq. (2.13)]; and UIL [Eq. (2.8)] with 72 pivots (upper curve) and 36 pivots (lower curve). (b) Corresponding derivatives.

$$j_d(-E) = D_i^{(2)}\left[\frac{dP_i^S}{dE_i}\right], \tag{3.2}$$

where the second-order energy-change moment is

$$D_i^{(2)}(E_i) = \frac{1}{2}\int_{-D}^{\infty}(E_f - E_i)^2 C_{if}\, dE_f . \tag{3.3}$$

The gradients shown in Fig. 2(b) are therefore expected to provide more reliable indicators of the extent of expected agreement between the corresponding rates.

This sensitivity is indeed confirmed in Figs. 3(a) and 3(b) which illustrate the quite different shapes for the var tions with E of $-j(-E)$, the downward energy-space c rent (2.3b), obtained from both approximations. The c rents (2.3b) are normalized to the exact QSS rate calcula from the numerical solution of Eq. (2.2) in Eq. (2.3b). though α_E is then by definition, constant with respect t variation, the E variation of the rate (2.3b) with the appro mate probabilities (2.8) and (2.13) indicates the sev breakdown of QSS, due to the differences displayed in F 2(a) and 2(b). The following points may now be noted.

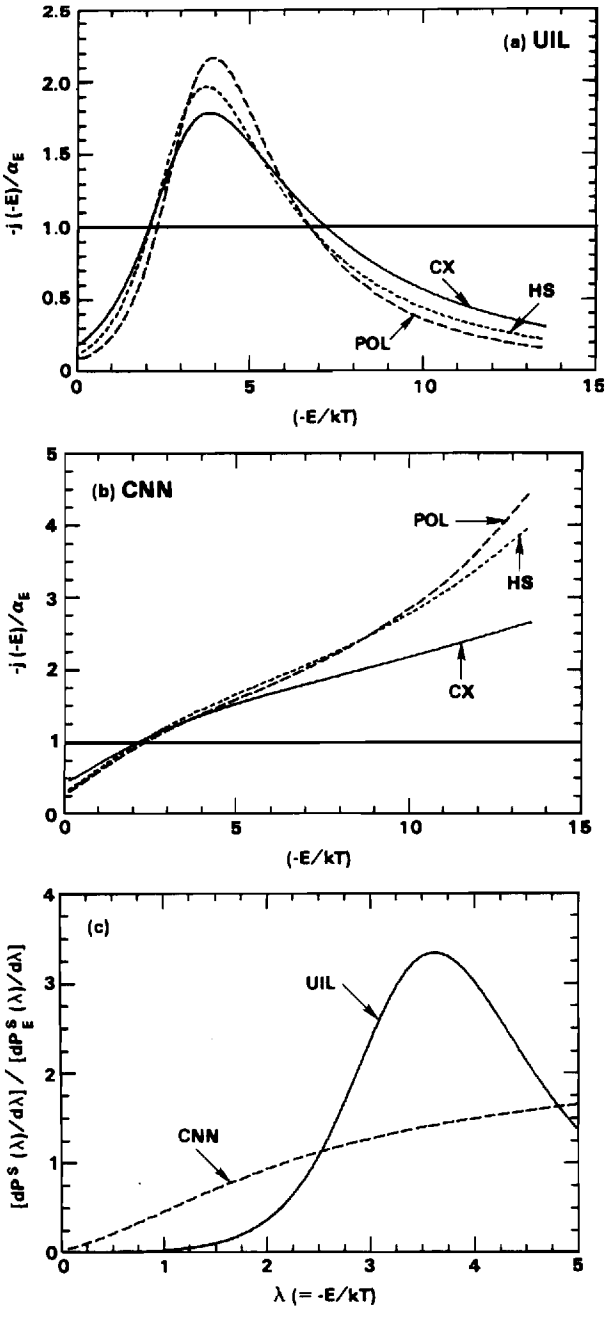

FIG. 3. Energy-space currents (2.3b), normalized to exact QSS rate α_E [Eq. (2.3b) with (2.2)] per unit $\tilde{N}_A\tilde{N}_B$ across bound energies ($-E/kT$): for model A–M interactions POL, HS, and CX. (a) UIL, with Eq. (2.8); (b) CNN, with Eq. (2.13); (c) ratio of approximate to exact derivatives, Eq. (3.4).

First, assigning the rate either at the dissociation li $E = 0$ (the $\mathscr{C}$–$\mathscr{B}$ interface) or at the lower association li $-S$ (the $\mathscr{B}$–$\mathscr{S}$ interface) represents a highly inaccur procedure for the case of non-QSS probabilities, as previo ly noted[4] for the diffusional results. Choosing the rate $\sim 2kT$ below the dissociation limit yields the exact QSS r for both approximations, a coincidence mainly due to agreement in Fig. 2(b) of the derivatives (dP_i^S/dE_i) $E_i \sim -2kT$.

Second, the different shape of Fig. 3(a) from that in 3(b) can be explained with the aid of Fig. 2(b). From (3.2), the ratio of the downward energy-space current to exact rate is

$$-j_d^{(A)}(E_i)/\alpha_E \approx \left[\frac{dP^S}{d\lambda}\right]_A \left[\frac{dP^S}{d\lambda}\right]_E^{-1}, \tag{3}$$

where A and E label approximate and exact quantities, spectively. As $\lambda = -E_i/kT$ increases to 2, Fig. 3(c) sh that the ratio (3.4) increases to unity for both CNN UIL. With further increase of λ, the CNN ratio continue increase while the UIL ratio increases until λ approa ~ 3.5 and then falls below unity past $\lambda \sim 7$. The diffe shapes in Figs. 3(a) and 3(b) are a direct reflection of variation for each approximation of the ratio (3.4) and firms the physical importance and significance of the gr ents (dP_i^S/dE_i).

In spite of its attractive illustrative features, the energy current (2.9) yields rates which are much sm than α_E by factors ranging from ~ 10 to $\sim 10^4$ as the parameter a of Eq. (3.1) varies from (1/3) for equal m to $10^{\pm 3}$. The simplified CNN result (2.14) varies fr factor of 3 higher for $a = 10^{-2}$, to a factor of 10 small $a = 1/3$, to a factor of 17 higher at $a = 10^3$, the limit for recombination in a gas.

As previously noted, the power expression (2.1), r than Eq. (2.3), must be used when approximate (non-C probabilities as Eq. (2.8) and (2.13) are adopted. Sinc QSS probabilities provided[2] a minimum α_E to Eq. (2.1 other approximate rates must be higher than α_E. Th indeed confirmed by Figs. 4(a) and 4(b), which also s that the CNN rates are much closer to α_E than the rates, as expected from the closer gradients in Fig. 2(b). maximum deviation occurs at $a = 1/3$ where the CNN are only $\sim 25\%$ higher than the exact QSS rates α_E. A the rates are normalized to the Thomson rate $\tilde{\alpha}_T$, as de in the previous reports.[3,4]

In addition to the exact QSS treatment, there are three accurate methods available for termolecular rates the previous variational procedure[2] which provides, in an alternative route to the QSS rates; (b) the previous

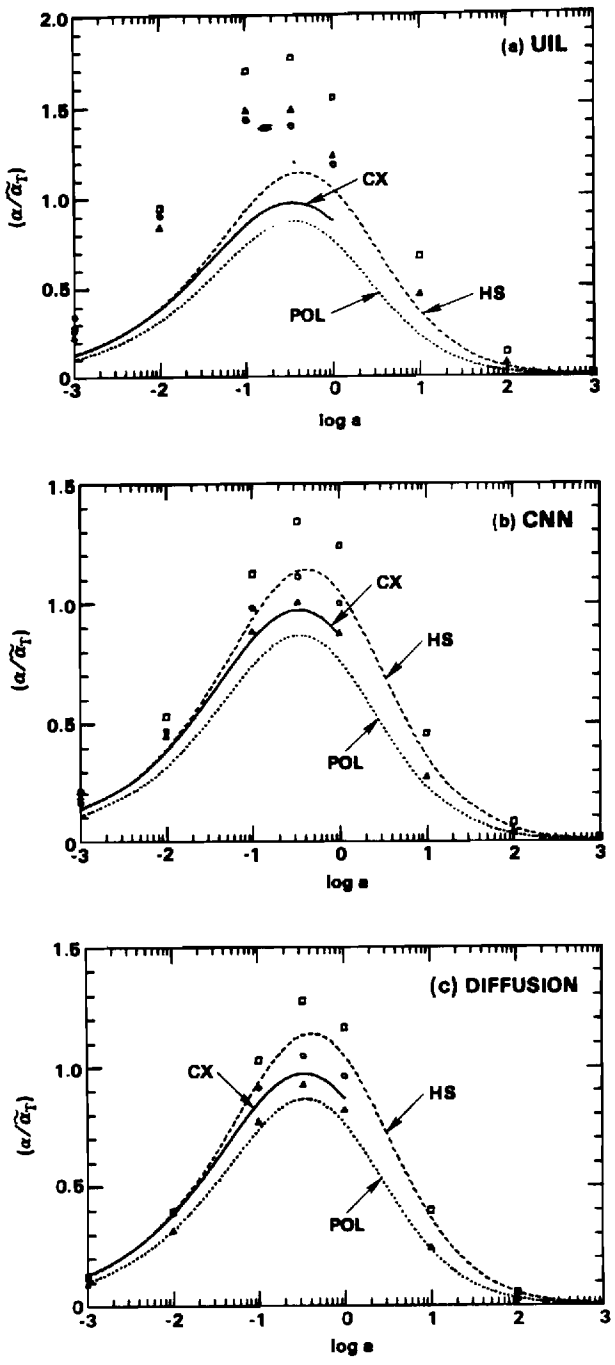

FIG. 4. Normalized partial rates $(M_A/M_{AB})(\tilde{\alpha}/\alpha_T)$ for termolecular recombination $A^+ + B^- + M \rightarrow AB + M$ resulting from $(A^+\text{–}M)$ collisions as a function of mass parameter a for various model interactions (CX and ○: symmetrical resonance charge transfer; HS and □: hard-sphere; POL and Δ: polarization attraction). (a) UIL, Eq. (2.1) with (2.8); (b) CNN, Eq. (2.1) with Eq. (2.13); (c) diffusion method, Eq. (2.1) with Eq. (3.6).

sional method[4] D; and (c) the present CNN method. Methods CNN and D are in effect similar in spirit in that CNN also includes upward and downward transitions, and also emphasizes the role of small energy changes between neighboring levels. The diffusion method, however, does not impose, as does CNN, an immediate cutoff to transitions which involve larger energy changes. The CNN probability (2.13) relies only on evaluation of the collision kernel $C_{n,n-1}$ via the relation

$$P_n^S = P_{n+1}^S + C_{n+1,n}^{-1}\left[\sum_{n=0}^{\infty} C_{n+1,n}^{-1}\right] \tag{3.5}$$

which is simpler to implement than the diffusion method,[4] for which

$$P_f^S(E_f) = P_i^S(E_i) + \left[\int_{E_i}^{E_f} \frac{dE}{D^{(2)}(E)}\right]\left[\int_{-s}^{0} \frac{dE}{D^{(2)}(E)}\right]^{-1} \tag{3.6}$$

which requires highly accurate[2] evaluation of the energy-change moment $D^{(2)}(E)$ given by Eq. (3.3).

Figure 4(c) shows the rates of the diffusion method obtained from calculations of $D_i^{(2)}$ which are more accurate than those previously determined in Ref. 4. Comparison between Figs. 4(b) and 4(c) indicates that comparable rates are achieved by the diffusion and CNN methods. The more sophisticated diffusion method, however, is, in principle, more accurate in the limits of small and large mass parameters a where the collision dynamics is weak so that the rates are then more sensitive to the stabilization probabilities P_i^S near the dissociation limit. The diffusion method is also more accurate for intermediate $a \sim 1/3$ since the larger energy transfers tend to be more influential and are included. In spite of these shortcomings, the CNN method yields rates, just slightly less good than the diffusion treatment.

IV. SUMMARY AND CONCLUSION

With the aid of an electrical diagram (Fig. 1) two extreme limits of collisional coupling are investigated in order to elucidate the role of various classes of transitions. A given level n is directly coupled only to its neighbor in CNN while, in UIL, each n is assumed coupled only to the fully dissociated and fully associated states of the reactant $\mathscr{C}$ and product $\mathscr{S}$ channels, respectively. The CNN approximation furnishes closer stabilization probabilities P_i^S and association rates α, thereby indicating that recombination tends to proceed more down an energy ladder of coupled levels than by larger energy jumps $\mathscr{C} \rightarrow n \rightarrow \mathscr{S}$ involving each intermediate level n. As in the case for all approximate P_i^S, the power equation (2.1) furnishes[7] the required rate (which is always higher than the exact QSS rate), rather than $j(-E_i)$ the energy-space current (2.3b) which holds[7] only for quasi-steady-state probabilities (2.2). The E_i variation of the energy-space currents $j(-E_i)$ deduced from non-QSS probabilities P_i^S is mainly determined by the derivatives (dP_i^S/dE_i), as in Eq. (3.4). When assessing via comparison with the exact QSS rate the effectiveness of the underlying physical mechanism in each approximate model (CNN, UIL, or diffusion) it is important to use the power expression (2.1). Otherwise, use of Eq. (2.9b), (2.14), or even of the energy-space currents (2.3b) as in Figs. 3(a) and 3(b) can lead to incorrect conclusions regarding the efficacy of the basic physical assumption.

In conclusion, the nearest-neighbor limit CNN appears to be a satisfactory approximation for termolecular ion–ion recombination over the full range of mass parameter and

interactions associated with (A^+–M) collisions. It is similar in spirit to the more sophisticated diffusion method, yields comparable rates, and yet it is much simpler to implement.

ACKNOWLEDGMENT

This research is supported by the U.S. Air Force Office of Scientific Research under Grant No. AFOSR-84-0233.

[1]D. R. Bates, Proc. R. Soc. London Ser. A 337, 15 (1974).
[2]M. R. Flannery, J. Chem. Phys. 89, 214 (1988).
[3]M. R. Flannery and E. J. Mansky, J. Chem. Phys. 88, 4228 (1988).
[4]M. R. Flannery, J. Chem. Phys. 87, 6947 (1987).
[5]D. R. Bates and A. E. Kingston, Proc. Phys. Soc. 83, 43 (1964).
[6]D. R. Bates and I. Mendaš, J. Phys. B 5, 1949 (1982).
[7]M. R. Flannery, J. Phys. B 18, L839 (1985).

Appendix A

Recombination Processes

M. R. Flannery

School of Physics

Georgia Institute of Technology

Atlanta, Georgia 30332-0430

U. S. A.

CONTENTS

1. SCOPE

The aim here is to survey the mechanisms basic to various types of recombination processes and provide some recent results. Most assume significance in astrophysics (interstellar medium, stellar and planetary atmospheres) and some in laboratory (Tokamak) fusion plasmas and in various types of lasers. They span a wide range in physical conditions e.g., the ranges $10 \leq T \lesssim 10^6$ in temperature T (^oK) and $1 \lesssim N \leq 10^{20}$ in particle density N (cm^{-3}). Recombination includes here not only electron-ion and ion-ion processes but also ion-atom (molecule) association. Most of the processes below may be characterized by the mechanism responsible for stabilization of an intermediate resonant collision complex. Typical two-body rates $k(cm^3\ s^{-1})$ for simple atomic and diatomic systems are indicated in parenthesis beside each process.

For *Termolecular Association* (TA)

$$A^+ + B + M \rightleftarrows (AB^+)^* + M \rightarrow AB^+ + M, \quad (10^{-28}\text{-}10^{-32})\ N\ cm^3 s^{-1} \qquad (1)$$

in a gas M of density N, stabilization of AB^* occurs via AB^* - M collisions at a quenching frequency $\upsilon_q \lesssim 10^{-9}\ N\ s^{-1}$, while *Radiative Association* (RA),

$$A^+ + B \rightleftarrows (AB^+)^* \rightarrow AB + h\upsilon\ , \quad (10^{-9}\text{-}10^{-17})\ cm^3 s^{-1} \qquad (2)$$

occurs via photon emission (vibrational and electronic) at a radiative rate $\upsilon_r \sim (10^3\text{-}10^6)\ s^{-1}$ depending on the type (vibrational or electronic) of stabilizing transition.

For *Dissociative Recombination* (DR),

$$e + AB^+ \rightleftarrows AB^* \rightarrow A^* + B\ , \quad (10^{-6}\text{-}10^{-7})\ cm^3 s^{-1} \qquad (3)$$

stabilization of AB^* occurs by quantal predissociation onto repulsive covalent excited molecular states at a dissociative frequency $\upsilon_d \sim 10^{15}\ s^{-1}$.

Emission of radiation provides the required stabilization in *Dielectronic Recombination* (DIR)

$$e + A^{Z+}(i) \rightleftarrows [A^{Z+}(k) - e]_{n,\ell} \rightarrow A^{(z-1)}(j;n\ell) + h\nu \ , \ (10^{-11}\ cm^3\ s^{-1}) \qquad (4)$$

which occurs at (resonant) electron energies much higher than the lower threshold energies for which the direct (non-resonant) *Radiative Recombination* (RR)

$$e + A^{Z+}(i) \rightarrow A^{(z-1)+}(i;n\ell) + h\nu \ , \ (10^{-12}\ cm^3\ s^{-1}) \qquad (5)$$

is more important. In contrast to the above formation of intermediate long lived scattering resonances in (1)-(4), *Termolecular Ion-Ion Recombination* (TR)

$$A^+ + B^- + M \rightarrow AB + M \ , \qquad (10^{-24}\text{-}10^{-25})\ N\ cm^3 s^{-1} \qquad (6)$$

of simple systems proceeds by non-resonant scattering since the Coulomb attraction cannot accomodate quasi-bound levels. The rates are fast since the third body M effectively utilizes the many (A^+-B^-) Coulombic superthermal encounters, which occur at large ion-ion separations $R \leq 3\ 70$ Å at room temperature. Elastic A^+-M and B^--M collisions are very efficient in removing most of the energy gained by A^+ and B^- from the Coulomb field so that the highly excited bound levels of AB so formed are then destroyed by multistep collisional cascades to stable levels. In parallel to the resonant scattering in (1), TA can also proceed via non-resonant (A^+-M) collisions which change the energy and angular-momentum of (A^+-B) relative motion.

Termolecular Electron-Ion Recombination

$$e + A^+ + M \rightarrow A(n) + M, \quad (10^{-26}\text{-}10^{-29})\ N\ cm^3 s^{-1} \tag{7}$$

also proceeds via collisions with the gas M, but at a much smaller rate, since elastic electron-atom M collisions cause only a small fraction (~2m/M) of energy to be transferred to M. Rates become larger for molecular M which absorb a much larger fraction of energy via rotational and vibrational excitation, and for molecular ions when dissociative recombination involving bound electrons can provide substantial enhancement.

As is well known, *Mutual Neutralization* (MN)

$$A^+ + B^- \rightarrow A^* + B\ , \qquad (10^{-7}\text{-}10^{-8})\ cm^3\ s^{-1} \tag{8}$$

proceeds by direct coupling of the diabatic ionic potential energy curve with the covalent curves, which however involve much smaller ion-ion separations $R \sim (10\text{-}50)$ Å to yield rates an order of magnitude smaller than for (6). The fact that the Coulombic interaction between the ions is strong at large separations where the (Landau-Zener) probability for curve crossing is weak ensures the dominance of termolecular process (6) over bimolecular process (8), even at modest pressures. Since collisions with M can form bound $(A^+\text{-}B^-)$ states which in turn promote more efficient curve crossing, MN can be considerably enhanced by an ambient gas. It does not occur parallel to TR (6) so that the effective rate for neutralization is then not simply the sum $(k_{TR} + k_{MN})$ of the individual rates.

In an electron-ion plasma of intermediate density $n_e \sim 10^{11}\ cm^{-3}$, recombination

$$e + A^+ + e \rightarrow A(n) + e + h\nu \tag{9}$$

proceeds by collisions into high n-levels, which become de-excited by e-A(n) collisions and radiative emission. State-to-states rates for DIR (4), RR (5), DR (3), and NSR (7) would all be relevant. Collisional-radiative recombination (CRR) then yields the familiar set of quasi-equilibrium (input = output) Master Equations to be solved for the individual excited state populations N_n in terms of the concentration of free electrons, ions and recombined atoms in the lowest stabilized states.

1.1 CURRENT STATUS OF RECOMBINATION

The present state of recombination is that theory (with reliable results) for most of the above processes involving simple atomic or diatomic systems is reaching maturity and is approaching a well defined Hi-Tech State. In particular the recent theoretical developments[1-3] of DIR indicate that DIR cross sections may be calculated to within the same degree of accuracy (~10%) as electron-ion inelastic collisions. Termolecular ion-ion recombination[4-6] of simple ion systems in a gas has been solved as a universal function of mass species, and gas density and temperature. Results for simple systems of general mass are available at low density. Dissociative recombination[8] of simple diatomic systems is in principle well known but lack of relevant molecular potential energy curves and branching ratios to final products prohibit rigorous quantal calculation. Ion-neutral reactions and termolecular electron-ion recombination for complex systems remain by comparision in a more exploratory condition, although substantial progress[9,10] has recently occurred.

Reliable experiments[8,11-13] exist for DR, TA and MN which proceed with measurable rates (10^{-7}-10^{-9} cm^3s^{-1}). Technical breakthroughs have recently permitted measurements on DIR[14,15] and RA[16] which proceed at much slower rates (10^{-10}-10^{-15}) cm^3s^{-1}, respectively. The influence of electric fields in the experiments is important, particularly for DIR and to a lesser extent for

DR. Theories of recombination in external fields are currently under development.

Although TR (6) is now well understood theoretically and proceeds at the largest rate of any recombination processes involving simple systems, reliable experimental measurement, apart from some historical data,[17] is as yet not forthcoming although some activity has recently emerged.[18] There are at present no measurements from a given laboratory which span the full range of gas pressures studied theoretically and which monitor the identity of ions as the pressure changes. The task is difficult in that the ions may well be clustered to high orders.

1.2 GENERIC KINETIC AND RESONANT-SCATTERING TREATMENT

Identify the interacting species in (1)-(9) as A, B and M with concentrations n_A, n_B and N, respectively. The two stage sequence common to TA(1), RA(2), DIR(3) and DR(5) is the formation of a long-lived unstable collision complex AB^*, or scattering resonance, followed by an irreversible stabilization mechanism, whether radiative as in RA and DIR, collisional as in TA or dissociative as in DR. The complex with energy degenerate to and lying within the continuum of dissociated A(i) + B(j) states is formed when the excess energy and angular momenta of internal and relative motion of A and B become redistributed among the internal degrees of freedom of AB^*. Following large perturbations in (A-B) close encounters, a quasi-equilibrium of these excited states of AB^* is established. Thus processes RA(1), TA(2), DR(3) and DIR(4) above may be conveniently analyzed in terms of the macroscopic two stage sequence

$$A + B \underset{\nu_d}{\overset{k^*}{\rightleftarrows}} AB^* \xrightarrow{\nu_s} \text{products} \qquad (10)$$

which involves the stabilization at frequency ν_s of quasi-bound resonant scattering states of AB^* formed at rate k^* ($cm^3 s^{-1}$) before AB^* can

redissociate (or autoionize) back to the initial or any other dissociated channel at frequency ν_d. For a quasi-steady-state density n^*_{AB} of the AB^*, the overall process then proceeds at a rate ($cm^3 s^{-1}$)

$$k = n^*_{AB}\nu_s = \left[\frac{\nu_s}{\nu_d+\Sigma\nu_s}\right] k^* \equiv P_s\, k^* \qquad (11)$$

where P_s is the probability of routing to a particular pair of stabilized products s. A negative temperature T dependence is anticipated for k since ν_d increases with T. As the density N of the gas M is raised, (11) for collisional association TA predicts an initial linear variation of k with N (when $\nu_d >> \nu_s \sim k_s N$) increasing towards a saturation value k^* (when $\nu_s >> \nu_d$) times the branching ratio $[\nu_s/\Sigma\nu_s]$ for that particular pair of products.

The reaction volume (cm^3)

$$K = n^*_{AB}/n_A n_B = k^*/\nu_d \qquad (12)$$

is pivotal in determining the T-dependence of the overall rate

$$k = \left[\frac{\nu_s K(T)}{k^* + \Sigma\nu_s K(T)}\right] k^* = K(T)\left[\frac{\nu_s \nu_d}{\Sigma\nu_s + \nu_d}\right] \qquad (13)$$

Note that K is not an equilibrium constant in the usual sense since AB^* is distributed only among those states satisfying energy and angular momentum conservation above the dissociation limit. It is given in usual notation by

$$K(T) = \frac{h^3}{(2\pi M_{AB} kT)^{3/2}} \frac{q(AB^*)}{q(A)q(B)} \frac{\omega_{AB}}{\omega_A \omega_B} \qquad (14)$$

where q is the internal partition function, or the number of quantum states available at temperature $T \sim \sum_i \exp(-E_i/kT)$, and where ω is the electronic statistical weight, associated with each reactant A and B and with the activated complex AB^* of reduced mass M_{AB}. While q(A) and q(B) are generally known, $q(AB^*)$ must include only those rotational-vibrational-electronic states of AB^* accessible at energies above the dissociation threshold of AB. It also includes states which satisfy conservation of total angular momentum produced from the orbital angular momentum for (A-B) relative motion and the combined internal angular momentum of the individual reactants.

The key quantities which characterize the T-dependence and rate limiting step of each of RA, TA, DIR and DR are therefore K(T) and the stabilization frequency ν_s. For polyatomic species, not only is calculation of K difficult but ν_s is uncertain to the extent that the type of transition (vibration or electronic) may not be established. This lack can involve at least two orders of magnitude difference in the rates.[10]

For cases RA, DIR, DR and TA, a microscopic state-to-state generalization, (phase-space or multichannel) of the basic premise underlying (11) can be written down in terms of all the relevant electronic, vibrational and rotational quantum numbers for the internal degrees of freedom i and j of A(i) and B(j), for the translational energy and angular momentum of A-B relative motion and for the total conserved angular momentum and energy. The simplified expression (11) however not only serves as a guide to experimentalists in elucidating the role, and extracting the rate peculiar to various stabilization mechanisms but is also capable of providing order-of-magnitude rates and the associated dependence on temperature T fairly reliably.

The intimate connection of (11), standard in chemical kinetics, with scattering theory is instructive. When the redissociation or autoionization channels in (1)-(5) are considered as a series of non-overlapping resonances

and when the non resonant background scattering is neglected, then Breit-Wigner resonance scattering theory with explicit inclusion of all multi-channels, consistent with energy and angular momentum conservation, can be applied. In order to preserve a simple notation to isolate the key connection, and to illustrate the essential technique, let AB^* exhibit only relative motion scattering resonances (quasi bound states) at (A-B) relative energies $E = E_r^*$. The cross section for the resonant reaction of A and B with internal energies $E_{A,B}$ is

$$\sigma(E;E_A,E_B) = \frac{\pi}{E}\left(\frac{h^2}{2M_{AB}}\right)\frac{\omega(AB^*)}{\omega(A)\omega(B)}\sum_r \frac{\Gamma_a\,\Gamma_s}{[(E_T-E_r^*)^2+\frac{1}{4}\Gamma^2]} \qquad (15)$$

where the total energy of the system is $E_T = E_A + E_B + E$, where the energy widths for stabilization and re-dissociation (autoionization) are related to the corresponding frequencies by

$$\Gamma_s = h\,\nu_s, \qquad \Gamma_d = h\,\nu_d \qquad (16)$$

where Γ is the total width $(\sum_d \Gamma_d + \sum_s \Gamma_s)$ for all dissociative (d) and stabilization channels (s). The electronic statistical weight of species X is $\omega(X)$. The rate of recombination for a Maxwellian distribution of relative energies E at temperature T is

$$k(T) = \left(\frac{8kT}{\pi M_{AB}}\right)^{1/2}\int_0^\infty \epsilon\,\sigma(\epsilon)\,\exp(-\epsilon)d\epsilon\;;\quad \epsilon = E/kT \qquad (17)$$

where M_{AB} is the reduced mass of (A-B). Since the Dirac delta function $\delta(x)$

is $\pi^{-1} \lim_{h\to o} h(x^2+h^2)^{-1}$, the rate (17) for sharp resonances $\Gamma << (E_T-E_r^*)$ then reduces to

$$k(T,E_A,E_B) = \frac{h^3}{(2\pi M_{AB}kT)^{3/2}} \frac{\omega_{AB}}{\omega_A\omega_B} \left[\sum_r \frac{\nu_d\nu_s}{(\Sigma\nu_s+\nu_d)} \exp-(E_r^*/kT) \right] \exp(E_A+E_B)/kT \quad (18)$$

On assuming that the frequencies are independent of the resonance positions E_r^*, then $\sum_r \exp(-E_r^*/kT)$ is then simply the partition function $q(AB^*)$ arising from all the resonance states of AB^*. On averaging over all internal states i and j of A and B and with the use of detailed balance, (12), (11) and (14) are then recovered since $\sum_{i,j} \exp(-E_A/kT) \exp(-E_B/kT)$ is the product $q(A)q(B)$ of the reactant partition functions. This connection provides a basis for (11) or (14) more quantitative than the earlier steady-state kinetic rate argument. The extension to include all multichannels directly is straight- forward, but the case of overlapping resonances existing in various polyatomic systems requires attention, and may well under approximation provide the rate (13) in current use.

Because of the long range Coulombic attraction in the entrance channels the remaining related processes (TR, TER), as indicated earlier, do not proceed via the resonating tight complex but rather by energy-changing collisions between M and (A^+-B^-) pairs. The collisions are effective for those pairs with separation $R \lesssim R_T = e^2/kT \sim 370$ Å at room temperature, which in a sense can be regarded to form an extremely large loose non-resonating complex with reaction volume $K = \frac{4}{3}\pi R_T^3$. At low gas density N, (13) predicts

$$k_{TR} \sim \frac{4}{3}\pi R_T^3 \nu_s = \frac{4\pi}{3} R_T^3 \langle v_{AB} \rangle N \sigma \quad (19)$$

where σ is the cross section for free-bound energy-changing (A^+-B^-)-M collisions, and emphasizes the characteristic linear N and the $T^{-5/2}$-T^{-3} dependencies. At high N, however, the rate does not converge to the saturation value k^* predicted by (13). The rate of approach of A^+ and B^- to R_T is limited by the transport rate, which decreases as N^{-1} and which becomes comparable to the reaction rate (19) within R_T at about ~1 atm. For TA(1) however the transport rate always remains much higher than the rate limiting step of reaction so that saturation to the thermal rate k^* is eventually obtained.

2. RADIATIVE AND TERMOLECULAR ASSOCIATION

2.1 *SIMPLE SYSTEMS*: The underlying physics of *Radiative Recombination* of simple system as

$$C^+(^2P_{1/2}) + H(^2S) \rightarrow CH^+(A\,^1\Pi) \rightarrow CH^+(X\,^1\Sigma) + h\nu \qquad (20)$$

becomes transparent in a semiclassical treatment,[19] where the cross section is

$$\sigma(E) = 2\pi \int_0^\infty P_r(E,\rho)\rho \, d\rho \qquad (21)$$

at relative energy E. The probability of radiative emission during a collision at impact parameter ρ is

$$P_r(E,\rho) = \int_{-\infty}^{\infty} G(t)A(t)dt = \oint_R^{\infty} G(R)A(R)dR/v_R \qquad (22)$$

where the radial speed at relative separation R is v_R with turning point R_T, and where G(R) is the probability that CH^+ during the collision is in state i ($A\,^1\Pi$), which radiates at a local rate

$$A(R) = \frac{4}{3} h^4 c^3 \, |M(R)|^2 \, \Delta E^3(R) \qquad (23)$$

to the stabilized state f($X\,^1\Sigma$). The molecular states, with wavefunctions $\psi_{i,f}$ and energy separation $\Delta E(R) = V_f(R) - V_i(R)$, are connected via the dipole

matrix element $M(R) = \langle \Psi_f(\underset{\sim}{r},R) | e\underset{\sim}{r} | \Psi_i(\underset{\sim}{r},R) \rangle$. Rates $k_{RA} = 1.3\ 10^{-17}\ cm^3\ s^{-1}$ obtained[19] for (20) over the temperature range $20 \leq T\ (^oK) \leq 1000$ do not, however, satisfactorily explain the discrepancy between the observed and theoretically deduced abundances of the radical CH^+ in diffuse interstellar clouds. A quantal treatment can in addition acknowledge the discrete vibrational levels of the intermediate electronic state $i(A\,^1\Pi)$ and can include quasi-bound resonances formed within the centrifugal barrier. These effects enhance[20] the semiclassical rates for (20) by ~ 25%, mainly at lower T. Also state i may support predissociating levels between the fine structure state $C^+\ (^2P_{1/2})$ and $C^+\ (^2P_{3/2})$ of the reactants. No full treatment has as yet been performed.

Termolecular Association

$$A^+ + B + M \rightarrow AB^+ + M \tag{24}$$

for formation of simple diatomics as He_2^+, Ne_2^+, etc. can be considered[21] as proceeding via a multistep series of collisions between $(A^+\text{-}B)$ pairs and M which change both the energy E and angular momentum L of relative $(He^+\text{-}He)$ motion to such an extent that bound stabilized levels are formed. At lower energies E there is an additional contribution from quasi-bound resonances[22] formed at positive E within the centrifugal barrier.

A multichannel generalization of (13) to simple (structureless) atomic systems yields the termolecular association rate[23]

$$k_{TA} = \int_0^\infty dE \int_0^{L^2_{max}} dL^2 \left[\frac{k_i^s K_i N}{k_i^* + k_i^s K_i N} \right] k_i^* \tag{25}$$

where subscripted-i rates refer to specific energy E and angular momentum L of A-B relative motion, where L_{max} is the maximum L of the complex at fixed E,

and where

$$k_i^s N n_i^* = \int_{R_i^-}^{R_o} n_i(R)\, \upsilon_i(R) d\underset{\sim}{R} \tag{26}$$

is the overall frequency for stabilization of all the $(A\text{-}B)_i$-pairs with internal separation R between the innermost turning point R_i^- of radial motion and the radial boundary $R_o(E,L)$ of the complex. The pair-distribution per unit interval $d\underset{\sim}{R}\, dE\, dL_i^2$ is $n_i(R)$, and $\upsilon_i(R) = k_q N$ is the frequency of $(A\text{-}B)_R^*$ - M quenching collisions with rate k_q at fixed (R, E_i, L_i^2). At low gas densities N this distribution can be taken as its equilibrium value $\tilde{n}_i$, since υ_i in (26) is already linear in N. When the quenching coefficient k_q is constant, and equal to some fraction β of the constant Langevin limiting rate for spiralling $(AB^*\text{-}M)$ collisions

$$k_L = 2\pi e(\alpha_M/M_s)^{1/2} \tag{27}$$

where α_M is the polarizability of M and M_s is the reduced mass of the $(AB^*\text{-}M)$ system, it then follows that

$$n^* = \int_o^\infty dE \int_o^{R_o(E)} d\underset{\sim}{R} \int_o^{R^2p^2} \tilde{n}_i(R) dL^2$$

$$= \frac{2}{\sqrt{\pi}} (kT)^{-3/2} \int_o^\infty \exp(-E/kT) dE \int_o^{R_o(E)} [E-V(R)]^{1/2}\, d\underset{\sim}{R} \tag{28}$$

For polarization attraction $V(R) \sim (\alpha_B e^2/2R^4)$ between A^+ and B of polarizability α_B and orbiting radius $R_o(E) = (\alpha_B e^2/2E)^{1/4}$, (28) yields

$$n^* = \frac{4}{3}\pi R_L^3 \frac{8}{\sqrt{\pi}} \tag{29}$$

where R_L is $(\alpha_B e^2/2kT)^{1/4}$ and $(8/\sqrt{\pi})$ arises from both the focusing effect and the enhancement of R_o at small E. The association rate at low N is then

$$k_{TA} = n^*[\beta(T,N)k_L]N \sim (10^{-28} - 10^{-31})N \text{ cm}^3 \text{ s}^{-1} \tag{30}$$

which exhibits the temperature dependence $\beta(T)\ T^{-3/4}$. The efficiency $\beta \sim 1$, but for He^+ - He charge transfer collisions the quenching rate $k_q \sim \langle v_{AM}\sigma_{AM}\rangle$ involves an additional $(kT)^{1/2}$ factor from v_{AM} and a factor $(kT)^{-1}$ from focusing effects so that $k_A \sim T^{-5/4}$ at low temperature.

2.2 *COMPLEX SYSTEMS*: Here, rates are much higher due to increase in the physical size and in the number of internal modes of the intermediate complex. For triatomic ionic systems as

$$C^+ + H_2 \underset{v_d}{\overset{k^*}{\rightleftarrows}} (CH_2^+)^* \xrightarrow{v_r} CH_2^+ + h\nu \tag{31a}$$

which initiates carbon phase chemistry in diffuse and dense interstellar clouds,[24] and for polyatomic complexes as in either

$$CH_3^+ + H_2 \rightleftarrows (CH_5^+)^* \rightarrow CH_5^+ + h\nu \tag{31b}$$

which is a precursor[9] to the formation of methane (CH_4), or in

$$CH_3^+ + H_2O \underset{v_d}{\overset{k^*}{\rightleftarrows}} (CH_3^+ \cdot H_2O)^* \xrightarrow{v_r} CH_3^+ \cdot H_2O + h\nu \tag{31c}$$

which can be photodissociated[24] to produce methanol (CH_3OH) in the interstellar medium, the "kinetic chemical" approach is as yet the only viable method. The collision duration is much longer than that for simple systems as (20) and there are simply too many degrees of freedom in the intermediate complex to consider in a full quantal state-to-state fashion. Moreover the complex offers a near continuum of closely spaced vibrational (and electronic) energies, overlapping resonances and many intramolecular processes so that a state-to-state method could not be considered as providing the most efficient or realistic description.

In order to isolate radiative association (RA) from termolecular association (TA) extremely low neutral densities $\lesssim 10^{10}$ cm^{-3} and temperatures T (10^{o}K-30^{o}K) are required. The mechanisms often proceed in parallel so that, in the coupled sequence,

$$A + B + (M) \underset{\upsilon_d}{\overset{k^*}{\rightleftarrows}} AB^* \xrightarrow{\upsilon_r} AB + h\upsilon \tag{32}$$

$$\underset{\upsilon_d}{\overset{k^*}{\rightleftarrows}} AB^* \xrightarrow{\upsilon_q} AB + M \tag{33}$$

radiative association occurs at the rate

$$k_{RA} = n^*_{AB}\, \upsilon_r = \left[\frac{\upsilon_r}{\upsilon_d+\upsilon_s}\right] k^* \tag{34}$$

and termolecular association at the rate

$$k_{TA} = n^*_{AB}\, \upsilon_q = \left[\frac{k_q M}{\upsilon_d+\upsilon_s}\right] k^* \,. \tag{35}$$

The frequency of stabilization of the complex, against *both* natural and collisional disruption at frequency υ_d, is

$$\upsilon_s = \upsilon_r + k_q N \quad , \tag{36}$$

the sum of the radiative decay frequency υ_r, and the frequency $k_q N$ for collisional quenching. At low densities $N(H_2,He) \sim (10^3\text{-}10^{10})$ cm^{-3} in interstellar clouds, $\upsilon_s = \upsilon_r << \upsilon_a$, so that the overall association is radiative controlled proceeding at rate

$$k_A = k_{RA} = K \upsilon_r \tag{37}$$

where the reaction volume is given by (14). At intermediate densities $(10^{10}\text{-}10^{16})$ cm^{-3}, υ_s still remains $<< \upsilon_a$, and association proceeds at rate

$$k_A = k_{RA} + k_{TA} = K (\upsilon_r + k_q N) \tag{38}$$

which increases with gas density N, until it saturates to the limiting rate $k_{TA} = k^*$ of collisional formation of the original complex. The rate (38) is determined by the character of the interaction between the transition channels within the complex and differences in temperature dependence are mainly controlled by the T-variation of the reaction volume K(T). Radiative stabilization rates υ_r for complex systems are also uncertain, but are expected to be $\upsilon_r \sim 10^3$ s^{-1} for vibrational transitions and $\upsilon_r \sim 10^5\text{-}10^6$ s^{-1} for electronic transitions. The larger electronic rates υ_r permits association in interstellar clouds to proceed faster than originally supposed.[9]

Typical values for the relevant rates are the Langevin limit $k^* \sim 10^{-9}$ cm^3 s^{-1}, $\upsilon_a \sim 10^7$ s^{-1}, $\upsilon_r \sim 10^3\text{-}10^5$ s^{-1} and the Langevin limit $\upsilon_q \sim 10^{-9} N$ s^{-1}.

Radiative rates $k_{RA} \sim (10^{-13}\text{-}10^{-11})$ cm^3 s^{-1} and termolecular rates $k_{TA} \sim 10^{-25}$ N cm^3 s^{-1} are then expected for complex systems at low gas densities N. Termolecular association therefore begin to compete with RA for $N \sim 10^{12}$ cm^{-3} while at higher $N \gtrsim 10^{15}$ cm^{-3}, TA becomes dominant.

Few experiments exist on RA, mainly due to the smallness of the rate $\sim 10^{-13}$ cm^3 s^{-1} and difficulty in achieving low temperatures ($T \sim 10^{o}K$) and densities ($N \lesssim 10^{9}$ cm^{-3}) needed for isolation of RA. The TRAP technique of Dunn and associates[16] represents a spirited effort while at higher $N \sim 10^{11}$ - 10^{13} cm^{-3}, the ICR (ion-cyclotron resonance)-experiment[25] measures the RA and TA combination (21). By contrast, many TA experimental studies at yet higher $N \gtrsim 10^{15}$ cm^{-3} exist for atmospheric species - the SIFT (selected ion flow tube) technique[12] being the major contributor. For TA, reasonable (order-of-magnitude) agreement exist with theory, particularly in the temperature variation. For RA, the few measurements of (24) and (25) do not agree with available theory and do not furnish information on the type (vibrational or electronic) of radiative stabilization. Interesting discrepancies between experiment and theory based on (42) and (43) for polyatomic species are discussed by Bates and Herbst.[10]

3. DISSOCIATIVE RECOMBINATION

3.1 *DIRECT PROCESS*

In the direct two stage mechanism (Fig. 1a)

$$e + AB^+(v_i) \underset{\upsilon_a}{\overset{k^*}{\rightleftarrows}} (AB^*)_r \xrightarrow{\upsilon_s} A^*+B, \quad k_{DR} \sim (300/T)^{1/2}\ 10^{-7}\ cm^3\ s^{-1} \qquad (39)$$

the electron of energy ϵ excites an electron of the ion-core AB^* and is then resonantly captured via a Franck-Condon (FC) vertical transition onto the repulsive state r of the double excited molecule (AB^*). Competition between reverse autoionization at nonlocal frequency υ_a and predissociation at

nonlocal frequency ν_s continue until the electronically excited neutral fragments accelerate past the stabilization point R_s. Beyond R_s the increasing energy of relative separation has reduced the total electronic energy to such an extent that autoionization is essentially precluded and the neutralization is then rendered permanent. The kinetic energy of the electron (in the field of AB^+) is effectively transferred here to motion of the nuclei not by direct collision but via a rearrangement in (39) of the whole electronic cloud. DR is a "*reactive*" process in the sense that the reactants and products involve different collision partners.

The autoionization character of AB^* for $R < R_s$ makes resonant capture originally possible, and the covalent repulsive character for $R > R_s$ makes neutralization finally permanent. For reasonable capture over a range of ϵ, the autoionization width $\Gamma_a \sim h\,\nu_a$ must not be too small, while large stabilization probabilities P_s demand small widths. The requirement of resonant capture without any energy transfer between electronic and nuclear motion is that the vertical difference in the potential-energy curves (PE^+ and PE^*) for XY^+ and XY^* equals ϵ (Fig. 1a). For thermal-energy electrons this requirement is best fulfilled when PE^* crosses PE^+ on the right side of its minimum (cf. Fig. 1a), as for most cases of doubly excited electronic states with more than four electrons. This energy-matching can consequently occur over the full range of ϵ.

Large capture rates depend therefore on good electron-electron communication (correlation) and on good vibrational overlap between the AB^+ bound and AB^*-continuum nuclear wavefunctions, an overlap which is sensitive to the initial vibrational level v_i of the ion and to the crossing of PE^* and PE^+. When the only crossings in Fig. 1a are provided by the upper repulsive PE^* curves, then the capture probability remains small for $v_i=0$ ions and thermal electrons, and becomes large only when these curves are accessed by more

energetic electrons $\epsilon \gtrsim 0.5$ eV, which imply however smaller Coulomb focused scattering cross sections $\sigma \sim \epsilon^{-1}$. This is the situation with H_2^+ (v_i=0) and He_2^+. Conversely, the overlap of AB^+ (v_i=2) in Fig. 1(a) with the lower PE^* is poor, relative to the much larger overlap with the upper curves. Note ϵ is measured from R on PE^+.

In keeping with (11), the recombination cross section for simple systems may be factored as

$$\sigma_{DR}(\epsilon) = \sigma_c(\epsilon)\ P_s(\epsilon) \tag{40}$$

where the cross section for capture at R_c is[26]

$$\sigma_c(\epsilon) = \frac{C}{\epsilon}\ |V(R_c)|^2 |\psi_v^+(R_c)|^2 [dR/d(PE^*)]_{R_c} \tag{41}$$

Here V(R) is the electronically-averaged interaction coupling the initial and intermediate molecular systems, ψ_v^+ is the vibrational wavefunction for $AB^+(v)$ and C is $(2\pi^3/m\ h)[\omega(AB)/\omega(AB^+)]$. The stabilization probability is given as in (11) by $\upsilon_s/(\upsilon_a+\Sigma_s\ \upsilon_s)$. By analogy with dissociative attachment, it may also be approximated by,[26]

$$P_s(\epsilon) = \exp[-\int_{t_c}^{t_s} [\Gamma_a(R)/h]dt] \tag{42}$$

where $\Gamma_a(R)$ is a *local* autoionization width (so that $\Gamma_a = h\ \upsilon_a$ is the probability of electron ejection per unit time) and where the integration is over the interval from the time t_c at formation of AB^* at R_c to the time t_s when stabilization at R_s is rendered permanent. This interval depends on the total energy and slope of PE^*. Although the *local* $\Gamma_a(R)$ in (42) is not strictly

appropriate to recombination at thermal ϵ, (43) remains useful as an estimate of the influence of autoionization. Thus P_s is reduced by an increase in number of open bound vibrational channels over which autoionization proceeds when electrons are emitted not only at energy $\epsilon_a = \epsilon$ but also at $\epsilon_a \neq \epsilon$ when the energy imbalance is absorbed by vibrational motion. It is enhanced not only by a reduction in the time interval, but also by an increase in the density of intermediate complexes and product channels, as with ion-clusters. The ϵ^{-1}-dependence of σ_c results in recombination rates (11) which decreases as $T_e^{-0.5}$. For typical diatomic molecular ions as Ne_2^+ or NO^+, dissociation occurs at frequencies $\nu_a \sim 10^{15}$ s^{-1}, large compared with $\nu_a \sim 10^{14}$ s^{-1} for autoionization, so that P_s is close to unity. At thermal energies Coulomb focusing dominates the capture so that $\sigma_c \sim \epsilon^{-1} \gtrsim 10^{-14}$ cm^2. Rates k_{DR} (Ne_2^+) $\sim 2\ 10^{-7}\ (300/T)^{0.5}$ cm^3 s^{-1} are then quite typical. As one proceeds through an ion sequence ($Ne_2^+ \rightarrow Xe_2^+$), the natural increase in σ_c is due both to the stronger interactions and larger vibrational amplitudes and P_s remains substantial. Owing to the increasing steepness of PE^*, it generally increases. Continued increase in σ_c however implies a corresponding increase in autoionization width so that P_s will eventually decrease, until it becomes limited to (ν_s/ν_a) as for the case of polyatomic systems.

3.2 *INDIRECT PROCESS*

In the following indirect additional mechanism for DR,[26]

$$e + AB^+(v) \rightleftarrows [AB^*(n,v)]_a \rightleftarrows (AB^*)_r \rightarrow A^* + B \qquad (43)$$

the electron is captured into attractive (a) vibrationally excited (v') Rydberg states (n) of AB^* which converge to the initial electronic state of AB^+ (Fig. 1b) and which are then coupled by configuration interaction to the dissociative channels. The first stage involves energy transfer from the

electron directly to vibrational excitation of the nuclei. In contrast to the broad ϵ-range enjoyed by the direct process (31), only selected energies ϵ' close to the Rydberg level (Fig. 1b) contribute to the indirect process which is therefore characterized by a series of narrow resonances (enhancements or dips) in the overall recombination cross section at the low electron energies $\epsilon \leq 1$ eV favored by this process.

The formal multichannel quantum theory of DR via the direct and indirect mechanisms can be constructed.[8] For full quantal calculations the following information is required as input: (a) identification and calculation of the relevant PE^+ and PE^* curves for the capture cross section including those for the vibrationally excited Rydberg state, (b) the quantum coupling between the autoionization and dissociation channels for the widths Γ_a and Γ_s and (c) the branching ratios to all possible products of dissociation. Since the coupling (b) appears as a resonance in the asymptotic phase of the electronic wavefunction the widths may be obtained either from direct electron-ion scattering calculations or from extrapolation of the properties of the Rydberg and valence bound states across the ionization threshold. The main theoretical problems are associated with the uncertainty of the role of the vibrationally excited Rydberg states and with the branching ratios which in turn involves solution of a set of coupled equations incorporating the interactions between the various products of dissociation. The "reactive" DR process combines therefore both electron-ion, ion-ion and neutral-neutral scattering technologies. Because of the sensitivity (as indicated above) of k_{DR} on the slopes, shapes and relative positions of PE^+ and PE^* and the lack of accurate PE curves for most systems, rigcrous calculation has been confined mainly[27,28] to H_2^+ and to some diatomic ions (N_2^+, O_2^+ and NO^+) of atmospheric significance.[8]

DR for even the simplest diatomic system $e+H_2^+$, although not quite typical, is instructive. The sole candidate in the direct process for $e-H_2^+(X^2\Sigma_g^+,v)$ recombination at low energies $\epsilon \leq 1$ eV is the lowest doubly excited $^1\Sigma_g\ (2p\sigma_u)^2$ state of H_2 which crosses the $^1\Sigma_g^+$ ion state in the vicinity of the v = 2 level, and which dissociates into ionic fragments $H^+ + H^-$. Because of the propensity rule $\Delta v' = 1$ for vibrational autoionization in (43), the recombination can be actively hindered by the higher vibrational levels v' of Rydberg states $(1s\sigma_g n\ell m)$ with intermediate $n \leq 8$, and the contribution from these levels is weak. However, the sequence, coupling the direct and indirect processes,

$$e + H_2^+ (v=0) \rightarrow H_2^{**} \rightarrow H_2\ (n, v\geq 2) \rightarrow H_2^{**} \rightarrow H_2^+ + e\ ,$$

does interfere destructively[27,28] with the direct process. The resulting resonant dips in the cross section have just been observed.[29] Rates for $e + H_2^+(v)$ can be given as $k_o\ (300/T)^\gamma\ 10^{-9}\ cm^3\ s^{-1}$ where (k_o,γ) have just been calculated[28] as (0.8,0.3), (6,0.5), (0.45,0.66), (0.66,0.32) and (1.1,0.77) for v = 0, 1, 2, 3 and 4, respectively.

The DR-rate for CH^+ (v=o) at 120°K was also calculated[28] to be ~ $1.12\ 10^{-7}\ cm^3\ s^{-1}$ in good agreement with a merged beam experiment.[8]

Even though measured DR rates for many ions of planetary and astrochemical interest can be used with reasonable confidence, severe disagreement exists for the simplest triatomic H_3^+ important to the Jovian atmosphere and to interstellar chemistry. The rate is expected to be small since the $^2A_1$ repulsive part of the PE^* curve of H_3 intersects the $^1A_1$ state of H_3^+ at 1 eV above the v=o level. Recent measurements[30] which vary from $2\ 10^{-8}\ cm^3\ s^{-1}$ at 100°K to $1\ 10^{-8}\ cm^3\ s^{-1}$ at 1000 K for v=o and 1 ions *are orders of magnitude higher* than the revised upper-limit rate[31] of $2\ 10^{-11}\ cm^3\ s^{-1}$ at

300 K. The merged beam experiment[30] detects the neutral products while the Flowing Afterglow Langmuir Probe (FALP) experiment[31] measures the loss of H_3^+ ions, and this may well be the source of the discrepancy.

Polyatomic ions and clusters offer many more additional degrees of freedom for capture of the electron, in both mechanisms. With increasing ion complexity, the multiplicity of readily excited internal modes of small energy separation makes the near resonant energy condition of the indirect process easier to attain by presenting a near continuum of closely spaced vibrational energies and trapping becomes more efficient over a broad range of ϵ'. This is confirmed by the large rates $k_{DR} \sim 2\ 10^{-6}\ (300/T)^{0.4}$ for dimer complexes $N_2^+ \cdot N_2$, $O_2^+ \cdot O_2$ and $CO^+ \cdot CO$, important in atmospheric chemistry. That polar clusters $H_3O^+ \cdot (H_2O)_n$ and $NH_4^+ \cdot NH_3$ with rates $k_{DR} \sim 3\ 10^{-6}$ cm^3 s^{-1} appear fairly insensitive to T, has as yet not been satisfactorily explained.

As systems become more complex ($Ne_2^+ \rightarrow Xe_2^+$), the resulting increase in the capture cross sections σ_c tends to be offset by a corresponding decrease in the stabilization probability P_s from near unity until stabilization becomes the rate limiting step. The rate from (11) is then

$$k_{RA} = K(T)\ \upsilon_s \tag{44}$$

where the reaction volume has now the interesting form[9]

$$K(T) = \frac{h^3}{(2\pi mkT)^{3/2}} \frac{\omega(AB^*)}{2\omega(AB^+)} \left[\int |\psi_v(R)|^2 \left[\frac{dR}{d(PE^*)}\right] \exp(-E/kT)dE \right] \tag{45}$$

which contains an effective Franck-Condon factor which essentially selects only that portion of the full internal partition function of AB^* that contributes to the capture by the vertical transition at $R = R_c$. Polyatomic systems relevant to interstellar cloud chemistry have recently been discussed by Bates.[9]

4. DIELECTRONIC AND RADIATIVE RECOMBINATION

Dielectronic recombination (DIR) at high temperatures ($\sim 10^6$K)

$$e(\epsilon\ell) + A^{Z+}(i) \underset{\upsilon_a}{\overset{k^*}{\rightleftarrows}} [A^{(z-1)+}(k)\text{-}e]_{n\ell} \xrightarrow{\upsilon_r} A^{(z-1)+}_{n\ell}(j) + h\upsilon \qquad (46)$$

is a resonant capture process into doubly excited Rydberg levels subsequently stabilized by radiative emission at frequency υ adjacent to, and usually on the lower frequency side of, the resonance transition

$$A^{Z+}(k) \rightarrow A^{Z+}(j) + h\upsilon_R \qquad (47)$$

of the recombining ion of charge Ze. These satellite lines are observed in solar and in high temperature fusion plasmas and provide valuable diagnosis of electron temperature, electron density and the various stages of ionization. The frequency shift which originates from core perturbation by the $n\ell$-electron is small for high Rydberg $n\ell$-levels but would be quite large for low-lying n levels. Since the product ion may be subsequently re-ionized by interaction with its environment the stabilization mechanism is not quite as secure as that for dissociative recombination.

Although stabilization of the high Rydberg ion mainly occurs at high electron temperatures T_e, by the inner-core transition (47) with the captured electron as a spectator, stabilization can also occur by a radiative transition $n\ell \rightarrow n'\ell'$ of the outer electron. This mechanism tends to be effective mainly at much lower temperatures ($\lesssim 10^{4}$K) characteristic of planetary nebulae. It is also effective for ions with low lying metastable levels, as in

$$e + O^{+}\,(^{4}S) \rightarrow O^{*}\,[2p^{3}(^{2}D)n'\ell'] \rightarrow O^{*}(^{2}D,n\ell) + h\upsilon \qquad (48)$$

The rate for dielectronic recombination (DIR) for an initial state i of the ion is, in the isolated resonance approximation (IRA), given by (16) as

$$k_{DIR}(T;i) = \left[\frac{h^{3}}{(2\pi mkT)^{3/2}}\right] \frac{1}{2g_{i}} \sum_{d} \sum_{f} g_{d} \left[\frac{\upsilon_{a}(d\rightarrow i)\upsilon_{r}(d\rightarrow f)}{\upsilon_{r}(d)+\upsilon_{a}(d)}\right] \exp(-E_{d}^{*}/kT) \qquad (49)$$

where g_i and g_d $(=2(2\ell+1))$ are the electronic statistical weights for state i of the recombining ion and for intermediate resonant state d $(=n\ell)$ at energy E_d^* above state i. Each resonant state d may autoionize back (via an Auger transition) to state i with frequency υ_a (d→i) or radiate with frequency υ_r (d→f) to bound levels f. The total radiative and Auger rates from d to all states are $\upsilon_r(d)$ and $\upsilon_a(d)$, respectively. The total DIR rate is obtained by summing over all possible initial states i, intermediate states d and final bound states f. Note that the factor $h^3/(2\pi mkT)^{3/2}$ in (49) is $(4\pi I_A/kT)^{3/2}$ $a_o^3 = 4.1212\ 10^{-16}\ T^{-3/2}\ cm^3$.

DIR within the past three years has been subjected to intense theoretical[3] and experimental[15] study. The existing calculations are based on either the Coulombic model, the distorted wave method and the relativistic configuration interaction method. For example, Chen[31] in a series of excellent papers has used the multiconfiguration Dirac-Fock model to evaluate the detailed transition energies and Auger and radiative rates. The calculations not only include the Coulomb r_{12}^{-1} interaction but also the Breit interaction and other quantum-electrodynamic corrections. A considerable amount of theoretical data has now been accumulated[3] for many different isoelectronic sequences - for cases when the number N of electrons in the initial ion is N = 1-5, 8-12, 18 and 19).

The autoionization frequency decreases with (n,ℓ) as $\nu_a \sim n^{-3} \exp(-a\ell^2)$ owing to a decrease in communication between the core and Rydberg electrons, and is independent of Z. The radiative frequency is $\nu_r \sim \alpha^3 Z^p$ for core decay (p = 4 or 1 with or without a change in core principal quantum number) and $\nu_r \sim \alpha^3 Z/n^3$ for outer electron decay. For small $n << 50$ and low ℓ, $\nu_r << \nu_a$ so that (49) is radiatively limited. At nebular temperatures $T \sim 10^4$ K the exponential in (49) restricts the summation to levels within ~ 0.15 eV of the ionization limit and ν_r is determined by outer electron decay. Since $\nu_a << \nu_r$ for large n, convergence can be obtained. Rates $k_{DIR} \sim (12\text{-}7)\ 10^{12}$ cm^3 s^{-1} for C^{2+}, N^{3+}, O^{4+} recombination at $T \sim 10^4$K which exceed the direct radiative contribution are typical.[3]

At high T ($\sim 10^7$ °K) ~ 1 keV characteristic of the solar corona, the full Rydberg series of autoionization levels must be included and core relaxation is the main radiative decay. For $n >> 50$, $\nu_a << \nu_r$ so that (49) is limited by autoionization. While the number of resonances increases as $2n^2$, only the low ℓ fraction are effective. Electric fields can however mix high ℓ-states with low ℓ-states so that DIR could be significantly enhanced. Typical rates[32] are ~ 3 10^{-11} cm^3 s^{-1} at 1 keV for F-like Se^{25+} - an X-ray laser candidate.

The separation ΔE (a.u.) between resonances of Rydberg series is $\sim Z^2/n^3$ which can become less than the radiative width $\Gamma_r = h\,\nu_r$. The detailed resonance structure is then smeared out by interaction with the radiation field and IRA breaks down. Bell and Seaton[2] have solved this problem by quantum defect theory which because of its close connection with Rydberg series is ideally suited to DIR. Thus DIR-cross sections can in principle be calculated to the same accuracy as electron-ion scattering cross sections (to within 10%).

For ions with low Z, Coster-Kronig (CK) channels, such as $1s2pn\ell \rightarrow 1s2s + e$ for He-like ions, become energetically accessible for large n.

This effect of autoionization to excited states of the recombining ion has generally been neglected in the fluorescence yield υ_r (d→f) $[\upsilon_r(d) + \upsilon_a(d)]^{-1}$ in all calculations of (49) until only recently. For example, the onset of the above CK transition for Be^{3+} ion is at $n^* = 3$, and n^* increases with Z (e.g., $n^* = 9$ for F^{7+}). Inclusion of CK transitions reduce[32] the peak values of the total DIR-rates for B^{3+}, N^{5+} and F^{7+} by 60%, 13% and 4%, respectively. This trend is correct since the relative contributions to DIR from high n-state (important at low Z) decrease with n, while the onset of CK-transitions occurs at higher n as Z increases. The CK-effects are not, of course, included in the largely historical semi-empirical formulae of Burgess[33] (for core decay $\Delta n = 0$) and of Merts et al.[34] (for $\Delta n = 1$). These formulae, although used quite generally by astrophysicists, over-estimate[32] small Z-rates by a factor of 3 and underestimate large Z-rates by as much as a factor of 2.

In addition to CK-transitions for low Z, some remaining problems appear to be (a) effects of external fields on DIR, (b) three-body density effects on k_{DIR} and (c) fine structure effects. For (c), fine structure states of the excited ion-core provide two Rydberg series of autoionization channels which can mutually interfere (as in the decay $3p_{3/2}\ (n\ell) \rightarrow 3p_{1/2}(\epsilon_1\ell) + 3s_{1/2}(\epsilon_2\ell)$ in Mg^+). A problem which appears to be solved is the coupling between resonant DIR and the following non-resonant radiative recombination (RR) which, while negligible for ions with low Z, becomes appreciable at high Z.

The subsequent chain of atomic processes in astrophysics was initiated by the basic (e-H^+) Radiative Recombination (RR) process

$$e + A^{z+}(i) \rightarrow A^{(z-1)}(n\ell) + h\upsilon \qquad (50)$$

into level $(n\ell)$. Since RR is a direct inverse of photoionization with cross section $\sigma_I^{n\ell}(h\upsilon)$, the RR rate by detailed balance is

$$k_R^{n\ell}(T) = \left[\frac{8kT}{\pi m}\right]^{1/2}\left[\frac{kT}{mc^2}\right]\left[\frac{g_{n\ell}}{2g_i}\right]\exp(I_{n\ell}/kT)\int_{I_{n\ell}/kT}^{\infty}\left[\frac{h\nu}{kT}\right]^2\sigma_I^{n\ell}(h\nu)\exp(-h\nu/kT)d(h\nu/kT) \tag{51}$$

where g_i and $g_{n\ell}$ are the electronic statistical weights of the initial ion and the recombined ion in level $n\ell$ with ionization potential $I_{n\ell}$. Various analytical forms for σ_I can be adopted e.g., when $(h\nu)^3\,\sigma_I(h\nu)$ equals its value $I_n^3\,\sigma_o^{n\ell}(I_n)$ at threshold then the rate is

$$k_R^{n\ell}(T) = 1.5\ 10^{-13}\left[\frac{300}{T}\right]^{1/2}\left[\frac{I_n}{I_H}\right]^2\left[\frac{g_{n\ell}}{2g_i}\right]\bar{\sigma}_o^{n\ell}(T)\ \text{cm}^3\ \text{s}^{-1} \tag{52}$$

where, in terms of the exponential integral E_1, the averaged cross section is

$$\bar{\sigma}_I^{n\ell}(T) = \sigma_o^{n\ell}\,[x_n \exp x_n]E_1(x_n), \quad x_n = I_n/kT \tag{53}$$

which reduces at low temperatures $kT \ll I_n$ to

$$\bar{\sigma}_I^{n\ell}(T) = \sigma_o^{n\ell}\,[1-(kT/I_n) + 2(kT/I_n)^2 - 6(kT/I_n)^3 + \ldots\ ] \tag{54}$$

The quantal cross section for photoionization of hydrogenic ions of charge Z by radiation of scaled energy $\omega(=h\nu/I_n)$ is

$$\sigma_I^{n\ell}(h\nu) = \sigma_K^n(\omega)\ G_{n\ell}(\omega) \rightarrow \begin{cases} \omega^{-3}, & h\nu \rightarrow I_n \\ \omega^{-\ell-7/2}, & h\nu \gg I_n \end{cases} \tag{55}$$

The departure from the (Kramer) semiclassical (high n and ℓ averaged) photoionization cross section[35]

$$\sigma_K^n(\omega) = \frac{2^6 a}{3\sqrt{3}} \left[\frac{n}{Z^2}\right] \left[\frac{I_n}{h\nu}\right]^3 \pi a_o^2 = 7.9\ n^2 Z^4 \omega^{-3}(\text{Mb}) \qquad (56)$$

where α is the fine structure constant (e^2/hc) is given by the bound-free Gaunt factor $G_{n\ell}$. The rate (14) is then

$$k_R^{n\ell}(Z,T) = \left[\frac{8kT}{\pi m}\right]^{1/2} \left[\frac{I_n}{kT}\right] \frac{1}{n} \left[\frac{2^S}{3\sqrt{3}}\right] (\alpha^3 \pi a_o^2) \left[\frac{g_{n\ell}}{2g_i}\right] F_{n\ell}(T^*) \qquad (57)$$

Departures of (57) from the above standard ($Z^2\ n^{-3}\ T^{-1/2}$) low temperature rule is provided by the function

$$F_{n\ell}(T^*) = \frac{1}{T^*} \exp(1/T^*) \int_1^\infty \frac{G_{n\ell}(\omega)}{\omega} \exp(-\omega/T^*) d\omega \qquad (58)$$

which decreases monotonically from $G_{n\ell}(1)$ as the scaled temperature T^* ($=kT/I_n$) increases. For interstellar clouds $kT \ll I_n$ and $F_{n\ell}(T^* \ll 1)$ tends to $G_{n\ell}(1)$ the threshold Gaunt factor. Note that (57) also provides the universal scaling law

$$k_R^{n\ell}(Z,T) = Z k_R^{n\ell}(1, T/Z^2) \qquad (59)$$

Recombination rates are greatest into low n levels and the $\omega^{-\ell-1/2}$ variation of $G_{n\ell}$ in (58) preferentially populates states with low $\ell \sim 2$-5. Highly accurate analytical fits for $G_{n\ell}(\omega)$ have been obtained[36] for $n \leq 20$ so that (57) is expressed in terms of known functions of fit parameters. This procedure (which does not violate the S_2 sum rule) has been extended[36] to non-hydrogen systems of neon-like Fe XVII, where $\sigma_I^{n\ell}(\omega)$ is a monotonically

decreasing function of ω.

Variation of the ℓ-averaged values, $n^{-2} \sum_{\ell=o}^{n-1} (2\ell+1) F_{n\ell}(T^*)$, is close[36] in both shape and magnitude with the corresponding semi-classical function $S(T^*)$ i.e., (58) with $G_{n\ell}(\omega) = 1$. Hence the ℓ-averaged recombination rate is

$$k_R^n(Z,T) = 1.1932\ 10^{-12} \left[\frac{300}{T}\right]^{1/2} \left[\frac{Z^2}{n}\right] F_n(T^*)\ \text{cm}^3\ \text{s}^{-1} \qquad (60)$$

where F_n can be calculated directly from (58) or be approximated as $G_n(1)$ $S(T^*)$. A computer program based on a three term expansion of G_n is also available.[37]

Tables exist[38] for the effective rate

$$k_E^{n\ell}(T) = \sum_{n'=n}^{\infty} \sum_{\ell'=o}^{n-1} k_R^{n'\ell'}\ C_{n'\ell',n\ell} \qquad (61)$$

of populating levels $n\ell$ of hydrogen by radiative recombination rate all levels $n' \geq n$ followed with probability $C_{i,f}$ for subsequent radiative cascade ($i \rightarrow f$) via all possible intermediate paths. Tables[38] also exist for the total rate

$$k_R^N = \sum_{n=N}^{\infty} n^{-2} \sum_{\ell=o}^{n-1} k_R^{n\ell} \qquad (62)$$

of recombination of levels N and above of hydrogen. They are useful in deducing time scales radiative of recombination and rates from (59) for complex ions.

When effective at higher temperatures, dielectronic recombination proceeds in general faster than RR. Since $k_R \sim Z^2$, RR can however become

competitive for highly charged ions. A unified treatment of DIR and RR has recently been presented.[39] The mutual interference of the corresponding amplitudes and continuum-continuum coupling is expected to be most important for individual transitions involving low-lying auto-ionization levels and is probably negligible for DIR arising from highly excited levels. If the photoionization cross section $\sigma_I^{n\ell}(h\nu)$ already includes the effects of autoionizing resonances, no further correction for DIR to RR may be necessary.

5. MUTUAL NEUTRALIZATION (MN)

Until fairly recently (1984), lack of agreement of various curve-crossing and Landau-Zener type theories with experiment for such a simple system as

$$H^+ + H^- \rightarrow H^*(n) + H \qquad (63)$$

remained embarassing, and agreement between the two main experiments remained very good. Then a 1983-theory[40] which included couplings (neglected in previous theories) to the n = 3 level still did not agree with measurement, until new experiments[41,42] were performed in 1984 and 1985. The process (63) is now apparently well understood, but careful quantum mechanics and experiment is required.

In dense interstellar clouds, MN of complex systems can be important and can produce qualitative changes[24] in the chemistry sequence. For example, when polycyclic aromatic hydrocarbons (PAH) exist in high abundance, the negative charge is carried not by electrons but by PAH^- so that MN, as in $C^+ + PAH^- \rightarrow C + PAH$, replaces dissociative recombination (DR) so that the C-abundance is enhanced.[24]

6. TERMOLECULAR RECOMBINATION

6.1 *ION-ION*:

The theory of termolecular ion-ion recombination and

$$A^+ + B^- + M \underset{k}{\overset{\alpha}{\rightleftarrows}} AB + M \tag{64}$$

of positive and negative atomic ions of concentrations $N_{A,B}(t)$ at time t in a gas M is also well established,[43] and is also suitable as a case study. The effective two-body association rate $\alpha(N,T)$ cm^3 s^{-1} and the dissociation frequency $k(N,T)$ s^{-1} are functions of gas density and are given by[43]

$$\alpha \tilde{N}_A \tilde{N}_B = \int_{-D}^{\infty} P_i^S \, dE_i \int_{-D}^{\infty} (P_i^S - P_f^S) \, C_{if} \, dE_f = k \tilde{n}_s \tag{65}$$

where P_i^S, which measures the departure from equilibrium, is the stochastic probability that a pair (A^+-B^-) with energy-distribution n_i over internal relative energy E_i of the pair is connected via a multistep series of energy (state)-changing collisions to a stabilized sink $\mathcal{S}$ of low lying fully associated pairs of concentration n_s (cf. Fig. 2). The sink $\mathcal{S}$ extends over the energy range $-S \geq E_i \geq -D$ where -D is the lowest energy level and where -S is that bound level below which P_i^S is unity. The one-way equilibrium rate C_{if} for $E_i \rightarrow E_f$ collisional transitions per unit interval $dE_i dE_f$ is $\tilde{n}_i \nu_{if}$, and the distribution n_i satisfies the input-output collisional Master Equation[43]

$$\frac{dn_i}{dt} = [\tau_c(t) - \tau_s(t)] \int_{-D}^{\infty} (P_i^S - P_f^S) \, C_{if} \, dE_f \tag{66}$$

where the departures from their steady equilibrium (tilda) values of the total

time-dependent concentrations of fully dissociated pairs (in block $\mathcal{C}$, $0 \leq E_i \leq \infty$ where $P_i^S \tilde{\simeq} 0$) and of fully associated pairs (in block $\mathcal{S}$ where $P_i^S \tilde{\simeq} 1$) are

$$\gamma_c(t) = N_A(t)N_B(t)/\tilde{N}_A\tilde{N}_B \; ; \quad \gamma_s(t) = n_s(t)/\tilde{n}_s \tag{67}$$

respectively. For quasi-steady-state (QSS) of the intermediate block $\mathcal{E}$ ($0 \geq E_i \geq -S$) of highly excited levels at time t, (66) vanishes so that (64) reduces to

$$\alpha \tilde{N}_A\tilde{N}_A = \int_{-E}^{\infty} dE_i \int_{-D}^{-E} (P_f^S - P_i^S)\, C_{if}\, dE_f \; , \tag{68}$$

for arbitrary energy -E in block $\mathcal{E}$.

6.1.1 *VARIATIONAL PRINCIPLE:* It has been recently proposed[44] that P_i^S are so distributed that the rate (65) is a minimum. This distribution leads exactly to the QSS-distribution given by (66) set to zero. Thus (65) provides a variational expression for the QSS condition, so that P_i^S may be determined (Fig. 3) variationally or from the direct solution of the integral equation (66). The Variational[44] and QSS[43] rates obtained are of course identical.

6.1.2 *DIFFUSION METHOD.* By performing a Fokker-Planck conversion of the integral equation (66), the resulting (but approximate) differential equation is identical with a diffusion equation in energy space which can be solved analytically for P_i^S (Fig. 3). Insertion in (65) yields a proposed diffusional method[45] which is highly accurate (Fig. 4).

6.1.3 *BOTTLENECK LIMIT.* On assuming that pairs above and below a bound level -E are in equilibrium with the fully dissociated and associated (blocks C and S, respectively (i.e., $P_i^S = 0$ for $E_i > -E$ and $P_i^S = 1$ for $E_i < -E$) then either (64) or (68) yield,

$$\alpha(-E)\ \tilde{N}_A\tilde{N}_B = \int_{-E}^{\infty} dE_i \int_{-D}^{-E} C_{if}\, dE_f \qquad (69)$$

the one-way equilibrium collisional rate across -E, which is then an upper limit to the exact rate. Variation of α with -E yields the least-upper-limit at the bottleneck energy E^* (see refs. [23] and [43]).

Other approximations such as Coupled Nearest-Neighbor (CNN) limit and Uncoupled Intermediate ℓ-block Levels (UIL), based on analogy of (65) and (66) with electrical networks recently proposed,[46] have also elucidated the modes of energy reduction.

6.1.4 *GAS DENSITY*

As the gas density N is raised non-equilibrium effects in internal separation R of A^+ and B^- must be considered. The appropriate input-output collisional-transport Master Equation satisfied by the distribution $n_i(\underset{\sim}{R})$ of $(A^+\text{-}B^-)$ pairs per unit interval $d\underset{\sim}{R}\, dE_i$ has been shown to satisfy the continuity equation[47]

$$\frac{d}{dt} n_i(R,t) = \frac{\partial n_i}{\partial t} + \frac{1}{R^2}\frac{\partial}{\partial R}\left[R^2 j_i^d(R)\right]_{E_i}$$

$$= -\int_{V(R)}^{\infty} \left[n_i(R)v_{if}(R) - n_f(R)v_{fi}(R)\right] dE_f \qquad (70)$$

where $j_i^d(R)$ $(= j_i^+ - j_i^-)$ is the net outward transport current of pairs expanding at R, where $v_{if}(R)$ is the frequency per unit interval $d\underset{\sim}{R}\, dE_i\, dE_f$ for $E_i \to E_f$ collisional transitions for ions at fixed separation R and where V(R) is the energy of interaction between A and B. Integration of (70) over all accessible R yields the standard Master Equation (66).

The question of reproducing the cumulative effects of multistep

energy-changing collisions by an accumulative strong collision within a loose collision complex of radial extent R_T can now be examined.[43] The rate of recombination within a sphere of radius R_T and the overall probability $P_i^A(R_T)$ of association within R_T are related by low gas density by

$$\alpha(R_T)\ \tilde{N}_A\tilde{N}_B = \int_0^\infty [4\pi R_T^2 \tilde{j}_i^-(R_T)]P_i^A(R_T)dE_i \quad , \tag{71}$$

which is expressed via (70) in terms of the stabilization probabilities P_f^S by[43]

$$\alpha(R_T)\ \tilde{N}_A\tilde{N}_B = \int_0^\infty dE_i \int_0^{R_T} dR \int_{V(R)}^0 C_{if}\ P_f^S\ dE_f \tag{72}$$

A strong-collision (or classical) treatment refers to the assignment $P_f^S = 1$ in (72).

Fig. 5 illustrates the ratio of the effective strong-collision rate, to α_E, the exact rate $\alpha\ (R_T \to \infty)$. Agreement can be obtained by assigning (de-facto) $R_T \tilde{\sim} 0.5\ R_e$. The underlying reason becomes apparent from Fig. 6. The exact probability P_i^{AE} that (E_i=0) dissociated pairs ultimately associate dominates the probability P_i^{RD} for ultimate redissociation (after bound levels are formed) for smaller $R_T << R_e = e^2/kT$, so that P_i^{AE} and the strong-collision probability P_i^{ST} (from (72) with $P_f^S = 1$) are essentially equal. Pairs with larger $R_T >> R_e$ are however mainly redissociated (Fig. 6). The strong collision rate at $R_T \sim 0.45$ is then twice the rate $\alpha(R_T)$ of (72). The remaining contribution from $R \geq R_T$ to the exact rate provides agreement with the strong collision rates.[43]

The concept of the above loose reaction complex is useful in showing[23] with the aid of (70) that the variation of recombination with gas density yields the familiar result

$$\alpha(N) = \frac{\alpha_{RN}\ \alpha_{TR}}{\alpha_{RN}+\alpha_{TR}} \tag{73}$$

where $\alpha_{TR}(N)$, the known rate for transport of pairs by diffusional-drift to within separation R_T, decreases as N^{-1}. The reaction rate α_{RN} by collision with M within $R \leq R_T$ increases initially linearly with N and saturates at higher N (~ 1 atm). The magnitude and density variation of (73), with accompanying theoretical procedures, agree with Monte-Carlo Computer Simulations for the recombination of rare gas-halide systems.[4,6] No benchmark measurements are available, but the two historical measurements at low and high N respectively in general agree[17] with (73).

6.2 Electron-Ion: The trapping radius concept is also useful to obtain classical rates (i.e., (72) with $P_f^S = 1$) not only for termolecular recombination (64) but also for electron and neutral stabilized electron-ion collisional recombination (9) and (7) respectively. The frequency $\nu_i(R) = \int_{V(R)}^{o} \nu_{if}(R)dE_f$ for formation of bound pairs is $v_{12}(R)\sigma N$, where v_{12} is the speed of $A^+ + B^-$ relative motion and σ is the cross section for AB^*-M deactivating collisions. On assuming constant cross section σ_o for such collisions, (72) reduces (with $P_f^S = 1$) exactly to

$$\alpha \tilde{N}_A \tilde{N}_B = \left[\int_o^\infty dE_i \int_o^{R_o} \tilde{n}_i(R)\, v_{12}(R)dR \right](\sigma_o N) \qquad (74)$$

$$= \left[\frac{8kT}{\pi M_{AB}}\right]^{1/2} \left[\frac{4}{3}\pi R_o^3\right] \left[1 + \frac{3}{2}\frac{R_e}{R_o}\right] \sigma_o N \qquad (75)$$

where R_e is e^2/kT. A classical version of the semiquantal bottleneck treatment (§ 6.1.3 above) yields, a priori, the trapping radius to be $R_o = 0.41\, R_e$. The rates α of termolecular recombination (64), and of e-e collisional recombination ($e + A^+ + e$) at electron temperature T_e and electron density n_e

are therefore,

$$\alpha_{TR}(T) = 0.32 \left[\frac{8kT}{\pi\mu M_{AB}}\right]^{1/2} \left[\frac{4}{3}\pi R_e^3\right] (\sigma_o N) \sim 2.3\ 10^{-25}\ (300/T)^{2.5}\ N(cm^3\ s^{-1}) \quad (76)$$

and

$$\alpha_{ee}(T) = 0.32 \left[\frac{8kT}{\pi m}\right]^{1/2} \left[\frac{4}{3}\pi R_e^3\right] (\frac{1}{9}\pi R_e^2) n_e \sim 2.7\ 10^{-20}\ (300/T)^{4.5}\ n_e(cm^3 s^{-1}) \quad (77)$$

respectively. In (77), σ_o for electron-electron collisions is taken as the Coulomb cross section ($\frac{1}{9}\pi R_e^2$) for energy changes $\geq \frac{3}{2}kT$. These expressions provide the correct order of magnitude and temperature dependence, and, in general, agree with experiment. In particular (76) agrees with the expression of Mansbach and Keck[48] derived from more elaborate analysis. At higher T_e and lower n_e, the highly excited levels collisionally formed within kT of the ionization limit become increasingly stabilized by radiative transitions. The resulting rate for collisional-radiative recombination can then be approximated as[49]

$$\alpha_{CR} = [3.8\ 10^{-9}\ T_e^{-4.5}\ n_e + 1.55\ 10^{-10}\ T_e^{-0.63} + 6\ 10^{-9}\ T_e^{-2.98}\ n_e^{0.37}]cm^3 s^{-1} \quad (78)$$

where the first term is (77), the second term is the radiative correction and the third term arises from collisional-radiative coupling. This expression agrees with the experimental data[49] to within 10% for a Lyman optically thick plasma with n_e and T_e in the range $10^9 \leq n_e\ (cm^{-3}) \leq 10^{13}$ and $2.50 \leq T_e\ (^oK) \leq 4000K$.

For termolecular ($e + A^+ + B$) collisional recombination only a small fraction $\delta = 2m/M_B$ can be transferred in e-B elastic collisions so that the

E_i-integration in (74) must be so restricted to give

$$\alpha_{eB}(T_e) = \left[\frac{8kT}{\pi m}\right]^{1/2} 4\pi R_o^3 (\sigma_o N) \int_o^{r_o} r^2 dr \int_o^{\delta/r} \left(1+\frac{1}{r\epsilon}\right) \epsilon e^{-\epsilon} d\epsilon \qquad (79)$$

with $R = r R_e$ and $\epsilon = E_i/kT$. Hence

$$\alpha_{eB}(T_e) = 4\pi\delta \left[\frac{8kT_e}{\pi m}\right]^{1/2} R_e^2 R_o (\sigma_o N) \sim [10^{-26}/M_C(AMU)] (300/T)^{2.5} N \qquad (80)$$

which agrees exactly with the diffusion result of Pitaevskii[50] and which is linear[51] in the trapping radius R_o. This result ($\sim 10^{-28}$ cm^3 s^{-1}) is in general agreement with experimental data for ($e + He^+ + Cs$) but is much smaller than that ($\sim 10^{-26}$) for ($e + He^+ + He$), which proceeds far more effectively[52] via formation of an intermediate complex He_2^* which then dissociates into neutral fragments.

The rate for ($e + A^+ + B$) is greatly increased[51] for a molecular gas B where energy reductions are effected mainly by rotational and vibrational transitions. Allowance for the discreteness of (e-A^+) Rydberg levels reduces α_{eM} and produces a sharper decrease with temperature.[53] When A^+ is a molecular ion XY^+ a dissociative recombination channel opens. Here the (e-XY^+) pairs formed in highly excited Rydberg molecular levels XY^* by collision with M, in addition to being collisionally and radiatively quenched to stable bound states of AB, may predissociate along repulsive curves X^*+Y i.e., by dissociative recombination involving bound electrons - the second half of the indirect mechanism.[43] The contribution from this *collisional dissociative recombination*[53] can dominate the contribution from direct collisional relaxation. That quantal curve-crossing is involved makes it

similar to the enhancement[6] of mutual neutralization ($A^+ + B^-$) by third bodies. In the limit of high gas density N, the recombination rate α_{eM} becomes transport limited, as in (73) for ion-ion recombination and decreases as N^{-1}. Because of the higher electron mobilities, its onset however occurs at much higher N. Between the linear low density region and the transport limited N^{-1} region only Monte Carlo simulations have been performed.[54] For ($e + A^+ + M$) recombination in a molecular gas the rotational and vibrational cross sections of Takayanagi[55] and of Takayanagi and Itikawa[56] and the recommended molecular constants[56] are invaluable.

Acknowledgements: This research is supported by the U.S. Air Force Office of Scientific Research under Grant No. AFOSR-84-0233.

REFERENCES

1. M. J. Seaton and P. J. Storey, in: Atomic Processes and Applications (P. G. Burke and B. L. Moiseivitsch, eds.), pp. 133-197, North-Holland, Amsterdam (1976).
2. R. H. Bell and M. J. Seaton, J. Phys. B 18, 1589-1629 (1985).
3. Y. Hahn and K. J. LaGattuta, Physics Reports 166, 195-268 (1988).
4. M. R. Flannery, in: Applied Atomic Collision Physics (E. W. McDaniel and W. L. Nighan, eds.), Vol. 3, pp. 141-172, Academic, New York (1982).
5. M. R. Flannery, Phil. Trans. R. Soc. London. Ser. A 304, 447-497 (1982).
6. D. R. Bates, in: Advances in Atomic and Molecular Physics (D. R. Bates and B. Bederson, eds.) Vol. 20, pp. 1-40, Academic, New York (1985).
7. M. R. Flannery, J. Chem. Phys. 88, 4228-4241 (1988).
8. See Contributions in: Proc. Intern. Workshop on Dissociative Recombination: Theory, Experiment and Applications (J. B. A. Mitchell and S. Guberman, eds.), World Scientific, New Jersey (1988).
9. D. R. Bates, in: Recent Studies in Atomic and Molecular Processes (A. E. Kingston, ed.), pp. 1-27, Plenum, New York (1987).
10. D. R. Bates and E. Herbst, in Reaction Rate Coefficients in Astrophysics (T. J. Miller and D. A. Williams, eds.) in press, Kluver, Dordrecht (1989).
11. J. B. A. Mitchell, in: Atomic Processes in Electron-Ion and Ion-Ion Collisions (F. Brouillard, ed.), pp. 185-222, Plenum, New York (1986).
12. D. Smith, in: Advances in Atomic and Molecular Physics (D. R. Bates and B. Bederson, eds.) Vol. 24, pp. 1-49, Academic, New York (1988).
13. K. Dolder and B. Peart, in: Advances in Atomic and Molecular Physics (D. R. Bates and B. Bederson, eds.) Vol. 22, Academic, New York (1986).
14. G. H. Dunn, in: Atomic Processes in Electron-Ion and Ion-Ion Collisions (F. Brouillard, ed.) pp. 93-116, Plenum, New York (1986).

15. See contributions in: Atomic Excitation and Recombination in External Fields (M. H. Hayfeh and C. W. Clark, eds.) pp. 439-452, Gordon and Breach, New York (1985).

16. S. E. Barlow, G. H. Dunn and K. Schauer, Phys. Rev. Letts. 52, 902-905; 53, 1610 (1984).

17. M. R. Flannery, in: Atomic Processes and Applications (P. G. Burke and B. L. Moiseiwitsch, eds.), pp. 407-466, North Holland, Amsterdam (1976).

18. H. S. Lee and R. Johnsen, Bull. Amer. Phys. Soc. 33(2), 149 (1988).

19. A. Gusti-Sugor, E. Roueff and H. van Regemorter, J. Phys. B 9, 1021-1034 (1976).

20. H. Abgrall, A. Giusti-Sugor and E. Roueff, Astrophys. Jour. 207, L69-L72 (1976).

21. D. R. Bates and C. S. McKibbin, Proc. Roy. Soc. A 33, 13-28 (1974).

22. A. D. Dickinson, R. E. Roberts and R. B. Bernstein, J. Phys. B 5, 355-365 (1976).

23. M. R. Flannery, in: Recent Studies in Atomic and Molecular Processes (A. E. Kingston, ed.) pp. 167-197, Plenum, New York (1987).

24. A. Dalgarno, in: Recent Studies in Atomic and Molecular Processes (A. E. Kingston, ed.) pp. 51-61, Plenum, New York (1987).

25. B. G. Anicich and W. T. Huntress, Jr., Astrophys. Jour. Supplem. Ser. 62, 553-672 (1986).

26. J. N. Bardsley and M. A. Biondi, in: Advances in Atomic and Molecular Physics (D. R. Bates and I. Esterman, eds.) Vol. 6, pp. 1-57, Academic, New York (1970).

27. A. Gusti-Sugor, J. N. Bardsley and C. Derkits, Phys. Rev. A 28, 682-691 (1983).

28. H. Nakamura, H. Takagi and K. Nakashima, in: reference 8.

29. H. Hus, F. Yousif, C. Noren, A. Sen and J. B. A. Mitchell, Phys. Rev. Letts. 60, 1006-1009 (1988).

30. H. Hus, F. Yousif, A. Sen and J. B. A. Mitchell, Phys. Rev. 38, 658-663 (1988).

31. D. Smith and N. G. Adams, J. Chem. Soc. Far. Trans. 2, 83 (1987); 2, 149 (1987).

32. M. H. Chen, Phys. Rev. A 34, 1079-1083 (1986).

33. A. Burgess, Astrophys. Journ. 141, 1588-1590 (1965).

34. A. L. Merts, R. D. Cowan and N. H. Magee, Los Alamos Scientific Laboratory Report No. LA-6220-MS, 1976.

35. H. A. Bethe and E. E. Salpeter, Quantum Mechanics of One- and Two-Electron Atoms, pp. 308-322, Plenum, New York (1977).

36. B. F. Rozsmyai and V. L. Jacobs, Astrophys. Jour. 327, 485-501 (1988).

37. D. R. Flower and M. J. Seaton, Computer Physics Communications 1, 31-34 (1969).

38. P. G. Martin, Astrophys. Jour. Supplem. 66, 125-138 (1988).

39. V. L. Jacobs, J. Cooper and S. L. Haan, Phys. Rev. A 36, 1093-1113 (1987).

40. V. Sidis, C. Kubach and D. Fussen, Phys. Rev. A 27, 2431-2446 (1983).

41. S. Szucs, M. Karema, M. Terao and F. Brouillard, J. Phys. B 17, 1613-1622 (1984).

42. B. Peart, M. A. Bennett and K. Dolder, J. Phys. B 18, L439-L444 (1985).

43. M. R. Flannery and E. J. Mansky, J. Chem. Phys. 88, 4228-4241 (1988).

44. M. R. Flannery, J. Chem. Phys. 89, 214-222 (1988).

45. M. R. Flannery, J. Chem. Phys. 87, 6947-6956 (1987).

46. M. R. Flannery, J. Chem. Phys. 89, 4086-4091 (1988).

47. M. R. Flannery, J. Phys. B 20, 3929-4938 (1987).

48. P. Mansbach and J. Keck, Phys. Rev. 181, 275-289 (1965).

49. J. Stevefelt, J. Boulmer and J. F. Delpech, Phys. Rev. A 12, 1246-1251 (1975).

50. L. P. Pitaevskii, Sov. Phys. - JETP 15, 919-921 (1962).

51. D. R. Bates, J. Phys. B 13. 2587-2599 (1980).

52. D. R. Bates, J. Phys. B 12, L35-L38 (1979).

53. D. R. Bates, J. Phys. B 14, 3525-3534 (1981).

54. W. L. Morgan, in: Recent Studies in Atomic and Molecular Processes (A. E. Kingston, ed.) pp. 149-166, Plenum, New York (1987).

55. K. Takayanagi, in: Advances in Atomic and Molecular Physics (D. R. Bates and I. Esterman, eds.), Vol. 1, pp. 149-194, Academic, New York (1965).

56. K. Takayanagi and Y. Itikawa, in: Advances in Atomic and Molecular Physics (D. R. Bates and I. Esterman, eds.), Vol. 6, pp. 105-153, Academic, New York (1970).

Figure Captions

Figure 1. Schematic representation of potential energy curves for dissociative recombination, $e + AB^+ \rightarrow A^* + B$, (a) via the direct (vertical transition) mechanism and (b) via the indirect (Rydberg) mechanism.

Figure 2. Schematic Diagram of energy blocks $\mathscr{E}$, $\mathscr{E}$ and $\mathscr{S}$ pertinent to recombination at low gas densities.

Figure 3. Stabilization probabilities: (E): quasi-steady-state[43] (V2): two-parameter Variational.[44] (D): Diffusion.[45]

Figure 4. $(A^+ + B^- + M)$ partial recombination rates $\left[\frac{M_A}{M_{AB}}\right] \alpha(a)$ normalized to Thomson's rate $\alpha_T(a)$ as a function of mass parameter $a = M_B M_g / M_A(M_A+M_B+M_g)$ for various (A^+-M) or (B^-M) interactions (CX: symmetrical resonance charge transfer; HS: hard-sphere; POL: polarization attraction). The full rates are $\alpha(a)\alpha_T(a) + \alpha(b)\alpha_T(b)$ where $b = (M_A/M_B)^2 a$ and where Thomson's rate is $\alpha_T(a) = \frac{4}{3} \pi R_e^3 (3\ kT/M_{AB})^{1/2} \sigma_{AM} N$. (Ref. 43.)

Figure 5. Variation of $\alpha(R_T)$, eq. (72) with $P_f^S = 1$, to exact rate, eq. (72) with $R_T \rightarrow \infty$, for ion-ion recombination of equal-mass species under various (A^+-M) interactions (cf. Fig. 4).

Figure 6. Probability for eventual association and re-dissociation of (A^+-B^-) pairs with zero internal energy. P^{AE} and P^{RD}: exact association and redissociation. P^{ST}: strong collision. The probabilities are normalized to Thomson's low density probability $P_T = R_T (\sigma_{AM} N)$. (Ref. 43).

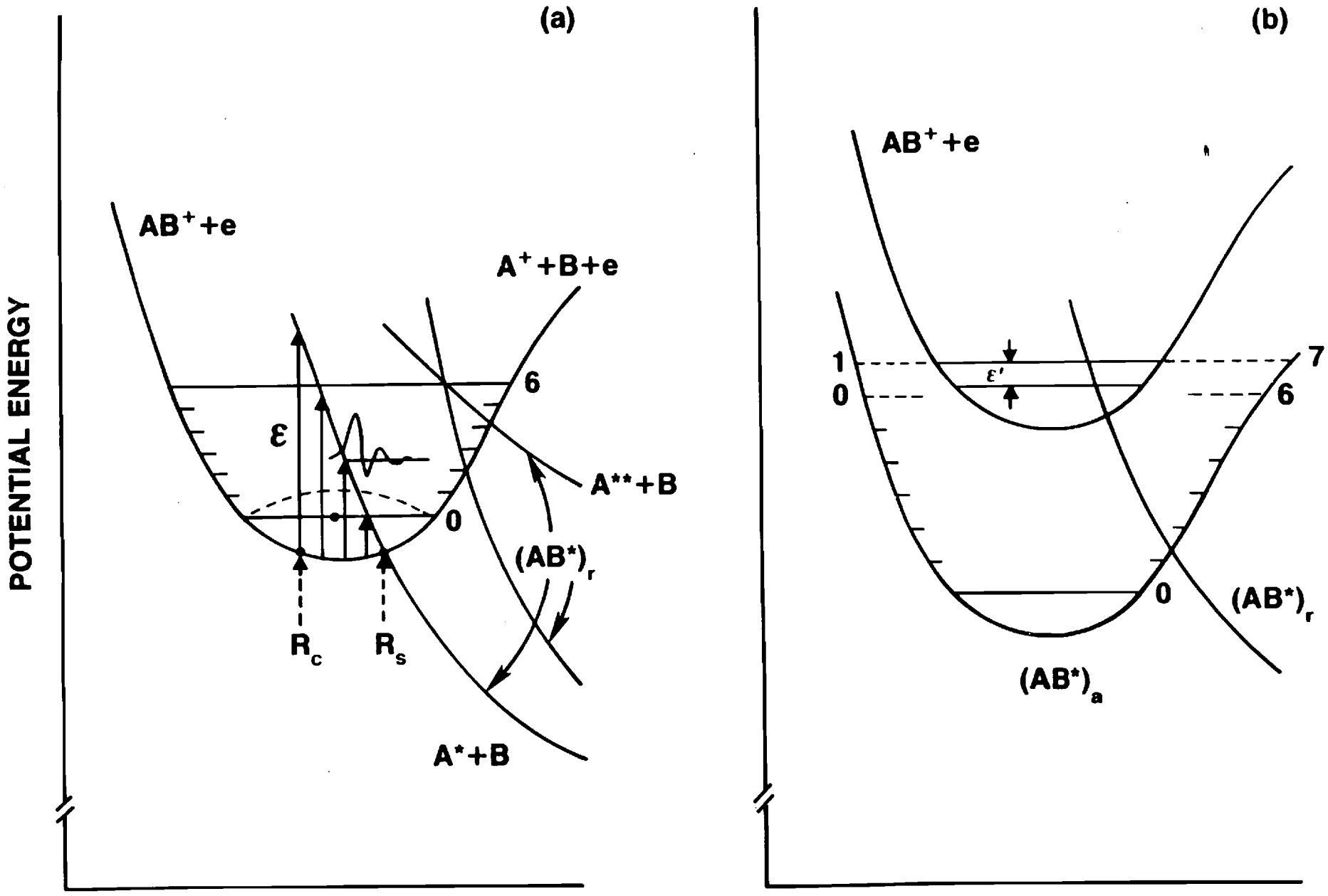
(a)
POTENTIAL ENERGY
AB⁺+e
A⁺+B+e
A**+B
(AB*)r
A*+B
ε
6
0
Rc
Rs
(b)
AB⁺+e
1
0
ε'
7
6
0
(AB*)r
(AB*)a

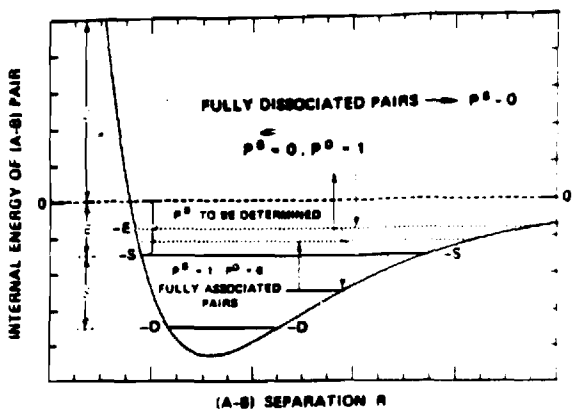

FIG. 2.

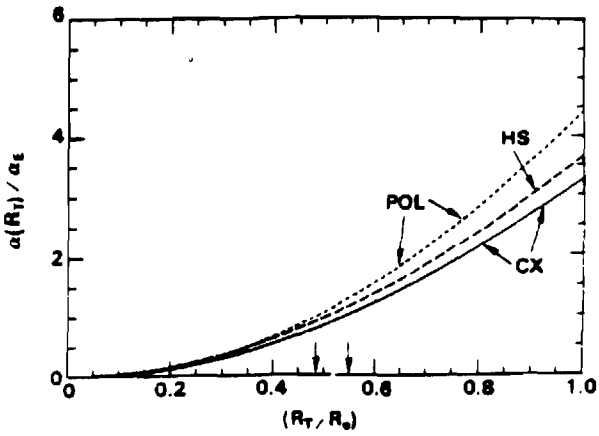

FIG. 5.

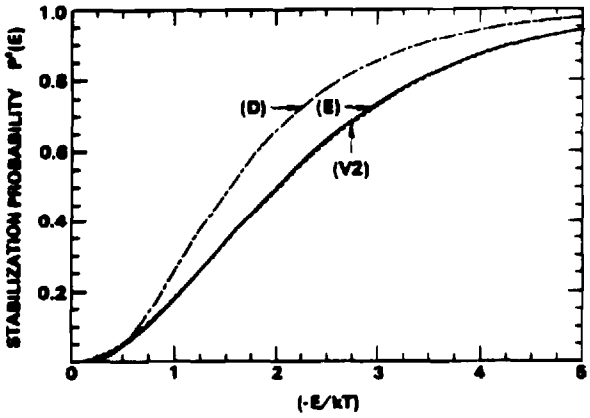

FIG. 3.

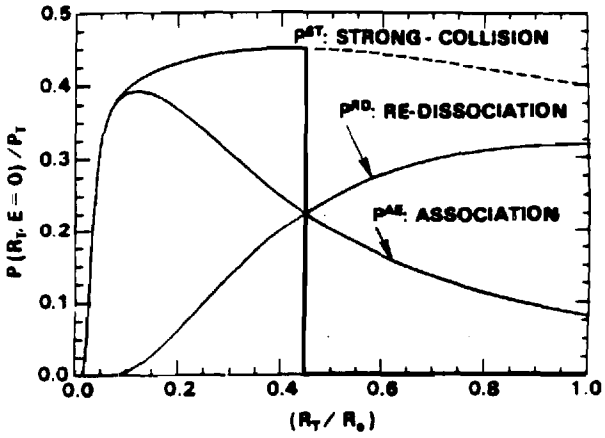

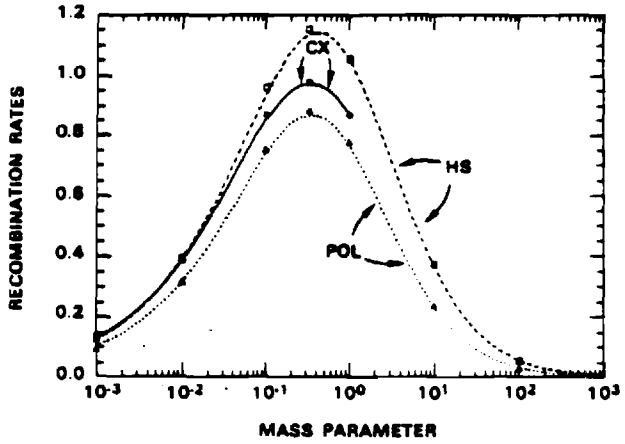

FIG. 4.

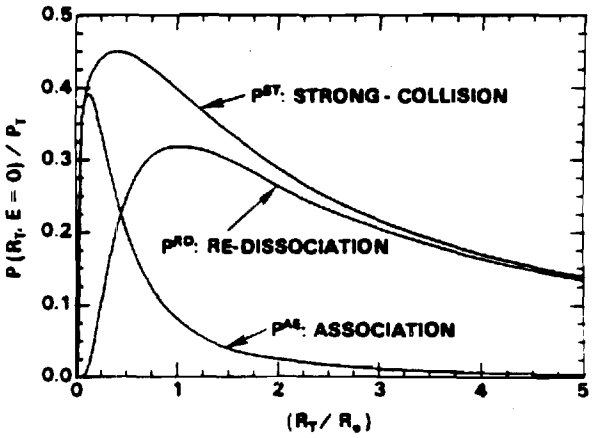

FIG. 6.

Appendix B

ELECTRON COLLISION CROSS SECTIONS INVOLVING EXCITED STATES

E. J. Mansky

School of Physics
Georgia Institute of Technology
Atlanta, Georgia 30332-0430 U.S.A.

Knowledge of the integral cross sections for the electron-impact excitation of atoms initially in a metastable state is of fundamental importance not only in determining the number densities of atoms in various excited states, but also in understanding the overall collision dynamics of energy transfer and excited-state diagnostics in partially ionized gases. Recently, the study of transitions between metastable states of He has been revitalized by experimental measurements at Kaiserslautern (Müller-Fiedler et al. 1984) of the differential cross sections, and at Madison (Rall et al. 1989) of the integral cross sections for the $2^3S \rightarrow 3^3L$ electronic excitations in helium. This signals a new era in experiments involving metastable states in that much more detailed information can now be obtained by modern measurements than was possible in the pioneering work of Phelps (1955). This has also marked a resurgence in theoretical activity in this area as well with recent distorted wave calculations (Mathur et al., 1987) and optical potential calculations (Vučić et al. 1987). In this note we will briefly summarize the original multichannel eikonal theory of Flannery and McCann (1974a,b,c, 1975a,b), together with the correction needed to account for the influence that distant trajectories have on the scattering amplitude for states dipole-coupled via an optically-allowed transition to the initial state (Mansky and Flannery 1989a). In particular, attention will be focused on the results for the $2^3S \rightarrow 3^3L$ transitions in He due to the recent experimental data which has become available.

The basic expression in the multichannel eikonal theory (MET) for the complex scattering amplitude for the transition $i \rightarrow n$ is (Flannery and McCann 1975a,c)

$$f_{ni}(\theta) = -(i)^{\Delta+1} \int_0^\infty J_\Delta(q'p) \, [I_1(\rho,\gamma(\theta)) - i \, I_2(\rho,\gamma(\theta))\rho \, d\rho \qquad (1)$$

where the integrals I_1 and I_2 are defined,

$$I_1(\rho,\tau(\theta)) = \int_{-\infty}^{\infty} dz\ \kappa_n(\rho,z)\ \frac{\partial C_n(\rho,z)}{\partial z}\ \exp[i\tau(\theta)z] \qquad (2a)$$

$$I_2(\rho,\tau(\theta)) = \int_{-\infty}^{\infty} dz\ [\kappa_n(\kappa_n-k_n) + \frac{\mu}{\hbar^2} V_{nn}]C_n(\rho,z)\ \exp[i\tau(\theta)z] \qquad (2b)$$

The other terms in equations (1) and (2) are: $q' = k_n \sin\theta$; $\tau(\theta) = k_n (1-\cos\theta)$; $\Delta \equiv m_i - m_n$, where $m_i(m_n)$ is the magnetic quantum number of state i(n); J_Δ is an ordinary Bessel function of order Δ; $\kappa_n^2 = k_n^2 - \frac{2\mu}{\hbar^2} V_{nn}$. The complex amplitude functions $C_n(\rho,z)$ in equation (2) are solutions of the following set of coupled first-order partial differential equations,

$$i\frac{\hbar^2}{\mu}\kappa_n \frac{\partial C_n(\rho,z)}{\partial z} + [\frac{\hbar^2}{\mu}\kappa_n(\kappa_n-k_n)+V_{nn}]C_n(\rho,z) = \sum_{j=1}^{N} V_{nj}C_j\ \exp[i(k_j-k_n)z] \quad (3)$$

which are solved subject to the asymptotic boundary condition condition, $C_n(\rho,z\to-\infty) = \delta_{ni}$ for the N states in the basis set (n = 1,2,...,N). For definitions of the remaining terms in equations (1-3) and a complete derivation of these equations see the original MET papers of Flannery and McCann (1974a,b,c, 1975a,b).

The main assumptions made in the derivation of (3) is that the trajectory for the relative motion of the electron in channel n is accurately characterized by a straight-line, and that the contribution of exchange to the inelastic integral cross section for channel n is negligible. The assumption of a straight-line trajectory for the relative motion of the projectile electron in $e^- + A^*$ collisions should be reliable due to the dominant nature of the long range part of the projectile-target electrostatic interaction in these collisions. However, in heavy particle collisions account must be taken of the curvature of the trajectory in order for accurate inelastic integral cross sections to be obtained. This has been done within the MET for applications in heavy particle collisions by McCann and Flannery (1976,1978).

Similarly, in electron-metastable atom collisions the neglect of electron exchange effects should not introduce a great deal of error (Vučić et al. 1987). This is due to the increased size of the target atom when the incident state is an excited state. Recall that for hydrogen (Bethe and Salpeter 1977), the mean value of r, the electron-nucleus distance, scales with n as, $\langle r\rangle = [3n^2 - \ell(\ell+1)]/2Z$. This increase results in a concomitant decrease in the electronic charge density $\rho(r)$ of the target atom, which results in a lowering of the probability of overlap of the projectile electron's wavefunction with that of the bound electron, thereby decreasing the importance of electron exchange when compared to the case of scattering from ground state targets (i.e., target atoms initially in the ground state).

In actual calculations the coupled PDE's (3) are solved over a finite 2-dimensional grid: $0 \le \rho \le \rho_{max}$, $-z_{max} \le z \le z_{max}$. The subsequent ρ-integration in (1) is then from $\rho = 0$ to $\rho = \rho_{max}$. Typical values of

z_{max} for ground state targets is 100-120 a_o, while for metastable targets (i.e., target atoms initially in a metastable state) z_{max} ranges from 250-300 a_o. The typical values of ρ_{max} range from 11 to 35 a_o for ground state targets, while for metastable targets the corresponding range is from 48 to 207 a_o. These ranges on z_{max} and ρ_{max} refer to 10-channel eikonal theory results for hydrogen and helium (Mansky and Flannery 1989a,b). While the above values of z_{max} and ρ_{max} for ground state targets is sufficient to insure convergence of the inelastic integral cross section to the corresponding Born value at high energy, in the case of metastable targets this is not the case. The contribution that trajectories, with impact parameters ρ in the range $\rho_{max} \leq \rho < \infty$, make to the scattering amplitude for metastable transitions (e.g., $2^3S \rightarrow 3^3L$, L = S,P,D) is not negligible at high energies. This is particularly true of metastable states dipole-coupled to the initial state via an optically-allowed transition. The correction to the scattering amplitude needed to account for these distant trajectories is given by (Mansky and Flannery 1989a),

$$f_{ni}^{(DMET)}(\theta) = \Gamma \int_0^{\rho_{max}} J_\Delta(q'\rho)[I_1(\rho,\tau) - i\, I_2(\rho,\tau)]\rho\, d\rho + f_{ni}^{(dipole)}(\theta)$$

$$= f_{ni}^{(MET)}(\theta) + f_{ni}^{(dipole)}(\theta), \text{ dipole-coupled transitions} \quad (4a)$$

$$= f_{ni}^{(MET)}(\theta), \text{ all other transitions} \quad (4b)$$

where,

$$f_{ni}^{(dipole)}(\theta) = \Gamma(i)^{\Delta+1} \frac{2\mu d'_{ni}}{\hbar^2} \frac{\alpha'}{q'^2+\alpha'^2} [x_1 J_{\Delta+1}(x_1)K_\Delta(x_1) - x_2 J_\Delta(x_2)K_{\Delta+1}(x_2)] \quad (5)$$

and $\Gamma \equiv -(i)^{\Delta+1}$, $\alpha' = \tau(\theta) - \alpha$, $\alpha = 2\mu(\epsilon_n - \epsilon_i)/\hbar^2(k_i + k_n)$, $d'_{ni} = \sqrt{3/4\pi}\, d_{ni}$, with d_{ni} denoting the dipole moment for the transition $i \rightarrow n$, and $x_1 \equiv q'\rho_{max}$, $x_2 \equiv \alpha'\rho_{max}$. The eigenenergies of the target atom are denoted ϵ_n, while $K_m(x)$ is a modified Bessel function of order m.

In this note the dipole correction (5) has been applied only to the $2^3S \rightarrow 2^3P_{o,\pm1}$ and $2^3S \rightarrow 3^3P_{o,\pm1}$ (Δ = 0,1) transitions within a 9-channel basis (2^3S, $2^3P_{o,\pm1}$, 3^3S, $3^3P_{o,\pm1}$ and $3^3D_{o,\pm1,\pm2}$). The present multi-channel eikonal theory results for these transitions are hereafter denoted DMET. However, to avoid confusion with Flannery and McCann's (1975) original MET results, the present results for the remaining triplet transitions will also be denoted DMET (with equations (4a) and (4b) in mind this should cause little confusion).

In figure 1 the present DMET results for the differential cross sections for the $2^3S \rightarrow 2^3P$ and $2^3S \rightarrow 3^3L$ (L = S,P,D) transitions at E = 20 eV

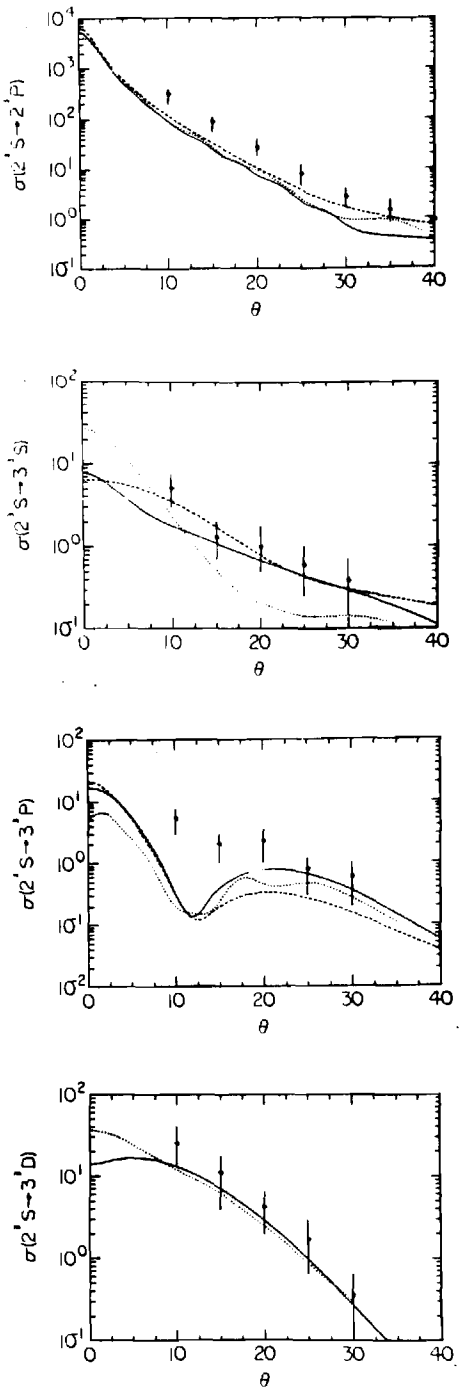

Figure 1. $e^- + He(2^3S \rightarrow n^3L)$ differential cross sections (πa_o^2/str.) at E = 20 eV; ___, present DMET results; -----, DW results (Mathur et al. 1987), ..., original MET results (Flannery and McCann, 1975b); o, experimental data (Muller-Fiedler et al. 1984).

are compared with the experimental data of Müller-Fiedler et al. (1984), the original MET results of Flannery and McCann (1975b) and (where available) the distorted-wave (DW) results of Mathur et al. (1987). The present DMET results for the $2^3S \rightarrow 3^3S$ and $2^3S \rightarrow 3^3D$ optically-forbidden transitions are clearly in excellent agreement with the experimental data. In particular, the agreement of the DMET results with experiment for the former transition is a direct result of the improved numerical solution of (3) used in the present results compared to that used in the original MET results. For the optically allowed $2^3S \rightarrow 2^3P$ and $2^3S \rightarrow 3^3P$ transitions, the present DMET results are seen to be underestimating the experimental data of Müller-Fiedler et al. This is also the case with the original MET results and the DW results. Interestingly however, all three theoretical results predict the existence of a deep diffractive minimum at about 12° in the $2^3S \rightarrow 3^3P$ DCS. No such behavior is seen however in the experimental data, leading one to question the theoretical results. While the DW results of Mathur et al. (1987) includes electron exchange within the primary, $2^3S \rightarrow 3^3P$, transition (with no couplings to other states), both the original MET results and the present DMET results neglect exchange but include couplings up to the 3^3D state. These points, taken together with the DCS experimental data for the n=4 triplet states (cf. Table 1), seem to indicate that the major physical mechanism missing from the theoretical results shown in figure 1 is coupling to the n=4 triplet states of helium. At least both dipole ($2^3S \rightarrow 4^3P$) and quadrupole ($2^3S \rightarrow 4^3S$, 4^3D) couplings should be included in a theoretical calculation in light of the relative magnitudes observed in the Kaiserslautern experiment between the DCS for the 3^3P state and the n=4 triplet states.

TABLE 1. Experimental Differential Cross Sections for $e^- + He(2^3S \rightarrow n^3L)$ (πa_o^2/str.) (Müller-Fiedler et al. 1984).

θ	2^3P	3^3S	3^3P	3^3D	$4^3S+4^3P+4^3D+4^3F$
10	300	4.9	5	25	10
15	85	1.4	1.9	10	6
20	26	.99	2.1	4	1.8
25	7.5	.60	.78	1.7	.78
30	2.8	.38	.58	.37	.50
35	1.6				
40	.82				

The DMET integral cross sections for the 2^3P and 3^3L (L=S,P,D) states are compared in figure 2 with the Born results of Flannery et al. (1975), the original MET results of Flannery and McCann (1975b) and (where available) the distorted-wave results of Mathur et al. (1987). Also, for the 2^3P and 3^3S states, the 5-state R-matrix results of Fon et al. (1981) and the Glauber theory results of Khayrallah et al. (1978) are shown, respectively. The above theoretical results are compared in figure 2 with the recent experimental data of Rall et al. (1989) for the 3^3S, 3^3P and 3^3D states. In the case of the 3^3S and the 3^3D states the experimental results are absolute apparent cross sections, so a direct comparison with theory will require the subtraction of the cascade contribution from the apparent measurements. Only the 3^3P results of Rall et al. (1989) are direct measurements. These were determined from the optical cross sections for

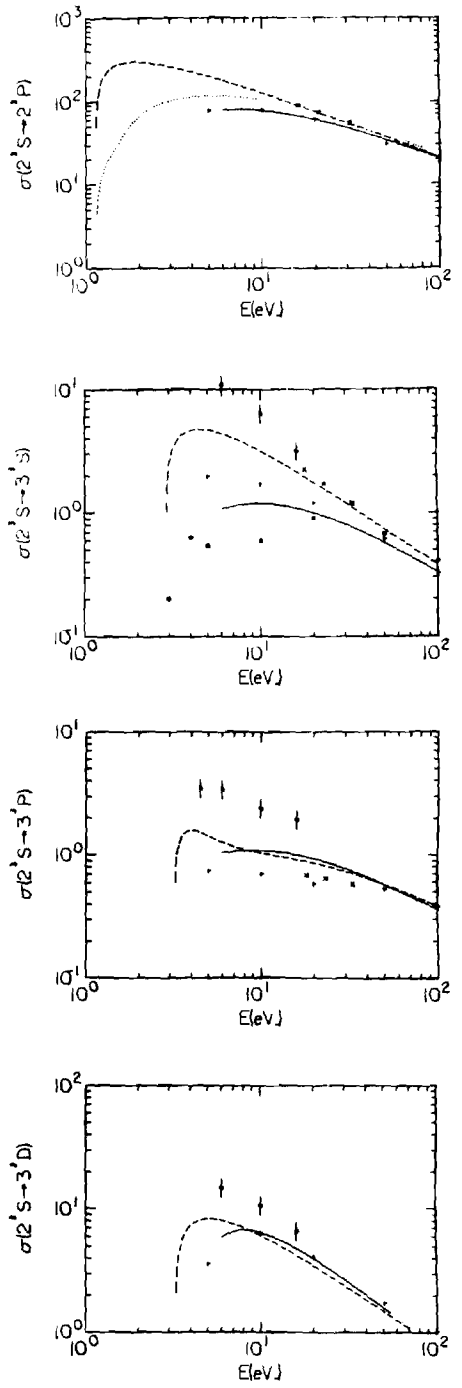

Figure 2. $e^- + He(2^3S \rightarrow n^3L)$ integral cross sections (πa_o^2). ---, Born results (Flannery et al. 1975); ___, present DMET results; +, original MET results (Flannery and McCann 1975b); x, DW results (Mathur et al. 1987); *, Glauber results (Khayrallah et al. 1978); ....., R-matrix results (Fon et al. 1981); o, experimental data (Rall et al. 1989).

the 2^3P and 3^3P and Einstein A coefficients (see Rall et al. (1989) for details). Clearly, further theoretical work will be required in order to convert the remaining apparent cross section measurements of Rall et al. to direct cross sections. However, the measurements of Rall et al. do confirm the basic trend, seen in both the MET and DMET, of the optically-forbidden $2^3S \rightarrow 3^3D$ cross section being larger than the optically-allowed $2^3S \rightarrow 3^3P$ cross section in the intermediate energy region.

ACKNOWLEDGEMENTS

This research is supported by AFOSR Grant No. 84-0233. Additional support from NATO and the Georgia Tech Research Corporation is also gratefully acknowledged.

REFERENCES

Bethe, H. A. and Salpeter E. E.,, 1977, Quantum Mechanics of One- and Two-Electron Atoms, Plenum Press (N.Y.)

Flannery, M. R. and McCann, K. J., 1974a, J. Phys. B: At. Mol. Phys. 7, L223-7

- 1974b, J. Phys. B: At. Mol. Phys. 7, 2518-32
- 1974c, J. Phys. B: At. Mol. Phys. 7, L522-7
- 1975a, J. Phys. B: At. Mol. Phys. 8, 1716-33
- 1975b, Phys. Rev. A 12, 846-55

Flannery, M. R., Morrison, W. F. and Richmond, B. L., 1975, J. Appl. Phys. 46, 1186-90

Fon, W. C., Berrington, K. A., Burke, P. G. and Kingston, A. E., 1981, J. Phys. B: At. Mol. Phys. 14, 2921-34

Khayrallah, G. A., Chen, S. T. and Rumble, J. R., 1978, Phys. Rev. A 17, 513-22

Mansky, E. J. and Flannery, M. R., 1989a, "The Multichannel Eikonal Theory of Electron-Hydrogen Collisions I. Excitation of H(1s)", to be submitted

- 1989b, "The Multichannel Eikonal Theory of Electron-Helium Collisions I. Excitation of He(1^1S)", to be submitted

Mathur, K. C., McEachran, R. P., Parcell, L. A. and Stauffer, A. D., 1987, J. Phys. B: At. Mol. Phys. 20, 1599-1608

McCann, K. J. and Flannery, M. R., 1975, J. Chem. Phys. 63, 4695-4707

- 1978, J. Chem. Phys. 69, 5275-87

Müller-Fiedler, R., Schlemmer, P., Jung, K., Hotop, H. and Ehrhardt, H., 1984, J. Phys. B: At. Mol. Phys. 17, 259-68

Phelps, A. V., 1955, Phys. Rev. 99, 1307-13

Rall, D. L. A., Sharpton, F. A., Schulman, M. B., Anderson, L. W., Lawler, J. E. and Lin, C. C., 1989, Phys. Rev. Lett. 62, 2253-6

Vučić, S., Potvliege, R. M. and Joachain, C. J., 1987, J. Phys. B: At. Mol. Phys. 20, 3157-70

Appendix C

THE NUMERICAL SOLUTION OF PARTIAL DIFFERENTIAL EQUATIONS IN ATOMIC SCATTERING THEORY

E. J. Mansky
School of Physics
Georgia Institute of Technology
Atlanta, Georgia 30332

ABSTRACT

The numerical solution of coupled partial and ordinary differential equations in electron-atom scattering theory are compared. In particular, a case study is made of the transition H(1s → 2s,2p) excited by electrons in the intermediate energy region. The results of the multichannel eikonal theory (MET) and the close coupling theory (CC) for this transition are compared and contrasted with experiment and each other. The principle conclusion is that the configuration space and angular momentum representations employed by the two theories provides information about the excitation process which is complementary. Specifically, the contrasting differences between the MET and CC results at small and large scattering angles for the modulus and phase angle of the complex scattering amplitudes $f_{ni}(\theta)$ sheds new light on the computational problems that need to be solved in order for the λ, R and I problem to be resolved.

I. INTRODUCTION

In this lecture the numerical solution of partial differential equations in electron-atom scattering theory will be discussed and contrasted with the problem of solving ordinary differential equations in scattering theory. In particular, the results obtained by the multichannel eikonal and close coupling theories for the electron impact excitation of hydrogen will be examined in detail. In Section II the partial differential equations of the multichannel eikonal theory are presented together with the ordinary differential equations of the close coupling theory. The advantages and limitations inherent in the representations employed by both theories is also discussed. In addition, the paralleli-

zability of the algorithms used in the numerical solution of the PDE's and the ODE's in the two theories is discussed in Section II. Section III contains a discussion of the results of the two theories for the integral and differential cross sections and the complex scattering amplitudes for the electron impact excitation of hydrogen. The conclusions are presented in Section IV together with a list of general references.

II. THEORY

Here we are concerned with the scattering of a structureless projectile B at a distance $\vec{R}$ from a target atom A with electronic coordinate $\vec{r}$. In this case, the time-independent Schrödinger equation is,

$$\mathcal{H}_i \psi_i = E_i \psi_i \tag{1}$$

where the Hamiltonian operator $\mathcal{H}_i$ is given by,

$$\mathcal{H}_i = \frac{-\hbar^2}{2m_A} \nabla_A^2 - \frac{\hbar^2}{2m_B} \nabla_B^2 - \frac{\hbar^2}{2m_e} \nabla_e^2 + V_{AB} + V_{Ae} + V_{Be} \tag{2a}$$

$$= \frac{-\hbar^2}{2m_T} \nabla_{CM}^2 - \frac{\hbar^2}{2\mu} \nabla_{AB}^2 - \frac{\hbar^2}{2m} \nabla_r^2 + V_{AB} + V_{Ae} + V_{Be} \tag{2b}$$

$$\equiv \mathcal{H}_{CM} + \mathcal{H}_i' \tag{2c}$$

In equation (2a) the first three terms on the right-hand side of the equation are the kinetic energy operators for the indicated particles, while in equations (2b,c) the separation into center-of-mass (CM) and relative motion terms are shown. As is well known, the separability of the CM and relative motion terms in this case allows one to write the system wavefunction Ψ_i as a product of a plane wave with a wavefunction ψ_i for the relative motion of projectile B in the field of force of target A. The target atom A in the present case is assumed to be hydrogenic, generalization to other cases is straightforward. The masses

in (2b) are defined as $m = m_e(m_A+m_B)/m_T$, $\mu = m_A m_B/(m_A+m_B)$ and $m_T = m_A + m_B + m_e$.

Therefore, Schrödinger's equation (1) now becomes,

$$\mathcal{H}'_i \psi_i = E' \psi_i \tag{3}$$

To solve (3) one generally expands the wavefunction ψ_i in a sum over eigenstates χ_n of the target A,

$$\psi_i = \sum_n F_n(\vec{r}_{AB})\, \chi_n(\vec{r}_{AB}, \vec{r}) \tag{4}$$

where F_n is the (unknown) wavefunction for the relative motion of projectile B a distance $\vec{r}_{AB}$ from target A (in channel n). In this lecture we are primarily concerned with contrasting the numerical solution of PDE's and ODE's in atomic scattering theory and hence the expansion given by (4) will be sufficient. However, if one is interested in resolving the spin structure of the target atom A, or the resonances in the cross section near threshold, additional terms (antisymmetrization, correlation, etc.) need to be added to (4). These additional terms will ultimately result in a larger set of coupled equations to be solved, but will not change in a material way our basic discussion of the numerical solution of coupled partial and ordinary differential equations in electron-atom scattering. References to calculations which do include the above effects are given in Section III.

Substitution of (4) into (3) results in the following set of coupled ordinary differential equations,

$$-\frac{\hbar^2}{2\mu} \nabla^2_{AB} F_n + \frac{\hbar^2 k_n^2}{2\mu} F_n - V_{nn} F_n = \sum_m{}' V_{nm}(\vec{r}_{AB}) F_m$$

$$- \sum_m \frac{\hbar^2}{2\mu} [F_m(\chi_n, \nabla^2_{AB} \chi_m) + 2 \vec{\nabla}_{AB} F_m (\chi_n, \vec{\nabla}_{AB} \chi_m)] \tag{5}$$

where the prime on the summation sign indicates omission of the term n=m, and the inner product (f,g) is defined.

$$(f,g) = \int f(\vec{r})\, g(\vec{r})\, d\vec{r}$$

To convert (5) into a set of PDE's, write $F_n(\vec{r}_{AB}) = A_n(\vec{r}_{AB})\, \exp[iS_n(\vec{r}_{AB})]$ and note that $r_{AB}^2 = \rho^2 + z^2$ with ρ, z, ϕ the usual cylindrical coordinates centered at A. This yields the following set of equations,

$$\Lambda_n \nabla_{AB}^2 A_n + 2 \vec{\nabla}_{AB} \Lambda_n \cdot \vec{\nabla}_{AB} A_n + \left\{ \nabla_{AB}^2 \Lambda_n + \left(k_n^2 - \frac{2\mu}{\hbar^2} V_{nn}\right) \Lambda_n \right\} A_n$$

$$= \sum_m{}' \frac{2\mu}{\hbar^2} V_{nm} \Lambda_m A_m - \sum_m \frac{2\mu}{\hbar^2} \vec{\beta}_{nm} \cdot \vec{\nabla}_{AB}(A_m \Lambda_m) \qquad (6)$$

with $\Lambda_n \equiv \exp[i\, S_n(\vec{r}_{AB})]$ and $\vec{\beta}_{nm} \equiv (\chi_n, \vec{\nabla}_{AB} \chi_m)$. After writing the gradient and Laplacian operators in (6) in terms of cylindrical coordinates, the coupled Hamilton-Jacobi partial differential equations are solved for the amplitude functions $A_n(\vec{r}_{AB})$. In these equations the eikonal phase $S_n(\vec{r}_{AB})$ is assumed to be known exactly. To obtain an equation for S_n set the term inside the curly brackets in (6) equal to zero,

$$\nabla_{AB}^2 \Lambda_n(\vec{r}_{AB}) + \left(k_n^2 - \frac{2\mu}{\hbar^2} V_{nn}\right) \Lambda_n(\vec{r}_{AB}) = 0 \qquad (7)$$

where the V_{nm} in (6) are the instantaneous electrostatic interaction between the projectile and target i.e., $V_{nm} = V_{nm}(\vec{r}_{AB}) = (\chi_n, V(\vec{r}_{AB}, \vec{r})\chi_m)$. Defining the local wavenumber $\kappa_n(\vec{r}_{AB}) \equiv k_n^2 - (2\mu/\hbar^2)\, V_{nn}$ and writing the Laplacian in (7) in spherical coordinates yields,

$$\frac{1}{r_{AB}^2} \frac{\partial}{\partial r_{AB}} \left[r_{AB}^2 \frac{\partial}{\partial r_{AB}} e^{iS_n(r_{AB})} \right] + \left[\frac{L_{AB}^2}{r_{AB}^2} + \kappa_n^2 \right] e^{iS_n(r_{AB})} = 0$$

$$\rightarrow i S_n'' + i \frac{2}{r} S_n' - (S_n')^2 + \omega_n^2 = 0 \qquad (8)$$

where the primes denote differentiation with respect to r_{AB} and L_{AB}^2 is the eigenvalue of the relative angular momentum operator $\vec{L}_{AB} = (\hbar/i)\ \vec{r}_{AB} \times \vec{\nabla}_{AB}$. The 'frequency' ω_n is defined, $\omega_n^2 \equiv (L_{AB}^2/r_{AB}^2) + \kappa_n^2$. Here we are interested in electron-atom collisions where the relative motion of the electron to a good approximation is a straight line. That is, we assume that the eikonal phase factor $S_n(\vec{r}_{AB})$ is a slowly varying function of $\vec{r}_{AB}$; or, equivalently, that the density of the classical ensemble of particles varies sufficiently slowly along the classical trajectory such that $S_n'' \sim 0$, and the L_{AB}^2 term in (8) can be ignored. In this case, the real part of (8) is integrated to give,

$$S_n(r_{AB}) \equiv S_n(\rho,z) = k_n z + \int_{-\infty}^{z} \left[[k_n^2 - \frac{2\mu}{\hbar^2} V_{nn}(\rho,z')]^{1/2} - k_n \right] dz' \qquad (9)$$

In the case of heavy particle collisions the curvature of the trajectory of the projectile must be included in the eikonal phase. An example of this type of calculation, for ion-molecule collisions, is the work of McCann and Flannery [26,27]. With the choice of (9) for the eikonal phase the coupled equations (6) are independent of A_n on the left-hand-side. In order to further simplify these 2nd-order partial differential equations for A_n, we in addition assume that the term $\nabla_{AB}^2 A_n$ is small and that the eigenstates χ_n are independent of $\vec{r}_{AB}$. The latter condition insures that the second summation on the RHS of (6) vanishes and is consistent with our omission of electron correlation effects in the wave-function expansion. These terms become important when there is significant configuration mixing in the target atom.

With the above approximations, the coupled equations (6) reduce to a set of first-order partial differential equations,

$$i\frac{\hbar^2}{\mu}\kappa_n\frac{\partial C_n(\rho,z)}{\partial z} + \left[\frac{\hbar^2}{\mu}\kappa_n(\kappa_n-k_n) + V_{nn}\right]C_n = \sum_j V_{nj}\,C_j\,\exp[i(k_j-k_n)z] \quad (10)$$

where $A_n(\rho,z) = C_n(\rho,z)\,e^{i\Delta_{in}\phi}\exp\{-i\int_{-\infty}^{z}(\kappa_n-k_n)dz'\}$, and $\Delta_{in} \equiv m_i-m_n$.

These equations are solved subject to the boundary condition $C_n(\rho,-\infty) = \delta_{ni}$. The coupled equations (10) are the basis of the multichannel eikonal theory (MET) of Flannery and McCann [11-16]. The three principal advantages of the semiclassical equations (10) are:

(i) The equations are first-order in z, hence the numerical techniques used for ordinary differential equations can be used to solve (10). This also means that no matrix diagonalization needs to be done in the numerical solution of (10), as is the case with 2nd-order ODE's.

(ii) The second variable ρ (the projectile's impact parameter) appears in (10) only as a parameter. This indicates that the coupled PDE's (10) will be readily parallelizable. While no calculations have yet been performed with (10) solved on a parallelizable machine, when this is done, a great deal of time should be saved. This is important since the numerical solution of (10) is the principle bottleneck in the MET calculations.

(iii) The memory and time required to solve (10) is a linear function of the number of eigenstates χ_n used in the basis set (4). This is in contrast to the case of 2nd-order ODE's where the time required for the matrix diagonalization is a *cubic* function of the number of elements in the matrix to be diagonalized. This in turn is a result of the direct methods used for the matrix diagonalization, and hence represents a major hurdle to the use of large basis sets in the solution of 2nd-order ODE's. The ultimate reason behind the difficulty in using large basis sets in solving 2nd-order ODE's by matrix techniques lies in the use of an angular momentum representation for the wavefunctions F_n rather than a

coordinate (i.e., configuration space) representation.

The main disadvantage of solving the 1st-order partial differential equations (10) is the fact that they must be solved over a 2-dimensional grid rather than a one-dimensional grid as is necessary in the solution of 2nd-order ODE's. A consequence of this is that the memory requirements are an order of magnitude larger for the former calculation as compared to the latter.

The close coupling 2nd-order ODE's which arise from using an angular momentum representation for $F_n(\vec{r}_{AB})$ in (4), are,

$$\left[\frac{d^2}{dr_{AB}^2} - \frac{\ell_i(\ell_i+1)}{r_{AB}^2} + \frac{2Z}{r_{AB}} + k_i^2\right] F_i(r_{AB})$$

$$= 2\sum_j V_{ij}(r_{AB})\, F_j(r_{AB}) + \int_o^\infty W_{ij}(r_{AB},r')\, F_j(r')dr'$$

$$+ \sum_{n\ell} \lambda_{n\ell}^{(i)}\, P_{n\ell}(r_{AB})\delta_{\ell\ell i} \qquad (11)$$

where ℓ_i is the orbital angular momentum quantum number of the projectile electron in state i, and the $\lambda_{n\ell}^{(i)}$ are Lagrange multipliers chosen such that the target orbitals $P_{n\ell}$ are orthogonal to the F_i. The matrix elements V_{ij} are the same as those defined previously, while the W_{ij} are the electrostatic matrix elements arising from inclusion of electron exchange (i.e., antisymmetrization) terms and correlation terms in the wavefunction expansion (4). The close coupling equations (11) are well known in the literature, hence their derivation need not be repeated here. However, attention is drawn to the following papers and reviews for those interested in further details [2,5-7,29].

Technically, the close coupling equations (11) are Fredholm ordinary integro-differential equations which, using the technique of Marriott [25], can be cast in the form of a larger set of purely ordinary differential equations. Then, after discretization of the Laplacian in (11), the problem is converted into one of matrix diagonalization.

The advantage of using the close coupling equations (11) is that very accurate inelastic cross sections can be obtained close to threshold - especially the resonance structure between the inelastic threshold and the threshold for ionization. However, as the energy crosses the ionization threshold (where the number of open channels becomes infinite), or in the case of transitions between excited states, the close coupling equations (11) become increasingly difficult to solve via matrix techniques due to the large number of basis states and partial waves ℓ_i required for convergence. This problem can partly be alleviated through the use of pseudo-states. Another way around the bottleneck of basis set size in the solution of (11) is through the use of multi-tasking on the CRAY-XMP. Important recent work in this regard is that of Sawey et al. [30]. Clearly further work on the numerical solution of (11), both by matrix diagonalization techniques and by solving the equivalent partial differential equations, is needed.

In this lecture we are interested in contrasting the numerical solutions of the coupled PDE's (10) with the ODE's (11). Hence we will only discuss the techniques used to solve numerically the PDE's (10), the techniques used to solve the close coupling equations (11) having been thoroughly described in [2,5,7]. In particular we will end Section II with a brief review of extrapolation methods used to solve 1st-order ordinary differential equations. A more complete discussion of the numerical solution of (10) including Runge-Kutta and predictor-corrector methods will be given in a forthcoming paper [22].

Extrapolation methods for ODE's

Consider the 1st-order ODE, $dy(t)/dt = F(t,y(t))$. When this is integrated for sufficiently small step sizes h, the solution of $y(t+h)$ can be written as a power series in h,

$$y(t+h) = y(t) + \sum_{i=1}^{m} \tau_i(t) h^i + \sigma(h^{m+1}) \qquad (13)$$

The goal of extrapolation methods is to eliminate the power series in h in (13) above by integrating the differential equation for a sequence of

step sizes $h_o, h_1, \ldots, h_m$, and then extrapolating the results to $h \to 0$. That is, the power series $\sum_i \tau_i(t)h^i$ is approximated by functions $R_m(t,h_i)$ which have m+1 unknowns. These unknowns are determined by the condition $R_m(t,h_j) = y(t+h_j)$, $j = 0,1,\ldots,m$. Hence the solution of the ODE $y(t)$ is approximated by $R_m(t,0)$.

The two principle extrapolation methods are by polynomials and by rational functions. In polynomial extrapolation the function $R_m(t,h_i) \equiv R_m^{(i)}(h)$ is an mth degree polynomial in h and is computed recursively by,

$$R_m^{(i)} = R_m^{(i+1)} + \frac{R_{m-1}^{(i+1)} - R_{m-1}^{(i)}}{(h_i/h_{i+m})-1}$$

In rational function extrapolation the $R_m^{(i)} = P_m(h)/Q_m(h)$ where $P_m(h)$ and $Q_m(h)$ are polynomials in h of degree μ and ν, respectively. The $R_m^{(i)}(h)$ are computed in this case recursively via

$$R_{-1}^{(i)} = 0, \quad R_o^{(i)} = y(t+h_i)$$

$$R_m^{(i)} = R_{m-1}^{(i+1)} + \frac{R_{m-1}^{(i+1)} - R_{m-1}^{(i)}}{(h_i/h_{i+m})^2 \left[1 - \dfrac{R_{m-1}^{(i+1)} - R_{m-1}^{(i)}}{R_{m-1}^{i+1} - R_{m-2}^{i+1}}\right] - 1}, \quad m \geq 1$$

The MET results discussed in Section III were obtained by solving the coupled 1st-order PDE's (10) using Bulirsch and Stoer's [4] method of rational extrapolation for ODE's. A full discussion of extrapolation techniques can be gound in Gear [17] and Dahlquist and Bjorck [10].

III. RESULTS

Before comparing the MET results obtained by solving the PDE's (10) with the close coupling equations (11) a short discussion on the practical numerical methods used to solve (10) are in order. To do this we quote the final expression used in the multichannel eikonal theory for

the complex scattering amplitude for the transition $i \rightarrow n$,

$$f_{ni}(\theta) = -(i)^{\Delta_{in}+1} \int_0^\omega J_{\Delta_{in}}(q'\rho)\,[I_1(\rho,\gamma(\theta)) - i\, I_2(\rho,\gamma(\theta))]\rho d\rho \qquad (14)$$

where the integrals I_1 and I_2 are defined,

$$I_1(\rho,\gamma) = \int_{-\omega}^{\omega} dz\, \kappa_n(\rho,z)\, \frac{\partial C_n(\rho,z)}{\partial z}\, \exp[i\gamma(\theta)z] \qquad (15a)$$

$$I_2(\rho,\gamma) = \int_{-\omega}^{\omega} dz\, [\kappa_n(\kappa_n - k_n) + \frac{\mu}{h^2} V_{nn}]C_n(\rho,z)\, \exp[i\gamma(\theta)z] \qquad (15b)$$

and refer the reader to the original literature [12,13,16] for the details. In equations (14,15) $q' = k_n \sin\theta$ and $\gamma(\theta) = k_n(1-\cos\theta)$ and $\Delta_{in} = m_i - m_n$. The 1st-order PDE's (10) are solved using Burlisch and Stoer's rational extrapolation technique for ODE's over a finite 2-dimensional grid: $o \leq \rho \leq \rho_{max}$, $-z_{max} \leq z \leq z_{max}$ for the amplitude functions $C_n(\rho,z)$. The values of ρ_{max} and z_{max} are varied until the cross section,

$$\int_0^{\rho_{max}} |C_n(\rho,z_{max})|^2 \rho d\rho \qquad (16)$$

is computed to within a tolerence ϵ (i.e., until subsequent evaluations change by less than an amount ϵ (%)). An additional criterion for the selection of optimal values of ρ_{max} and z_{max} is that the MET integral cross section, computed from the scattering amplitude (14) should converge to the 1st Born approximation at high incident energies. For this to be achieved it was found necessary to solve (20) using a non-linear grid in z in order that the rapid variation of C_n and $\partial C_n/\partial z$ near $z = 0$ be accurately represented. This was needed so that the subsequent evaluations of I_1, I_2 were accurate. The nonlinear grid in z used was:

$z_i = 3\tan(i\delta)$, $i = -N_z,\ldots,N_z$ with $\delta = \tan^{-1}(z_{max}/3)/N_z$. However, since I_1 and I_2 must be evaluated numerically from the tabulated solution of the coupled equations (10), the most efficient way of solving (10) is to make the grid points z_i used to solve (10) and the pivots used in the evaluation of I_1, I_2 *identical*. This avoids the need to interpolate w.r.t. z in the quadrature of I_1 and I_2 (interpolation w.r.t. ρ must still be done however). In the MET calculations discussed below, integrals I_1, I_2 were evaluated using Simpson's rule with the nonlinear pivots z_i chosen above and with weights $\omega_i = r_i\delta\ \sec^2(i\delta)$, where r_i are the usual Simpson's rule weights and N_z is the number of points used to discretize the z-range $[o,z_{max}]$. Hence while the number of points required for an accurate evaluation of I_1, I_2 is much larger using Simpson's rule as compared with using a higher-order quadrature method, the amount of time saved by eliminating the need to interpolate w.r.t. z more than makes up for the increased number of grid/ pivot points z_i required.

In figure 1 the real and imaginary parts of the amplitude function $C_n(\rho,z)$ for the 1s state of hydrogen are shown as an example of the type of behavior exhibited by the solutions of equation (10). For a more extensive exhibition of the solutions of the semiclassical equations (10) see [22].

In the remainder of Section III an overview of the MET results for e^-+H collisions will be given. This will include differential and integral cross sections as well as the complex scattering amplitudes. For a complete update and discussion of the present MET see Mansky and Flannery [23,24]. It should be clear that by comparing the results obtained for a wide range of physical observables, from the solution of equations (10) and (11), one not only gets an idea of the success or failure of a particular theory over a wider range of physical conditions, but also insight into the accuracy of the numerical solution of the coupled equations underlying a given theory. That is, by varying z_{max} and ρ_{max} in the semiclassical equations (10) until the integral cross sections computed from (14), for all states in the basis set, have

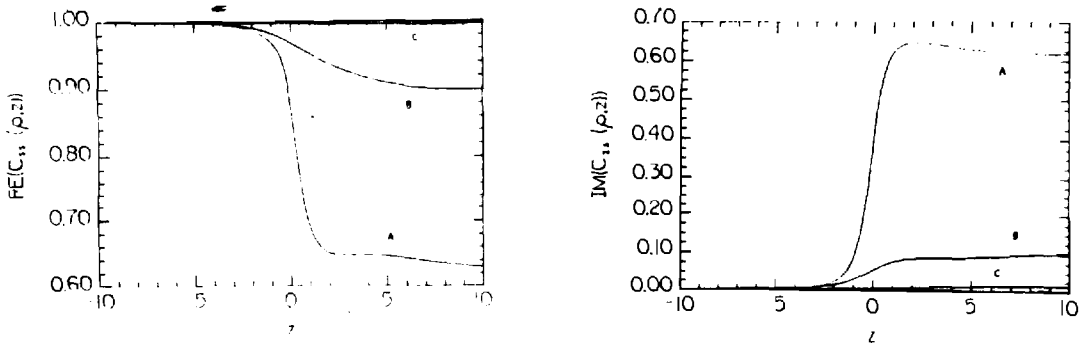

Figure 1: Real and imaginary parts of the MET amplitude function $C_{1s}(\rho,z)$ versus $z(a_o)$ for e^-+H collisions at E = 54.40 eV.

converged to their corresponding 1st Born approximation values in the limit of high energy, one obtains an idea of the minimum size 2-dimensional grid required to solve the coupled PDE's (10). These values of ρ_{max}, z_{max} can then be used to solve (10) for all other energies of interest. Note that a similar argument can be made about the numerical solution of the coupled ODE's (11) where the appropriate parameters are r_{max} and ℓ_{max} - the maximum value of the independent variable r_{AB} and the largest partial wave ℓ_i retained in the expansion.

The MET differential and integral cross sections are defined as,

$$\sigma_n(\theta) = \frac{k_n}{k_i} |f_{ni}(\theta)|^2 \qquad (17a)$$

$$\sigma_n = \int_0^{2\pi} d\phi \int_0^{\pi} \sin\theta \, d\theta \, \sigma_n(\theta) = 2\pi \int_0^{\pi} \sigma_n(\theta) \sin(\theta) d\theta \qquad (17b)$$

where the complex scattering amplitude for the transition i → n is given by (14). In figures 2,3 the integral and differential cross sections for

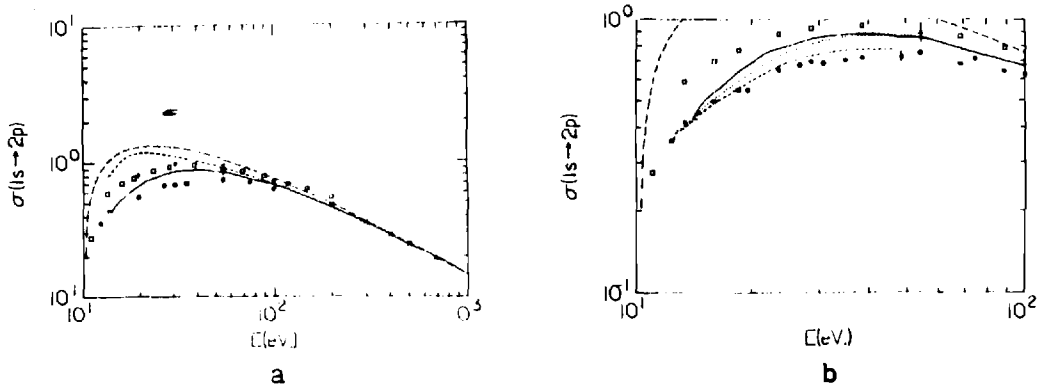

Figure 2a: Integral cross section σ_{2p} in units of πa_o^2 versus E (eV.). 1st Born (- - -), MET [23] (___), 3-state close coupling [18] (-----), DWSBA [20] (X), AVCC-18 state [9] (*), unitarized Born [31] (+), experimental data of Long et al. [21] as renormalized by Bransden and McDowell [3] (□), experimental data of Long et al. [21] as renormalized by van Wyngaarden and Walters [34] (0), experimental data of Williams [32] (Δ).

Figure 2b: Same as Fig. 2a except with AVCC-11 state (.....) [8].

e^-+H(1s → 2p) collisions are shown (results for other transitions in hydrogen are given in [23]). The MET results are in good overall agreement with experiment in figure 2, and clearly converge to the Born cross section at high energy. In particular, the agreement (cf. figure 2b) with the absolute measurement of Williams [32] at 54.40 eV is noteworthy. The differences between the original algebraic variational close coupling results of Callaway [8], and the same results as renormalized by van Wyngaarden and Walters [34], is a choice of normalization (i.e., normalization to experiment at 11 eV versus the pseudostate close coupling calculations of van Wyngaarden and Walters [35] at 350 eV). On the other hand, the differences between the 3-state close coupling results of Kingston, Fon and Burke [18] (cf. figure 2a) and the MET results is an indication of the lack of convergence w.r.t. basis set size in the former calculation. The importance of basis set size is evident in comparing the 3-state close coupling results of Kingston, Fon and Burke and the 18-state AVCC results of Callaway et al. [9] (cf. figure 2b). While the MET results are in good agreement with the results of Callaway et al. for energies $E \geq 70$ eV, the differences observed in figure 2 at lower energies is due to the neglect of electron exchange terms in the MET. This is also evident in figure 3 by the rapid decrease of the MET

differential cross sections $\sigma_{2s}(\theta)$, $\sigma_{2p}(\theta)$ at scattering angles $\theta > 40^{o}$ when compared to the close coupling results of Kingston, Fon and Burke [18] and van Wyngaarden and Walters [34]. The agreement between the MET and the experimental data of Williams [32] for $\theta \leq 20^{o}$ in figure 3 also indicates that the choices for z_{max} and ρ_{max} in the solution of (10) were correct.

From figure 3 one would conclude that electron exchange effects are only important at large scattering angles. This is incorrect. While a definitive calculation has not yet been done, the ongoing problem of theory to reproduce the experimental data for the λ, R and I parameters indicates that theory is still not handling adequately the numerical solution of the coupled equations (10) or (11). In figure 4 we show the λ, R and I parameters for e^{-}+H(1s $\rightarrow$ 2p) collisions at E = 54.40 eV and scattering angles $\theta \leq 50^{o}$. Clearly the MET results accurately reproduce the experimental data of Williams [32] only for $\theta \leq 20^{o}$, while at the level of $\sigma_{2p}(\theta)$ the corresponding angular range was $\theta \leq 40^{o}$. In contrast, the two close coupling results shown in figure 4 are in good agreement with experiment out to approximately 40^{o}. However, at larger scattering angles ($\theta \geq 60^{o}$) the close coupling results fail to reproduce the second experimental minimum in the λ parameter observed around 100^{o} and the magnitude of the R parameter in the range $70^{o} \leq \theta \leq 120^{o}$. These facts taken together indicate that while the values of z_{max}, ρ_{max} used to solve (10) in the MET are adequate at the level of differential and integral cross sections, the small z behavior of the amplitude functions still needs refinement for physical observables directly dependent on the complex scattering amplitude $f_{ni}(\theta)$. For completeness, the λ, R and I parameters are defined,

$$\lambda = |f_{o}|^{2}/[\,|f_{o}|^{2} + 2|f_{+1}|^{2}] \qquad (18a)$$

$$R = \sqrt{[\lambda(1-\lambda)/2]}\,\cos(\beta_{1} - \beta_{o}) \qquad (18b)$$

$$I = \sqrt{[\lambda(1-\lambda)/2]}\,\sin(\beta_{1} - \beta_{o}) \qquad (18c)$$

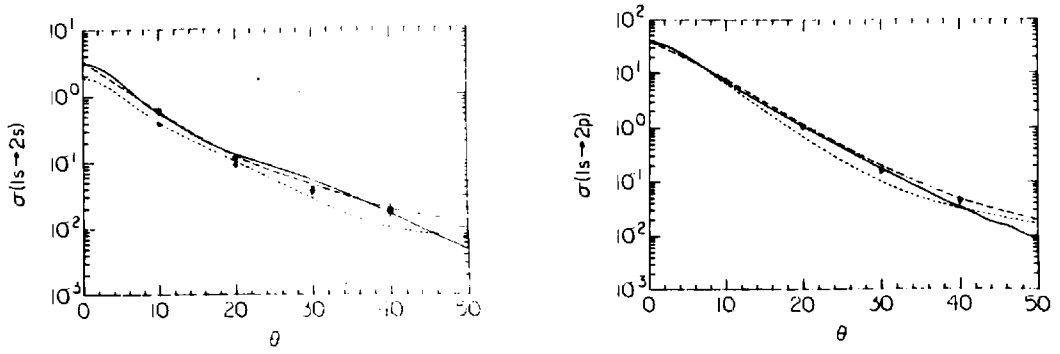

Figure 3: Differential cross sections $\sigma_{2s}(\theta)$, $\sigma_{2p}(\theta)$ in a_o^2/str. vs. θ for E = 54.40 eV. MET [23] (___), 3-state close coupling [18] (---), pseudostate close coupling [35] (----), experimental data of Williams [23] O (via sum), □ via ratio).

where $f_m(\theta) = |f_m(\theta)| \exp[i\beta_m(\theta)]$ and $f_m(\theta)$ denotes the complex scattering amplitude for $2p_m$ magnetic substate. For a complete discussion of the angular correlation and polarization correlation parameters in electron-atom scattering see Andersen et al. [1]. For more on the problem of the λ, R and I parameters in e^-+H collisions see Morgan [28].

To better understand what part of the solution of the PDE's (10) needs improvement, in regards to the λ, R and I problem discussed above, and where the electron exchange terms in (11) become important, we show the MET results for the scattering amplitudes $f_{2p_o}(\theta)$ and $f_{2p_1}(\theta)$ at E = 54.40 eV in figures 5 and 6, respectively. These are compared in figures 5,6 with the close coupling results of Kingston, Liew and Burke [19]. Two things are evident in these figures. First, that the electron exchange terms in the close coupling equations (11) manifest themselves quite differently in the modulus and phase angle of the scattering amplitude. For example, the phase angles for the singlet and triplet spin channels for the $f_{2p_o}(\theta)$ scattering amplitude differ from each other appreciably for $\theta \geq 30^o$, while for the $f_{2p_1}(\theta)$ they don't begin to differ greatly until $\theta \geq 40^o$. On the other hand, the modulii for the singlet

and triplet spin channels of the $f_{2p_o}(\theta)$, $f_{2p_1}(\theta)$ scattering amplitudes only differ appreciably for $\theta \leq 20^o$, $\theta \leq 30^o$, respectively. That is, electron exchange terms are important at small scattering angles for the moduli of scattering amplitudes, while for the corresponding phase angles, they are important only at large scattering angles. This indicates that unraveling the relative contributions that direct and exchange terms make to a given scattering amplitude at a specific angle will be difficult.

The second point to note from figure 5 is that the MET results for the $f_{2p_o}(\theta)$ amplitude agrees quite closely at all angles with the triplet spin channel results of Kingston, Liew and Burke. On the other hand in figure 6 the MET results only agree with the singlet spin channel results over a limited angular range. In particular the MET results exceed both the singlet and triplet spin channel results for $|f_{2p_1}(\theta)|$

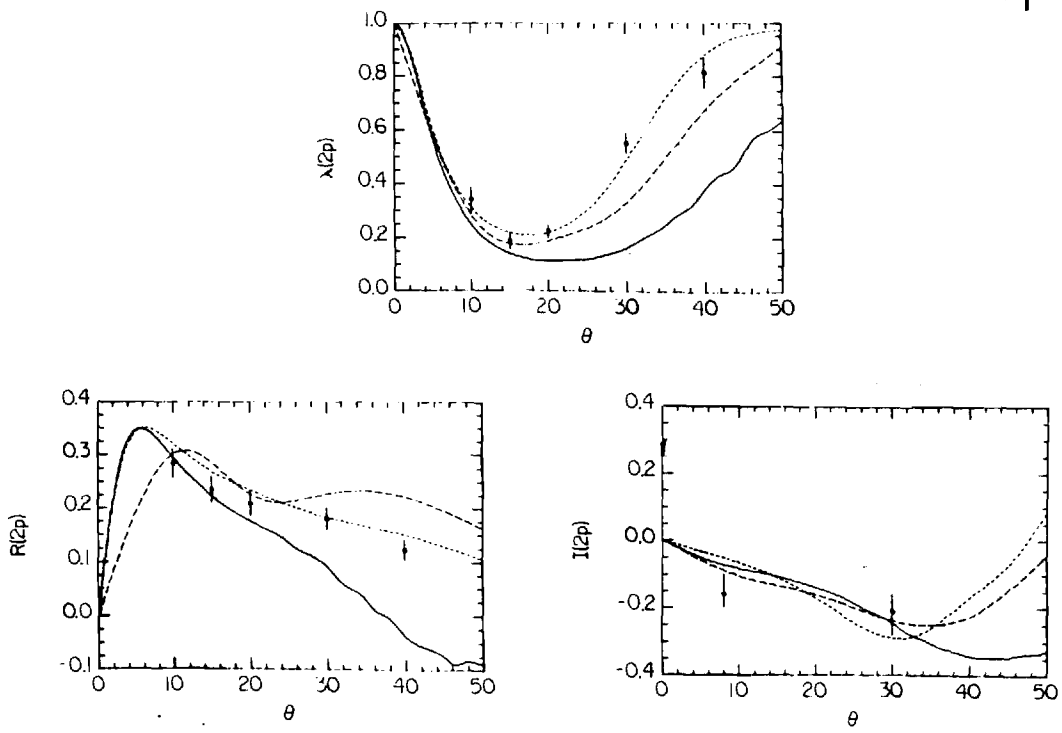

Figure 4: λ, R and I parameters for the 2p state at E = 54.40 eV. MET [23] (___), 3 state close coupling [18] (---), pseudostate close coupling [35] (-----), experimental data of Williams [32,33] O (λ, R from [32], I from [33]).

for $\theta \leq 20^{o}$. Note that we should not expect to see the MET results in figures 5,6 lying between the singlet and triplet spin channel results of Kingston, Liew and Burke. Rather, the observed behavior of the modulii and phase angles of the MET scattering amplitudes in figures 5,6 is a direct result of a complicated interplay between the z-behavior of the amplitude functions $C_n(\rho,z)$ and eikonal phases $S_n(\rho,z)$. A detailed discussion of these topics is beyond the scope of this lecture, but will be the subject of a forthcoming paper.

IV. CONCLUSIONS AND GENERAL REFERENCES

In this lecture we have contrasted solving coupled PDE's with ODE's in electron-atom collision theory. The principle conclusion of this lecture is that the solutions of (10) and (11) are complementary. That is, the configuration space representation employed by the MET, and the angular momentum representation employed by close coupling theories, complement one another, both in terms of information they provide about the scattering event, and in the energy ranges over which they are valid. This is important since it means that by solving (10) *and* (11) one gains additional insight into a particular excitation process that would not be obtained otherwise. This proved useful for example in the discussion of

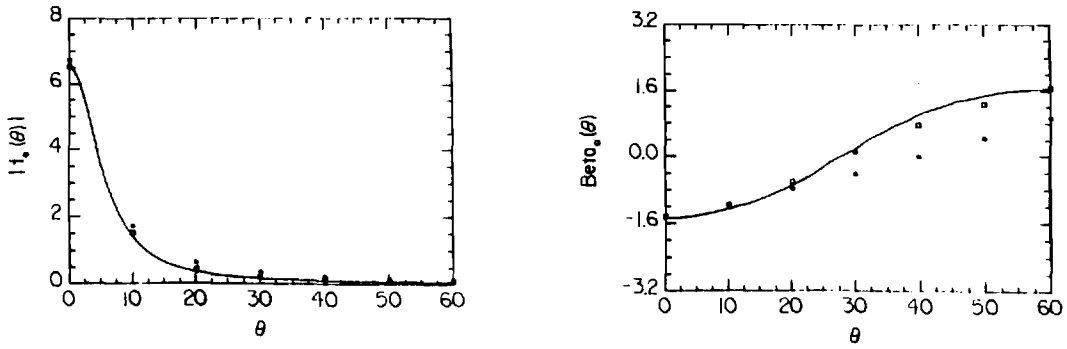

Figure 5: Modulus $|f_0|$ (in a_0) and phase angle β_0 (in radians) for $f_{2p}(\theta)$ vs. θ for E = 54.40 eV. MET [23] (___), 3 state close coupling [19] O (singlet) □ (triplet).

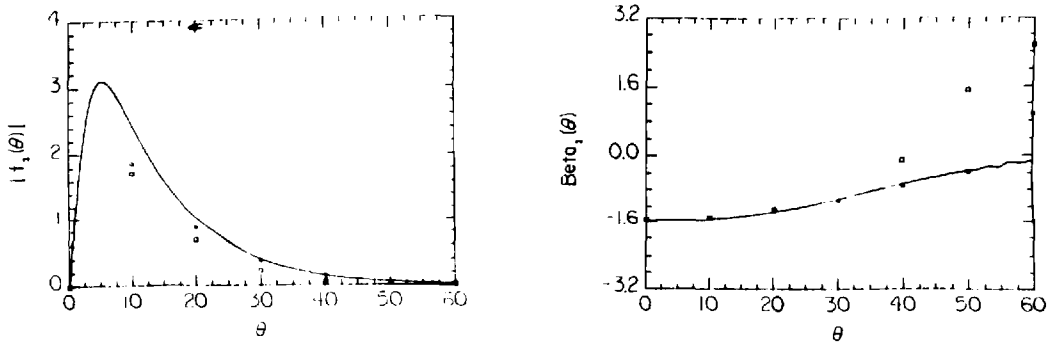

Figure 6: Same as Fig. 5 except for $f_{2p_1}(\theta)$.

the λ, R and I problem in Section III. We end this lecture with a short list of general references which we have found useful on the subject of coupled ordinary and partial differential equations.

- Collatz, L., 1960, The Numerical Treatment of Differential Equations 3rd ed., Springer-Verlag.
- Dahlquist, G., 1956, Math. Scandinavica 4 33-50, 1959, Trans. Roy. Inst. Tech., Stockholm, No. 130.
- Dahlquist, G., and Bjorck, A., 1974, Numerical Methods, Prentice Hall.
- Gear, C. W., 1971, Numerical Initial Value Problems in Ordering Differential Equations, Prentice-Hall.
- Henrici, P., 1962, Discrete Variable Methods for Ordinary Differential Equations, Wiley.
- Ince, E. L., 1956, Ordinary Differential Equations, Dover.
- Olver, P. J., 1986, Applications of Lie Groups to Differential Equations, Springer-Verlag.

Acknowledgements

This work is supported by AFOSR under grant no. 84-0233. The invitation to lecture, and the partial support received from Oak Ridge National Laboratory are also gratefully acknowledged.

References

1. Anderson, N., Gallagher, J. W., and Hertel, I. V., 1988, Phys. Rep. 165, 1-188.
2. Berrington, K. A., Burke, P. G., Le Dourneuf, M., Robb, W. D., Taylor, K. T. and Lan Vo Ky, 1978, Comp. Phys. Comm. 14, 367-412.
3. Bransden, B. H., and McDowell, M. R. C., 1978, Phys. Rep. 46, 249-394.
4. Bulirsch, R., and Stoer, J., 1966, Numer. Math. 8, 1-13.
5. Burke, P. G., and Eissner, W. B., 1983, Chapter 1 (p. 1-54) in Atoms in Astrophysics, Plenum Press (Burke, P. G., Eissner, W. B., Hummer, D. G. and Percival, I. C., eds.).
6. Burke, P. G., and Robb, W. D., 1971, Adv. Atom. Mol. Phys. 11, 143-214.
7. Burke, P. G., and Seaton, M. J., 1971, Methods in Comput. Phys. 10, 1-80.
8. Callaway, J., 1985, Phys. Rev. A 32, 775-83.
9. Callaway, J., Unnikrishnam, K., and Oza, D. H., 1987, Phys. Rev. A 36, 2576-84.
10. Dahlquist, G., and Bjorck, A., 1974, Numerical Methods, Prentice-Hall.
11. Flannery, M. R., and McCann, K. J., 1974, J. Phys. B: At. Mol. Phys. 7, L223-7.
12. ibid., J. Phys. B: At. Mol. Phys. 7, 2518-32.
13. ibid., J. Phys. B: At. Mol. Phys. 7, L522-7.
14. ibid., Phys. Rev. A 10, 2264-72.
15. ibid., 1975, J. Phys. B: At. Mol. Phys. 8, 1716-33.
16. ibid., Phys. Rev. A 12, 846-55.
17. Gear, C. W., 1971, Numerical Initial Value Problems in Ordinary Differential Equations, Prentice-Hall.
18. Kingston, A. E., Fon, W. C., and Burke, P. G., 1976, J. Phys. B: At. Mol. Phys. 9, 605-18.
19. Kingston, A. E., Liew, Y. C., and Burke, P. G., 1982, J. Phys. B: At. Mol. Phys. 15, 2755-66.
20. Kingston, A. E., and Walters, H. R. J., 1980, J. Phys. B: At. Mol. Phys. 13, 4633-62.

21. Long, R. L., Cox, D. M., and Smith, S. J., 1968, J. Res. NBS A 72, 521-35.
22. Mansky, E. J., 1989, J. Comput. Phys., to be submitted.
23. Mansky, E. J., and Flannery, M. R., 1989, "The Multichannel Eikonal Theory of Electron-Hydrogen Collisions I. Excitation of H(1s)", J. Phys. B, to be submitted.
24. ibid., "The Multichannel Eikonal Theory of Electron-Helium Collisions I. Excitation of He(1^1S)", J. Phys. B, to be submitted.
25. Marriott, R., 1958, Proc. Phys. Soc. (Lon.) 72, 121-9.
26. McCann, K. J., and Flannery, M. R., 1975, J. Chem. Phys. 63, 4695-4707.
27. ibid., 1978, J. Chem. Phys. 69, 5275-87.
28. Morgan, L. A., 1982, J. Phys. B: At. Mol. Phys. 15, 4247-57.
29. Percival, I. C., and Seaton, M. J., 1957, Proc. Camb. Phil. Soc. 53, 654-62.
30. Sawey, P. M. J., Berrington, K. A., Burke, P. G., and Kingston, A. E., 1989, 16th Int. Conf. on the Phys. of Electronic and Atom. Coll. (N.Y.) Abstracts of contrib. papers 214.
31. Somerville, W. B., 1963, Proc. Phys. Soc. (Lon.) 82, 446-55.
32. Williams, J. F., 1981, J. Phys. B: At. Mol. Phys. 14, 1197-1217.
33. ibid., 1986, Aust. J. Phys. 39, 621-32.
34. van Wyngaarden, W. L., and Walters, H. R. J., 1986, J. Phys. B: At. Mol. Phys. 19, L53-8.
35. ibid., J. Phys. B: At. Mol. Phys. 19, 929-68.

Appendix D

ITERATIVE SOLUTION OF LARGE LINEAR SYSTEMS AND HEAVY PARTICLE COLLISIONS: ION-ION RECOMBINATION

E. J. Mansky
School of Physics
Georgia Institute of Technology
Atlanta, Georgia 30332

ABSTRACT

The solution of large sparse linear systems of algebraic equations arising from the discretization of coupled Boltzmann partial integro-differential equations, which model ion-ion recombination processes in dense gases, is discussed. The advantages and limitations of various representations of these equations is provided. A detailed analysis is given of the derivation and structure of the coefficient matrix $\mathcal{A}$ of the resultant algebraic equations. The need for preconditioning the algebraic equations through the calculation of the condition number of the matrix $\mathcal{A}$ is highlighted. Approximate methods of computing termolecular recombination rate coefficients via the Debye-Smoluchowski equation and diffusion models in energy space are also briefly discussed.

I. INTRODUCTION

In this lecture the numerical solution of large sets of linear algebraic equations by iterative methods will be discussed with particular application to problems in heavy particle collisions. The physical problem specifically addressed is that of ion-ion recombination at arbitrary gas densities. The determination of the rate of recombination is governed by the solution of a pair of coupled Boltzmann-like integro-differential equations (IDE's). The derivation of these coupled Boltzmann equations from a more basic perspective involving the BBGKY hierarchy of equations is reviewed in Section II. The solution of these coupled IDE's provides a general framework for discussing the problem of computing chemical reaction rates in dense plasmas. This is provided in

Section II along with a detailed discussion of the advantages and limitations of transforming the IDE's into a set composed solely of differential equations (DE's) or integral equations (IE's). In all three representations the problem of numerically solving the coupled Boltzmann equations reduces to one of solving a set of simultaneous linear algebraic equations composed of a large, sparse, real, positive definite, non-symmetric, ill-conditioned matrix. The solution of these algebraic equations by iterative techniques is highlighted in Section II.

Historically, until the advent of supercomputers, the direct solution of the coupled Boltzmann equations was generally avoided through the use of simplifying approximations because of the difficulty in solving large sets of algebraic equations. In Section III the link between the coupled Boltzmann equations and it's approximations is given. In particular the formulation of the problem in terms of diffusion equations (in energy space) and Debye-Smoluchowski equations is accentuated in Section III. The conclusions of this lecture and a list of general references is given in Section IV.

II. BOLTZMANN EQUATION TREATMENT OF IONIC RECOMBINATION

The overall goal of the type of calculations described in this lecture is the prediction from a microscopic viewpoint, of the rate of chemical reactions in dense gases. The proto-type chemical reaction we are primarily interested in is that of ion-ion recombination at arbitrary gas densities,

$$X^+ + Y^- + Z \xrightarrow{\alpha} [XY]^* + Z \qquad (1)$$

whereby free ions (X^+,Y^-) are converted into diatomic molecules XY (usually in some metastable state denoted by *). We will assume that the number density of third bodies Z is arbitrary, but that the free ion number densities is sufficiently low so that the interaction potential between ions is strictly Coulombic. This will necessarily exclude from discussion dynamic screening effects in dense plasmas. We will also not discuss the related problem of ion-atom association,

$$X^+ + Y + Z \rightarrow [XY^+]^* + Z$$

which is an important mechanism by which molecular ions are formed in interstellar media and in laboratory plasmas. To solve both problems from a microscopic standpoint will require a great deal of information on the full three-body sector of phase space which is beyond the scope of this lecture to provide. Anyway, before the latter two problems can be solved, a complete understanding of the solution of the termolecular recombination rate in the limit of low ionic density and arbitrary gas density will be needed.

We are interested in computing in this lecture microscopic reaction rates which the reader should take to mean that the reaction rates will be expressed in terms of the phase space distribution functions f_N for the N particles comprising the three component plasma (positively and negatively charged particles as well as neutral species) undergoing termolecular recombination. Our starting point is the BBGKY hierarchy of equations,

$$\frac{\partial f_s}{\partial t} = - \mathcal{H}_s f_s + n\ell_s f_{s+1} \qquad s = 1,2,3,\ldots,N-1 \qquad (2)$$

which is a set of coupled equations for the s-particle reduced distribution functions $f_s = f_s(x_1,x_2,\ldots,x_s;t) = V^{-(N-s)} \int dx_{s+1} \int dx_{s+2} \ldots \int dx_N\, f_N(x_1,\ldots,x_N;t)$ with V denoting the total volume of phase space and $x_i:(\vec{r}_i,\vec{p}_i)$ denotes the 6-dimensional phase space point for particle i. In equation (2), the Hamiltonian operator for s particles of equal mass m is defined,

$$\mathcal{H}_s = \sum_{i=1}^{s} \frac{\vec{p}_i}{m} \vec{\nabla}_{\vec{r}_i} + \frac{\vec{\mathcal{F}}_i}{m} \cdot \vec{\nabla}_{\vec{p}_i} - \sum_{1 \leq i < j \leq s} \theta_{ij} \qquad (3)$$

where $\vec{\mathcal{F}}_i$ is the external force on particle i, and the interaction operator between particles i and j, is

$$\Theta_{ij} = \frac{\partial \phi_{ij}}{\partial \vec{r}_i} \cdot \vec{\nabla}_{\vec{p}_i} + \frac{\partial \phi_{ij}}{\partial \vec{r}_j} \cdot \vec{\nabla}_{\vec{p}_j} \tag{4}$$

with the interaction potential between particles i and j denoted ϕ_{ij}. The phase-mixing operator $\mathscr{L}_s$ in the BBGKY equations (2) is defined,

$$\mathscr{L}_s = \sum_{i=1}^{s} \int dx_{s+1}\, \Theta_{i,s+1} \tag{5}$$

and the number density n in (2) is n = N/V. For a detailed derivation of the BBGKY hierarchy (2) the reader is referred to the statistical mechanical literature (Akhiezer et al. [1], Balescu [3,4], Chapman and Cowling [13], Ferziger and Kaper [18] and Tolman [41]).

Since in ionic recombination we are interested in the formation of diatomic molecules, it is natural to assume that the most important reduced distribution functions in the three component plasma are those for one and two particles. Hence we will truncate the BBGKY hierarchy of equations at f_3 and concentrate on the equations for f_1, f_2. Also, since we are interested only in the recombination of positively and negatively charged particles to form neutral diatomic molecules, it follows that the main determining factor in computing α, the rate of reaction (1) will be the pair correlation function $g_2^{(+-)}$ between X^+ and Y^-. From this we conclude that a separate BBGKY hierarchy (2) will be required for each component of the plasma. These hierarchies for the three component plasma are,

$$\dot{f}_1^{(+)} = -\mathscr{K}_1^{(+)} f_1^{(+)} + \mathscr{L}_1^{(++)} f_2^{(++)} + \mathscr{L}_1^{(+-)} f_2^{(+-)} + \mathscr{L}_1^{(+n)} f_2^{(+n)} \tag{6a}$$

$$\dot{f}_1^{(-)} = -\mathscr{K}_1^{(-)} f_1^{(-)} + \mathscr{L}_1^{(-+)} f_2^{(-+)} + \mathscr{L}_1^{(--)} f_2^{(--)} + \mathscr{L}_1^{(-n)} f_2^{(-n)} \tag{6b}$$

$$\dot{f}_1^{(n)} = -\mathscr{K}_1^{(n)} f_1^{(n)} + \mathscr{L}_1^{(n+)} f_2^{(n+)} + \mathscr{L}_1^{(n-)} f_2^{(n-)} + \mathscr{L}_1^{(nn)} f_2^{(nn)} \tag{6c}$$

$$\dot{f}_2^{(++)} = -\mathcal{H}_2^{(++)} f_2^{(++)} + \mathcal{L}_2^{(+++)} f_3^{(+++)} + \mathcal{L}_2^{(++-)} f_3^{(++-)} + \mathcal{L}_2^{(++n)} f_3^{(++n)} \quad (7a)$$

$$\dot{f}_2^{(+-)} = -\mathcal{H}_2^{(+-)} f_2^{(+-)} + \mathcal{L}_2^{(+-+)} f_3^{(+-+)} + \mathcal{L}_2^{(+--)} f_3^{(+--)} + \mathcal{L}_2^{(+-n)} f_3^{(+-n)} \quad (7b)$$

$$\dot{f}_2^{(+n)} = -\mathcal{H}_2^{(+n)} f_2^{(+n)} + \mathcal{L}_2^{(+n+)} f_3^{(+n+)} + \mathcal{L}_2^{(+n-)} f_3^{(+n-)} + \mathcal{L}_2^{(+nn)} f_3^{(+nn)} \quad (7c)$$

$$\dot{f}_2^{(--)} = -\mathcal{H}_2^{(--)} f_2^{(--)} + \mathcal{L}_2^{(--+)} f_3^{(--+)} + \mathcal{L}_2^{(---)} f_3^{(---)} + \mathcal{L}_2^{(--n)} f_3^{(--n)} \quad (7d)$$

$$\dot{f}_2^{(-n)} = -\mathcal{H}_2^{(-n)} f_2^{(-n)} + \mathcal{L}_2^{(-n+)} f_3^{(-n+)} + \mathcal{L}_2^{(-n-)} f_3^{(-n-)} + \mathcal{L}_2^{(-nn)} f_3^{(-nn)} \quad (7e)$$

$$\dot{f}_2^{(nn)} = -\mathcal{H}_2^{(nn)} f_2^{(nn)} + \mathcal{L}_2^{(nn+)} f_3^{(nn+)} + \mathcal{L}_2^{(nn-)} f_3^{(nn-)} + \mathcal{L}_2^{(nnn)} f_3^{(nnn)} \quad (7f)$$

where the superscripts +, -, n indicates a positively or negatively charged particle or a neutral species, respectively, and the dots indicate differentiation w.r.t. time.

The set of coupled equations (6,7) are closed by use of the cluster expansion (Ferziger and Kaper [18]) wherein the 3 particle distributions f_3 are written as functionals of the 1 and 2-particle distribution functions. The latter functions are written in turn as functionals of f_1 thereby closing the set of equations (6,7). For a detailed derivation of these equations see Mansky [35] and Flannery and Mansky [28]. Since we are primarily interested in the numerical aspects of the problem of computing ionic recombination rates α in this lecture, we will omit the details of the subsequent reduction of the coupled equations (6,7) to the working equations (8), but refer the reader to the above two references as well as two earlier important papers of Flannery's [24,25].

Therefore, after reduction, the final steady state working equations are

$$\left[\frac{1}{r} - \lambda\right] \frac{\partial \rho^+(r,\lambda)}{\partial r} + \frac{1}{r}\left[\frac{1}{r} - 2\lambda\right][\rho^+(r,\lambda) - \rho^-(r,\lambda)] = \Gamma' \int_{-\infty}^{1/r} \rho^+(r,\mu) F(\lambda,\mu;r)\, d\mu - \Gamma' \rho^+(r,\lambda) \mathcal{F}(r,\lambda) \quad (8a)$$

$$-\left[\frac{1}{r} - \lambda\right] \frac{\partial \rho^-(r,\lambda)}{\partial r} = \Gamma' \int_{-\infty}^{1/r} \rho^-(r,\mu) F(\lambda,\mu;r)\, d\mu - \Gamma' \rho^-(r,\lambda) \mathcal{F}(r,\lambda) \quad (8b)$$

$$\left[\frac{1}{r} - \lambda\right] \frac{\partial \rho^{+}(r,\lambda)}{\partial r} = \Gamma' \int_{-\infty}^{1/r} \rho^{+}(r,\mu) F(\lambda,\mu;r)\, d\mu - \Gamma'\, \rho^{+}(r,\lambda)\mathcal{F}(r,\lambda) \qquad (8c)$$

$$-\left[\frac{1}{r} - \lambda\right] \frac{\partial \rho^{-}(r,\lambda)}{\partial r} - \frac{1}{r}\left|\frac{1}{r} - 2\lambda\right|[\rho^{+}(r,\lambda) - \rho^{-}(r,\lambda)] = \Gamma' \int_{-\infty}^{1/r} \rho^{-}(r,\mu) F(\lambda,\mu;r)\, d\mu - \Gamma'\, \rho^{-}(r,\lambda)\mathcal{F}(r,\lambda) \qquad (8d)$$

where equations (8a,b) are valid for region I: $-\infty < \lambda \leq \frac{1}{2r}$ and (8c,d) are valid for region II: $\frac{1}{2r} \leq \lambda \leq \frac{1}{r}$ (see figure 1). The functions $\rho^{(\pm)}(r,\lambda)$ represented the number density of ion-pairs expanding (+) and contracting (-) at a given relative separation r and internal energy λ in phase space. The ρ's are just the ratio of the number density of ion-pairs undergoing recombination to the equilibrium number density (i.e., $\rho^{(\pm)}(r,\lambda) = n^{(\pm)}(r,\lambda)/n_{eq}$). The working equations (8) are written in terms of dimensionless natural variables which are defined,

$$r = r_{12}/R_e, \qquad \lambda = -E_i/kT, \qquad \mu = -E_f/kT$$

where $R_e = e^2/kT$ and $\Gamma' \equiv \Gamma\, e^{-\lambda}$, $\Gamma = \frac{\Lambda_{mfp}}{2\sqrt{\pi}}\Gamma_o$, $\Lambda_{mfp} = R_e/\lambda_{mfp}$, $\lambda_{mfp} = (N(Z)Q^D)^{-1}$. Hence the dependence on gas density in (8) is contained in the constant Γ, which also depends on the masses via,

$$\Gamma_o \equiv \begin{cases} [(1+c)/c]^{3/2} & \text{, charge transfer} \\ (1+a)^2/a^{3/2} & \text{, hard sphere} \\ \sqrt{3/2}\,(1+a)^{5/2}/a^{3/2} & \text{, polarization} \end{cases}$$

and,

$$\mathcal{F}(r,\lambda) \equiv \int_{-\infty}^{1/r} F(\lambda,\mu;r)\, d\mu$$

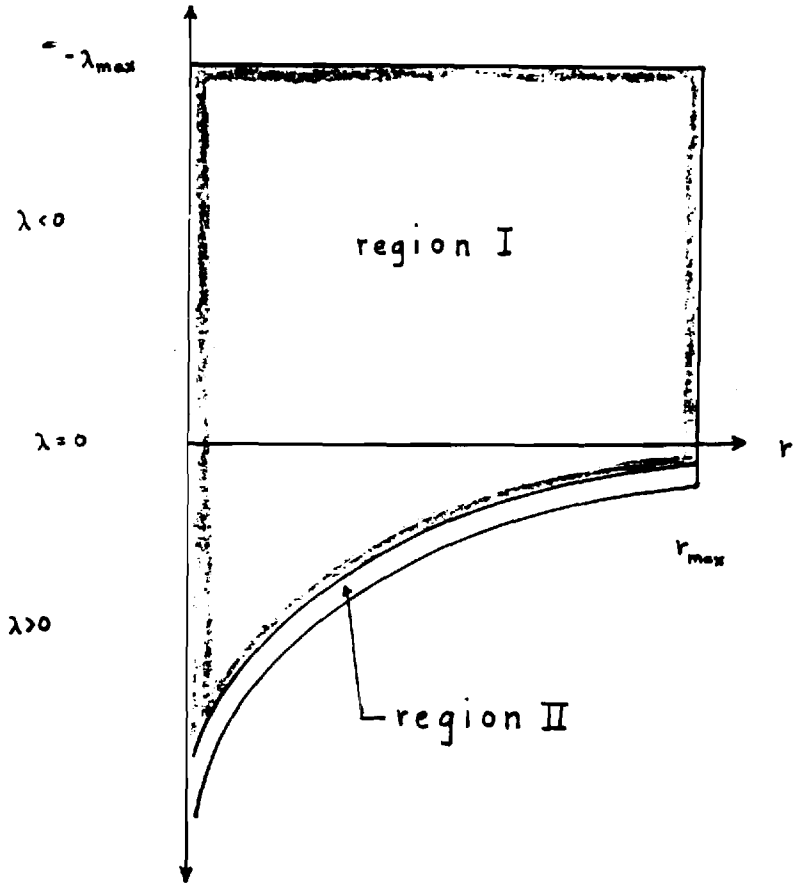

Figure 1: Illustration of λ, r phase space domain of equation (8).

The detailed formulae for the energy-change rate coefficients $F(\lambda,\mu;r)$ for the energy transfer mechanisms of charge-transfer, hard sphere and polarization collisions need not concern us here, but can be found in the original literature Flannery [21-23] and Flannery and Mansky [27]). In the definition of Γ_o the mass ratio parameters are defined,

$$a = m_2 m_3 / m_1 (m_1+m_2+m_3)$$

$$c = m_1/m_2$$

where m_2, m_2 and m_3 are the masses of X^+, Y^- and Z, respectively.

The functions $\rho^{\pm}(r,\lambda)$ are not completely determined by the working equations (8) until their associated boundary conditions are specified,

$$\rho^{\pm}(r,\lambda\to-\infty) = 1 \tag{9a}$$

$$\rho^{\pm}(r\to\infty,\lambda) = 1 \quad \text{for } \lambda \leq 0 \tag{9b}$$

$$\rho^{+}(r=o,\lambda) = \rho^{-}(r=o,\lambda) \tag{9c}$$

$$\rho^{+}(r,\frac{1}{r}) = \rho^{-}(r,\frac{1}{r}) \tag{9d}$$

Before we convert the working equations (8) into a set of practical, numerical equations we will discuss the relative computational merits of transforming the integro-differential equations (8) into equivalent differential equations or integral equations.

Technically, the working equations (8) are coupled Volterra partial integro-differential equations (PIDE's). They are 1^{st}-order in r and 1-dimensional in λ meaning that the highest derivative in r appearing in (8) is the first, while only single integrals w.r.t. λ appear. To convert (8) into a set of PDE's define the functions $\tilde{\rho}^{\pm}(r,\lambda)$ by

$$\rho^{\pm}(r,\lambda) = \frac{1}{F(\mu,\lambda;r)} \frac{\partial\tilde{\rho}^{\pm}(r,\lambda)}{\partial\lambda} \tag{10}$$

yielding,

$$(\frac{1}{r}-\lambda) \frac{\partial}{\partial r}\left[\frac{1}{F(\mu,\lambda;r)} \frac{\partial\tilde{\rho}^{+}(r,\lambda)}{\partial\lambda}\right] + \frac{\frac{1}{r}\left[\frac{1}{r}-2\lambda\right]}{F(\mu,\lambda;r)}\left[\frac{\partial\tilde{\rho}^{+}(r,\lambda)}{\partial\lambda} - \frac{\partial\tilde{\rho}^{-}(r,\lambda)}{\partial\lambda}\right]$$

$$+ \Gamma' \frac{\mathcal{F}(r,\lambda)}{F(\mu,\lambda;r)} \frac{\partial\tilde{\rho}^{+}(r,\lambda)}{\partial\lambda} = \Gamma'[\tilde{\rho}^{+}(r,\frac{1}{r}) - \tilde{\rho}^{+}(r,-\infty)] \tag{11a}$$

$$-(\frac{1}{r}-\lambda) \frac{\partial}{\partial r}\left[\frac{1}{F(\mu,\lambda;r)} \frac{\partial\tilde{\rho}^{-}(r,\lambda)}{\partial\lambda}\right] + \Gamma'\frac{\mathcal{F}(r,\lambda)}{F(\mu,\lambda;r)} \frac{\partial\tilde{\rho}^{-}(r,\lambda)}{\partial\lambda} = \Gamma'[\tilde{\rho}^{-}(r,\frac{1}{r})-\tilde{\rho}^{-}(r,-\infty)] \tag{11b}$$

$$(\frac{1}{r}-\lambda) \frac{\partial}{\partial r}\left[\frac{1}{F(\mu,\lambda;r)} \frac{\partial\tilde{\rho}^{+}(r,\lambda)}{\partial\lambda}\right] + \Gamma'\frac{\mathcal{F}(r,\lambda)}{F(\mu,\lambda;r)} \frac{\partial\tilde{\rho}^{+}(r,\lambda)}{\partial\lambda} = \Gamma'[\tilde{\rho}^{+}(r,\frac{1}{r})-\tilde{\rho}^{-}(r,-\infty)] \tag{11c}$$

$$-\left(\frac{1}{r}-\lambda\right)\frac{\partial}{\partial r}\left[\frac{1^{-}}{F(\mu,\lambda;r)}\frac{\partial\tilde{\rho}^{-}(r,\lambda)}{\partial\lambda}\right]+\Gamma'\frac{\mathcal{F}(r,\lambda)}{F(\mu,\lambda;r)}\frac{\partial\tilde{\rho}^{-}(r,\lambda)}{\partial\lambda}-\frac{\frac{1}{r}\left|\frac{1}{r}-2\lambda\right|}{F(\mu,\lambda;r)}\left[\frac{\partial\tilde{\rho}^{+}}{\partial\lambda}-\frac{\partial\tilde{\rho}^{-}}{\partial\lambda}\right]$$

$$=\Gamma'[\tilde{\rho}^{-}(\cdot,\tfrac{1}{r})-\tilde{\rho}^{-}(r,-\infty)] \qquad (11d)$$

Performing the indicated differentiation w.r.t. r and rearranging terms results in the following set of coupled hyperbolic 2nd-order partial differential equations,

$$\frac{\left[\frac{1}{r}-\lambda\right]}{F(\mu,\lambda;r)}\frac{\partial^{2}\tilde{\rho}^{+}(r,\lambda)}{\partial r\partial\lambda}+\left[\frac{\frac{1}{r}\left[\frac{1}{r}-2\lambda\right]}{F(\mu,\lambda;r)}-\frac{\left[\frac{1}{r}-\lambda\right]F'(\mu,\lambda;r)}{(F(\mu,\lambda,;r))^{2}}+\frac{\Gamma'\mathcal{F}(r,\lambda)}{F(\mu,\lambda;r)}\right]\frac{\partial\tilde{\rho}^{+}(r,\lambda)}{\partial\lambda}$$

$$-\frac{\frac{1}{r}\left[\frac{1}{r}-2\lambda\right]}{F(\mu,\lambda;r)}\frac{\partial\tilde{\rho}^{-}(r,\lambda)}{\partial\lambda}=\Gamma'[\tilde{\rho}^{+}(r,\tfrac{1}{r})-\tilde{\rho}^{+}(r,-\infty)] \qquad (12a)$$

$$-\frac{\left[\frac{1}{r}-\lambda\right]}{F(\mu,\lambda;r)}\frac{\partial^{2}\tilde{\rho}^{-}(r,\lambda)}{\partial r\partial\lambda}+\left[\frac{\Gamma'\mathcal{F}(r,\lambda)}{F(\mu,\lambda;r)}+\frac{\left[\frac{1}{r}-\lambda\right]F'(\mu,\lambda;r)}{(F(\mu,\lambda,;r))^{2}}\right]\frac{\partial\tilde{\rho}^{-}(r,\lambda)}{\partial\lambda}$$

$$=\Gamma'[\tilde{\rho}^{-}(r,\tfrac{1}{r})-\tilde{\rho}^{-}(r,-\infty)] \qquad (12b)$$

$$\frac{\left[\frac{1}{r}-\lambda\right]}{F(\mu,\lambda;r)}\frac{\partial^{2}\tilde{\rho}^{+}(r,\lambda)}{\partial r\partial\lambda}+\left[\frac{\Gamma'\mathcal{F}(r,\lambda)}{F(\mu,\lambda;r)}-\frac{\left[\frac{1}{r}-\lambda\right]F'(\mu,\lambda;r)}{(F(\mu,\lambda,;r))^{2}}\right]\frac{\partial\tilde{\rho}^{+}(r,\lambda)}{\partial\lambda}$$

$$=\Gamma'[\tilde{\rho}^{+}(r,\tfrac{1}{r})-\tilde{\rho}^{+}(r,-\infty)] \qquad (12c)$$

$$-\frac{\left[\frac{1}{r}-\lambda\right]}{F(\mu,\lambda;r)}\frac{\partial^{2}\tilde{\rho}^{-}(r,\lambda)}{\partial r\partial\lambda}+\left[\frac{\frac{1}{r}\left|\frac{1}{r}-2\lambda\right|}{F(\mu,\lambda;r)}+\frac{\left[\frac{1}{r}-\lambda\right]F'(\mu,\lambda;r)}{(F(\mu,\lambda,;r))^{2}}+\frac{\Gamma'\mathcal{F}(r,\lambda)}{F(\mu,\lambda;r)}\right]\frac{\partial\tilde{\rho}^{-}(r,\lambda)}{\partial\lambda}$$

$$- \frac{\frac{1}{r}\left|\frac{1}{r} - 2\lambda\right|}{F(\mu,\lambda;r)} \frac{\partial\tilde{\rho}^{+}(r,\lambda)}{\partial\lambda} = \Gamma'[\tilde{\rho}^{-}(r,\tfrac{1}{r}) - \tilde{\rho}^{-}(r,-\omega)] \qquad (12d)$$

with the boundary conditions at the turning point ($\lambda = 1/r$) and in the continuum ($\lambda \to -\omega$) incorporated into the RHS of (12). Equations (12a,b) are valid only in region I, while (12c,d) are valid only in region II. Note that primes on $F(\mu,\lambda;r)$ in (12) denote differentiation w.r.t. r, and that $F(\mu,\lambda;r) = F(\lambda,\mu;r)$.

To convert (8) into an analogous set of coupled integral equations, define the functions $\bar{\rho}^{\pm}(r,\lambda)$ by,

$$\rho^{\pm}(r,\lambda) = \int_0^r \bar{\rho}^{\pm}(r',\lambda)dr' \qquad (13)$$

yielding,

$$\left(\frac{1}{r} - \lambda\right)[\bar{\rho}^{+}(r,\lambda) - \bar{\rho}^{+}(o,\lambda)] + \frac{1}{r}\left(\frac{1}{r} - 2\lambda\right)\int_0^r [\bar{\rho}^{+}(r',\lambda) - \bar{\rho}^{-}(r',\lambda)]dr'$$

$$= \Gamma' \int_{-\infty}^{1/r} d\mu\, F(\lambda,\mu;r) \int_0^r \bar{\rho}^{+}(r',\mu)dr' - \Gamma'\,\mathcal{F}(r,\lambda) \int_0^r \bar{\rho}^{+}(r',\lambda)dr' \qquad (13a)$$

$$-\left(\frac{1}{r} - \lambda\right)[\bar{\rho}^{-}(r,\lambda) - \bar{\rho}^{-}(o,\lambda)] = \Gamma' \int_{-\infty}^{1/r} d\mu F(\lambda,\mu;r) \int_0^r \bar{\rho}^{-}(r',\mu)dr'$$

$$- \Gamma'\mathcal{F}(r,\lambda)\int_0^r \bar{\rho}^{-}(r',\lambda)dr' \qquad (13b)$$

$$\left(\frac{1}{r} - \lambda\right)[\bar{\rho}^{+}(r,\lambda) - \bar{\rho}^{+}(o,\lambda)] = \Gamma' \int_{-\infty}^{1/r} d\mu\, F(\lambda,\mu;r) \int_0^r \bar{\rho}^{+}(r',\mu)dr'$$

$$- \Gamma'\,\mathcal{F}(r,\lambda) \int_0^r \bar{\rho}^{+}(r',\lambda)dr' \qquad (13c)$$

$$-\left(\frac{1}{r}-\lambda\right)\left[\bar{\rho}^{-}(r,\lambda)-\bar{\rho}^{-}(o,\lambda)\right]-\frac{1}{r}\left|\frac{1}{r}-2\lambda\right|\int_{o}^{r}\left[\bar{\rho}^{+}(r',\lambda)-\bar{\rho}^{-}(r',\lambda)\right]dr'$$

$$=\Gamma'\int_{-\omega}^{1/r}d\mu\ F(\lambda,\mu;r)\int_{o}^{r}\bar{\rho}^{-}(r',\mu)dr'-\Gamma'\,\mathcal{F}(r,\lambda)\int_{o}^{r}\bar{\rho}^{-}(r',\lambda)dr' \quad (13d)$$

Rearranging terms in (13) to show the couplings present between the integral equations gives,

$$\left(\frac{1}{r}-\lambda\right)\bar{\rho}^{+}(r,\lambda)+\left[\frac{1}{r}\left(\frac{1}{r}-2\lambda\right)+\Gamma'\,\mathcal{F}(r,\lambda)\right]\int_{o}^{r}\bar{\rho}^{+}(r',\lambda)dr'$$

$$-\Gamma'\int_{-\omega}^{1/r}d\mu\ F(\lambda,\mu;r)\int_{o}^{r}\bar{\rho}^{+}(r',\mu)dr'-\frac{1}{r}\left(\frac{1}{r}-2\lambda\right)\int_{o}^{r}\bar{\rho}^{-}(r',\lambda)dr'$$

$$=\left(\frac{1}{r}-\lambda\right)\bar{\rho}^{+}(o,\lambda) \quad (14a)$$

$$-\left(\frac{1}{r}-\lambda\right)\bar{\rho}^{-}(r,\lambda)+\Gamma'\,\mathcal{F}(r,\lambda)\int_{o}^{r}\bar{\rho}^{-}(r',\lambda)dr'$$

$$-\Gamma'\int_{-\omega}^{1/r}d\mu\ F(\lambda,\mu;r)\int_{o}^{r}\bar{\rho}^{-}(r',\mu)dr'=-\left(\frac{1}{r}-\lambda\right)\bar{\rho}^{-}(o,\lambda) \quad (14b)$$

$$\left(\frac{1}{r}-\lambda\right)\bar{\rho}^{+}(r,\lambda)+\Gamma'\,\mathcal{F}(r,\lambda)\int_{o}^{r}\bar{\rho}^{+}(r',\lambda)dr'$$

$$-\Gamma'\int_{-\omega}^{1/r}d\mu\ F(\lambda,\mu;r)\int_{o}^{r}\bar{\rho}^{+}(r',\mu)dr'=\left(\frac{1}{r}-\lambda\right)\bar{\rho}^{+}(o,\lambda) \quad (14c)$$

$$-\left(\frac{1}{r}-\lambda\right)\bar{\rho}^{-}(r,\lambda)+\left[\frac{1}{r}\left|\frac{1}{r}-2\lambda\right|+\Gamma'\,\mathcal{F}(r,\lambda)\right]\int_{o}^{r}\bar{\rho}^{-}(r',\lambda)dr'$$

$$-\Gamma'\int_{-\omega}^{1/r}d\mu\ F(\lambda,\mu;r)\int_{o}^{r}\bar{\rho}^{-}(r',\mu)dr'-\frac{1}{r}\left|\frac{1}{r}-2\lambda\right|\int_{o}^{r}\bar{\rho}^{+}(r',\lambda)dr'$$

$$=-\left(\frac{1}{r}-\lambda\right)\bar{\rho}^{-}(o,\lambda) \quad (14d)$$

where the boundary condition at r = o has been incorporated into the RHS of (14). The three representations of the coupled Boltzmann equations (equations (8), (12) and (14)) all require the same number of quadratures to obtain a solution - namely two each for $\rho^{+}(r,\lambda)$ and $\rho^{-}(r,\lambda)$. However, our reason for giving the details of the transformation between representations (cf. equations (10), (13)) is to highlight the different types of boundary conditions required in each case. In the case of the PDE's (12), it is clear from (10) that the required boundary conditions on $\tilde{\rho}^{\pm}(r,\lambda)$ should be global in energy and local in r, while in the case of (14) the boundary conditions on $\bar{\rho}^{\pm}(r,\lambda)$ should be local in energy and global in r. We use the word global to indicate that the integrand of an integral w.r.t. the specified degree of freedom is required as a boundary condition. Otherwise it is called a local boundary condition (e.g., equation (9) is local in both r and λ). Therefore, from (10) and (13) it is clear that the boundary conditions for the PDE and IE representations are of a mixed nature, and will be difficult to implement numerically. It should be clear however that in all three cases (eqs. (8), (12) and (14)), after discretization, the basic problem numerically is the same - namely one of solving a set of simulataneous algebraic equations for the PIDE representation (8) (these are the practical equations mentioned earlier), and leave it to the reader to write down the corresponding sets of equations for the other representations (12), (14).

Numerical Solution of PIDE's

To convert the coupled PIDE's (8) into algebraic equations, four steps need to be taken:

(i) Replace all derivatives with finite differences. If the PIDE is part of an initial value problem, the choice of either forward or backward differences will depend on the boundary conditions.

(ii) Replace all integrals with quadrature sums. The choice of quadrature rule is crucial in determining the overall stability and convergence rate of the resulting algorithm. The type of quadrature rule chosen in turn depends on the global behavior of the

integrand over all of phase space. Hence, for a multidimensional kernal, this step can easily be the most time consuming one in preparing for the full solution.

(iii) Impose all boundary conditions on the algebraic equations resulting from steps (i) and (ii). Make sure that the boundary conditions used lead to a well-posed problem with a non-singular coefficient matrix.

(iv) Finally, choose a technique for solving the resultant set of algebraic equations which takes advantage as much as possible of the structure of the coefficient matrix. Compute the condition number of the coefficient matrix and determine whether the algebraic equations need preconditioning.

Therefore, discretizing $r \to r_i = \{o, r_1, r_2, \ldots, r_{max} \equiv r_{N_r}\}$ with $N_r + 1$ equally spaced points (step size h), and replacing integrals with quadrature sums (with weight functions ϕ_k) yields the following for (8),

$$T_{ij} \frac{[\rho^+_{i+1,j} - \rho^+_{i-1,j}]}{2h} + \mathcal{G}_{ij}(\rho^+_{ij} - \rho^-_{ij}) + \Gamma'_j \mathcal{F}_{ij}\rho^+_{ij} - \Gamma'_j \sum_k \phi_k F_{jki}\rho^+_{ik} = 0 \tag{15a}$$

$$-T_{ij} \frac{[\rho^-_{i+1,j} - \rho^-_{i-1,j}]}{2h} + \Gamma'_j \mathcal{F}_{ij}\rho^-_{ij} - \Gamma'_j \sum_k \phi_k F_{jki}\rho^-_{ik} = 0 \tag{15b}$$

$$T_{ij} \frac{[\rho^+_{i+1,j} - \rho^+_{i-1,j}]}{2h} + \Gamma'_j \mathcal{F}_{ij}\rho^+_{ij} - \Gamma'_j \sum_k \phi_k F_{jki}\rho^+_{ik} = 0 \tag{15c}$$

$$-T_{ij} \frac{[\rho^-_{i+1,j} - \rho^-_{i-1,j}]}{2h} - |\mathcal{G}_{ij}|(\rho^+_{ij} - \rho^-_{ij}) + \Gamma' \mathcal{F}_{ij}\rho^-_{ij} - \Gamma'_j \sum_k \phi_k F_{jki}\rho^-_{ik} = 0 \tag{15d}$$

where $\Gamma_j \equiv \Gamma e^{-\lambda_j}$, $F_{jki} = F(\lambda_j, \mu_k; r_i)$, $\mathcal{F}_{ij} = \mathcal{F}(r_i, \lambda_j)$, $\mathcal{G}_{ij} = \frac{1}{r_i}\left(\frac{1}{r_i} - 2\lambda_j\right)$,

$|\mathcal{G}_{ij}| = \frac{1}{r_i}\left|\frac{1}{r_i} - 2\lambda_j\right|$, $T_{ij} = \frac{1}{r_i} - \lambda_j$ and $\rho^{\pm}_{ij}$ denotes $\rho^{\pm}(r_i,\lambda_j)$.

It will prove convenient to rearrange equations (15) into the order (15a,c), followed by (15b,d), so that the resultant coefficient matrix is positive definite (Golub and van Loan [30]). Then applying the boundary conditions on r yields,

$$-(1-\delta_{io})T_{ij_1}\rho^{+}_{i-1,j_1} - 2h\sum_{k_1}\left[\Gamma'_{j_1}\phi_{k_1}F_{j_1k_1i} - \delta_{k_1j_1}(\mathcal{G}_{ij_1} + \Gamma'_{j_1}\mathcal{F}_{ij_1})\right]\rho^{+}_{ik_1}$$

$$- 2h\,\Gamma'_{j_1}\sum_{k_2}\phi_{k_2}F_{j_1k_2i}\,\rho^{+}_{ik_2} - 2h\,\mathcal{G}_{ij_1}\,\rho^{-}_{ij_1} + (1-\delta_{N_r})\rho^{+}_{i+1,j_1}$$

$$= \delta_{io}\rho^{+}(r=o,\lambda_{j_1}) + \delta_{iN_r}\rho^{+}(r_{max},\lambda_{j_1}) \qquad (16a)$$

$$-(1-\delta_{io})T_{ij_2}\rho^{+}_{i-1,j_2} - 2h\,\Gamma'_{j_2}\sum_{k_1}\phi_{k_1}F_{j_2k_1i}\,\rho^{+}_{ik_1}$$

$$- 2h\sum_{k_2}\left[\Gamma'_{j_2}\phi_{k_2}F_{j_2k_2i} - \delta_{k_2j_2}\,\Gamma'_{j_2}\mathcal{F}_{ij_2}\right]\rho^{+}_{ik_2} + (1-\delta_{iN_r})\rho^{+}_{i+1,j_2}$$

$$= \delta_{io}\rho^{+}(r=o,\lambda_{j_2}) + \delta_{iN_r}\rho^{+}(r_{max},\lambda_{j_2}) \qquad (16b)$$

$$(1-\delta_{io})T_{ij_1}\rho^{-}_{i-1,j_1} - 2h\sum_{k_1}\left[\Gamma'_{j_1}\phi_{k_1}F_{j_1k_1i} - \delta_{k_1j_1}\,\Gamma'_{j_1}\mathcal{F}_{ij_1}\right]\rho^{-}_{ik_1}$$

$$- 2h\,\Gamma'_{j_1}\sum_{k_2}\phi_{k_2}F_{j_1k_2i}\,\rho^{-}_{ik_2} - (1-\delta_{N_r})\rho^{-}_{i+1,j_1}$$

$$= \delta_{io}\rho^{-}(r=o,\lambda_{j_1}) + \delta_{iN_r}\rho^{-}(r_{max},\lambda_{j_1}) \qquad (16c)$$

$$(1-\delta_{io})T_{ij_2}\rho^{-}_{ij_2} - 2h\,|\mathcal{G}_{ij_2}|\rho^{+}_{ij_2} - 2h\,\Gamma'_{j_2}\sum_{k_1}\phi_{k_1}F_{j_2k_1i}\,\rho^{-}_{ik_1}$$

$$- 2h\sum_{k_2}\left[\Gamma'_{j_2}\phi_{k_2}F_{j_2k_2i} - \delta_{k_2j_2}(|\mathcal{G}_{ij_2}| + \Gamma'_{j_2}\mathcal{F}_{ij_2})\right]\rho^{-}_{ik_2} - (1-\delta_{iN_r})\rho^{-}_{i+1j_2}$$

$$= \delta_{io}\rho^{-}(r=o,\lambda_{j_2}) + \delta_{iN_r}\rho^{-}(r_{max},\lambda_{j_2}) \qquad (16d)$$

and where the indices are defined: $1 \le i \le N_r-1$, $-N_c \le j_1 \le N_{b_1}$, $N_{b_1} \le j_2 \le N_{b_2}$ and $-N_c \le k_1 \le N_{b_1}$, $N_{b_1} \le k_2 \le N_{b_2}$. The energy range $[-\infty, \frac{1}{r}]$ has been discretized into three grids: $[-\lambda_{max},o]$, $[o, \frac{1}{2r_i}]$, $[\frac{1}{2r_i}, \frac{1}{r_i}]$ composed of $N_c + 1$, $N_{b_1} + 1$ and $N_{b_2} - N_{b_1}$ points, respectively. The total number of points in the energy grid is $N_c + N_{b_2}$. Hence the subscripts j_1, k_1 indicate that the energy is restricted to region I: $[-\lambda_{max}, \frac{1}{2r_i}]$, while j_2, k_2 indicate that the energy is restricted to region II: $[\frac{1}{2r_i}, \frac{1}{r_i}]$. The parameter λ_{max} represents the largest free ion energy considered. More details on the energy grid are given below.

Now, before applying the boundary conditions on λ (equations 9a,d)), a word is needed on continuity conditions. In equation (8) the λ,r phase space is divided into 2 regions. Since we assume that the unknowns $\rho^{\pm}(r,\lambda)$ are smooth functions of λ and r, we must insure that the computed solutions of (16) are continuous across the boundary between regions I and II. We do this by recognizing that (16a,b) are 2 equations for the *same* unknown when $j_1 = j_2 = N_{b_1}$. Therefore, we can add the two equations together and divide by 2. This insures that we will not have an overdetermined system of equations. In the case where j_1 and j_2 don't equal N_{b_1}, the appropriate terms from the k_1 and k_2 summations (i.e., the

last in k_1 and the first in k_2) must be added together in (16a,b). These two steps will insure that $\rho^+(r,\lambda)$ is continuous at $\lambda = 1/2r$. Analogous additions in equations (16c,d) will likewise insure that $\rho^-(r,\lambda)$ will be continuous at $\lambda = 1/2r$. Therefore, applying the steps above to insure continuity in the solution, and the boundary conditions on λ yields the following set of practical algebraic equations,

$$-(1-\delta_{io})T_{ij_1}\rho^+_{i-1,j_1} - \sum_{k_1}{}' \mathcal{A}^{(i)+}_{j_1k_1}\rho^+_{ik_1} - \mathcal{C}^{(i)+}_{j_1N_{b_1}}\rho^+_{iN_{b_1}} - \sum_{k_2}{}' \mathcal{A}^{(i)+}_{j_1k_2}\rho^+_{ik_2}$$

$$- 2h\,\mathcal{E}_{ij_1}\rho^-_{ij_1} + (1-\delta_{iN_r})\rho^+_{i+1,j_1} = \mathcal{B}^{(i)+}_{j_1} \qquad (17a)$$

$$-(1-\delta_{io})T_{ij_2}\rho^+_{i-1,j_2} - \sum_{k_1}{}' \mathcal{A}^{(i)+}_{j_2k_1}\rho^+_{ik_1} - \mathcal{C}^{(i)+}_{j_2N_{b_1}}\rho^+_{iN_{b_1}} - \sum_{k_2}{}' \mathcal{A}^{(i)+}_{j_2k_2}\rho^+_{ik_2}$$

$$+ (1-\delta_{iN_r})\rho^+_{i+1,j_2} = \mathcal{B}^{(i)+}_{j_2} \qquad (17b)$$

$$(1-\delta_{io})T_{ij_1}\rho^-_{i-1,j_1} - \sum_{k_1}{}' \mathcal{A}^{(i)-}_{j_1k_1}\rho^-_{ik_1} - \mathcal{C}^{(i)-}_{j_1N_{b_1}}\rho^-_{iN_{b_1}} - \sum_{k_2}{}' \mathcal{A}^{(i)-}_{j_1k_2}\rho^-_{ik_2}$$

$$- (1-\delta_{iN_r})\rho^-_{i+1,j_1} = \mathcal{B}^{(i)-}_{j_1} \qquad (17c)$$

$$(1-\delta_{io})T_{ij_2}\rho^-_{i-1,j_2} - 2h\,|\mathcal{E}_{ij_2}|\,\rho^+_{ij_2} - \sum_{k_1}{}' \mathcal{A}^{(i)-}_{j_2k_1}\rho^-_{ik_1} - \mathcal{C}^{(i)-}_{j_2N_{b_1}}\rho^-_{iN_{b_1}}$$

$$- \sum_{k_2}{}' \mathcal{A}^{(i)-}_{j_2k_2}\rho^-_{ik_2} - (1-\delta_{iN_r})\rho^-_{i+1,j_2} = \mathcal{B}^{(i)-}_{j_2} \qquad (17d)$$

where the coefficient matrix $\mathcal{A}$ and column vector $\mathcal{B}$ are defined as,

$$\mathcal{A}^{(i)+}_{j_1k_1} = 2h\left[\Gamma'_{j_1}\,\phi_{k_1}\,F_{j_1k_1i} - \delta_{k_1j_1}(\mathcal{G}_{ij_1} + \Gamma'_{j_1}\,\mathcal{F}_{ij_1})\right] \tag{18a}$$

$$\mathcal{A}^{(i)+}_{j_1k_2} = 2h\,\Gamma'_{j_1}\,\phi_{k_2}\,F_{j_1k_2i} \tag{18b}$$

$$\mathcal{A}^{(i)+}_{j_2k_1} = 2h\,\Gamma'_{j_2}\,\phi_{k_1}\,F_{j_2k_1i} \tag{18c}$$

$$\mathcal{A}^{(i)+}_{j_2k_2} = 2h\left[\Gamma'_{j_2}\,\phi_{k_2}\,F_{j_2k_2i} - \delta_{k_2j_2}\,\Gamma'_{j_2}\,\mathcal{F}_{ij_2}\right] \tag{18d}$$

$$\mathcal{A}^{(i)-}_{j_1k_1} = 2h\left[\Gamma'_{j_1}\,\phi_{k_1}\,F_{j_1k_1i} - \delta_{k_1j_1}\,\Gamma'_{j_1}\,\mathcal{F}_{ij_1}\right] \tag{18e}$$

$$\mathcal{A}^{(i)-}_{j_1k_2} = 2h\,\Gamma'_{j_1}\,\phi_{k_2}\,F_{j_1k_2i} \tag{18f}$$

$$\mathcal{A}^{(i)-}_{j_2k_1} = 2h\,\Gamma'_{j_2}\,\phi_{k_1}\,F_{j_2k_1i} \tag{18g}$$

$$\mathcal{A}^{(i)-}_{j_2k_2} = 2h\left[\Gamma'_{j_2}\,\phi_{k_2}\,F_{j_2k_2i} - \delta_{k_2j_2}(|\mathcal{G}_{ij_2}| + \Gamma'_{j_2}\,\mathcal{F}_{ij_2})\right] \tag{18h}$$

and,

$$\mathcal{B}^{(i)+}_{j_1} = \delta_{io}\rho^{+}(r=o,\lambda_{j_1}) + \delta_{iN_r}\rho^{+}(r_{max},\lambda_{j_1}) + \delta_{N_{b_2}k_2}\,2h\Gamma'_{j_1}\phi_{N_{b_1}}F_{j_1N_{b_2}i}\rho^{+}_{iN_{b_2}}$$

$$+ \delta_{k_1-N_c}\rho^{+}_{i,-N_c}\,2h\left[\Gamma'_{j_1}\,\phi_{-N_c}\,F_{j_1-N_ci} - \delta_{-N_cj_1}(\mathcal{G}_{ij_1} + \Gamma'_{j_1}\,\mathcal{F}_{ij_1})\right] \tag{19a}$$

$$\mathcal{B}^{(i)+}_{j_2} = \delta_{io}\rho^{+}(r=o,\lambda_{j_2}) + \delta_{iN_r}\rho^{+}(r_{max},\lambda_{j_2}) + \delta_{k_1-N_c}\,2h\Gamma'_{j_2}\phi_{-N_c}F_{j_2-N_ci}\rho^{+}_{i-N_c}$$

$$+ \delta_{k_2N_{b_2}}\rho^{+}_{iN_{b_2}}\left[2h\,\Gamma'_{j_2}\,\phi_{N_{b_2}}F_{j_2N_{b_2}i} - \delta_{k_2j_2}\,\Gamma'_{j_2}\,\mathcal{F}_{ij_2}\right] \tag{19b}$$

$$\mathcal{B}^{(i)-}_{j_1} = \delta_{io}\rho^{-}(\underline{r}=o,\lambda_{j_1}) + \delta_{iN_r}\rho^{-}(r_{max},\lambda_{j_1}) + \delta_{N_{b_2}k_2}\, 2h\Gamma'_{j_1}\phi_{N_{b_2}}F_{j_1N_{b_2}i}\rho^{-}_{iN_{b_2}}$$

$$+ \delta_{k_1-N_c}\rho^{-}_{i,-N_c}\, 2h\left[\Gamma'_{j_1}\,\phi_{-N_c}\,F_{j_1-N_c i} - \delta_{k_1j_1}\,\Gamma'_{j_1}\,\mathcal{F}_{ij_1}\right] \tag{19c}$$

$$\mathcal{B}^{(i)-}_{j_2} = \delta_{io}\rho^{-}(r=o,\lambda_{j_2}) + \delta_{iN_r}\rho^{-}(r_{max},\lambda_{j_2}) + \delta_{k_1-N_c}\, 2h\Gamma'_{j_2}\phi_{-N_c}F_{j_2-N_c i}\rho^{-}_{i,-N_c}$$

$$+ \delta_{j_2N_{b_2}}\, 2h|\mathcal{G}_{ij_2}|(\rho^{+}_{i,N_{b_2}} - \rho^{-}_{i,N_{b_2}})$$

$$+ \delta_{k_2N_{b_2}}\, 2h\left[\Gamma'_{j_2}\,\phi_{N_{b_2}}\,F_{j_2N_{b_2}i} - \delta_{k_2j_2}\,\Gamma'_{j_2}\,\mathcal{F}_{ij_2}\right]\rho^{-}_{iN_{b_2}} \tag{19d}$$

The elements of the coefficient matrix $\mathcal{A}$ which govern the continuity of the solutions $\rho^{\pm}$ at the boundary between regions I and II are denoted by $\mathcal{C}$ in (17) and are defined,

$$\mathcal{C}^{(i)+}_{j_1N_{b_1}} = 4h\,\Gamma'_{j_1}\phi_{N_{b_1}}F_{j_1N_{b_1}i} - \delta_{j_1N_{b_1}}\,2h\,\Gamma'_{j_1}\mathcal{F}_{ij_1} \tag{20a}$$

$$\mathcal{C}^{(i)+}_{j_2N_{b_1}} = 4h\,\Gamma'_{j_2}\phi_{N_{b_1}}F_{j_2N_{b_1}i} \tag{20b}$$

$$\mathcal{C}^{(i)-}_{j_1N_{b_1}} = 4h\,\Gamma'_{j_1}\phi_{N_{b_1}}F_{j_1N_{b_1}i} - \delta_{j_1N_{b_1}}\,2h\,\Gamma'_{j_1}\mathcal{F}_{ij_1} \tag{20c}$$

$$\mathcal{C}^{(i)-}_{j_2N_{b_1}} = 4h\,\Gamma'_{j_2}\phi_{N_{b_1}}F_{j_2N_{b_1}i} \tag{20d}$$

The index i in (17) is defined as before, while in (17a,c) j_1 is defined: $-N_c+1 \le j_1 \le N_{b_1}$, and in (17b,d) j_2 is defined: $N_{b_1}+1 \le j_2 \le N_{b_2}-1$. The primes on the k_1 and k_2 summations in (17) denote that the λ boundary terms are omitted (i.e., $k_1 = -N_c$ and $k_2 = N_{b_2}$). The primes also

indicate that the terms with $k_1 = N_{b_1}$ and $k_2 = N_{b_2}$ have been factored-out of the summation (and are represented by the $\mathcal{C}$ terms).

The algebraic equations (17) can be written in the familiar matrix notation,

$$\mathcal{A}\,\rho = \mathcal{B} \tag{21}$$

where $\mathcal{A}$ and $\mathcal{B}$ are given by (18,19), respectively, and ρ is the unknown column vector composed of the discretized elements of ρ^+ first, then ρ^-. The known column vector $\mathcal{B}$, composed of boundary conditions on $\rho^{\pm}$, has been written in full detail in (19) in order to show exactly how each boundary condition contributes to the problem. In practice, after application of (9), (19) will simplify considerably. From (18) it is clear that the coefficient matrix $\mathcal{A}$ is non-symmetric due to the presence of the $\mathcal{G}_{ij}$ and $|\mathcal{G}_{ij}|$ terms. The overall structure of the coefficient matrix is shown in figure 2.

The energy grid chosen was nonlinear due to the skew discontinuity present in the kernals $F(\lambda,\mu;r)$ (Flannery [22,23]). In particular, we use the 3tan(u) prescription of Bates and Mendaš [8] for the pivot points used in the Simpson's rule quadratures in (17). That is, the weights and pivots used in the energy quadratures are defined for the three grids as,

$$\lambda_k = 3\tan(k\xi), \qquad \phi_k = r_k\,\xi\,\sec^2(k\xi)$$

with,

(i) continuum part of region I: $-\lambda_{max} \le \lambda \le 0 \qquad -N_c \le k \le 0$

$$\xi = \tan^{-1}(\lambda_{max}/3)/N_c$$

$$r_k = \begin{cases} 1 & , k = -N_c,\ 0 \\ 4 & , k = \text{even integer in } (-N_c,0) \\ 2 & , k = \text{odd integer in } (-N_c,0) \end{cases}$$

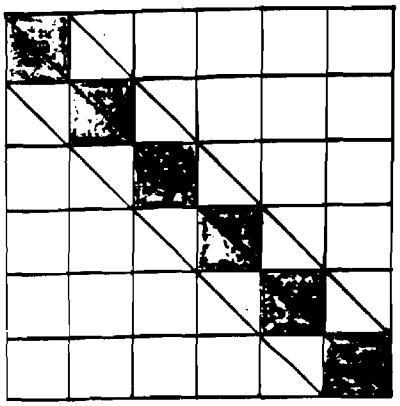

a.

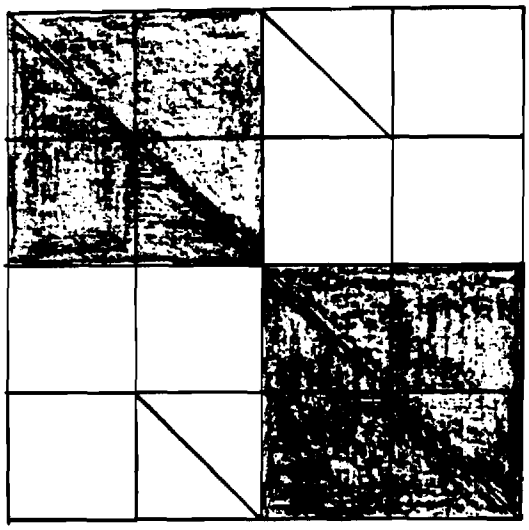

b

Figure 2: Structure of coefficient matrix $\mathcal{A}$ in equation (21). a) block tri-diagonal in r, b) non-symmetric, positive-definite in λ.

(ii) bound state part of region I: $0 \leq \lambda \leq \frac{1}{2r_i}$ $\quad 0 \leq k \leq N_{b_1}$

$$\xi = \tan^{-1}(1/6r_i)/N_{b_1}$$

$$r_k = \begin{cases} 1 & , k = 0, N_{b_1} \\ 4 & , k = \text{even integer in } (0,N_{b_1}) \\ 2 & , k = \text{odd integer in } (0,N_{b_1}) \end{cases}$$

and,

(iii) region II: $\frac{1}{2r_i} \le \lambda \le \frac{1}{r_i}$ $\quad N_{b_1} \le k \le N_{b_2}$

$$\lambda_k = 3\tan[\xi_{min} + (k-N_{b_1})\xi] \qquad \phi_k = r_k\, \xi\, \sec^2[\xi_{min} + (k-N_{b_1})\xi]$$

$$\xi_{min} = \tan^{-1}(1/6r_i) \qquad \xi = [\tan^{-1}(1/3r_i) - \tan^{-1}(1/6r_i)]/(N_{b_2}-N_{b_1})$$

$$r_k = \begin{cases} 1 & , k = N_{b_1}, N_{b_2} \\ 4 & , k = \text{even integer in } (N_{b_1}, N_{b_2}) \\ 2 & , k = \text{odd integer in } (N_{b_1}, N_{b_2}) \end{cases}$$

Denoting the total number of points in the energy quadrature by $N_\lambda \equiv N_c + N_{b_2} - 2$, and the total number of simultaneous equations in (21) by $N \equiv (N_r-1)\, 2\, N_\lambda = 2(N_r-1)(N_c+N_{b_2}-2)$. A typical value for N is 20,988 for $N_r = 100$, $N_c = 36$ and $N_{b_2} = 72$. Hence, due to the very large sparse nature of the coefficient matrix $\mathcal{A}$, the use of direct techniques like Gaussian elimination to solve (21) will be totally out of the question because of the time and memory requirements involved. Therefore iterative techniques like Lanczos algorithms (Cullum and Willoughby [15], Golub and van Loan [30], accelerated successive overrelaxation methods (Young [42], Hageman and Young [32]) and Tchebychev iteration (Manteuffel [36,37]) should be used to solve (21).

Consequently, before continuing our discussion of the solution of (21), we will review some of the iterative techniques used to deal with large linear systems. For readers interested in a complete treatment consult the books listed in section IV - especially those by Young and Hageman and Young.

Iterative Methods for Large Linear Systems

Solve the matrix equation Ax = B where A is an N x N real, symmetric positive definite matrix, and x, B are column vectors of length N. Decompose A into three parts: a) it's diagonal elements (D), (b) all elements below the diagonal (C_L) and (c) all elements above the diagonal

(C_u). That is, we can write $A = D - C_L - C_u$. Now, scale the problem so the diagonal elements of the new coefficient matrix are 1. This can be done by multiplying by $D^{1/2}$,

$$(D^{-1/2} A D^{-1/2})(D^{1/2} x) = D^{-1/2} b \tag{22}$$

$$\rightarrow D^{-1/2}(D - C_L - C_u)D^{-1/2} = D^{-1/2} D D^{-1/2} - D^{-1/2}C_L D^{-1/2} - D^{-1/2} C_u D^{-1/2}$$

$$= I - L - L^t \tag{23}$$
$$\equiv I - B$$

where I is the identity matrix and $L \equiv D^{-1/2} C_L D^{-1/2}$, $B \equiv L + L^t$. Then, from (22), defining the column vectors $u \equiv D^{1/2} x$, $c \equiv D^{-1/2} b$ allows the original problem to be case into the suggestive form,

$$u = B u + c \tag{24}$$

which is then solved iteratively.

Two of the most widely used iterative methods are the Jacobi method,

$$u^{(n+1)} = B u^{(n)} + c \tag{25a}$$

and the Gauss-Seidel method,

$$u^{(n+1)} = L u^{(n+1)} + L^t u^{(n)} + c$$
$$= \mathcal{L} u^{(n)} + k \tag{25b}$$

where $k = (I - L)^{-1} c$, $\mathcal{L} = (I-L)^{-1} L^t$ and in (25) $u^{(n)}$ denotes the nth iteration of u. More recently variants on the Gauss-Seidel method have been developed to speed the convergence of the iteration procedure. One of the variants is the successive overrelaxation method (SOR),

$$u^{(n+1)} = \omega\,(L\,u^{(n+1)} + L^t\,u^{(n)} + c) + (1-\omega)\,u^{(n)}$$
$$= \mathcal{L}_\omega\,u^{(n)} + k_\omega \qquad (25c)$$

with $\mathcal{L}_\omega = (I - \omega L)^{-1}\,(\omega L^t + (1-\omega)I)$, $k_\omega = \omega(I-\omega L)^{-1}\,c$. The parameter ω is known as the acceleration parameter. When $\omega = 1$ (25c) reduces to the Gauss-Siedel method (25b). A generalization of the SOR method involves 2 SOR sweeps for each iteration of u, and is called the symmetric successive overrelaxation method (SSOR),

$$u^{(n+1/2)} = \mathcal{L}_\omega\,u^{(n)} + k_\omega^{(for.)} \qquad (25d)$$

$$u^{(n+1)} = \mathcal{U}_\omega\,u^{(n+1/2)} + k_\omega^{(back.)} \qquad (25e)$$

where the operator $\mathcal{L}_\omega$ is defined above, and $\mathcal{U}_\omega = (I - \omega L^t)^{-1}(\omega L + (1-\omega)I)$ and $k_\omega^{(for.)} = \omega(I - \omega L)^{-1}\,c$, $k_\omega^{(back.)} = \omega(I - \omega L^t)^{-1}\,c$. Equations (25d,e) can be combined into one iteration step by defining the operator $\mathcal{S}_\omega = \mathcal{U}_\omega\,\mathcal{L}_\omega$,

$$u^{(n+1)} = \mathcal{S}_\omega\,u^{(n)} + k_\omega \qquad (25f)$$

where $k_\omega = \omega\,(2-\omega)(I-\omega L^t)^{-1}(I-\omega L)^{-1}\,c$.

In the SOR and SSOR methods one must choose an acceleration parameter ω which will be optimal for a given coefficient matrix A. Two widely used methods of acceleration are Chebyshev acceleration and conjugate gradient acceleration. Writing the basic iteration procedure (24) as $u^{(n+1)} = \mathcal{G}\,u^{(n)} + k$, Chebyskev acceleration is defined,

$$u^{(n+1)} = \rho_{n+1}[(\gamma\,\mathcal{G}\,u^{(n)} + k) + (1-\gamma)u^{(n)}] + (1-\rho_{n+1})u^{(n-1)} \qquad (26a)$$

where $\gamma = 2/[2-M(\mathcal{G})-m(\mathcal{G})]$ and,

$$\rho_{n+1} = \begin{cases} 1 & , n = s \\ (1 - \sigma^2/2)^{-1} & , n = s+1 \\ [1 - (\sigma/2)^2 \rho_n]^{-1} & , n \geq s+2 \end{cases}$$

with $\sigma = [M(\mathcal{G})-m(\mathcal{G})]/[2 - M(\mathcal{G})-m(\mathcal{G})]$, $M(\mathcal{G})$ = maximum eigenvalue of matrix $\mathcal{G}$, $m(\mathcal{G})$ = minimum eigenvalue of $\mathcal{G}$. The integer s is initially zero, then increased as the adaptive procedure proceeds (Grimes et al. [31]). That is, one can reassign the overrelaxation parameter ρ several times during the iteration process. A disadvantage of Chebyshev acceleration is that it requires estimates of the smallest and largest eigenvalues of $\mathcal{G}$ to be made.

Conjugate gradient acceleration is defined,

$$u^{(n+1)} = \rho_{n+1} (\gamma_{n+1} \delta^{(n)} + u^{(n)}) + (1 - \rho_{n+1})u^{(n-1)} \qquad (26b)$$

$$\delta^{(n+1)} = \rho_{n+1} (\gamma_{n+1} \mathcal{G} \delta^{(n)} + (1-\gamma_{n+1}) \delta^{(n)}) + (1 - \rho_{n+1})\delta^{(n-1)} \qquad (26c)$$

where $\delta^{(n)}$ is a pseudo-residual vector given by: $\delta^{(n)} = \mathcal{G} u^{(n)} + k - u^{(n)}$. The acceleration parameters ρ and γ are defined,

$$\rho_{n+1} = \begin{cases} 1 & , n = 0 \\ \dfrac{1}{1 - \left[\dfrac{\gamma_{n+1}}{\gamma_n \rho_n}\right] \dfrac{\delta^{(n)t} W^t W \delta^{(n)}}{\delta^{(n-1)t} W^t W \delta^{(n-1)}}} & , n \geq 1 \end{cases}$$

$$\gamma_{n+1} = \left[1 - \frac{\delta^{(n)t} W^t W \mathcal{G} \delta^{(n)}}{\delta^{(n)t} W^t W \delta^{(n)}}\right]^{-1}$$

where W is a nonsingular symmetrization matrix. For the Jacobi method $W = D^{1/2}$, while for the SSOR method $W = (1/\omega) D^{-1/2}(D - \omega C_L^t)$. While the

conjugate gradient acceleration method doesn't require estimation of the eigenvalues of $\mathcal{G}$, the number of arithmetic operations required for it's implementation is greater.

We have necessarily been selective and brief in our discussion of iterative methods due to the vastness of this area of linear algebra. The discussion of this subsection is based upon appendix A in the technical report of Grimes et al. [31]. Two excellent books which provide good introductions to this area are Young [42] and Hageman and Young [32] (others can be found in the list of general references in section IV). As for software which implements the iterative techniques discussed above (as well as others not discussed here), excellent packages are the ITPACK library (Grimes et al. [31]) and the package of Lanczos algorithms of Cullum and Willoughby [15].

So far we have only discussed iterative techniques for symmetric coefficient matrices $\mathcal{A}$. However, the central numerical problem of this lecture is to solve equation (21) for a large, sparse non-symmetric matrix $\mathcal{A}$. Unfortunately there is much less known in linear algebra about iterative techniques for non-symmetric matrices. One way to handle non-symmetric matrices $\mathcal{A}$ is to consider (instead of (21) for example) the associated equation $\mathcal{A}^t\mathcal{A}\rho = \mathcal{A}^t\mathcal{B}$, where $\mathcal{A}^t\mathcal{A}$ is a symmetric coefficient matrix. However, in many practical applications the condition number of $\mathcal{A}^t\mathcal{A}$ is much greater than that of $\mathcal{A}$ - thereby indicating that this technique will not necessarily yield a problem which will converge rapidly using one of the iterative techniques discussed above. Another way to deal with non-symmetric problems is to develop the appropriate generalizations of (25,26) directly (Young and Jea [43], Manteuffel [36,37]). However, these generalizations require knowledge of the eigenvalue spectrum of $\mathcal{G}$ which is difficult to obtain in practice. In summary then, while some progress has been made in linear algebra towards handling the non-symmetric case, much more work needs to be done in devising criteria by which one can select acceleration parameters which will be optimal for a given general coefficient matrix $\mathcal{G}$.

Returning now to our discussion of the numerical solution of (21) for non-symmetric $\mathcal{A}$, we will need to know the condition number $\kappa(\mathcal{A})$ for

the coefficient matrix $\mathcal{A}$ before using one of the iterative techniques above. The condition number of a matrix $\mathcal{A}$ is defined: $\kappa(\mathcal{A}) = ||\mathcal{A}|| \cdot ||\mathcal{A}^{-1}||$. Computing the condition number of the coefficient matrix in a given problem (e.g., equation (21)) is necessary because the iterative techniques discussed above (like SSOR) work best for well-conditioned matrices (i.e., those with small κ). Otherwise, the number of iterations required for convergence will increase greatly, and since κ provides a measure of the sensitivity of a given problem to round-off errors and perturbations, if κ is too large for a given $\mathcal{A}$, then iterative techniques will not work due to accumulation of round-off errors. Physically, the condition number of a matrix $\mathcal{A}$ provides a measure of the distance between $\mathcal{A}$ and the set of angular matrices. Hence, when $\kappa(\mathcal{A})$ is very large the matrix $\mathcal{A}$ is considered ill-conditioned, which means that the numerical solution u, of (24) say, will be very sensitive to round-off error which are unavoidably accumulated during the iteration process. More details about condition numbers in linear algebra can be found in Golub and van Loan [30].

Using the routine LFCRG in the IMSL library [33] to estimate the condition number $\kappa_1(\mathcal{A})$, via the algorithm of Cline et al. [14], of the coefficient matrix of equation (17) we find that $\kappa_1(\mathcal{A}) \simeq 4.20\ 10^{19}$. In contrast $\kappa_1(\mathcal{A}) = 1751.1$ for the coefficient matrix $\mathcal{A}$ resulting from the discretization of the quasi-equilibrium integral equation (29). This indicates that the condition number for the coefficient matrix of (17) needs to be reduced approximately 16 orders of magnitude before the iterative techniques (25,26) will become effective. This can be accomplished either by row scaling (Golob and van Loan [30]) or pre-conditioning (Faber and Manteuffel [17]) the coefficient matrix. Unfortunately, these calculations have not been completed at the time of writing but will be reported in a forthcoming paper (Flannery and Mansky [28]). Hence, it is still an open question whether the iterative techniques discussed above are effective in solving (17). However our discussion of the condition number $\kappa_1(\mathcal{A})$ of $\mathcal{A}$ given by (18) has revealed the underlying reason why the earlier work of [8], failed to converge quickly as a function of gas density N(Z). Also, by illustrating the structure of the coefficient matrix in figure 2 and equation (18), a

deeper insight into the role the gas density plays in the nonlinear pressure regime is obtained. In fact once the problem of the ill-condition of $\mathcal{A}$ is solved, a number of other problems in chemical physics should become ameniable to the iterative techniques discussed in this lecture including the prediction of microscopic three-body ion-neutral association rates (Bates and McKibben [7]), and the inclusion of non-thermal effects into ion-ion recombination (Bates et al. [6]).

Before ending section II we wish to discuss the numerical solution of integral equations briefly. This is necessary because much of the numerical analysis of PIDE's relies heavily upon the expertise gained in solving related one-dimensional integral equations. The IE we will use as an example will be the quasi-equilibrium integral equation arising in ion-ion recombination. We will necessarily be brief since the numerical analysis of integral equations (even one-dimensional ones) is a vast field and we only wish to highlight points about the numerical treatment of IE's which are related to our earlier discussion of PIDE's. For a complete discussion of the numerical treatment of IE's see Baker [2].

In discussing the quasi-equilibrium theory of ion-ion recombination it will prove useful to define the functions $\rho^S(r,\lambda)$ and $\rho^D(r,\lambda)$,

$$\rho^D(r,\lambda) = \frac{1}{2}\left[\rho^+(r,\lambda) - \rho^-(r,\lambda)\right] \tag{27a}$$

$$\rho^S(r,\lambda) = \frac{1}{2}\left[\rho^+(r,\lambda) - \rho^-(r,\lambda)\right] \tag{27b}$$

which describe physically the net and total numbers of ion pairs undergoing recombination at a given relative separation r and internal energy λ. Substituting (27) into (8) yields two coupled PIDE's valid for $-\infty < \lambda \leq \frac{1}{r}$,

$$\left(\frac{1}{r} - \lambda\right)\frac{\partial \rho^D(r,\lambda)}{\partial r} + \frac{1}{r}\left(\frac{1}{r} - 2\lambda\right)\rho^D(r,\lambda) = \Gamma' \int_{-\infty}^{1/r} \rho^S(r,\mu)F(\lambda,\mu,;r)d\mu - \Gamma' \mathcal{F}(r,\lambda)\rho^S(r,\lambda) \tag{28a}$$

$$\left(\frac{1}{r} - \lambda\right) \frac{\partial \rho^S(r,\lambda)}{\partial r} + \frac{1}{r}\left|\frac{1}{r} - 2\lambda\right|\rho^D(r,\lambda) = \Gamma' \int_{-\infty}^{1/r} \rho^D(r,\mu)F(\lambda,\mu,;r)d\mu$$

$$- \Gamma' \mathcal{F}(r,\lambda)\rho^D(r,\lambda) \qquad (28b)$$

In the quasi-equilibrium theory the motion of the center of mass of the ion pairs is taken to be in thermodynamic equilibrium with the third bodies, while a quasi-equilibrium distribution in highly excited internal energy states of the ion pairs is established effectively instantaneously due to collisions with the much more numerous third bodies. In the establishment of this distribution it is assumed that the distribution of separations of ion pairs does not effect the quasi-equilibrium distribution in internal energy. That is, the r dependence of the distributions $\rho^+(r,\lambda)$, $\rho^-(r,\lambda)$ is not influenced by the recombination proceeding in the plasma. Hence we can assume that the r-distributions of contracting and expanding ion pairs is in thermodynamic equilibrium, thereby implying that $\rho^D(r,\lambda) = 0$. This results in (28b) indicating that $\rho^S(r,\lambda)$ is a constant w.r.t. r. Multiplying (28a) by r^2 and integrating w.r.t. r yields the quasi-equilibrium integral equation for the distribution over internal energy states $\rho^S_{QE}(\lambda)$,

$$\int_{-\infty}^{\epsilon} F(\lambda,\mu)\rho^S_{QE}(\mu)d\mu = \rho^S_{QE}(\lambda) \int_{-\infty}^{\omega} F(\lambda,\mu)d\mu \qquad (29)$$

where ω is the maximum binding energy of an ion pair, and ϵ is the stabilization energy of an ion pair. We refer the reader to the original literature (Bates and Moffett [12], Bates and Flannery [5], Bates and Mendaš [11], and Flannery [22,23]) for the details.

Equation (29) is valid only in the low gas density limit where the flow of contracting and expanding ion pairs balance, at higher gas densities however a net contraction of ion pairs occurs so that the full PIDE (8) must be solved. We quote the expression for the recombination rate coefficient α for the low density limit from the original literature cited above,

$$\alpha/\alpha_T = \Gamma_o \int_{-\infty}^{\upsilon} d\lambda \int_{\upsilon}^{\omega} d\mu \; F(\lambda,\mu)[\rho_{QE}^S(\lambda) - \rho_{QE}^S(\mu)] \qquad (30)$$

where $\upsilon = -E/kT$ is an arbitrary energy level, and α_T is the Thomson rate coefficient (Thomson [40]). From (30) it is clear that once IE (29) is solved for the $\rho_{QE}^S(\lambda)$, a bi-cubic spline quadrature will yield α.

To solve the quasi-equilibrium integral equation (29) we impose the boundary conditions: $\rho_{QE}^S(\lambda \leq o) = 1$, $\rho_{QE}^S(\lambda \geq \epsilon) = 0$ yielding,

$$\int_o^{\epsilon} \rho_{QE}^S(\mu)\; F(\lambda,\mu)d\mu - \rho_{QE}^S(\lambda) \int_{-\infty}^{\upsilon} F(\lambda,\mu)d\mu = \int_{-\infty}^{o} F(\lambda,\mu)d\mu \qquad (31)$$

When (31) is discretized the result is a system of algebraic equations similar to (21) which can be solved either by iterative methods (SSOR) or direct techniques (Gaussian elimination), due to the much smaller size coefficient matrix $\mathcal{A}$ in the quasi-equilibrium case. As an example of the type of results obtained, we show in figures 3 and 4 the quasi-equilibrium distribution $\rho_{QE}^S(\lambda)$ and recombination rate α/α_T, respectively for the energy-transfer mechanisms of charge-transfer, hard-sphere and polarization collisions. We should also mention that, in addition to the smaller size, the quasi-equilibrium coefficient matrix is also symmetric - a fact which greatly helps in the numerical solution of (29). We have not discussed the numerical solution of the PIDE (28) in the same detail as that of (8), even though they are equivalent, because it results in a system of algebraic equations with a non-symmetric, nonpositive-definite coefficient matrix $\mathcal{A}$ - a problem much more difficult than (17). Finally, the quadrature rule used to determine the weights and pivots used in solving the quasi-equilibrium integral equation (31) were the same nonlinear Simpson's rule weights and pivots of Bates and Mendaš [8] discussed earlier. We conclude section II with a summary of the types of IE's found in the literature.

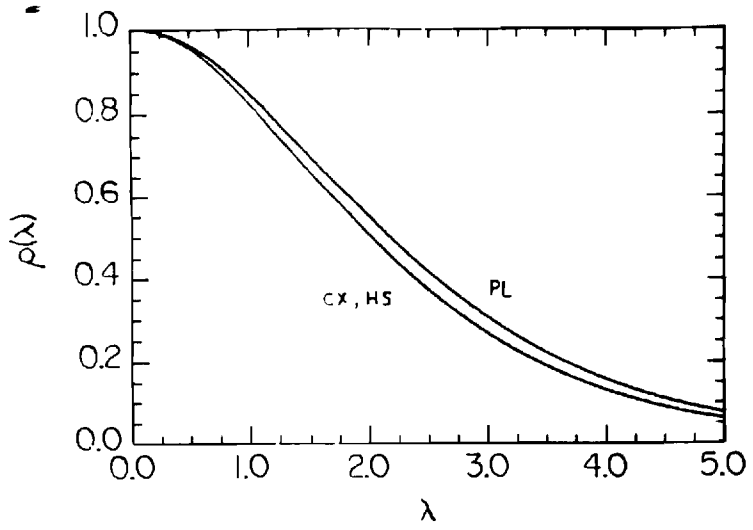

Figure 3: Quasi-equilibrium distribution function $\rho_{QE}(\lambda)$ for the case of a = 1/3 (m_1=m_2=m_3), and energy-change mechanisms of charge-transfer (CX), hard-sphere (HS) and polarization (PL) collisions.

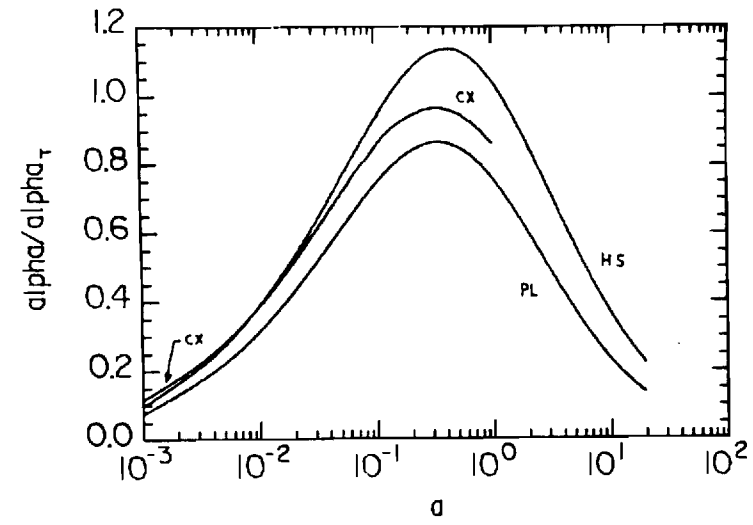

Figure 4: Quasi-Equilibrium recombination rate coefficient (α/α_T) versus mass ratio parameter (a) for energy-change mechanisms of charge-transfer (CX), hard-sphere (HS) and polarization (PL) collisions.

Numerical Solution of IE's

The three basic types of integral equations are Fredholm equations,

$$\int_a^b K(x,y)f(y)dy = g(x)f(x)$$

and Volterra equations of the first kind,

$$\int_o^t K(t,s)f(s)ds = g(t)$$

and second kind,

$$f(t) - \int_o^t K(t,s)f(s)ds = g(t)$$

where g is a known function, f is the unknown function and K is the kernal of the integral equation. We have already encountered Fredholm equations and Volterra equations of the 2nd-kind in (29) and (8), respectively. We will not encounter Volterra integral equations of the 1st-kind in this lecture. However, upon discretization, all three types of IE's above reduce to a problem of solving a system of linear algebraic equations. The particular technique used to solve the algebraic equations depends upon the structure of the coefficient matrix $\mathcal{A}$, which in turn depends on the behavior of the kernal K. Recalling our steps in the numerical solution of PIDE's, we find that steps (ii) - (iv) also provide a good prescription for the numerical solution of one-dimensional IE's. We have been brief in our summary of the numerical treatment of integral equations due again to the breadth of the area. For a complete introduction to the numerical solution of IE's see Baker [2] and Delves and Mohamed [16]. For an excellent account of Volterra equations see Linz [34].

III. Approximate Treatments of Ionic Recombination

As stated in the introduction, until the advent of super-computers, the direct solution of the PIDE's arising from the Boltzmann equation treatment of ionic recombination, was generally avoided due to the difficulty in solving systems of algebraic equations composed of 1000 or more equations and unknowns. The paper (Bates and Mendaš [9]) which originally derived the coupled PIDE's (8) solved them by a power series expansion in $\Lambda_{mfp.}$ which converged slowly with gas density and whose coefficients were difficult to compute in general. As discussed in section II, the slow convergence rate of the power series solution of (8) is directly related to the ill-conditioned nature of the coefficient matrix $\mathcal{A}$ in (21). Hence other methods of solving for the recombination rate α are needed. One such method which has proven quite successful is the Monte Carlo simulation of ion-ion recombination processes (Bates and Mendaš [10], and Morgan et al. [38]). We will not cover this type of calculation in this lecture since our main interest is in discussing techniques which lead to PDE's or PIDE's.

In this section we will discuss the Debye-Smoluchowski and diffusion equation approaches to ionic recombination. The starting point for the Debye-Smoluchowski equation is the macroscopic continuity equation for the number density of ion pairs, undergoing recombination of time t and separation R,

$$\frac{dn(\vec{R},t)}{dt} = \frac{\partial n(\vec{R},t)}{\partial t} + \vec{\nabla} \cdot \vec{J}(\vec{R},t) = 0 \qquad (32)$$

for $R \geq S \equiv$ sink radius, and is solved subject to the asymptotic boundary condition $n(R \to \infty,t) = \tilde{N}(X^+)\,\tilde{N}(Y^-)$ where $\tilde{N}$ is the equilibrium number density. The net current $\vec{J}(\vec{R},t)$ of ion pairs expanding at time t is,

$$\vec{J}(\vec{R},t) = -D\,\vec{\nabla}\,n(\vec{R},t) + (K/e)(\vec{\nabla}\,V)\,n(\vec{R},t) \qquad (33)$$

where V(R) is the interaction potential between X^+ and Y^-, and D, K are

the relative diffusion and mobility coefficients of X^+ and Y^- in a background gas Z. The introduction of a sink, with an assigned local three-body reaction rate α_3 at the surface, allows one to avoid dealing with the complicated collision kernels $F(\lambda,\mu;r)$ and full PIDE nature of (8) by replacing the problem with a phenomenological model. After substituting the current (33) into (32), and discretizing, the problem reduces to a boundary value problem involving a time-dependent diffusion equation in R. An example of the resultant solution is given in figure 5 which shows the time-dependent number density of ion pairs n(R,t) versus R for a specified sink radius. For further details on the Debye-Smoluchowski equation and ion-ion recombination see Flannery and Mansky [29].

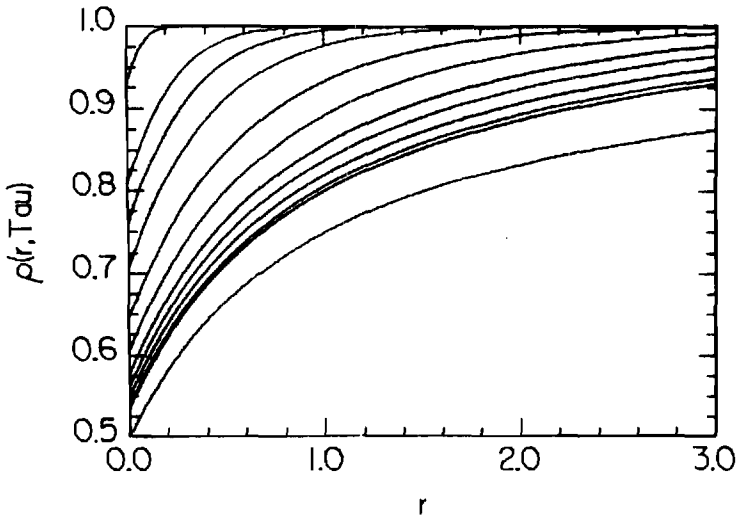

Figure 5: Solution of Debye-Smoluchowski equation for $\rho = n(r,\tau)/N_o \exp(-V/kT)$ $r \equiv R/S-1$, $\tau \equiv Dt/S^2$. τ ranges (from the top curve down) from 0.05, 0.5, 1, 2, 5, 10, 20, 30 to 100. The lowest curve is the steady state (equilibrium) distribution. Assigned parameters are S = 0.5, $\alpha_\infty/\alpha_{TR}$ = 0.5 (see [29] for details).

Diffusion equations in energy have also been used to model ionic recombination since the work of Pitaevskii [39]. In fact, the quasi-equilibrium theory of ion-ion recombination discussed in section II can be considered a Markov process (Flannery [19]). Writing the quasi-equilibrium integral equation (29) in terms of energies E, E_i (with the time-dependence reinserted - see Flannery [30], p. 17),

$$\frac{\partial n(E,t)}{\partial t} = N(Z) \int_{-E_s}^{\infty} n(E_i,t)\ K(E_i,E)dE_i - n(E,t) \int_{-D}^{\infty} K(E,E_i)dE_i \qquad (34)$$

Combining the integrals in (34) and Taylor series expanding the resultant integrand results in the Fokker-Planck equation,

$$\frac{\partial n(E,t)}{\partial t} = -\frac{\partial}{\partial E}\left[A_1 n(E,t)\right] + \frac{1}{2}\frac{\partial^2}{\partial E^2}\left[A_2\ n(E,t)\right] \qquad (35)$$

where,

$$A_n = N(Z) \int_{-D}^{\infty} (E_f - E_i)^n\ K(E,E_f)dE_f$$

and one assumes that the energy-transfer between the ion-pairs and third bodies is small so that the Taylor series expansion of (34) converges. This necessarily limits the diffusion model to electron-ion recombination processes. As an example of the type of results obtained by the energy space diffusion equation, we show in figure 6 the steady-state distribution $\rho(\lambda)$ obtained by Pitaevskii compared with the corresponding results of the quasi-equilibrium theory. While Pitaevskii's treatment only becomes accurate in the limit of electron-ion recombination, it's similarity with the quasi-equilibrium results in figure 6, for the case of equal mass constitutents, is striking. For a more complete discussion of energy space diffusional theories of termolecular recombination see Flannery [26].

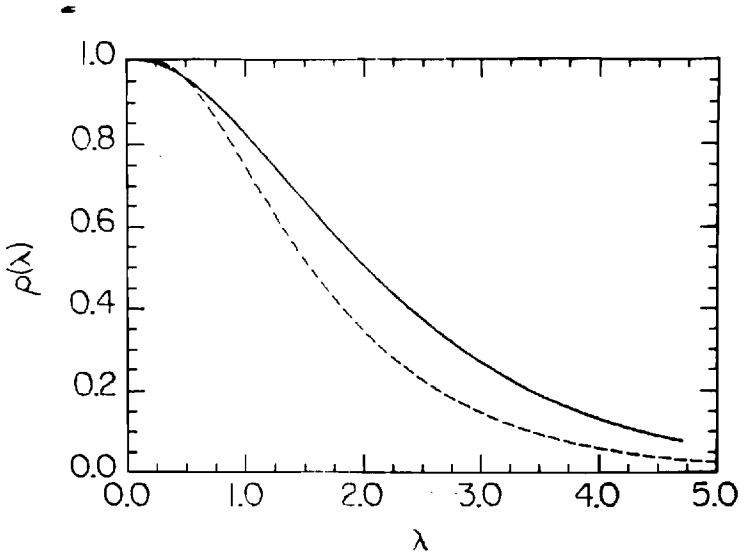

Figure 6: Comparison of quasi-equilibrium distribution (___) and Pitaevskii's distribution (---_ for the case of a = 1/3 and charge-transfer collisions.

IV. Conclusions and General References

In this lecture we have provided a detailed prescription for handling numerically the coupled partial integro-differential equations which arise from the Boltzmann equation treatment of ionic recombination. We have also given a brief summary of some of the approximate methods of treating ionic recombination. The reason for our detailed treatment of PIDE's is that there is little in either the physics or mathematics literature on how to tackle the problem of solving numerically a system of multi-dimensional PIDEs (i.e., systems with more than 1 independent variable). In this lecture we have tried to fill this gap.

Our main conclusion is that iterative techniques are numerically the most efficient way of solving the large systems of algebraic equations which result from PIDE's like (8). While this is not entirely unexpected, it is the first time techniques like the SSOR have been applied to problems in ionic recombination. With resolution of the problem of the ill-conditioning of $\mathcal{A}$ in (21), a number of long-standing

problems in chemical physics will be able to be solved. We end this lecture with a list of general references which we have found useful on the subject of solving numerically IE's and PIDE's.

- Baker, C. T. H., 1977, The Numerical Treatment of Integral Equations, Oxford University Press.
- Cullum, J. K., and Willoughby, R. A., 1985, Lanczos Algorithms for Large Symmetric Eigenvalue Computations, Vol. I, Theory, Vol. II, Programs, Birkhäuser (Boston).
- Delves, L. M. and Mohammed, J. L., 1985, Computational Methods for Integral Equations, Cambridge University Press.
- Feldstein, A., and Sopka, J. R., 1974, SIAM J. Numer. Analy. 11, 826-46.
- Golub, G. H., and van Loan, C. F., 1983, Matrix Computations, Johns Hopkins University Press.
- Hageman, L. A., and Young, D. M., 1981, Applied Iterative Methods, Academic Press.
- Linz, P., 1985, Analytical and Numerical Methods for Volterra Equations SIAM Press, (Philadelphia).
- Young, D. M., 1971, Iterative Solution of Large Linear Systems, Academic Press.
- Young, D. M., and Jea, K. C., 1980, Lin. Algebra Appl. 34, 159-94.
- Wilkinson, J., 1965, The Algebraic Eigenvalue Problem, Oxford Univ. Press.

Acknowledgements

This work is supported by AFOSR under grant No. 84-0233. The invitation to lecture, and the partial support received from Oak Ridge National Laboratory are also gratefully acknowledged.

References

1. Akhiezer, A. I., Akhiezer, I. A., Polovin, R. V., Sitenko, A. G., and Stepanov, K. N., 1975, Plasma Electrodynamics, Vol. 1, Linear Theory, Pergamon Press.
2. Baker, C. T. H., 1977, The Numerical Treatment of Integral Equations, Oxford University Press.

3. Balescu, R., 1963, Statistical Mechanics of Charged Particles, Interscience - Wiley.
4. ibid., 1975, Equilibrium and Nonequilibrium Statistical Mechanics, Wiley.
5. Bates, D. R., and Flannery, M. R., 1968, Proc. Roy. Soc. (Lon.) A 302, 367-83.
6. Bates, D. R., Hays, P. B., and Spevak, D., 1971, J. Phys. B: At. Mol. Phys. 4, 962-8.
7. Bates, D. R., and McKibbin, 1974, Proc. Roy. Soc. (Lon.) A 339, 13-28.
8. Bates, D. R., and Mendaš, I., 1975, J. Phys. B: At. Mol. Phys. 8, 1770-5.
9. ibid., 1978, Proc. Roy. Soc. (Lon.) A 359, 275-85.
10. ibid., 1978, Proc. Roy. Soc. (Lon.) A 359, 287-301.
11. ibid., 1982, J. Phys. B: At. Mol. Phys. 15, 1949-56.
12. Bates, D. R., and Moffett, 1966, Proc. Roy. Soc. (Lon.) A 291, 1-8.
13. Chapman, S. and Cowling, T. G., 1970, The Mathematical Theory of Non-Uniform Gases, Cambridge University Press, 3rd. ed.
14. Cline, A. K., Moler, C. B., Stewart, G. W., and Wilkinson, J. H., 1979, SIAM J. Numer. Analy. 16, 368-75.
15. Cullum, J. K., and Willoughby, R. A., 1985, Lanczos Algorithms for Large Symmetric Eigenvalue Computations, Vol. I, Theory, Vol. II, Programs, Birkhäuser (Boston).
16. Delves, L. M., and Mohamed, J. L., 1985, Computational Methods for Integral Equations, Cambridge University Press.
17. Faber, V., and Manteuffel, T. A., 1989, p. 37-61, in Transport Theory, Invariant Imbedding and Integral Equations, (P. Nelson, V. Faber, T. A. Manteuffel, D. A. Seth and A. B. White, Jr., eds.) Marcel Dekker.
18. Ferziger, J. H., and Kaper, H. G., 1972, Mathematical Theory of Transport Processes in Gases, North-Holland.
19. Flannery, M. R., 1971, Ann. Phys. (N.Y.) 67, 376-88.
20. ibid., 1972, Chap. 1, p. 1-90, in Case Studies in Atomic Collision Physics, Vol. 2, (E. W. McDaniel and M. R. C. McDowell, eds.), North-Holland.

21. ibid., 1973, Ann. Phys. (N.Y.) 79, 480-517.
22. ibid., 1980, J. Phys. B: At. Mol. Phys. 13, 3649-64.
23. ibid., 1981, J. Phys. B: At. Mol. Phys. 14, 915-34.
24. ibid., 1982, Phil. Trans. Roy. Soc. (Lon.) A 304, 447-97.
25. ibid., 1987, J. Phys. B: At. Mol. Phys. 20, 4929-38.
26. ibid., 1987, J. Chem. Phys. 87, 6947-56.
27. Flannery, M. R., and Mansky E. J., 1988, J. Chem. Phys. 88, 4228-41.
28. ibid., 1989, "Kinetic Theory Foundations of Ion-Ion Recombination", J. Chem. Phys., to be submitted.
29. ibid., 1989, Chem. Phys. 132, 115-36.
30. Golub, G. H., and van Loan, C. F., 1983, Matrix Computations, Johns Hopkins University Press.
31. Grimes, R. G., Kincaid, D. R., and Young, D. M., 1979, ITPACK 2.0 User's Guide, CNA-150, Center for Numerical Analysis, Univ. Texas (Austin).
32. Hageman, L. A., and Young, D. M., 1981, Applied Iterative Methods, Academic Press.
33. IMSL Math/Library User's Manual, Vol. 1, 1989.
34. Linz, P., 1985, Analytical and Numerical Methods for Volterra Equations, SIAM Press (Philadelphia).
35. Mansky, E. J., 1985, Ph.D. thesis, Georgia Institute of Technology.
36. Manteuffel, T. A., 1977, Numer. Math. 28, 307-27.
37. ibid., 1978, Numer. Math. 31, 183-208.
38. Morgan, W. L., Whitten, B. L., and Bardsley, J. N., 1980, Phys. Rev. Lett. 45, 2021-4.
39. Pitaevskii, L. P., 1962, Soviet Phys. JETP 15, 919-21.
40. Thomson, J. J., 1924, Phil. Mag. 47, 337-78.
41. Tolman, R. C., 1938, The Principles of Statistical Mechanics, Oxford University Press.
42. Young, D. M., 1971, Iterative Solution of Large Linear Systems, Academic Press.
43. Young, D. M., and Jea, K. C., 1980, Lin. Algebra Appl. 34, 159-94.